INDIAN JOURNAL OF PHYSICS

VOL. XVII

AND

PROCEEDINGS

OF THE

Indian Association for the Cultivation of Science, Vol. XXVI

(Published in Collaboration with the Indian Physical Society)

Indian Journal of Physics.

(With Eight Plates)

PRINTED BY DINABANDHU GANGULEE, B.A., SUPERINTENDENT, CALCUTTA
UNIVERSITY PRESS, 48, HAZRA ROAD, BALLYGUNGE, CALCUTTA, AND
PUBLISHED BY THE SECRETARY, INDIAN ASSOCIATION FOR
THE CULTIVATION OF SCIENCE,
210, Bowbazar Street, Calcutta.

1944

Price Rs. 12 or £1-2-6

CONTENTS

PART I

PAGE

1. Application of Photon Statistics to the Specific Heat of Monatomic Solid—By B. N. Biswas 1
2. Study of the Band-pass Effect by Cathode-ray Oscillograph—By S. P. Chakravarti 7
3. Propagation of Elastic Waves through Electrolytic Solutions—By A. K. Dutt and B. B. Ghosh 19
4. On the Nature of Latent Images formed in Photographic Emulsions due to Light-absorption and to the Passage of Ionising Particles —By D. M. Bose 27
5. Fluid flow through Porous Media, Part II. Porosity, Permeability and average Grain Size of Consolidated Sands—By N. C. Sen Gupta and Mg. Thein Nyun 39
6. On the Ultra-violet Absorption of the Dyestuffs in Solution and Influence of Neutral Salts on the same—By Krishnadas Chowdhury and Chitta Ranjan Bose 43
7. On the Nature of Dynatron type Negative Impedances at Frequencies from 1 to 40 Megacycles/Second—By S. P. Chakravarti and P. N. Das 51

PART II

8. Spectrum of Active Nitrogen in the Schumann Region—By B. M. Anand, P. N. Kalia and Mela Ram 69
9. Electrical Properties of Indian Mica—By S. Datta, J. Sen Gupta and P. C. Mahanti 79
10. String under Intermittent impulses and Experimental verifications of Kar's Theory of Intermittent action—By H. G. Mane and B. N. Biswas 97
11. A Note on Elementary Theory of Thermal Diffusion—By R. N. Rai and D. S. Kothari 103
12. A Vibrographic Study of the Output of a Single-phase Half-wave Power Rectifier—By T. Tirunarayanachar 107
13. Volume Rectification of Crystals—By S. R. Khastgir 111
14. The advantage of using Orthogonalised terms in a Polynomial for Curve fitting—By V. Satakopan 115
15. The Atmospheric Absorption Curves and their dependence on the nature of the Primary Cosmic Rays—By S. K. Chakravarti ... 121

PART III

PAGE
16. A study of Absorption lines of Potassium vapour under varying conditions of Temperature and Pressure—By D. K. Bhattacharya and S. P. Sinha 131
17. The Band Spectrum of Phosphorus, Part I, Rotational Structure—By K. Narahari Rao 135
18. Intensity distribution in Molecular Spectra ; Class I, System HgCl and HgBr—By M. G. Sastry 141
19. The Band Spectrum of Phosphorus, Part II, Alternating intensity and Nuclear Spin—By K. Narahari Rao 149
20. Dipole moments of the Chief Constituents of Lac Resin—By G. N. Bhattacharya 153
21. On the Axial Length of Phloroglucin Dihydrate—By C. R. Bose and Ranjit Kumar Sen 163
22. On the Theory of Performance of wide and Ultra-violet band Lattice type Crystal Band-pass filters containing stabilised negative impedance element—By S. P. Chakravarti 167

PART IV

23. Electrical Energies of two Cylindrical Charged particles—By G. P. Dube 189
24. A Note on Oscillating Rotator—By K. Basu 193
25. On the presence of Phosphorus in Solar Atmosphere—By K. Narahari Rao 197
26. The Dielectric constant of Ionised air in a Discharge Tube in the range of wavelengths 80 cm.-1500 cm.—By Nurul Alam and S. R. Khastgir 204
27. A new Ultra-violet Band system of Antimony Monoxide (SbO)—By A. K. Sen Gupta 216
28. Transformation of Diazocyanides—By M. A. Saboor 223
29. Spectrum of Doubly-ionised Cadmium—By K. C. Majumdar 229

PART V

30. On Whistling Meteors—By S. R. Khastgir 239
31. Development of γ and δ Bands of Nitric oxide in Active Nitrogen and Lyman bands in Helium-Nitrogen mixture—By B. M. Anand ... 246
32. On the Experimental study of the Effect of Transverse H.F. Electric field on the Viscosity of Liquids—By B. N. Singh and S. Ghosh 252
33. Radium content of Ceylon Thorianite—By P. K. Sen Chowdhury ... 257
34. On Sargent curves for Artificially β-active Nuclei—By P. K. Sen Chowdhury 262
35. Studies of Electrical Interference to Radio Reception—By S. C. Majumdar, S. M. Sen and S. R. Khastgir 271

PAGE

36. Influence of Common Ion on the Dissociation of Some Strong Electrolytes, Part I Sulphuric acid and Bisulphates—By N. Rajeswara Rao 283
37. Experiments in Scattered light. Angles of First minimum.—By R. V. Tambankar and G. R. Paranjpe 287
38. Effect of temperature on the Electrolytic dissociation in Strong Electrolytes. Part I. Nitric Acid—By N. Rajeswara Rao ... 295

PART VI

39. A Note on Dirac Equations and the Zeeman Effect—By S. N. Bose and K. Basu 301
40. Influence of Temperature on the Intensities of Raman lines due to some Organic Liquids—By S. C. Sircar and S. B. Sanyal ... 309
41. A Self-consistent Method of Determining the Mass of Mesotron—By K. C. Kar and R. R. Roy 316
42. The Theory of Neutron-proton Scattering—By K. C. Kar and R. R. Roy 321
43. Molecular Association in Oxyacids—By N. Rajeswara Rao ... 236
44. Study of Electrolytic Dissociation in Strong Electrolytes by Raman Effect. Trichloracetic acid—By N. Rajeswara Rao ... 332
45. Fluid Flow through Porous Media, Part III. Air Permeability of consolidated Sands partly Saturated with water—By N. C. Sen Gupta 338
46. On the Theory of Emission of α-particles from Radio-active Nuclei—By G. P. Dube and S. N. Jha 344
47. Study of Electrolytic Dissociation in Strong Electrolytes by Raman Effect. Miscellaneous substances, Phosphoric acid, Bicarbonates and Perchloric acid—By N. Rajeswara Rao... 357

AUTHOR INDEX

AUTHOR	SUBJECT	PAGE
Alam, Nurul and Khastgir, S. R.	The Dielectric Constant of Ionised Air in a Discharge Tube in the range of Wave lengths 80 cm—1500 cm. ...	204
Anand, B. M., Kalia, P. N. and Mela Ram	Spectrum of Active Nitrogen in the Schumann region ...	69
Anand, B. M.	Development of δ and γ bands of Nitric Oxide in Active Nitrogen and Lyman bands in Helium-Nitrogen mixture ...	246

AUTHOR	SUBJECT	PAGE
Basu, K.	A note on Oscillating Rotator ...	193
Bhattacharya, D. K. and Sinha, S. P.	A study of Absorption lines of Potassium Vapour under Varying conditions of Temperature and Pressure ...	131
Bhattacharya, G. N.	Dipole Moments of chief Constituents of Lac resin ...	153
Biswas, B. N.	Application of Photon Statistics to the Specific heats of a Monatomic solid ...	1
Bose, C. R. and Sen, Ranjitkumar.	On the Axial length of Phloroglucin Dihydrate	163
Bose, D. M.	On the nature of Latent Images formed in Photographic Emulsions due to Light absorption and to passage of Ionising particles ...	27
Bose, S. N. and Basu, K.	A note on Dirac equations and the Zeeman Effect ...	301
Chakravarti, S. K.	The Atmospheric Absorption Curves and their dependence on the nature of Primary Cosmic rays ...	121
Chakravarti, S. P.	Study of Band-pass effect by Cathode ray Oscillograph ...	
Chakravarti S. P. and Das, P. N.	On the frequency of Dynatron type Negative impedances at frequencies from 1 to 40 Mega cycles/sec. ...	51
Chakravarti, S. P.	On the Theory of performance of wide Ultra-violet band Lattice type Crystal Band pass filters containing Stabilised Negative Impedance element ...	168
Chowdhury, Krishnadas and Bose, C. R.	On the Ultra-violet Absorption of Dye-stuff in solution and the Influence of Neutral salt on the same ...	43
Datta, A. K. and Ghosh, B. B.	Propagation of Elastic wave through Electrolytic solutions ...	19
Datta, S., Sengupta, J. and Mahanti, P. C.	Electrical properties of Indian Mica	79
Dube, G. P.	Electrical energies of Two Cylindrical charged particles ...	189
Dube, G. P. and Jha, S. N.	On the Theory of Emissions of α-particles from Radio-active Nuclei ...	344
Kar, K. C. and Roy, R. R.	A Self-consistent Method of determining the Mass of Mesotron ...	316
Kar, K. C. and Roy, R. R.	The theory of Neutron-Proton scattering ..	321
Khastgir, S. R.	Volume Rectification of Crystals ...	111
Khastgir, S. R.	On Whistling Meteors ...	239

AUTHOR	SUBJECT	PAGE
Majumdar, S. C., Sen, S. M. and Khastgir, S. R.	Studies of Electrical Interference to Radio Reception	271
Majumdar, K. C.	Spectrum of Doubly-ionised Cadmium	229
Mane, H. G. and Biswas, B. N.	String under Intermittent Impulses and experimental verification of Kar's theory of Intermittent action	97
Rai, R. N. and Kothari, D. S.	A note on Elementary theory of Thermal diffusion	103
Rao, K. Narahari	The Band spectrum of Phosphorus, Part I, Rotational Structure	135
Rao, K. Narahari	The Band spectrum of Phosphorus, Part II, Alternating intensity and Nuclear spin	149
Rao, K. Narahari	On the presence of Phosphorus in Solar Atmosphere	197
Rao. N. Rajeswara	Influence of Common Ion on the Dissociation of some strong Electrolytes	283
Rao, N. Rajeswara	Effect of temperature on the Electrolytic dissociation in Strong Electrolytes, Part I, Nitric Acid	295
Rao, N. Rajeswara	Molecular Association in Oxyacids	326
Rao, N. Rajeswara	Study of Electrolytic Dissociation in Strong electrolytes by Raman Effect. Trichloracetic acid	332
Rao, N. Rajeswara	Study of Electrolytic Dissociation in Strong electrolytes by Raman Effect. Miscellaneous substances, Phosphoric acid, Bicarbonate, and Perchloric acid	357
Saboor, M.A.	Transformation of Diazocyanides	223
Sastry, M. G.	Intensity distribution in Molecular Spectra, Class I, System of Hp Cl and HgBr	141
Satakopan, V.	The advantage of using Orthogonalised terms in Polynomial for curve fitting	115
Sen Chowdhury, P. K.	Radium content of Ceylon Thorianite	257
Sen Chowdhury, P. K.	On Sargent curves for artificially β-active nuclei	262
Sen Gupta, A. K.	A new Ultra violet band system of Antimony Monoxide (SbO)	216
Sen Gupta, N. C. and Nyun, Mg. Thein	Fluid flow through Porous Media, Part II, Porosity, Permeability and Average grain size of Consolidated sand	39

AUTHOR	SUBJECT	PAGE
Sen Gupta, N. C.	Fluid flow through Porous Media, Part III, Air permeability of Consolidated Sands partly Saturated with water ...	338
Singh, B. N. and Ghosh, S.	On the Experimental Study of the Effect of Transverse H. F. Electric field on the Viscosity of Liquids ...	252
Sirkar, S. C. and Sanyal, S. B.	Influence of Temperature on the Intensities of Raman lines due to some Organic Liquids ...	309
Tambankar, R. V. and Paranjpe, G. R.	Experiments in Scattered light, Angles of First Minimum ...	287
Tirunarayanachar, T.	A Vibrographic study of the Output of a Single-phase Half-wave Power Rectifier ...	107

SUBJECT INDEX

SUBJECT	AUTHOR	PAGE
Absorption lines of Potassium vapour under Varying conditions of Temperature and Pressure, A study of	D. K. Bhattacharyya and S. P. Sinha ...	131
Active Nitrogen in Schumann Region, Spectrum of	B. M. Anand, P. N. Kalia and Mela Ram ...	69
Atmospheric Absorption Curves and their dependence on the nature of Primary Cosmic Rays, The	S. K. Chakravarti ...	121
Band-pass Effect by Cathode Ray Oscillograph, Study of	S. P. Chakravarti ...	7
Band-pass Filters containing stabilised Negative Impedance, On the theory of Performance of wide and Ultra-violet band Lattice type crystal	S. P. Chakravarti ...	168
Band Spectrum of Phosphorus. The. Part I, Rotational Structure	K. Narahari Rao ...	135
Band Spectrum of Phosphorus. The. Part II, Alternating Intensity and Nuclear spin.	K. Narahari Rao ...	149
Band System of Antimony Monoxide (SbO). A new Ultra-violet.	A. K. Sen Gupta ...	216
Bands of Nitric Oxide in Active Nitrogen and Lyman-bands in Helium-Nitrogen mixture, Development of δ and γ	B. M. Anand ...	246

SUBJECT	AUTHOR	PAGE
Cylindrical charged particles, Electrical Energies of two	G. P. Dube	189
Diazocyanides, Transformation of,	M. A. Saboor	223
Dipole moments of chief Constituents of Lac Resin	G. N. Bhattacharya	153
Dielectric constant of Ionised air in Discharge tubes in the range of Wave lengths 80 cm—1500 cm. The	Nurul Alam and S. R. Khastgir	204
Dirac Equations and the Zeeman effect, A note on	S. N. Bose and K. Basu	301
Dissociation of strong Electrolytes, Influence of Common Ion on the,	N. Rajeswara Rao	283
Doubly ionised Cadmium, Spectrum of,	K. C. Majumdar	229
Dynatron type Negative Impedance at frequencies from 1 to 4 Mega cycles/sec, On the nature of	S. P. Chakravarty and P. N. Das	51
Dye-stuffs in solution and the Influence of Neutral salt on the same, On the ultra-violet absorption of the	Krishnadas Chowdhury and C. R. Bose	43
Elastic wave through Electrolytic Solution, Propagation of	A. K. Datta and B. B. Ghosh	19
Electrolytic Dissociation in Strong Electrolytes, Effect of Temperature on the, Part I, Nitric Acid	N. Rajeswara Rao	205
Electrolytic Dissociation in Strong Electrolytes by Raman Effect, Study of Trichloracetic Acid	N. Rajeswara Rao	332
Electrolytic Dissociation in Strong Electrolytes by Raman Effect, Study of. Miscellaneous substances, Phosphoric acid, Bicarbonates and Perchloric acid.	N. Rajeswara Rao	357
Emissions of α-particles from Radio-active nuclei. On the Theory of	G. P. Dube and S. N. Jha	344
Fluid flow through Porous Media, Part II, Porosity, Permeability and Average grain size of Consolidated sand	N. C. Sengupta and Mg. Thein Nyan	39
Fluid flow though Porous Media, Part III, Air Permeability of Consolidated Sands partly Saturated with water	N. C. Sengupta	338
Indian Mica. Electrical properties of	S. Datta, J. Sengupta and P. C. Mahanti	79

SUBJECT	AUTHOR	PAGE
Latent images formed in Photographic Emulsions due to Light-absorption and to the passage of Ionising particles, On the nature of	D. M. Bose	27
Mesotron, A self-consistent Method of determining the Mass of	K. C. Kar and R. R. Roy	316
Molecular Association in Oxyacids	N. Rajeswara Rao	326
Molecular Spectra, Intensity distribution in, Class I, System of HgCl and Hg Br.	M. G. Sastry	141
Neutron-Proton Scattering, The Theory of	K. C. Kar and R. R. Roy	321
Orthogonalised terms in Polynomial for curve fitting, The advantage of using	V. Satakopan	115
Oscillating Rotator, A note on	K. Basu	193
Phloroglucin Dihydrate, On the axial lengths of	C. R. Bose and R. K. Sen	163
Power Rectifier, A Vibrographic study of the output of a Single-phase, Half-wave	T. Tirunarayanchar	107
Radium content of Ceylon Thorianite	P. K. Sen Chowdhury	257
Raman Lines due to some Organic liquids, Influence of Temperature on the Intensities of	S. C. Sirkar and S. B. Sanyal	309
Radio Reception, Studies of Electrical interference to,	S. C. Majumdar, S. M. Sen and S. R. Khastgir	271
Sargents curves for Artificially β-active Nuclei, On	P. K. Sen Chowdhury	262
Scattered light, Experiments in, Angles of First minimum	R. V. Tamhankar and G. R. Paranjpe	287
Solar Atmosphere, On the presence of Phosphorus in	K. Narahari Rao	197
Specific Heat of Monatomic solid, Application of Photon Statistics to the	B. N. Biswas	1
String under Intermittent pulses and experimental verification of Kar's theory of Intermittent action.	H. D. Mane and B. N. Biswas	97
Thermal Diffusion, A note on Elementary theory on	R. N. Rai and D. S. Kothari	103
Volume Rectification of Crystal	S. R. Khastgir	111
Viscosity of Liquids, On the experimental study of the effect of transverse H. F. electric field on the	B. N. Singh and S. Ghosh	252
Whistling Meteors, On	S. R. Khastgir	239

APPLICATION OF PHOTON STATISTICS TO THE SPECIFIC HEAT OF A MONATOMIC SOLID

By B. N. BISWAS

(Received for publication, Aug. 24, 191[illegible])

ABSTRACT. In the present paper, the statistics of photons, as developed by the author in a previous paper, has been applied to derive an expression for the specific heat of a monatomic solid, the molecules of which are endowed with three degrees of freedom. The expression thus found is similar to Debye's expression for the specific heat of a monatomic solid. Expressions for the entropy and free energy of the solid have also been worked out.

SUMMARY OF STATISTICS OF PHOTONS

Black radiation contained in a chamber at any temperature is assumed to consist of photons in thermal equilibrium The whole of the phase space representing them is divided into cells of volume h^3.

Number of cells contained in the energy layers $h\nu$ and $h(\nu+d\nu)$ in the phase space

$$V \times 4\pi\nu^2 \times d\nu \qquad \dots \quad (1)$$

where V is the volume of the black chamber.

The total number of cells to be considered in the phase space within the energy layers $h\nu$ and $h(\nu+d\nu)$

$$= \frac{8\pi V.\nu^2.d\nu}{c^3} \qquad \dots \quad (2)$$

in view of polarisation.

In this domain of the phase space, some cells will remain empty, some will contain one representative point, some two, and so on.

C_r = number of cells containing r representative points ($r = 0, 1, 2, \dots$)

$$= \frac{8\pi V.\nu^2}{c^3}\left(1 - e^{-\frac{h\nu}{kT}}\right)e^{-r\frac{h\nu}{kT}}. \qquad \dots \quad (3)$$

The total number of photons represented in the same phase space,

$N = C_1 + 2C_2 + 3C_3 + \dots$

$$= \frac{8\pi V.\nu^2.d\nu}{c^3}\left(1 - e^{-\frac{h\nu}{kT}}\right)\left[e^{-\frac{h\nu}{kT}} + 2.e^{-2\frac{h\nu}{kT}} + 3.e^{-3\frac{h\nu}{kT}} + \dots\right]$$

$$= \frac{8\pi V.\nu^2.d\nu}{c^3} \times \frac{1}{e^{h\nu/kT} - 1}. \qquad \dots \quad (4)$$

Total amount of energy associated with photons of frequency

$$E=\frac{8\pi V.\nu^2.d\nu}{c^3}\times\frac{h\nu}{e^{h\nu/kT}-1}. \qquad \ldots (5)$$

Entropy of the same photons,

$$S=\frac{8\pi k.V.\nu^2d\nu}{c^2}\left\{\frac{\frac{h\nu}{kT}}{e^{h\nu/kT}-1}-\log\left(1-e^{-\frac{h\nu}{kT}}\right)\right\}. \qquad \ldots (6)$$

Free energy of the same photons,

$$F=\frac{8\pi V.k.T.\nu^2}{c^3}\log\left(1-e^{-\frac{h\nu}{kT}}\right). \qquad \ldots (7)$$

STATISTICAL THEORY OF SPECIFIC HEAT OF A MONATOMIC SOLID

The molecular weight of a monatomic solid contains N atoms, N being Avogadro's number. Hence the system has 3N degrees of freedom. The degree of freedom is defined here by the number of independent terms contained in the expression for its energy. Thus the expression for the heat content of a monatomic solid would consist of 3N terms. In order to derive the law of partition of energy in this case, from the principles of statistics of photons, quantised waves in ether having been replaced by photons, the solid, as a whole, is assumed to be a continuous elastic medium in which energy is associated with two types of waves, longitudinal and transverse. Each of these two types of waves is assumed to be quantised. Hence it can be replaced by photons. Longitudinal waves of frequency ν are replaced by photons, called afterwards as longitudinal photons of frequency ν, each of energy $h\nu$ and momentum $h\nu/C_L$ where C_L is the velocity of the longitudinal wave in the elastic solid and is equal to $\sqrt{K+\frac{4}{3}n/\rho}$. Similarly, transverse waves, by photons of frequency ν, called transverse photons, each of energy $h\nu$ and momentum $h\nu/C_T$ where C_T is the velocity of the transverse waves in the solid and is equal to $\sqrt{n/\rho}$; K is the bulk modulus of elasticity and n the coefficient of rigidity and ρ the density of the medium.

The expression for the energy of the solid would, in the light of the assumptions made above, include as many independent terms as the number of cells required in the phase space to represent all the photons in the phase space, the energy of a cell being equal to the energy of photons, the representative points of which are enclosed by the cell. Hence their total number must be 3N.

Thus, 3N = number of cells for longitudinal photons
+ number of cells for transverse photons

$$=4\pi V\int_0^{\nu}\frac{1}{C_T^3}+\frac{2}{C_L^3}\,d\nu. \qquad (8)$$

From (1) and (2), the upper limit must be a definite quantity as the L.H.S.E. is definite. The upper limit obviously depends on the nature of the substance in view of 3N being independent of the nature of the substance, V, of course, stands for the volume of the solid.

or,

$$3N = \frac{4\pi V \nu_m^3}{3}\left[\frac{1}{C_L^3} + \frac{2}{C_T^3}\right]$$

$$\nu_m^3 = \frac{9N}{4\pi V\left[\frac{1}{C_L^3} + \frac{2}{C_T^3}\right]}, \qquad \dots \quad (9)$$

Energy associated with both types of photons of frequency ν is, according to (5),

$$= 4\pi V\left[\frac{1}{C_L^3} + \frac{2}{C_T^3}\right] \times \frac{h\nu^3}{e^{h\nu/kT} - 1}\, d\nu. \qquad \dots \quad (10)$$

Heat content of the solid

$$= 4\pi V\left[\frac{1}{C_L^3} + \frac{2}{C_T^3}\right] \int_0^{\nu_m} \frac{h\nu^3}{e^{\frac{h\nu}{kT}} - 1}\, d\nu$$

$$= \frac{9N}{\nu_m^3} \int_0^{\nu_m} \frac{h\nu^3}{e^{\frac{h\nu}{kT}} - 1}. \qquad \dots \quad (11)$$

On putting $\frac{h\nu}{kT} = \epsilon$, $\frac{h\nu_m}{k} = \theta$ and $\frac{\theta}{T} = \epsilon_m$, we have

$$U = 9RT\left(\frac{T}{\theta}\right)^3 \int_0^{\epsilon_m} \frac{\epsilon^3 . d\epsilon}{e^{\epsilon} - 1} \qquad \dots \quad (11a)$$

$$C_v = \frac{dU}{dT} = 9R\frac{T^3}{\theta^3} \times \int_0^{T} \frac{e^{\epsilon}\epsilon^4}{(e^{\epsilon} - 1)^2}\, d\epsilon$$

$$= 3R\left[\frac{12}{x^3}\int_0^x \frac{\epsilon^3}{e^{\epsilon} - 1}\, d\epsilon - \frac{3x}{e^x - 1}\right], \qquad \dots \quad (11b)$$

putting $x = \epsilon_m = \frac{\theta}{T}$,

which is the same as Debye's expression for the specific heat of a monatomic solid.

From (6) and (9) we have entropy of the solid,

$$S = \frac{9Nk}{\nu_m^3}\left[\int_0^{\nu_m}\left\{\frac{\frac{h\nu^3}{kT}}{e^{\frac{h\nu}{kT}} - 1} - \nu^2 \log\left(1 - e^{-\frac{h\nu}{kT}}\right)\right\}.d\nu\right] \qquad \dots \quad (12)$$

excluding the constant term,

$$= \frac{9NkT}{\theta^3} \int_0^{\epsilon_m} \frac{\epsilon^3 . d\epsilon}{e^{\epsilon} - 1} - \frac{9NkT^3}{\theta^3} \int_0^{\epsilon_m} \epsilon^2 . \log\left(1 - e^{-\epsilon}\right) . d\epsilon \qquad \ldots \quad (12a)$$

on making the same substitutions as before.

$$S = \frac{12NkT^3}{\theta^3} \int_0^{\frac{\theta}{T}} \frac{\epsilon^3}{e^{\epsilon} - 1} . d\epsilon - 3Nk \log\left(1 - e^{-\frac{\theta}{T}}\right) \qquad \ldots \quad (12b)^*$$

which is the general expression for the entropy of the solid, excluding the constant term.

APPROXIMATIONS AT LOW AND HIGH TEMPERATURES

(*i*) *Low temperature*—

At very low temperatures, $T << \theta$, consequently equation (12*a*) assumes the following form :

$$S = \frac{9N.kT^3}{\theta^3} \int_0^{\infty} \frac{\epsilon^3}{e^{\epsilon} - 1} d\epsilon - \frac{9N.kT^3}{\theta^3} \int_0^{\infty} \epsilon^2 . \log\left(1 - e^{-\epsilon}\right) . d\epsilon$$

$$= \frac{4\pi^4}{5} \times \frac{N.k.T^3}{\theta^3} \qquad \ldots \quad (12c)\dagger$$

excluding the constant terms.

(*ii*) *High temperature*—

$$T >> \theta$$

Equation (12*a*) assumes the following form :

$$S = \frac{9NkT^3}{\theta^3} \int_0^{\epsilon_m} \frac{\epsilon^3 . d\epsilon}{e^{\epsilon} - 1} - \frac{9NkT^3}{\theta^3} \int_0^{\epsilon_m} \epsilon^2 . \log\left(1 - e^{-\epsilon}\right) . d\epsilon$$

$$= 4Nk + 3Nk \log \frac{T}{\theta} \qquad \ldots \quad (12d)\ddagger$$

excluding the constant term.

From (7) and (9) we have free energy of the solid

$$F = \frac{9N.kT}{\nu_m^3} \int_0^{\nu_m} \nu^2 . \log\left(1 - e^{-\frac{h\nu}{kT}}\right) d\nu, \text{ excluding the constant term.}$$

$$= 9kT\left(\frac{T}{\theta}\right)^3 \int_0^{\epsilon_m} \epsilon^2 . \log\left(1 - e^{-\epsilon}\right) d\epsilon \qquad \ldots \quad (13)$$

$$= 3NkT \log\left(1 - e^{-\frac{\theta}{T}}\right) - \frac{3NkT^4}{\theta^3} \int_0^{\frac{\theta}{T}} \frac{\epsilon^3}{e^{\epsilon} - 1} . d\epsilon \qquad \ldots \quad (14)$$

which is the general expression for the free energy, excluding the constant term.

---

* *Vide* p. 591, *The Principles of Statistical Mechanics*, *Tolman*, equation (137.36).

† *Vide* p. 591, *Tolman*, equation (137.37).

‡ *Vide* p. 590, *Tolman*, equation (137.34).

(*i*) *Low temperature, i.e.*, $T << \theta$

The equation (13) assumes the following form :

$$F = 9NkT\left(\frac{T}{\theta}\right)^3 \int_0^{\infty} \epsilon^2 . \log(1 - e^{-\epsilon}) . d\epsilon$$

$$= -\frac{NkT^4\pi^4}{5\theta^3} \tag{15}$$

excluding the constant term.

(*ii*) *High temperature, i.e.*, $T >> \theta$.

From (13) we have

$$F = 9NkT\left(\frac{T}{\theta}\right)^3 \int_0^{\frac{\theta}{T}} \epsilon^2 . \log \epsilon . d\epsilon$$

$$= 3NkT \log \frac{\theta}{T} - NkT, \tag{16}$$

excluding the constant term.

PHYSICAL LABORATORY,
RAJARAM COLLEGE,
KOLHAPUR.

REFERENCE

[1] Biswas, B. N., *Jour. Ind. Math. Soc.*, New Series, Vol. 3, No. 3 (1938).

2

STUDY OF THE BAND-PASS EFFECT BY CATHODE-RAY OSCILLOGRAPH

By S. P. CHAKRAVARTI

(Received for publication, September 26, 1942)

ABSTRACT. The paper relates to study of the important phenomenon of "band-pass effect" by cathode-ray oscillograph method developed by the author utilizing Wood's phase angle measurement.

Measurements were carried out both on low-pass and high-pass filter sections terminated in stabilised negative impedance; and gain or attenuation, phase-shift angle and sign of phase-shift angle of the resulting band pass arrangement were obtained by oscillograph method.

The method not only enabled the phase-shift angle at different frequencies to be obtained with sufficient accuracy and comparative ease, but the variation of the sign of phase-shift angle as the frequency altered could be visually observed. Comparison between this method and a well-known non-oscillographic method has been made.

The method developed here is applicable to determination of gain or attenuation, phase-shift angle and sign of phase-shift angle of all types of wave-filter and network.

1. INTRODUCTION

It was experimentally discovered by the author (1938) about six years ago that both low-pass and high-pass *symmetrical* filter sections of any type terminated in stabilized negative impedances of magnitude more or less equal to their maximum characteristic impedance in the transmission band become "converted" to *unsymmetrical* band-pass filters and in addition, amplification was obtained over the transmitted band. Thus the two effects, namely the "band-pass effect" and "amplification effect," were simultaneously obtained. The band-pass effect was, however, more important than the latter effect. Use of negative impedance of magnitude greater and less than the maximum characteristic impedance in the transmission band for termination purpose had the effect of adjusting gain in the transmission band, transmission band-width and sharpness of cut-off of the resulting band-pass arrangement.

It has been found (Chakravarty, 1941) that the cause of the band-pass effect lies in (*a*) the nature of variation of the network gain or loss of the 'equivalent' network (formed from the original filter section and the negative impedance termination) with frequency and (*b*) the nature of variation of the reflection gain or loss between characteristic impedance of the original filter section and negative impedance of the termination with frequency. It has further been found that the former variation contributes little to the band-pass effect whereas the latter variation contributes mainly to it. The nature of variation of reflection gain or loss with frequency which intensifies the "band-pass effect" is again largely due to variation of negative impedance of the termination with frequency.

The present paper arose out of the desire to examine the "band-pass effect" by an *entirely different* method—by observing patterns on the screen of cathode-ray oscillograph and measuring various lengths and angles thereon. It has been possible by the oscillographic method developed to determine attenuation or gain, angle of phase-shift and sign of the angle of phase-shift at various frequencies for the resulting band-pass arrangement. Both low-pass and high-pass symmetrical filter sections have been considered. Advantages and disadvantages of this oscillographic method over other methods have been fully discussed.

2 CATHODE-RAY OSCILLOGRAPH METHOD

The diagram of connections for study of the band-pass effect by a cathode-ray oscillograph of Standard Telephones and Cables Co.'s make is shown in Figs. 1(*a*) and 1(*b*). Fig. 1(*a*) shows the beat-frequency audio-oscillator (model 70 D), manufactured by Clough Brengle Co.) feeding into a low-pass filter section terminated in a stabilized negative impedance *as well as* the connections from the input and output terminals of the filter section to the plates of the oscillograph

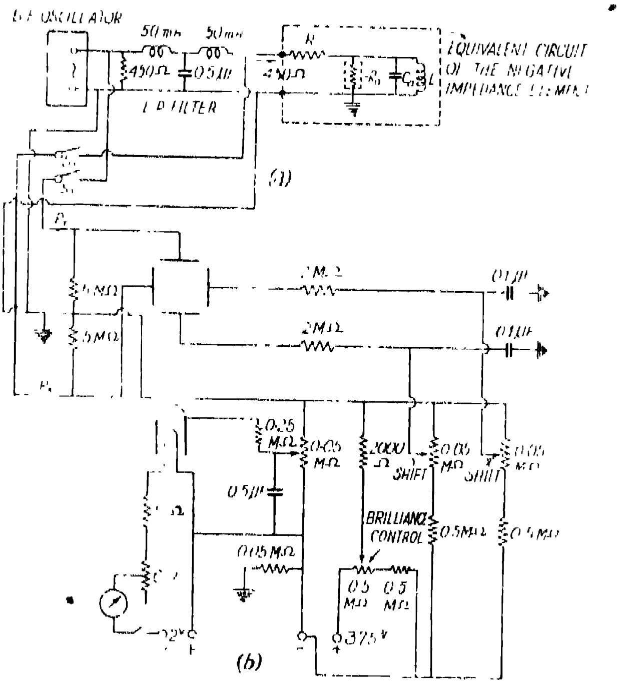

FIG. 1

The plate-to-plate capacitance (for each pair of plates of the cathode-ray oscillograph) is 10 to 12 $\mu\mu$ F and its impedance at 1 Kc/s is 15.8 to 13.2

megohms respectively shunting the input and output impedances of the filter. The anode-filament capacitance of the AC/SG tube together with stray capacitances in parallel and choke inductance both shunting the negative resistance are about 50 $\mu\mu$F and 40 H respectively and their impedance at 1 Kc/s is therefore 3.2 and 0.25 megohms respectively. A high resistance has to be connected across each pair of plates for steadying or stabilizing purpose and has to be of such value that the positive and negative impedances connected across input and output terminals of the filter section respectively are not appreciably altered. A resistance of 5 megohms has been used. Switches S_1 and S_2 enable one to examine only either input or output as desired.

Fig. 1(*b*) shows the circuit of the oscillograph with various controls, designed for the experiment.

Case I. When V_1=effective input voltage (to vertical deflector plates) and V_2=effective output voltage (to horizontal deflector plates), and V_1 and V_2 are of the same phase (*i.e.*, there is no phase-shift in transmission through the filter section).

At first only V_1 is applied across the vertical deflector plates and length of trace measured in cms. Then only V_2 is applied across the horizontal deflector plates and length of trace obtained in cms. Subsequently) the two voltages with no phase-shift between them applied simultaneously across their respective plates will give the resultant—a straight line of length $\sqrt{l_1^2+l_2^2}$ diagonally across the screen at an angle α (to the horizontal) given by

$$\alpha=\tan^{-1}\frac{l_1}{}.$$

Measurement of the lengths of traces l_1 and l_2 (in cms.) corresponding to $2V_1$ and $2V_2$ respectively or of the angle α will give the attenuation or gain directly. If the length of trace in vertical or horizontal direction is directly proportional to voltage at all frequencies and the constant of proportionality same for both directions at all frequencies, attenuation or gain can be obtained in decibels directly from the ratio of lengths. If not, voltages corresponding to lengths have to be obtained from calibration curves.

Case II. When V_1 and V_2 differ in phase.

In this case also, V_1 and V_2 are first applied separately to the respective pairs of plates of the cathode-ray oscillograph and lengths of traces are measured in cms. to obtain attenuation or gain in decibels as $20 \log_{10} l_1/l_2$.

Further, when both V_1 and V_2 are applied simultaneously, an elliptical trace whose dimensions depend upon the phase angle of V_1 and V_2 and their relative values is obtained.

The phase angle is obtained directly from lengths of traces due to V_1 and V_2 on screen, (*i.e.*, $l_1/2$ and $l_2/2$ respectively) as well as from the major and minor axes of the ellipse. If ϕ is the phase-shift between the voltages, then $$\phi=\sin^{-1}\frac{a.b}{4V_1V_2}\,(\text{Wood})^{*3}=\sin^{-1}\frac{a.b}{l_1l_2},$$

where a = major axis of the ellipse, and b = minor axis of the ellipse.

When frequencies higher than 0.4 to 0.5 Mc/s are involved in wave-filters, direct application of V_1 and V_2 to the respective pairs of plates is not desirable. V_1 and V_2 are then applied to two exactly similar super-heterodyne amplifiers (consisting of high-frequency amplifier, mixer and intermediate-frequency amplifier stages) with the same local oscillator giving same gain and phase-shift and the corresponding I.F. voltages V'_1 and V'_2 are applied to the respective pairs or plates of the oscillograph. It is necessary in this case to have linear relation between r.f. input voltage to super-heterodyne system and i.f. output voltage as well as between i.f. output voltage and deflection in cms. on the screen of the oscillograph.

At high frequencies, direct application of V_1 and V_2 to the plates causes instability and loss by radiation and does not give linear relation between voltage applied and deflection on the screen.

At very high frequencies, in addition, the difference in distance between the deflector plates introduces an error in the phase angle measurement due to "Hollmann Phase Effect" (Hollman, 1933). The time of flight of the electron being d/V (where d = axial interplate distance and V = velocity of the beam), the phase angle is $\phi\pm\frac{\omega d}{V}$.

The method evolved here is convenient for finding out gain or attenuation, phase-shift angle, sign of phase-shift angle, etc., at various frequencies for any network or filter section. The advantages and disadvantages of this method are discussed in section 5.

3. LOW-PASS FILTER TERMINATED IN STABILISED NEGATIVE IMPEDANCE ELEMENT

A low-pass H-type filter section (total series inductance = 100 mH and total shunt capacitance = 0.5 μF) of nominal characteristic impedance 450 ohms and cut-off frequency 1500 c. p. s. was terminated by a negative impedance of magnitude nearly same as the nominal characteristic impedance obtained from AC/SG screen-grid tube under secondary emission condition.

Table I gives the results of observation on the traces on the screen of cathode-ray oscillograph. Negative sign in column under 'gain or attenuation' (Table I) signifies gain.

It will be seen from Table I that for first five frequencies (marked with asterisks) the pattern on combining voltage has been observed to be a straight line signifying that there is no phase-shift introduced in transmission at those frequencies. The length of the straight line is almost equal to $\sqrt{l_1^2+l_2^2}$ (where l_1 and l_2 are in cms.).

---

* V_1 and V_2 in the equation stand for corresponding lengths of traces due to them.

TABLE I

Frequency in c.p.s.	l_1 in cms. (corresponding to $2V_1$)	l_2 in cms (corresponding to $2V_2$)	Gain or attenuation db	Nature of pattern on combining voltages	Axes for elliptical pattern a cms.	Axes for elliptical pattern b cms.	Phase shift ϕ
*50	3.50	4.20	−1.58	Straight line 5.4 cms. at 40°			0°
*80	5.40	5.90	−.748	7.9 at ,,		*	0°
*100	5.30	6.00	−.984	8.0 ,, ,,			0°
*200	4.90	5.00	−.172	7.0 ,, ,,			0°
*300	3.70	4.90	−2.412	6.2 ,, ,,			0°
400	3.70	5.10	−2.75	Ellipse with major axis inclined to horizontal at 40°	6.00	0.70	12° 18′
500	3.50	5.10	−3.288	,, ,,	6.00	0.90	17°
600	3.50	5.00	−3.106	,, ,,	5.70	0.95	18°
700	3.50	4.00	−2.922	,, 50°	5.40	1.10	20° 24″
800	3.30	4.40	−2.542	,, ,	4.60	1.30	24° 42′
900	2.90	3.00	−2.542	,, ,,	4.00	1.35	28° 15′
1000	2.80	3.60	−2.008	,, 60°	3.70	1.35	28° 30′
2000	2.00	1.30	3.742	,, 140°	1.80	1.10	40° 44′
3000	2.00	1.10	5.102	,, 150°	1.80	1.10	65°
4000	2.00	0.90	12.766	,, 155°	2.50	0.60	75° 24′
5000	2.00	0.60	12.766	,, 160°	2.00	0.50	65° 15′
6000	2.70	0.40	16.178	,, 165°	2.50	0.30	44°
8000	2.70	0.10	30.158	,, 175°	2.50	0.20	90°

Fig. 2 shows the attenuation or gain and phase-shift with frequency of the band-pass arrangement. The cut-off frequencies are 500 to 1000 c. p. s. The phase-shift ϕ varies linearly with frequency over the transmission band of the band-pass arrangement.

As the frequency is altered from 50 c. p. s. to 8000 c. p. s., the pattern on the screen of cathode-ray oscillograph undergoes remarkable variation. Up to 300 c. p. s., the pattern appears to the eye to be a straight line which may be a much elongated ellipse in which the minor axis has been negligibly small. At 400 c. p. s. and near about the ellipse is an elongated one with major axis at 40° to the horizontal. As frequency increases up to 1000 c. p. s. and near about, the ellipse broadens out gradually with major axis making larger and larger angle with the horizontal. Subsequently, after 2000 c. p. s. the broadening decreases, the ellipse getting thinner and thinner and the major axis makes angles larger than 90° with the horizontal so as to rotate itself to the second quadrant.

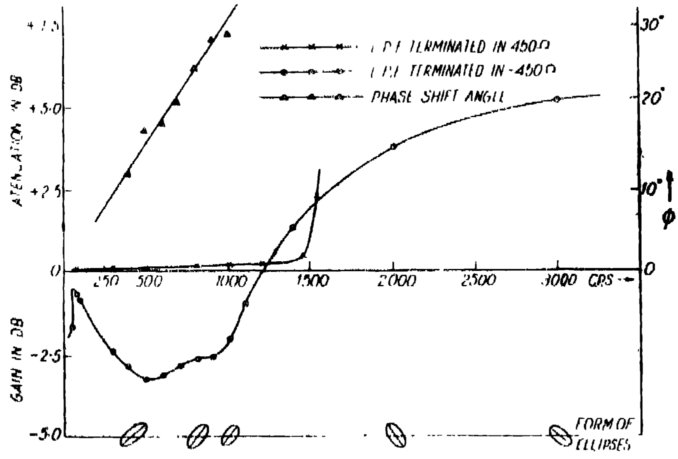

Fig. 2

As the phase angle ϕ between the voltages increases, the ellipse becomes broader ; and as ϕ decreases it becomes narrower. The rotation of ellipse will depend upon the sign of the phase-angle with variation of frequency (*i.e.*, the phase-angle may be ' lagging ' at some frequencies and ' leading ' at others).

It will be seen that within the transmission band (500-1000 c. p. s.) ϕ increases linearly with frequency but remains same with regard to sign (*i.e.*, ellipse is not rotated).

4. HIGH-PASS FILTER TERMINATED IN STABILISED NEGATIVE IMPEDANCE ELEMENT

A high-pass H-type filter section (total series capacitance = 0·075 μF and total shunt inductance = 50 mH) of nominal characteristic impedance 814 ohms and cut-off frequency about 1330 c. p. s. was terminated by a negative impedance of 814 ohms obtained in a similar manner as before.

Table II gives the results of observation on the traces on the screen of cathode ray oscillograph. Negative sign in column under gain or attenuation (Table II) signifies gain.

It will be seen from Table II that for four frequencies (marked with asterisk) it is likely that the pattern is much elongated ellipse with negligibly small minor axis appearing to be a straight line since the length of the line is $<\sqrt{l_1^2+l_2^2}$.

Fig. 3 shows the attenuation or gain and phase shift with frequency of the band-pass arrangement. The cut-off frequencies are 2150 and 4000 c. p. s. Since the sign of ϕ in the transmission band is negative (as explained below), ϕ plotted on negative scale will show a linear variation with frequency over the transmission band.

TABLE II

Frequency in c.p.s.	l_1 in cms corresponding to $2V_1$	l_2 in cms corresponding to $2V_2$	Gain or attenuation db	Nature of pattern on combining voltages	Axes for elliptical patterns		Phase-shift ϕ
					a cms.	b cms.	
*500	3.55	0.60	14.9	St. line 3.1 cms at 10° to horizontal			0°
*600	3.15	0.65	13.7	Do.			0°
700	3.15	0.70	13.1	Ellipse with major axis inclined to horizontal at 15°	3.00	.35	26° 42′
800	3.15	0.85	10.95	Do	3.00	.45	31° 18′
900	2.95	1.00	9.4	at 20°	3.00	.60	37° 48′
1000	2.90	1.20	7.7	at 22°	3.00	.80	44°
1100	2.80	1.30	6.7	,, 25°	2.80	.90	44°
1200	2.70	1.45	5.6	,, 25°	2.85	1.00	46° 48′
1300	2.50	1.70	3.5	,, 30°	2.80	1.20	54° 1′
1400	2.42	1.75	2.9	,, 30°	2.70	1.42	65°
1500	2.30	2.00	1.2	,, 35°	2.05	1.60	67°
1800	1.90	2.43	2.1	,, 60°	2.42	2.00	90°
2000	1.75	2.60	−3.4	,, 80°	2.60	1.85	90°
2400	1.65	2.85	−4.8	,, 105°	2.90	1.60	81° 6′
2800	1.65	2.90	−4.9	,, 120°	3.10	1.25	54°
3600	1.70	2.95	−4.8	,, 130°	3.30	1.10	46° 12′
4000	1.80	2.00	−4.13	,, 130°	3.35	1.00	40° 18′
4200	1.90	2.65	−3.1	,, 130°	3.30	.90	36° 15′
5500	2.02	2.11	−.40	,, 132°	3.30	.50	21° 15′
6000	2.00	2.05	−.20	,, 135°	3.15	.33	14° 30′
*7000	1.50	1.50	0	St. line 1.95 cms at 135°	—	—	0°
*7500	1.60	1.50	.55	St. line 2.0 cms at 135°	-	—	0°

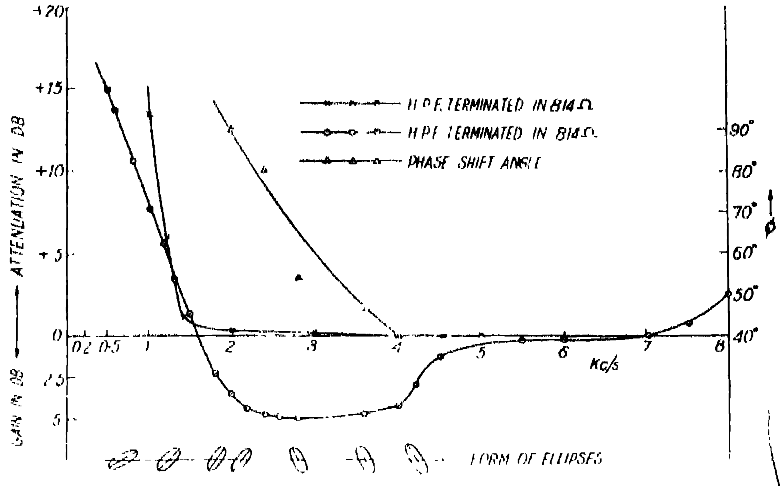

FIG. 3

Here also as the frequency is altered the pattern on the screen of cathode ray oscillograph undergoes remarkable variation. φ increases with frequency and has the same sign up to 2000 c. p. s. and near about. Thereafter φ decreases and also changes in sign. φ, however, has the same sign within the transmission band.

5. DISCUSSION ON MEASUREMENTS BY CATHODE-RAY OSCILLOGRAPHIC METHOD

The oscillographic method employed here utilizes the method of phase-angle determination evolved by Wood (1932), and is capable of giving gain or attenuation as well as phase-angle and its sign with sufficient accuracy both over low and high frequency ranges.

Another cathode ray oscillograph method which might have proved suitable for the purpose was developed by F. de la C. Chard (1938), for measuring gain or attenuation as well as phase angle. It suffers from several disadvantages as follows:—

(1) It requires two pairs of magnetic deflection coils with a number of accessories; (2) the mutual inductance between deflection coils causes inaccuracy specially at higher frequencies; (3) there is also liability of loss by radiation from coils at high frequencies; (4) to find out whether current in coil B say leads or lags that in coil A (that is, to find out the sign of phase-angle) the direction of rotation of the cathode-ray beam has to be observed by viewing the tube screen through a stroboscopic disc (requiring an induction motor rotating a single-holed disc at 1470 r.p.m.); and (5) further the cathode-ray tube should not be of the type which gives a long-sustained afterglow.

The non-oscillographic method developed by Messrs. Hinton, Rendall and White (1920), for measurement of phase-shift angle is capable of giving both gain or attenuation as well as phase-shift angle but requires a special type of transformer, two exactly similar linear amplifiers, a third linear amplifier for combined voltages and a calibrated thermionic voltmeter. For higher frequencies good balancing and great deal of care in circuit design are necessary. If only gain or attenuation is desired but not the phase-shift angle, measurement requires only a calibrated thermionic voltmeter.

Table III shows the results of observation on the same high-pass filter (total series capacitance $=0.25$ μF and total shunt inductance $=150$ mH; nominal characteristic impedance $=770$ ohms and cut-off frequency $=400$ c. p. s.) terminated by -700 ohms (negative impedance) by oscillographic method employed here as well as non-oscillographic method of Messrs. Hinton, Kendall and White. The negative sign in Table III signifies gain.

TABLE III

f in c. p. s.	Oscillographic method		Non-oscillographic method	
	Gain or attenuation db	Phase-shift in degrees	Gain or attenuation in db	Phase-shift in degree
[illegible]00	[illegible]	0	15.0	0°
400	7.5	38°	8.3	30°
600	2.0	41° 30′	2.0	10°
800	−3.5	14°	2.8	43° 30′
900	−5.7	46° 48′	−5.1	40°
1000	0.3	75° 21′	7.4	76° 30
1200	−0.7	65°	−7.5	66°
1400	−0.7	50°	7.3	66°
1600	−0.5	50° 18′	−7.3	55° 30′
2000	−2.7	46° 48′	2.1	46°
3000	1.6	41	1.0	43°
4000	−1.5	30°	−0.8	28° 30′
5000	−1.1	20° 24′	−0.5	19°
10,000	−0.8	0°	0	0°
12,000	−0.5	0°	0	0°
15,000	0	0°	0.5	0°

It will be seen from Table III that there is some discrepancy between gain or attenuation measurements by the two methods and that the non-oscillographic method gives larger gain and better sharpness of cut-off. Further a closer agreement between phase-shift angles measured by the two different methods will be observed.

By comparing the two methods it will be seen that in oscillographic method both gain and phase-shift can be determined from *four* observations per frequency whereas in the method developed by Messrs. Hinton, Rendall and White (1929) both gain and phase-shift can be obtained from *three* observations per frequency but a larger number of equipments (some of special features) as stated above as well as skilful manipulation are necessary. The oscillographic method gives one a visual picture as to how the ellipse undergoes alteration in shape (*i.e.*, broadens out or narrows down) as phase-shift angle increases or decreases with frequency and as to how the ellipse rotates as the sign of ϕ changes with variation of frequency. Thus the oscillographic method has *distinct* advantage over the other method at least regarding the examination of the phase-shift problem.

The disadvantages of the oscillographic method are as follows:—

1. Measurement of lengths of traces on the cathode-ray oscillograph screen is liable to inaccuracy. By means of two adjusters the thickness of lines on the screen can be reduced to less than 0.6 mm. and the whole length can be brought to equally good brilliancy. As the ellipse becomes more and more elongated, measurement of minor axis is liable to introduce great error. Measurement of voltages by thermionic voltmeter for gain or attenuation and phase determinations can give better accuracy.

2. It will be seen that if frequency band involved is large, direct determination of attenuation or gain and phase-angle from lengths measured on the screen of cathode-ray oscillograph is liable to error for reasons discussed below. The wide band difficulty is involved in case of high-pass filter terminated in stabilised negative impedance.

The length of the trace (vertical or horizontal) may not be directly proportional to the a.c. voltage impressed across the plates for all voltages over the frequency range involved and the constant of proportionality may not be the same for traces in vertical and horizontal directions.

An experiment has been carried out to test the relation between length of trace and voltage impressed across the plates for the S. T. C. Co.'s cathode-ray oscillograph (Type 4050A—filament current = 0.9A, anode voltage = 350V, and shield voltage = 25V with respect to filament) used at 1000 and 8000 c. p. s. Table IV shows the results of the experiment.

TABLE IV

Frequency 1000 c. p. s.				Frequency 8000 c. p. s.			
Vertical		Horizontal		Vertical		Horizontal	
Impressed volts	Deflection cms.	Impressed volts	Deflection cms.	Impressed volts	Deflection cms.	Impressed volts	Deflection cms.
3.1	1.0	3.3	1.0	2.9	1.0	3.6	1.0
6.6	2.0	7.1	2.0	6.4	2.0	7.4	2.0
9.9	3.0	10.6	3.0	9.8	3.0	11.2	3.0
13.2	4.0	14 0	4.0	13.3	4.0	14.8	4.0
16.4	5.0	17.4	5.0	17.0	5.0	18.7	5.0

It will be seen from Table IV that the variation is more or less linear in all cases but slight discrepancies occur in the variation for two directions as well as at different frequencies.

6. ACKNOWLEDGMENTS

The whole of the experimental work was carried out at the Kanodia Electrical Communications Engineering Laboratories, Department of Applied Physics, University of Calcutta. Many thanks from the author are due to Prof. P. N. Ghosh, Sc.D., Ph.D., for taking kind interest and giving him all facilities for research work.

REFERENCES

Chakravarti, 1938, *Phil. Mag.*, **26**, 473
Chakravarti, 1941, *Wireless Engineer*, **18**, 103.
Chard F de La, 1938, *J. I. E. E.*, **83**, 681
Hinton, Rendall and White, 1920, *Electrical Communication*, **8**, 30
Hollman, 1933, *Wireless Engineer and Experimental Wireless* **10**, 430 , see also
Hollman and Von Ardenne, 1932, *Electronics*, **5**, 318.
Wood, 1932, *Rev. Sci. Instruments*, **3**, 378.

PROPAGATION OF ELASTIC WAVES THROUGH ELECTROLYTIC SOLUTIONS*

By A. K. DUTTA

AND

B. B. GHOSH

(Received for publication, October 1, 1942)

ABSTRACT The change of supersonic velocity and hence the change of compressibility of different electrolytic solutions with concentration have been studied by previous workers from the standpoint of the ionic theory of Debye. They have so far observed only a rise of supersonic velocity with concentration and have explained minor characteristics of the curve. It has been shown here that heavy alkali halides show at first a decrease of velocity with concentration and then an increase of velocity. This effect is enhanced at higher temperatures. Inasmuch as this behaviour is of opposite nature to the general behaviour of the other electrolytes, the compressibility-concentration relationship bears a close relationship with the viscosity-concentration relationship. These similarities have been critically considered

Two papers on the variation of supersonic velocity with the concentration of electrolytic solutions have drawn some attention. One of them by Szalay[1] gives measurements of supersonic velocity on LiCl, NaCl, KCl, KBr, Li_2SO_4, $MgSO_4$, $ZnSO_4$, $CdSO_4$ and $Al_2(SO_4)_3$. He has observed that the velocity increases with the concentration linearly. The rate of increase of velocity seemed to have no relationship with the valency of the ions. Considering the respective densities he observed that the compressibility decreases with the concentration in electrolytes. He has, however, tried to show that the percentage decrease of compressibility $d\beta/\beta$ at any concentration falls within definite ranges according to the concentration and the ionic valency.

Falkenhagen and Bachem[2] have tried to show in another paper the relationship of the variation of compressibility with concentration from the standpoint of the ionic theory of Debye and Falkenhagen. From the experimental data on the variation of supersonic velocity with concentration and the densities at the corresponding concentrations, they worked out the compressibilities of different salts at different concentrations and plotted the respective curves. These curves show a slight inclination towards the axis. Thus the curves are of the type $\beta=\beta_0+A'C+B'C^{3/2}$ where A' is large and negative and B' is of a smaller order and positive. In essence, Falkenhagen and Bachem have compared the coefficient B' with a constant derived from the ionic theory, the

---

Communicated by the Indian Physical Society.

larger coefficient A′, which determines the general slope of the curves has been left out of consideration. The basis of comparison in Falkenhagen and Bachem's work is as follows:—

The apparent molar compressibility of a solution $\phi(k)$ can be determined when the concentration, the densities and compressibilities of the solvent and the solution are known. Thus the apparent molar compressibility is given by the relationship

$$\phi(\bar{k}_2) = -\frac{(\delta V/\delta p) - (-\delta V_1/\delta p)}{n_2}$$

where V and V_1 are the volumes of solution and solvent and n_2 is the number of moles dissolved,

or
$$\phi(\bar{k}_2) = \frac{\beta V - \beta_1 V_1}{n_2}$$

where β and β_1 are the compressibilities of the solution and solvent,

or
$$\phi(\bar{k}_2) = \beta\frac{1000}{c} - \frac{\beta_1}{d_1}\left(\frac{1000d}{c} - M_2\right)$$

where M_2 is the molar wt. of the solute. Hence knowing β, β_1, d, d_1, c, M_2, $\phi(\bar{k}_2)$ can be experimentally determined and a graph of $\phi(\bar{k}_2)$ against c or $\sqrt{c}$ can be drawn.

Now, $\phi(\bar{k}_2)$ is related with the partial molar compressibility $\bar{k}_2$ which varies with the concentration according to a definite law determined by the ionic theory of Debye and Falkenhagen.

Thus $\bar{k}_2$, the partial molar compressibility

$$-\frac{\partial}{\partial n_2}\left(-\frac{\partial V}{\partial p}\right) = \frac{\partial}{\partial n_2}\left(\beta V\right) = \frac{\partial}{\partial n_2} n_2\left[\phi(\bar{k}_2)\right]$$

since β_1 and V_1 corresponding to the solvent are constants.

or
$$\bar{k}_2 = \phi(\bar{k}_2) + n_2\frac{\delta\phi(\bar{k}_2)}{\delta n_2}$$

$$= \phi(\bar{k}_2) + c\frac{\delta\phi(\bar{k}_2)}{\delta c}.$$

If $\bar{k}_2$ is of the form $a + m\sqrt{c} = a + \frac{3}{2}b\sqrt{c}$, it can be also written as

$$\bar{k}_2 = a + b\sqrt{c} + c.\frac{b}{2\sqrt{c}} = (a + b\sqrt{c}) + c.\frac{\delta}{\delta c}(a + b\sqrt{c}).$$

Comparing the two equation for $\bar{k}_2$ thus obtained one gets,

$$\phi(\bar{k}_2) = a + b\sqrt{c} \quad \text{when} \quad \bar{k}_2 = a + \tfrac{3}{2}b\sqrt{c}.$$

Now, according to ionic theory, an expression for k_2 can be obtained in the form

$$k_2 = k_2^0 - \Sigma\nu_i RT \frac{\delta}{\delta p}(\beta - \beta_1) + \frac{\varepsilon(\Sigma\nu_i z_i^{\,2})^{\frac{3}{2}}}{D^{\frac{3}{2}}\,T^{\frac{1}{2}}}\sqrt{c}\,,$$

where the second term is negligible compared with the third, so that k_2 is roughly of the form $k_2 = a + m\sqrt{c}$ where m is the constant from the ionic theory and can be calculated when the valency of the electrolyte is known. This value of 'm' derived from the ionic theory can be compared with the coefficient $(3/2)\,b$ in the equation for partial compressibility, where b is obtained from the graph of apparent molar compressibility drawn against $\sqrt{c}$.

In the results calculated by Falkenhagen and Bachem, the values are of the same order. But as Bachem[3] points out in a later paper, the coefficient of the same valency does not remain constant as demanded by theory.

However, since

$$\phi(k_2) = \frac{-\delta V/\delta p - \delta V_1/\delta p}{n_2} = a + b\sqrt{c}$$

it is apparent that in the relationship $\beta = \beta_0 + A'C + B'C^{\frac{3}{2}}$ the coefficient A' is composed of the coefficient 'a' in the equation for apparent molar compressibility and the coefficient B' is composed of the coefficient 'b' in the former equation. As we have mentioned previously that in the equation for compressibility A' is large and of a higher order than B', we compare by the method of Falkenhagen and Bachem a secondary effect on the course of the compressibility curve, and the general nature of the variation of compressibility with concentration remains beyond the scope of the ionic theory alone. This remains yet an open problem.

It was considered by us that the compressibility of a liquid medium or a solution would be dependent on the intermolecular cohesive force existing in the medium and this characterises as well the viscosity of the medium. Thus some short of interdependence was expected by us between the compressibility and the viscosity of the solution. In the case of electrolytic solutions it is well known that with most electrolytes the relative viscosity of the solution (compared to water) increases with concentration, and the viscosity is always greater than that of the solvent, whereas in the case of some electrolytes, specially, with the heavy-molecule alkali halides, the relative viscosity at first decreases and then increases with concentration and the viscosity of the solution is very often lower than the viscosity of water. It was, therefore, expected that although the compressibility of most of the electrolytes decreases with concentration, *i.e.*, the velocity increases with concentration, some heavy alkali halide solution might show a decrease of velocity with concentration and thus perhaps an increase of compressibility with concentration. It should be noted in this connection that the variation of density with concentration is quite regular without having any maximum or minimum for all the electrolytes. Hence the shape of the compressibility curves is determined primarily by the shape of the velocity curves. With this view we have measured the velocity of supersonic waves in some electrolytic solutions which show abnormal viscosity and have taken our measurements at different temperatures. It will be evident from the graphs of relative velocity against concentration, that these solutions show abnormal behaviour with regard to the velocity as well, although under not exactly the same condition of temperature and concentration.

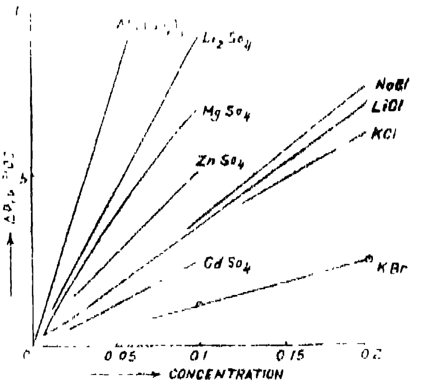

FIG. 1

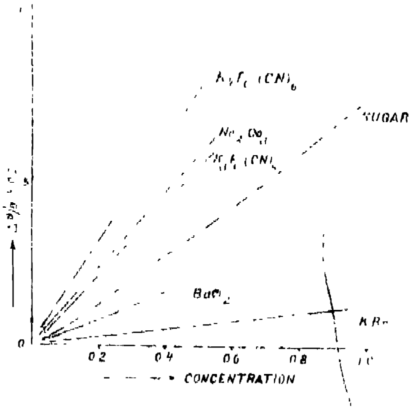

FIG. 1*a*

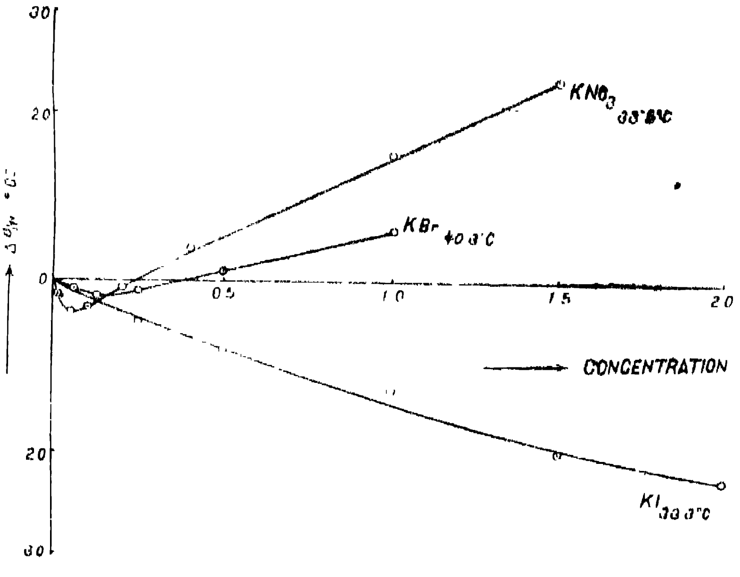

FIG. 2

Figs. 1 and 1*a* show the relative velocity of supersonic waves in electrolytes as obtained by Szalay and by Falkenhagen and Bachem. In Fig. 2 the relative velocity of supersonic waves in particular electrolytes selected by us for their abnormal viscosity curve have been plotted. They show a decrease of velocity with concentration at the lower concentration ranges and then an increase of velocity. In all other electrolytes so far studied by other workers this peculiarity has not been noted. Further, the course of the velocity-concentration graph changes appreciably at different temperatures. The decrease of relative velocity with concentration, which may be considered as abnormal, is enhanced at higher temperatures. These are shown in graphs 3, 3*a*, 3*b*. It will be seen, for example, with KI at higher temperatures, that the compressibility is very much increased compared to that of

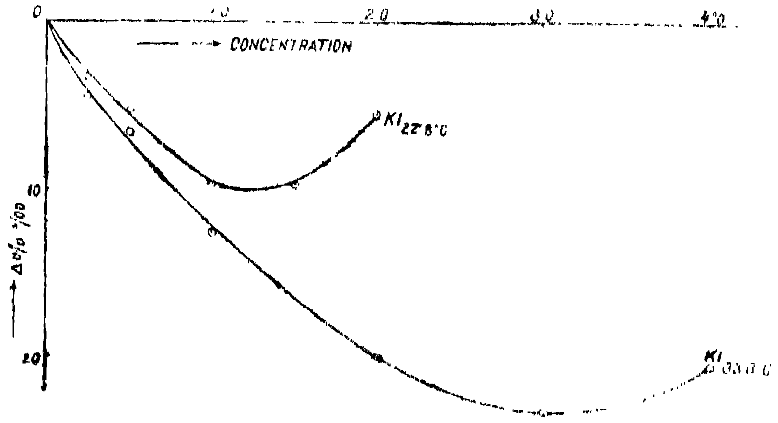

FIG. 3

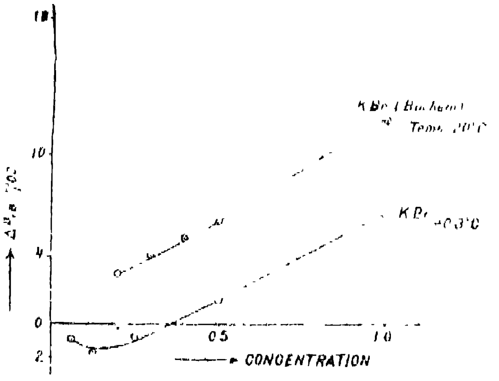

FIG. 3*a*

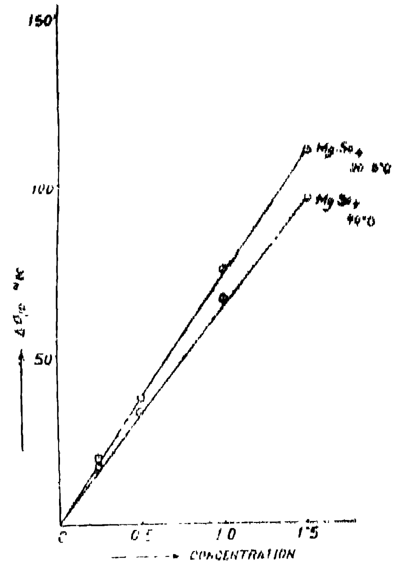

FIG. 3*b*

water. Our ideas up to the present were that the compressibility always decreases when an electrolyte is dissolved in water. The finding is thus corroboratory to the idea obtained from the study of relative viscosity concentration curves that electrolytes fall into two distinct groups according as they increase or tend to decrease the viscosity of water when dissolved. The variation with temperature of the relative viscosity-concentration curves are drawn in Fig. 4, for comparison, from which it will be apparent that there is a peculiar difference in the two classes of electrolytes both from the standpoint of viscosity and the velocity of elastic waves. Other workers have so far failed to note this peculiarity.

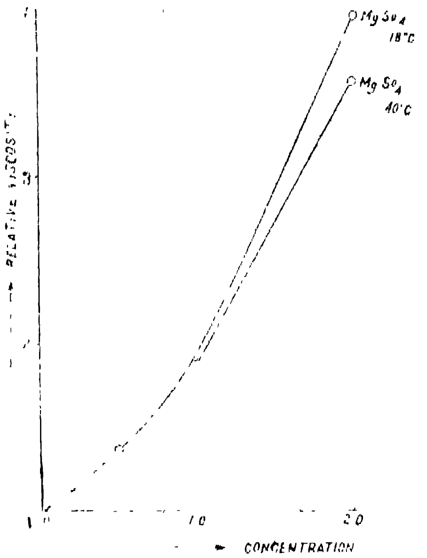

FIG. 4

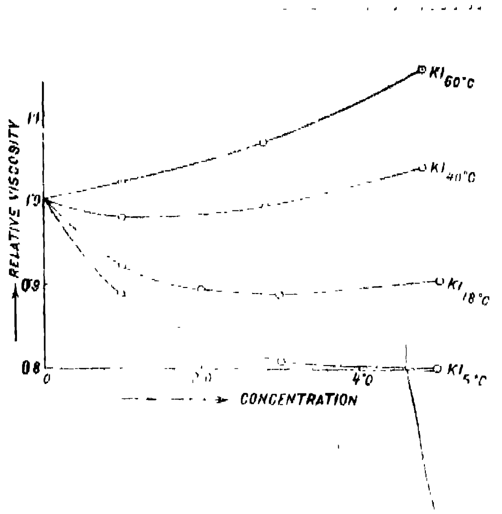

FIG. 4a

It is interesting to note that at a higher temperature the percentage-variation of velocity of both KI and $MgSO_4$, the two typical cases, decreases. This indicates a decrease of cohesional force between the components of the solution at a higher temperature and one would expect a decrease of relative viscosity as well with the rise of temperature. But whereas $MgSO_4$ shows the decrease in relative viscosity, KI shows an increase of relative viscosity with the rise of temperature. Since this increase of viscosity in the case of KI is not due to the increase of cohesional force between the components as proved by a decrease of relative velocity, *i.e.*, an increase of relative compressibility with temperature, one is almost forced to the conclusion that with KI type of molecules, the dimension of each moving component increases with temp., *i.e.*, the KI molecules attach more water molecules around the ions as the temperature increases. This becomes plausible in view of the fact that at the higher temperature, the association in water breaks up more easily or is already broken up and thus water molecule can be attached to the KI ions in solution. The idea of attachment of water molecules to heavy alkali halide ions was also suggested by Prins[5] when working on X-rays of electrolytic solutions. The idea fits in with the finding that the compressibility in KI is greater than that of pure water as against the general behaviour of other group of electrolytes and further that the increase of compressibility is more pronounced the higher the temperature.

The relationships brought forth in the above work call for a diversion of procedure in tackling with the compressibility of electrolytic solutions. So far, attempts have been made to look into the compressibility data from the ionic standpoint. But our work reveals that compressibility of electrolytic solutions might be better understood if we look into it from an angle from which viscosity of the solution might as well be viewed. This requires a better understanding of the phenomenon of viscosity of solutions. Attempts are being carried out in this direction.

Our thanks are due to Prof. D. M. Bose, Director, for his kind interest in the work.

REFERENCES

[1] A. Szalay, *Phys. Zeit*, **35**, 630 (1934)

[2] Falkenhagen and Bachem, *Zeit. Electro. Chem.*, **41**, 570 (1935)

[3] Bachem, *Zeit. f. Phys.*, **101**, 541 (1937)

[4] *International Critical Tables*, Vol. 5.

[5] Prins, *Zeit. f. Phys.*, **56**, 617 (1929)

4

ON THE NATURE OF THE LATENT IMAGES FORMED IN PHOTOGRAPHIC EMULSIONS DUE TO LIGHT ABSORPTION AND TO THE PASSAGE OF IONISING PARTICLES*

By D. M. BOSE

(*Received for publication, October 1, 1942*)

ABSTRACT. In this paper a comparison is made between the mechanism of latent image formation in silver halide grains present in photographic emulsions by photons and by ionising particles. It is shown that in the former the action of light proceeds from the surface of the grains inwards, while the energy transferred by ionising particles is a volume effect, starting the process of latent image formation from inside to the surface of silver halide grains. Thus the one favours the formation of surface and other of internal latent images. From this difference some of the observed differences in the action of photons and ionising particles can be explained, *e.g.*, emulsions with large grained particles will be more sensitive to photons than those with fine grained particles and *vice versa* for ionising particles. For the same transference of energy by photons and ionising particles to silver halide grains, the former will be more effective. The *rôle* of optical desensitisors in increasing the sensitiveness of fine grained emulsion to the action of ionising particles is also discussed.

An account is given of the theoretical deduction of H and D curve by Webb, which is based upon the assumption that the photographic emulsion contains silver halide grains with different degrees of photon sensitiveness.

Experimental evidence is discussed which shows that similar variation in sensitiveness to the action of ionising particles exists in silver halide grains in photographic emulsions. A theoretical H and D curve is deduced for the action of ionising particles and is compared with an experimental curve drawn for Ilford Halftone plates containing tracks of protons and α particles of different energies.

INTRODUCTION

It is well-known that a photographic plate consists of an emulsion of silver halide crystals in a film of gelatine. When such a plate is exposed to a light source of suitable wave-length, some of the silver halide crystals absorbing the light radiation become developable, *i.e.*, under the action of developers the affected silver halide grains are reduced to silver, which is deposited in the form of black grains. It is supposed that a latent image has been formed on the photographic plate which is acted upon by developing solutions. Large numbers of investigations have been directed towards elucidating the nature of the latent image formed due to light-absorption. Another subject which has been recently much discussed and which has an important bearing on our present review is the question of the sensitiveness of the photographic emulsion. If the different

---

Communicated by the Indian Physical Society.

strips of a photographic film are exposed to a light source of constant intensity but the time of exposure is increased in a geometric progression, the plate, when developed, will show patches of different degrees of blackness or opacity. A curve is then drawn giving a relation between the density of deposit as function of the total quantity of light incident, *H*. Such a curve is known as H and D curve, which is a measure of the light sensitivity of the given film. Attempts have been made to interpret theoretically the dependence of the density of deposit in the exposed film on the integrated light intensity. Such interpretation can be made on two different assumptions: (*a*) the silver halide grains are all of the same sensitiveness, and (*b*) the different grains have different light sensitiveness, *i.e.*, they require the absorption of different numbers of photons to become developable.

Latent images are also formed in such films under the action of ionising particles. Investigations have been undertaken to find out how far the Reciprocity law holds good under such conditions. We are, however, more interested in studying the density of deposit of silver grains along the tracks of some of the ionising particles like α-particles, protons, and deuterons. It has been found that not all photographic emulsions are suitable for recording the tracks of ionising particles. Some like Ilford R_1 plates record only the tracks of α-particles, others like Ilford R_2 record, in addition, the tracks of protons and deuterons, while a third kind Ilford New Halftone plates records, in addition, tracks of mesotrons. It is further found that fast plates are not suited for this type of work, but on the other hand fine grained slow plates with large gradation like process plates and halftone plates are more suited. Further, it has been noted that the sensitiveness of plates like Imperial Process and Ilford R_2 to protons is considerably increased by bathing these plates in a dilute solution of pinakryptol yellow which is known to act as desensitisor of plates to the action of light. Another result has been obtained by the action of ionising particles on photographic emulsion which has a direct bearing on the question of the variability in the sensitiveness of silver halide grains in photographic emulsions. Thus, while it is found that the number of silver grains deposited per unit length of ionising tracks of α-particles is independent of the energy of the α-particle (Th C′ 8·95 MV, Po 5.40 MV), the number is found to be dependent on energy of protons and mesotrons. In the latter case it is found that within the certain energy-range the mean grain number is inversely proportional to the energy of proton particles. (Chowdhuri, 1941.) It is the purpose of the present paper to make a comparative study of the nature of the latent images formed under the action of light-absorption and of ionising particles. Further, the question will also be discussed in light of results obtained with photons and with ionising particles as to the variability in sensitiveness of silver halide grains.

The subject will be treated as follows :—

A—Latent image due to photon absorption :

§ 1—Mott and Gurney's theory ;

§2—Surface and internal latent images and chemical methods of distinguishing between them ,
§3—Distribution of sensitivity amongst silver halide grains ;
§4—Webb's theoretical deduction of H and D curves.
B—Latent image due to the action of ionising particles :
§5—Energy transfer to silver halide grains by ionising particles ,
§6—Evidence on the variability of sensitiveness amongst silver halide grains rendered developable by ionising particles ;
§7—Theoretical deduction of the H and D curve for ionising particles and comparison with experimental results

A

§1. *Theory of latent image due to light absorption.*—When light is incident on silver halide grains, absorption starts from the outer boundary surface of the halide grain and proceeds inwards. According to the photochemical equivalence law, each photon absorbed will decompose one molecule of AgBr. The absorption takes place in the Br ion which leads to the release of the valence electron. According to the theory of Gurney and Mott (1938) this released electron will be raised to the conduction level of the AgBr crystal, where it is free to move about until it comes to the surface of the crystal and gets trapped on a so-called 'sensitive spot.' Each grain can have one or more sensitive spots which are supposed to be minute specks of silver sulphide, on which a trace of silver metal may have been deposited during the process of ripening. The concentration of a few such released electrons on a sensitive spot produces a strong local field in which some of the Ag^+ ions in the crystal grain move up and are deposited as silver atoms. This is the mechanism of the formation of latent image under light-absorption. The question as to the number of light quanta required to be absorbed before a latent image becomes developable will be discussed later.

When such an exposed plate is acted upon by a developer, the latter begins to act on the surface at the interface between the silver halide grain and the gelatine, the reduction spreading through the mass of the grain. It is supposed that the latent image acts as a heterogeneous catalyst which serves to distinguish between exposed and unexposed grains.

§2. So far we have considered only latent images formed on the interface of the silver halide grains. Recent investigations have shown that with increasing light intensity, latent images can also be formed inside silver halide grains. It is not possible by using normal developers to distinguish between surface and inner latent images. The technique which has been used by Berg, Marriage and Stevens (1941) for this purpose is as follows :-

(*a*) For surface latent image—Use a developer which contains as far as possible no alkali halide solvent, such as a glycine developer. With such a developer only the surface latent image is developed.

(*b*) For inner latent image—First use a bleacher to dissolve away only the surface latent image. This bleacher should not contain a silver halide solvent. Best results are obtained by using a solution of potassium bichromate in dilute sulphuric acid.

It is probable that a desensitisor like pinakryptol yellow acts as an oxidiser and bleaches the surface latent image.

An internal developer solution is made up, which contains a silver halide solvent in such concentration that the surface of the silver halide grain is etched away, exposing gradually the internal latent image which is then reduced by the developing solution.

With such a pair of developers, the relative concentration of surface and internal latent images as function of the intensity of exposure has been studied. It is found that the concentration of the internal to the surface latent image increases with the intensity of exposure.

Ordinary commercial developers usually contain sodium sulphite which is a silver halide solvent and with such developers it is not possible to distinguish between internal and external latent images.

§3. *Sensitivity of silver halide grains to light exposure*.—It is known from absolute sensitivity measurements that in an emulsion the most sensitive grains are rendered developable by the incidence of a few light quanta varying from one to twenty.

Recently a discussion has taken place in the Journal of Optical Society of America whether from a mathematical analysis of the H and D curve any information could be obtained as to the number of quanta required to form the latent image. Webb (1940) maintained that the conclusion arrived at must depend upon the basic assumption made in deriving the theoretical expression employed. It is shown how the assumption that all the grains require a fixed minimum number *r* of light quanta to acquire a latent image leads to the conclusion that only a small number of quanta is required for the formation of the latent image. It was further shown that if the alternative assumption is made that the grains in an emulsion have a wide range of sensitivity, the conclusion that a small number of quanta would be required for latent image formation would not follow. This statement led to a discussion between Webb and Silberstein which need not be considered here. To settle the question experimentally Webb and Evans (1941) performed an experiment in which H and D curves drawn for a film with strips exposed to intermittent light exposures *H* of different frequencies and intensities were compared to two similar curves due to (*a*) continuous exposures of intensity equal to that of the flash period of the intermittent exposure and (*b*) an exposure equal to the average intensity of the intermittent exposure. From a study of these curves the authors came to the conclusion that there were at least some grains in this emulsion which required between several hundreds to a thousand light quanta to produce developability.

§4. Having thus found an experimental verification of the assumption of the variability in light sensitivity of silver halide grains in a photographic emulsion, Webb (1941) proceeds to derive a theoretical expression for the variation of density of silver deposited in a photographic plate as function of exposure (H and D curve). We give a short account of his theory :

If during an exposure the number of light quanta incident per cm^2 on a photographic plate be E, then each silver halide grain receives on an average y units where $y = cE$: the maximum value of c is πa^2, the area of each grain. The number of photons absorbed by different grains will deviate from the average y, due to (*i*) inhomogeneity in size distribution of silver halide grains in the emulsion and (*ii*) fluctuation in the energy distribution in the incident light wave front. The probability that any grain receives n quanta, is given by Poisson's formula $w_n = \frac{e^{-y} \cdot y^n}{n!}$. Supposing now there is only one class of grains which require the absorption of at least r quanta to acquire developability, and if K is the total number of grains affected per cm^2 due to the given light exposure, then $\frac{K}{N} = \sum_{n=r}^{\infty} \frac{e^{-y} \cdot y^n}{n!}$; N is the total number of grains per cm^2.

If now there are different classes of grains requiring different number of light quanta, and the sensitivity distribution amongst them is given by a function f(r) such that $\sum_{r_{min}}^{r_{max}} f(r) = 1$;

Then the fraction of the grains rendered developable due to an average exposure y is

$$\frac{K}{N} = \sum_{r_{min}}^{r_{max}} f(r) \sum_{n=r}^{\infty} \frac{e^{-y} \cdot y^n}{n!}. \qquad \ldots \quad (1)$$

The form of f (r) selected by Webb is $f(r) = a.\ exp.\left[-k\left(ln\frac{r}{r_0}\right)^2\right]$

where
$$\frac{1}{a} = \sum_{r_{min}}^{r_{max}} exp.\left[-k\left(ln\frac{r}{r_0}\right)^2\right]$$

k is a parameter governing its overall latitude, and r_0 the maximum sensitivity.

For $\frac{K}{N}$ we can also write $\frac{D}{Dm}$, where D is the density ($\log_{10}.\frac{1}{transmission}$) for an exposure E.

Webb has compared his theoretical formula with the H and D curves of three different kinds of plates and has obtained the following values for the constants:

Plates	blue-sensitive	Average grain size, cm^2.	k	r_0	r_{min}
I.	Low Speed	0.115×10^{-8}	2.9	8	4
II.	Medium	0.300	.18	2.0	4
III.	High	0.700	.07	1/16	4

It will be noticed that for the same intensity of exposure E, the average number of quanta received per grain $y = cE$, is about six times for a grain in a high speed emulsion as compared to that for a low speed one. On the other hand it is found that overall gradation is much greater in the low speed plate; further, even in the high speed plates there are some grains which require the absorption of several thousands of light quanta to acquire developability. The H and D curve for the low speed plate is given in Fig. 1, Curve I, which is obtained on exposure to light of wave-length 4330 Å.

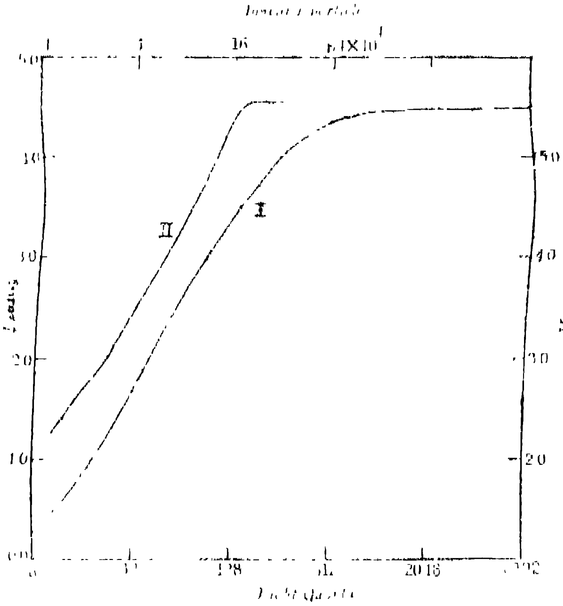

FIG. 1

The left hand vertical and bottom numbers refer to Curve I.

Abscissa—Mean number of light quanta absorbed per silver halide grain, λ = 4360 Å.

Ordinate—Mean density of developed plate

The right hand vertical and top numbers refer to Curve II.

Abscissa—Mean energy absorbed per silver halide grain from ionising particle, in terms of light quanta units, λ = 4360 Å

Ordinate—Number of silver halide grains deposited per 10^{-3} cm. length of track of ionising particles.

§5. *Latent image formed by the action of ionising particles.*—When an ionising particle of mass substantially greater than that of an electron passes through a material medium, with not too great a velocity, so that the loss by radiation can be neglected, the energy lost by the particle will be chiefly due to collision with the bound electrons of the atoms in the material medium. The probability of transfer of energy by nuclear collision is small for ionising particles with small mass and small effective charge. The energy loss per unit length suffered by the particle is given by the following non-relativistic equation :

$$-\left(\frac{dT}{dx}\right)_{\text{coll.}} = 2\pi e^4 . z^2 . \frac{\sigma}{T} . \frac{M}{m} ln\left(\frac{4m}{M} . \frac{T}{I}\right) \quad \ldots \quad (2)$$

T—kinetic energy of particle, whose mass is M.

ez—charge on particle.

σ—NZ= No. of electrons per unit volume of the medium.

I—$13.6\ Z$= ionisation potential of the atoms.

If we express T in electron volts, and express M in terms of proton mass, then the energy loss of a particle of energy V electron-volts in a crystal of silver bromide is given by the formula

$$\text{Energy loss} = 6.01 .\ 10^2 z^2 .\ \frac{M}{V}\, ln \left(1.04 \times 10^{-6} .\frac{V}{M} \right) \quad .. \quad (3)$$

The energy which is transferred in this way to the atoms of a silver halide grain will go to raise some of the bound electrons to the higher excitation levels including the conduction level of the AgBr crystal. Some of these will eventually be trapped on the sensitive spots present in the grain. Our knowledge about the mechanism of production of latent images in silver halide grains by ionising particles is not so detailed as of that formed by light-absorption.

Certain differences are however apparent. In the case of light-absorption, the process starts from the surface layer of the absorbing grain, and therefore the electron raised to the conduction level has a fair chance of being trapped on a sensitive spot which, it is assumed, is generally to be found on the surface. And the amount of energy absorbed is proportional to the surface area, *i.e.*, to a^2. For this reason also emulsions containing large-sized grains can more easily form latent images than those with small-sized grains.

In the case of the formation of latent images by the action of ionising particle, the ionisation produced is a volume rather than a surface one. If a is the radius of a silver halide grain considered to be spherical, then the average path of an ionising particle in such a grain is $p = \frac{4}{3}\ a$. The electrons which are set free by such a process have to traverse much longer paths before they can get trapped on the sensitive spots lying on the surface of the grains. The ionisation produced is proportional to the radius a, while the chance of meeting a sensitive spot on the surface is inversely proportional to a^2. This may be the explanation why slow Process and Halftone plates are more suited as detectors of ionising particles compared to fast plates containing large-sized silver halide grains.

It is worth investigating by the method described in §2 the relative ratio of surface to internal latent image formed in silver halide grains by the action of ionising particles. If it is found that the latter is much greater, then our interpretation of the relatively higher efficiency of emulsions containing small silver halide grains is valid. This would also explain the increase in sensitivity to the action of ionising particles produced by optical desensitisors like pinakryptol yellow, which by destroying the surface sensitive spot allows the internal latent images to come into prominence.

[Note added in proof—

H. Wambacher has recently published a report (Phot. Korr., **77**, 52, 1941) on the action of pinakryptol yellow (P) on photographic emulsion. From the very short summary given in Chem. Abs. (**36**, 5435, 1942) it appears that (*i*) emulsions treated with P before exposure give relatively small grains and (*ii*) with emulsion exposed to visible radiation and then treated with P, both the density and the number of developed grains diminish. These results are in agreement with our conclusions.]

The developers used for developing such plates like Elon-hydroquinone recommended by Wilkins (1940) contain sodium sulphite, which is a solvent for silver bromide. With such developers both internal and surface latent images are acted upon. It is proposed to undertake an experiment to determine the ratio of internal to the surface latent images produced by the action of ionising particles.

§5. We shall now consider in detail the developability produced in silver halide grains by the passage of ionising particles. In this case we have to consider a linear rather than a surface distribution of silver halide grains. We consider such particles to be spherical in shape and of radius of the order of 0.15×10^{-4} cm. All the particles whose centres lie within a cylinder of radius a are supposed to lie along the track of an ionizing particle whose trajectory is the axis of the cylinder.

The number of silver halide grains per unit length is not a constant, but is subject to a statistical fluctuation about its mean value s_0, given by Poisson's formula $w(s) = \frac{e^{-s_0} \cdot s_0^s}{|s}$. Further, if l is the length of the track of the ionizing particle through a grain, the energy transferred to it by collision is $-\frac{\partial T}{\partial x} \cdot l$; the value of l varies between o and $2a$. The energy transferred to each grain will fluctuate about the mean value $-\left(\frac{\partial T}{\partial x}\right)p$, where $p = 4/3.a$ is the average path of the ionising particles through the grains. The value of $\frac{\partial T}{\partial x}$ is given by formula (2). It is however not possible to make use of this formula, since the value of T is not known at each point on the particle track. We can however obtain indirectly an expression for the average energy transferred by the ionising particle to each silver halide grain on its path.

If T is the kinetic energy of the particle and L is its range in the emulsion, then the average energy loss per unit length is $\frac{T}{L}$. During the average path p of the ionising particle in each grain, the energy transferred is $\frac{T}{L} \cdot p \cdot \frac{\sigma_1}{\sigma_2}$, where σ_1 is the number of electrons per unit volume of a silver halide crystal and σ_2 is the number of electrons per unit volume of the photographic emulsion, *viz.*, $\sigma_2 = \Sigma n_k z_k$; where there are in the emulsion $1 \ldots k$ kinds of atoms of atomic numbers $z_1 \ldots z_k$ and their numbers present per unit volume are $n_1 \ldots n_k$ respectively.

It is found experimentally (Chowdhuri, 1941) that the number of grains deposited along tracks of α-particles of energy varying from 5.3 MV to 8.0 MV is an approximate constant independent of the particle energy. On the other hand the mean grain number along the tracks of protons for the energy range between 4MV to 10 MV varies inversely as the proton energy.

Thus we find that in spite of fluctuations in the number of silver halide grains along the tracks of ionising particles and the variation in the path traversed by the ionisation particles, certain mean values are obtained which indicate that the mean grain number deposited is inversely proportional, within a certain range, to the energy transferred to the silver halide grains

It is found that the energy received per grain increases with the diminution of the energy of ionising particle, and this is accompanied by an increase in the number of silver grains developed per unit length along the track. This indicates that the number of silver halide grains which become developable increases with the increase in energy received by them by collision with the ionising particle, *i.e., the silver halide grains present in the emulsion possess different degrees of sensitiveness.*

§7. We shall deduce an expression for the number of silver grains deposited along the track of ionising particles similar to that obtained by Webb for absorption of light quanta. We shall then give for comparison an empirical curve connecting the mean grain number deposited along the track of ionising particle as function of the mean energy absorbed by the silver halide grains

Let s be the number of halide grains per unit length in the emulsion, and s_0 the mean grain number; the value of s can be obtained by actually counting with a high magnification microscope along different directions on the plate If $f(r)$ is the fraction of the grains requiring r units of energy to acquire developability (measured either in electron volts or by the equivalent number of photons of a given wave-length), then the number k of grains rendered developable per unit length by the absorption of the mean energy r is given by $\frac{k}{s} = \int_{r_{\min}}^{r} f(r)dr$; where $r_{\min}$ is the minimum amount of energy required to make a silver halide grain developable when struck by an ionising particle.

If for any kind of charged particle and for a particular range of energy the mean energy received by the silver halide grains r is greater than the amount $r_{\max}$ required to make the least sensitive of the grains developable, then within that range k the mean grain number deposited is independent of the energy of the ionising particle. This is the case we find for α-particles emitted by Po and ThC′ with energy-range from 5 to 9 MV. We shall, following Webb

assume that
$$f(r) = a\, e^{-k\left(ln\frac{r}{r_0}\right)^2}.$$

Then
$$\frac{k}{s} = a\int_{r_{\min}}^{\bar{r}} e^{-k\left(ln\frac{r}{r_0}\right)^2}.\, dr \qquad \ldots \quad (4)$$

is the theoretical form of the H and D curve for the formation of latent images due to ionising particels. *A priori* it can be said that the constants k, and r_0 for the same kind of emulsion will not be the same both for the action of photons and ionising particles. Further, as mentioned above, s is not a constant, but may vary for different tracks on the emulsion.

We shall now give an empirical H and D curve for ionising particles which is based upon the data given in Table I, part of which is taken from a paper by Miss Chowdhuri (1941), who has obtained a curve showing the relation between the mean grain spacing in Ilford Halftone plates of tracks of protons and α-particles of different energies.

TABLE I

Energy in 10^6 eV	Range in air in cm	Quanta absorbed per grain	Mean number of grains per 10^{-8} cm
Proton 1	2.3	8.36×10^4	1.5
2	7.1	6.06 ,,	4.0
3	14.1	4.00 ,,	3.57
4	24.0	3.20 ,,	3.43
5	34.0	2.83 ,,	3.03
6	47.0	2.45 ,,	2.96
7	61.0	2.21 ,,	2.78
8	77.2	1.99 ,,	2.70
9	95.5	1.82 ,,	2.60
10	115	1.67 ,,	2.50
particle 5.40	3.87	26.7 ,,	5.55
8.05	8.62	20.0 ,,	5.55

Column 1 gives the energies of proton and α-particles, whose ranges in R cm in air is given in Column 2, Column 3 gives the mean energy absorbed by silver halide grains expressed in terms of the equivalent number of light quanta of wave length 4300°Å (energy 2.86 eV).

This is obtained from the formula,

$$r=\frac{T}{R}\cdot\frac{R}{L}\cdot p\cdot\frac{\sigma_1}{\sigma_2}\cdot\frac{\lambda e}{h.c} \qquad (5)$$

where T—particle energy in electron volt,

R—range of particle in air,

$\frac{L}{R}$—ratio of ranges in the emulsion and in air $=7.2\times10^{-4}$,

p=mean path of the ionising particle in the silver halide grains -0.2×10^{-4} cm.

$\frac{\sigma_1}{\sigma_2}$ = the ratio of electrons present in unit volumes of silver bromide crystal, and of the emulsion $=19.7$

$\frac{300hc}{\lambda e}$ =energy in electron-volt of photon of wave-length λ.

Column 4 gives the mean grain number per 10^{-3} cm of track in the photographic emulsion which is equal to $\frac{10}{m.g.s.}$ and is taken from Miss Chowdhuri's paper.

Fig. 1, Curve II is drawn from the data collected in Table I, and is of the shape to be expected from a sensitivity distribution curve of the form given by Webb. The experimental data are not sufficiently accurate nor sufficiently closed spaced in the region 4 to 30×10^4 quanta to enable us to determine the constants of the sensitivity distribution function. A comparison of the Curves I and II, drawn for sensitivity distribution curves of similar types of slow fine-grained plates as function of the number of light quanta and of collision energy absorbed, respectively, shows that light quanta are about 10 to 100 times more effective than ionising particles. This is what is to be expected considering the nature of the action of the two agents.

Bose Institute
Calcutta.

REFERENCES

Berg, Marriage, and Stevens (1941), *J. Opt. Soc. Am.*, **31**, 385
Chowdhuri, Biva (1941), *Trans. Bose Res. Inst.*, **15**.
Gurney and Mott (1938), *Proc. Roy. Soc. A.*, **164**, 151.
Silberstein, L. (1941), *J. Opt. Soc. Am.*, **31**, 343.
Webb, *ibid.*, **31** (1941), 348 and 550.
Webb and Evans (1941), *ibid.*, **31**, 355.
Wilkins, T. R. (1940), *J. of App. Phys.*, **11**, 3

FLUID FLOW THROUGH POROUS MEDIA. PART II. POROSITY, PERMEABILITY AND AVERAGE GRAIN SIZE OF CONSOLIDATED SANDS*

By N. C. SEN GUPTA

AND

Mg. THEIN NYUN

(*Received for publication, November 18, 1942*)

ABSTRACT Permeabilities, porosities and particle size distribution curves of twenty-three sand core samples were obtained. It was observed that with increase in the average particle diameter the porosity at first increased and then tended to attain a constant limiting value. Permeability, K, on the other hand increased continuously with the average diameter, *d*, and the approximate relation $K \propto d^2$ was obtained.

INTRODUCTION

A previous paper[1] dealt with the question of measuring true permeability of sand cores using gases. Measured permeabilities were found to diminish with an increase in the rate of flow and results obtained using hydrogen were higher than those obtained with oxygen. Preliminary measurements using liquids† showed that the latter gave lower permeabilities than those obtained using gases without any correction.

In the present paper relations between permeability, porosity and average grain size of twenty-three sand cores have been studied.

EXPERIMENTAL

The core samples used in these experiments were obtained from four different oil wells. Permeabilities were measured by finding the rate of flow of dry oxygen at low pressure gradients and constant temperature and were calculated from the formula :–

$$K = \frac{2Vp\eta L}{(p_2^2 - p_1^2)A}, \qquad (1)$$

where V is the volume of gas flowing per unit time at atmospheric pressure p, p_2 the pressure of the entering and p_1 that of the issuing gas, η is the viscosity of the gas at the temperature of the measurement, L is the thickness and A is the cross-section of the cylindrical core. The permeability values were not corrected for any error, *e.g.*, due to slip or kinetic energy effect[1] since approximate values were considered to be sufficiently accurate for present purposes.

---

* Communicated by Prof. J. N. Mukherji.

† This work was interrupted by the Japanese invasion but may be continued elsewhere later.

Porosities were determined by Melcher's method.[2]

Particle-size distribution curves were drawn from data found using Puri's Siltometer.[3] The curves generally showed one maximum, but occasionally there were two maxima. Representative curves of the two different types are shown in figure 1

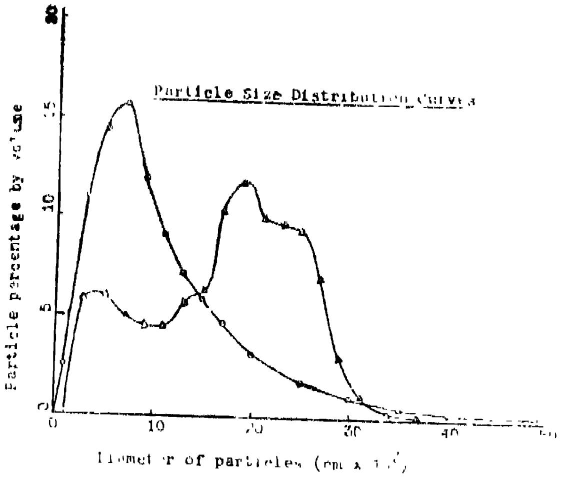

Figure 1

Average grain diameter, $\bar{d}$ was calculated from the particle-size distribution curves from the relation

$$\bar{d}=\left(\frac{100}{\Sigma P_i/d_i^3}\right)^{1/3}, \qquad \cdots \quad (2)$$

where P_i is the percentage, by volume, of particles having diameter d_i. Since the value of $\bar{d}$ is mainly determined by the percentage of smaller particles, a smaller value of $\bar{d}$ indicates the presence of a large percentage of particles having diameters smaller than 0.002 cm.

RESULTS AND DISCUSSION

The relation between the average effective diameter and the porosity, *f*, is shown in figure 2 and that between the diameter and the permeability on a log-log scale in figure 3.

Figure 2 gives a more or less 'S' shaped curve. The porosity appears to attain a constant limiting value at very large particle diameters. This maximum value of the porosity is 22.5 %. It is of interest to note in this connection that when spherical particles of uniform size are arranged to build a hexagonally close-packed structure the porosity equals 25.95%. Other types of arrangements show higher porosities.

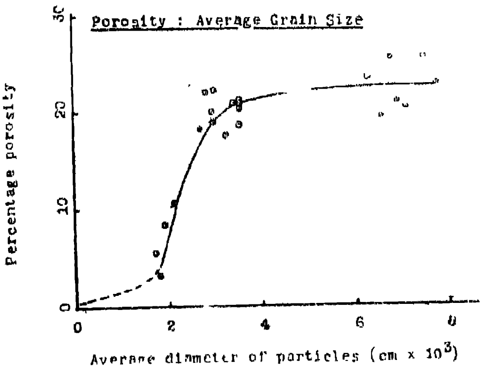

Figure 2

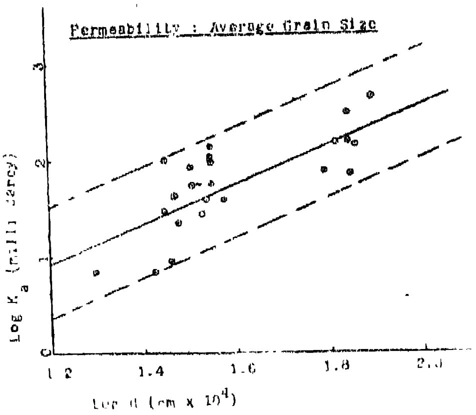

Figure 3

When the particle diameter tends to become negligibly small, porosity also tends to be very small. It may be considered that when $\bar{d}$ approaches zero, f assumes a lower limiting value. The curve can be represented by an equation of the type :—

$$\frac{f - f_{\text{min.}}}{f_{\text{max.}} - f} = d^n, \qquad \dots \quad (3)$$

where f is the porosity corresponding to the average diameter $\bar{d}$, $f_{\text{max.}}$ and $f_{\text{min.}}$ are the maximum and minimum porosities and n is a constant. The value of n appears to be nearly 6 in this particular instance.

The variation of porosity with the average diameter can be explained only when the size and shape of the particles and their spatial arrangements are known. For example, fine particles, if present in appreciable amount, will cement the pores formed by the arrangement of the bigger particles. Further, small particles in sand are generally less symmetrical than the big ones, and when closely packed, will provide a sand with lower porosity. It appears that no experimental work on this topic, using consolidated oil-sands, has yet been reported.

The points plotted in figure 3 fall on a very broad band indicated by the dotted lines. Assuming that log K varies linearly as log $\bar{d}$, the slope of the statistical line drawn through the points is 2.05 which shows that the empirical relation

$$K = \text{Const. } \bar{d}^2, \qquad \dots \quad (4)$$

where K is the permeability corresponding to the average diameter d, is approximately obtained. When the spatial arrangement of the particles is not altered, the permeability of a system containing spherical particles of uniform size will diminish as the square of the diameter of the particles. The scattering of the points in figure 3 from the straight line might be due to a variation in the shape and size of the particles and to their spatial arrangements. The individual effects of these factors cannot be discussed until further measurements have been carried out.

This work was carried out in the Research Laboratories of the Burmah Oil Co. (Burma Concessions), Ltd., at Khodaung, Upper Burma, under the general direction of Mr. A. Reid, Senior Fields Chemist. Authors' thanks are due to the Manager of the Company for permission to publish this work.

Colloid Research Laboratory,
University College of Science,
92, Upper Circular Road, Calcutta.

REFERENCES

[1] Sengupta, N. C., and Mg. Thein Nyun, *Ind. J. Phys.* **16**, 119 (1942).
[2] Melcher, A. F., *A.I.M.E.*, **65**, 469 (1921)
[3] Puri, A. N., *The Punjab Irrigation Inst. Research Publication*, **5**, 1 (1933).

ON THE ULTRA-VIOLET ABSORPTION OF THE DYESTUFFS IN SOLUTION AND THE INFLUENCE OF NEUTRAL SALTS ON THE SAME

By KRISHNADAS CHOWDHURY

AND

CHITTARANJAN BOSE

(Received for publication, August 12, 1942)

ABSTRACT. The paper deals with the ultra-violet absorption of a large number of fluorescent dyestuff solvents, namely, succinyl eosin, pinakryptol yellow in glycerine, acriflavine in alcohol, pinaflavol in alcohol, aniline orange in alcohol, 'rose Bengal' in alcohol, pinakryptol green in alcohol, succinyl fluorescein in glycerine. The absorption curves for each of these dyestuff are given. The effect of quenching element, namely, potassium iodide, has also been studied for acriflavine, succinyl fluorescein and pinakryptol yellow. With this particular type of quenching element it has been found that practically there is no change in the nature of absorption curves.

INTRODUCTION

A large amount of experimental work has been done by the different workers on the absorption of the dyestuff in different solvents. The existing literature on the subject reveals that the great majority of the investigators in that particular domain confined their investigations in the visible region of the spectrum. Very few quantitative measurements have been made in the ultra-violet region of the spectrum. It is well known that a quantitative measurement of absorption spectra of solutions of pure compounds can be made relatively easily, and it not only furnishes a method of identification of the substances but also serves as a basis of a theoretical treatment of their molecular structure, as is evident from the recent investigations of Mayneord,[1] Fisher[2] and others.

Mitra[3] and Grisebach[4] measured the absorption coefficient of a few dyestuffs in solution in the ultra-violet region and tried to establish a relation between the absorption curves in the near ultra-violet and polarisation curves of the fluorescent radiations emitted by these dyestuffs in solution under the excitation of light of various wave-lengths. In view of the meagre accurate data on the ultra-violet absorption, as well as, to find out whether there is any resemblance between the two sets of curves, as was reported by Grisebach and Mitra, it was thought desirable to make a systematic observation on the ultra-violet absorption of a large number of fluorescent dyestuffs in solutions.

EXPERIMENTAL ARRANGEMENTS

The absorption coefficients were determined by a calibrated rotating sector photometer (Adam Hilger) used in conjunction with a quartz spectrograph. The source of light for the quantitative measurements has normally been a condensed tungsten-steel spark, about 4 mm. gap, the necessary potential being obtained from an X-ray induction coil with mercury interrupter in the primary. The results were in a few cases verified by the measurements of the absorption with a sensitive Moll thermopile and a galvanometer system.

A parallel beam of light from a point source of quartz mercury lamp was allowed to fall on a cell containing the dyestuff in solution through a suitable filter, which allowed only monochromatic radiation to pass. The intensities of the incident and transmitted light were measured with the help of a Moll thermopile and galvanometer. The absorption coefficients were measured from the well-known relation :—

$$I = I_0 e^{-ad},$$

where I and I_0 are the transmitted and incident intensity, respectively, of light, *d*, thickness of the cell containing the solution and a, the absorption coefficient.

The results of our observations in the case of both the experimental arrangements, thermoelectric and photographic, are given below for a comparative study. It will be evident that the agreement is fairly satisfactory.

TABLE I

Dyestuffs in alcoholic soln	Absorption coefficient for λ 4358 A	
	Thermoelectric	Photographic
Succ. fluorescein	$.42_2$	.40
Pinakryptol	$.29_5$	.30
Aniline orange	$.24_8$	.25
Pinaflavol	$.44_7$	.45

RESULTS

We have investigated the absorption of the following flourescent dyestuffs in alcoholic and glycerine solutions. The figures within brackets indicate the concentrations.

1.	Succinyl fluorescein ...	... (1.120000)
2.	Succinyl eosin ...	... (1.70000)
3.	Pinaflavol ...	... (1.200000)
4.	Aniline orange ...	... (1.50000)
5.	Acriflavine ...	... (1.50000)
6.	Pinakryptol yellow ...	... (1.100000)
7.	Pinakryptol green ...	... (1·125000)
8.	Rose Bengal ...	... (1.100000)

All the above compounds were purified in the usual way. The results are shown graphically by the following curves (Figs. 1 to 8). As regards the resemblance between the two sets of curves, *viz.*, absorption and polarisation curves, as already reported in our introduction, we shall return to this point in another communication.

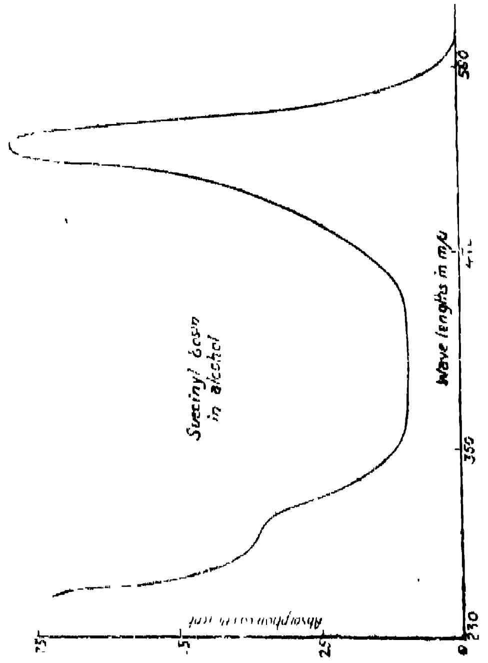

FIG. 2

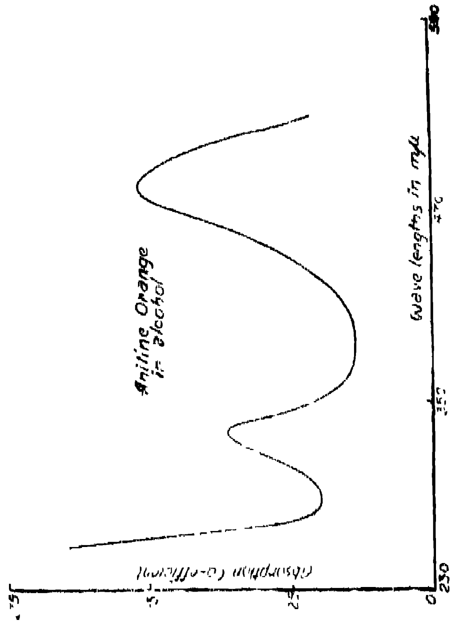

FIG. 4

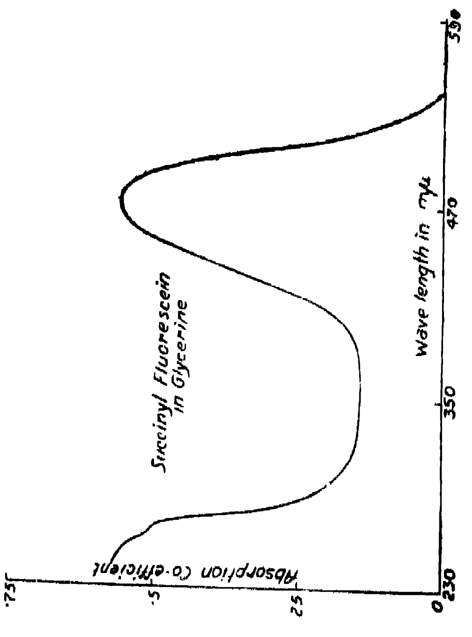

FIG. 1

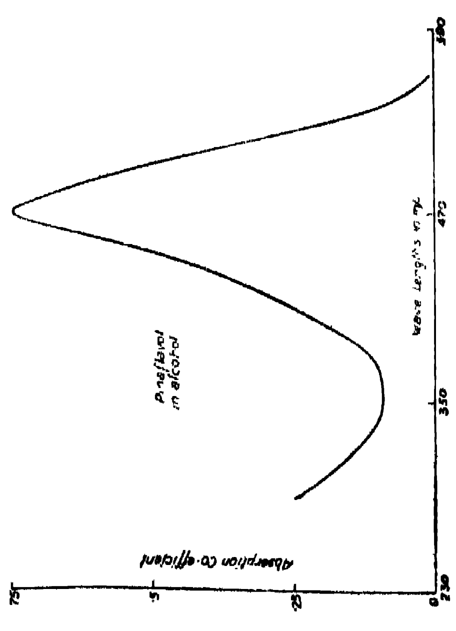

FIG. 5

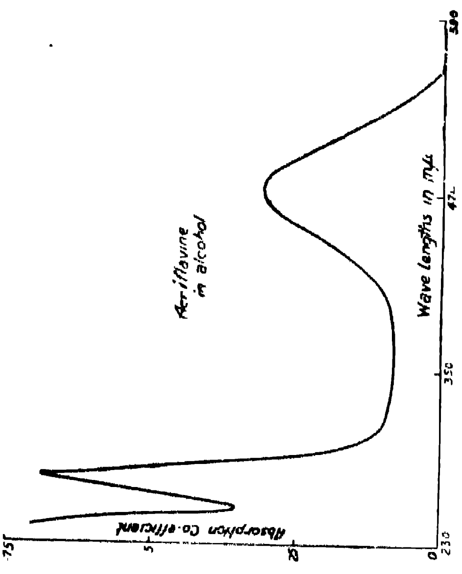

FIG. 5

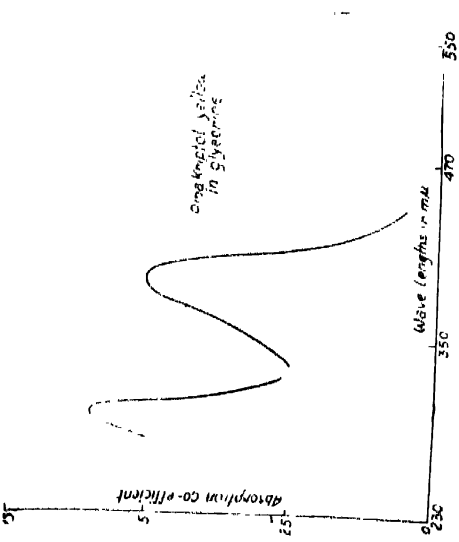

FIG. 6

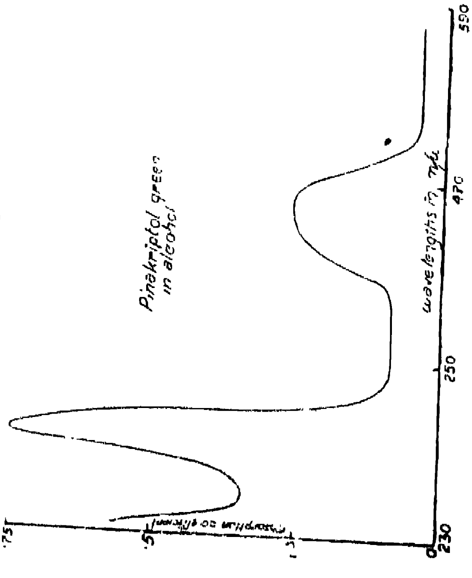

FIG. 7

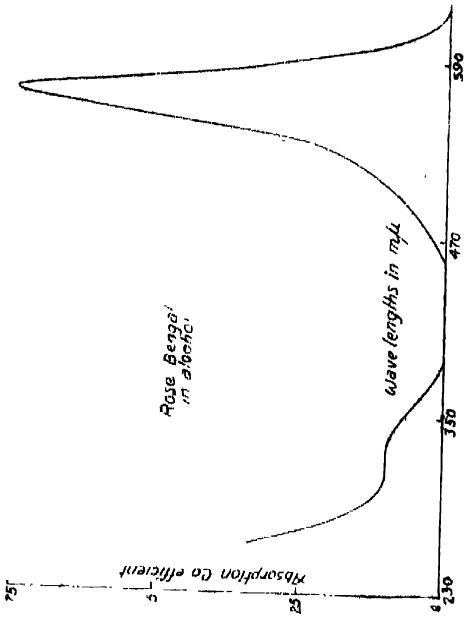

FIG. 8

INFLUENCE OF FOREIGN NEUTRAL SALTS ON THE ABSORPTION OF THE DYESTUFFS IN SOLUTION

The quenching of the flourescence of the dyestuffs in solution by foreign neutral salts is quite well known and has been investigated by a large number of workers. It appears that the majority of them are of the opinion that the phenomena of quenching are due to de-activating collisions of the second kind between the dyestuff molecules in the excited state and the negative ions of the added salts. The main argument in favour of the physical interpretation of the quenching effect is the increase of polarisation of the fluorescent radiation emitted by the dyestuffs in solutions, as was observed by Perrin,[5] Franck,[6] Mitra,[7] and others. But there may be an alternative explanation, *viz.*,—gradual "complex formation" due to the association of the molecules of the dyestuffs and those of the quencher with the gradual addition of the foreign substance—these complex molecules being non-fluorescent. These molecules, if any, will reveal their presence by a change (or by a new band) in the absorption spectrum of the dyestuff in presence of the quencher. So, unless one studies the influence of the foreign neutral salts on the absorption of the dyestuffs and demonstrates the absence of any such influence, the aforesaid alternative explanation, *viz.*,—gradual complex molecular formation, and consequent decrease in the number of emitting dyestuffs molecules, which is exhibited by a decrease in intensity of the flourescent radiation, cannot be ruled out of the field.

The idea of complex molecular formation is not new. It is well known that as the concentration of the fluorescent substance is increased, the intensity of the fluorescent radiation also increases up to a maximum value, then the intensity falls down on further increase of the concentration of the fluorescent substance. That is, there is a definite concentration for a dyestuff for which the intensity of the fluorescent radiation is maximum. When the concentration is further increased, the resulting intensity of the fluorescent light dwindles down. In order to explain this concentration-quenching, Lewschin[8] assumed the formation of complex molecules which are non-fluorescent unlike the mother molecules. In support of his assumption he showed that when the concentration of fluorescent dyestuffs is increased over that aforesaid maximum value, considerable alteration of the absorption spectrum of the dyestuff takes place.

One finds that Lampert,[9] and Mitra[10] measured the absorption co-efficient of a few dyestuffs in solution for both pure and after the addition of varying amounts of neutral salts. Besides these, no systematic investigations have been made on the subject so far. In view of the importance of the subject on the mechanism of quenching, we thought it prudent to investigate this point along with our absorption measurements.

It has already been mentioned that the intensity of the fluorescent radiation of the dyestuffs in solution suffers appreciable diminution when neutral salts are added to the solvent medium. The investigations of Perrin,[11] West, Jetty and Muller[12] indicate that the order of the extinguishing power of the different ions is as follows :—

$$I' > CNS' > Br' > Ce' > SO_4'' > NO_3'$$

which is practically the order of their deformability, that is, of the ease of displacement of an electron in the peripheral shell of the ion. This shows that iodide ions exert the greatest quenching influence on the fluorescing dyestuff molecules. In view of this, we have investigated at present the influence of KI on the absorption of a few dyestuffs in solution.

Our experimental procedure was as follows. A solution of the dyestuff, in alcohol of requisite concentration, was taken and its absorption at different wave-lengths was determined in the usual way by the rotating sector photometer.

Then to the same solution of the dyestuff, potassium iodide solution of known concentration was added drop by drop, till the fluorescence was quenched completely, as observed visually, the concentration, *c* of KI being determined from the number of drops added.

Then one cell of the photometer was filled up with the quenched dyestuff solution and the other cell with the KI solution of concentration *c*.

For the present, we have investigated the influence of iodide ions on succ. fluorescein, succ. eosin, acriflavine and pinakryptol yellow. The results are shown graphically by the accompanying curves (Figs. 9-11).

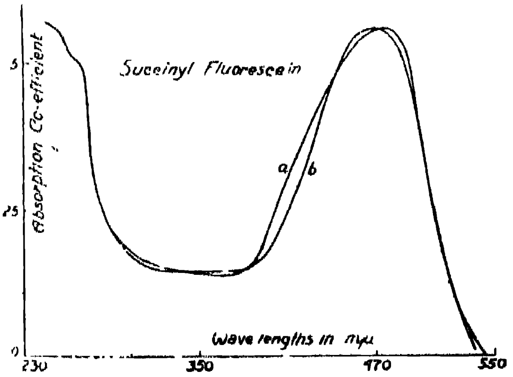

FIG. 9

Acriflavin
a—without KI
b—with KI

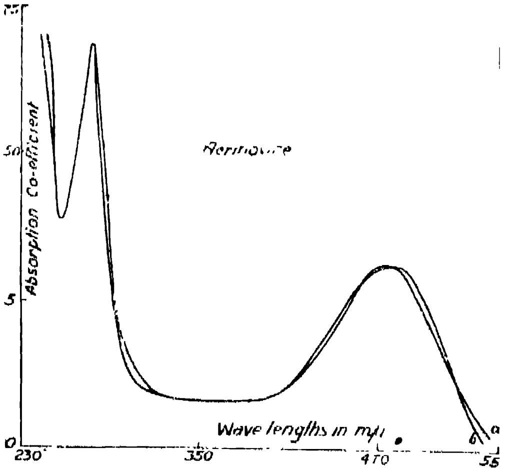

FIG. 10

Succ. flurescein
a—without KI
b—with KI

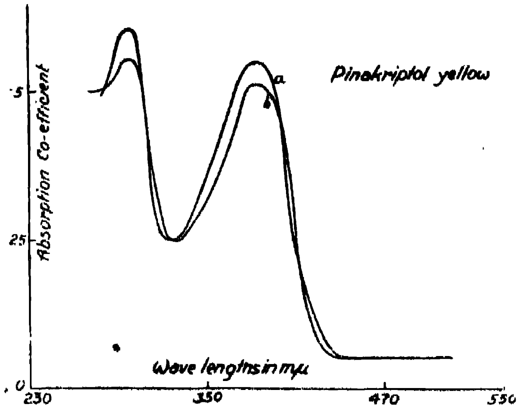

FIG. 11

Pina Kryptol yellow
a—without KI
b—with KI

The graphs show that there is practically no change in the nature of the absorption curves on the addition of the foreign neutral salt. This shows that quenching of the flourescent radiation on the addition of foreign salts takes place through collision of the second kind between the dyestuff molecules and the ions of the added salts.

In conclusion, it gives us great pleasure to thank Prof. S. N. Bose for his kind interest and Dr. S. M. Mitra for his kind guidance throughout the work.

PHYSICS LABORATORY,
UNIVERSITY OF DACCA.

REFERENCES

[1] Mayneord, *Proc. Roy. Soc. A*, **152**, 299 (1935).
[2] Fisher, *Proc. Roy. Soc. A*, **154**, 703 (1936).
[3] Mitra, *Thesis* (1938), Dacca.
[4] Grisebach, *Zeit. fur Phys.*, **101**, 13 (1936).
[5] Perrin, *Thesis* (1929), Paris.
[6] Frank, *Zeit. fur Phys.*, **69**, 100 (1931)
[7] Mitra, *Zeit. fur Phys.*, **92**, 61 (1934).
[8] Lewschin, *Zeit. fur Phys.*, **42**, 230 (1927).
[9] Lampert, *Thesis* (1938), Berlin.
[10] Mitra, *Thesis* (1938), Dacca.
[11] Perrin, *Comp. Rend.*, **184**, 1121 (1927).
[12] West, Jetty and Muller, *Proc. Roy. Soc.*, **121**, 294 (1928)

7

ON NATURE OF DYNATRON TYPE NEGATIVE IMPEDANCES AT FREQUENCIES FROM 1 TO 40 MEGACYCLES/SECOND

By S. P. CHAKRAVARTI

AND

P. N. DAS

(Received for publication, October 6, 1942)

ABSTRACT. The paper relates to investigations on the nature of dynatron type negative impedances obtained from screen-grid tubes operated under secondary emission condition over the range 1-40 Mc/s and forms an extension of a previous work by the first author.

A suitable method for the measurement of "$-R_n$," "C_n" and "C_{nf}" has been evolved. Measurements of "$-R_n$," "C_n" and "C_{nf}" have been carried out over the range 1-40 Mc/s and discussion as to the nature of variation of $/R_n/$ and C_{nf} with frequency has been made. Dependence of $/R_n/$, C_n and C_{nf} upon the amplitude of the operating h.f. voltage (*i.e.*, that applied between anode and filament) or superimposed h.f. voltage has been shown.

A discussion on the nature of variation of $/R_n/$ of screen-grid tubes under secondary emission condition with frequency over a large frequency range has been made. Considering a substantially large frequency range and allowing for the effect of the amplitude of impressed or superimposed h.f. voltage, it has been found that the mean curve derived from the experimental curve indicates the law that the internal resistance decreases in general with increase of frequency from very low to very high frequencies.

Further, a discussion on the dielectric constant K of electronic medium between anode and filament of screen-grid tubes under secondary emission condition and its dependence upon the amplitude of impressed or superimposed h.f. voltage as well as upon the frequency has been made. Allowing for the effect of h.f. voltage amplitude, it has been found that the curves of variation of 'K' with frequency are wavy showing peaks and depressions and that the values of 'K' are less than unity at frequencies greater than 11 Mc/s for some tubes and 14 Mc/s for others.

Linearity of the negative impedance element (taken as a whole) has been investigated since this forms the essential requirement for the use of the element in circuits and networks.

Phase shift caused by the negative impedance element (as a whole) has been calculated from measurement of $/R_n/$ and C_n as well as measured directly by cathode-ray oscillograph method.

INTRODUCTION

In a previous work the first author (Chakravarti, 1940) has made comparative studies of "stability," "magnitude and angle of impedance," "linearity" and "phase-distortion" for dynatron, transitron and feed-back types of negative impedance element over the frequency range, 0.5 Kc/s to 1.0 Mc/s.

From stability point of view, the transitron type has been found to be the best of the three. The dynatron type obtained from screen-grid tube can be maintained stable by keeping plate and screen-grid voltage variations as well as filament current variations within limits and suppressing the oscillations set up by closing the negative element terminals through network or apparatus or any impedance, as discussed in previous works (Chakravarti, 1938 and 1940). The feed-back type of negative impedance can be made stable by proper adjustment of the amplifier performance.

The negative impedance element of any type cannot be regarded as non-reactive except at very low frequencies. In the first author's paper (Chakravarti, 1940) entitled 'On Nature of Negative Resistance Sections,' the dynatron types of negative impedance element have been taken more or less non-reactive up to 50 Kc/s. A good agreement of the results calculated on that basis with the actual measurements has confirmed that the above view point could be maintained without much error up to 50 Kc/s.

The correct equivalent of the negative impedance element (of dynatron and transitron types) at a higher frequency will be a negative resistance ($-R_a$) shunted by the effective capacitance (C_a) equal to anode-filament capacitance (C_{af}) added on to self-capacitance of choke as well as other stray capacitance in wiring, valve base, etc., and by an inductance (L_c) inserted to block the a.c. from traversing the path of H.T. source. As impedance due to 'L_c' is very large, the (effective) equivalent of the negative impedance element untuned to any frequency will be $-R_a$ shunted by C_a. For all types of negative impedance over the range 0.5 Kc/s—1.0 Mc/s the impedance magnitude has been found to decrease in general with increase of frequency though not in a smooth curve.

From the linearity point of view, the dynatron type has appeared to be best suited for use in a.c. circuits over the range 0.5 Kc/s—1.0 Mc/s. The transitron type has been more of non-linear nature, whereas the linearity of the feed-back type has been found to depend upon that of the amplifier.

For dynatron and transitron types the angle of phase-shift has been proportional to $1/\omega$ up to 0.5 Mc/s but varies in a non-linear way with $1/\omega$ between 0.5 and 1.0 Mc/s.

Before proceeding to the scheme of measurements undertaken at present, it is desirable to survey the works of various authors on internal (a.c.) resistances and interelectrode capacitances of thermionic tubes as well as on dielectric constants of ionized medium therein.

The problems relating to (*a*) variation of dielectric constant (*vide* Bergman and During, 1929; Benner, 1929; Benham. 1931; Sil, 1932; Prasad and Varma, 1936; Imam and Khastgir, 1937; Hollmann and Thoma, 1938; Khastgir and Serajuddin, 1939, and Basak,* 1941) of electronic medium in diode, triode, and screen-grid tube (operated under normal condition) with frequency and agreement or otherwise of the measured values with Eccles-Larmor, Benner and Lorentz theories and (*b*) variation of internal resistance and interelectrode capacitances (*vide* Benner, 1929; Hartshorn, 1931; Mitra and Sil, 1932; Baker, 1933; Hollmann and Thoma, 1938: Rao, 1940; Khastgir, 1941, and Basak, 1941) of triodes (operated under normal condition and also as dynatron) and screen-grid tubes (operated under normal condition) with frequency have received attention of the majority of workers. A few workers, however, have interested themselves on the dependence of the interelectrode capacitances of thermionic tubes upon the operating conditions (*vide* Moullin, 1933 ; Dye and Jones, 1933 ; Bell, 1935 ; Moullin, 1937, and Jones, 1937).

It will be noted that none of the above studies has related to internal resistance, anode-filament capacitance and dielectric constant of ionized medium for a screen-grid tube operated *under secondary emission condition*. The first author in a previous paper (Chakravarti, 1940) has measured among other things the variation of the magnitude of negative (internal) resistance as well as negative impedance with frequency over the range 0.5 Kc/s—1.0 Mc/s for screen-grid tubes under secondary emission condition.

The present paper relates to extension of work on the nature of dynatron type negative impedance obtained from screen grid tube over the range 1-40 Mc/s, since this alone of all types of negative impedance has proved suitable from all points of view for use in communication circuits at frequencies up to 1 Mc/s.

The work undertaken has consisted of the following :—

(*a*) Measurements of $-R_a$, C_a and C_{af} over range 1-6 Mc/s.

(*b*) Measurements of $-R_a$, C_a and C_{af} over range 6-15 Mc/s.

(*c*) Measurements of $-R_a$, C_a and C_{af} over range 20-40 Mc/s.

(*d*) Measurements of the effect of h.f. voltage amplitude (applied to negative impedance element) on $/R_a/$ and C_{af}.

(*e*) Discussion on variation of $/R_a/$ with frequency for screen-grid tube under secondary emission condition.

(*f*) Discussion on dielectric constant of electronic medium under secondary emission condition and its dependence upon frequency and h.f. operating voltage.

(*g*) Measurements of the linearity of the negative impedance element at 3, 10 and 30 Mc/s.

(*h*) Determination of phase-shift caused by the negative impedance element over range 1-17 Mc/s by cathode-ray oscillograph method developed by the first author.

Four screen-grid tubes of British, American and Continental makes worked under secondary emission condition have been employed for (*a*), (*b*), (*c*), (*d*), (*e*) and (*f*) measurements, while only AC/SG tube has been used for (*g*).

METHOD OF MEASUREMENT OF NEGATIVE RESISTANCE, EFFECTIVE CAPACITANCE AND ANODE-FILAMENT CAPACITANCE

The negative resistance and the shunting effective capacitance of the negative impedance element at a desired frequency (the parallel inductance of choke being of such impedance as to cause no appreciable error when neglected) could be obtained by two measurements of impedance magnitude of the element, one at the desired frequency and another at slightly higher or slightly lower frequency such that values of negative resistance and effective capacitance at this second frequency could be regarded same as those at the first frequency. The impedance could be obtained directly by observing the h.f. voltage drop across the negative element and the h.f. current flowing into the element.

For instance, if negative resistance and shunting effective capacitance at 3 Mc/s ($\omega = 2\pi \times 3 \times 10^6$ r.p.s.) are desired, the impedance of the element (Z) at 3 Mc/s is first obtained. We then have the equation

$$\frac{1}{Z^2} = A^2 = \frac{1}{R_n^2} + \omega^2 C_n^2, \qquad \ldots \quad (i)$$

'A' being the admittance.

Next, the impedance of the same element (Z') is measured at slightly higher frequency, say, 3.005 Mc/s ($\omega = 2\pi \times 3.005 \times 10^6$) so that the values of the components may be regarded almost the same. Then the new equation will be

$$\frac{1}{Z'^2} = A'^2 = \frac{1}{R_n^2} + \omega'^2 C_n^2. \qquad \ldots \quad (ii)$$

From (i) and (ii), $|R_n|$ and C_n can be obtained.

For this method, (a) the number of observations required is doubled, (b) the h.f. source must be able to give the value of desired frequency f (Mc/s) *plus* or *minus* 1 to 5 Kc/s accurately over the whole range; and (c) input impedance of the valve voltmeter must be very large compared to the impedance of the element at all frequencies over the range 1-40 Mc/s.

Due to difficulty of obtaining a suitable thermionic voltmeter which would fully satisfy the condition (c) above for the frequency range 1-40 Mc/s, this method was abandoned in favour of a new method evolved by the authors for the purpose.

Fig. 1 shows the circuit diagram and the equivalent circuit. The blocking condenser (C) and shunting choke (L), being of negligibly small and considerably large impedance respectively at the frequencies concerned, have been left out in the equivalent circuit. The impedances of the measuring instruments I_1, I_2 and I_3 are negligibly small at the frequencies concerned.

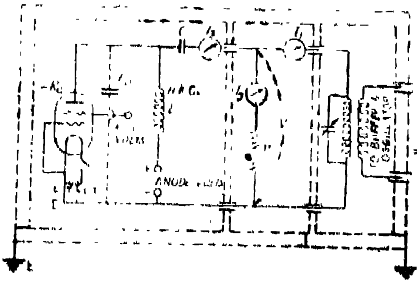

FIG. 1(a)

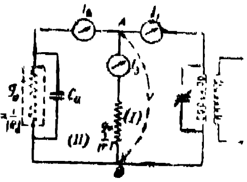

FIG. 1(b)

Let V = voltage between points A-B in the circuit ; g = conductance (magnitude) of arm I of the parallel impedance A-B ; g_a = conductance (magnitude) of negative resistance portion of arm II of the parallel impedance A-B; and C_a = total effective capacitance shunting the negative resistance.

Conductance is ordinarily a scalar quantity, but when negative resistance is involved, the idea of the direction of conductance cannot be avoided. For instance, if a voltage V be applied to terminals 1-2 of a positive resistance 'R' with 1 positive and 2 negative, the direction of current is from 1 to 2 and if the same voltage be applied to terminals 1-2 of negative resistance of the same magnitude 'R' with 1 positive and 2 negative the direction of current is from 2 to 1. The direction of conductance is also reversed in the two cases. In the following calculations, only magnitudes and not directions have been considered for all quantities and consequently the same applies to the case of conductance.

Then
$$V = \frac{I_3}{g} \qquad \text{(1)}$$

$$V = \frac{I_2}{\sqrt{g_a^2 + \omega^2 C_a^2}} \qquad \text{(2)}$$

$$V = \frac{I_1}{\sqrt{(g+g_a)^2 + \omega^2 C_a^2}} \qquad \text{(3)}$$

From (2) and (1),
$$g_a^2 + \omega^2 C_a^2 = \frac{I_2^2}{I_3^2} \cdot g^2 \qquad \text{(4)}$$

From (3) and (1),
$$(g+g_a)^2 + \omega^2 C_a^2 = \frac{I_1^2}{I_3^2} \cdot g^2 . \qquad \text{(5)}$$

Subtracting (4) from (5),
$$g^2 + 2gg_a = \frac{g^2}{I_3^2}(I_1^2 - I_2^2)$$

$$2gg_a = g^2 \left[\frac{I_1^2 - I_2^2 - I_3^2}{I_3^2} \right]$$

$$\therefore \quad g_a = \frac{g}{2} \left[\frac{I_1^2 - I_2^2 - I_3^2}{I_3^2} \right] \text{ in magnitude} \qquad \text{(6)}$$

and from (4)
$$C_a = \frac{1}{\omega} \sqrt{(I_2^2/I_3^2) . g^2 - g_a^2} \, . \qquad \text{(7)}$$

The value of 'r' and therefore of 'g' at frequencies involved can be accurately known. I_1, I_2 and I_3 can be accurately measured up to 40 Mc/s by Sullivan u.h.f. thermo-milliammeters. Hence the magnitude of g_a and R_a can be known with accuracy. C_a depending on g, g_a, I_2, I_3 and ω can be determined accurately.

Since self-capacitance of the choke together with stray capacitances of wiring, tube base, etc., can also be determined by similar arrangement after removing the tube from its base, C_{af} which is the (hot) anode-filament capacitance can be found out. H.F. power to the measuring arrangement has been supplied from a suitably controlled master oscillator through a buffer stage to obtain stability of the source frequency. The voltage output of the master oscillator decreases with increase of frequency. Great deal of care has been taken in the lay-out of the circuit and screening the different portions and leads as well as the measuring instruments at high and ultra-high frequencies.

MEASUREMENTS OF "$-R_a$," "C_a" AND "C_{af}" OVER RANGE 1-6 Mc/s

Measurements were carried out on dynatrons obtained from four different screen-grid tubes—(1) SG 215 (Mazda), (2) AC/SG (Mazda), (3) A 442 (Philips) and (4) 32 (RCA-American)—over the range 1-6 Mc/s working under conditions set forth in the next paragraph. The tubes SG 215, AC/SG and 32 were new whereas A 442 was in intermittent use for last few years. SG 215, A 442 and 32 were battery-heated tubes whereas AC/SG was an indirectly heated type. Table I gives details of the anodes (from which secondary emission takes place) and anode-cathode distances collected from broken specimen.

TABLE I

Tube	Type of anode structure	Approx. anode dimensions	Approx. width between plates if rectangular	Anode material	Anode-cathode distance (cms)
SG 215	Two rectangular plates	1½″ × ½″ each	1/8″	Pure nickel	0.51
AC/SG	Do	Do	Do	Do.	0.46
A 442	Do.	5/8″ × 3/8″ each	3/16″	Alloy of iron, nickel molybdenum and cobalt found on spectroscopic analysis	0 64
32	Circular plate	diameter 1″, length 3/4″	,,	Pure nickel	0.88

For SG 215 the screen-grid, plate and control-grid voltages were 80, 40 and 0 volts respectively, the filment current was 0.15 A and a.c. resistance from static characteristic was $-{}_0R_a = -22.86 \times 10^3$ ohms; for AC/SG the screen-grid, plate and control-grid voltages were 60, 28 and 0 volts respectively, the filament current was 1.0 A and a.c. resistance (static) was -15×10^3 ohms; for A 442 the screen-grid, plate and control-grid voltages were 100, 50, and 0 volts repectively the filament current was .06A and a.c. resistance (static) was—69.23×10^3 ohms; and for 32 tube the screen-grid, plate and control grid voltages were 68, 22 and 0 volts respectively, the filament current was .06 A and a.c. resistance (static) was -150×10^3 ohms.

Table II shows the values of $-R_a$, C_a and C_{af} obtained at different frequencies from observations of various currents and known conductance ' g.' Measurements on each tube were made at a constant h.f. voltage at all the frequencies,

TABLE II

Frequency in Mc/s.	SG 215 H.F. Voltage=12.5'			AC/SG H.F. Voltage=12.5'			A 442 H.F. Voltage=12.5"			32 H.F. Voltage=8.0"		
	$-R_a$	C_a	C_{af}	$-R_a$	C_a	C_{af}	$-R_a$	C_a	C_{af}	$-R_a$	C_a	C_{af}
	ohms	μμF	μμF	ohms	μμF	μμF	ohms	μμF	μμF	ohms	μμF	μμF
2	−12500	60.6	48.3	−15620	40.5	37.7	−4250	97.7	85.9	−8410	52	40.2
3	−5210	74.0	35.0	−5430	68.0	29.0	−3125	82.2	43.2	−5710	57	18.0
4	−2070	70.6	34.3	−1390	66.3	30.0	−1835	72.5	36.2	−3700	43	6.7
5	−512	65.5	27.7	−868	53.4	15.6	−567	79.8	42.0	−2580	22	10.0
5·5	−735	37.6	2.6	−1100	35.6	0.6	−1100	79.1	44.1	−2500	22.1	11.0

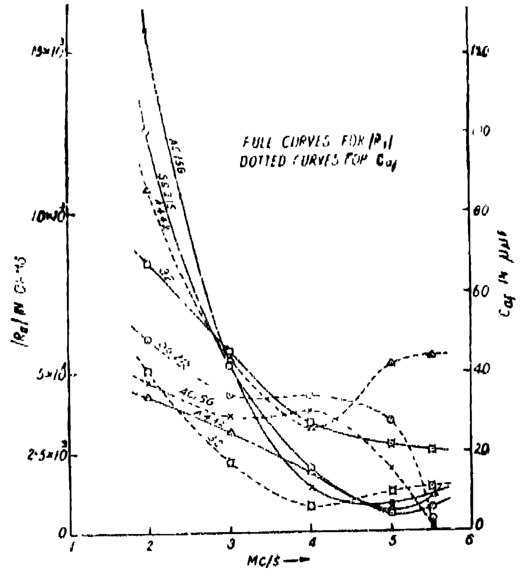

FIG. 2

Variation of R_a and C_{af} with frequency.—Fig. 2 shows the variation of $/R_a/$and C_{af} with frequency for all tubes over the range 1-6 Mc/s. It will be seen that for all tubes $/R_a/$ decreases smoothly with frequency up to 5 Mc/s and for three of them (except 32) it tends to increase again between 5 and 5.5 Mc/s. It will be observed that for SG 215 and AC/SG C_{af} decreases at first slowly up to 4 Mc/s and then rapidly between 4 and 5.5 Mc/s ; and for A 442 and 32 it decreases smoothly up to 4 Mc/s and then increases subsequently.

MEASUREMENT OF "$-R_a$", "C_a" AND "C_{af}" OVER RANGE 6-15 Mc/s

Measurements were made on dynatrons obtained from the four tubes mentioned in Section 3 over the range 6-15 Mc/s. The working conditions and a.c. resistance (static) were the same as those mentioned in Section 3.

Table III shows the measured values of $-R_a$, C_a and C_{af} at different frequencies. Measurements on each tube were made at a constant h.f. voltage at all the frequencies.

TABLE III

Frequency in Mc/s	SG 215 H.F. Voltage=4.1"			AC/SG H.F. Voltage = 3.2"			A 442 H.F. Voltage 4.1"			32 H.F. Voltage=2.74"		
	$-R_a$	C_a	C_{af}	$-R_a$	C_a	C_{af}	$-R_a$	C_a	C_{af}	$-R_a$	C_a	C_{af}
	ohms	μμF	μμF	ohms	μμF	μμF	ohms	μμF	μμF	ohms	μμF	μμF
6	−980	39	1.5	−2360	50.7	13.2	−3330	54.6	17.1	−720	50.3	12.8
8	−2700	42.5	4.5	−1300	45.2	7.2	−1770	42.4	4.4	−260	41.8	3.8
10	−1180	46.7	8.5	−1040	62	23.8	−1560	47.2	9.0	−360	45.2	7.0
12	−310	37.8	2.6	−220	40.1	4.9	−328	43.3	8.1	−880	39.4	4.2
14	−310	33.8	8.3	−250	26	0.5	−230	32.0	6.5	−1110	26.8	1.3

Variation of $/R_a/$ and C_{af} with Frequency

Fig. 3 shows the variation of $/R_a/$ and C_{af} with frequency for all tubes over the range 6-15 Mc/s. It will be seen that $/R_a/$ for A 442 and AC/SG decreases more or less smoothly with increase of frequency, for SG 215 it increases to a maximum value at 8 Mc/s and then decreases smoothly with increase of frequency and for 32 tube it decreases to a minimum value and then increases smoothly with increase of frequency. The variation of $/R_a/$ with frequency for SG 215 appears to be exactly opposite to that of 32.

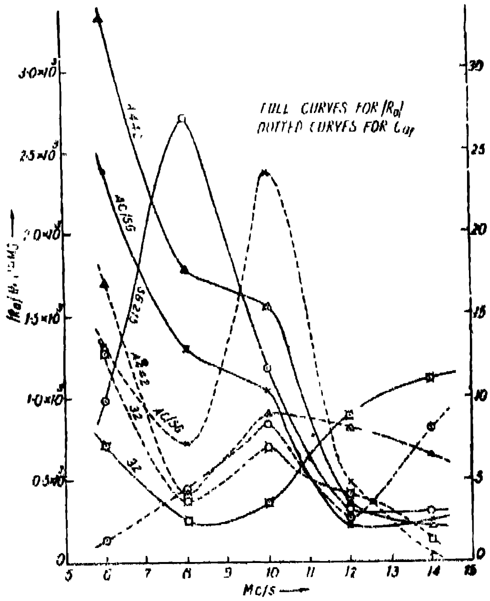

FIG. 3

It will be observed that the nature of variation of C_{af} with frequency for all tubes over the range 6-15 Mc/s is similar to a combination of resonance and anti-resonance characteristics. For AC/SG, A 442 and 32 tubes C_{af} decreases with frequency to a minimum at 8 Mc/s, then increases till 10 Mc/s and subsequently decreases. For SG 215, it increases till 10 Mc/s, then decreases till 12 Mc/s and subsequently increases again.

MEASUREMENTS OF "$-R_a$," "C_a" AND "C_{af}" OVER RANGE 20-40 Mc/s

Measurements were carried out on dynatrons obtained from the same four tubes mentioned in Sections 3 and 4 over the range 20-40 Mc/s. The working conditions and a.c. resistance (static) were the same as those mentioned in Section 3.

Table IV shows the measured values of $-R_a$, C_a and C_{af} at different frequencies. Measurements on each tube were made at a constant h.f. voltage at all the frequencies.

TABLE IV

Frequency in Mc/s	SG 215 H. F. Voltage = 0.3"			AC/SG H. F. Voltage = 0.4"			A 442 H. F. Voltage = 0.4"			32 H. F. Voltage = 0.4"		
	$-R_a$ or R_a	C_a	C_{af}	$-R_a$ or R_a	C_a	C_{af}	$-R_a$ or R_a	C_a	C_{af}	$-R_a$ or R_a	C_a	C_{af}
	ohms	$\mu\mu F$	$\mu\mu F$	ohms	$\mu\mu F$	$\mu\mu F$	ohms	$\mu\mu F$	$\mu\mu F$	ohms	$\mu\mu F$	$\mu\mu F$
20	−286	109	47	−400	147	85	−185	76.7	14.7	−345	84	22.0
22.5	−196	109	42	−137	140	73	−175	76.7	9.7	−339	87.7	20.7
25	−126	184	114	−182	82.8	12.8	−169	119	49	−180	91.0	21.0
27.5	−126	184	114	−116	122	52	−150	109	40	−139	102	32
30	−56	178	99	−43	115	36	−84	115	36	−83	93.4	14.4
32.5	−126	201	115	−54	153	67	−79	147	61	−100	92.4	6.4
35	−101	248	158	+143	108	18	−104	162	72	−107	95.8	5.8
37.5	−98	311	205	+36	87	14 ?	−36	187	81	−103	116	10.0
40	+20	120	8	+714	89.2	14 ?	+44	75	73 ?	−54	123	11.0

On the Positive sign of the Resistance component measured at some of the high frequencies

It will be seen from Table IV that only for 32 the resistance component has been found to be negative up to 40 Mc/s, for SG 215 and A 442 it has been negative up to 37.5 Mc/s and for AC/SG it has been negative up to 32.5 Mc/s.

This deviation for some of the tubes at frequencies higher than a certain value may be due to one or both of the causes given below.

(1) The values of I_1, I_2 and I_3 obtained at frequencies above 37.5 and 32.5 Mc/s for SG 215 and A 442 and AC/SG respectively may not have been correct due to loss by radiation from tube systems, portions of circuit, etc., at these high frequencies.

(2) A very large amplitude oscillation (or possibly a very large amplitude oscillation with amplitude increasing with time as in a negative resistance circuit) whose frequency is the same as or near about that of the impressed h.f. voltage may have been set up due to either the "amplification effect" of the type found by the first author elsewhere or the "resonance" effects in the tube system or due to both the causes and caused impairment or break-down of the negative resistance condition.

Variation of $/R_a/$ and C_{af} with frequency

Fig. 4 shows the variation of $/R_a/$ and C_{af} with frequency for all tubes over the range 20-40 Mc/s. It will be observed that the variation of both $/R_a/$ and C_{af} with frequency over this range is more complex than that over 1-6 Mc/s and 6-15 Mc/s ranges.

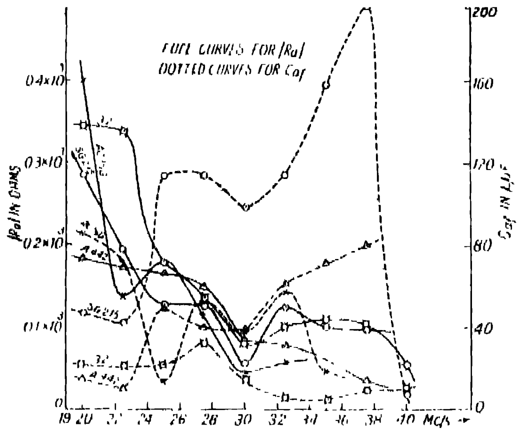

FIG. 4

For SG 215, AC/SG and 32, $/R_a/$ first decreases then increases to decrease again presenting a wavy characteristic; and for A 442 it decreases with frequency though not in a smooth curve.

For SG 215, AC/SG and A 442, C_{af} varies with frequency in a wavy manner whereas for 32 it first increases and then decreases with frequency.

DEPENDENCE OF $/R_a/$, C_a AND C_{af} UPON THE OPERATING H. F. VOLTAGE AMPLITUDE

$/R_a/$, C_a and C_{af} were measured at different values of V, keeping the frequency constant. V was obtained accurately from the product of I_3 and r.

Tables V, VI and VII show the results of measurement at 3, 10 and 30 Mc/s respectively for the four dynatron units operated under conditions mentioned in Section 3.

TABLE V (at 3 Mc/s)

S G. 215				AC/SG				A 442				32			
V	$-R_a$	C_a	C_{af}	V	$-R_a$	C_a	C_{af}	V	$-R_a$	C_a	C_{af}	V	$-R_a$	C_a	C_{af}
volts	ohms	μμF	μμF	volts	ohms	μμF	μμF	volts	ohms	μμF	μμF	volts	ohms	μμF	μμF
6.1	−3900	66.3	27.3	6.1	−4460	58.3	19.3	3.0	−1500	87.6	48.6	10	−4000	28.6	16.0
12.5	−5210	74.0	35.0	12.5	−5430	68	29.0	6.0	−6250	75.2	36.2	20	−3970	31.2	24.7
16.3	−4310	63.2	24.2	18.5	7040	61.6	22.6	7.3	−5020	75.6	36.6	25	−3330	11.4	7.4
20.0	−4390	61.8	22.8	21.3	−6410	60.9	21.9	8.0	−5100	76.9	37.9	40	−4330	15.7	12.5
23.8	−4170	63.2	24.2	25.0	−5950	61.3	22.3	10.4	−5350	76.8	37.8	50	−4440	16.2	13.0
27.5	−5320	62.2	23.2	28.8	−4310	64.6	25.6	12.1	−4690	76.7	37.7	—		—	—
30.0	−5100	63.5	24.5	—	—	—	—	—	—	—	—	—			

TABLE VI (at 10 Mc/s)

SG 215				AC/SG				A 442				32			
V	$-R_a$	C_a	C_{af}	V	$-R_a$	C_a	C_{af}	V	$-R_a$	C_a	C_{af}	V	$-R_a$	C_a	C_{af}
volts	ohms	μμF	μμF	volts	ohms	μμF	μμF	volts	ohms	μμF	μμF	volts	ohms	μμF	μμF
1.59	− 357	91.5	53.3	1.59	− 442	78.5	40.3	1.59	− 233	75.5	37.3	1.59	− 443	87.8	49.6
2.30	− 478	58.6	20.4	2.3	− 521	46.0	7.8	2.3	− 478	63.8	25.6	2.3	− 402	54.4	16.2
3.19	− 588	39.2	1.0	3.19	− 1042	56.8	18.0	3.19	− 541	46.6	8.4	2.74	− 361	45.2	7.0
4.07	−1140	46.0	7.8	4.07	− 735	49.4	11.2	4.07	− 1500	47.0	8.8	3.19	− 384	46.1	7.9
4.78	− 555	43.6	5.4	4.78	− 653	45.4	7.2	4.78	− 840	43.3	5.1	4.16	−1770	40.1	1.9
5.31	− 653	43.6	5.4	5.31	− 492	39.3	1.1	5.31	− 735	42.4	4.2	5.2	−1610	39.0	0.8
6.28	− 478	41.2	3.0	6.18	− 442	39.4	1.2	6.28	521	43.0	4.8				

TABLE VII (at 30 Mc/s)

SG 215				AC/SG				A 442				32			
V	$-R_a$	C_a	C_{af}	V	$-R_a$	C_a	C_{af}	V	$-R_a$	C_a	C_{af}	V	$-R_a$	C_a	C_{af}
volts	ohms	μμF	μμF	volts	ohms	μμF	μμF	volts	ohms	μμF	μμF	volts	ohms	μμF	μμF
0.12	−158	191	112	0.14	−122	258	179	0.20	−127	188	109	0.27	− 54.6	117	38.0
0.20	−104	210	131	0.21	−108	199	120	0.29	−120	156	77	0.47	− 85	93.0	14.0
0.27	− 56	178	99	0.27	− 58	189	110	0.35	− 84	124	45	0.61	−117	86.9	7.9
0.33	− 55	142	63	0.35	− 38	121	42	0.46	− 84	98	19	0.77	−263	65.0	25.0
0.40	− 46	97	18	0.40	− 43	115	36	0.55	− 80	90	11	0.93	−104	71.3	31.3
0.46	− 59.5	114	35	0.50	− 46	101	22	0.65	− 80	80	1	1.08	− 96	57.2	17.2
0.53	− 66.6	104	25	0.56	− 44	84.4	5.4					1.20	− 86	54.5	14.5
0.65	− 63	93.2	14.2	0.63	− 42	82.0	3.0								

Variation of $/R_a/$ *and* C_{af} *with H.F. Voltage Amplitude*

Measurements in Tables V, VI and VII show the variation of $/R_a/$ and C_{af} with h.f. voltage at 3, 10 and 30 Mc/s respectively.

At 3 Mc/s, C_{af} for all tubes decreases in general with increase of voltage—first increasing, then decreasing with slight increase subsequently; and $/R_a/$ for all tubes except 32 at first increases and then decreases, giving peaky curves. For 32, $/R_a/$ remains constant, then decreases and subsequently rises roughly to the initial values.

At 10 Mc/s, for C_{af} for SG 215 and AC/SG at first decreases and then increases slightly to decrease again and for A 442 and 32 it decreases with increase of voltage; and $/R_a/$ for all tubes increases initially to a peak value to decrease subsequently.

At 30 Mc/s, C_{af} for all tubes except 32 decreases in general with increase of voltage and for 32 it first decreases and subsequently increases with increase of voltage; and $/R_a/$ for all tubes except 32 at first decreases in general with increase of voltage (though not in a smooth curve) and then remains roughly constant and for 32 it first decreases, then rises to a peak value to decrease again.

7. DISCUSSION ON THE NATURE OF VARIATION OF $/R_a/$ WITH FREQUENCY

According to Hartshorn, the internal resistance of a triode decreased with increase of frequency.

Mitra and Sil worked out a variation of internal resistance with frequency which differed entirely from Hartshorn's theory. According to their calculation the internal resistance of a triode would be independent of frequency for frequencies lower than a certain value, say '*f*' Mc/s, and would increase gradually with increase of frequency for values higher than '*f*' Mc/s.

Rao found that the internal resistance of triodes used by him at first decreased with increase of frequency till 1.6 or 2.0 Mc/s (depending upon the tube) and then increased steadily with increase of frequency. Basak found that the resistance of anode—screen-grid space of a screen-grid tube under normal condition decreased with increase of frequency over the range 0.5—1.0 Mc/s.

Hollman and Thoma showed that the resistance of electronic medium inside a thermionic valve would decrease with increase of frequency from very low to very high frequencies.

It will be noted that measurements of internal resistance were carried out by majority of workers over frequency ranges which were not large enough for any definite deduction as to the general nature of variation of $/R_a/$ with frequency to be made, and further the effect of amplitude of h.f. voltage impressed between plate and filament on $/R_a/$ was not considered at all, since this would also modify the nature of variation of $/R_a/$ with frequency unless the h.f. voltage amplitude was adjusted to the same value at all frequencies.

The present work along with the first author's previous work relates to variation of $/R_a/$ of screen-grid tubes *under secondary emission* condition with frequency over the range 0.5 Kc/s—40 Mc/s as well as its variation with h.f. voltage amplitude at various frequencies in the range. Compared to triodes and screen-grid tubes worked under normal condition, the conditions in screen-grid tubes under secondary emission condition affecting the internal resistance and dielectric constant are as follows :—(1) The time of stay of the electrons (T) is somewhat longer (*i.e.*, 0.1×10^{-8} sec., 0.1×10^{-8} sec., 0.11×10^{-8} sec., and 0.2×10^{-8} sec. calculated for SG 215, AC/SG, A 442 and 32 respectively) ; (2) the thermionic current is comparatively smaller and (3) there is more uniform distribution of electrons in anode-filament space.

From measurements performed with time of stay, thermionic and filament currents, control grid voltage, screen-grid and anode voltages and h.f. voltage kept constant at all frequencies, it has been found that the law of variation indicated by the *mean curve* derived from the experimental curve is that the internal resistance decreases with increase of frequency (according to the inverse square law) from very low to very high frequencies in agreement with Hollmann and Thoma as well as Hartshorn. Several "turning points" (more or less of the nature mentioned by Khastgir with reference to Rao's work) are noticeable in the experimental curve if drawn over a sufficiently large frequency range. From these turning points, as frequency increases, the curve can be seen to rise slightly over a frequency band of width varying from less than 1 Mc/s to 8 Mc/s (giving an increase of resistance with increase of frequency over this band) and subsequently to fall at higher frequencies.

If measurement be started from one of these "turning point frequencies" or a frequency higher than this, the internal resistance will be found to increase with increase of frequency over a band width of 7 to 8 Mc/s. If measurement be started from a frequency less than the turning point frequency but is not continued beyond that point, an opposite law of variation will be obtained ; and if measurement be continued beyond the turning point frequency results similar to those of Rao will be found.

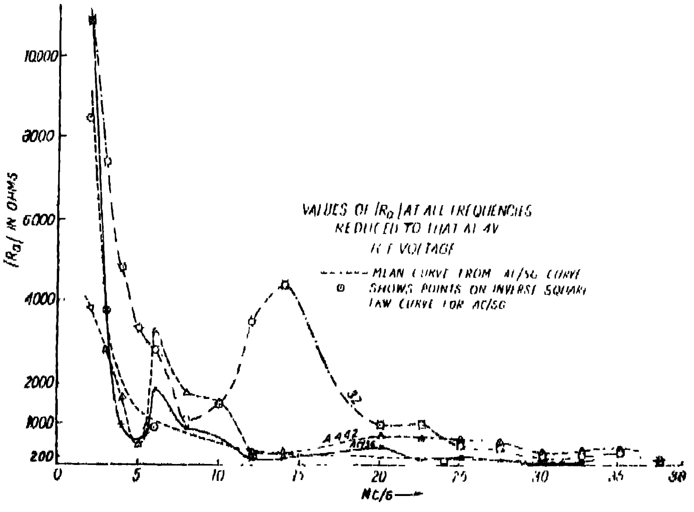

FIG. 5

FIG. 5 shows the variation of $/R_a/$ with frequency (the values of $/R_a/$ at all frequencies having been reduced to those at 4 volts h.f. voltage amplitude) over the range 1-40 Mc/s for AC/SG, A 442 and 32 tubes. Taking the mean curve for AC/SG (drawn plain-dotted) it will be seen to pass almost through all the points lying on the inverse square law curve thereby satisfying the relation $/R_a/ \propto \frac{1}{\omega^2}$ in accordance with the law of conductivity $\sigma \simeq \frac{Ne^2\omega^2T^3}{12m}$ (when ωT is sufficiently small) given by Hollmann and Thoma.

DISCUSSION ON DIELECTRIC CONSTANT OF ELECTRONIC MEDIUM UNDER SECONDARY EMISSION CONDITION AND ITS DEPENDENCE UPON H.F. OPERATING VOLTAGE AND FREQUENCY

The dielectric constant of the electronic medium between anode and filament of screen-grid tubes under secondary emission condition has been estimated over the range 1-40 Mc/s, from values of C_{af} under ' filament on ' or ' hot condition ' (as given in Tables II, III, IV, V, VI and VII) and values of C'_{af} under ' filament off ' or ' cold condition ' (as measured by connecting anode-filament capacitance in parallel to the capacitance element of a standard oscillatory circuit and observing frequency-change thereby).

In the past, the dielectric constant of the electronic medium in a screen-grid tube (under normal condition) with increase of frequency has been measured by Prasad and Verma and also by Imam and Khastgir. Prasad and Verma carried out their measurements over the range 0.57-3.7 Mc/s and found their results agreeing with the Eccles-Larmor theory. Imam and Khastgir experimented over the range 60-75 Mc/s and found that dielectric constant of electronic medium between anode and filament decreased as frequency was increased from 60 to 64 Mc/s and then increased with further increase of frequency up to 75 Mc/s. Their measurements between 64-75 Mc/s did not satisfy the Eccles-Larmor theory. Imam and Khastgir further examined the effect of increasing filament current, screen-grid voltage and anode voltage on the dielectric constant.

As in the previous section the measurement of dielectric constant needed to be carried out over a sufficiently large frequency range and the effect of amplitude of h.f. voltage impressed between plate and filament should also have been considered.

The present studies relate to (1) the variation of the dielectric constant of the electronic medium under secondary emission condition with the increase of h.f. voltage applied between anode and filament, keeping filament current, anode voltage, control-grid and screen-grid voltages same at all frequencies; and (2) the variation of the dielectric constant of the electronic medium under secondary emission condition with increase of frequency keeping filament current, anode voltage, control-grid and screen-grid voltages same at all frequencies.

Variation of dielectric constant with h.f. operating voltage. It will be seen from Fig. 6*a* that (*a*) at 3 Mc/s the dielectric constant varies with increase of h.f.

voltage in a wavy manner though the variation is small; (*b*) at 10 Mc/s it decreases with increase of h.f. voltage though not in a smooth curve; and (*c*) at 30 Mc/s it decreases rapidly with increase of h.f. voltage for AC/SG and A 442 but varies in a wavy manner for 32 tube, the variation being larger than that at 3 Mc/s. It may be said that at 10 and 30 Mc/s the dielectric constant is much greater than unity at smaller values of h.f. voltage and becomes in general less than unity at higher values of h.f. voltage.

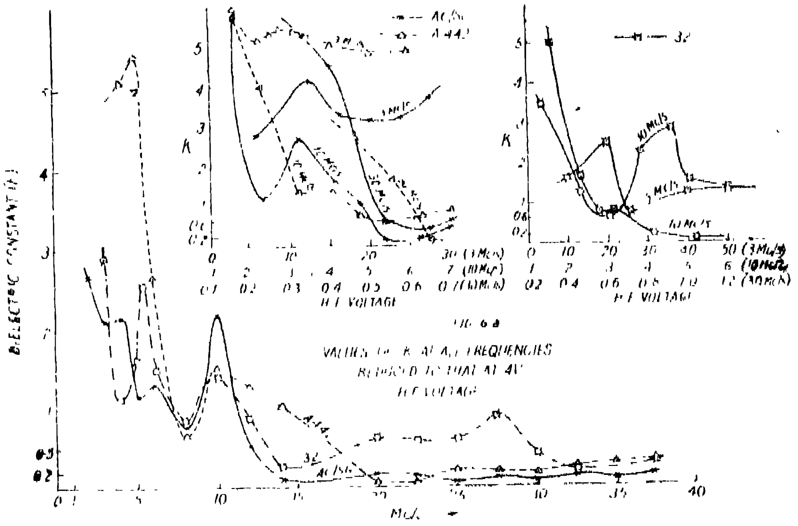

FIG. 6

Variation of dielectric constant with frequency. It will be observed from Fig. 6*b* (the values of dielectric constant having been reduced to that at 4V h.f. voltage amplitude) that (*a*) the curves of variation between 1-40 Mc/s are wavy showing peaks and depressions and (*b*) the value of 'K' is less than unity between 7-9 Mc/s as well as after 11 Mc/s for AC/SG and 32 and after 14 Mc/s for A 442. The Eccles-Larmor theory does not hold good for the measurements undertaken.

It has already been observed by some of the previous workers for electronic atmosphere in other types of vacuum tube that the dielectric constant could be sometimes less than, sometimes greater than and sometimes equal to unity. The present case appears to confirm this view-point for the anode-filament space of screen-grid tube under secondary emission condition over 1-40 Mc/s range. The effect of much smaller thermionic current and of the time of stay of the electrons shorter compared to the period of h.f. oscillation at lower frequencies has been to give very high values of dielectric constant (greater than unity) at these frequencies. As frequency increases above 10 Mc/s, the time of stay of the electrons (in this case) approaches the period of h.f. oscillation. This fact together with more uniform distribution of electrons in anode-filament space appears to give very low values of dielectric constant (much less than unity) at frequencies higher than 10 Mc/s.

LINEARITY OF NEGATIVE IMPEDANCE ELEMENT OVER RANGE 1-40 Mc/s

The variation of $/R_a/$, C_a and $C_{a/}$ with h.f. voltage has been considered in Section 6. When negative impedance has to be used in a circuit or network, the dependence or independence of the magnitude of negative impedance *as a whole* rather than that of its components upon the amplitude of h.f. voltage impressed is of very great importance.

The magnitude of negative impedance (that is $/Z/$) has been computed from the measured values of $/R_a/$ and effective capacitance C_a.

Tables VIII, IX and X show the magnitude of negative impedance as whole as the h.f. voltage is increased at 3, 10 and 30 Mc/s respectively.

TABLE VIII (at 3 Mc/s)

SG 215		AC/SG		A442		32	
V volts	|Z| ohms	V volts	|Z| ohms	V volts	|Z| ohms	V volts	|Z| ohms
6.1	785	6.1	892	3.0	601	10.0	1684
12.5	711	12.5	773	6.0	702	20.0	1563
16.3	824	18.5	855	7.3	697	25.0	2707
20	812	21.3	864	8.6	684	40.0	2656
23.8	843	25.0	856	10.4	685	50.0	2635
27.5	843	28.8	807	12.1	684		
30.0	825						

TABLE IX (at 10 Mc/s)

SG 215		AC/SG		A442		32	
V volts	|Z| ohms	V volts	|Z| ohms	V volts	|Z| ohms	V volts	|Z| ohms
1.59	229	1.59	184	1.59	156	1.59	168
2.30	236	2.30	160	2.30	221	2.30	236
3.19	334	3.19	270	3.19	285	2.74	252
4.07	331	4.07	295	4.07	330	3.19	257
4.78	305	4.78	309	4.78	337	4.16	388
5.31	318	5.31	313	5.31	334	5.2	395
6.28	301	6.28	298	6.28	302		

TABLE X (at 30 Mc/s)

S. G. 285		AC/SG		A 442		32	
V volts	|Z| ohms	V volts	|Z| ohms	V volts	|Z| ohms	V volts	|Z| ohms
0.12	27.4	0.14	20.3	0.20	27.5	0.27	34.9
0.20	25.0	0.21	25.9	0.29	32.7	0.47	47.4
0.27	27.5	0.27	25.3	0.35	38.1	0.61	54.1
0.33	30.9	0.35	28.7	0.46	45.5	0.77	78.0
0.40	35.1	0.40	31.5	0.55	47.5	0.93	60.5
0.46	36.5	0.50	34.6	0.65	48.1	1.08	66.6
0.53	40.5	0.56	35.9			1.20	63.0
0.65	42.2	0.63	35.2				

It will be seen from the tables VIII and IX that at 3 and 10 Mc/s the impedance magnitude for all dynatrons has generally been lower at low voltages and increases to almost constant value at voltages beyond 4 to 6 dbs above the initial voltage. The dynatrons obtained from SG 215, AC/SG and A 442 could be regarded for most purposes as linear impedances at the above frequencies. Table X shows that alteration in impedance-magnitude at 30 Mc/s for voltage variation of 14 dbs is greater than that at 3 and 10 Mc/s for the same variation of voltage.

PHASE-SHIFT CAUSED BY NEGATIVE IMPEDANCE ELEMENT OVER RANGE 1-17 Mc/s

The phase-shift caused by negative impedance element obtained from AC/SG tube has been measured by the "Cathode-Ray Oscillograph Method" employed by the author in a previous paper (Chakravarti, 1943).

A resistance (which is purely non-reactive at frequencies involved) is connected in series with the negative impedance element and fed from the h.f. source by the usual circuit arrangement. The voltage drops across the non-reactive resistance and the negative impedance element are applied to two exactly similar superheterodyne linear amplifiers with the same local oscillator and the corresponding I.F. Voltage outputs are applied to the respective pairs of plates of the oscillograph. The phase-shift caused by negative impedance element has been obtained from the phase difference measured between the two applied voltages. The phase-shift under similar conditions has also been calculated from the measured values of $|R_n|$ and C_n given in section 3 and 4.

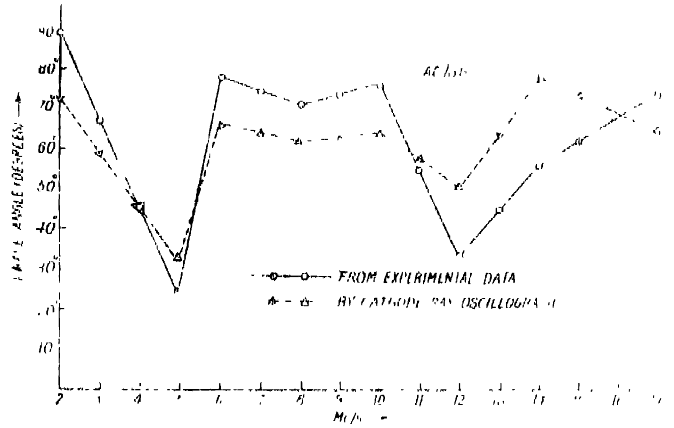

FIG. 7

Fig. 7 shows the phase-shift for AC/SG at different frequencies as obtained by cathode-ray oscillograph method as well as calculated from measured values given in Sections 3 and 4. It will be seen that over the range 1-17 Mc/s the variation of phase-shift is irregular since both R_n and C_n have been found to vary differently over different portions of the frequency range. Between 1 and 5 Mc/s, the phase-shift angle varies inversely as ω and between 5 and 6 Mc/s it varies directly as ω. Between 6 and 17 Mc/s it remains roughly constant except for a decrease at 12 Mc/s.

ACKNOWLEDGMENT

The whole of the experimental work has been carried out at the Kanodia Electrical Communication Engineering Laboratories, Department of Applied Physics, University of Calcutta. The authors desire to thank very heartily Prof. P. N. Ghosh, Sc.D., Ph.D., for his kind encouragement and interest during the progress of work.

REFERENCES

Baker, 1933, *J. I.E.E.*, **72**, 196.

Bargmann and During, 1929, *Ann. d. Phys.*, **1**, 1041.

Basak, 1941, *Ind. J. Phys.*, **15**, 343.

Bell, 1935, *Marconi Review*, **57**, 18.

Benham, 1931, *Phil. Mag.*, **11**, 457.

Benner, 1929, *Ann. d. Physik* **3**, 993.

Chakravarti, 1938, *Phil. Mag.*, **26**, 173

Chakravarti, 1940, *Phil. Mag.*, **30**, 201

Chakravarti, *Ind. J. Phys.* in press.

Dye and Jones, 1933, *J. I.E.E.*, **72**, 169.

Hertshorn, 1931 *Wireless Engineer*, **8**, 413.

Hollmann and Thoma, 1938, *Ann. d. Physik*, **6**, 32

Imam and Khastgir, 1937, *Ind. J. Phys.* **11**, 37.

Jones, 1937, *J.I.E.E.*, **81**, 658.

Khastgir and Serajuddin, 1939, *Phil. Mag.*, **28**, 532

Khastgir, 1941, *Ind. J. Phys.*, **15**, 317

Mitra and Sil, 1932, *Phil. Mag.*, **13**, 1081.

Moullin, 1933, *J.I.E.E.*, **73**, 186

Moullin, 1937, *J.I.E.E.*, **81**, 667.

Prasad and Verma, 1936, *Zeits. f. Phys.*, **99**, 78

Rao, 1940, *Ind. J. Phys.*, **14**, 217

Sil, 1933, *Phil. Mag.*, **16**, 1114 and 1124.

SPECTRUM OF ACTIVE NITROGEN IN THE SCHUMANN REGION

BY B. M. ANAND, P. N. KALIA

AND

MELA RAM

(Received for publication, Nov. 12, 19[illegible])

Plate I

ABSTRACT A review of the theories of active nitrogen is given. Experiments by the authors to study the emission and absorption spectrum of the afterglow in the Schumann region with one metre normal incidence vacuum spectrograph are described. Spectroscopic evidence which is produced, is against the atomic hypothesis and supports the molecular nature of the phenomenon.

The phenomenon of afterglow of nitrogen was discovered by E. P. Lewis (1900) by passing condensed electric discharges in tubes through which nitrogen was flowing. He observed that the gas continued to glow with a yellow colour as it came out of the region of discharge. The luminosity, however, steadily diminished until it entirely disappeared. The nitrogen in this form is capable of reacting with several substances very easily and vigorously and has, therefore, been given the name of active modification of nitrogen by Lord Rayleigh (1904) who has done a great deal of experimental work to elucidate its nature.

At one time Lord Rayleigh believed that the constitution of active nitrogen was similar to that of ozone. Under the action of the discharge some of the N_2 molecules decompose into atoms and combine with molecules to give what may be called tri-nitrogen (N_3), according to the equation

$$N_2 + N_1 = N_3$$

and further that N_3 combines with N_1 to form $2N_2$,

$$N_3 + N_1 = 2N_2$$

and in doing so radiates light.

As the change of volume experimentally observed in the process of conversion is, however, quite different from that expected on this basis, and further the more recent measurements of Wrede on pressure changes also do not support it, the hypothesis so far has not found any favour.

Saha and Sur (1924) then put forward a new hypothesis. According to them the Lyman-Birge-Hopfield bands lying in the vacuum region arise from a level which is metastable and the energy content of the molecule in this state was considered to be of the order of 8 volts or so. Saha and Sur suggested that the excited molecule parts with its energy by a collision of the second type with another molecule which when it returns to the normal state gives rise to the phenomenon of afterglow. At the time when this suggestion was made, knowledge of the molecular spectrum of nitrogen was very meagre and therefore in the light of the analysis of the band spectrum of nitrogen which he carried out, Birge (1924) modified this hypothesis, and to the extent that an energy-content of 11·4 volts was assigned to the metastable state. He also suggest that the function of impurities which are found to be necessary for the production of active nitrogen, is to absorb the free electrons, which would otherwise permit an easy and direct passage to the normal state.

From an analogy with active hydrogen which is known to be atomic hydrogen, a handy explanation suggests itself that active nitrogen is also atomic in nature. Indeed, Lewis had suggested that chemical and luminescence phenomena are due to the energy set free by the recombination of two atoms. This would mean that the molecule formed by the recombination of two atoms possesses the energy of dissociation in the form of the energy of excitation.

For obvious reasons with our present-day knowledge of molecules such an idea without further modification would not be tenable. Sponer (1925), therefore, tried to explain away the difficulties by introducing the hypothesis that the discharge dissociates the molecule into two atoms, and when two of such atoms recombine in the presence of a third particle, phenomena associated with the active stage occur. The extraordinarily long life of the afterglow is thus due to the rare occurrence of such collisions. The third partner in such collisions may be a normal nitrogen molecule of any other foreign molecule or atom which takes up the dissociation energy which is liberated and given out eventually as radiation. The strongest bands in active nitrogen have their upper states corresponding to $v' = 11$, 12 of the $B(^3\Pi)$ of N_2 and are situated in the visible region giving rise to the golden yellow colour of the afterglow. According to Spener, therefore, the energy of excitation of these bands corresponds to the heat of dissociation of N_2.

The three body collision hypothesis did not come in direct contradiction with any experimental facts. Indeed, it is supported by the decay curves which indicate that the decay of the afterglow is either a bimolecular or a trimolecular reaction. But as further spectroscopic data became available, the value 11.6 volts assigned by Sponer for the dissociation of N_2 molecule in two atoms in ^4S states, was found to be too high.

These circumstances led Cario and Kaplan (1929) to develop a new hypothesis, which was really a modification and combination of the previous views, for it required the presence of metastable atoms and metastable molecules as well as a three body collision. According to this hypothesis, atomic nitrogen is formed by the discharge. As two such atoms combine in a three body collision with a molecule of nitrogen, dissociation energy amounting to 9.5 volts is liberated and this is sufficient either to take the molecule to the metastable state (which requires only 8 volts) or to excite any other atom (the third body) taking part in the collision, but is not sufficient to excite the afterglow. The necessary equation is as follows:

$$N_2 + N_1 + N_1 = N_2 + N'_2$$

N'_2 indicates the nitrogen molecule in the metastable state ($A^3\Sigma$). When two such excited molecules N'_2 collide together, an energy of 16 volts goes towards the dissociation of one of the two molecules and is used up in changing the two atoms from a normal state to a metastable state. Thus

$$N'_2 + N'_2 = N_2 + N'_1 + N'_1$$

N'_1 and N'_1 indicate two metastable atoms. The total enegy of 16 volts is more than sufficient to dissociate a molecule which requires only 9.5 volts. The rest 6.5 volts is divided between the two atoms, each one being loaded with an amount of energy nearly 3.3 volts. Compton and Boyce have shown from spectroscopic investigations that for the nitrogen atom, the two metastable states (^2D and ^2P) have the energy-values of 2.37 and 3.56 volts respectively.

According to Cario and Kaplan (1920) the afterglow is given out when a metastable molecule collides with a metastable atom of either type. Thus

$$N_2{}^3\Sigma(8) + N^2P(3.56) = N_2{}^3\Pi B_{12}(11.56)$$
$$N_2{}^3\Sigma(8) + N^2D(2.37) = N_2{}^3\Pi B_6(10.37).$$

These are excited levels involved in the production of the afterglow corresponding to 11.56 and 10.37 volts, giving rise to certain bands of the first positive system selectively intensified.

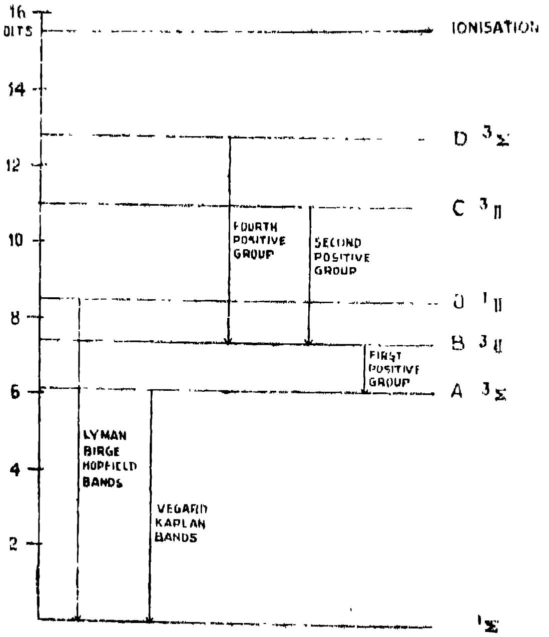

Electronic Levels of N2

FIG. 1

In the light of further work on the analysis of the molecular spectrum of N_2 and also on the basis of the work done by Okubo and Hamada (1933*a*) on the excitation of spectrum by active nitrogen it becomes at once apparent that this hypothesis needs modification. According to the original theory of Cario the values of energies available in active nitrogen were 8.0 ($A^3\Sigma$), 10.37 ($B_6{}^3\Pi$) and 11·56 ($B_{12}{}^3\Pi$). The lines observed by Okubo and Hamada have an excitation potential of 9.5 volts or less.

The discovery of Vegard-Kaplan (1930) bands (Fig. 1) also put the question of energy values in doubt. Vegard observed bands in solid nitrogen which he later also associated with certain bands in the spectrum of Aurora Borealis. Kaplan (1930) by designing a special discharge tube showed that they could be observed in N_2 gas and after working out the vibration analysis proved conclusively that the lower state of this system corresponds to the normal state of the molecule. The value for $A^3\Sigma$ thus comes out as 6.14 volts. In the light of these works, the energy values of $A^3\Sigma$ and $B^3\Pi$ are modified to 6.14 and 7·34 volts respectively.

As a result of series of experiments carried out in oxygen-nitrogen mixtures excited by rapidly interrupted weak discharges Kaplan has obtained an afterglow which has been called by him Auroral afterglow to differentiate it from the usual Lewis-Rayleigh phenomenon. It gives the auroral green line due to oxygen λ5577 ($^1S_0$—$^1D_2$). According to Kaplan the metastable nitrogen molecules in $A^3\Sigma$ state are present only in the Auroral glow and not in the Lewis-Rayleigh glow. When the pressure is high the Auroral glow gives out in addition the forbidden lines of nitrogen corresponding to $^2P \rightarrow {}^4S$ and $^2D \rightarrow {}^4S$ transitions, proving the existence of metastable nitrogen atoms in the afterglow. The metastable nitrogen atoms are not produced directly but are supposed to be produced by the dissociation of the molecules.

Kaplan and Rubens (1940) have studied the behaviour of the Auroral glow with time and have observed that the intensity of the forbidden line λ 3467 (^2P—^4S) increases with time in the early phase of the afterglow. To explain this, they have postulated the existence of some molecules whose number increases with the time elapsed and their rapid predissociation causes the appearance of the forbidden lines. These temporal effects have also been observed in nitrogen-helium mixtures and the large intensity of the forbidden line has been explained as due to either the prevention of diffusion of metastable nitrogen atoms to the walls or the increased predissociation of molecular nitrogen in the presence of helium.

Hebb and Sponer (1941) have now proposed a modification of the old triple collision hypothesis, according to which the energy of the afterglow is stored partly as the energy of dissociation of nitrogen molecule into normal atoms and partly as the excitation energy of metastable ^2D atoms. A ^2D atom recombines with a normal atom in the presence of a third body directly into $B\ ^3\Pi$ state which is the upper state of the afterglow bands.

From the review of the present theories of active nitrogen which has been given above, it would appear that the view, that atoms of nitrogen in some state are present in active nitrogen, is generally finding favour. This hypothesis, however, up to this time lacks a direct experimental confirmation. It may be mentioned that Cario (1934) and Kaplan (1934) have cited the results of Wrede (1929) and others on the observation of the pressure changes due to the diffusion of the products of the discharge, in support of their hypothesis of the presence of atoms of nitrogen. But, as has been pointed out by Saha and Mathur (1936), these experiments only prove the existence of these entities in the region of the discharge and it remains an open question whether they are also present in active nitrogen in the side tube. Kichlu and Acharya (1929) did not succeed in getting any line of nitrogen at 8200 on their plates though such long exposure were given that even the weakest bands of the first positive group were clearly visible up to 8900. The experiments described in the present paper were undertaken to photograph the spectrum of the afterglow of nitrogen in the Schumann region at about λ 1700 Å where the resonance lines of atomic nitrogen due to the transitions $2p^3—2p^2\ 3s$, $2p^2\ 3d$ are situated.

EXPERIMENTAL

Nitrogen obtained from a commercial cylinder is collected in a large glass jar provided with a side tube at the bottom and placed in a water trough. By means of a tube put at the top it could be drawn out and passed through freshly cut chips of phosphorus contained in a bottle in order to remove traces of oxygen. After passing successively through calcium chloride tower, a phosphorus pentoxide tube and a capillary tube for partial regulation of the stream, the nitrogen entered the discharge tube provided with three electrodes (E, E_2, E_3), E_3, E_2 being connected together and earthed. The gas is excited by a condensed discharge provided by a 16000-volt transformer with capacity and spark gap. The special construction of the discharge tube is shown in Fig. 2. The

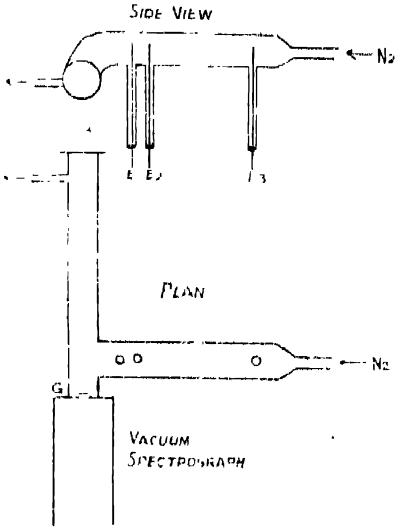

FIG. 2

end G is sealed on to the one-metre vacuum grating spectrograph of this laboratory. The passage between the slit and the tube is closed with a fluorite plate. The observation tube, about 30 cms. long, is collimated with respect to the spectrograph and is put in such a way that no light of the discharge enters the slit. The gas is drawn out by an oil pump which sends the gas back to the reservoir. A number of stop-cocks are put in the circuit for adjustment of pressure, etc. The arrangement is perfectly automatic and needs looking after only occasionally. Exposure is started after the gas has attained the characteristic yellow colour of active nitrogen as observed by the first positive group. The vacuum spectrograph has a dispersion of about 17.5A per millimetre in the first order and is adjusted to take spectrum between 100A and 2000A in one exposure. In the present case the fluorite plate restricted the short wave-length limit to about 1250A. The Schumann plates used were prepared in this laboratory.

Several photographs of the spectrum of active nitrogen with varying lengths in one case extending to 53 hours of exposure were taken. In none of these plates was there even the slightest trace of the lines of atomic nitrogen. The experiment of course cannot be advanced as an argument against the hypothesis Cario and Kaplan according to which the atoms of nitrogen may exist in metastable state ^2D and ^2P of $2p^3$ configuration and may not exist in any of the states belonging to the configuration $2p.^23s$. But it does show that the analogy of the parallel properties of active hydrogen and active nitrogen cannot be stretched too far, inasmuch as active hydrogen shows Balmer lines strongly and would, if the experiment were tried, also show the Lyman series.

A crucial test should be to observe the absorption spectrum of active nitrogen in the Schumann region where the resonance lines of atomic nitrogen are situated. According to Cario and Kaplan's theory, active nitrogen is composed of atoms in the states $2p^3$ (^2D, ^2P) and the absorption experiment should show the following multiplets in reversal ;

$2p^2.3s$ / $2p^3$	$^2P_{3/2}$ 31156	$^2P_{1/2}$ 31236	^2D 17701
$2p^3$ ^2D 98143	1492.6	1494.7	1243.2
$2p^3$ ^2P 88537	1742.7	1745.3	1411.9

The apparatus employed to test this point was essentially the same as described before. The phosphorus bottle was, however, dispensed with and in addition more effective drying arrangements were used. For continuous spectrum the radiations from a hydrogen discharge tube taking 90 *ma.* at 1500 volts was used. This tube was sealed end-on to the tube through which the afterglow was streaming, and to avoid the mixing up of the two gases a fluorite window was provided. A fluorite window was also sealed on to the slit of the spectrograph. The length of the afterglow, through which the radiations from the hydrogen tube passed and fell on the slit of the one-metre vacuum grating spectrograph, was about 14 cms. The glow was very bright and was steadily maintained at a pressure of about 7 mm. The electrodes of the discharge tube near the spectrograph were carefully earthed, so that the afterglow streamed through a field-free space. The active nitrogen was formed by a condensed discharge from a 20,000 volts transformer taking about 300 watts. The Schumann plates used were prepared in the laboratory and an exposure of five hours was found to be enough.

RESULTS

Plate 1 shows two of the spectrograms taken. "a" shows the discharge alone from the hydrogen without any active nitrogen. This particular spectro-

List of the fourth positive bands of CO observed in active nitrogen

λ in Å Observed by authors	Observed by Knauss	Assignment by Birge (v', v'')	λ in Å Observed by authors	Observed by Knauss	Assignment by Birge (v', v'')
2262.3		5–14	1724.5	—	4–0
	2191	2–11	1713.3	-	0–3
—	2171	5–13 1–10	1705.7	—	3–5
2150.9	—	4–12	1670.7	1669	1–3
2068.0	—	4–11	1654.3	1653	0–2
2044.0	—	3–10	1649.0	1648	3–4 6–6
2034.1	-	6–12	1631.2	—	2–3 5–5
2010.6	—	5–11	1613.4	—	4–1
1991.0		4–10	1597.3	1597	0–1
1970.2		3–9	1577.3	1574	2–2 5–4
1931.3	—	1–7			
1914.8	—	0–6 7–11	1561.4	1558	1–1 4–3
1898.4	—	3–8	1543.5	1542	3–2
1879.0	—	2–7	—	1528	5–3
1859.2	—	1–6	—	1496	6–3
1811.1	1810	2–6	—	1493	3–1
1792.2	1793	1–5	—	1464	4–1
1775.1	—	0–4	1453	—	6–2
1730.2	—	1–4	1411	1410	6–1

gram was taken with an exposure of 3 hours. The continuous spectrum goes right upto the beginning of the Lyman H_2 bands starting at 1674 and can still be observed at 1550A. It is perfectly free from any emission lines. Spectrogram " b " is that of the light after passing through the afterglow. The usual γ- and δ-bands of NO and the fourth positive bands of CO observed by Knauss (1928) are clearly visible in emission but there is absolutely no trace of any absorption of nitrogen lines and we are definitely of the opinion that an increase of the length of the absorbing column would not bring out the looked for absorption lines, as in the present experiment the whole of the region of the strongest intensity in the afterglow was being utilized for absorption.

Attention may be drawn to the presence of the 4th positive bands of CO on our plates. No CO was introduced in the tube containing active nitrogen, as was done by Knauss. These bands must, therefore, be attributed to the combination of the traces of oxygen present as impurity with the carbon from greases, etc.

The list given above comprises of most of the bands of the fourth positive group of CO observed by Knauss and in addition gives a large number of bands not recorded by him. Knauss mentions that he experienced great difficulty in photographing these bands and as the intensity was very low the slit had to be kept very wide. In our experiments the bands come out easily and with short exposures. The accuracy of measurements for most of the bands is within 1A. The conclusion of Knauss that only those bands of CO are developed in the afterglow whose initial vibration states run from 1 to 6, is confirmed by observation on much larger number of bands recorded in the present work. This fixes up the excitation energy between 8.0 and 9.0 volts.

DISCUSSION

The absence of absorption lines of nitrogen in the ^2D and ^2P states does not support the theory of Cario and Kaplan mentioned before, nor the more recent speculation of Hebb and Sponer (1941). This result, however, appears to support the viewpoint of Saha and Mathur that the atoms occur only in the region of the discharge and the two excited atoms of nitrogen form an extremely stable state of the molecule which produces the L. R. afterglow on collision with neutral molecule. This view is essentially the same as proposed by Debeau, (1942) a short while ago, in consequence of some experiments on pressure changes in the afterglow.

In this experiment, electrodeless discharge in a bulb containing nitrogen at .5 m.m. pressure, produced active nitrogen in another connected bulb, and at the same time increased the pressure of the system to almost double its value before passing the discharge. On cooling a small portion of the active nitrogen bulb by liquid air, the intensity of the afterglow increased near the cooled portion and within thirty seconds completely disappeared from the entire bulb. The pressure of the system, however, was reduced to its value before the discharge. On removing the liquid air, the pressure regained its double value and the glow

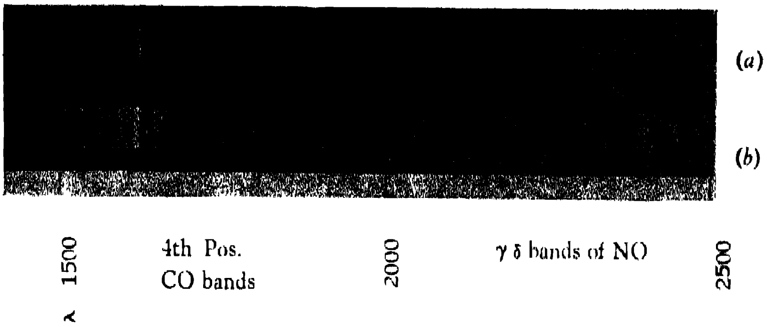
(a)
(b)
λ 1500
4th Pos. CO bands
2000
γ δ bands of NO
2500

reappeared first at the cooled portion and subsequently filling the bulb. The large pressure changes have been ascribed to the complete dissociation of nitrogen molecules. The products of dissociation consist of atoms in the normal state possessing energy equal to 7.35 volts and the excited metastable atoms in the ^2D state. The recombination of these atoms forms a collision complex loaded with 9.8 volts energy. This complex on colliding with neutral nitrogen molecules raises them to certain levels of B $^3\Pi$ state, which give rise to the afterglow. To explain the effects of liquid air he assumes that the life of these complex molecules increases with decrease of temperature, a corresponding decrease occurs in the number of atoms and causes the large reduction of pressure observed. The increased concentration of (NN) complex at the cooled surface is responsible for the increased intensity of the glow, which soon disappears due to the scarcity of more atoms to form the collision complex. The reverse process occurs on removing the liquid air.

This interesting experiment of the freezing out of the active component of the afterglow supports the recent hypothesis of Saha and Mathur (1936). The (NN) complex of Debeau is really identical with the proposed "some stable state of molecule loaded with an energy content of 9.8 volts" of Saha and Mathur. This "extremely stable molecule" or the (NN) collision complex loaded with about 10 volts energy, having a long life time, persists in the afterglow space, collides with neutral nitrogen molecules giving rise to the active nitrogen phenomenon. In our experiments with the Lewis-Rayleigh glow the excitation of a large number of CO bands of the fourth positive group, and γ and δ bands of NO, clearly showed the activity of the afterglow. But the non-appearance of any emission or absorption lines of atomic nitrogen, in our plates definitely proves the absence of ^2D, ^2P atoms in the afterglow. In view of this spectroscopic evidence against the atomic hypothesis, we conclude that the afterglow phenomenon of Lewis-Rayleigh is primarily due to the activity of some unknown molecular state of nitrogen. This would also appear to be supported by the experiments of Kneser recently confirmed by Lord Rayleigh (1940b) that a definite increase in the luminosity of this afterglow is obtained by the introduction of neutral nitrogen molecules.

It may be that under the conditions for the excitation of forbidden lines in the Auroral glow of Kaplan this particular molecular state predissociates to form the required excited atoms. But of course no evidence for or against such a supposition is provided by the present experiments. That atoms are present in the region of the discharge does not lead us very far, because they must be present even without the formation of active nitrogen. The chief problem, therefore, from the point of view of the phenomenon of active nitrogen is the identification of the stable molecular state of Saha and Mathur or the molecular complex of Debeau.

The authors are very thankful to Dr. P. K. Kichlu for his helpful discussions and advice which was always freely available during the course of these experiments. We take this opportunity of expressing our indedtedness to Prof. J. B. Seth for his kind interest and encouragement in our work.

GOVERNMENT COLLEGE,
LAHORE.

REFERENCES

Birge, 1924, *Nature*, **114**, 642.
Cario and Kaplan, 1929, *Z. f. Phys.*, **58**, 769.
Cario, 1934, *Z. f. Phys.*, **89**, 523.
Debeau, 1942, *Phys. Rev.*, **61**, 668.
Hebb and Sponer, 1941, *Phys. Rev.*, **59**, 925.
Kaplan, 1934, *Phys. Rev.*, **45**, 675.
Kaplan, 1936, *Phys. Rev.*, **49**, 67.
Kaplan, 1937, *Phys. Rev.*, **51**, 143.
Kaplan, 1939, *Phys. Rev.*, **56**, 558.
Kaplan and Rubens, 1940, *Phys. Rev.*, **58**, 188.
Kichlu and Acharya, 1929, *Proc. Roy. Soc.*, **123A**, 168.
Knauss, 1928, *Phys. Rev.*, **32**, 417.
Lewis, 1900, *Astrophys. J.*, **12**, 8.
Lewis, 1904, *Astrophys. J.*, **20**, 49.
Okubo and Hamada, 1933a, *Phil. Mag.*, **15**, 103; 1933b, *Astrophys. J.*, **77**, 130.
Rayleigh, 1935, *Proc. Roy. Soc.*, **151A**, 567.
Rayleigh, 1940a *Proc. Roy. Soc.*, **176A**, 1; 1940b, *Proc. Roy. Soc.*, **176A**, 16.
Saha and Mathur, 1936, *Proc. Nat. Acad. Sc.*, **6**, 120.
Saha and Sur, 1924, *Phil. Mag.*, **48**, 421.
Sponer, 1925, *Z. f. Phys.*, **34**, 622.
Strutt, 1911a, *Proc. Roy. Soc.*, **85A**, 219.
Strutt, 1911b, *Proc. Roy. Soc.*, **86A**, 56, 105, 262.
Strutt, 1912, *Proc. Roy. Soc.*, **87A**, 179.
Vegard, 1930, *Skrifter utgitt av Det Norske Videnskaps Akad.* i, *Oslo*, **2**, 24.
Vegard, 1933, *Nature*, **132**, 682.
Wrede, 1929, *Z. f. Phys.*, **54**, 53.

9

ELECTRICAL PROPERTIES OF INDIAN MICA

I—POWER FACTOR

By S. DATTA, J. SEN GUPTA

AND

P. C. MAHANTI

(*Received for publication, November 24, 1942*)

ABSTRACT. In this paper, the results of measurements of power factor of a large number of samples of mica of different qualities available in different parts of India are reported and their suitability as electrical insulants in electrical industry is discussed.

INTRODUCTION

Mica occupies a unique position as an electrical insulant amongst the raw materials for the manufacture of electrical apparatus. Owing to many desirable physical and chemical properties which it possesses, its superiority over other solid dielectrics is but little doubted. In fact, mica, for its exceptional insulating properties, is considered an indispensable element for the growth of electrical industry, especially when a flexible insulating medium to sustain very high electrical, mechanical and thermal stresses is necessary, although there are limitations to the size of pieces in which it is available.

This valuable electrical insulation is a crystalline mineral, which occurs in various forms and is very widely dispersed throughout the various terrestrial strata. But it is relatively in few localities that the mica used in electrical industry is obtained in sufficiently large dimensions and quantities to be of any commercial importance. Such localities lie in India, Canada, the United States, Guatemala, Argentina, Brazil, Madagascar, Tanganyika, South Africa, Russia, Northern Australia and Norway. But amongst these countries, India is the greatest producer of good quality sheet mica and at present provides more than 80 per cent of the world's demand of this important and unique mineral. With the growing enterprise for the manufacture of electrical apparatus in India, it is realised that the electrical properties of mica available in the different localities of this vast country should be studied with a view to ascertaining their suitability for different service requirements.

It is proposed to study in a series of investigations those electrical properties, *viz.*, power factor, dielectric constant (or permitivity), dielectric strength and resistivity, which are of importance to the electrical industry. It is also interesting to enquire how these properties are influenced by variations of temperature, humidity and frequency. Much work has, however, been done in the past by a large number of foreign workers in this direction. The results of the early investigators show wide variations from one another due to many experimental difficulties. But the recent works of Dannatt and Goodall (1930), of Lewis, Hall and Caldwal (1931), of Hartshorn and Ruston (1939), and of Hackett and Thomas (1941), are very reliable and supply us with much useful information regarding these properties of mica in general. Little attempts have, however, been made to carry out a comparison of the properties of different kinds of mica produced in different parts of India. Such information is expected to be of great importance to the development of electrical industries in this country. In the present paper are reported the results of measurements of power factor of Indian mica of different kinds available through the Geological Survey of India.

THE MICA OF ELECTRICAL INDUSTRY

To the mineralogists, the following eight different varieties of mica are so far known. They are—

(1) Muscovite or potassium mica,
(2) Paragonite or sodium mica,
(3) Zinwaldite or lithium-iron mica,
(4) Lepidolite or lithium mica,
(5) Phlogopite or magnesium mica,
(6) Biotite or magnesium-iron mica,
(7) Lepidomelane or ferric-iron mica,
(8) Roscoelite or vanadium mica.

These different varieties are classified into two principal groups, namely, the granitic group and the pyroxenic group, according to the nature of their geological formation. The first four varieties belong to the granitic group while the last four, to the pyroxenic group. The members of each group are different in chemical composition but they may, in general, be regarded as orthosilicates of aluminium with alkali metals (potassium, sodium or lithium), magnesium, iron and fluorine present in varying amounts. They are characterised by perfect basal cleavage, yielding readily very thin, strong and flexible splittings. Amongst these varieties, only the muscovite and the phlogopite mica find applications as electrical insulants and represent, therefore, the mica of electrical industry. They are available in abundance and in suitable sizes for commercial purposes.

Of the world's known deposits of mica, muscovite occurs in a larger number of countries than phlogopite. In fact, commercially important deposits of muscovite mica are found in India, United States, Russia, Norway, Argentina, Brazil, Tanganyika and Guatemala, while those of phlogopite mica only in Canada and Madagascar. There are, however, many other countries in which either of these two varieties or both are found to occur but they do not hold out any commercial prospect.

The approximate chemical formula of muscovite is given as $KH_2Al_3(SiO_4)_3$ while that of phlogopite as $KH(MgF)_3.Mg_3Al(SiO_4)_3$. Besides being almost chemically inert, these two varieties of mica possess many useful mechanical properties, such as a high degree of flexibility, elasticity, toughness, hardness and ability to withstand heat, for which they are often preferred to other solid dielectrics for use in electrical industry. They have, however, important differences, which greatly affect their suitability for particular conditions of service. In fact, phlogopite is distinctly inferior to muscovite as regards rigidity, hardness, toughness and elasticity and does not also split so readily. But it is generally more flexible than muscovite and can withstand higher temperatures. The surface of individual splittings of muscovite is smooth whereas the splittings of phlogopite have a fine crinkled surface, which is useful for certain purposes. But muscovite mica, because of its superior electrical and many mechanical properties, is more in demand than phlogopite in electrical industry.

Almost all the mica deposits in India belong to the muscovite variety with biotite in frequent association with it, the solitary exception so far known, being a small occurrence of phlogopite in the State of Travancore in Madras. The economic selection of the correct type of Indian mica for specific engineering purposes requires, however, a knowledge of their occurrence and classification, besides an acquaintance with their electrical properties.

OCCURRENCE OF MICA IN INDIA

There are many localities in India where muscovite mica occurs in the granitic pegmatites associated with mica schists. Bihar, Madras and Rajputana are at present the three important mica-producing centres. Amongst them, Bihar is the largest and produces about more than 75 per cent of the total production of mica in India. Madras comes next in importance while the mica deposits in Rajputana have only recently been commercially exploited. In addition to these three principal centres of mica deposits occurrences of mica have also been recorded in other parts of India.

The important mica centres in Bihar lie in the districts of Hazaribagh, Gaya and Monghyr. Hazaribagh contains the best mica reserve in India. Kodarma in this district is the largest centre of block mica while Giridih claims to be the largest centre for the finest class of mica splittings. Mica deposits in Manbhum and Bhagalpur districts have been of late commercially exploited. There are also occurrences of mica in Singhbhum, Palamau and Santal Parganas.

It may be mentioned here that the present Bihar mica field was included within the province of Bengal till 1912. Mica produced in this belt was therefore called and in fact is still known commercially as Bengal mica. At present Bengal proper does not produce any mica of commercial value, only a scanty occurrence of it having been recorded in the district of Bankura some years ago.

The chief mica deposits in Madras occur in the district of Nellore. There are a large number of mica mines in this area. Deposits in other districts, *viz.*, Nilgiris, Coimbatore and Malabar, are not commercially very important. Mica occurs also in the States of Travancore and Mysore. The most important centre of mica mining in Travancore is Eraniel. Travancore mica is principally phlogopite. Mica-bearing rocks in Mysore lie in the districts of Hassan, Mysore and Sringeri Jahgir. An occurrence of mica is also recorded in Coorg.

The third important mica deposit in India occurs in Rajputana in Central India. The major part of this deposit falls within the British territory of Ajmere-Merwara. There are however many States in Rajputana, namely, Jaipur, Tonk, Kishengarh, Sirohi, Udaipur, Shahpura and Jodhpur, where deposits of good quality mica have been found and in some cases commercially exploited. In addition to Rajputana, there are a few other States in Central India, such as Tehri, Gwalior, Jhabua, Rewah and Jashpur, where occurrences of mica have been also reported.

Mica deposits in the Central Provinces occur in the districts of Balaghat and Bilashpur, and also in Nandgaon and Bastar States. But they do not appear promising commercially. The Patiala State and the Kangra district in the Punjab as well as Garhwal in the United Provinces contain also good deposits of mica. In the newly-formed province of Orissa, occurrences of mica have been found in the districts of Sambalpur and Ganjam and also in the States of Mayurbhanj, Bamra, Ganpur and Bonai.

It is next of importance to enquire into the classification of the mica produced in the aforesaid localities.

CLASSIFICATION OF INDIAN MICA

Indian mica may in general be designated after the name of the province or locality of its occurrence. It is however usual to classify the muscovite mica, which is India's principal production, into two main types according to its colour, namely, ruby muscovite and green muscovite. The colour of ruby muscovite varies usually from light brownish-red in thin splittings to dark ruby-red in thick plates. Green muscovite varies from green to greenish-brown and sometimes to dark in very thick plates. Besides these two types, white and brown muscovite micas are also found in certain localities. Clear muscovite mica of any kind is, however, colourless in very thin splittings. The special feature of Bihar mica is its characteristic ruby colour. Green, brown and white micas are also occasionally found in Bihar. Madras mica is characteristically of the green muscovite type with only one exception, namely, that of Kalichedu mine, where pale ruby type is found. Rajputana mica belongs to both ruby and green types.

According to quality, each type of muscovite mica may be further subdivided into various kinds, such as clear, stained, spotted, slightly stained, heavily stained, slightly spotted, heavily spotted, stained and spotted, etc., depending upon the presence of impurities and inclusion in it. This method of classification is also adopted in trade.

In the present investigation different samples of mica of different kinds, which could be secured from different localities, have been tested for their power factor, whose knowledge is of fundamental importance for their use in electrical industry.

POWER FACTOR

It is well known that a perfect dielectric has only one electrical property, namely, that of specific inductive capacity or permitivity. When a sinusoidal voltage is impressed, the current that flows through it, leads the voltage in phase by $\pi/2$ radians. But in none of the solid dielectrics this ideal phase relationship between their current and voltage is satisfied. In fact, the phase difference between them is found to be slightly less than $\pi/2$. This defect from the ideal phase relationship is known as the "loss angle" of a dielectric while the sine of this angle gives a measure of its power factor. Thus if the loss angle of the dielectric is denoted by δ, its power factor is given by sin δ. When δ is very small, sin δ may also be replaced by tan δ. A knowledge of the power factor gives at once an idea of the power loss in the dielectric. The larger the value of power factor, the greater is the magnitude of the dielectric loss. Hence the importance of power factor measurements of dielectrics for ascertaining their usefulness in electrical industry is evident.

The power factor or the dielectric loss of mica, available in different parts of the world, has been the subject of a very large number of investigations. As early as 1912 Symons Walker (1912) made an attempt to estimate its value for different kinds of mica. Since then the experimental technique and methods of its measurement have been much improved and very reliable data of its value are available. Amongst the several investigators, Dye and Hartshorn (1924) estimated the power factor of the muscovite variety of Indian mica known as Bengal ruby, Madras green and Madras brown micas of different qualities, namely, clear, stained and spotted. But they used a method which does not admit of great accuracy. Using a Schering bridge, Dannatt and Goodall (1930) obtained very accurate data of power factor of ruby and green varieties of clear muscovite mica as well as of amber mica and studied the effects of temperature, stress and frequency on their power factor over a range covering the working conditions met with in electrical engineering practice. Unfortunately, these authors do not explicitly mention the geographical origin of the samples of mica tested by them. But it is very probable that some of them were taken from India. Lewis, Hall and Caldwell (1931) carried out power factor test on a large number of samples of micas, fairly representative of the major sources of the world's supply of mica. A few samples of clear and stained muscovite micas from India were also included in their list. The method used by these authors for evaluating the value of power factor was similar in principle to that employed by Dye and Hartshorn. Very recently Hartshorn and Rushton (1939), have investigated the power losses in mica subjected to the action of an alternating voltage at frequencies 50 to 4,000 cycles per second. The variations of the losses with moisture content, temperature, frequency, voltage and thickness have been also studied in detail in the case of typical samples of clear ruby mica.

From above it is evident that an extensive study of the power factor of mica available in different localities in India, which is the world's largest source of mica supply, is still wanting. To obtain the data of power factor within reasonable accuracy, a proper choice of the method of measurement is essential in addition to the careful preparation of the test condenser.

METHOD OF MEASUREMENT

A condenser is formed with the dielectric under test as the medium between its electrodes and its power factor is then evaluated. Several methods have been devised for the purpose. Earlier workers used wattmeter methods which suffered from errors inherent in such deflectional methods. They were not suitable for measurements at high voltages and the range of frequencies at which such instruments could be used was also very limited. Later on, several investigators calculated the value of power factor from measurements of the capacitance and the equivalent shunt or series resistance of the test condenser at a known frequency by using several bridge methods. Although the capacitance could be measured with considerable precision, there was great uncertainty in determining the equivalent shunt or series resistance because of the errors due to residuals in a bridge network. To avoid these errors, a resonance-capacitance method has also been used by a number of workers. Very recently, Hartshorn and Ward (1936) have devised a novel and ingenious method for the measurement of power factor of insulating materials over a wide range of radio-frequencies. This method employs capacitance-variation in a tuned circuit with a thermionic voltmeter as a detector of resonance. A cylindrical condenser of very small range of capacity whose variation follows a simple linear law is used to secure sharpness of resonance. Power factor of the test condenser and hence of the insulating material is obtained as a ratio of two capacitance readings. Thus frequency is not involved in the calculation of power factor. It is this property which enables the method to be employed over a wide range of frequencies. The errors due to residual inductance and resistance even at the highest frequency are eliminated by a careful design of the apparatus and by following a careful procedure in making the measurements.

A simple but a very accurate bridge method of measuring power factor when a precision condenser of negligible or known dielectric loss is available is that devised by Schering in 1920. Since then it has been considerably modified by several investigators to use it over wide ranges of voltage and frequency but is still known as the Schering bridge. In fact, it is used widely at present for accurate measurements of power factor. Like all bridge methods, it consists essentially of a Wheatstone network. The source of e.m f. is an alternating one either at power or any desired higher frequency. The nature of detector employed depends upon the frequency at which measurement is to be made, Usually, a vibration galvanometer is used directly at power frequency while a headphone at higher frequencies up to about 1000 cycles per second. Cathode-ray and heterodyne null detectors are employed at still higher frequencies and are more sensitive null detectors than others. The electrostatic screening and the Wagner-earthing are the two notable features of the Schering bridge. The former shields the bridge from the influence of external electrostatic fields while the latter eliminates the errors due to electrostatic coupling between various arms of the bridge and due to earth capacities of the various parts of the apparatus.

Many commercial forms of the modified Schering bridge are at present available. One such commercial bridge manufactured by Messrs. British Physical Laboratories, Ltd., London, which claims a high degree of precision for capacitance and power factor measurements, has been used in the present investigation.

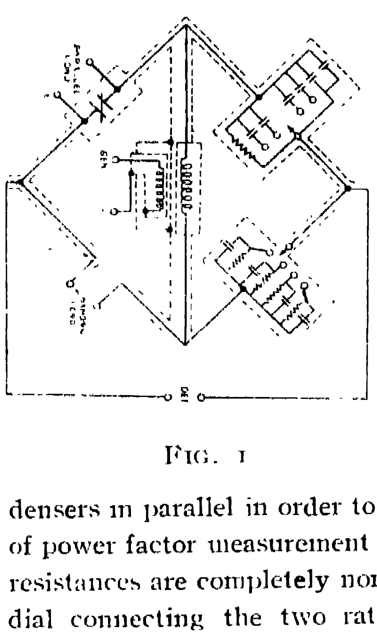

FIG. 1

The general arrangement of the bridge is shown in Fig. 1. The ratio arm across which the power factor condenser is connected has a value of 30,000 ohms. The other ratio arm consists of four independent resistance units of values 30,000, 3,000, 300 and 30 ohms. These resistances have suitable mica condensers in parallel in order to give a constant value of RC so that the accuracy of power factor measurement may be obtained over the entire range. All the resistances are completely non-inductive and have an accuracy of 0.01%. The dial connecting the two ratio arms indicates multiplying factors of values 1, 10, 100 and 1000. A high-precision variable air condenser which is employed as a standard of capacity forms one of the two remaining bridge arms. This condenser is designed to give a constant power factor with capacity and hence it has a constant loss with frequency. Its dial consists of a worm drive having no back-lash and its scale is direct reading in micro-microFarads from 0 to 1140. Using the multiplying factors, capacities up to 1.14 F can be measured in four ranges. The capacity dial is accurate within ±0.1%. The power factor standard consists of a variable condenser having a logarithmic change of capacity with the angle of rotation. Its dial is also direct reading in % from 0 to 0.06 with an accuracy of ±0.05%. The logarithmic characteristic of the scale enables to obtain good reading near the zero point. The bridge can be used on 50 to 10,000 cycles frequency range. The calibration of the power factor dials corresponds to one kilo-cycle.

Supply to the bridge is taken through a transformer from a beat frequency oscillator fed from an A.C. supply of 220 V. at 50 cycles and capable of giving a frequency range of 25 to 10,000 cycles per second within an accuracy of ±1%.

The balance indicator is a General Radio cathode-ray null detector of the visual type which can be used with bridges operating at any frequency between 25 cycles and 20 kilo-cycles. It employs a tuned degenerative amplifier which is entirely free from any electromagnetic or electrostatic pick up and does not itself radiate any appreciable electromagnetic field. One of its advantages is its ability to indicate, separately, the effect of adjusting the resistive or reactive controls of the bridge. It indicates also whether one of these controls, selected as desired, is off-balance in a positive or a negative direction. The bridge output is applied to the vertical deflecting plates of the cathode-ray tube through the amplifier while the bridge generator voltage is applied to its horizontal plates through an adjustable phase-shifting network. An elliptical pattern is produced on the screen when the bridge is out of balance. But on balancing, this is reduced to a horizontal straight line. The observable sensitivity of the detector is about 200-300 microvolts at 1000 cycles.

As indicated by dotted lines in Fig. 1, sufficient care has been taken to shield completely each arm of the bridge including the condensers, resistances, connecting leads, etc. The two windings of the transformer are electrostatically shielded from one another while the transformer itself is contained in a cast-iron box which gives complete magnetic shielding against external fields.

PREPARATION OF TEST CONDENSER

It has been mentioned in the previous section that for ascertaining the power factor of a dielectric, a test condenser is prepared by inserting the sample between two electrodes. But the value of power factor is liable to be greatly affected by the nature of such electrodes because of the contact resistance and capacitance of measurable amounts that exist in many cases. A proper choice of electrodes which would make intimate contact with the test sample is, therefore, very essential.

A considerable amount of information regarding the properties of electrode contacts and their effects on the measurements of dielectric properties are now available. Such information obtained previous to 1924 was summarised by Hartshorn in 1926. Churcher (1929) and his co-workers on behalf of the Electrical Research Association undertook a detailed investigation into contact effects between electrodes and dielectrics and recommended electrodes of mercury or of graphite (in the form of Aquadag) backed with metal plates for obtaining best results. It was also found that in certain cases graphite backed with mercury gave better contact than that obtained with mercury alone. Later on, Hartshorn and Ward at the National Physical Laboratory as well as Sharpe and O'Kane at the Applied Electricity Laboratory of Liverpool University found independently that although the results obtained in the above investigation were satisfactory for measurements at power frequencies, errors in measurements at higher frequencies could not be explained on the basis of the then knowledge of electrode contact. This led them to undertake a further investigation into the subject and they published their results (Hartshorn, Ward, Sharpe and O'Kane, 1934) jointly in 1934. They are of opinion that for general purposes mercury electrodes are the most satisfactory for measurements of permitivity and power factor of insulating materials in sheet form, although a film of graphite between mercury and test sample may improve the contact as previously noted by Churcher and his co-workers. They have further found that thin tin-foil applied with a trace of vaseline as an adhesive is a good substitute for mercury. Graphite electrodes backed with metal plates are easy to apply but should be employed with sufficient care at audio frequencies and not at all at radio frequencies.

For measurements of permitivity and power factor of mica, several of the early investigators prepared the test condenser by simply pressing two sheets of tin foil into contact with the sample, one on either side of it, without the use of any adhesive. There was, therefore, much uncertainty in securing intimate contact between the sample and the electrodes. Others used electrodes of mercury. Unless special precautions are taken, air bubbles are apt to form on the surface of the sample and so vitiate results. It may be mentioned here that the usual method of floating the test specimen on mercury with an upper mercury electrode is impracticable in the case of mica because of the thinness and flexibility of the samples. Another method consisted in inserting the sample into the gap of a parallel-plate air condenser of known dimensions. This is also not free from many serious objections. Dye and Hartshorn (1924) used both the air gap and the mercury electrode methods. In the latter case, the mercury electrodes were contained in ebonite dams and found to be very satisfactory. Dannatt and Goodall (1930) employed electrodes of mercury as well as of graphite in the form of Aquadag. They found that much of the trouble due to uncertainty of contact between the sample and the electrodes was due to a film of contamination present on the surface of mica specimen. Considerable improvement was effected by washing the surfaces with methylated ether just before the application of electrodes. In the case of graphite electrodes this method of treatment gave very satisfactory results. But for mercury electrodes, more elaborate precautions were necessary in order to obtain consistent results. Perfectly clean mercury had to be used and a somewhat tedious routine of washing surfaces, first with methylated spirit and then with methylated ether and finally drying them at 30°-40°C, was evolved. In the opinion of these authors, careful use of graphite electrodes gives accurate and consistent results. Lewis and his co-workers. (Lewis Hall and Caldwell, 1931) used tin foils as electrodes and linseed oil as an adhesive.

In preparing the test condenser in the present investigation due considerations were given to the fact that, since a large number of samples had to be tested, the electrodes should be so chosen that they would admit of easy manipulation without sacrificing accuracy. From this point of view it was decided to use thin tin foils as electrodes with a trace of linseed oil as an adhesive. Extreme care was taken to prepare a test-piece before applying the electrodes to it. From each block of a given sample of mica under test, several thin pieces approximately 2 cm. by 1 cm., were cut or split. They were then carefully examined and any loose layer, if present, was removed from them. The average thickness of each piece was measured with the help of a dial gauge. To minimise the effect of contact resistance, pieces of thickness less than 2 mils were rejected. Before fixing the electrodes the surfaces of each piece were first carefully cleaned with methylated spirit and linseed oil spread over them. With a clean and dry cloth, the oil was wiped out from each face. The slight trace of oil that still remained over the faces helped the thin tin foils to adhere to them. Thus the presence of any air pocket between the surfaces of the test piece and the electrodes was avoided. A somswhat similar process was adopted by Lewis, Hall and Caldwell, who found that the effect of introducing two films of oil of unknown thickness into the test condenser is not very appreciable on the values of power factor.

EXPERIMENTAL PROCEDURE

The method of substitution was employed for measurements which were made at the room temperature varying from about 30°C to 36°C on different days during the period of investigation. A standard air condenser was connected to the unknown or fourth arm of the bridge. The ratio of the resistances in the ratio arms was kept fixed at a definite value throughout the operations. Balance was obtained once with the bridge standard condenser alone in the third arm and then with the test condenser connected across it. It is well known that under the above conditions of balance, we have,

firstly, $C/C_s = R_2/R_1$ ... (1)

and $\phi - \phi_s = \phi_2 - \phi_1,$ ... (2)

and secondly, $C/C'_s + C_T = R_2/R_1$ ... (3)

and $\phi - \phi_T = \phi'_2 - \phi_1,$ ... (4)

where C and ϕ = capacity and power factor of the standard air condenser respectively ;

C_s and C'_s = capacity of the bridge standard condenser before and after substitution, respectively ;

C_T = capacity of the test condenser ;

ϕ_s = constant power factor of the bridge standard condenser ;

ϕ_T = power factor of the test condenser ;

$\phi_2 - \phi_1$ and $\phi'_2 - \phi_1$ = difference of power factor of the balancing arms of the bridge, before and after substitution, respectively ;

and R_2/R_1 = ratio of resistances in the ratio arms of the bridge.

From equations (1) and (3) and from (2) and (4), we have

$$C_T = C_s - C'_s \qquad \ldots (5)$$

and $\phi_T - \phi_s = \phi_2 - \phi'_2$ ... (6)

But assuming ϕ_s to be negligible in comparison to ϕ_T, we get

$$\phi_T = \phi_2 - \phi'_2 . \qquad \ldots (7)$$

It is evident from equations (5) and (7) that the capacity and power factor of the test condenser can be obtained directly from the difference of capacity and power factor dial readings of the bridge before and after substitution.

In actual practice, the ratio of the resistances in the ratio arms of the bridge was kept fixed at unity and the standard air condenser was given a suitable value which was kept unaltered during the two operations. Hence C and ϕ were maintained also constant. Balance under each condition was obtained by adjusting the bridge standard condenser as well as the power factor standard condenser at the maximum input of the bridge and at the maximum gain of the detector. After each balance, the capacity and power factor dial readings were noted.

From each sample of mica, several test condensers were prepared as described already and the values of their factor were measured on different days. The power factor of each test condenser was found to be substantially constant. The slight variations, wherever noticed, may be attributed to variations in the room temperature and atmospheric humidity. Incidentally, it may be mentioned here that the effect of humidity on power factor while considered to be too small by Dannatt and Goodall (1930) was thought to be of appreciable magnitude by Hartshorn and Ruston (1939). In the present measurements, we have not, however, made any careful study to ascertain any correlation between power factor and humidity but hope to undertake this investigation in future.

A few test readings were also taken with the bridge in order to check the experimental accuracy of the measuring system. We know that if r is the small effective series resistance in the condenser, the power factor is given by $r\omega c$. Using a standard condenser and non-inductive resistances of known values, the change in power factor could thus be calculated very readily. This change was also ascertained from the difference of the power factor dial readings of the bridge. The deviation in each case was found to be within ±4.5%. This order of accuracy may be considered fairly tolerable in the present series of measurements which aim mainly at a comparative study of power factor of the different kinds of mica available in the different parts of this country. It may be mentioned further that the series resistances used with the standard condenser were assumed to be truly non-inductive. Presence of any inductance would, however, increase the effective capacity. But this effect, if present at all, can legitimately be overlooked at the frequency of one kilo-cycle per second. This is borne out by the observed data which are in all cases less than their calculated values. The presence of any series inductance effect would have influenced the observed values in the opposite sense. The effect due to the presence of self-capacity of non-inductive resistances is also negligible at the above frequency.

EXPERIMENTAL RESULTS

Tables I-IX contain the data of power factor of mica obtained from different parts of India. In Column 1 is given the designation adopted by the Geological Survey of India for each kind and quality of mica as well as the name of the

TABLE I
Bihar Mica
Bengal Ruby Mica

Designation and colour	Quality	Average thickness (in mils)	Number of samples tested	Power factor	
				Spread %	Average %
Ruby Red ...	Clear ...	4	6	0.0092—0.0106	0.0102
		6	6	0.0098—0.0110	0.0104
		8	6	0.0094--0.0112	0.0106
C—Red ...	Stained ...	4	6	0.0103—0.0238	0.0152
		6	6	0.0101—0.0259	0.0186
		8	8	0.0109—0.0257	0.0176
D—Red ...	Stained ...	5	6	0.0192—0.0300	0.0262
		7	9	0.0182—0.0319	0.0251
		9	7	0.0228—0.0267	0.0249
A—Red ...	Stained and slightly spotted.	4	7	0.0116—0.0192	0.0143
		6	8	0.0105—0.0205	0.0152
		8	10	0.0107—0.0210	0.0146
F—Red ...	Stained and slightly spotted.	4	7	0.0107—0.0203	0.0142
		6	8	0.0140—0.0185	0.0162
		8	7	0.0102—0.0232	0.0128

TABLE II
Madras Mica

Designation and colour	Quality	Average thickness (in mils)	Number of samples tested	Power factor	
				Spread %	Average %
Madras Green ...	Clear ...	4	6	0.0102—0.0122	0.0114
		6	6	0.0104—0.0124	0.0116
		8	6	0.0102—0.0126	0.0118
C—Green ...	Stained ...	5	6	0.0160—0.0313	0.0229
		7	6	0.0151—0.0316	0.0235
		9	7	0.0174—0.0300	0.0258
D—Green ...	Stained ...	5	8	0.0255—0.0384	0.0320
		7	8	0.0250—0.0400	0.0308
		9	6	0.0278—0.0341	0.0309
A—Green ...	Stained and slightly spotted	6	7	0.0232—0.0394	0.0288
		9	8	0.0203—0.0404	0.0274
		12	10	0.0189—0.0382	0.0307
F—Green ...	Stained and slightly spotted.	4	8	0.0112—0.0174	0.0137
		6	7	0.0120—0.0171	0.0146
		8	7	0.0112—0.0177	0.0158
M 177—Green (Palamani Mines, Nellore).	Stained and spotted.	3	5	0.0297—0.0357	0.0318
		5	6	0.0282—0.0362	0.0320
		7	6	0.0265—0.0366	0.0319
M 242—Green (Kandali Mine, Nellore).	Slightly stained with black metallic spots.	3	6	0.0141—0.0272	0.0202
		5	6	0.0152—0.0263	0.0200
		7	6	0.0134—0.0265	0.0194
M 236—Green (Kalichedu Mining Co., Nellore).	Stained and slightly spotted.	4	5	0.0174—0.0188	0.0183
		6	5	0.0135—0.0218	0.0191
		8	6	0.0132—0.0234	0.0182

TABLE III

Rajputana Mica

Designation and colour	Quality	Average thickness (in mils)	Number of samples tested	Power factor	
				Spread %	Average %
0.273—Green (Jaitaram district, Jaipur).	Slightly stained.	3	5	0.0143—0.0170	0.0170
		5	6	0.0147—0.0171	0.0165
		7	5	0.0153—0.0173	0.0167
6552—Green (Jaipur).	Stained with black metallic spots.	4	5	0.0192—0.0219	0.0205
		6	7	0.0175—0.0233	0.0208
		8	7	0.0159—0.0377	0.0227
N756—Green (Tehri, Central India).	Slightly stained with black metallic spots.	4	5	0.0183—0.0192	0.0186
		6	6	0.0181—0.0191	0.0185
		8	6	0.0178—0.0198	0.0187
K162—Green (Daulatapura, Kishengarh).	Stained with black metallic spots.	4	5	0.0189—0.0285	0.0220
		6	5	0.0190—0.0281	0.0225
		8	6	0.0177—0.0328	0.0234
L333—Red (Udaipur).	Stained ...	3	7	0.0151—0.0199	0.0174
		5	5	0.0153—0.0198	0.0172
		7	5	0.0158—0.0186	0.0171
N758—Red (Dudpura near Beawar).	Stained and slightly spotted.	3	5	0.0143—0.0247	0.0188
		5	5	0.0140—0.0280	0.0194
		7	5	0.0151—0.0244	0.0193
N759—Red (Shahpura).	Stained with metallic spots.	4	7	0.0172—0.0240	0.0208
		6	6	0.0166—0.0226	0.0205
		8	7	0.0163—0.0245	0.0206

TABLE IV

Travancore Mica

Designation and colour	Quality	Average thickness (in mils)	Number of samples tested	Power factor	
				Spread %	Average %
M 624—Red	Stained and spotted.	3	5	0.0278—0.0379	0.0329
		5	5	0.0283—0.0386	0.0342
		8	6	0.0202—0.0387	0.0318
L 999—Red (Tippermalai Mines).	Heavily stained and spotted.	3	5	0.0558—0.0886	0.0731
		5	7	0.0428—0.0884	0.0750
		7	7	0.0422—0.1010	0.0772
R 41—Red	Stained and heavily spotted.	3	5	0.0413—0.0833	0.0731
		4	6	0.0420—0.0962	0.0735
		6	6	0.0366—0.0956	0.0728
M 25—Red	Heavily stained (Phlogopite).	4	7	0.0496—0.1150	0.0800
		6	7	0.0494—0.1142	0.0813
		8	8	0.0522—0.1082	0.0829

TABLE V

Mysore Mica

Designation and colour	Quality	Average thickness (in mils)	Number of samples tested	Power factor	
				Spread %	Average %
M 620 —Green	Clear	3	6	0.0103—0.0164	0.0114
		4	6	0.0102—0.0177	0.0119
		5	8	0.0108—0.0181	0.0118

TABLE VI

Orissa Mica

Designation and colour	Quality	Average thickness (in mils)	Number of samples tested	Power factor	
				Spread %	Average %
M 894—Red (Sambalpur)	Stained	3	5	0.0142—0.0245	0.0197
		5	6	0.0136—0.0261	0.0205
		7	6	0.0132—0.0264	0.0207

TABLE VII

U. P. Mica

Designation and colour	Quality	Average thickness (in mils)	Number of samples tested	Power factor	
				Spread %	Average %
I 581—Green (Garhwal).	Clear	3	5	0.0307—0.0537	0.0421
		5	5	0.0387—0.0566	0.0473
		7	6	0.0245—0.0761	0.0429

TABLE VIII

Punjab Mica

Designation and colour	Quality	Average thickness (in mils)	Number of samples tested	Power factor	
				Spread %	Average %
I 306 —Red (North of Patiala)	Stained and slightly spotted.	4	8	0.0204—0.0386	0.9094
		6	8	0.0226—0.0365	0.2024
		8	10	0.0162—0.0553	0.0291

TABLE IX

Summary of Results

Source	Designation and colour	Kind or quality	Power factor	
			Average %	Spread %
Bihar	Bengal Ruby	Clear	0.0104	0.0092—0.0112
	C—Red	Stained	0.0173	0.0101—0.0259
	D—Red	Stained	0.0252	0.0182—0.0319
	A—Red	Stained & slightly spotted	0.0147	0.0105—0.0210
	F—Red	Stained & slightly spotted	0.0144	0.0102—0.0232
Madras	Muscovite Green.	Clear	0.0116	0.0102—0.0126
	C—Green	Stained	0.0241	0.0151—0.0316
	D—Green	Stained	0.0313	0.0250—0.0400
	A—Green	Stained & slightly spotted	0.0294	0.0189—0.0460
	F—Green	Stained & slightly spotted	0.0144	0.0112—0.0177
	M177—Green	Stained and spotted	0.0319	0.0265—0.0366
	M242—Green	Slightly stained with black metallic spots.	0.0198	0.0134—0.0272
	M236—Green	Stained & slightly spotted	0.0187	0.0132—0.0234
Rajputana	0273—Green	Slightly stained	0.0165	0.0143—0.0173
	N756—Green	Slightly stained with black metallic spots.	0.0186	0.0178—0.0198
	6552—Green	Stained with black metallic spots	0.0216	0.0159—0.0377
	K162—Green	Stained with black metallic spots	0.0227	0.0177—0.0328
	L333—Red	Stained	0.0172	0.0151—0.0190
	N758 Red	Stained and slightly spotted	0.0192	0.0140—0.0280
	N759 Red	Stained with metallic spots	0.0206	0.0163—0.0245
Travancore	M624—Red	Stained and spotted	0.0329	6.0202—0.0387
	R41—Red	Stained and heavily spotted	0.0732	0.0366—0.0962
	L999—Red	Heavily stained and spotted	0.0752	0.0422—0.1010
	M25—Red	Phlogopite, heavily stained	0.0815	0.0494—0.1150
Mysore	M620—Green	Clear	0.0118	0.0102—0.0181
Orissa	M894—Red	Stained	0.0203	0.0132—0.0264
U.P.	1581—Green	Clear	0.0440	0.0245—0.0761
Punjab	1306—Red	Stained and slightly spotted	0.0293	0.0162—0.0533

particular locality or mine of its occurrence contained within parentheses. It has not been possible to supply the latter information in every case. Column 2 gives the quality of each kind of mica tested. To carry out the test, the samples were first grouped into lots according to their thickness. The average thickness of the samples of a particular lot and the number of samples included in it, as well as the data of power factors spread and of average power factors of each such lot are given in columns 3, 4, 5 and 6 respectively. The power factor data have been expressed in percentage.

Finally, in Table IX are collected together for comparison the data of power factor obtained from measurements on the different samples, irrespective of their thickness, for each kind or quality of mica tested during the present investigation. It may be noted that excepting one quality of phlogophite mica obtained from Travancore, the others belong to the muscovite variety.

DISCUSSION

From Table IX, it is easily seen that the average power factor of clear muscovite mica, excepting that obtained from the United Provinces, is very small although the green variety of both Madras and Mysore has a slightly higher value than the ruby variety of Bihar, known popularly as the Bengal ruby mica. The clear 1581-green mica available at Garhwal in the United Provinces shows, however, a comparatively larger value of power factor, which is even greater than that of the stained and spotted mica samples of other provinces included in the present investigation. It may be noted here that the value of power factor of clear muscovite mica of the different grades or varieties seems to be of the right order of magnitude at the frequency of our measurements. Amongst the previous investigators, Lewis, Hall and Caldwell (1931) found the spread of power factor for clear Indian ruby mica to lie between 0.01 to 0.02%. Furthermore, Dannatt and Goodall (1930) have observed that although the power factor of the green variety is about three times as large as that of the ruby at the power frequency of 60 cycles per second, they have nevertheless nearly the same value at a frequency of 800 cycles per second. This latter observation is well supported by the present data.

It is difficult to compare the power factor values of the stained and spotted micas with those reported by other investigators since the power factor is known to be very much influenced by the amount of stain or spot present in the samples under test. It is also not known whether these investigators used micas of the same localities as used in the present measurements. Very likely, they did not. It is, however, found from present data that the power factor of muscovite mica, either stained, spotted, or both, is higher than that of clear mica as has been observed by several other investigators. The sample of phlogopite mica has a still higher value of power factor.

The uses to which virgin mica is put are well known. It is used to insulate small commutator segments, condensers, heating elements and miscellaneous punched parts and washers. The grade of mica suitable for condenser insulation varies according to the service for which the condenser is designed. For D.C. and general testing and standardising purposes, mica of particularly high insulation is preferred. For every high-voltage condensers, mica of the highest electric strength must be used, while, for high-frequency condensers, low-loss mica is to be selected.

Dannatt and Goodall (1930) have found that clear ruby mica possesses outstanding superiority over the green variety inasmuch as it has not only a small power factor but also small variation of power factor and capacitance with temperature as well as small change of power factor and permitivity with frequency. These properties mark it as an almost ideal material for the insulation of precision condensers and allied apparatus. The clear green mica has also exceptionally good insulating properties. In fact it is as good as ruby mica for high-quality commercial insulating material. The only point against its use in precision condenser is that its power factor varies, as has been noted already, with frequency and probably attains a steady value only at very high frequencies.

The stained and spotted micas which have been put to test in the present measurements show that the power loss in them is not very large and, in fact, it is fairly tolerable. They are, therefore, not unsuited for use in commercial condensers of the Dubiliar types for radio purposes where great precision is not warranted. A few condensers were actually constructed with some of these mica samples and put to service where they were found satisfactory throughout the year under varying conditions of temperature and atmospheric humidity. It is hoped that more definite conclusions, regarding the uses to which the stained and spotted micas available in many parts of India could be put, may be drawn after our study of their different electrical and physical properties is complete.

In conclusion, the authors gratefully acknowledge their indebtedness to Dr. C. S. Fox, Director, Geological Survey of India, for supplying practically all the mica-samples which have been put to test in the present investigation and also for his kind interest and suggestions. They also wish to acknowledge their thanks to Prof. P. N. Ghosh, Head of the Department of Applied Physics, Calcutta University, for allowing them all facilities to carry out the investigation and for his helpful discussions and to Mr. S. P. Chakravarti for his kind encouragement.

REFERENCES

Churcher, Dannatt and Dalgleish, 1929, *J.I.E.E.*, **67**, 271

Dannatt and Goodall, 1930, *J.I.E.E.*, **69**, 490

Dye and Hartshorn, 1924, *Proc. Phys. Soc.*, **37**, 42.

Hackett and Thomas, 1941, *J.I.E.E.*, **88**, *Part I*, 95

Hartshorn and Rushton, 1939, *E.R.A.*, *Report, Ref. L/T00*, **24**

Hartshorn and Ward, 1936, *J.I.E.E.*, **79**, 597

Hartshorn, Ward, Sharpe and O'Kane, 1934 *J.I.E.E.*, **75**, 730

Lewis, Hall and Caldwell, 1931, *B.S.J.R.*, **7**, 403.

Walker, 1912, *J.I.E.E.*, **48**, 671.

STRING UNDER INTERMITTENT IMPULSES AND EXPERIMENTAL VERIFICATION OF KAR'S THEORY OF INTERMITTENT ACTION

By H. G. MANE AND B. N. BISWAS

(Received for publication, Sept. 8, 194.)

ABSTRACT. Kar's theory of intermittent action as applied to bowed string by Biswas has been experimentally verified

The experiment consists of two parts :

(1) A string has been subjected to intermittent impulses at a point near one end by means of a toothed rubber wheel rotated by a motor, and the vibration recorded photographically by a Vibroscope It is observed that the trace on the photographic paper is a two-step Zig-zag

(2) Helmholtz's law of velocity of the bowed point has also been verified by photographically recording the vibration of the region struck by the wheel provided with a pin along its circumference fixed perpendicular to the plane of the wheel It is observed from the photo that the forward velocity of the region is equal to that of the wheel.

These two experiments therefore conclusively prove that the action of the bow and that of the toothed wheel are similar in nature

It was observed long ago by Helmholtz that when a string is bowed, not far from one end, the vibrations at any point can be represented by a simple two step zig-zag curve. He also showed that when the bow is moved perpendicularly on the string, the velocity of the bowed point in the upward direction is equal to that of the bow. He investigated the motion of the string by using a vibroscope and explained the action of the bow. Later on, Raman (1919) investigated the motion of the bowed string more exhaustively and was able to demonstrate the equality of the velocity of the bow with that of the bowed point. Kar's theory of intermittent action was applied to bowed string by Biswas who showed that if intermittent impulses of regular period be imparted to a string under tension, the motion of the string is the same as that given by Helmholtz. The present problem is therefore undertaken to verify experimentally the theory given by Biswas (1930). This theory clearly explains the action of the bow when it is moved perpendicularly across the string.

THE EXPERIMENTAL PORTION CONSISTS OF TWO PARTS

Part 1.—Intermittent impulses of regular period are imparted to the string under tension by using a toothed rubber wheel mounted on an axle which is held horizontally between two clamps. The wheel is set into rotation by means of a motor driven by a battery of constant e.m.f. The motion of any point of the string is recorded by using a vibroscope in the usual manner. It is observed that the trace of the motion on the photographic paper is a two step zig-zag curve.

Part 2.—The toothed wheel is provided with a pin along its circumference fixed perpendicularly to the plane of the wheel, rotated and allowed to strike the string. The simultaneous record of the motion of the wheel and that of the string is obtained photographically in the usual manner by means of the vibroscope.

INDEX OF PARTS OF THE APPARATUS USED

W—Rubber wheel.
S_1 and S_2—Wooden shutters.
M_1 and M_2—Metallic strips attached to the shutters S_1 and S_2.
S—Photographic slide.
C_1 and C_2—Clamps for holding the string.
T—Tension screw.
Q—Tilting screw
U—Wooden board to which the wheel is attached. It is hinged on one side and can be tilted by the screw Q.
L—Condensing lens.
A—Arc lamp.
M—Low horse power motor.
Rh—Rheostat.
Ws—Wooden stand for the wheel.
Is$_1$ and Is$_2$—Iron stands to which the clamps C_1 and C_2 are attached.
O_1 and O_2—Openings at the back of the vibroscope provided with black pieces of cloth.
Vs—Vibroscope stand.
V—Vibroscope.
P—Pan in which weights are placed.
B—Wooden board to which iron stands Is$_1$ and Is$_2$ are fixed.
R—Resistance for the arc lamp.
Wb—Wooden bar fixed at the top of the iron bars Is$_1$ and Is$_2$.
Wa—Pulley fixed to the axle.

* EXPERIMENTAL

Part 1

Method.—The string is held between two metallic jaws which are clamped to two iron bars Is$_1$ and Is$_2$ fixed to a wooden board B (Fig. 1). The vibroscope V fixed to a wooden stand Vs is placed just behind the string and parallel to it. The vibroscope is provided with two wooden shutters S_1 and S_2 which can be adjusted so as to form a very fine slit just behind a point of the string whose motion is to be recorded. A photographic slide S similar to the ordinary photographer's slide provided with two small metallic rollers at the bottom to minimise friction, runs between two grooves of the vibroscope. It is dragged along the grooves by a piece of string, one end of which is fixed to the slide. The string passes over a pulley and at the other end a pan P is attached to add weights.

---

* This part is carried out by Mr. H. G. Mane alone.

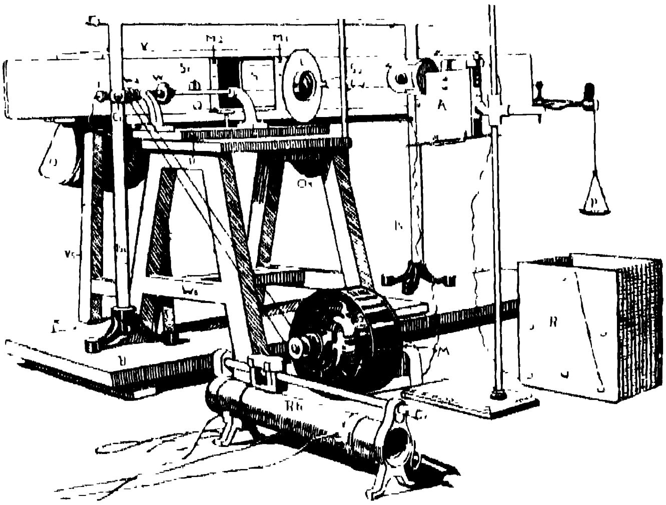

FIG. 1

The string is excited by a toothed rubber wheel W held between two metallic jaws. A small piece is first cut from a plane rubber sheet and is then cut on a lathe. The circumference is then divided into 32 equal parts (this number is found to be suitable with the material at hand) by means of a divider. The teeth are then cut by a razor blade. Great care must be taken while cutting the teeth as the length and the depth of each tooth must be the same. The teeth are then polished and any defect in them is removed by using a fine file.

The wheel is then mounted on an axle which is held horizontally between two clamps which are fixed to a wooden board. This board is hinged on one side to another wooden stand. At the unhinged edge there is a milled screw Q which is used for adjusting the pressure of the wheel on the string. The whole stand is then placed on the wooden board carrying the iron stands and the string.

To excite the string, the height of the string is adjusted and the clamps are fixed to the iron bars. The wheel is then fixed to the axle against the desired point of the string. To maintain the vibrations of the string, the speed and the pressure of the wheel are to be adjusted. The first is done by adjusting the current from the battery and the second by using the screw Q.

When the vibrations of the string are maintained, the shutters are arranged so as to form a very fine slit just behind the point whose motion is to be recorded.

The slit is illuminated by condensing the light from an arc lamp. The loaded photographic slide is then inserted into the vibroscope through the left hand opening, is opened inside the vibroscope and then released. The plate then runs through the grooves on account of the weights placed in the pan. In this way the motions of several points of the string are recorded photographically. The photographs are shown below :—

LENGTH OF THE STRING 60 CMS

Plate No.	Struck pt. distance from one end	Observed pt distance from the other end	Plate.
1	1/3	1/3	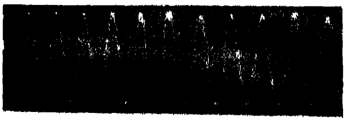
2	13 cms	1/3	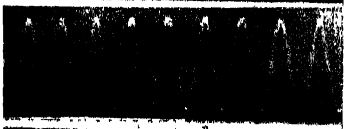
3	1/5	1/5	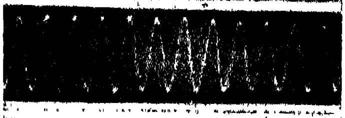
4	1/6	1/5	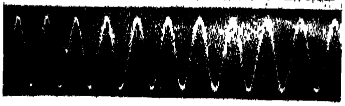
5	1/6	1/4	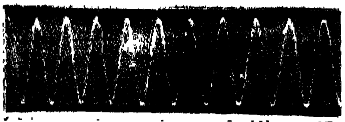
6	1/8	1/4	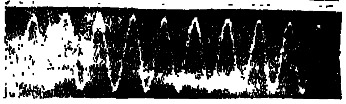

FIG. 2.

Part 2

To show the applicability of Helmholtz's law of velocity to the present case.

A thin pin is fixed to the rubber wheel against one of its teeth and perpendicular to the plane of the wheel. The wheel is then fixed to the axle against the desired point of the string. The shutters are adjusted to form a fine slit just near the wheel. The slit is illuminated by the arc lamp and the vibrations of the string are maintained as explained previously and the photograph of the point struck by the wheel is taken. In this way several photographs of the motion of the wheel and that of the corresponding points of the string are taken.

It is observed that the record of the motion of the pin and that of the motion of the string are coincident. The photographs are shown below :—

LENGTH OF THE STRING 60 CMS

Plate No.	Struck pt. distance from one end.	Plate
1	1/4	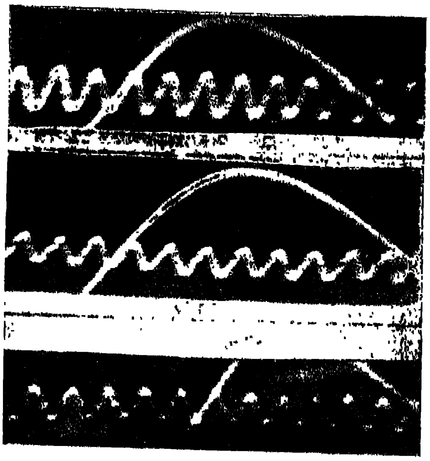
2	1/5	
3	1/6	

FIG. 3

CONCLUSION AND DISCUSSION

The photographs obtained in the two parts of the experimental portion show that Kar's theory of intermittent action as applied to the bowed string by Biswas is true. The action of the bow is similar to that of the wheel. When the wheel is rotating, the part of the string in contact with the wheel is carried along with the particular tooth in the forward direction, it then slips and begins to move in the downward direction till it is caught by the next tooth and the process is repeated. The investigations are being continued to solve other allied problems such as to find the relation between the upward and downward velocities and the position of the point of observation, etc.

Finally, we express our heartfelt thanks to Dr. Kar of Presidency College, Calcutta, for the kind interest he took in our investigations.

PHYSICAL LABORATORY,
RAJARAM COLLEGE, KOLHAPUR.

REFERENCES

Raman, C. V., 1914, *Ind. Assoc. for Cult. of Sc Bull.*, No. 11.
Also see Raman, C. V., 1918, *Indian Assoc. for Cult. of Sc. Bull.*, No. 15 (),
And Mitra, M. N., 1927, *Ind. J. Phys.*, Vol. 1, Part 3.
Biswas, B. N., 1930, *Jour. Ind. Math Soc.*, Vol. 18.

11

A NOTE ON THE ELEMENTARY THEORY OF THERMAL DIFFUSION

By R. N. RAI

AND

D. S. KOTHARI

(Received for publication, January 13, 1943)

ABSTRACT. An elementary derivation of the co-efficient of thermal diffusion and its change of sign with concentration is discussed. The results have been compared with the experimental results of Grew.

The phenomena of thermal diffusion was predicted independently by Enskog and Chapman about 20 years ago, but it did not attract much attention until the work of Clusius and Dickel (1938, 1939) which has made it the most effective method for the separation of isotopes. The convection currents set up in the Clusius-Dickel vertical column progressively build up, due to thermal diffusion, the separation of the constituents, and one is reminded in this connection of Linde's method of regenerative cooling by Joule-Thomson effect which, prior to Linde's work, was only of laboratory interest. It was supposed for a long time that, unlike the case of ordinary diffusion, no elementary theory of thermal diffusion was possible and hence the recent paper of Fürth (1942) discussing thermal diffusion from elementary considerations is of some interest. As Fürth has shown, the simple treatment brings out most of the essential features of Enskog-Chapman's analysis, and in this connection it is interesting to observe that the simple theory also provides an immediate explanation of the recent experiment of Grew (1942) on the change of sign of thermal diffusion factor for a neon-ammonia mixture.

Let us consider a binary mixture in which the concentration and temperature gradients are present only along one direction, say the z-axis. If n_1 and n_2 denote the concentration of the two types of molecules and T the temperature, all functions of z (n_1, n_2 will also be functions of time), then the pressure p will be

$$p = k(n_1 + n_2)T = \text{constant}. \qquad \dots \quad (1)$$

If Γ_1 and Γ_2 represent the net flow of molecules of types one and two respectively along the positive z-direction, then we have in the usual way

$$\Gamma_1 = -\Gamma_2 = -\frac{\lambda_1}{3}\frac{d}{dz}(c_1 n_1) + un_1 = \frac{\lambda_2}{3}\frac{d}{dz}(c_2 n_2) - un_2, \qquad \dots \quad (2)$$

where u is the velocity of mass motion, λ_1, λ_2 the mean free paths and c_1, c_2

the mean velocities of molecules of types one and two respectively. The mutual rate of diffusion q_{12} is defined as

$$q_{12}=\frac{\Gamma_1}{n_1}-\frac{\Gamma_2}{n_2}=\Gamma_1\left(\frac{1}{n_1}+\frac{1}{n_2}\right)=\frac{n_1+n_2}{n_1 n_2}\Gamma_1.$$

Substituting for Γ_1 and u from (2), using (1) and replacing n_1 and n_2 by the partial concentrations γ_1, γ_2 defined by

$$\gamma_1=\frac{n_1}{n_1+n_2},\ \gamma_2=\frac{n_2}{n_1+n_2},$$

we have $$q_{12}=-\frac{D}{\gamma_1\gamma_2}\left\{\frac{d\gamma_1}{dz}+k_T\frac{d(\log T)}{dz}\right\},$$

where $$D=\tfrac{1}{3}(\gamma_1\lambda_2 c_2+\gamma_2\lambda_1 c_1),$$

and $$k_T=\gamma_1\gamma_2\left\{\frac{\lambda_2 c_2-\lambda_1 c_1}{2(\gamma_1\lambda_2 c_2+\gamma_2\lambda_1 c_1)}\right\},$$

k_T is called the thermal diffusion ratio. Writing as usual

$$\frac{1}{\lambda_1}=\pi(n_1\sigma_1^2+n_2\sigma_{12}^2)\quad\text{and}\quad\frac{1}{\lambda_2}=\pi(n_2\sigma_2^2+n_1\sigma_{12}^2),$$

where σ_1 is the collision diameter for mutual collision between type-one molecules, σ_2 the same for type-two and σ_{12} the collision diameter for collision between type-one and type-two.

Thus we have $$k_T=\frac{\gamma_1\gamma_2}{2}\,\frac{a_1\gamma_1-a_2\gamma_2}{b_1\gamma_1^2+b_2\gamma_2^2+b_{12}\gamma_1\gamma_2}, \qquad \ldots (3)$$

where $$a_1=m_1^{\frac{1}{2}}\sigma_1^2-m_2^{\frac{1}{2}}\sigma_{12}^2,\quad a_2=m_2^{\frac{1}{2}}\sigma_2^2-m_1^{\frac{1}{2}}\sigma_{12}^2,$$

$$b_1=m_1^{\frac{1}{2}}\sigma_1^2,\qquad b_2=m_2^{\frac{1}{2}}\sigma_2^2,$$

and $$b_{12}=(m_1^{\frac{1}{2}}+m_2^{\frac{1}{2}})\sigma_{12}^2,$$

m_1, m_2 are the molecular masses of the two components.

Let us now assume that the two components differ from one another only to a small extent, *i.e.*, $m_1-m_2=\Delta m$, $\sigma_1-\sigma_2=\Delta\sigma$ and $\sigma_{12}-(\sigma_1+\sigma_2)/2=\Delta S$, then, we have to the first order

$$k_T=\frac{\gamma_1\gamma_2}{2}\left\{\frac{\Delta\sigma}{\sigma}+\frac{1}{2}\frac{\Delta m}{m}-2(\gamma_1-\gamma_2)\frac{\Delta S}{\sigma}\right\}. \qquad \ldots (4)$$

In the case of an isotropic mixture $\Delta\sigma=\Delta S=0$, and

$$k_T=0.5\,\gamma_1\gamma_2\frac{\Delta m}{2m}. \qquad \ldots (5)$$

This may be compared with the expression

$$k_T=0.35\,\gamma_1\gamma_2\frac{m_1-m_2}{m_1+m_2}=0.35\,\gamma_1\gamma_2\frac{\Delta m}{2m},$$

given by Furry, Clark-Jones and Onsager (1939).

Writing (4) in the form

$$k_t = \gamma_1(1-\gamma_1)\{a+b(1-2\gamma_1)\},$$
$$= b\gamma_1(1-\gamma_1)\{(1+q)-2\gamma_1\},$$

where $a=\frac{1}{2}\left(\frac{\Delta\sigma}{\sigma}+\frac{1}{2}\frac{\Delta m}{m}\right)$, $b=\frac{\Delta S}{\sigma}$, and $q=a/b$,

we notice that

(1) $k_t = 0$ for $\gamma_1=0$, $\gamma_1=1$, and $\gamma_1=\alpha_0=(1+q)/2$;

and (2) $\frac{dk_t}{d\gamma_1}=0$ for values of γ_1 given by

$$6\gamma_1^2-2(q+3)\gamma_1+(q+1)=0.$$

Denoting the two values of γ_1 by α_1 and α_2 we have

$$\alpha_1+\alpha_2=\frac{q+3}{3}=\frac{2(\alpha_0+1)}{3},\quad \alpha_1\alpha_2=\frac{q+1}{6}=\frac{\alpha_0}{3}, \qquad \dots \quad (6)$$

which gives $$\alpha_1=\frac{1+\alpha_0-\sqrt{1+\alpha_0+\alpha_0^2}}{3}=\frac{1+\alpha_0-x}{3},$$

and $$\alpha_2=\frac{1+\alpha_0+\sqrt{1-\alpha_0+\alpha_0^2}}{3}=\frac{1+\alpha_0+x}{3}, \qquad \dots \quad (7)$$

where $$x=\sqrt{1+\alpha_0+\alpha_0^2}\,.$$

Further, denoting by y_1 the value of k_t for $\gamma_1=\alpha_1$ and by y_2 the value corresponding to $\gamma_1=\alpha_2$, we have

$$y_1=\frac{2}{27}(1+\alpha_0-x)\,(2-\alpha_0+x)\,(2\alpha_0-1+x),$$

and $$y_2=\frac{2}{27}(1+\alpha_0+x)\,(2-\alpha_0-x)\,(2\alpha_0-1-x). \qquad \dots \quad (8)$$

We reproduce the experimental curve due to Grew[1] for the neon-ammonia mixture. From the curve we notice that $\alpha_0=0.75$, $\alpha_2=0.27$, $\alpha_0=0.86$ and, as is reasonable, assuming the ordinates to be proportional to k_t, we have

$$y_1/y_2=-5.2.$$

The simple theory given above requires that

$$\tfrac{1}{2}(\alpha_1+\alpha_2)=\tfrac{1}{3}+\alpha_1\alpha_2, \qquad \dots \quad (9)$$

$$\alpha_0=3\alpha_1\alpha_2, \qquad \dots \quad (10)$$

and $$\frac{y_1}{y_2}=\frac{(1+\alpha_0-x)\,(2-\alpha_1+x)\,(2\alpha_0-1+x)}{(1+\alpha_0+x)\,(2-\alpha_0-x)\,(2\alpha_0-1-x)}. \qquad \dots \quad (11)$$

Substituting Grew's values of α_1, α_2 (10) requires α_0 to be 0.74 whereas Grew's value is 0.75. Further, substituting the observed value of α_0 we obtain $y_1/y_2=-6.9$, whereas the observed value of the ratio is about -5.2.

---

[1] The value of the separation at the bottom of the figure is given by Grew to be -2.5. This is presumably -5

In connection with the above agreement, it must be remarked that the discussion given above is crude though extremely simple. For example, at some stages of the argument, the elastic model of the molecule is assumed, whereas in taking σ_{12} not equal to $(\sigma_1 + \sigma_2)/2$, we consider the force-field model. Again, in the case of the neon-ammonia mixture $\Delta\sigma/\sigma$ cannot really be regarded as a small quantity. However, it seems that such defects must be present in any elementary treatment of thermal diffusion.

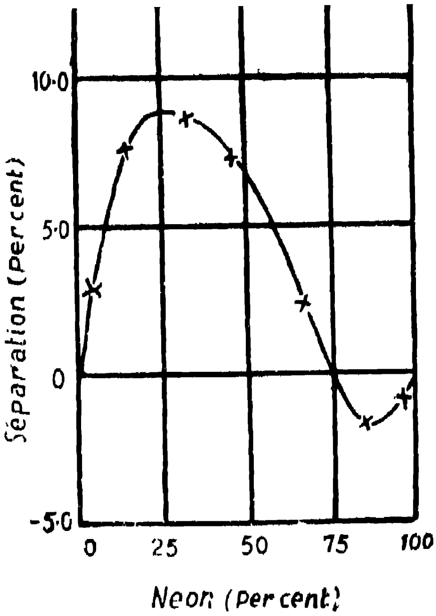

FIG. 1

It will be seen that for the existence of a reversal of sign of k_T with concentration it is necessary that $0 < (1+q)/2 < 1$, *i.e.*, *a* must be numerically less than *b*.

In the case of the neon-ammonia mixture, the value of *a* is contributed almost entirely by $\sigma_1 - \sigma_2$, the contribution due to mass difference though of opposite sign is relatively very small. The following mixtures are also expected to show reversals of the type observed by Grew: (1) N_2 and NO, (2) A and CO_2.

REFERENCES

Clusius, K., and Dickel G., 1938, *Naturwiss*, **26**, 546; 1930, **27**, 148.
Furry, Clark-Jones and Onsager, 1939, *Phys. Rev.*, **55**, 1083.
Fürth, R., 1942, *Proc. Roy. Soc. A* **179** 461
Grew, K. E., 1942, *Nature*, **150**, 320.

A VIBROGRAPHIC STUDY OF THE OUTPUT OF A SINGLE-PHASE HALF-WAVE POWER RECTIFIER

By T. TIRUNARAYANACHAR

(Received for publication, Dec. 16, 1942)

ABSTRACT. A simple device for studying the efficacy of design of filter circuits employed in power units is described. Instead of the usual cathode-ray oscillograph and a linear time base, the arrangement consists of an electromagnetically excited wire, the vibrations being recorded by a vibrograph, devised by the author (Tirunarayanachar, 1932). Vibrograms taken in the study of the wave-form and ripple-components of a single phase half-wave power rectifier output are given in support of the method suggested. The arrangement is specially suited for studying the ripple components in the output. The applicability of the method in wave-form investigation is being further studied.

INTRODUCTION

A thermionic rectifier allows a current flow in one direction only and offers infinite resistance to the current flow when the polarity is reversed; so that if the input current is a symmetrical A.C. of the form $I_0 \sin \omega t$ ($\omega = 2\pi f$, where f is the frequency of the supply mains), then the output from a single-phase half-wave rectifier is a current of the form :

$I = I_0 \sin \omega t$ between $t = 0$ to $t = \frac{T}{2}$; the output current is zero from $t = \frac{T}{2}$ to $t = T$.

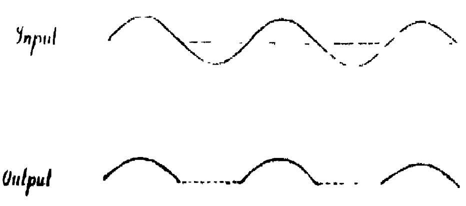

FIG. 1

In order to get a detailed picture of the output current, it must be resolved into its various components by the application of Fourier's theorem. $f(x)$ can be represented by the infinite series:

$$f(x) = A_0 + \sum_{n=1}^{\infty} A_n \cos nx + \sum_{n=1}^{\infty} B_n \sin nx,$$

where

$$A_0 = \frac{1}{T} \int_0^T f(x)\, dx$$

$$A_n = \frac{2}{T} \int_0^T f(x) \cos nx\, dx$$

$$B_n = \frac{2}{T} \int_0^T f(x) \sin nx\, dx,$$

In this case $f(x)=I_0 \sin \omega t$ between the limits $t=0$ to $t=\frac{T}{2}$; $f(x)=0$ between $t=\frac{T}{2}$ and $t=T$. On evaluating the Fourier coefficients for all values of n from 1 to ∞ by working out the definite integrals given above, we get for the instantaneous value of the rectified output current I, the result :

$$I=I_0\left[\frac{1}{\pi}+\tfrac{1}{2}\sin \omega t-\frac{2}{3\pi}\cos 2\omega t-\frac{2}{15\pi}\cos 4\omega t-\ldots\ldots\right].$$

The analysis shows that the rectified output consists of a D.C. of value I_0/π having superposed upon it an A.C. of supply frequency and having amplitude $I_0/2$ together with a series of even harmonics whose amplitudes go on decreasing rapidly.

A cathode-ray oscillograph together with a linear time-base is generally used for studying the wave-form of such output current. This paper gives an account of the results obtained by a study of the output current using a sonometer in conjunction with a vibrograph.

EXPERIMENTAL ARRANGEMENT AND RESULTS

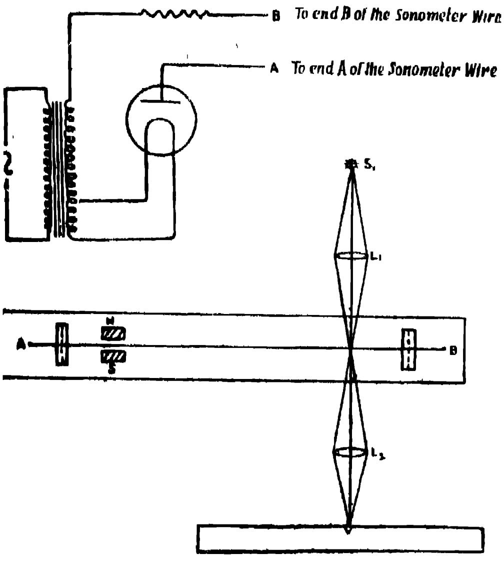
B To end B of the Sonometer Wire
A To end A of the Sonometer Wire
S₁
L₁
N
S
A
B
L₂

FIG. 2

Fig. 2 shows the experimental arrangement employed in the study of the problem. The rectifier used was a Tungar rectifier. It is a soft valve rectifier similar to that of a mercury vapour rectifier: but the tube in a Tungar contains pure argon gas at a pressure of three to eight cm. of mercury column. The tube operates at a low voltage and can handle large currents. A small current from the output of such a rectifier is passed through a sonometer wire AB. A portion of the wire lies between the poles N, S, of a permanent magnet mounted so that it can be slid along the length of the wire. When the frequency of anyone of the ripple components in the output coincides with one of the possible harmonic frequencies of the wire, a large resonant vibration occurs. The point of observation is illuminated by the source S_1 and the optical system L_1. L_2 focuses the shadow on the slit of the vibrograph, immediately behind which is the photographic plate shot at right angles to the direction of vibrations. Tuning can be effected by varying the tension and length of the wire. The method is a very elegant one and by suitably placing the permanent magnet, *i.e.*, by the proper control of the point of mechanical excitation of the wire, it is easy to obtain resonance with the ripple components in the output. Curves F, G, in the plate indicate vibrograms obtained in that way and they correspond to frequencies *f* and 2*f*.

Strings excited by electromagnetic means have in the past been utilised for the study of symmetrical audiofrequency currents, notably by D. W. Dye (1924) in the design of a standard sonometer. The vibrographic records taken by the author seem to suggest that the method can also be applied for the study of assymetrical currents as in the case of the output of single-phase half-wave rectifier.

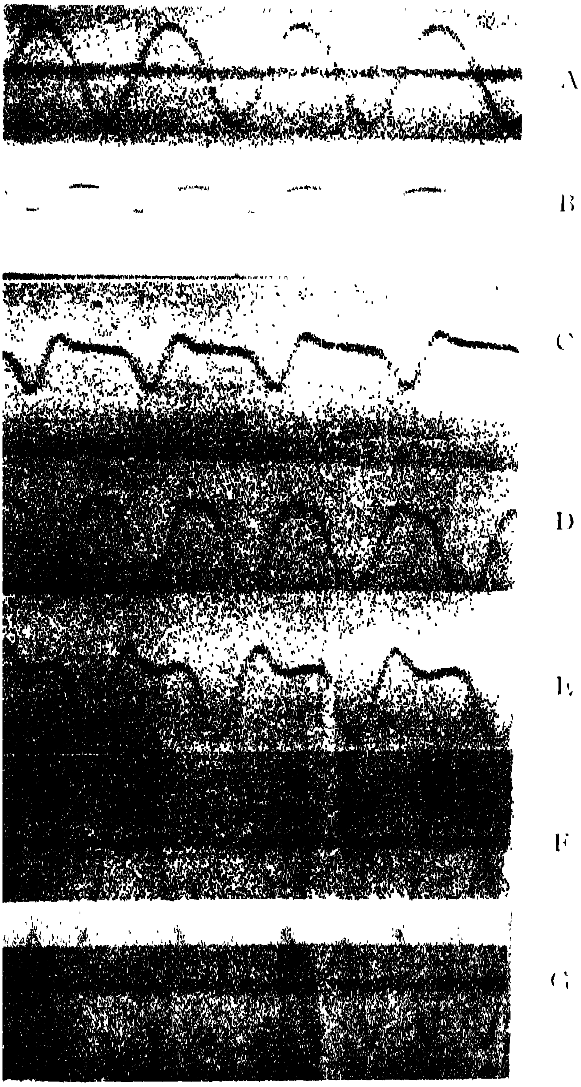

FIG. 3

In taking a vibrogram care must be taken in choosing the point of excitation as well as the point of observation on the wire. All harmonics which have a node at the point of excitation will be absent from the resultant form. Since the amplitudes of the higher harmonics go on rapidly decreasing, their effect on the wave-form becomes small, beyond a certain number. Curve A is the wave-form of the input symmetrical A.C. Curves B, C, D and E represent the wave-form of the rectified output, the point of observation is different in each case for a chosen point of excitation. Curves C and E show the assymetric effect remarkably well. The lower halves of the curves correspond to the half period when there is no current through the wire; on account of the inertia of the vibrating system, those parts are present.

CONCLUSION

In conclusion, the author wishes to suggest that besides the study of the wave-form, the arrangement is particularly suitable for testing the efficiency of filter circuits designed for smoothing the raw output of an H. W. rectifier. The power required for excitation of the wire in the case of a properly designed instrument like the Dye standard sonometer is of the order of only one milliwatt, for giving visible loops at lower frequencies. It is enough if the test is conducted for the presence of the fundamental ripple component only, for if the filter is designed to cut off the fundamental ripple component from the output, it would be a more efficient filter in cutting off the higher harmonic components.

ACKNOWLEDGMENT

The author wishes to thank Prof. A. Venkata Rao Telang, for the facilities afforded in conducting the experiments.

INTERMEDIATE COLLEGE,
BANGALORE.

REFERENCES

Dye, 1924, *N. P. L. Reports*, **26**, 85.

Tirunarayanachar, 1932, *Rev. Sci. Inst.*, **3**, 12.

13

A NOTE ON VOLUME RECTIFICATION OF CRYSTALS

By S. R. KHASTGIR

(Received for publication, Feb. 20, 1943)

Recently a paper has been published on volume rectification by B. K. Sen (1942). The paper appears to be an elaboration of what was reported by the same author (1937) about five years ago. Deaglio (1938) at that time, in a note published in Nature, made a clear statement about volume rectification which is only a natural consequence of the lack of symmetry in *polar* crystals. He also referred to the experimental evidence of such volume rectification in his experiments with carborundum and made the present position with regard to the rectifying properties of crystals abundantly clear. Yet it has been concluded by Sen in his recent paper that "the volume rectification effect is not confined to crystals like carborundum, zincite and silicon alone, which have no centres of symmetry but that it is also exhibited by crystals like galena, iron-pyrites and pyrolusite, possessing centres of symmetry." In view of such conclusion, a brief review of the subject is given here to leave no room for any misunderstanding about the existence of volume rectification in *polar* crystals.

My experiments with Das-Gupta (Khastgir, 1935) showed that when carborundum, zincite or silicon crystal was placed between two mercury electrodes giving large contact areas, there was considerable rectification. Similar experiments with symmetrical crystals like iron-pyrites, galena, etc., showed no rectification. The carborundum crystal under examination exhibited one plane face and other facets and it consisted of at least two crystals twinned together. Of the symmetrical crystals, the iron-pyrites and magnetite crystals used in these experiments could be regarded as single crystals. The results of these experiments strongly *suggested* asymmetric conductance in crystals having no centres of symmetry. The fact that the rectification observed in carborundum, zincite and silicon crystals did not change, when one of the crystal surfaces was heated, seemed also to support this suggestion. As there was no experimental test that the surface effect was entirely eliminated in our experiments, the evidence of volume rectification in polar crystals was not regarded as conclusive. Crucial tests were therefore considered necessary. Such a crucial test was made a few months later by Deaglio (1935) who performed two sets of experiments. In the first set of experiments, the plane natural face of the carborundum crystal which was perpendicular to the axis of six-fold symmetry and the face opposite to it, scraped and made plane, were coated with gold or platinum by cathodic sputtering. The I-V characteristic curve obtained with such crystal between two electrodes making large contact areas showed considerable rectification. No electrolytic polarisation was observed but there was photo-electric effect on the crystal surface. The observed rectification was considered as *mainly* due to rectification of the "barrier layer"-type. In the second set of experiments, both the faces of a carborundum single crystal were scraped and made smooth. The electrodes were gold or platinum films deposited on the scraped surfaces. There was no trace of any electrolytic polarisation and there was also no evidence of any Dember effect or any internal photo-electric effect. The characteristic curves were then drawn for two different thicknesses of the same crystal keeping the contact-areas the same. The rectification observed was opposite in sign to that observed in the first set of experiments. When curves were drawn showing *current* against *voltage per cm.* for the two different thicknesses of the crystal, they were found to be almost identical. This showed that the observed rectification was not due to any surface effect. There was thus no room for any doubt as to the existence of volume rectification, at least in carborundum crystals.

This asymmetric conductivity was studied later in the experiments of Khastgir and Chakravarty (1937) when the potential fall in the body of the carborundum crystal was observed for an applied voltage sending current in the two opposite directions. With carborundum, the potential distribution was found to be different for the two opposite directions. In the single crystals of iron-pyrites and magnetite, however, the potential distribution remained exactly the same for the two opposite directions of the current.

It is likely that Tissot (1910) and Pierce (1912) also detected volume rectification years ago in some crystals. They showed that with a certain group of crystals, even relatively large polished plates between metallic electrodes made very sensitive detectors. It is evident that the rectification observed by them in the symmetrical crystals was a *surface* effect: whereas, in the crystals with no centres of symmetry, the effect must have been a combination of *surface* and *volume* rectification.

On the theoretical side, R. de L. Kronig (1926) showed in a general way that the crystal rectification could be due to asymmetric binding of the ions into positions of equilibrium by restoring forces, not symmetrical for equal and opposite displacements. Considering the isothermal variation of the electrical resistance with the applied voltage (which was called "electro-resistive" effect), Osterberg (1930) also gave a theoretical treatment of rectification in carborundum crystals. The resistance was shown theoretically to change, on reversing the sign of the applied voltage by an amount depending upon the electro-resistive constants of the crystal. Carborundum crystals were actually found to rectify current in the manner predicted along the direction of the axis of six-fold symmetry.

In conclusion, it can be said that Sen's observations of the rectification effect in symmetrical crystals like galena, iron-pyrites, pyrolusite, etc., placed between mercury electrodes of large contact areas, merely showed that the surface effects were not eliminated in his experiments.

PHYSICS DEPARTMENT,
DACCA UNIVERSITY

REFERENCES

Deaglio, 1935, Comptes Rendus, **200**, 1303; see also *Atti R. Acad. Delle Scienze* (class Physics) LXX (1936).

Deaglio, 1938, *Nature*, **141**, 1011

Khastgir, 1935, *Nature*, **135**, 148; see also Khastgir and Das Gupta, 1935, *Ind. Jour. Phys.*, **9**, 258

Khastgir and Chakravarty, 1937, *Zeitschrift für Physik*, **105**, 88.

Krönig, 1929, *Nature*, **123**, 314.

Osterberg, 1936, *Phys. Rev.* **50**, 1187.

Pierce, 1912, *Electrician* **69**, 66.

Sen, 1937, *Nature*, **140**, 1102.

Sen, 1942, *Ind. Jour. Phys.*, **16**, 329

Tissot, 1912, *L Electrician*, **39**, 331.

THE ADVANTAGES IN USING ORTHOGONALISED TERMS IN A POLYNOMIAL FOR CURVE-FITTING

BY V. SATAKOPAN

(Received for publication, December 6, 1941)

ABSTRACT. The paper briefly discusses the relationships between the least squares solutions of Polynomial Constants obtained by using :—

(1) ordinary power terms (solutions discussed by S. M. Kerawala (1941) and

(2) orthogonalised terms (R. A. Fisher's method),

when the polynomial is fitted to a series of observations

It is shown how all the constants of polynomials up to the rth degree obtained by using simple power terms can be determined from the $(r+1)$ constants obtained from the orthogonal terms.

The advantages of using the orthogonalised terms instead of ordinary power terms are also indicated.

S. M. Kerawala (1941), in an interesting paper which appears in a recent issue of the Indian Journal of Physics has discussed the least squares solutions of the constants of polynomials up to the fifth degree fitted to series of observations y_1, y_2,… ………., y_n corresponding to the values of the independent variate x_1, x_2,…………, x_n varying by equal intervals.

Writing the polynomials up to the fifth degree in the form,

$$
\begin{aligned}
&y=a_{00}\\
&y=a_{01}+a_{11}x\\
(1)\qquad &y=a_{02}+a_{12}x+a_{22}x^2\\
&y=a_{03}+a_{13}x+a_{23}x^2+a_{33}x^3\\
&y=a_{04}+a_{14}x+a_{24}x^2+a_{34}x^3+a_{44}x^4\\
&y=a_{05}+a_{15}x+a_{25}x^2+a_{35}x^3+a_{45}x^4+a_{55}x^5,
\end{aligned}
$$

it will be seen that there are in all 21 coefficients a_{00}, a_{01},……, a_{55}, in the set of polynomials up to the fifth degree. For a set of polynomials up to the rth degree there will be $\frac{(r+1)(r+2)}{2}$ coefficients. But not all of these coefficients are independent as some of them repeat themselves and a few others are connected by simple relationships with others, and so, for a complete determination of the least squares solutions of all the polynomials it is not necessary to determine all the coefficients independently. Kerawala has shown that 12 different values are sufficient to determine completely all the 21 constants for the set of polynomials up to the 5th degree. He has also computed tables to facilitate the computation of the 12 values for series up to $n=30$.

It may however be pointed out that by using the orthogonalised terms for the polynomials instead of the simple power terms as in (I) above, the number of independent values that are necessary to determine completely the least squares solutions of all constants of polynomials up to the rth degree can be reduced still further to only $(r+1)$. Six values will thus enable us to determine all the 21 coefficients required for polynomials up to the 5th degree. Tables (Fisher and Yates, 1938 pp. 54-60) are also available for facilitating the determination of the six constants for values of n up to 52.

Assuming the polynomials to be fitted is of the rth degree it can be chosen in the form

$$\text{(II)} \qquad y = A_0\phi_0(x) + A_1\phi_1(x) + A_2\phi_2(x) + \dots\dots\dots + A_r\phi_r(x)$$

where $\phi_r(x)$ is a function of the rth power in x, the independent variate. For simplicity we shall assume here that x is measured in unit intervals from its mid-point so that for n values it will vary

$$\text{(1) from} - \frac{n-1}{2} \text{ to } + \frac{n-1}{2}, \text{ if } n \text{ is odd.}$$

$$\text{(2) from} - n/2 \text{ to } + n/2, \quad \text{if } n \text{ is even.}$$

Now if $\phi_0(x)$, $\phi_1(x)$,........., etc. be chosen to satisfy the condition

$$\text{(III)} \qquad S\{\phi_r(x)\phi_s(x)\} = 0 \qquad \text{when } r \neq s$$

the summation extending over the range of the variate x, the least squares solutions of the constants are very easy to determine. The polynomials $\phi_0(x)$, $\phi_1(x)$,... are known as Tchebycheff's polynomials. The general form of such polynomials is connected by the reduction formula (Allan, 1930, p. 312).

$$\text{(IV)} \qquad \phi_r(x) = 2(2r-1)x\,\phi_{r-1}(x) - (r-1)^2\{n^2-(r-1)^2\}\phi_{r-2}(x)$$

and their expressions for $r=0, 1, \dots\dots, 10$, are given by Allan (1930, p. 319). It will be seen that these are the same as the orthogonal polynomials mentioned by Kerawala as Condon's Polynomials in p. 250 of his paper quoted above. An arithmetical procedure for fitting these polynomials to a set of n observations has been developed by Fisher (Fisher, 1936, p. 156).

The least squares solutions of the constants A_0, A_1,......, A_r are given by

$$\text{(V)} \qquad A_p = \frac{S\{y\phi_p(x)\}}{S\{\phi_p(x)\}^2} \quad \text{......(Allan, 1930, p. 311).}$$

Using Kerawala's notation that

$$\eta_r = S(yx^r)$$

the least square solutions of the constants up to A_5 are as shown below (Fisher, 1936, p. 150).

$$A_0=\eta_0/n$$

$$A_1=\frac{12}{n(n^2-1)}\eta_1$$

$$A_2=\frac{180}{n(n^2-1)(n^2-4)}\left(\eta_2-\frac{n^2-1}{12}\eta_0\right)$$

$$\text{(VI)}\qquad A_3=\frac{2800}{n(n^2-1)\ldots(n^2-9)}\left(\eta_3-\frac{3n^2-7}{20}\eta_1\right)$$

$$A_4=\frac{44100}{n(n^2-1)\ldots(n^2-16)}\left(\eta_4-\frac{3n^2-13}{14}\eta_2+\frac{3(n^2-1)(n^2-9)}{560}\eta_0\right)$$

$$A_5=\frac{698544}{n(n^2-1)\ldots(n^2-25)}\left(\eta_5-\frac{5(n^2-7)}{18}\eta_3+\frac{15n^4-230n^2+407}{1008}\eta_1\right).$$

It may be interesting to note that these solutions exactly correspond to the values of a_{00}, a_{11}, a_{22}, a_{33}, a_{44} and a_{55} respectively (Kerawala, 1941, p. 274) in the expressions (I) above and these six values are sufficient to determine all the 21 coefficients involved therein. For, the orthogonal property of the ϕ's used make the least squares solutions of A_0, ..., A_5 independent of each other and hence the process of increasing the degree of curve fitted simply amounts to the addition of one more term to the expression for the previous degree. Thus, if a parabola is already fitted to a series of observations and is given by

$$y=A_0\ \phi_0(x)+A_1\phi_1(x)+A_2\phi_2(x),$$

then the cubic curve fitted to the same set of observations is obtained by simply adding $A_3\phi_3(x)$ to the right-hand side of the above equation. Now, if we remember that the least squares solution of a polynomial fitted to a series of observations should be the same whatever may be the form of the polynomial used, it is seen that a_{0r}, a_{1r},......, a_{rr} the least squares solutions of a polynomial of the rth degree should be equal to the coefficients of various powers of x in

$$A_0\phi_0(x)+A_1\phi_1(x)+\ldots\ldots+A_r\phi_r(x).$$

Writing the expressions $\phi_0(x)$, $\phi_1(x)$,......, etc. in full for each degree of the curve fitted and collecting the coefficients of various powers of x, we have, for polynomials up to the 5th degree:

$$y=A_0=\eta_0/n \qquad \therefore\quad A_0=a_{00} \qquad \ldots\ (1)$$

$$y=A_0+A_1x \qquad \therefore\quad a_{01}=A_0\,;\ a_{11}=A_1 \qquad \ldots\ (2)$$

$$y=A_0+A_1x+A_2\left(x^2-\frac{n^2-1}{12}\right) \qquad \ldots\ (3)$$

$$=\left(A_0-\frac{n^2-1}{12}A_2\right)+A_1x+A_2x^2,$$

(VII) $\therefore \quad a_{02}=A_0-\frac{n^2-1}{12}A_2;$

$a_{12}=A_1$ and $a_{22}=A_2.$

$$y=A_0+A_1x+A_2\left(x^2-\frac{n^2-1}{12}\right)+A_3\left(x^3-\frac{3n^2-7}{20}x\right) \quad \ldots \quad (4)$$

$$=\left(A_0-\frac{n^2-1}{12}A_2\right)+\left(A_1-\frac{3n^2-7}{20}A_3\right)x+A_2x^2+A_3x^3$$

$\therefore \quad a_{03}=A_0-\frac{n^2-1}{12}A_2, \quad a_{13}=A_1-\frac{3n^2-7}{20}A_3;$

$a_{23}=A_2; \quad a_{33}=A_3.$

$$y=A_0+A_1x+A_2\left(x^2-\frac{n^2-1}{12}\right)+A_3\left(x^3-\frac{3n^2-7}{20}x\right)$$
$$+A_4\left(x^4-\frac{3n^2-13}{14}x^2+\frac{3(n^2-1)(n^2-9)}{560}\right) \quad \ldots \quad (5)$$

$\therefore \quad a_{04}=A_0-\frac{n^2-1}{12}A_2+\frac{3(n^2-1)(n^2-9)}{560}A_4;$

$a_{14}=A_1-\frac{3n^2-7}{20}A_3;$

$a_{24}=A_2-\frac{3n^2-13}{14}A_4;$

$a_{34}=A_3; \quad a_{44}=A_4.$

$$y=A_0+A_1x+A_2\left(x^2-\frac{n^2-1}{12}\right)+A_3\left(x^3-\frac{3n^2-7}{20}x\right) \quad \ldots \quad (6)$$
$$+A_4\left(x^4-\frac{3n^2-13}{14}x^2+\frac{3(n^2-1)(n^2-9)}{560}\right)$$
$$+A_5\left(x^5-\frac{5(n^2-7)}{18}x^3+\frac{15n^4-230n^2+407}{1008}x\right)$$

$\therefore \quad a_{05}=A_0-\frac{n^2-1}{12}A_2+\frac{3(n^2-1)(n^2-9)}{560}A_4;$

$a_{15}=A_1-\frac{3n^2-7}{20}A_3+\frac{15n^4-230n^2+407}{1008}A_5;$

$a_{25}=A_2-\frac{3n^2-13}{14}A_4; \quad a_{35}=A_3-\frac{5(n^2-7)}{18}A_5;$

$a_{45}=A_4; \qquad a_{55}=A_5.$

The above equations bring out the connection between the least squares solutions of orthogonalised terms and ordinary terms in polynomials up to the fifth degree fitted to a series of n observations. All the equalities given by Kerawala on p. 250 among the 21 coefficients also follow from the above relationships. Hence it is clearly seen that the six coefficients A_0, A_1, $A_2, \ldots, A_5$ are sufficient, if determined, to find the least squares solutions of the 21 coefficients of expressions (I). It is also evident that in general the $(r+1)$ coefficients $A_0, A_1, \ldots, A_r$ will be sufficient to determine all the $\frac{(r+1)(r+2)}{2}$ coefficients in a set of polynomials up to the rth degree.

These orthogonal polynomials are well-known among statisticians and have been used widely by statistical workers for curve-fitting because of the elegant arithmetical procedure for fitting developed by Fisher (4, pp. 151-56). Tables of the functions up to $n=52$ have also been published since, to facilitate rapid computation of A_0 etc., for series of values up to $n=52$, by Fisher and Yates.[2] It will also be seen that the values of ξ_1, ξ_2, $\xi_3, \ldots, \xi_5$ given in these tables agree with the values given for a_{11}, a_{22}, $a_{33}, \ldots, a_{55}$ of Kerawala's tables up to $n=30$, as they should.

The more obvious advantage of using the orthogonalised terms in the polynomial worth mentioning here is the ease with which the sum of squares of residuals can be computed if it is desired to test the goodness of fit. It is not proposed to prove here the results involved, though simple, for which a reference may be made to Allan (1930). It has been shown therein that sum of squares of the residuals after fitting a curve of rth degree is given by

$$\text{(VIII)} \qquad S(y^2)-S\{A_0\phi_0(x)\}^2-S\{A_1\phi_1(x)\}^2-\ldots\ldots-S\{A_r\phi_r(x)\}^2$$

where S denotes the summation over the various points of the series. The form at once makes it clear that for each degree of the curve fitted the reduction in the sum of squares is given by the expression

$$A^2S\{\phi(x)\}^2$$

and this enables us also to allocate the total reduction in sum of squares to various individual degrees of the curve fitted with one degree of freedom for each in the analysis of variance. But for the orthogonal property of the terms involved it would not be possible to do so without laborious computations.

One more use of the orthogonalised terms may also be mentioned here. As the coefficients A_0, $A_1, \ldots, A_r$ are independent of one another, they yield a series of independent constants that usefully serve to represent main features of the sequence as indicated by Professor Fisher. He (Fisher, 1936) has suggested that for any series, a', b', c', d', e', f' obtained the following formulae may be taken as a set of independent constants to represent the general distribution features of the series and used in regressional work. These constants have been found very useful in practice for studying distribution features of a variate and the regression functions obtained by correlating these constants with a dependent variate have shown very interesting results (Fisher, 1923, and Kalamkar *et al*, 1940).

$$\begin{aligned}
A_0 &= a' \\
A_1 &= \frac{6}{n-1}\, b' \\
A_2 &= \frac{30}{(n-1)(n-2)}\, c' \\
A_3 &= \frac{140}{(n-1)(n-2)(n-3)}\, d' \\
A_4 &= \frac{630}{(n-1)(n-2)\ldots(n-4)}\, e' \\
A_5 &= \frac{2772}{(n-1)(n-2)\ldots(n-5)}\, f'.
\end{aligned} \tag{IX}$$

It is, therefore, advantageous in many ways to use the orthogonalised terms in a polynomial while fitting it to a series rather than using the ordinary power terms. In view of the enormous amount of arithmetical labour saved if tables are available the tables which are already available up to $n=52$ have now been extended up to $n=75$ by the author of this note and will be published shortly.

Kerawala's paper has, however, thrown much light on the relationships between the least squares solutions of coefficients of ordinary power terms and orthogonalised terms in a polynomial fitted to a series.

METEOROLOGICAL OFFICE,
POONA 5.

REFERENCES

Allan, F. E., 1930, *Proc. Roy. Soc. Edin.*, **50**, Part III, No. 24.

Fisher, R. A., 1923, *Phil. Trans. Roy. Soc. Lond. B.*, **213**, 89.

Fisher, R. A., 1936, *Statistical Methods for Research Workers* (Oliver and Boyd London), 6th edition.

Fisher, R. A., and Yates, F., 1938, *Statistical Tables, Tables XXIII*, 54 (Oliver and Boyd, London).

Kalamkar, R. J., and Satakopan, V., 1940, *Ind. Jour. Agri. Sci.*, **10**, 960.

Kerawala, S. M., 1941, *Ind. J. Phys.*, **24**, 241.

THE ATMOSPHERIC ABSORPTION CURVES AND THEIR DEPENDENCE ON THE NATURE OF THE PRIMARY COSMIC RAYS

By S. K. CHAKRABARTY

(Received for publication, Jan 13, 1943)

ABSTRACT. With a view to testing the possibility of interpreting the observed results on the absorption of cosmic rays in the atmosphere in terms of incoming electrons or positrons, the nature of the absorption curves produced by soft primaries has been calculated. Two different hypotheses have been assumed for the energy spectra of the primary, *viz*, (*a*) that the number of particles having energy E varies as $E^{-(\delta+1)}$ and (*b*) that only discrete sets of isoenergetic particles, produced through the annihilation of different atoms which are found in abundance in the interstellar space exist The theoretical curves when compared with the observed Bangalore-Peshwar difference curve show that near the top of the atmosphere a good deal of difference in the absorption co-efficient between theory and observation exists. In this region however, the number of counts is much less than the actual ionization and the observations are also inaccurate

A comparison of the absorption coefficient at large depths and also the sea-level latitude effect indicate definitely that the primary cosmic rays *must* contain protons. Whether electrons exist at all in the primary and if so whether hypothesis (*a*) or (*b*) approaches reality can only be determined by further observations made at closer intervals particularly, between 0° and 20°N. The observational results at Agra and Bangalore suggest, however, that even the protons in the primary cannot have a continuous energy spectrum

An application of the results of the cascade theory of showers can be made in the theoretical interpretation of the observed absorption curves in the atmosphere specially at high altitudes. Recent developments of cosmic-ray theory and experiments have made it possible to get deeper into the problem of the energy spectra of the various sorts of rays and the nature as well as the spectra of their primary. The high altitude measurements of the cosmic-ray intensity at different latitudes have been made by several authors [Bowen, Millikan and Neher (1938), Millikan, Neher and Pickering (1942), Neher and Pickering (1942)]. On the other hand the latitude effect at sea-level was also observed by Gill (1939), Compton and Turner (1937) and also by Millikan and Neher (1935). All these results show definitely that the cosmic-ray intensity is not the same at different places and is smallest for places near the equator. This is known as the latitude effect of cosmic radiation. The difference curves obtained by Millikan and others must all be produced by *charged* primary cosmic rays whose individual energies lie between definite limits depending on the geomagnetic latitudes of the places of observation and are given by the results of Störmer's theory as developed by Lemaitre and Vallarta. It is observed that all these difference curves have the same general shape and are in several respects similar to the theoretical absorption curves of the cascade theory. One is, therefore, tempted to conclude that these observed absorption curves are due to shower-formation by charged primary particles (electrons and positrons) having energies lying between certain well-defined limits. From the results of their observation Bowen, Millikan and Neher have derived a form for the primary energy spectrum incident at the top of the atmosphere. Naturally, from the atmospheric absorption curves measured at a small number of stations one cannot expect to derive a continuous spectrum for the primary rays. The curve derived by Bowen, Millikan and Neher is only a plausible one drawn in order to fit the observed results. The theoretical difference curves as calculated with the results of Bhabha and Heitler (1937) and those of Carlson and Oppenheimer (1937) when compared with the observed difference curves of Bowen, Millikan and Neher (1937) gave a qualitative agreement, but there was quite an appreciable amount of systematic difference between observation and theory. The maxima of the observed curves occurred at depths much less than the calculated ones. At the present time several authors are inclined to believe that up to date evidence is quite good for interpreting the observed results in terms of incoming protons *instead of* electrons. The main reasons they put forward are that the rate of rise of the ionization in the first metre of water of the atmosphere is a good deal more rapid than they can account for, by the cascade theory. Moreover the number of electrons which are usually obtained at depths of two or three metres of water below the top is according to them very much less than would be required by the cascade theory if the incoming rays are electrons. In view of the qualitative nature of the results obtained by Bhabha and Heitler and also by Carlson and Oppenheimer, and specially due to their inadequate treatment of the collision-loss it was difficult to say whether the above-mentioned differences were really due to the rough approximations made in the theory. The results obtained by Serber (1938) which have lately been used for theoretical calculations, when compared with those obtained by Bhabha and the present author (Bhabha and Chakrabarty, 1942) suggest that at least two of the above-mentioned difficulties may possibly be removed when the accurate results of the cascade theory are used. It is the purpose of the present paper to examine whether calculations based on the accurate results of the cascade theory can be compared with the observed curves and thereby to test whether the results of observation can be interpreted in terms of incoming electrons and positrons. Such a comparison will give an idea as to the nature and history of the primary cosmic rays before they enter the earth's atmosphere, which possibly bear the impress of the origin of cosmic rays.

The observational data so far obtained relating to the variation of the intensity of cosmic rays with altitude at different latitudes were not suitable for comparison with the theoretical results. When the measuring instruments are electroscopes or single counters which respond to rays reaching them from all directions instead of merely from the vertical, the analysis becomes much more complicated, especially in the equatorial latitudes. For comparison with the theoretical curves which give results for vertically incident primaries, the previous authors have applied Gross-transformation to the observed results or the inverse of the Gross-transformation to the theoretical results. But the uniformity of the primary radiation in azimuth, assumed in the derivation of the Gross equation does not really exist and the non-uniformity increases as one approaches the equator. This will be evident from the variation of the allowed cone with latitude, obtained by Lemaitre and Vallarta (1936). A consequence of this property is that the electroscope or single counter data cannot be used for any fine structure analysis of the primary, since the difference curves cannot be then considered as due to charged primaries lying between *sharply defined limits*. To overcome this difficulty Neher and Pickering (1942) have, however, used two counters as a cosmic-ray telescope to record the radiation coming from a definite direction. It may be doubted wheather the counter data do actually give the intensity of the radiation and in order to obtain the intensity at any altitude electroscopes should be used. The difference that may arise between counter and electroscope records have been tested, and Neher and Pickering conclude from their results of observation that the counting rates at any place, after proper adjustments, can fairly accurately be taken as proportional to the intensity of the cosmic rays at the corresponding position. A similar conclusion was also arrived at previously by Korff, Curtiss and Astin (1938).

Vertical coincidence measurements have been made by Neher and Pickering* only at Bangalore, Agra and Peshwar. We shall, however, use these results for the purpose of comparing the theoretical results deduced in the present paper.

Two different hypotheses have been postulated regarding the nature of the energy spectra of primary charged particles which are assumed for the present to be electrons or positrons. The possibility of the existence of protons in the primary will, however, be discussed at the end. The first hypothesis is (*a*) that the primary particles can have all possible energies and according to previous authors [Blackett (1941), Hilbery (1941), Johnson (1938), Heitler (1937)], the spectra can be represented by the equation,

$$f(E_0)dE_0=\delta I\cdot\frac{k^{\delta}}{E_0{}^{\delta+1}}\,dE_0 \qquad \dots \quad (1)$$

where δ lies between 1 and 2 and $f(E_0)dE_0$, gives the number of particles having energies between E_0 and E_0+dE_0. Following Johnson and Blackett we shall take for the primary energy spectrum the form given by (1) where $\delta=1.87$. k is, however, a constant quantity of the dimensions of energy, and may be suitably adjusted to give a good fit of the observed data with those calculated. The form (1) is also analogous to the one assumed by Heisenberg and

---

* Bhabha has informed me in a private communication that the angle subtended by their counters was so large that even this cannot be called a vertical measurement. In fact Millikan's two and three counter telescopes, which Neher and Pickering have used, record rays which pass through at an angle of as much as 45° from the vertical

Euler (1938) for the energy-spectrum of the mesons. The nature of the primary spectrum obtained by Millikan and others, however, can be made to coincide with (1) for values of $E_0 \geq 7 \times 10^9$. *e.v.* [*cf.* Hilbery (1941)]. Since for the purpose of comparison, with the results of observation, made in this paper we are concerned mainly with values of $E_0 > 7 \times 10^9$. *e.v.*, the results obtained with (1) will be nearly the same as that obtained with a primary distribution given earlier by Millikan and others.

The second hypothesis regarding the nature of the primary cosmic rays is (*b*) that the primary spectrum is not continuous but has lines or bands in which the the energy of the particles lie.

Since $f(E_0)dE_0$ is the number of charged particles (electrons or positrons) having energies lying between E_0 and $E_0 + dE_0$ and incident vertically on the top of the atmosphere, the average number of particles $C(a, t)$, say, produced at a depth t, in radiation units, below the top of the atmosphere and coming in the vertical direction is given by

$$C(a, t) = \int f(E_0) N(y_0, t) dE_0 \qquad (2)$$

where $N(y_0, t)$ is the average number of particles produced at a depth t by a primary particle of energy β exp. y_0, incident vertically on the top of the atmosphere. β represents the mean collision loss corresponding to the material in which the shower is produced. The function $N(y_0, t)$ has been deduced in a previous paper by Bhabha and the present author. The value of a, however, depends on the geomagnetic latitude of the place of observation and can be easily deduced from the Lemaitre-Vallarta function. Substituting the values of $N(y_0, t)$ and simplifying, we get

$$C(a, t) = \frac{1}{2\pi i} \int_{\sigma - i\infty}^{\sigma + i\infty} \delta I . \left(\frac{k}{a} \right)^{\delta} . \left(\frac{a}{\beta} \right)^{S-1} . \left\{ \frac{1}{g_0(S)} \right\}^{S-1}$$

$$\times \frac{1}{(S-1)} . \frac{1}{(\delta - S + 1)} . \frac{D-\lambda}{\mu-\lambda} e^{-\lambda t} . dS$$

$$= \delta I . \left(\frac{k}{\beta} \right)^{\delta} . \frac{1}{2\pi i} \int_{\sigma - i\infty}^{\sigma + i\infty} exp. \left\{ (S - 1 - \delta) y_a - \lambda t \right\}$$

$$\times \frac{1}{(S-1)(\delta+1-S)} \left\{ \frac{1}{g_0(S)} \right\}^{S-1} . \frac{D-\lambda}{\mu-\lambda} . dS \qquad \ldots \quad (3)$$

where

$$y_a = \log(a/\beta) \qquad . \quad (4)$$

and λ, μ, $g_0(S)$, etc., are all functions of S and are given in a previous paper (Bhabha and Chakrabarty, 1942). The integral on the right side of (3) can be evaluated quite accurately by the saddle point method and the method of such evaluation has been given previously (Chakrabarty, 1942). But $C(a, t)$ is not the quantity, which can be compared directly with the results of observation, since in the observed absorption curves in any particular latitude exists also the particles produced by the uncharged primaries and also by any other charged particles which are not electrons or positrons or do not multiply according to the cascade process. If α_1 and α_2 are the values of α at two different latitudes then $C(\alpha_2, t) - C(\alpha_1, t)$ will give the difference curve which should compare with the observed difference curve corresponding to the latitudes of the places of observations, which obviously represents the effect of the latitude sensitive part of the primary cosmic rays having energies lying between α_2 and α_1 if it consisted only electrons and positrons. In Table I are given the values of α and y for some different places of observations. The geomagnetic latitude of the places of observation are also given in the second row of the table.

TABLE I

Place of observation	Bangalore	Agra	Peshwar	San Antonio	Oklahoma City	Omaha	Bismark
Magnetic latitude	3°N	17° 3N	25°N	38° 5N	45°N	51°N	57°N
α in B e v.	15.30	12.80	11.39	7.55	4.3	2.9	1.39
y_α	5.001	4.820	4.706	4.294	3.732	3.338	2.602

The values of $C(\alpha, t)$ as obtained from (3) for different values of α (*i.e.*, of y_α), and t can be obtained from Table II where the values of $1.80 \times 10^5.I^{-1}k^{-\delta}\beta^{\delta}.C(\alpha, t)$ have been given. These values give immediately the theoretical difference curve between any two given places of observations listed in Table I.

TABLE II

Values of $1.80 \times 10^5.I^{-1}k^{-\delta}\beta^{\delta}.C(\alpha, t)$ for different values of y_α and t

y_α \ t	1	2	3	4	5	6	8	10	12	15
5.001	87.5	218.4	324.6	375.6	360.0	308.2	186.4	94.9	42.9	12.1
4.820	119.1	280.0	404.2	446.8	419.2	352.8	201.2	99.7	46.0	12.6
4.706	137.6	312.4	455.2	499.0	466.6	383.4	220.6	106.0	48.4	12.8
4.294	216.0	553.0	715.0	715.0	616.2	487.8	258.4	119.2	50.9	—
3.732	644.0	1148.0	1280.0	1130.0	891.2	672.4	317.6	136.2	58.0	—
3.338	1226.0	1845.0	1839.0	1530.0	1139.0	803.6	368.2	166.6	...	—

If Millikan's hypothesis be accepted then in view of the results of Bowen and Wise (1939) on the abundance of the atoms in space, the primary cosmic rays should mainly consist of five definite cosmic-ray bands, arising out of the complete transformation of helium, carbon, nitrogen, oxygen and silicon atoms into cosmic rays. In Table III are given the values of the energy of the primaries that may be obtained from different atoms, together with the lowest value of the latitude ϕ_0 at which such rays may be incident on the top of the earth's atmosphere in the *vertical* direction.

TABLE III

Element	He	C	N	O	Si
E_0 in B.e.v.	1.0	5.6	6.6	7.5	13.2
y_0	2.915	4.000	4.160	4.288	4.853
ϕ_0	54°N	13°N	40°N	38°N	16°N

Since the primary consists of discrete sets of isoenergetic particles, we have on this hypothesis

$$C(a, t) = \Sigma I(y_0) N(y_0, t) \tag{5}$$

where $I(y_0)$ is the intensity of the primary having energy β exp. y_0 and the summation is to be taken for all values of y_0 given in Table III for which $E_0 \geq a$. Hence, as in the previous case,

$$C(a_2, t) - C(a_1, t) \tag{6}$$

will give the theoretical difference curves. The values of I in this case will be proportional to the relative abundance of the different elements in space. In Table IV we have given the values of $N(y_0, t)$ for different values of y_0 corresponding to the different elements. With equations (5) and (6) it will then be possible to get the theoretical difference curves for any pair of latitudes lying in the northern hemisphere or, better say, between 3°N to 54°N.

TABLE IV

Values of $N(y_0, t)$ for different values of y_0 and t

y_0 \										15
2.915	3.14	2.82	1.82	1.08	0.628	0.369	—	—	—	—
4.000	3.88	6.21	6.25	1.77	3.08	2.14	0.806	0.280	0.0947	0.0165
4.288	4.19	7.40	7.97	6.61	4.90	3.33	1.32	0.047	0.0154	0.0285
4.853	4.86	9.90	12.6	12.1	9.88	7.21	3.26	1.28	0.464	0.0894

One very important difference exists between the two hypotheses which will possibly be sufficient to determine whether the primary cosmic radiation has a continuous energy spectrum or it only consists of discrete sets as postulated in hypothesis (*b*). It is apparent from Tables I and II that on the hypothesis (*b*) no difference should exist between the vertical coincidence curves taken at (*i*) Peshwar and Agra, (*ii*) Oklahoma City and Omaha, and also possibly between (*iii*) Bismark and any other higher latitudes, but on the hypothesis (*a*) differences must exist in these cases also. The observations made at the first pair of stations, *viz.*, Peshwar and Agra, made by Neher and Pickering (1942) puts a strong evidence against the hypothesis (*b*) whereas their observations taken at Agra and Bangalore invalidates both the hypotheses. Similar observations should be made at other latitudes also before making any definite conclusion on this point. The theoretical difference curves for other latitudes can be easily obtained from Tables II and IV.

In Fig. 1 we have plotted the Bangalore-Peshwar difference curve as given by Neher and Pickering.*The theoretical curves as obtained for the two hypotheses have also been drawn. The ordinates of the theoretical curves are so adjusted (such adjustments will possibly give the values of *k* and I) that all the curves give the same maximum intensity. It will appear from the figure that the theoretical difference curves based on the hypothesis (*a*) and (*b*) are nearly identical so that a comparison of these curves only will give no indication as to the validity of either of the hypotheses. When compared with the observed curves it is significant that the observed rate of rise of the ionization in the first metre of water equivalent of the atmosphere is more rapid than the theoretical estimates based on the cascade theory. It may be noted, however, that in this region the observed data are possibly much less than the actual ionization and this is due to the use of counters instead of electroscopes for observations, since at these altitudes groups of particles must become increasingly prevalent and these register but once in the counter whereas they will give their true value in an electroscope. Such a difference between the counter and electroscope data at high altitudes has also been noticed by Neher and Pickering Hence to compare more accurately it is necessary to make observations with counter-controlled electroscopes, or any other device which will record the *true ionization produced only by vertical rays*.

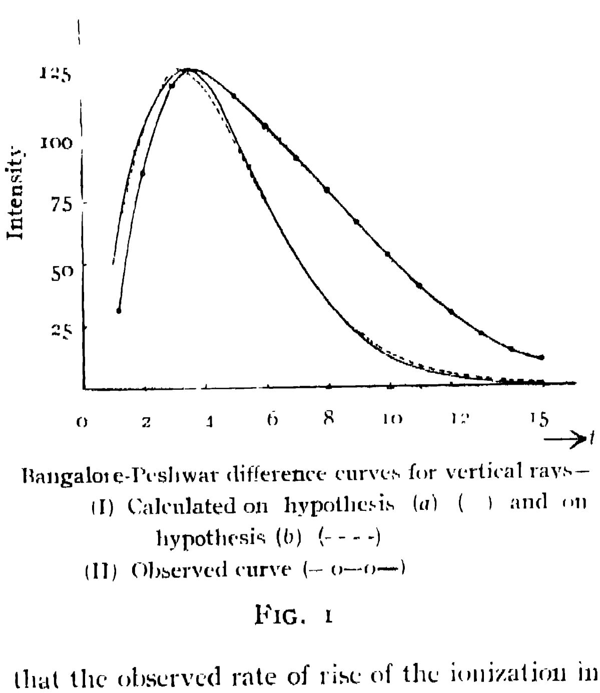

Bangalore-Peshwar difference curves for vertical rays—
(I) Calculated on hypothesis (*a*) ( ) and on hypothesis (*b*) (- - - -)
(II) Observed curve (— o—o—)

FIG. 1

---

* For reasons mentioned above this cannot be compared with the theoretical curves. This has, however, been introduced to show qualitatively the order of the difference at large depths.

Figure 1 will also show that the discrepancy mentioned by previous authors as regards the position of the maximum disappears almost completely. Beyond the maximum the actual ionization is much more than can be explained by the cascade theory. Since these curves represent the ionization produced by primary particles in a definite range of energy the discrepancy in the apparent absorption co-efficient at large depths cannot be explained by the presence of a few primary particles of very high energy. Consequently, to account for the difference between the observed and theoretical estimates of the ionization at great depths it is necessary to postulate the creation of charged particles by processes other than the cascade process, for which the primary must be charged particles within definite range of energy. The excess ionization observed has been suggested by several authors as due to mesons and their decay particles. If such an explanation is to be accepted then it is necessary to postulate that mesons are somehow produced at least in part by charged particles. These results suggest that the primary cosmic rays should also consist of protons. The experiments of Schein, Jesse and Wollan (1941) lend support to this view.

Although the observed Agra-Bangalore difference curve cannot be explained by hypothesis (*a*) there exists a serious difficulty in accepting the hypothesis (*b*). The energy of some of the most energetic rays are known to be more than a thousand times the mass of the heaviest known atom and as such, hypothesis (*b*) cannot explain the existence of such particles. The validity of either of the two hypotheses can only be tested by making further observations at closer latitudes. If, however, the discrepancy mentioned above between the theoretical and the observed curves on the left of the maximum persists even with more accurately obtained observational results, it may be necessary to accept the view that electrons and positrons are not at all present in the primary cosmic rays, and the charged primary particles are entirely protons. In that case, however, in order to explain the observed facts it will be necessary to admit the existence of hitherto unknown process which allows a complete absorption of protons in the very upper layers of the atmosphere and a consequent production of mesons, electrons or γ-rays.

The latitude effect at sea-level has been observed by several authors. But from the results already published (Bhabha and Chakrabarty, 1942, Table III) it will be clear that even for a primary particle (electron or positron) with energy as high as 40. B.e.v, there is a very little probability of its effect being felt at sea level. Consequently the sea-level latitude effect cannot be produced by primary electrons or positrons, and requires the existence of protons in the primary cosmic rays. This conclusion will be altered if we assume that electrons can produce mesons or some other particles which require a lower energy to penetrate the atmosphere than by the cascade process.

It is therefore essential that protons or at least some charged particles other than electrons or positrons *must* exist in the primary cosmic rays. A similar conclusion was also arrived at by Johnson (1930) from other considerations. Whether electrons or positrons do exist at all in the primary cannot, however, be definitely established unless further observational data, taken at closer latitudes, are available. A few observations made at closer intervals between the equator and say 20° N will give definite indications as to the possibility of either of the two hypotheses and will also indicate whether electrons do exist in the primary. The results of the measurements of Neher and Pickering (1942) at Agra and Bangalore, however, suggest that even the protons in the primary cosmic rays cannot have a continuous energy spectrum.

DEPARTMENT OF APPLIED MATHEMATICS,
UNIVERSITY OF CALCUTTA

REFERENCES

Bhabha and Heitler, 1937, *Proc. Roy. Soc.*, **159**, 432.

Bhabha and Chakrabarty, 1942, *Proc. Ind. Aca. Sci.*, **15**, 464.

Blackett, 1941, *Proc. Phys. Soc.*, **53**, 203.

Bowen, Millikan and Neher, 1937, *Phys. Rev.*, **52**, 80; 1938, *Phys. Rev.*, **53**, 855.

Bowen and Wise, 1939 *Bull. Lick Observatory*, **19**, 1

Carlson and Oppenheimer, 1937, *Phys Rev.*, **51**, 220.

Chakrabarty, 1942, *Proc. Nat. Inst. Sci. Ind.*, **8**, 331.

Compton and Turner, 1937, *Phys. Rev.*, **52**, 799.

Gill, 1939, *Phys. Rev.*, **55**, 1151.

Heisenberg and Euler, 1938, *Ergeb. Exakt. Naturwiss.*, **17**, 1.

Hilbery, 1941, *Phys. Rev.*, **60**, 1.

Heitler, 1937, *Proc. Roy. Soc.*, **161**, 261.

Johnson, 1938, *Phys. Rev.*, **53**, 499; 1939, *Rev. Mod. Phys.*, **11**, 20,

Korff, Curtiss and Astin, 1938, *Phys. Rev.*, **53**, 11.

Lemaitre and Vallarta, 1936, *Phys. Rev.*, **50**, 493.

Millikan Neher and Pickering, 1942, *Phys. Rev.*, **61**, 397.

Millikan and Neher, 1935, *Phys. Rev.*, **47**, 205

Neher and Pickering, 1942, *Phys. Rev.*, **61**, 407.

Serber, 1938, *Phys. Rev.*, **54**, 320.

ERRATA

Dipole Moments of Palmitic Acid, Aleuritic Acid and Alkyl Esters of Aleuritic Acid—By G. N. Bhattacharya, Ind. J. Phys., Vol. XVI

P. 372, line 7 from the bottom—

read ' p ' *instead of* ' P ' in the formula $P = \frac{\epsilon - 1}{\epsilon + 2} \cdot \frac{1}{d}$

P. 372, line 6 from the bottom—*read* ' ϵ ' *instead of* ' C '

P. 372, line 3 from the bottom—*read* $P_1 = M_1\left(p_2 + \frac{p_{12} - p_2}{w}\right)$

instead of $P_1 = M_1\left(P_2 + \frac{P_{12} - P_2}{w}\right)$

P. 372, line 2 from the bottom—*read* ' p_{12} and p_2 ' *instead of* ' P_{12} and P_2 '

P. 375, line 12 from the top—*read* ' carbon atom ' *instead of* ' carbonation '

P. 376, under reference 3—*read* ' Reinhold ' *instead of* Reihnold '

P. 376, under reference 18—*read* ' Swietonslawski ' *instead of* ' Swietoslwaski. '

16

A STUDY OF ABSORPTION LINES OF POTASSIUM VAPOUR UNDER VARYING CONDITIONS OF TEMPERATURE AND PRESSURE

By D. K. BHATTACHARYA

AND

S. P. SINHA

(*Received for publication, February 11, 1943*)

Plate II

ABSTRACT. The absorption spectra of potassium vapour under varying conditions of temperature and pressure have been studied using a hydrogen continuum as the background. It is observed that the number of absorption lines increases with the increase in the partial vapour pressure.

INTRODUCTION

Professor Saha remarked in 1924: "There seems to be at present a wide divergence of views regarding the magnitude of pressure in the reversing layers of stars." From the existing record of the number of lines in the Fraunhofer spectrum in case of hydrogen, sodium, magnesium and calcium, he postulated that the pressure in the outer layers of the photosphere was such that the orbits beyond the sixth were rarely developed. He also considered the well-known formula

$$n \propto (T/P)^{\frac{1}{6}}$$

where n is the order number of the lines developed,
T is the temperature, and
P is the vapour pressure,

and concluded that the number of lines would increase as the pressure diminished. Datta and Roy (1930) made an attempt to have experimental support of Saha's hypothesis. But their source of continuous radiation was not so satisfactory as is available at present. Hence experiments with potassium in nitrogen gas, using hydrogen continuum as the background, have been undertaken by us to see the behaviour of the absorption lines of the element potassium, under varying conditions of temperature and pressure.

EXPERIMENT

The scheme of the arrangement is indicated in the annexed diagram where S is a small quartz spectrograph, C is a hydrogen discharge tube (Fig. 1) for a continuous source both supplied by Adam Hilger, Ltd. TT is a metal tube in which a metal cell G open at both ends containing potassium was introduced.

The tube TT was first covered with a single layer of asbestos paper and then a piece of nichrome wire was wound round it. Finally, a sheet of asbestos paper was rolled round the tube so that there might not be any fluctuation in temperature due to external disturbances. The rest of the diagram is self-explanatory. M is a mercury manometer, A1, A2, A3, A4, are vacuum stopcocks and D is a gas washing bottle partly filled with strong sulphuric acid. Nitrogen was selected to be introduced whenever any change in the total pressure in the observation tube TT was desired, as any combination of alkali metals with nitrogen is unknown. The flow of nitrogen from the cylinder had to be regulated before connecting the cylinder to the pressure tube at H. The end F was connected to a suitable suction pump and, before heating, the tube TT was thoroughly evacuated by running the pump for a long time and the stopcock A1 was kept closed for nearly 24 hours. There was practically no change in the readings of the manometer within that period. Photographs were taken only when temperatures desired became stationary. Though with varying temperature vapour pressure of potassium was altered within the observation tube TT, its indication could not be detected in the manometer. So we had to make an estimate of the partial pressures of the vapour of potassium by calculating the pressure by the empirical formla (Johnston *et al*, 1928) $\log_{10} p = -52.23\ A/T + B$, where p is the pressure in mm. and T is the temperature on absolute scale. The values of A and B for potassium are 84.9 and 7.183.

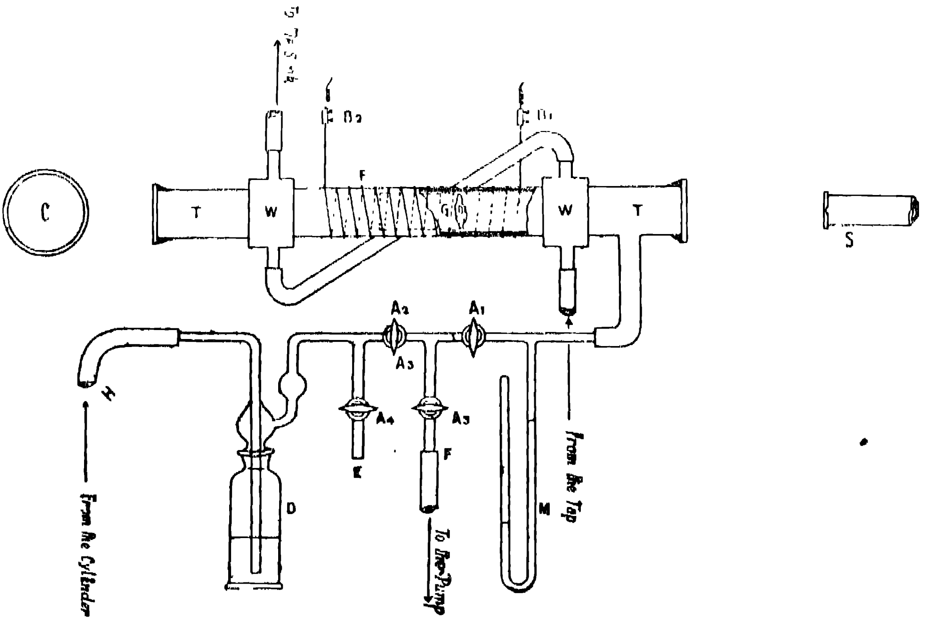

Fig. 1

Alterations in the total pressure could only be read in the manometer when nitrogen gas was introduced, *i.e.*, only when the pressure-communicating medium was present.

TABLE I

Spectrum	Temperature	Partial vapour pressure of potassium	Total pressure in mm.	Number of lines developed	Visual estimate of intensity of the line $\lambda=4045.6$
a	388°C	3 mm.	0.1 mm.	0	0
			30.0	3	2
b			66.0	8	4
			106.0	3	6
c			140.0	7	6
			260.0	7	8
d			400.0	7	8
			680.0	7	10
e	433°C	21 mm.	0.1	6	1
			30.0	10	1
f			66.0	10	3
			106.0	10	3
g			143.0	10	5
			263.0	10	5
h			400.0	10	8
			760.0	10	10
i			850.0	10	10
			940.0	10	10
j	545°C	58 mm.	0.1	10	1
			30.0	13	2
k			66.0	13	4
			106.0	13	7
l			143.0	13	8
			263.0	13	8
m			400.0	14	8
			760.0	14	8
n			860.0	14	8
o	695°C	400 mm.	0.1	10	very faint
			30.0	13	1
p			120.0	13	2
q			220.0	13	3
			300.0	14	4
r			390.0	14	4
			480.0	14	5
s			615.0	14	5
t			680.0	14	5
			760.0	15	6
u			106.0	15	5
			140.0	15	5

RESULTS

The results of the experiment are entered in Table I. The figures in sixth column give the variation of the intensity of the line ${}^2S_{\frac{1}{2}} - (2)\,{}^2P_{\frac{1}{2},\frac{3}{2}}$, *i.e.*, $\lambda = 4045.6$Å. The intensity of other absorption lines varies in exactly the same way. From the figures it is quite apparent that intensity of each line increases with total pressure. The rate of increase in intensity is greater at low pressures than at high pressures. Again we notice in column 5 that the number of lines also increases with total pressure. But here we also notice that after a certain value of total pressure is reached the number of absorption lines becomes almost constant. An inspection of column 2 and 5 read with figures in column 3 shows that the number of absorption lines at high partial vapour pressure is greater than at low partial vapour pressure. Thus number of lines at partial vapour pressure 3 mm. varies from 0 to 7, at partial vapour pressure 21 mm. varies from 6 to 10, at partial vapour pressure 58 mm. varies from 10 to 14 and at partial vapour pressure 400 mm. varies from 10 to 15. From these we conclude that greater number of absorption lines can be seen when the temperature, *i.e.*, when partial pressure of the vapour of the metal is increased. It is also clear that partial vapour pressure of the metal which depends upon the temperature of the tube has greater influence on the number of absorption lines than the total pressure. The effect of total pressure on the intensity of the lines, however, cannot be doubted.

It is also to be noted that two sharp absorption lines on both sides of the line ${}^2S_{\frac{1}{2}} - (3)\,{}^2P_{\frac{1}{2},\frac{3}{2}}$, *i.e.*, $\lambda = 3447{\cdot}2$Å were clearly seen in the negative taken at temperature 695°C, though their presence is not indicated in the print marked u (Plate II).

More detailed study of the main problem of this paper together with that of the lines referred to in the last paragraph is considered necessary before attempting to give any explanation of the phenomena.

Our thanks are due to Professor S. P. Prasad for giving us every facility in conducting this piece of work.

Department of Physics,
Science College, Patna.

REFERENCES

Datta and Roy, 1930, *Ind. Jour. Phys.*, **5**, 365.
Johnson *et al*, 1928, *International Critical Tables*, **3**, 205.
Saha, M. N., 1924, *Nature*, 155.

PLATE II A

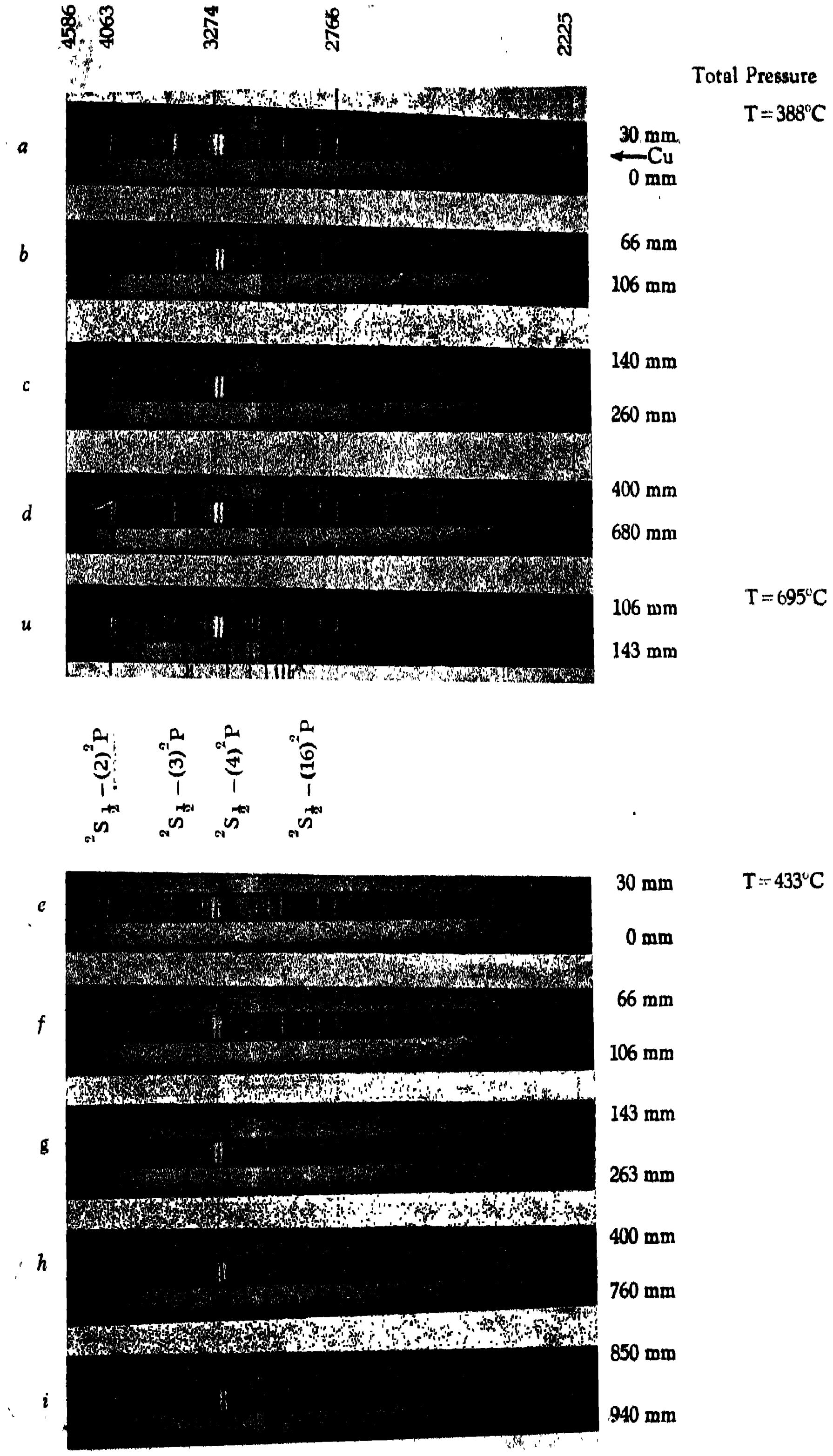
4586
4063
3274
2766
2225
Total Pressure
T = 388°C
a
30 mm
←Cu
0 mm
b
66 mm
106 mm
c
140 mm
260 mm
d
400 mm
680 mm
u
106 mm
143 mm
T = 695°C
$^2S_{\frac{1}{2}} - (2)^2P$
$^2S_{\frac{1}{2}} - (3)^2P$
$^2S_{\frac{1}{2}} - (4)^2P$
$^2S_{\frac{1}{2}} - (16)^2P$
e
30 mm
0 mm
T = 433°C
f
66 mm
106 mm
g
143 mm
263 mm
h
400 mm
760 mm
i
850 mm
940 mm

ATTACHARYA & SINHA

PLATE II B

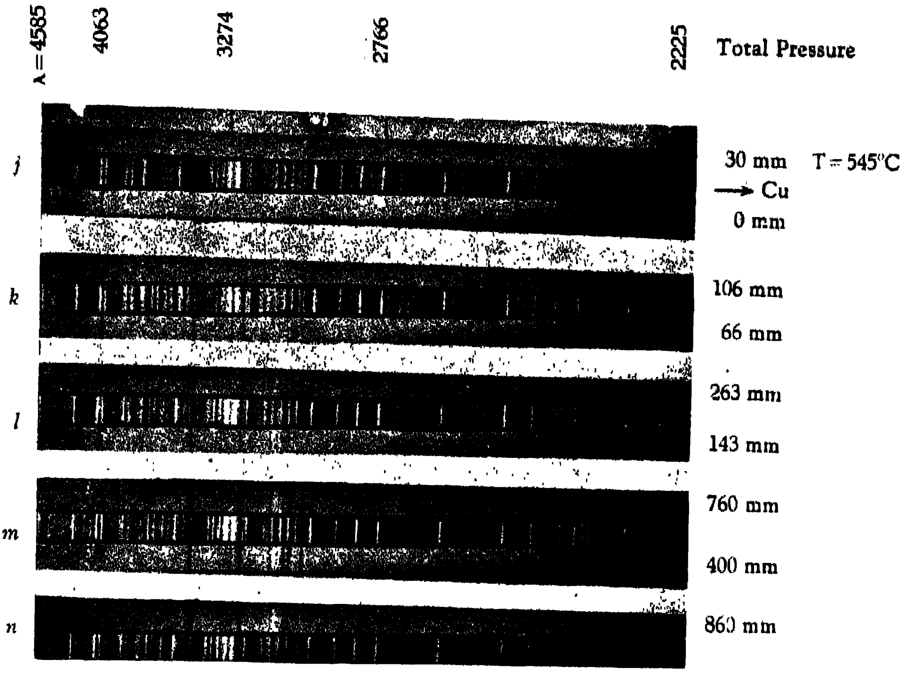

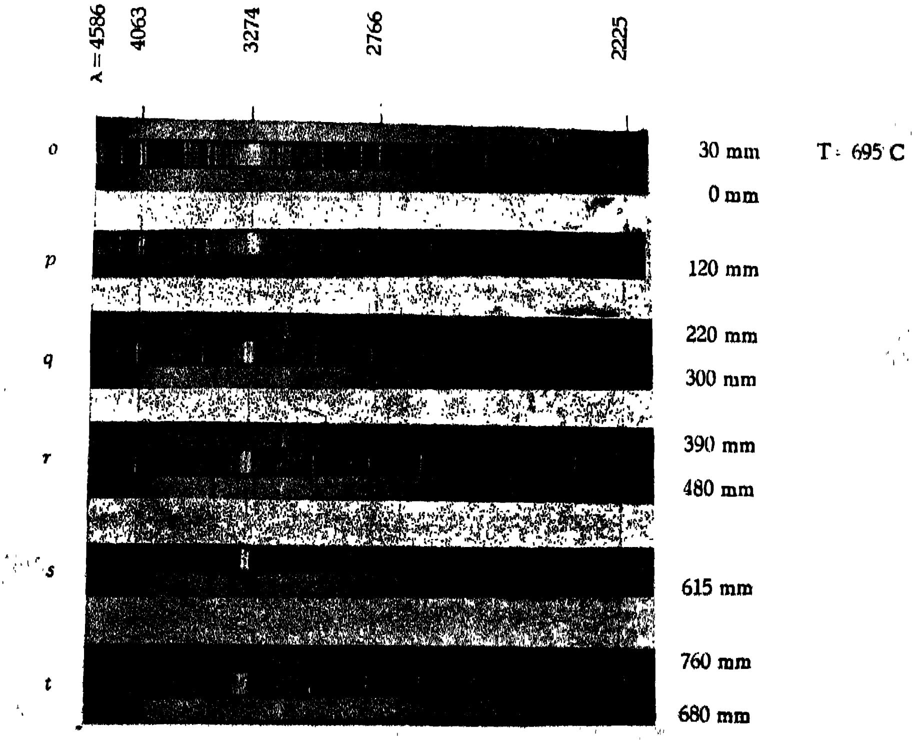

THE BAND SPECTRUM OF PHOSPHORUS PART I ROTATIONAL STRUCTURE

By K. NARAHARI RAO

(Received for publication, Jan. 30, 1943)

ABSTRACT. The band spectrum of phosphorus, as excited in a discharge tube, has been photographed with a Hilger large quartz Littrow spectrograph and the bands (9,21), (5,21), (5,18) and (4,18) have been measured. The analysis of their rotational structure has led to the following values of the constants (in cms.$^{-1}$).

$B'_4=0.2346$ $B''_{18}=0.2799$
$B'_5=0.2323$ $B''_{21}=0.2736$
$B'_9=0.2255$

The constant for $v'=9$ agrees with that obtained by Herzberg and also by Ashley, the others being newly obtained. The absence of any perturbations in the rotational structure of the bands (5,21) and (5,18) has shown that the perturbations pointed out by Herzberg must be only vibrational.

INTRODUCTION

While the band spectrum of nitrogen has been very extensively studied, investigations on that of phosphorus are comparatively few. The P_2 molecule is well known to emit an extensive and typical band spectrum ranging from λ 3500 down to the very extreme ultraviolet till about λ1900. The lower region of emission does not appear to have been adequately investigated. Apart from the very early work, the more recent and important investigations on this band spectrum consist chiefly of those of Jakowlewa (1931), Herzberg (1932), Ashley (1933) and Jenkins (1935). Jakowlewa was the first to suggest the vibrational analysis of the spectrum. Herzberg confirmed and extended the vibrational analysis. He also reported the rotational structure of the bands with the initial levels $v'=8$, 9, 10, 11. The most important points in the work of Herzberg, however, were the detection of perturbation in the vibrational levels $v'=2$ and 5 and of the phenomenon of predissociation exhibited by the P_2 molecule.

Herzberg plotted the difference between the observed and the calculated $\nu(v',0)$ values against the vibrational quantum number v' and found the differences at $v'=2$ and 5 to be abnormal, and beyond what might be accounted for as possible errors of measurement. So he concluded that the vibrational levels $v'=2$ and 5 are strongly perturbed.

Ashley redetermined the rotational structure of the (8,27), (8,28), and (9,28) bands previously analysed by Herzberg and in addition, she made the fine structure analysis of the (6,22) and (6,23) bands lying further towards the ultraviolet. The bands were photographed in the second order of a 21-foot concave grating, a more accurate evaluation of the rotational constants being thereby obtained. The chief aim of her work was the estimation of the alternation ratio of the intensities of the rotational lines in the spectrum. A more direct method of determining this ratio was attempted later by Jenkins. The ratio arrived at was 3 : 1 within limits of experimental error in the case of (6,22), (9,28), (9,29) and (10,31) bands, while in the (5,21) band Jenkins got the ratio to be between 3.4 to 3.5 : 1. This larger ratio which is theoretically inadmissable was interpreted by him as due to strong perturbations in the band (5,21) or to another fainter band that may perhaps lie underneath this.

If the anomalous value is due to a strong perturbation it would be expected that similar anomalies might occur in other bands involving the vibrational level $v'=5$ which is reported by Herzberg to exhibit strong perturbations.

It is therefore found desirable to examine the rotational structure and determine the alternating intensity ratio in the case of bands having this perturbed vibrational level. The present part deals with the fine structure analysis of the (9,21), (5,21), (5,18) and (4,18) bands. Two of these have $v'=5$. The above four bands have been selected for study, as they are free from overlapping by other bands and, as such, are suitable for analysis even under the comparatively low dispersion used. The results of the determination of the intensities of the rotational lines and of the alternation ratio will be reported in a succeeding part.

EXPERIMENTAL

The phosphorus bands have been excited in an ordinary H-shaped discharge tube of the type used by Sastry (1941). Preliminary trials with tubes of different bore have shown that the bands could be excited conveniently in a tube with the central portion having a bore of about 2 mm. The container was filled with red phosphorus and the electrodes were aluminium rods. An uncondensed discharge from a 1/4 kilo-watt transformer was passed. It was found essential to heat the container frequently in order to get the spectrum free from nitrogen and other impurity bands. Overheating of the tube, however, had to be avoided as in such a case the discharge ceased to pass. The tube was continuously evacuated with a Hyvac pump which was protected from the phosphorus vapour by a series of absorbing towers containing potassium hydroxide, calcium chloride and ice-cooled buffers. Care was taken to see that phosphorus did not deposit itself on the quartz window by cooling the wider portion of the tube behind the window.

The instrument used for photographing the spectrum was the Hilger large quartz Littrow spectrograph of type E1, with a dispersion of 3.5 A.U. per mm. in the region investigated. With a very narrow slit width, exposures of about 30-40 minutes gave good photographs showing well-defined rotational structure.

ROTATIONAL CONSTANTS

Table I

Structure of the band (9,21)

J	R Branch	P Branch	R(J)−P(J) = Δ_2F'	R(J−1) −P(J+1) = Δ_2F''	J	R Branch	P Branch	R(J)−P(J) = Δ_2F'	R(J−1) −P(J+1) = Δ_2F''
29	35,788.0	35,760 7	27.3		53	708.8	660.1	48.7	58.1
30	785 2	758.1	27.1	33.3	54	702.6	653.0	49.6	58.4
31	783.2	754.7	28.4	33.4	55	699 8	650.4	49.4	59.5
32	780.2	751.8	28.4	35.1	56	604.7	643.1	51.7	60.3
33	777.6	748.0	29.6	34.9	57	690 9	639.5	51.4	63.4
34	775.6	745.3	30.3	36.7	58	683.0	631.3	51.7	63.2
35	772.0	740.9	31.1	38.8	59	681.0	627.7	53.3	63.8
36	769.7	736.8	32.9	38.3	60	673 2	619.2	54.0	65.2
37	767.0	733.7	33.3	—	61	670.7	615 8	54.9	65.4
38	763.7	—	—	41.6	62	663.0	607.8	55.2	66.7
39	760.7	725.4	35.3	42.6	63	660.1	604.0	56.1	69.5
40	758.1	721.1	37.0	43.8	64	—	593.5		
41	754.7	716.9	37.8	45.4	65	656.8			
42	751.8	712.7	39.1	45.9	66	646.2			
43	748.0	708.8	39.2	47.4	67	639.5			
44	745.3	704.4	40.9	48.2	68	635.7			
45	740.9	699.8	41.1	50.6	69	627.7			
46	736.8	694.7	42.1	50.0	70	624.8			
47	733.7	690.9	42.8	51.4	71	615.8			
48	—	685.3	—	52.7	72	609.3			
49	725.4	681.0	44.4	—	73	604.0			
50	719 3	673.2	46.1	54.7	74	601.4			
51	716.9	670.7	46.3	56.3	75	597.0			
52	711.1	663.0	48.0	56.8					

Table II

Structure of the band (5,21)

J	R Branch	P Branch	R(J)−P(J) = Δ_2F'	R(J−1) −P(J+1) = Δ_2F''	J	R Branch	P Branch	R(J)−P(J) = Δ_2F'	R(J−1) −P(J+1) = Δ_2F''
43	34,005.8				61	940.4	883.0	57.4	67.4
44	002.4			48.9	62	935.8	877.4	58 4	67.7
45	33,999.6	33,956.9	42.7	48.8	63	931.3	872.7	58.6	68.6
46	996.5	953.6	42.9	50.5	64	927.3	867.2	60.1	69.8
47	992.7	949.7	43.6	51.7	65	922.6	861 5	61.1	
48	989.7	944.8	44.9	52.3	66	918.3			
49	985.8	940 4	45.4	53.9	67	913.0			
50	—	935.8	—	54.5	68	908.2			
51	—	931.3	—	—	69	903.5			
52	—	927.3	—	—	70	899.2			
53	971.2	922.6	48.6	—	71	893.3			
54	968.6	918.3	50.3	58.2	72	888.5			
55	964.1	913.0	51.1	60.4	73	883.0			
56	—	908.2	—	60.6	74	877.4			
57	956.9	903.5	53.4	—	75	872.7			
58	953.6	899.2	54.4	63.6	76	867.2			
59	949.1	893.3	55.8	65.1	77	861.5			
60	944.8	888.5	56.3	66.1	78	856.5			

TABLE III

Structure of the band (5, 18)

	R Branch	P Branch	$R(J)-P(J) = \Delta_2F'$	$R(J-1) - P(J+1) = \Delta_2F''$	J	R Branch	P Branch	$R(J)-P(J) = \Delta_2F'$	$R(J-1) - P(J+1) = \Delta_2F''$
29	36,005.3	35,976.7	28.6	—	51	931.6	883.5	48.1	59.0
30	002.5	973.3	29.2	35.3	52	926.8	876.6	50.2	59.0
31	000.0	970.0	30.0	35.9	53	922.4	872.6	49.8	59.8
32	35,997.7	966.6	31.1	37.0	54	917.9	867.0	50.9	60.7
33	991.5	963.0	31.5	39.0	55	913.0	861.7	51.3	62.4
34	992.1	958.1	33.4	39.2	56	908.5	855.5	53.0	62.9
35	987.3	955.3	32.0	39.7	57	903.4	850.1	53.3	64.2
36	986.0	952.4	33.6	39.2	58	898.9	844.3	54.6	65.0
37	983.3	948.1	35.2	42.7	59	893.4	838.4	55.0	66.4
38	981.0	943.3	37.7	43.9	60	887.4	832.5	54.9	67.8
39	976.7	939.4	37.3	45.4	61	883.5	825.6	57.9	68.9
40	973.3	935.6	37.7	45.1	62	876.6	818.5	58.1	—
41	970.0	931.6	38.4	46.5	63	872.6	—	—	—
42	966.6	926.8	39.8	47.6	64	868.5	—	—	—
43	963.0	922.4	40.6	48.7	65	861.7	—	—	—
44	958.7	917.9	40.8	50.0	66	858.4	—	—	—
45	955.3	913.0	42.3	50.2	67	850.1	—	—	—
46	952.4	908.5	43.9	51.9	68	844.3	—	—	—
47	948.1	903.4	44.7	—	69	838.4	—	—	—
48	943.3	—	—	54.7	70	832.5	—	—	—
49	939.4	893.4	46.0	54.4	71	825.6	—	—	—
50	935.6	888.9	46.7	55.9	72	820.8	—	—	—

TABLE IV

Structure of the band (4, 18)

J	R Branch	P Branch	$R(J)-P(J) = \Delta_2F'$	$R(J-1) - P(J+1) = \Delta_2F''$	J	R Branch	P Branch	$R(J)-P(J) = \Delta_2F'$	$R(J-1) - P(J+1) = \Delta_2F''$
33	35,544.9	35,513.4	31.5	—	53	472.8	423.8	49.0	58.9
34	542.0	510.5	31.5	39.2	54	468.6	418.6	50.0	59.3
35	539.3	505.7	33.6	39.7	55	464.0	413.5	50.5	60.8
36	536.5	502.3	34.2	41.0	56	458.3	407.8	50.5	—
37	533.1	498.3	34.8	42.1	57	454.6	—	—	62.3
38	530.2	494.4	35.8	43.0	58	449.6	396.0	53.6	65.2
39	526.7	490.1	36.6	44.1	59	444.4	389.4	55.0	66.8
40	524.2	486.1	38.1	44.8	60	440.4	382.8	57.6	—
41	520.6	481.9	38.7	46.7	61	434.8	—	—	69.0
42	517.1	477.5	39.6	47.8	62	429.6	371.4	58.2	—
43	513.4	472.8	40.6	48.5	63	423.8	—	—	—
44	510.5	468.6	41.9	49.4	64	420.7	—	—	—
45	505.7	464.0	41.7	52.2	65	413.5	—	—	—
46	502.3	458.3	44.0	51.1	66	407.8	—	—	—
47	498.3	454.6	43.7	52.7	67	396.4	—	—	—
48	494.4	449.6	44.8	53.9	68	396.0	—	—	—
49	490.1	444.4	45.7	54.0	69	389.4	—	—	—
50	486.1	440.4	45.7	55.3	70	386.0	—	—	—
51	481.9	434.8	47.1	56.5	71	380.1	—	—	—
52	477.5	429.6	47.9	58.1	72	373.9	—	—	—

ROTATIONAL STRUCTURE

The phosphorus bands due to the P_2 molecule possess a simple rotational structure, the electronic transition involved being $^1\Sigma - ^1\Sigma$. The predicted branches in a $^1\Sigma - \Sigma$ band are only a single P and a single R, the Q branch being forbidden. The fact that only the strong lines of the P branch need be assumed to be in coincidence with the strong lines of the R branch and similarly for the weak lines was of valuable help in deriving the analysis. The stronger lines are assigned odd values of J. In Tables I to IV the structure of the bands as divided into the R and P branches is given. These tables also contain combination differences. It is seen that the values of Δ_2F' agree for the (9,21) band and the (9,28) (*cf.* Ashley) justifying the assignment of a common initial vibrational level. Similarly, the agreement of Δ_2F'' values in the case of (4,18) and (5,18) bands confirms that the bands have a common final level. A difficulty is experienced during the analysis of the (5,21) band. At the tail end of the band, the assignment could be arrived at easily. But when the classification was extended towards the head of the band (beyond ν 33,956.0) the differences were found to be out of step. This at first suggested the existence of strong perturbations in this region. But, the analysis arrived at for the (5,18) band involving the level $v'=5$ extends very far towards the head of the band and does not show the definite existence of any perturbation. It is, therefore, considered that the difficulty in extending the analysis of the (5,21) band is due to the probable overlapping of a fainter band occurring just in this region. That this is plausible, is obvious from the photograph of the band also. Just after ν 33,056.9 there is seen in the picture a distinct change in the spectrum suggestive of an overlapping.

For determining the rotational constants the following formula for the second differences is used (*cf.* Jevon's Report on Band Spectra):

$$\Delta_2F = 4B_v(J+\tfrac{1}{2}) + 8D_v(J+\tfrac{1}{2})^3.$$

The value of D_v was at first estimated from the usual relation $D_e = -\frac{4B_e{}^3}{\omega_e{}^2}$, in which ω_e was taken from the equation given by Herzberg and an approximate preliminary value was adopted for B_e. Then the term $8D_v(J+\tfrac{1}{2})^2$ was subtracted algebraically from the corresponding $\Delta_2F/(J+\tfrac{1}{2})$. The resulting value of $4B_v$ obtained for different J values were then averaged. The absolute values of the combination differences were plotted against J in order to check the absolute numbering of the rotational quantum number. Only those points lying on the curve were taken for evaluating the constants. The procedure for the upper state as well as the lower was the same. Values of B_e and α are also calculated. The resulting constants are given in the following table which contains also those due to Herzberg and Ashley for comparison:

	$v''=21$	$v''=18$	$v'=9$	$v'=5$	$v'=4$
B cm.$^{-1}$	0.2736	0.2799	0.2255	0.2323	0.2336

Author		Herzberg	Ashley
B_e'	0.2420	0.24197	0.2415
α'	0 0017	0.0017	0.00164
B_e''	0.3187	0.31424	0.3057
α''	0.0021	0 0019	0.00165

SUMMARY

The rotational structure of four bands, two of which involve the initial vibrational level $v'=5$, has been examined. The structure does not reveal any rotational perturbations and it is concluded that the perturbations shown by Herzberg must be only vibrational. The constants for $v'=4$, 5 and $v''=18$, 21 are newly obtained.

The author is indebted to Dr. K. R. Rao for his advice and guidance in the course of these investigations.

SOLAR PHYSICS LABORATORY
KODAIKANAL.

REFERENCES

Ashley, 1933, Nuclear Spin of Phosphorus from Band Spectrum Analysis, *Phys. Rev.*, **44**, 919.

Herzberg, 1932, Band Spectrum, Predissociation and Structure of the P_2 Molecule, *Ann. d. Physik*, **15**, 677.

Jakowlewa, 1931, Fluorescence and Absorption Spectra of Phosphorus Vapour, *Zeits. f Physik*, **69**, 548.

Jenkins, 1935, Alternating Intensities in the Spectrum of P_2, *Phys. Rev.*, **47**, 783 (Letter).

Sastry, M. G., 1941, The Ultraviolet Band Spectrum of Mercuric Chloride and Bromide, *Proc. Nat. Inst. Sci. Indi.*, **7**, 351, 359.

INTENSITY-DISTRIBUTION IN MOLECULAR-SPECTRA: CLASS I SYSTEMS OF HgCl AND HgBr

By M. G. SASTRY

(Received for publication, Dec. 11, 1942)

Plate III

ABSTRACT. Using the slit-width method and a calibrated quartz Kipp and Zonen standard ribbon lamp, the "peak intensities" have been determined for the bands of the Class I system of $HgCl^{35}$ and $HgBr^{31}$ lying in the region between λ2650 and λ2400. The transition probabilities for the various bands in each system have hence been derived. These experimental values have been found to agree with Condon's theoretical considerations. The Morse energy function was assumed for drawing the potential energy curves. The effective temperature of the source has been estimated assuming Maxwell-Boltzmann distribution.

INTRODUCTION

The intensity distribution in bands extending over long spectral regions is but little investigated and only in the case of a few molecules have quantitative data been obtained. Ornstein (1928), Elliot (1930), Johnson and Tawde (1932), and Tawde (1934) among others made accurate measurement of the intensities of certain band systems due to lighter molecules. Mercury chloride and mercury bromide are comparatively heavier molecules, giving rise to prominent band systems in the ultra-violet in the region between λ2700-2400 and quantitative estimate of the intensities of these are considered to be of value in relation to the Franck-Condon theory (Jevons). The present paper gives the results of such determination with respect to the Class I systems of these two molecules HgCl and HgBr.

EXPERIMENTAL

The intensity technique and the photographic procedure adopted in the present case are essentially the same as those used by Johnson and Tawde (1932). For work in the ultra-violet region in which the bands were situated, a quartz standardised ribbon lamp calibrated by a monochromater down to λ2400 and supplied by Kipp and Zonen was used. The bands were obtained in a discharge tube as described in the previous papers by the author (Sastry, 1941). Photographs were taken with a Hilger medium quartz spectrograph and Ilford special rapid plates were used throughout. With the usual precautions in adjusting the times of exposure and in developing the plates the grain effect is found negligible. Plates with varying times of exposure were used to calculate the intensities of the weaker as well as the stronger band heads. The calibration marks were given on the same plate using the slit-width method. The density marks and the spectrum are shown in Figs. 1 and 2 of Plate III.

Microphotometer curves were taken of the band system and of the different intensity marks, successively along the entire wave-length range on a single photographic sheet at a single setting of the microphotometer. The Curve corresponding to the spectrum was thus superposed on those corresponding to the intensity marks in an exact manner with respect to the wave-length. This special procedure considerably facilitated the evaluation of the densities at the

TABLE I

I and I/ν^4 values for $HgCl^{35}$

Weight	v' \ v''	0	1	2	3	4	5	6	7	8	9	10
1401.4	0	1000.0 401.7	1427.0 589.8	344.5 146.8	188.3 82.5	177.4 70.9	110.0 51.5	103.0 49.2	—	—	—	—
877.2	1	759.2 292.2	—	353.4 145.3	377.7 159.3	241.9 105.2	173.0 77.5	117.0 53.8	92.6 43.9	—	—	—
684.8	2	223.0 83.7	328.6 127.1	179.5 71.4	147.9 60.5	202.2 85.0	215.5 93.3	145.5 64.8	116.0 53.3	97.2 45.7	—	—
553.1	3	56.0 20.4	302.2 113.0	139.5 53.7	218.0 86.2	87.7 35.6	110.1 40.1	140.3 60.4	94.9 41.9	115.0 53.5	90.5 42.3	—
322.3	4	21.4 7.5	50.5 20.5	211.1 78.6	79.3 30.4	120.4 49.8	85.5 34.6	66.1 27.6	70.8 30.3	—	—	92.7 43.0
202.4	5	10.6 3.6	30.5 10.7	144.3 52.0	129.6 48.1	71.9 27.4	71.4 27.9	81.3 32.7	—	—	—	—
142.5	6	1.4 0.5	12.4 4.2	34.9 12.2	140.0 50.3	79.3 29.2	84.2 32.0	36.2 114.1	—	—	—	—
95.8	7	—	1.7 0.7	16.4 5.6	60.0 20.9	108.5 38.8	—	78.7 29.8	—	—	—	—
83.3	8		—	3.4 1.1	23.2 7.9	66.6 23.1	57.8 20.6	—	81.4 30.6	—	—	—
54.3	9	—	—	—	4.6 1.5	46.1 15.5	57.8 20.0	48.7 17.3	—	—	—	—
42.0	10	.	—	—	.	6.3 2.0	58.0 20.0	36.6 12.6	21.0 7.4	—	—	.
28.4	11	—	—	—	—	—	8.5 2.8	50.2 16.8	25.7 8.8	—	—	—
19.7	12		—	—	..	.		9.4 2.5	34.0 11.4	16.9 5.8	—	—
14.4	13	—	—	—	—	—	—	—	7.7 3.1	20.3 6.7	13.1 4.6	—
2.8	14	—	—	—	—	—	—	—	—	—	—	8.1 2.8

proper wave-lengths. A photograph of one such set of typical curves taken on a plate of HgCl is shown in Plate III, Fig. 3. The values of the optical density log (u/u_0) for the different steps are calculated for a particular wave-length, say λ, at which the band head is situated. In finding the true density of the band head at any point the density of the background of the photographic plate at that point is subtracted from that of the band head at the same point. Plotting the density values of the intensity marks against log I (where $I = E_\lambda d\lambda \times w$) the density curve was obtained. From this curve the intensity corre-

TABLE II

I/ν^4 and I values $HgBr^{81}$

Weight	v' \ v''	0	1	2	3	4	5	6	7	8	9
2720.0	0	1000.0 450.4	1420.0 652.8	1075.0 503.7	792.7 378.4	691.3 336.4	452.6 224.6	343.7 173.7		—	
2621.4	1	1535.0 676.1	738.9 331.3	—	671.4 312.9	839.9 399.0	762.6 369.1	651.2 321.0	422.4 212.0	—	—
2576.3	2	1058.0 455.0	769.5 337.7	945.0 422.1	527.3 240.0	266.5 123.2	075.8 177.5	652.2 313.9	515.8 302.1	410.5 205.0	—
2000.5	3	730.7 306.8	917.7 392.9	458.7 200.4	566.5 252.2	486.2 220.3	235.1 108.2	—	660.2 320.6	408.8 199.1	—
1629.9	4	449.4 184.8	1670.0 699.3	486.7 207.8	599.2 260.6	—	615.5 277.4	—		—	—
887.8	5	—	651.2 266.8	769.3 320.4	296.7 126.1	—	—	—	156.0 71.0	222.4 103.5	—
706.0	6	—	275.7 110.5	794.9 324.4	·	—	—	271.7 119.2	—	—	—
580.0	7	—	—	432.4 172.6	640.9 260.6	358.8 151.9	347.7 146.8	—	—	—	—
344.4	8	—	—	—	447.1 178.0	—	—	—	—		—
217.6	9	—	—	—	26.0 19.1	410.5 166.4	126.7 50.9	—	—	—	—
141.5	10	—	—	—	—	304.9 156.6	263.8 104.2	—	—	—	—
125.1	11	—	—	—		95.9 37.3	225.0 87.1	96.6 38.0	·		—
151.7	12	—	—	—	—	—	188.7 71.6	207.6 80.1	—	—	—
160.5	13	—	—	—	—	—	—	199.0 75.3	221.4 85.2	·	—
140.1	14	—	—	—	—	—	—	—	204.8 77.3	163.6 62.8	—
53.5	15	—	—	—	—	—	—	—	—	53.15 19.96	86.9 33.3

TABLE III

Transition Probabilities, HgCl

v' \ v''	0	1	2	3	4	5	6	7	8	9	10	11
0	.29	.42	.11	06	.04	04						
1	.33	.	.17	.18	12	.09	06	.05				
2	.12	.19	.10	.09	12	.14	09	08	.07			
3	.04	.20	.10	16	.06	.08	.11	08	09	.08		
4	.02	06	.24	09	15	.11	.09	.09	—	—	.15	
5	.02	.05	26	.24	.13	.14	16					
6	.	.05	.09	35	20	.22	.09					
7	—	.00	.06	22	.41	—	.31					
8			01	.09	28	25	—	.37				
9				.03	29	37	32					
10					.05	48	30	.18				
11						.10	.59	.31				
12							.13	.58	.29			
13								[illegible]	.47	32		
14											1.0	

TABLE IV

Transition Probabilities, HgBr

v' \ v''	0	1	2	3	4	5	6	7	8	9	10	11	12
0	17	.26	19	14	12	08	.06						
1	.26	.15	-	.12	.15	.14	.12	.08					
2	.18	.13	16	.09	.05	.07	.12	.12	08				
3	.15	.20	.10	.13	.11	.05	—	.16	10				
4	11	.43	.13	.16	—	.08							
5		.30	.36	.14	-	-	—	.08	.12				
6		.16	.46	—	.22	—	.17						—
7			.30	.45	-	.25							
8			.	.52	.48								
9				.05	.57	.23							
10					.26	74							
11						.70	.30						
12						.47	.53						
13							.47	53					
14								.55	.45				
15									.37	.44			

sponding to the density of the band head at λ was read off. On account of the rapidly varying sensitivity of the plate it was found necessary to plot a separate density curve for each wave-length at which a band head was situated and as many curves were drawn as there were band heads whose intensities had to be determined.

The final values of the intensities thus obtained for all the band heads of the Class I systems of HgCl are shown in Table I on the scale of 1000 for the (0,0) band. Table II gives similar values in the case of HgBr.

Immediately below the numbers denoting the intensities in the above tables are given the I/ν^4 values of the bands, ν being calculated from the vibration constants given at the end.

The $\Sigma \frac{I}{\nu^4}$ values corresponding to the initial state v' are given in the same tables under column "Weight." The quotient of the I/ν^4 values of any band and the "Weight" of the initial state represents the transition probability. These probabilities are given in Tables III and IV for HgCl and HgBr.

THEORETICAL

The potential energy curves (Figs. 4 and 5) drawn to scale for the upper and

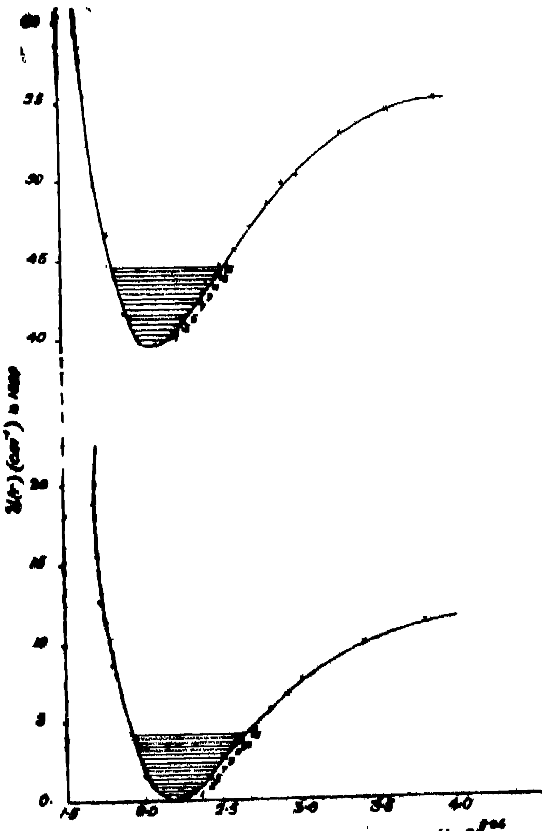

Fig. 4 Potential Energy Curve HgCl

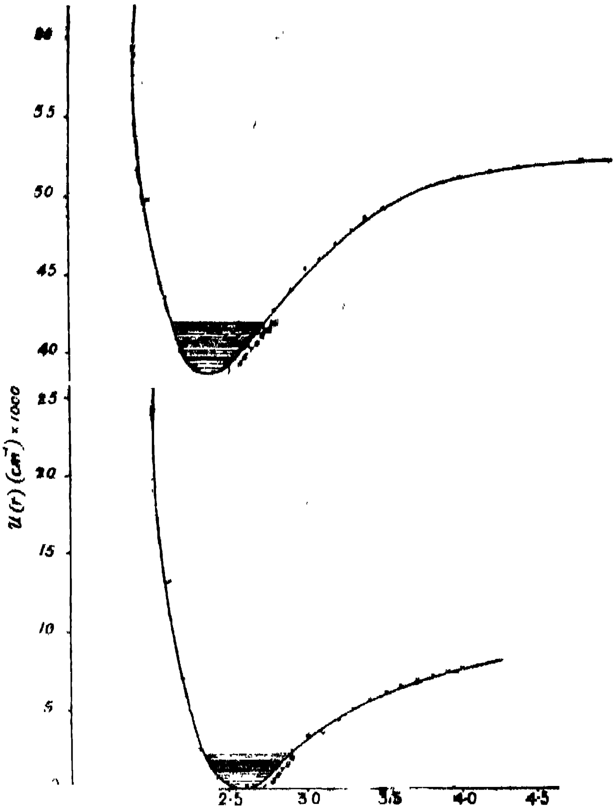

Fig 5. Potential Energy Curve $HgBr^{81}$

lower states involved in the emission of the Class I systems of $HgCl^{35}$ and $HgBr^{81}$ are drawn with the aid of the Morse function

$$U(r) = D_e\left[1 - e^{-a(r - r_e)}\right]^2$$

in which the constants (Sastry, 1941) are found to be for HgBr

$D'_e = 13740$ $a' = 1.81$ $r'_e = 2.36$

$D''_e = 8863$ $a'' = 1.83$ $r''_e = 2.53$

and for HgCl

$D'_e = 17040$ $a' = 1.75$ $r'_e = 2.06$

$D''_e = 12660$ $a'' = 1.74$ $r''_e = 2.17$.

The vibrational constants employed in the above calculation are given below (Wieland, 1927).

	$HgCl^{35}$	$HgBr^{81}$
ν_e	39700·5	38754·4
ω'_e	341·4	228.5
$x'_e\omega'_e$	1.71	·95
ω''_e	292·5	186.5
$x''_e\omega''_e$	1.69	·975

From these curves, the parabola representing the maximum probability of transition was derived by the graphical method suggested by Condon (Jevons, p. 70). This parabola is superposed in its correct position on the data given in Tables III and IV for HgCl and HgBr. In the case of HgCl the parabola is narrower than HgBr and the distribution agrees well with the experimental values.

In HgBr the parabola is slightly out of step with the experimental values. This might be due to the superposition of the unresolved isotopic band heads, which in the case of bromine are of equal intensity the abundance ratio of the Br^{79} and Br^{81} being 1 : 1. More probably it is due to the inadequacy of the Morse function.

A peculiar feature that is noticed in the theoretical derivation of the parabola in both band systems is that one arm is developed more than the other: this feature is in very good agreement with experiment which shows distinctly that the sequences of bands in both HgCl and HgBr towards the violet end are better developed than towards the red.

EFFECTIVE TEMPERATURES

The first column in Tables I and II gives the number of molecules in the various initial vibrational states. Assuming that this is a distribution in thermal equilibrium at temperature T of the source, we have, according to Maxwell-Boltzmann,

$$N = N_0 e^{-E_v/kT}$$

so that

$$hc\left[\omega'_e(v'+\tfrac{1}{2}) - x'_e\omega'_e(v'+\tfrac{1}{2})^2\right] = kT.\log_e\frac{N_0}{N'_{v+\frac{1}{2}}}$$

Substituting the various constants for $HgCl^{35}$ system

$$341.1(v'+\tfrac{1}{2}) - 1.71(v'+\tfrac{1}{2})^2 = 1.6083\,T\log_e\frac{N_0}{N'_{v+\frac{1}{2}}}$$

The numbers N_0 and $N'_{v+\frac{1}{2}}$ are given by the 'Weights' corresponding to the respective initial vibrational levels. Plotting the vibrational energy against the ratio $\log_e\frac{N_0}{N'_{v+\frac{1}{2}}}$ the absolute temperatures are obtained directly. The effective temperatures thus derived in the case of HgCl is about 1500Å and for HgBr 1800Å.

The author desires to express his very grateful thanks to Prof. K. R. Rao for his kind interest and guidance during the course of this work, and to the Andhra University for the award of a research fellowship.

ANDHRA UNIVERSITY,
GUNTUR.

REFERENCES

Elliot, 1930, *Dissertation Utrecht.*

Jevons, *Report on Band Spectra.*

Johnson and Tawde, 1932, *Proc. Roy. Soc. Lond. A.*, **137**, 575.

Ornstein *et al*, 1928, a number of papers in *Proc. Phy. Soc.* (*London*) *and publications* (*Utrecht*).

Tawde, 1934, *Proc. Phys. Soc. Lond.*, **46**, 324.

Sastry, 1941, *Proc. Nat. Inst. Sci.* (*India*), **7**, 351 and 359.

Wieland, 1927, *Helv. Acta Phys.*, **2**, 46 and 77.

THE BAND SPECTRUM OF PHOSPHORUS—PART II : ALTERNATING INTENSITY AND NUCLEAR SPIN

By K. NARAHARI RAO

(*Received for publication, March 5, 1943*)

Plate IV

ABSTRACT. Elaborate quantitative measurements have been made of the alternating intensities of the rotational structure lines in the case of the bands (5,21), (5,18), (9,21), and (6,22). The (5,21) band alone gave the anomalous value 3.3 while for the others, the ratio on an average is 3.0. Such a high value (3.4 to 3.5) was obtained for this band also by Jenkins (1935). But the anomaly cannot be ascribed to any effect of perturbations, as the (5,18) band does not show the anomaly and the rotational structure has not revealed any perturbations. The intensity ratio leads to a value of $\frac{1}{2}h/2\pi$ for the nuclear spin of phosphorus as determined by Ashley (1933) and Jenkins (1935).

From a study of the rotational structure of the bands of phosphorus involving the level $v'=5$, the author has considered in a previous paper (Rao, 1943) the possibility of a perturbation of rotational lines associated with the initial vibrational level 5 which has been reported by Herzberg (1932) to show strong perturbations. The present part deals with the determination of the alternating intensities of the lines in the bands (5,21), (5,18), (9,21) and (6, 22) in relation to the nuclear spin of phosphorus. Two of the above bands chosen for study have the initial vibrational level 5. As such, the results of the determination of the alternating intensity ratio of the above bands throw light on the question of perturbation of the level $v'=5$. The method employed for determining the intensities of the lines is a direct one using a standardised quartz lamp and varying slit widths.

EXPERIMENTAL

The experimental arrangement for exciting the bands is the same as that described in the previous paper of the author. The phosphorus bands were photographed with a quartz Littrow spectrograph on Ilford Special Rapid plates. With the usual precautions in adjusting the times of exposure and in developing the plates, the grain effect is found to be negligible.

For the purpose of deriving the blackening-intensity curves of the plate at any wavelength, density marks were given with varying slit widths on the same plate as the one utilised for recording the band spectrum of phosphorus. The slit is calibrated by a Hilger photo-measuring micrometer. The slit widths employed were 0.10, 0.25, 0.63 and 1.58 mms. The slit of the spectrograph was directly illuminated from a distance of about half a metre by a quartz standardised lamp, calibrated at Utrecht. The lamp was run on 220 volts D.C.

from high-capacity batteries and a steady current of 16 amperes was sent. The exposures for the density marks were 25 minutes each. (Plate IV.)

The calibration curve of the lamp gave the relation $E_\lambda : \lambda$ in the spectral region investigated and for the current at which the lamp was worked (*i.e.*, for the corresponding temperature of the filament). The value of $E_\lambda : \lambda$ for the regions investigated have been given in the tables supplied by the manufacturer along with the lamp. From these values and the dispersion curve $d\lambda/dm : \lambda$ of the quartz spectrograph (drawn separately) a curve is drawn in two different regions between $E_\lambda/d\lambda/dm$ and λ appropriate to the standard lamp (at the temperature at which it is worked) used in conjunction with the particular spectrograph employed.

The energy falling over a given region of the plate at any wavelength is given by E_λ $(d\lambda/dm)$ W where W is the slit-width.

Microphotometer curves were taken for the band system under study and of the different intensity marks successively on a single photographic sheet at a single setting of the microphotometer. Forty-nine times magnified microphotometer records are obtained separately for the individual bands. The curves corresponding to each band in the spectrum are thus superposed on those corresponding to the intensity marks in an exact manner with respect to the wavelength. This special procedure considerably facilitated the evaluation of the densities at the proper wavelengths. The curve of the (5,18) band is given in Fig. 1 as an illustration.

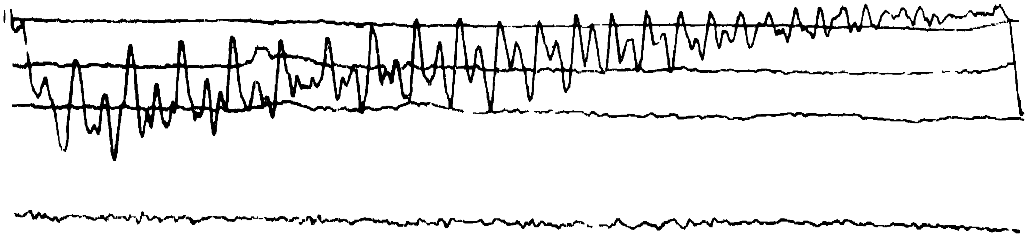

(5,18) band (P_2 molecule)

FIG. 1

The values of the optical density log (u_0/u) ('u_0' being the perpendicular distance of the zero line to the blank plate line and 'u' the distance from the zero line to the point corresponding to which the intensity is required to be evaluated) for the different steps and the line (whose intensity is required) are calculated for a particular wavelength, say λ_1, at which the line under study is situated. The density is plotted against log I (where $I = E_\lambda . d\lambda/dm . W$) From this curve, the intensity corresponding to the density of the line is read off. On account of the variation of sensitivity of the plate, a separate density curve for each wavelength at which a line is situated has to be drawn. As many curves are to be drawn as there are lines whose intensities are to be evaluated. Here each band extends to about 10 Angstrom units at the most.

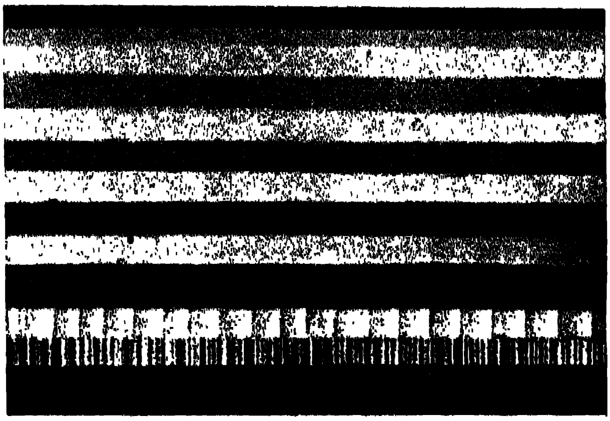

So in order to minimise the more laborious and tedious calculations one curve is drawn for each band and the intensities of all the lines in the band are read off from that curve.

The intensities thus obtained for all the lines in the band are corrected for the continuous background. The intensity at the depression just preceding the peak corresponding to a particular line is subtracted from the peak intensity to get the actual value of the intensity of the line correcting for the background.

In this manner, the intensities of all the lines (strong and weak) in each band are evaluated. (The influence of frequency in not considered as it does not affect the alternating intensity ratio.) In a particular band the ratio between the sum of all the intensities of the strong lines and that of an equal number of the weak lines lying in between the two gives the mean ratio of the intensity of the strong to the weak lines. This process is utilised for the determination of the mean ratio to minimise errors due to the blends of the P and R branches.

In evaluating the ratio for the various bands those portions of the spectrum only where the structure is well open are chosen. A final value of the ratio of the strong to the weak lines is obtained by finding out the average of the values determined for individual bands.

A large number of plates (more than forty to fifty in all) were taken varying the times of exposures of the standard lamp and the discharge through phosphorus and an equally large number of microphotometer records were also made for the different bands. Only those plates for which the microphotometer record of the lines in the band lies in between the curves for the density marks are utilised for calculating the intensities in the manner indicated above. Great care is taken to see that such developer and hypo solutions are used which are filtered free from dust particles, the developer being of uniform standard in strengths for all the plates. The values obtained for the bands studied are shown in the table given below :

Bands v', v''	Alternating intensity ratio
5,21	3.3
5,18	3.0
6,22	3.1
9,21	2.9
	Average of the last three values is 3.0

The table of alternating intensity ratios given above shows that the intensity ratio is approximately 3.0 for all the bands with the exception of (5,21) which gives a higher ratio. But that this is not due to any effect of strong perturbation (reported by Herzberg as associated with the vibrational level $v'=5$) is obvious as the (5,18) band does not give an anomalous value. The larger value of the (5,21) band must be ascribed to the probable overlapping of a fainter band which has given rise to a difficulty in elucidating the rotational structure.

NUCLEAR SPIN

It is known that the ratio of the intensity of the strong to that of the succeeding weak line in the case of the rotational structure of the bands due to the symmetrical molecules is given by the expression $(I+1)/I$ where I is the spin moment of the nucleus. The experimentally determined ratio 3.0 for the P_2 molecule obtained in the above investigation leads to $I=\frac{1}{2}$, the same as that arrived at by Asley (1933) and Jenkins (1935).

The author is indebted to Dr. K. R. Rao for his advice and guidance in the course of these investigations.

Solar Physics Laboratory,
Kodaikanal.

REFERENCES

Ashley, 1933, *Phys. Rev.*, **44**, 919.
Jenkins, 1935, *Phys. Rev.*, **47**, 783.
Herzberg, 1932, *Ann. der Phys.*, **15**, 677.
Rao, K. Narahari, 1943, *Ind. J. Phys.*, **17**, 135.

DIPOLE MOMENTS OF THE CHIEF CONSTITUENTS OF LAC AND ROSIN

BY G. N. BHATTACHARYA

(Received for publication, March 22, 1943)

ABSTRACT. Dipole moment of abietic acid, the chief constituent of rosin, has been determined from measurements on its dilute solutions in 1, 4 dioxane. Similar measurements have also been made on dilute dioxane solutions of pure lac resin (reinharz) and soft lac resin, the two main constituents of lac. The temperature of measurements was 25°C for all of them. The values obtained for the dipole moment of abietic acid, soft lac resin and pure lac resin are 1.35, 4.61 and 7.45 Debye units respectively.

INTRODUCTION

Rosin and lac are two very important natural resins. The chief constituent of rosin is abietic acid and it forms more than 90% of American rosin (Ellis, 1935). Considerable work has been done on the constitution of abietic acid by various investigators (Tschirch and Studer, 1904; Ruzicka and Meyer, 1922; Haworth, Letsky and Marvin, 1932; Bardhan and Sengupta, 1932) and there is still some minor controversy on the position of two double bonds and the carboxyl group regarding the structure proposed by Ruzicka and his co-workers (Ruzicka, Ankersmit and Frank, 1932; Ruzicka, Waldmann, Meier and Hösli, 1933). But the empirical formula $C_{20}H_{30}O_2$ for this acid has been established now. Shellac, however, has been shown to consist of two main fractions regarding its solubility in diethyl ether. The fraction which is insoluble in ether has been termed 'Reinharz' or 'Pure lac resin' or 'α-lac', and has been shown by Palit and Bhattacharya (1939) to consist entirely of a dibasic acid of molecular weight 1900. By treating this pure resin with very strong caustic alkali (5N KOH) and then decomposing the potassium salt with dilute sulphuric acid a white crystalline acid was obtained by Harries and Nagel (1922). This acid has been termed aleuritic acid and its constitution has been definitely established as 9, 10, 16 tri-hydroxy-palmitic acid by these authors. Dialysis experiments (Palit, 1939) with shellac solutions in alcohol have shown that soft resin and pure resin of lac are separate bodies and further experiments with these fractions showed that they could not be further fractionated. This fact shows that pure lac resin or soft lac resin is not a mixture of substances of varying molecular weights, as was previously considered (Verman and Bhattacharya, 1934; Shaeffer, Weinberger and Gardner, 1938; Shaeffer and Gardner, 1938), but that they are most probably homogeneous bodies. The structure of pure lac resin, however, is not yet known but a few tentative proposals have been put forward by a few workers from time to time.

The ether-soluble fraction of shellac which is often called soft lac resin or simply 'soft resin' from its tarry consistency has been shown by Palit and Bhattacharya (1930) to consist of a monobasic acid of molecular weight 530. Subsequent work at this Institute (1940) on the constitution of this fraction of lac showed that the molecule has one hydroxyl group and one carboxyl, and probably the empirical formula is $C_{31}H_{56}O_5$. It is apparent therefore that these substances cannot be included in the category of those whose structures have been established beyond doubt except perhaps abietic acid. Nevertheless the object of undertaking the dielectric study of these substances lies in the search for a very satisfactory explanation of the anomalous solubility of these substances in some of the organic solvents. Palit (1940) has very recently put forward an explanation for this anomalous solubility from a study of the solubility of a few natural resins in different mixed solvents. It has been observed in that connection that many of the non-solvents for a particular resin may be rendered good solvents for the same by adding some 'polar-helpers' to those non-solvents. From the current conceptions regarding solvation of large molecules and subsequent dissolution (Sheppard, Carver and Houck, 1928; Hildebrand, 1936) it may be inferred that either the molecules of these resins are themselves polar in nature or the different constituent bodies act as polar substances towards these mixed solvents, the polar-helpers thus acting as solubilisers. The determination of dipole moments of the chief constituents of rosin and lac is therefore of considerable interest. In a previous paper the author (Bhattacharya, 1942) has reported the results of dipole measurement on aleuritic acid and its alkyl esters in dioxane. The high value of electric moment of aleuritic acid reported in that paper has given impetus to carry on the work further. But the extreme difficulty which is attendant with the purification of such resinous substances must not be under-estimated. The process of purification of abietic acid or aleuritic acid by repeated crystallisation, though laborious and very tedious, must be considered a simple matter when compared with the process of purification of the constituents of lac resin, *viz.*, pure resin and soft resin. Their purity cannot be checked by determining the melting point as is usually done in the case of crystalloids and the determination of the refractive index was also a meagre help in this matter. The elimination of other constituent bodies from a particular sample leaving only the desired fraction was the only process which was resorted to with extreme carefulness in these purification methods.

Wilson and Wenzke's (1934) finding that the solvent 1, 4 dioxane when used for the determination of electric moments gives correct values of moments of fatty acids had led many workers to use this solvent subsequently for the same purpose. The same solvent has been used in these experiments also, and it is perhaps the only suitable solvent for lac constituents.

PREPARATION OF MATERIALS

Dioxane.—The dioxane used in these experiments was American produce bottled by A. Boake Roberts & Co., Ltd., of England and was purified according to the method already described in a previous paper (Bhattacharya, 1942). The various physical constants of the material are as follows:

$$\text{F.P.}=11^\circ.6\ \text{C},\ n^{25}=1.4198,\ d^{25}=1.0282,\ \epsilon^{25}=2.2024.$$

Abietic acid.—Abietic acid manufactured by J. D. Riedel—E. de Häen A. G. of Germany was recrystallised six times from dilute methyl alcohol. After four crystallisations, the melting point of the sample became practically constant at 160°C. After two more crystallisations the sample was finally washed with the same dilute alcohol which was being used for crystallisation and it was dried in a vacuum-desiccator. Typical clusters of abietic acid crystals were obtained after a few crystallisations. The sample was then kept under vacuum to avoid oxidation.

A second sample was also used by crystallising twice from dilute methyl alcohol abietic acid obtained from American wood rosin by the method of Steele (1922). The two samples, however, gave practically the same values of polarisation.

Pure lac resin.—Pure lac resin (Reinharz) of about 92-95% purity was first prepared according to the method suggested by Palit (1942). It was powdered, mixed up with silver sand and then extracted with diethyl ether in a soxhlet apparatus for the removal of final traces of soft resin. Finally the sample was extracted with petroleum ether in the same soxhlet apparatus for the removal of any trace of shellac-wax that might have been left. The criterion of the final stages of soxhlet extraction was obtained from the complete evaporation of a few drops of the extracted liquid from a clean glass slide without leaving any stain on it. When this was achieved, the resin was dissolved in alcohol, filtered free from sand, precipitated again from a large volume of distilled water and then drawn into fibres on softening from the boiling water. These fibres were dried in air, powdered in a mortar and then finally dried in a vacuum-oven at 40°C.

Soft lac resin.—Soft lac resin was first obtained by soxhlet extraction with ether from kusmi shellac. This soft resin was then dissolved in pure ethyl acetate and boiled with decolourising charcoal to remove any colouring matter. The resin was then boiled with petroleum ether under a reflux vigorously stirring from time to time. Petroleum ether was renewed several times till this liquid evaporated on a clean glass slide without leaving a stain. The resin was then heated at 105°C in a vaccum-oven in order to free it from any adherent solvent.

EXPERIMENTAL

The experimental cell was made of pyrex glass according to the design of Sayce and Briscoe. The apparatus and the method used has been described previously (Bhattacharya, 1942).

Density measurements were made with a pyknometer of approximately 25 cc. capacity and the refractive index measurements were carried out with a Zeiss-Abbe Refractometer according to the method suggested by the author in a previous paper (Bhattacharya, 1940).

All the measurements were carried out at 25°C.

SYMBOLS

The symbols used in the equations and tables are : w, the weight fraction of the solute; d^{25}, the density of the solution at 25°C ; ϵ, the dielectric constant of the solution. P_1, the polarisation of the solute ; P_∞, the polarisation of the solute at infinite dilution ; MR_D, the molar refraction for the sodium D-line ; μ, the dipole moment ; T, the absolute temperature ; p, the specific polarisation ; p_2, the specific polarisation of the solvent ; p_{12}, the specific polarisation of the mixture or solution, M_1, the molecular weight of the solute.

CALCULATIONS

Polarisations were calculated using Sugden's formula (Sugden, 1934) for specific polarisation instead of molar polarisation,

$$p=\frac{\epsilon-1}{\epsilon+2}\cdot\frac{1}{d}.$$

The total polarisation is calculated from the relation,

$$P_1=M_1\left(p_2+\frac{p_{12}-p_2}{w}\right).$$

Polarisations at infinite dilutions were obtained by employing the graphical extrapolation method using P_1—w curves.

Molar refraction for abietic acid was calculated as the sum of the atomic refractions (Swietonslawski, 1920 ; Getman, 1937) for the sodium D-line. For pure lac resin and soft resin, however, the electronic polarisations were calculated from refractive index measurements.

The contributions of the atomic polarisations to polarisations at infinite dilutions were neglected. The dipole moments were calculated from the relation,

$$\mu=.0127\times10^{-18}\sqrt{(P_\infty-MR_D)T}\ .$$

ACCURACY

Density measurements may be considered to be accurate to 0.01%, Dielectric constant values are probably accurate to 0.03%.

RESULTS

TABLE I

Dielectric constants, densities, weight fractions and polarisations
Solvent—Dioxane

Abietic acid				*Soft lac resin*				*Pure lac resin*			
w	d	ϵ	P_1	w	d	ϵ	P_1	w	d	ϵ	P_1
0.000000	1.0281	2.2024	—	0.000000	1.0281	2.2024	—	0.000000	1.0281	2.2024	—
0.004012	1.0284	2 2062	126·9	0 003060	1.0283	2.2188	575	0.003310	1.0284	2.2155	1647
0.004732	1.0284	2.2065	124·2	0.006175	1.0284	2.2357	577	0.007153	1.0290	2.2308	1618
0.008193	1.0286	2.2101	127·1	0.010338	1.0286	2.2559	556	0.008824	1.0292	2.2382	1641
0.012087	1.0289	2.2143	128·5	0.015948	1.0290	2.2862	557	0.012723	1.0296	2.2569	1702
0.016954	1.0293	2.2196	129·1					0.018949	1.0301	2.2804	1652

TABLE II

Substance	n	d	$\frac{n^2-1}{n^2+2}\frac{M}{d}$
Pure resin ...	1.5240	1.172	495
Soft resin ...	1.4950	1.107	137

TABLE III

Substance	MR_D	P_∞	$\mu \times 10^{18}$
Abietic acid ...	88.7	126.7	1.35
Soft lac resin ...	137	580	4.61
Pure lac resin ...	495	1650	7.45

DISCUSSION

For abietic acid the molecular weight is 302, but no such exact figure is available for either pure resin or soft resin since the composition is not yet definitely known. But actual determination of the molecular weight both by the Rast method as well as by the F.P. method using dioxane (Bhattacharya and Sen, 1939) has yielded an average value of 1900 for pure resin and 520 for soft resin. These values have been taken in these experiments. For abietic acid the molar refraction was obtained from the constituent atomic refractions corresponding to the sodium D-line, taking the Ruzicka structure. Controversy on the position of the two double bonds or the carboxyl group, however, would not affect the value of its molar refraction at all. For pure resin and soft resin, however, the molar refraction has actually been determined from refractive index and density measurements. Density of pure resin has been determined to be 1.172 and of soft resin 1.107.

The value of moment obtained for abietic acid is only 1.35 Debye units. The structure of this acid as given by Ruzicka and his co-workers is as follows:

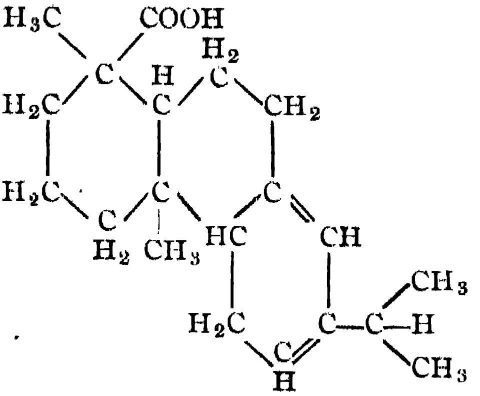

It is difficult to comment on the low value of dipole moment of abietic acid from its complex structure when so many unknown factors are present and to try to do so will be wild speculation. But we may reasonably assume from this value of moment and the formula $(CH_3)_2CH(CH_3)_2C_{14}H_{16}COOH$ that here the acid group provides the dipole. We are only concerned with the value of moment for the present.

Soft lac resin has given a value of 4.61 Debye units. Work at this Institute (1940) has revealed that a molecule of this resin contains one free hydroxyl, one free carboxyl, one lactone group and one double bond. The position of this hydroxyl or the carboxyl has not yet been finally ascertained but a tentative structure has been reported as follows :—

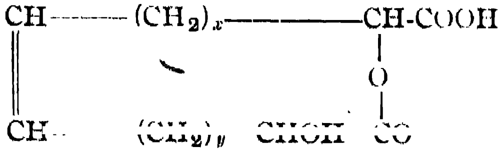

where $x+y=25$.

This structure gives 508 as the value of the molecular weight of soft resin, but for want of sufficient evidence, the average value obtained experimentally for soft resin, *viz.* 520, has been used. This uncertainty in the molecular weight values of pure and soft resins of lac will naturally make corresponding variation in the dipole moment values but that variation will probably remain within the limits of experimental error.

Pure resin of lac has been found to have a moment of 7.45 Debye units. Its constitution is still unknown but as has already been said on saponification with very strong caustic alkali it yields aleuritic acid whose constitution is now known. Harries and Nagel (1922) reported the isolation of another acid from pure resin which they named shellolic acid and to which they ascribed the empirical formula $C_{15}H_{20}O_6$. Research workers in India, England and America, however, failed to isolate this acid. Harries and Nagel consider that the resinous character of pure lac resin owes its origin to the splitting off of water from the molecules of aleuritic acid and shellolic acid forming lactides. Nothing more is known about the constitution of pure resin up till now.

Shellac as such was not used for the study of its dipole moment since shellac may be looked upon as a solid solution of pure resin in soft resin in the unimolecular proportion. This view may be arrived at from the following considerations:

(1) A simple alcoholic solution of shellac may be separated into its constituents, *viz.*, soft resin and pure resin, by dialysis. If shellac had been a homogeneous chemical compound this separation by such a simple physical process might not have been possible.

(2) Shellac can easily be separated into its constituents by simple extraction with solvents such as moist ether, ethyl acetate, etc.

(3) Average 'molecular weight' of shellac (if such a term is justified in the case of a mixture) as determined by Rast method using camphor or by the F. P. method using dioxane lies within 1000-1100, whereas pure resin and soft resin gives about 1900 and 520 respectively. It is also known that shellac contains about 70% of its weight of pure resin and 30% soft resin. Combining these two facts we can easily see that pure resin and soft resin are simply mixed up to form shellac. Thus, in one gm. of shellac, there are $\frac{0.7}{1900}$ gm. mol. of pure resin and $\frac{0.3}{520}$ gm. mol. of soft resin. That is, one gm. of shellac contains in all $\frac{0.7}{1900}+\frac{0.3}{520}$ gm. mol., or $\frac{934}{988}\times 10^{-3}$ gm. mol., if the individual molecules are in an uncombined state. The average 'molecular weight' of shellac, therefore, comes to be $\frac{988}{934}\times 10^{3}$ or 1058, *i.e.* 1060, say. The experimentally determined value for shellac also corresponds to near about this figure. The determination of dipole moment of shellac was therefore not undertaken as it is considered that its behaviour towards a solvent may be understood from the behaviour of its constituents.

It should be clearly understood, however, that polarity alone cannot give an idea of the intermolecular forces when a solute is placed inside a solvent, but that solvation is more probable when both the solute and the solvent are polar than when they are non-polar or even when one is polar and the other is not. For a better understanding of the dissolution phenomena of large molecules Coltof (1937) has recently shown that three actions, *viz.*, swelling, dispersion and ballast action of the solvents must be clearly understood. Even the same solvent behaves differently with different solutes. He thinks that the atomic groups in the solvent and solute molecules are responsible for this behaviour and a complete understanding of the behaviour of a large number of solvents towards a particular solute may lead to the making up of mixtures of non-solvents which are good solvents of the same solute. Polarity is certainly a very important factor in this behaviour, but any one physical constant such as dielectric constant, polarisability or the electric moment cannot be the only criterion for its solubility. The fact remains, however, that pure lac resin is more polar than the soft resin and that the polarity of abietic acid is of the order of a simple fatty acid.

ACKNOWLEDGMENT

It is a pleasant duty to acknowledge gratefulness to Dr. H. K. Sen, Director of this Institute, for his kind interest. Thanks are also due to my colleague, Dr. S. R. Palit, for kindly supplying me with a sample of abietic acid made from American wood rosin by the method of Steele.

Physical & Physico-Chemical Laboratories,
Indian Lac Research Institute,
Namkum, Ranchi (Bihar).

REFERENCES

Bardhan, J. C., and Sengupta, S. C., 1932, Resin acids, Part II Synthesis of retene *J.C.S.*, 2798.

Bhattacharya, G. N., 1940, A Note on the Refractive Index of Shellac, *Ind. J. Phys.*, **14**, 237; 1942, Dipole Moments of Palmitic Acid, Aleuritic Acid and Alkyl Esters of Aleuritic Acid, *Ind. J. Phys.*, **16**, 369.

Bhattacharya, G. N., and Sen, H. K., 1939, Dioxane as Cryoscopic Solvent for Shellac, *Proc. Ind. Sci. Cong.*, Part III, 100.

Coltof, W., 1937, Solubility Properties of some Highly Polymeric Substances, *Jour. Soc. Chem. Ind.* (*Trans.*), **56**, 363.

Ellis, C., 1935, Abietic Acid, *The Chemistry of Synthetic Resins* (Reinhold Pub. Corp.), Vol. 1, 764.

Getman, F. H., 1937, Specific and Molar Refractions, *Outlines of Theoretical Chemistry*, 86.

Harries, C., and Nagel, W., 1922, Aleuritic Acid, *Chem. Umschau.*, **29**, 135, and *Chem. Soc. Abs.*, **122** (i) 522, *Wiss. Veröffent Siemens—Konzern*, **1**, 178, Untersuchungen über die Schellolsäure, *Ber. der. Deut. Chem. Ges.*, **55** B, 3833.

Haworth, R. D., Letsky, B. M., and Marvin, C. R., 1932, Syntheses of Alkylphenanthrenes, *J. C. S.*, 1784.

Hildebrand, J. H., 1936, Polarity, *Solubility*, Chap. IV, 77.

Indian Lac Research Institute, 1938, Constitution of Shellac, *Annual Report*, 3, 1940, Constitution of lac-soft Resin, *Annual Report*, 5.

Nagel, W., 1927, Untersuchungen über die Natur des Schellacks : die Konstitution der Aleuritinsäure, *Ber. der. Deut. Chem. Ges.*, **60**, 605.

Palit, S. R., 1940, Physical Chemistry of Resin Solution, Part II, Nature of Resin Solutions in Organic Solvents, *Jour. Ind. Chem. Soc.*, **17**, 537; Physical Chemistry of Resin Solutions, Part I, Anomalous Solubility of Shellac and other Resins in Organic Solvents, *Jour. Ind. Chem. Soc.*, **17**, 308; 1942, A Simple Method for the Preparation of Pure Lac Resin, *Jour. Ind. Chem. Soc. Ind.* and *New Edn.*, **5**, 25.

Palit, S. R., and Bhattacharya, G. N., 1939, A Note on the Basicity and Molecular Weight of Shellac, *J. Ind. Chem. Soc.*, **16**, 258.

Ruzicka, L., and Meyer, J., 1922, Higher Terpene Derivatives, Part II, Abietic Acid, *Helv. Chim. Acta*, **5**, 315, and *Amer. Chem. Abs.*, **16**, 2500.

Ruzicka, L., Ankersmit, P. J, and Frank, B., 1942, Polyterpenes and Polyterpenoids, LXXIII, *Helv. Chim Acta*, **15**, 1289.

Ruzicka, L., Waldmann, H., Meier, P J, and Hösli, H., 1933, Polyterpenes and Polyterpenoids, LXXVIII, Position of the Carboxyl and Double Bond in Abietic Acid *Helv. Chim. Acta*, **16**, 169.

Shaeffer, B. B., Weinberger, H., and Gardner, W. H., 1938, Nature and Constitution of Shellac, Part XIII, *Ind. Eng. Chem.*, **30**, 451.

Shaeffer, B. B., and Gardner, W. H., 1938, Nature and Constitution of Shellac, Part XII, *Ind. Eng. Chem.*, **30**, 333.

Sheppard, S. E., Carver, E. K., and Houck, R. C., 1928, Plasticity and Solvation of Cellulose Esters, *Colloid Symposium Monograph*, Vol. 5, 243.

Steele, L. L., 1922, Abietic Acid and Certain Metal Abietates, *Jour. Amer. Chem. Soc.*, **44**, 1333.

Sugden S., 1934, The Dielectric Behaviour of Dipole Substances, General Discussions, *Trans. Farad. Soc.*, **30**, 720

Swietoslawski, W., 1920, Atomic Refractions, *Jour. Amer. Chem. Soc.*, **42**, 1945.

Tschirch. A, and Studer B., 1904, American Colophony, *J. C. S*, **86** (i), 79

Verman, L. Bhattacharya, R, 1934, Isolation of Pure Lac Resin, *Lond. Shel. Res. Bur. Tech. Paper*, 1, 9.

Wilson, C J., and Wenzke, H. H., 1934, Dipole Moment of Higher Fatty Acids, *Jour. Chem. Phys.*, **2**, 546.

ON THE AXIAL LENGTHS OF PHLOROGLUCIN DIHYDRATE CRYSTALS

By C. R. BOSE

AND

RANJITKUMAR SEN

(Received for publication, April 28, 1943)

ABSTRACT. The axial lengths of Phloroglucin Dihydrate crystals have been accurately determined. The values obtained are $a=6.740$ A.u., $b=8.090$ A.u., $c=13.604$ A.u. The axial ration determined from goniometric measurements of the crystal are $a:b:c :: .8334 : 1 : 3.366$. The density of the crystal is found to be 1.453 gms. per c.c

On examining the axial ratios of Phloroglucin Dihydrate crystal given in Groth's Chemische Kristallographie (Vol. IV, p. 89) and the ratios of axial lengths found from X-ray study (Banerjee and Ahmed, 1938) a discrepancy appeared which was much higher than the limits of accuracy usually attained in such experiments. So it was thought useful to repeat these measurements.

The axial lengths were measured from rotation and oscillation photographs in a cylindrical camera of diameter 8.3 cms. Both copper and iron K_α radiations from a Hadding tube were used for this purpose.

A small crystal was mounted successively with the three crystallographic axes parallel to the rotation axes by the help of a Czapski two circle theodolite goniometer. In order to eliminate uncertainties in the determination of the diameter of the camera due to want of axial symmetry of the camera if any, fine aluminium powder was dusted on the crystal. The diameter of the camera was thus determined accurately from the aluminium lines for each photograph separately. This also removes any error arising in the process of mounting the film in the camera.

To obtain the layer line distances, the distance between pairs of corresponding spots on two layers of the same order one above and one below the equatorial line was measured. Half of the mean of these distances was taken as the layer line distance for that order. The axial lengths were thus calculated separately from different layer lines for the three axes. The mean values of the axial lengths thus obtained were

$$a=6.744 \text{ A.U}, \quad b=8.093 \text{ A.U.}, \quad c=13.615 \text{ A.U.}$$

These values of the axial lengths were used for indexing the diffraction spots whose positions were accurately determined. Very accurate values of the axial lengths were thus obtained. Very small crystals were used so that the diffraction spots were appreciably small. With the help of the calibrated diameter of the camera the angles of reflection of these spots were calculated. The results of the measurements are given in Table I where the first column gives the indices of the planes, the second gives 2θ, the third and the fourth give d and $\frac{1}{d^2}$ or $\frac{h^2}{a^2}+\frac{k^2}{b^2}+\frac{l^2}{c^2}$ respectively, whence a, b and c have been calculated.

TABLE I

Planes	2θ	d	$\frac{1}{d^2}$	Axial lengths		
				a	b	c
600	86°36′	2.122	793	6.733	—	—
006	30°39′	2.264	.195	—	—	13.589
080	99°5′	1.012	.977	—	8.096	—
008	69°15′	1.702	.345	—	—	13.616
.00(10)	90°37′	1.361	.540	—	—	13.610
630	95°45′	1.039	.963	6.745	8.085	—
650	113°6′	.922	1.083			
290	124°48′	868	1.325	6.736	8.090	—
510	70°44′	1.320	.566			
401	54°45′	1.674	.357	6.746	—	13.595
400	54°19′	1.687	351			
402	56°7′	1.637	.373	—	—	13.615

Mean value of the axial lengths :—

$a=6.740$ A.U., $b=8.090$ A.U, $c=13.604$ A.U.

The crystals were also studied by a two circle theodolite goniometer. A few good crystals with well-developed faces were chosen and each was mounted successively with the three crystallographic axes vertical and the interfacial angle between the corresponding zone faces were measured by the horizontal circle. The mean values from the measurement of several crystals are given below :—

$$m : m\ (110) : (1\bar{1}0) = 79°32'$$

$$r : r\ (101) : (\bar{1}01) = 27°47'$$

The interfacial angles as quoted by Groth :—

$$m : m\ (110) : (1\bar{1}0) = 79°1'$$

$$r : r\ (101) : (\bar{1}01) = 27°8'$$

The axial ratio $a : b$ obtained from our measurement of the interfacial angle (110) : (110) came out to be .8324 : 1

The axial ratio $b : c$ obtained from the interfacial angle $(1\bar{0}1)$ came out to be 1 : 3.366

Thus from the interfacial angles we have :—

$$a : b : c :: .8324 : 1 : 3.366$$

The axial ratios from the X-ray measurements are

$$a : b : c :: .8333 : 1 : 3.362$$

The ratios from the Groths' quoted values are

$$a : b : c :: 8261 : 1 : 3\ 4172$$

The density of the crystal was determined by Retger's suspension method from a solution of zinc sulphate in water. Very small particles from flawless crystals were used. Several observations were taken and the mean value of the density was found to be 1.453 gms. per c.c. The number of molecules per unit cell thus came out to be 4. The density of the crystal was also calculated from the mean value of the axial lengths determined by us and was found to be 1.442 gms. per c.c.

Our grateful thanks are due to Prof. S. N. Bose for his kind interest in the work and to Dr. K. Banerjee for suggesting the problem and guidance.

DACCA UNIVERSITY.

REFERENCE

Banerjee and Ahmed, 1938, *Ind. Journ. Phys.*, **12**, 249.

ON THE THEORY OF PERFORMANCE OF WIDE AND ULTRA-WIDE BAND LATTICE TYPE CRYSTAL BAND-PASS FILTERS CONTAINING STABILISED NEGATIVE IMPEDANCE ELEMENTS

By S. P. CHAKRAVARTI

(Received for publication, April 18, 1943)

ABSTRACT. The paper relates to the theory of performance of wide and ultra-wide band lattice type crystal band-pass filter sections containing crystal, capacitance, inductance and stabilized negative impedance elements developed by the author elsewhere. One typical section of each of th eClasses I and II has been chosen for consideration.

The typical lattice section of Class I consists of a series resonant element in the series arm and a crystal (mounted between two electrodes) connected in series with a stabilised negative impedance element in the lattice arm. Five important cases have been considered. Nature of reactances in series and lattice arms for the five cases with their subcases has been investigated, and the possibility of attenuation peak and '' or waviness in total insertion-loss characteristics has been discussed. The lattice section has been reduced to an equivalent T-section for calculation purpose. Characteristic impedance and its nature have been discussed. The cut-off frequencies have been determined and the attenuation and phase constants of the section have been obtained.

The typical lattice section of Class II consists of a crystal (mounted between two electrodes) connected in parallel to a stabilised negative impedance element in the series arm and a crystal (mounted between two electrodes) connected in series with a stabilised negative impedance element in the lattice arm. Four important cases have been considered. Nature of reactances in series and lattice arms for the four cases with their subcases has been investigated. The lattice section has been reduced as before to an equivalent T-section. Characteristic impedance and its nature have been discussed. The cut-off frequencies have been determined and the attenuation and phase constants of the section have been obtained.

I. INTRODUCTION

The simplest type of crystal band-pass filter is the ladder section (Mason, 1934) consisting of crystal and capacitance elements which gives a small transmission band-width. By using a lattice section (Mason, 1934) employing crystal and capacitance elements, it is possible to get a larger band-width which is still much less than the requirement. Lattice section (Mason, 1934, 1937 ; Stanesby and Broad, 1939, 1941 ; Stanesby, 1942) using crystal, capacitance and inductance elements is capable of giving much larger band-width than the lattice section without the inductance element, but this still remains much narrower for majority of requirements of the modern communication systems. Besides, the use of inductance coils of comparatively lower 'Q' value gives large attenuation in the transmission band.

The author in a previous paper (Chakravarti and Dutt, 1940) developed wide band and ultra-wide band low-loss lattice type crystal band-pass filters containing crystal, capacitance, inductance and stabilised negative impedance elements. The characteristic impedance and total insertion loss characteristics of such lattice sections have been measured and the sharpness of cut-off on the two sides has been compared to that of lattice sections using crystal, capacitance and inductance elements.

The wide and ultra-wide band crystal band-pass filters so developed have considerable applications in several types of modern communication systems—for example, as band-pass filters in television and broad band carrier current systems and as band-pass filters and band-pass couplings in multi-channel radio telephone transmission and reception systems. By reducing the band-width to less or somewhat less than that required for the above communication systems (which is possible by the methods developed), they are capable of being utilized for various other useful purposes in short-wave and medium wave radio systems.

The present paper relates to further investigation regarding the performance of wide and ultra-wide band lattice type crystal band-pass filter sections (designated as Class I and Class II types in the author's previous paper) using crystal, capacitance, inductance and stabilized negative impedance elements.

II. WIDE AND ULTRA-WIDE BAND LATTICE TYPE CRYSTAL BAND-PASS FILTER SECTION—CLASS I

Consider a typical Class I lattice section in which a series resonant element (consisting of an inductance and a capacitance connected in series) is in the series arm and a crystal (mounted between two electrodes) connected in series with a stabilized negative impedance element is in the lattice arm [Fig. 1(*a*)]

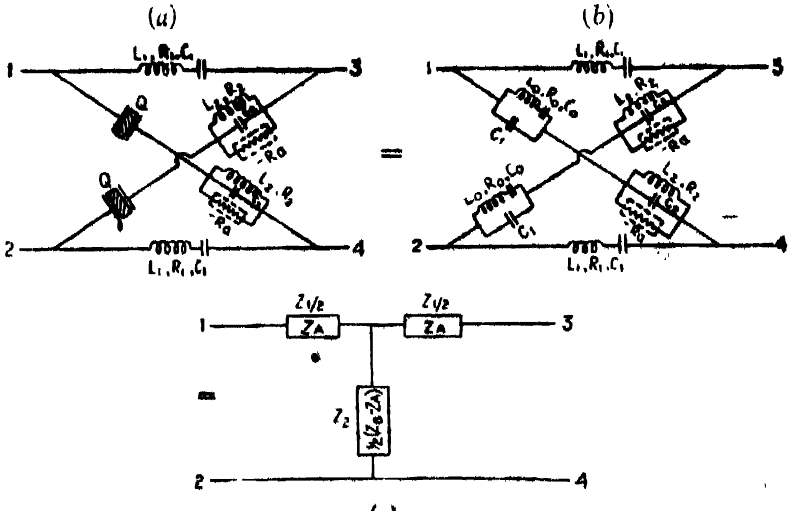
(*a*) (*b*) (*c*)

FIG. 1

1. DIFFERENT CASES

Five important cases may arise as follows—(1) in which the negative impedance element is detuned to the crystal frequency as well as to the resonance frequency of the series resonant element; (2) in which the negative impedance element is tuned to the resonance frequency of the series resonant element but the crystal frequency is different; (3) in which the negative impedance element is tuned to the crystal frequency but the resonance frequency of the series resonant element is different; (4) in which the series resonant element is tuned to the crystal frequency but the negative impedance element is tuned to a different frequency; (5) in which the negative impedance element is tuned to the crystal frequency as well as the resonance frequency of series resonant element.

Suppose F_1 = resonance frequency of the series resonant element (in the series arm), F_2 = resonance frequency of the parallel resonant element incorporated in the stabilized negative impedance element (in the lattice arm), f_0 = resonance frequency of the crystal (in the lattice arm), and F_0 = overall frequency (or anti-resonance frequency) of the crystal (in the lattice arm). Then in case (1) F_1, F_2 and F_0 (or f_0) are all different; in case (2) $F_1 = F_2$ but F_0 (or f_0) is different; in case (3) $F_2 = F_0$ (or f_0) and F_1 is different; in case (4) $F_1 = F_0$ (or f_0) and F_2 is different; and in case (5) $F_1 = F_2 = F_0$ (or f_0)

2. NATURE OF REACTANCES IN SERIES AND LATTICE ARMS

Fig. 2 shows the reactance-frequency characteristics of the series and lattice arms drawn for the five cases mentioned above. The curve marked I refers to the characteristic of the series resonant element in the series arm; the curve marked II_1 refers to that of the negative impedance element in the lattice arm, and the curve marked II_2 refers to that of the crystal (mounted between electrodes) in the lattice arm.

The nature of the reactance characteristic of the negative impedance element in the lattice arm follows from the following calculations. The impedance of the negative impedance element is given by

$$_N Z_2 = \frac{j\omega L_2 R_a}{R_a(1-\omega^2 L_2 C_2) - j\omega L_2} \quad \ldots \quad (1)$$

The reactance component of $_N Z_2$ can be shown to be

$$j_N X_2 = j . \frac{\omega L_2 R_a^2 (1-\omega^2 L_2 C_2)}{R_a^2 R_a^2 (1-\omega^2 L_2 C_2)^2 + \omega^2 L_2^2} \quad \ldots \quad (2)$$

$$= -j . \frac{L_2 C_2 \left(\omega L_2 - \frac{1}{\omega C_2}\right)}{C_2^2 \left(\omega L_2 - \frac{1}{\omega C_2}\right)^2 + \frac{L_2^2}{R^2}}, \quad \ldots \quad (2a)$$

on dividing both numerator and denominator by $\omega_2 R_a^2$.

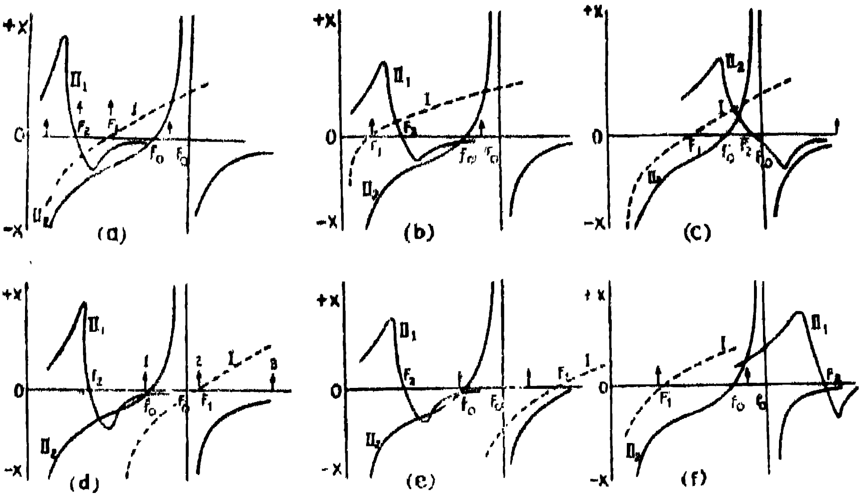

CASE (1) WHEN F_1, F_2, AND F_0 (OR f_0) ARE DIFFERENT.

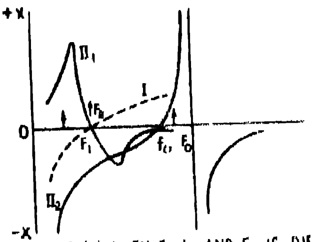

CASE (2) WHEN $F_1 = F_2$, AND F_0 IS DIFFERENT

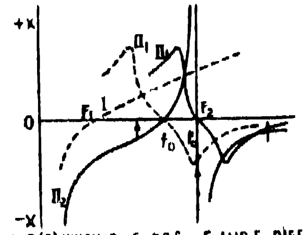

CASE (3) WHEN $F_0 = F_2$ OR $f_0 = F_2$ AND F_1 DIFFERENT.

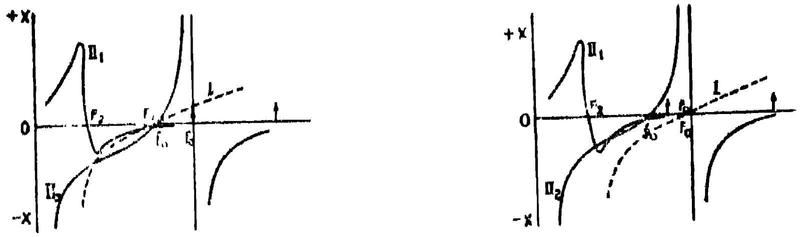

CASE (4) WHEN $f_0 = F_1$ OR $F_0 = F_1$ AND F_2 IS DIFFERENT

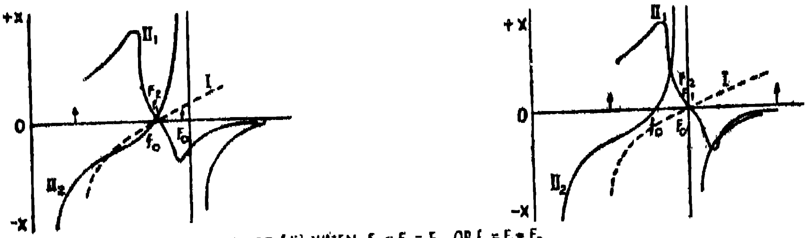

CASE (5) WHEN $F_0 = F_1 = F_2$ OR $f_0 = F_1 = F_2$

FIG. 2

•Assume that the total shunting capacitance C_2 has been kept more or less constant at a suitable value (*i.e.*, by means of an external capacitance) when h.f. voltage of varying frequency is impressed on the negative impedance element; that the resonance frequency of L_2-C_2 parallel combination associated with the negative impedance element is 'F_2' Mc/s. Therefore with h.f. voltage of varying frequency applied to the negative impedance element, the magnitude of the resistance component *only* has to be taken to change with ω according to the approximate relation $/R_n/ = \frac{m}{\omega^2}$ [found by the author elsewhere (Chakravarti and Das, 1943)] where m is a constant. Then

$$ {}_sX_2 = -\frac{L_2C_2\left(\omega L_2 - \frac{1}{\omega C_2}\right)}{C_2^2\left(\omega L_2 - \frac{1}{\omega C_2}\right)^2 + \frac{L_2^2}{m^2}\,\omega^4} \qquad \ldots \quad (3) $$

When $\omega < \frac{1}{\sqrt{L_2C_2}}$, $\omega L_2 - \frac{1}{\omega C_2}$ will be negative and hence ${}_sX_2$ will be positive; when $\omega = \frac{1}{\sqrt{L_2C_2}} = 2\pi F_2$, ${}_sX_2 = 0$; and when $\omega > \frac{1}{\sqrt{L_2C_2}}$, $\omega L_2 - \frac{1}{\omega C_2}$ will be positive and hence ${}_sX_2$ will be negative.

Starting from a point before F_2 as the frequency is increased the magnitude of the positive reactance has been found to increase till a frequency say $F_2 - f'$ and then to decrease rapidly to zero value at F_2. After the resonance frequency F_2 is passed, the reactance is of negative sign and its magnitude at first increases till a certain frequency say $F_2 + f''$ and then decreases to low value as the frequency is further increased. The form of the reactance curve is shown in Fig. 3.

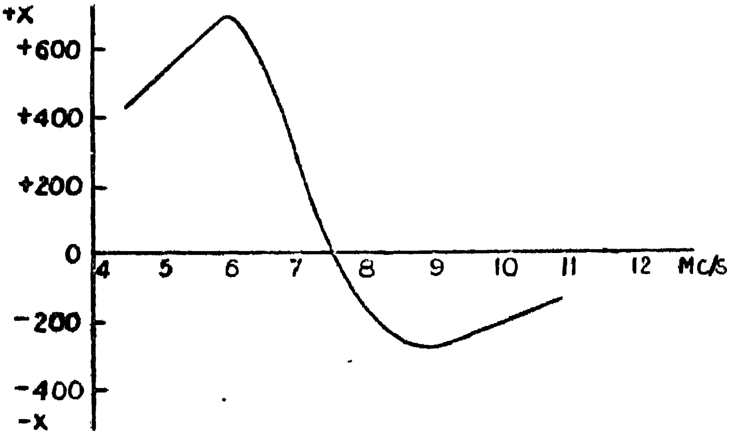

FIG. 3

The nature of the reactance characteristic of a typical negative impedance element can be seen from figures in Table I. $L_2 = 10 \times 10^{-6}$H; $C_2 = 44 \times 10^{-12}$F; $R_a = 2 \times 10^3$ ohms at 5 Mc/s, 1.4×10^3 ohms at 6 Mc/s, 0.9×10^3 ohms at 7.6 Mc/s, 0.8×10^3 ohms at 8 Mc/s and 0.68×10^3 ohms at 9 Mc/s, 0.5×10^3 ohms at 10 Mc/s and $F_2 = 7.6$ Mc/s roughly.

TABLE I

Frequency Mc/s	L_2C_2	$\omega L_2 - \frac{1}{\omega C_2}$	$C_2^2\left(\omega L_2 - \frac{1}{\omega C_2}\right)^2 + \frac{L_2^2}{R_a^2}$	$_NX_2$ ohms
5	440×10^{-18}	-406	3.25×10^{-10}	$+540$
6	440×10^{-18}	-223	1.40×10^{-10}	$+691$
7.6	440×10^{-18}	0	1.23×10^{-10}	0
8	440×10^{-18}	$+54$	1.76×10^{-10}	-135
9	440×10^{-18}	$+167$	2.63×10^{-10}	-279
10	440×10^{-18}	$+270$	5.6×10^{-10}	-213

It will be noted that such a variation of the reactance of negative impedance element as shown above added on to the typical variation of the reactance of a crystal agrees well with the variation of the measured value of total reactance 'X_2' in the lattice arm with frequency for the untuned case given in Fig. 8, on page 305 of the author's previous paper (Chakravarti and Dutt, 1940).

It will be seen from the reactance diagrams drawn for different cases in Fig. 2 that the performance of wide band and ultra-wide band band-pass filters depends not only upon the values of F_1, F_2 and F_0 (or f_0) but upon their location in the frequency spectrum with respect to one another.

Further, in all cases and sub cases the probable cut-off frequencies indicated on the diagrams are on the basis that the impedances in series and lattice arms are purely reactive. In actual practice the impedances have resistance components as well and the results get modified. For example, if the series resonant element in the series arm be taken to contain no resistance, it is evident that at F_1 the reactance is zero and Z_A (where Z_A is the total impedance in each series arm of the lattice section) is also zero. Hence the characteristic impedance of the lattice section becomes zero giving a cut-off frequency at F_1. On the other hand, if the series resonant element in the series arm has a resistance component, the characteristic impedance of the section at F_1 is not zero; and the total insertion loss characteristic will be characterised by reflection effects giving the 'effective cut-off frequency' somewhat different from F_1.

Take case (1) in which F_1, F_2 and F_0 (or f_0) are different. (*a*) shows the condition when $F_2 < F_1 < F_0$ (or f_0), and F_2 and F_1 are nearer to each other. It will be observed that the reactance in the series arm and the total reactance in the lattice arm are of the same sign between F_2 and F_1 with the magnitude of the latter reactance greater than that of the former and further the reactance in the series arm becomes zero at F_1. Consequently it can be expected that there will be large attenuation and/or waviness in the total insertion loss characteristic between F_2 and F_1. This condition may give rise to two band-pass filters having almost adjoining transmission bands or a single band-pass filter of larger band-width with waviness about F_1 according as the resistance component of the impedance in the series arm is negligible or has appreciable value and also according as F_2 is farther away or much nearer to F_1;

(*b*) shows the condition when $F_1 < F_2 < F_0$ (or f_0), and F_1 and F_2 are nearer to each other. The probable positions of cut-off frequencies are indicated by arrows. In this case the transmission band-width will be large and the cut-off will be equally sharp on both the sides. The total insertion loss characteristic over the transmission band is expected to be fairly even;

(*c*) shows the condition when $F_1 < f_0 < F_2 < F_0$, and F_1 and F_2 are nearer to f_0. The probable positions of cut-off frequencies are indicated by arrows. In this case the transmission band-width will be large and the cut-off will not be equally sharp on both the sides;

(*d*) shows the condition when $F_2 < F_0$ (or f_0) $< F_1$, and F_1 is nearer to F_0. The transmission band-width may be small as indicated by arrows 1-2, or may be large as indicated by arrows 1-3 with waviness in the total insertion loss characteristic about F_1. The sharpness of cut-off is expected to be unequal on the two sides;

(*e*) shows the condition when $F_2 < F_0$ (or f_0) $< F_1$, and F_1 is far away from F_0. This condition is expected to give small transmission band-width and the sharpness of cut-off may be more or less the same on both the sides ;

(*f*) shows the condition when $F_1 < F_0$ (or f_0) $< F_2$, and F_2 is far away from F_0. This condition may be suitable for wide and ultra-wide band band-pass filters. The nearer F_2 is to F_0, the larger will be the transmission band-width. The sharpness of cut-off is expected to be the same on the two sides.

Take case (2) in which $F_1 = F_2$, and F_0 or f_0 is different. This case refers to F_1 (or F_2) being less than F_0, but a similar diagram could be made for F_1 (or F_2) being greater than F_0. It will be seen that at F_1 (or F_2) the reactance of series arm becomes zero and the characteristic impedance will become zero unless modified by the resistance component of the series arm impedance. This condition may give rise to two band-pass filters having adjoining transmission bands or a single band-pass filter of larger band-width with waviness in the total insertion loss characteristic about F_1 (or F_2) for reasons given in (*a*) of case (1).

Take case (3) in which $F_0 = F_2$, or $f_0 = F_2$, and F_1 is different and less than F_2. It will be seen that when $f_0 = F_2$ the band-width is indicated by arrows (placed on the frequency axis). When $F_0 = F_2$ the band width is smaller and indicated by arrows (placed along the frequency axis at a lower level). The sharpness of cut-off is expected to be different on the two sides.

Take case (4) in which $F_0 = F_1$ or $f_0 = F_1$, and F_2 is different and less than F_1. It will be seen that when $F_0 = F_1$, or $f_0 = F_1$ the expected band-width may be more or less the same and is indicated by the arrows on the two diagrams. The sharpness of cut-off is expected to be different on the two sides.

Take case (5) in which $F_0 = F_1 = F_2$, or $f_0 = F_1 = F_2$. It will be seen that when $f_0 = F_1 = F_2$, the band-width (marked by arrows) is slightly smaller than when $F_0 = F_1 = F_2$. The sharpness of cut-off is expected to be similar on both the sides.

3. ON POSSIBLE ATTENUATION PEAK AND WAVINESS IN TOTAL INSERTION-LOSS CHARACTERISTICS IN CERTAIN CASES

If the reactances in series and lattice arms are of opposite signs and same in magnitude over the transmission band, the characteristic impedance in the transmission band is a pure resistance of magnitude same as that of one of the reactances. If Z_A and Z_B are the total impedances in each series and each lattice arms respectively, suppose $Z_A = +jX$ and $Z_B = -jX$. Then $Z_0 = \sqrt{Z_A Z_B} = \sqrt{X^2}$, so that the magnitude of characteristic impedance is $/X/$. When terminated by non-reactive impedance 'X', the reflection loss in the transmission band is zero and the total insertion loss or gain will be due to network loss or gain respectively.

If the reactances in series and lattice arms are of opposite signs but very much unequal in magnitudes, the characteristic impedance will be a pure resistance of value smaller or larger than $/X/$. When still terminated by non-reactive impedance 'X,' there will be reflection loss (depending upon the magnitudes of the impedances) to be added on to the network attenuation or gain.

If one of the reactances say in series arm is zero and the other one in lattice arm either of positive or of negative sign, the characteristic impedance is zero. When terminated by non-reactive impedance 'X,' there will be very large reflection loss giving a kind of attenuation peak in the total insertion-loss characteristic. This may be modified by the resistance component of the series arm impedance (if appreciable) since in that case the characteristic impedance will not be zero but will contain both resistance and reactance components.

If both the reactances are of the same sign and their magnitudes are nearly equal or unequal, the characteristic impedance is purely reactive. When terminated by a non-reactive impedance 'X,' there will be large reflection loss with reflection phase shift giving large attenuation as well as waviness in the total insertion loss characteristic. The condition discussed here is typical for the attenuation band of a band-pass filter.

The waviness in the total insertion loss characteristic due to reflection effects could be noticed in the curve for I(1)D type band-pass filter shown in Fig. 7 (page 304) of the author's previous paper (Chakravarti and Dutt, 1940).

4. EQUIVALENT T-SECTION OF THE ORIGINAL LATTICE SECTION

A general section (in which the negative impedance element is detuned to the crystal frequency as well as to the resonance frequency of series arm) is shown in Fig. 1(*a*) and its effective equivalent is shown in Fig. 1(*b*). Neglect R_1, R_0 and R_2, the resistance components in the various inductances.

If Z_A be the total impedance in *each* series arm and Z_B the total impedance in *each* lattice arm, then we have

$$Z_A = j\left(\omega L_1 - \frac{1}{\omega C_1}\right) \qquad \ldots \quad (4)$$

$$Z_B = \frac{-\dfrac{j}{\omega C_0}(1-\omega^2 L_0 C_0)}{1-\omega^2 L_0 C' + \dfrac{C'}{C_0}} + \frac{j\omega L_2 R_a}{R_a(1-\omega^2 L_2 C_2) - j\omega L_2} \quad \dots \quad (5)$$

For a crystal mounted between two electrodes,

$$\frac{C'}{C_0} = k \quad \dots \quad (6)$$

where 'k' is about 140 for the type of quartz crystal used by the author. The expression for Z_B can be simplified by putting $C_0 k$ for C' from (6) as follows :—

$$Z_B = \frac{-\dfrac{j}{\omega C_0}(1-\omega^2 L_0 C_0)}{1 + k - k\omega^2 L_0 C_0} + \frac{j\omega L_2 R_a}{R_a(1-\omega^2 L_2 C_2) - j\omega L_2} \quad \dots \quad (7)$$

Since '1' can be neglected in comparison to 'k' in the denominator of the first term on the R.H.S. of equation (7) without appreciable error

$$Z_B \simeq -\frac{j}{\omega C_0 k} + \frac{j\omega L_2 R_a}{R_a(1-\omega^2 L_2 C_2) - j\omega L_2} \quad \dots \quad (8)$$

Now since the lattice section in Fig. 1(*b*) is equivalent to the T-section in Fig. 1(*c*), the various results for the lattice section can be obtained from those of the equivalent T-section.

If Z_1 and Z_2 be the total series and total shunt impedances of the equivalent T-section respectively in Fig. 1(*c*), then (deducing from Figs. 24A and 24B, Appendix 'D,' page 281, of Transmission Circuits for Telephonic Communication by K. S. Johnson) we have

$$Z_1 = 2Z_A = 2j\left(\omega L_1 - \frac{1}{\omega C_1}\right) \quad \dots \quad (9)$$

$$Z_2 = \tfrac{1}{2}(Z_B - Z_A) = \tfrac{1}{2}\left[\frac{\omega^2 L_2^2 R_a}{R_a^2(1-\omega^2 L_2 C_2)^2 + \omega^2 L_2^2} - j\left\{\frac{1}{\omega C_0 k} - \frac{\omega L_2 R_a^2(1-\omega^2 L_2 C_2)}{R_a^2(1-\omega^2 L_2 C_2)^2 + \omega^2 L_2^2} + \left(\omega L_1 - \frac{1}{\omega C_1}\right)\right\}\right] \quad \dots \quad (10)$$

5. CHARACTERISTIC IMPEDANCE

The characteristic impedance 'Z_0' of the T-section is given by

$$Z_0 = \sqrt{Z_1 Z_2 + \frac{Z_1^2}{4}}$$

$$= \sqrt{\left(\omega L_1 - \frac{1}{\omega C_1}\right)\left[\frac{1}{\omega C_0 k} - \frac{\omega L_2 R_a^2(1-\omega^2 L_2 C_2)}{R_a^2(1-\omega^2 L_2 C_2)^2 + \omega^2 L_2^2} - \frac{j\,\omega^2 L_2^2 R_a}{R_a^2(1-\omega^2 L_2 C_2)^2 + \omega^2 L_2^2}\right]} \quad \dots \quad (11)$$

The imaginary term under the radical sign $\left|\dfrac{\omega^2 L_2^2 R_a}{R_a^2(1-\omega^2 L_2 C_2)^2 + \omega^2 L_2^2}\right|$ is a small fraction of the first real term $\left|\frac{1}{\omega C_0 k}\right|$ over a large frequency band, as it can be shown by the example given below. The second real term is much smaller than the first one. As ω increases, the first real term becomes smaller and smaller with the result that after a certain frequency limit the imaginary term becomes quite appreciable compared to it.

Take a typical wide band lattice section of class I having a comparatively smaller band-width so that $|R_a|$ could roughly be taken to vary from 2×10^3 ohms to $0{\cdot}8 \times 10^3$ ohms over the band under consideration. For this section suppose $F_1 = 5.0$ Mc/s, $f_0 = 7.17$ Mc/s, $F_0 = 7{\cdot}24$ Mc/s, $F_2 = 7.6$ Mc/s, $L_1 = 10 \times 10^{-6}$H, $C_1 = 101.6 \times 10^{-12}$F, $C_0 = .011 \times 10^{-12}$F, $L_2 = 10 \times 10^{-6}$H, $C_2 = 44 \times 10^{-12}$F, $|R_a| = 2 \times 10^3$ ohms at 5 Mc/s, 1.4×10^3 ohms at 6 Mc/s, 1.0×10^3 ohms at 7.3 Mc/s and 0.8×10^3 at 9 Mc/s and $k = 140$.

Then the ratio of the first real term to the imaginary term under radical sign in (11) is given by

$$N = \frac{1}{\omega C_0 k} \Big/ \frac{\omega^2 L_2^2 R_a}{R_a^2(1-\omega^2 L_2 C_2)^2 + \omega^2 L_2^2} = \frac{R_a^2(1-\omega^2 L_2 C_2)^2 + \omega^2 L_2^2}{\omega^3 C_0 L_2^2 R_a k}. \quad \ldots \quad (12)$$

It will be seen that $N = 135$ at 5 Mc/s, $N = 34$ at 6 Mc/s, $N = 17$ at 7 Mc/s, $N = 16$ at 7.3 Mc/s., and $N = 16$ at 9 Mc/s.

Hence the imaginary term may be dropped out in comparison to the real terms under the radical sign at least over the frequency range 5.0-9.0 Mc/s (the lower limit has been chosen from the consideration that at 5 Mc/s, Z_0 will be zero). Similar calculations can be obtained for almost all other sections of this class.

$$\therefore \quad Z_0 \sim \sqrt{\left(\omega L_1 - \frac{1}{\omega C_1}\right)\left[\frac{1}{\omega C_0 k} - \frac{\omega L_2 R_a^2(1-\omega^2 L_2 C_2)}{R_a^2(1-\omega^2 L_2 C_2)^2 + \omega^2 L_2^2}\right]} \quad \ldots \quad (13)$$

which is purely non-reactive and depends upon ω.

6. NATURE OF THE CHARACTERISTIC IMPEDANCE

$\omega L_1 - \frac{1}{\omega C_1}$ will be negative for values of $\omega < \frac{1}{\sqrt{L_1 C_1}}$; it will be zero for $\omega = \frac{1}{\sqrt{L_1 C_1}} = 2\pi F_1$ and will be positive for $\omega > \frac{1}{\sqrt{L_1 C_1}}$.

Therefore Z_0 will be pure reactance for frequencies less than F_1, it will be zero at F_1 and will be almost pure resistance between F_1 and a frequency f_2 since the reactance component will be negligibly small between these limits. At frequencies greater than f_2, the reactance component of Z_0 becomes appreciably large compared to the resistance component and hence Z_0 becomes an impedance of more and more reactive nature.

The characteristic impedance of the wide band section mentioned above over the range 5-9 Mc/s is shown in Table II.

TABLE II

f in Mc/s ...	5	6	7	7·3	9
Z_0 in ohms ...	0	1386	1794	1852	2100

It will be seen that Z_0 increases with 'f' (at first increasing rapidly and later on slowly) over the range 5-9 Mc/s which is the transmission band of the section as shown in the following sections.

7. CUT-OFF FREQUENCIES

By referring to the section on the "Nature of reactances in series and lattice arms," it may be predicted that one of the cut-off frequencies will lie at or near about F_1 and another of the cut-off frequencies near about the other edge of the band over which Z_0 is more or less non-reactive.

Since Z_0 is expected to be non-reactive over the transmission band, both Z_1 and Z_2 are to be purely reactive and of opposite signs over the same band. From (9), Z_1 is purely reactive. From equation (10), Z_2 has both resistance and reactance components; but since

$$\left| \frac{\omega^2 L_2^2 R_a}{R_a^2(1-\omega^2 L_2 C_2)^2 + \omega^2 L_2^2} \right|$$

has been neglected in comparison to

$$\left| \frac{1}{\omega C_0 k} \right|$$

in section 5 on 'characteristic impedance,' it should be similarly done *as well* in equation (10) to obtain Z_2 as purely reactive.

Therefore, for calculation of the cut-off frequencies (*i.e.* the limits between which Z_0 is more or less non-reactive),

$$Z_1 = 2j\left(\omega L_1 - \frac{1}{\omega C_1}\right), \qquad \text{[same as (9)]}$$

$$\text{and } Z_2 \simeq -\frac{j}{2}\left[\frac{1}{\omega C_0 k} - \frac{\omega L_2 R_a^2(1-\omega^2 L_2 C_2)}{R_a^2(1-\omega^2 L_2 C_2)^2 + \omega^2 L_2^2} + \left(\omega L_1 - \frac{1}{\omega C_1}\right)\right]. \qquad \dots \quad (14)$$

$$\text{If } \frac{Z_1}{Z_2} = 0, \text{ then } \omega^2 = \frac{1}{L_1 C_1}, \text{ or } f_1 = \frac{1}{2\pi\sqrt{L_1 C_1}} = F_1. \qquad \dots \quad (15)$$

Hence lower cut-off frequency $f_1 = 5·0$ Mc/s for the section taken.

$$\text{If } \frac{Z_1}{Z_2} = -4, \text{ then } \frac{1}{\omega C_0 k} = \frac{\omega L_2 R_a^2(1-\omega^2 L_2 C_2)}{R_a^2(1-\omega^2 L_2 C_2)^2 + \omega^2 L_2^2}, \text{ ultimately}$$

or $$\omega^4(C_2 + C_0 k)L_2^2 C_2 R_a^2 - \omega^2(2R_a^2 C_2 - L_2 + C_0 k R_a^2)L_2 + R_a^2 = 0.$$

Solving the biquadratic equation and putting $2\pi f_2$ for ω, we have

$$f_2 = \frac{1}{2\pi}\left[\frac{(2R_a^2C_2 + R_a^2C_0k - L_2) \pm \{(2R_a^2C_2 + R_a^2C_0k - L_2)^2 - 4R_a^4C_2(C_2 + C_0k)\}^{\frac{1}{2}}}{2L_2C_2R_a^2(C_2 + C_0k)}\right]^{\frac{1}{2}} \qquad \ldots \quad (16)$$

where 'f_2' is the real admissible value.

Taking values of C_0, L_2, C_2 and k and appropriate value of $|R_a|$ at the frequency concerned, $\omega = \sqrt{3226 \times 10^{12}} = 56.8 \times 10^6$ *r.p.s.*,

$$\because \qquad f_2 = 0.06 \text{ Mc/s.}$$

Hence the cut-off frequencies of the typical section considered are 5.0 and 0.06 Mc/s, or F_1 and f_2 Mc/s. It may be said that if F_0 be the overall frequency of the crystal in the lattice arm, the cut-off frequencies of the section are *very roughly* $F_0 - \frac{B}{2}$ and $F_0 + \frac{B}{2}$ where $\frac{B}{2} \simeq 2{,}03$ Mc/s.

8. ATTENUATION AND PHASE CONSTANTS

The ratio of the current at the input (I_1) to the current at the output (I_2) when the equivalent T-section is terminated in Z_0 in the transmission band is given by

$$\frac{I_1}{I_2} = 1 + \frac{Z_1}{2Z_2} + \frac{Z_0}{Z_2}$$

$$= 1 - \frac{2\left(\omega L_1 - \frac{1}{\omega C_1}\right)}{\left[\frac{1}{\omega C_0k} - \frac{\omega L_2R_a^2(1 - \omega^2L_2C_2)}{R_a^2(1 - \omega^2L_2C_2)^2 + \omega^2L_2^2} + \left(\omega L_1 - \frac{1}{\omega C_1}\right)\right]}$$

$$+ j \cdot \frac{2Z_0}{\left[\frac{1}{\omega C_0k} - \frac{\omega L_2R_a^2(1 - \omega^2L_2C_2)}{R_a^2(1 - \omega^2L_2C_2)^2 + \omega^2L_2^2} + \left(\omega L_1 - \frac{1}{\omega C_1}\right)\right]} \qquad \ldots \quad (17)$$

Let $l = \frac{1}{\omega C_0k} - \frac{\omega L_2R_a^2(1 - \omega^2L_2C_2)}{R_a^2(1 - \omega^2L_2C_2)^2 + \omega^2L_2^2}$ and $m = \omega L_1 - \frac{1}{\omega C_1}$.

Then from (13), $\qquad Z_0 \simeq \sqrt{lm}$.

The equation (17) can be written as

$$\frac{I_1}{I_2} = 1 - \frac{2m}{l+m} + j.\frac{2\sqrt{lm}}{l+m} = \frac{l-m}{l+m} + j.\frac{2\sqrt{lm}}{l+m}. \qquad \ldots \quad (18)$$

If P = propagation constant $= \log_e(I_1/I_2) = \alpha + j\beta$ where α = attenuation constant and β = phase constant of the section, then

$$\alpha = \log_e \sqrt{\left(\frac{l-m}{l+m}\right)^2 + \frac{4lm}{(l+m)^2}} = \log_e \sqrt{\frac{(l-m)^2 + 4lm}{(l+m)^2}} = \log_e 1 = 0. \quad (19)$$

Hence there is no attenuation in the transmission band, F_1 to f_2 Mc/s. Actual measurements of network attenuation have shown *low loss* in the transmission band for the sections of this class. Further,

$$\beta = \tan^{-1} \frac{2\sqrt{lm}}{l-m}. \qquad \dots \quad (20)$$

Table III shows the values of β over the frequency range 5-9 Mc/s for the lattice section considered.

TABLE III

f in Mc/s ...	5	6	7	7.22	9
β in degrees...	0	9° 18′	14° 6′	14° 48′	21° 24′

III. WIDE AND ULTRA-WIDE BAND LATTICE TYPE CRYSTAL BAND-PASS FILTER SECTION—CLASS II

Consider a typical class II ultra-wide band section in which a crystal (mounted between electrodes) connected in parallel to a stabilised negative impedance element is in the series arm and a crystal (mounted between two electrodes) connected in series with a stabilised negative impedance element is in the lattice arm [Fig. 4(*a*)].

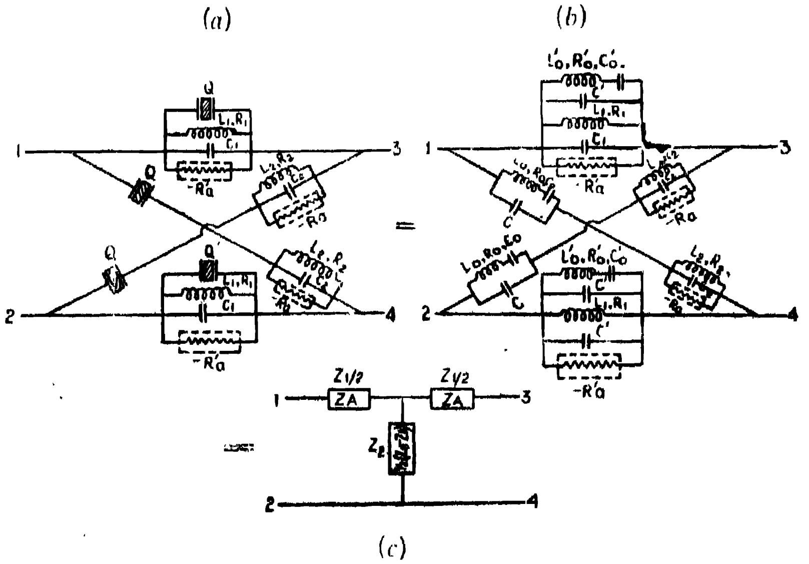

FIG. 4

1. DIFFERENT CASES

Four important cases may arise as follows—(1) in which the resonance frequency of the *equivalent* parallel resonant circuit formed from L_1-C_1 combination associated with the stabilised negative impedance element and equivalent circuit of the crystal (mounted between two electrodes) in the series arm, the frequency of the crystal in the lattice arm and the resonance frequency of the parallel resonant circuit in the stabilised negative impedance element in the lattice arm are all different; (2) in which the resonance frequency of the *equivalent* parallel resonant circuit referred to above in the series arm is equal to the resonance frequency of the parallel resonant circuit incorporated in negative impedance element in the lattice arm, and the frequency of crystal in the lattice arm is different; (3) in which the resonance frequency of the *equivalent* parallel resonant circuit (referred to above) in the series arm is equal to the frequency of the crystal (resonance or anti-resonance frequency) in the lattice arm, and the resonance frequency of the parallel resonant circuit incorporated in negative impedance element in the lattice arm is different; and (4) in which the resonance frequency of the *equivalent* parallel resonant circuit (referred to above) in the series arm, the resonance frequency of the parallel resonant circuit incorporated in negative impedance element in the lattice arm and the frequency of the crystal in the lattice arm are all the same.

Suppose $F_1 =$ resonance frequency of the *equivalent* parallel resonant circuit (referred to above) in the series arm, $F_2 =$ resonance frequency of the parallel resonant circuit in the stabilised negative impedance element in the lattice arm, $f_0 =$ resonance frequency of the crystal in the lattice arm and $F_0 =$ over all frequency (or anti-resonance frequency) of the crystal in the lattice arm. Let f'_0 and F'_0 be the corresponding frequencies of the crystal in the series arm. Then in case (1) F_1, F_2 and F_0 (or f_0) are all different; in case (2) $F_1 = F_2$ but F_0 (or f_0) is different; in case (3) $F_1 = f_0$ or F_0 but F_2 is different; and in case (4) $F_1 = F_2 = F_0$ (or f_0).

2. NATURE OF REACTANCES IN SERIES AND LATTICE ARMS

Fig. 5 shows the reactance-frequency characteristics of the series and lattice arms drawn for the four cases mentioned above. The curve marked I refers to the characteristic of the negative impedance element together with crystal (mounted between electrodes) in parallel in the series arm; the curve marked II_1 refers to that of the crystal (mounted between electrodes) in the lattice arm and the curve marked II_2 refers to that of the negative impedance element in the lattice arm.

The nature of the reactance characteristic of the negative impedance element together with crystal (mounted between electrodes) in parallel in the series arm can be shown to follow from the consideration given below.

The impedance of the crystal (mounted between electrodes) in the series arm is given by

$$Z'_1 = \frac{-j/\omega C'_0(1-\omega^2 L'_0 C'_0)}{1-\omega^2 L'_0 C' + C'/C'_0}. \tag{21}$$

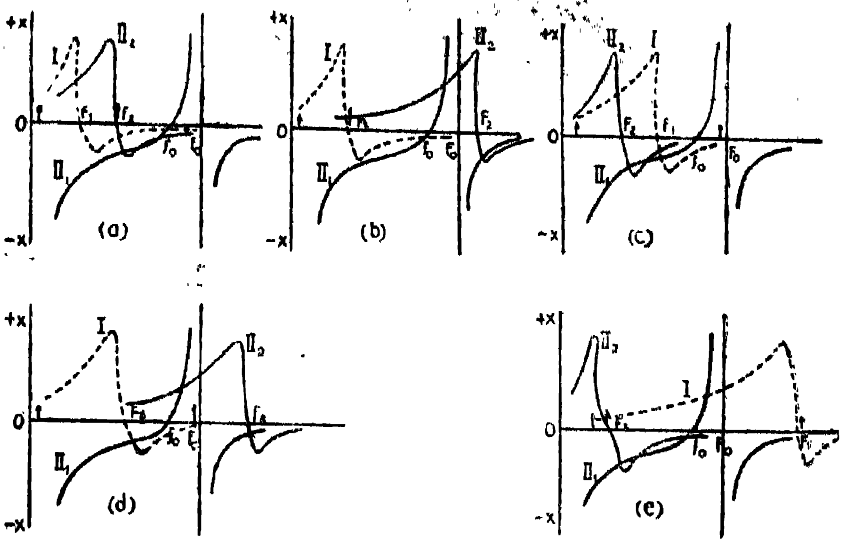

CASE (1)- F1, F2, AND F0 (OR f0) IS DIFFERENT

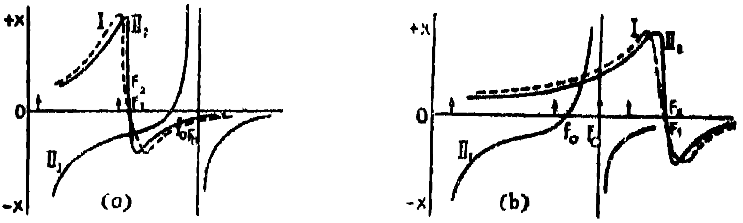

CASE (2) -F1=F2 AND F0 (OR f0) IS DIFFERENT

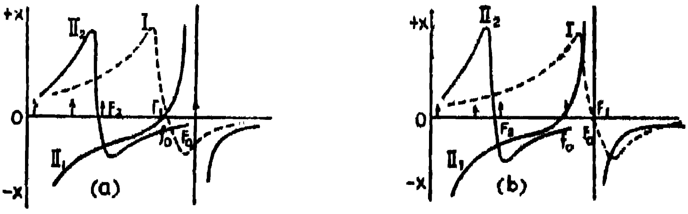

CASE (3) -F1 = f0 OR F0 AND F2 IS DIFFERENT

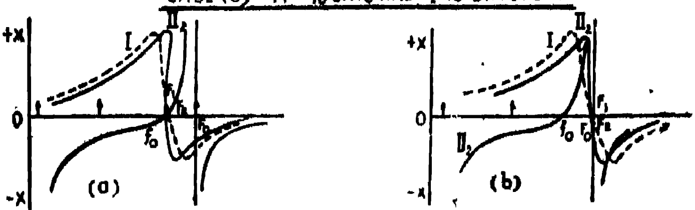

CASE 4 - WHEN F1=F2=F0 OR f0

FIG. 5

Substituting C'_0k for C' in (21) and neglecting '1' in comparison to 'k' in the denominator, we have

$$ {}_0Z'_1 \simeq -\frac{j}{\omega C'_0 k} . \qquad \dots \quad (22)$$

Hence the impedance of the crystal (mounted between electrodes) may be approximately regarded as purely reactive due to a capacitance C'_0k, and the usual equivalent circuit of the crystal (mounted between electrodes) may be replaced by the effective capacitance C'_0k. Since this capacitance is shunting the capacitance C_1 of the L_1-C_1 parallel resonant circuit of the negative impedance element in the series arm, the total capacitance in parallel resonant circuit is now $C_1+C'_0k$. Hence the reactance component of the negative impedance element shunted by the crystal in the series arm can be written as follows similar to that in equation (3).

$$ {}_kX'_1 = \frac{L_1(C_1+C'_0k)\left|\omega L_1 - \frac{1}{\omega(C_1+C'_0k)}\right|}{(C_1+C'_0k)^2\left[\omega L_1 - \frac{1}{\omega(C_1+C'_0k)}\right]^2 + \frac{L_1^2}{m}\omega^4} \qquad \ldots (23)$$

When $\omega < \frac{1}{\sqrt{L_1(C_1+C'_0k)}}$, $\omega L_1 - \frac{1}{\omega(C_1+C'_0k)}$ will be negative and hence ${}_kX'_1$ will be positive; when $\omega = \frac{1}{\sqrt{L_1(C_1+C'_0k)}} = 2\pi F_1$, ${}_kX'_1 = 0$; and when $\omega > \frac{1}{\sqrt{L_1(C_1+C'_0k)}}$, $\omega L_1 - \frac{1}{\omega(C_1+C'_0k)}$ will be positive and hence ${}_kX'_1$ will be negative. As frequency is increased from a point before F_1, the magnitude of the positive reactance has been found to increase at first till a frequency $F_1-\phi'$ and then to decrease rapidly to zero value at F_1. After the resonance frequency is passed the reactance is of negative sign and its magnitude at first increases till a certain frequency $(F_1+\phi'')$ and then decreases to low value as the frequency is further increased. It will be noted that the nature of variation of the reactance of the negative impedance element shunted by the crystal (mounted between electrodes) in the series arm is *similar* to that of the negative impedance element in the lattice arm.

In all cases and sub-cases discussed below the cut-off frequencies indicated are for conditions in which the effects of resistance components of the impedances in series and lattice arms have been neglected. If the impedances are taken to consist of both resistance and reactance components, the effective cut-off frequencies will be different.

Take case (1) in which F_1, F_2 and F_0 (or f_0) are all different. (*a*) shows the condition when $F_1 < F_2 < f_0$ (or F_0), and F_1 and F_2 are nearer to each other. The probable positions of cut-off frequencies are indicated by arrows. It will be seen that at F_1 Mc/s the characteristic impedance will be zero unless the resistance component of the impedance in the series arm has an appreciable value. The condition can give a very wide band with slight reflection effect about F_1.

(*b*) shows the condition when $F_1 < f_0$ (or F_0) $< F_2$, and F_1 and f_0 and also F_2 and F_0 are nearer to each other. The probable positions of cut-off frequencies are indicated by arrows. This condition is expected to give a band-pass filter of lesser band-width than that of (*a*).

(*c*) shows the condition when $F_2 < F_1 < f_0$ or F_0. If F_1 and f_0 are nearer to each other, the band-width is expected to be very large.

(*d*) shows the condition when $F_1 < f_0$ (or F_0) $< F_2$, and F_2 is farther from F_0. This condition will give a very wide band band-pass filter of cut-off frequencies marked by arrows.

(*e*) shows the condition when $F_2 < f_0$(or F_0)$<F_1$, and F_1 is farther from F_0. This condition will give a very wide band band-pass filter of cut-off frequencies marked by arrows. There may be slight waviness in the total insertion loss characteristic between f_0 and F_0.

Case (2) shows the condition when $F_1 = F_2$, and F_0 (or f_0) is different. The band-widths are marked by arrows when F_1 (or F_2) is less than f_0 and also when F_1 (or F_2) is greater than F_0. The band-width in the latter case may be less than that of the former case if there be a large attenuation in the total insertion loss characteristic about F_0.

Case (3) shows the condition when $F_1 = f_0$, and F_2 is different as well as when $F_1 = F_0$, and F_2 is different. Two band-pass filters of different transmission band widths can be obtained under this condition and they could be made to give a single band-pass filter of larger band-width by altering the condition slightly in certain ways.

Case (4) shows the condition when $F_1 = F_2 = f_0$ and also when $F_1 = F_2 = F_0$. It will be seen that in the former case there may be two band-pass filters one of large and another of small transmission band width whereas in the latter case there may be only one band-pass filter. The probable cut-off frequencies of the band-pass filters are indicated by arrows.

Among the subcases of case (1) the sharpness of cut-off is expected to be more or less the same on both the sides in (*c*), (*d*) and (*e*) and different on both the sides in (*a*) and (*b*). For case (2), it is expected to be nearly the same in (*b*) and different in (*a*) on both the sides. For case (3) it is expected to be different for the band-pass filter involving the lower frequency range and same for the one involving the higher frequency range on both the sides. For case (4) it is expected to be different for the band-pass filter involving the lower frequency range and same for the one involving the higher frequency range on both the sides in (*a*), and it is expected to be different on both the sides in (*b*).

3. EQUIVALENT T-SECTION OF THE ORIGINAL LATTICE SECTION

A general section in which the resonance frequency of the equivalent parallel resonant circuit in the stabilised negative impedance element in the series arm, the frequency of the crystal in the lattice arm and the resonance frequency of the parallel resonant circuit in the stabilised negative impedance element in the lattice arm are all different, is shown in Fig. 4(*a*) and its effective equivalent is shown in Fig. 4(*b*). Neglect the resistances in various inductances in series and lattice arms (that is, neglect R'_0, R_1, R_0 and R_2).

If Z_A be the total impedance in *each* series arm and Z_B the total impedance in *each* lattice arm, then we have

$$Z_A = \frac{j\omega L_1 R'_a}{R'_a[1-\omega^2 L_1(C_1+C'_0 k)] - j\omega L_1} \quad \ldots \quad (24)$$

$$Z_B = -\frac{j}{\omega C_0 k} + \frac{j\omega L_2 R_a}{R_a(1-\omega^2 L_2 C_2) - j\omega L_2}. \quad \ldots \quad (25)$$

If Z_1 and Z_2 be the total series and total shunt impedances respectively of the equivalent T-section in Fig. 4(*c*), then

$$Z_1 = \frac{2j\omega L_1 R'_a}{R'_a[1-\omega^2 L_1(C_1+C'_0 k)] - j\omega L_1} \quad \ldots \quad (26)$$

$$Z_2 = \tfrac{1}{2}\left[-\frac{j}{\omega C_0 k} + \frac{j\omega L_2 R_a}{R_a(1-\omega^2 L_2 C_2) - j\omega L_2} - \frac{j\omega L_1 R'_a}{R'_a[1-\omega^2 L_1(C_1+C'_0 k)] - j\omega L_1} \right]. \quad \ldots \quad (27)$$

4. CHARACTERISTIC IMPEDANCE

Separating the real and imaginary portions in the expressions on the R.H.S. of equations (26) and (27) and putting

$$a = \frac{\omega^2 L_1^2 R'_a}{R'^2_a[1-\omega^2 L_1(C_1+C'_0 k)]^2 + \omega^2 L_1^2} \quad \ldots \quad (28)$$

$$b = \frac{\omega L_1 R'^2_a[1-\omega^2 L_1(C_1+C'_0 k)]}{R'^2_a[1-\omega^2 L_1(C_1+C'_0 k)]^2 + \omega^2 L_1^2} \quad \ldots \quad (29)$$

$$a' = \frac{\omega^2 L_2^2 R_a}{R_a^2[1-\omega^2 L_2 C_2]^2 + \omega^2 L_2^2} \quad \ldots \quad (30)$$

and
$$b' = \frac{\omega L_2 R_a^2[1-\omega^2 L_2 C_2]}{R_a^2[1-\omega^2 L_2 C_2]^2 + \omega^2 L_2^2} \quad \ldots \quad (31)$$

we have
$$Z_1 = 2(a+jb) \quad \ldots \quad (32)$$

and
$$Z_2 = \tfrac{1}{2}\left[(a'-a) + j\left(b' - b - \frac{1}{\omega C_0 k} \right) \right]. \quad \ldots \quad (33)$$

Therefore finally the characteristic impedance of the equivalent T-section is given by

$$Z_0 = \sqrt{\left[aa' - bb' + \frac{b}{\omega C_0 k} \right] + j\left[a'b + ab' - \frac{a}{\omega C_0 k} \right]} \quad \ldots \quad (34)$$

5. NATURE OF THE CHARACTERISTIC IMPEDANCE

In order to estimate the relative values of real and imaginary terms under the radical sign in (34) over a frequency range, it is desirable to consider a typical ultra-wide band section of class II. Take a section in which $L_1 = 10 \times 10^{-6}$H, $C_1 = 19 \times 10^{-12}$F, $C'_0 = .015 \times 10^{-12}$F, $k = 140$, $|R'_a|^* = 2 \times 10^3$ ohms, $L_2 = 100 \times 10^{-6}$H, $C_2 = .28 \times 10^{-6}$F, $C_0 = .011 \times 10^{-12}$F, $|R_a|^\dagger = 7.05 \times 10^3$ ohms, $F_2 = 30$ Kc/s, $F_1 = 11.5$ Mc/s, $f_0 = 7.17$ Mc/s and $F_0 = 7.24$ Mc/s.

Table IV shows the values of a, b, a', b' and Z_0 as well as of the real and imaginary terms under the radical sign in (34).

TABLE IV

Frequency in Mc/s	$\frac{1}{\omega C_0 k}$	a	b	a'	b'	$aa' - bb' + \frac{b}{\omega C_0 k}$	$a'b + ab' - \frac{a}{\omega C_0 k}$	Approximate $\|Z_0\|$ ohms
.05	22.6×10^5	0.005	3.15	43×10^{-3}	−16.0	68×10^5	-0.113×10^5	2607
.5	2.26×10^5	0.5	31.5	18×10^{-5}	−1.15	72.45×10^5	-1.16×10^5	2690
1	1.13×10^5	2	63	4.6×10^{-5}	−0.6	71.2×10^5	-2.26×10^5	2668
2	$.56 \times 10^5$	9	134	1.12×10^{-5}	0.27	80.4×10^5	-5.4×10^5	2840
3	$.377 \times 10^5$	21	202	0.5×10^{-5}	−0.19	76.8×10^5	-7.98×10^5	2780
4	$.28 \times 10^5$	13	292	0.29×10^{-5}	−0.14	81.8×10^5	-12.04×10^5	2910
5	$.226 \times 10^5$	77	383	0.19×10^{-5}	−0.12	88.1×10^5	-17.7×10^5	2983
6	$.188 \times 10^5$	144	529	0.125×10^{-5}	−0.095	100.5×10^5	-27.36×10^5	3240
7	$.16 \times 10^5$	240	627	0.09×10^{-5}	−0.08	100.3×10^5	-38.4×10^5	3286
8	$.14 \times 10^5$	483	871	0.073×10^{-5}	−0.071	122.4×10^5	-67.6×10^5	3741
10	$.113 \times 10^5$	1600	806	0.046×10^{-5}	−0.058	91.1×10^5	-180.8×10^5	4527

It will be seen from Table IV that the imaginary term under the radical sign in (34) varies from 0.16% to about 27% of the real term under the same sign over the range 50 Kc/s—6Mc/s and therefore Z_0 may be regarded more or less as pure resistance between those limits. At frequencies higher than 6 Mc/s, the imaginary term becomes greater and greater percentage of the real term and Z_0 will be an impedance with both resistance and reactance components, and further beyond a certain frequency Z_0 will be highly reactive giving conditions for the attenuation band. Further it will be noted that the magnitude of Z_0 varies in a wavy manner in the transmission band—at first increasing, then decreasing, then increasing, again decreasing and finally increasing with frequency. At least for the frequency range over which Z_0 is more or less of non-reactive type, Z_1 and Z_2 can roughly be taken to be pure reactances of opposite signs. Hence over this range,

---

* Magnitude of negative resistance in series arm at 5 Mc/s.

† Magnitude of negative resistance in lattice arm at 5 Mc/s. It will be noted that in actual case, $|R_a|$ for both series and lattice arm will vary irregularly with frequency over such an ultra-wide band (*i.e.*, 30 Kc/s–11.5 Mc/s) as under consideration at present. The values of $|R_a|$ taken from the mean curve (following the inverse square law) for this large range are liable to introduce great errors. Hence $|R_a|$ at 5 Mc/s has been taken for both cases in calculation.

$$Z_1 \simeq j.2b \qquad \cdots \quad (35)$$

$$Z_2 \simeq -\frac{j}{2}\left[b + \frac{1}{\omega C_0 k} - b'\right]. \qquad \cdots \quad (36)$$

The characteristic impedance Z'_0 arrived at from (35) and (36) will be

$$Z'_0 = \sqrt{\left[\frac{b}{\omega C_0 k} - bb'\right]} \qquad \cdots \quad (37)$$

which can be compared to the value Z''_0 obtained by neglecting $a'b + ab' - \dfrac{a}{\omega C_0 k}$ in (34),

$$Z''_0 = \sqrt{\left[aa' - bb' + \frac{b}{\omega C_0 k}\right]}; \qquad \cdots \quad (38)$$

Z'_0 is nearly equal to Z''_0, since aa' is very small.

6. CUT-OFF FREQUENCIES

If $\dfrac{Z_1}{Z_2} = 0$, then $b = 0$, *i.e.*, $\dfrac{\omega L_1 R'^2_a[1 - \omega^2 L_1(C_1 + C'_0 k)]}{R'^2_a[1 - \omega^2 L_1(C_1 + C'_0 k)]^2 + \omega^2 L_1^2} = 0$

which means $\omega = 0$ or $\omega = \dfrac{1}{\sqrt{L_1(C_1 + C'_0 k)}}$.

The value $\omega = 0$ is inadmissible. Hence one of the cut-off frequecies say, 'f_1', is given by

$$f_1 = \frac{1}{2\pi\sqrt{L_1(C_1 + C'_0 k)}}. \qquad \cdots \quad (39)$$

In the case of the ultra-wide band section considered above $f_1 = 10.93$ Mc/s.

If $\dfrac{Z_1}{Z_2} = -4$, then $j.2b = 2j\left[b + \dfrac{1}{\omega C_0 k} - b'\right]$, or $\dfrac{1}{\omega C_0 k} = b'$,

or $$\omega^4(C_2 + C_0 k)L_2^2 C_2 R_a^2 - \omega^2(2C_2 R_a^2 + C_0 k R_a^2 - L_2)L_2 + R_a^2 = 0 \qquad \cdots \quad (40)$$

on evaluating b' from (31). Solving the biquadratic and putting $\omega = 2\pi f_2$, we have

$$f_2 = \frac{1}{2\pi}\left[\frac{(2C_2 R_a^2 + C_0 k R_a^2 - L_2)L_2 \pm \sqrt{(2C_2 R_a^2 + C_0 k R_a^2 - L_2)^2 L_2^2 - 4R_a^2 L_2^2 C_2(C_2 + C_0 k)}}{2L_2^2 C_2 R_a^2(C_2 + C_0 k)}\right]^{\frac{1}{2}} \qquad \cdots \quad (41)$$

where 'f_2' is the real admissible value.

Taking $C_2 = 0.28 \times 10^{-6}$F, $L_2 = 100 \times 10^{-6}$H, $C_0 = .011 \times 10^{-12}$F, $k = 140$, $|R_a| = 7.05 \times 10^3$ ohms from the data given for the ultra-wide band section,

$$f_2 = \frac{1}{2\pi}\sqrt{353.5 \times 10^8}$$

$$= 30 \text{ Kc/s.}$$

Hence the cut-off frequencies of the ultra-wide band section considered are roughly 30 Kc/s and 10.93 Mc/s. If $\frac{F_0+F'_0}{2}$ Mc/s be the arithmetic mean of the overall frequencies of the crystals in series and lattice arms, then the cut-off frequencies will be $\frac{F_0+F'_0}{2}-3B'$ and $\frac{F_0+F'_0}{2}+2B'$Mc/s where B′ varies from 2.12 to 2.22 Mc/s.

7. ATTENUATION AND PHASE CONSTANTS

The ratio of the current at the input (I_1) to the current at the output (I_2) when the T-section is terminated by Z_0 in the transmission band is given by

$$\frac{I_1}{I_2}=1+\frac{Z_1}{2Z_2}+\frac{Z_0}{Z_2}\,.$$

Taking Z_1, Z_2 and Z_0 from equations (35), (36) and (38) respectively we have

$$\frac{I_1}{I_2}=1-\frac{2b}{b+\dfrac{1}{\omega C_0 k}-b'}+j\,.\,\frac{2\sqrt{aa'-bb'+b/\omega C_0 k}}{b+\dfrac{1}{\omega C_0 k}-b'}$$

$$=\frac{\dfrac{1}{\omega C_0 k}-b-b'}{b+\dfrac{1}{\omega C_0 k}-b'}+j\,.\,\frac{2\sqrt{aa'-bb'+b/\omega C_0 k}}{b+\dfrac{1}{\omega C_0 k}-b'}\,. \qquad \ldots \quad (42)$$

It will be seen from Table IV that $|b'|$ is very small except over a small portion of the transmission band near the lower cut-off frequency and aa' and bb' are also very small in comparison to $\frac{1}{\omega C_0 k}$.

Therefore

$$\frac{I_1}{I_2}\simeq\frac{\dfrac{1}{\omega C_0 k}-b}{b+\dfrac{1}{\omega C_0 k}}+j\,.\,\frac{2\sqrt{b/\omega C_0 k}}{b+\dfrac{1}{\omega C_0 k}}. \qquad \ldots \quad (43)$$

If the propagation constant $P=\log_e(I_1/I_2)=\alpha+j\beta$, where α and β are attenuation and phase constants respectively, then

$$\alpha=\log_e\frac{\sqrt{\left(\dfrac{1}{\omega C_0 k}-b\right)^2+\dfrac{4b}{\omega C_0 k}}}{\sqrt{\left(b+\dfrac{1}{\omega C_0 k}\right)^2}}=\log_e\frac{\sqrt{\left(b+\dfrac{1}{\omega C_0 k}\right)^2}}{\sqrt{\left(b+\dfrac{1}{\omega C_0 k}\right)^2}}=\log_e 1=0..(44)$$

$$\beta=\tan^{-1}\frac{4b}{\omega C_0 k}\Bigg/\left(\frac{1}{\omega C_0 k}-b\right)\simeq\tan^{-1}4b \qquad \ldots \quad (45)$$

since $b<<\frac{1}{\omega C_0 k}$.

Hence there is no attenuation in the transmission band of the section. Actual measurements of network attenuation have shown *low loss* in transmission band for sections of this class.

The phase-shift angle (in degrees) is almost the same at all frequencies in the transmission band, as shown in Table V.

TABLE V

f in Mc/s	.05	.5	1	2	3	4	5	6	7	8	10
tan β	12.5	126	252	536	808	1168	1532	2116	2508	3496	3224
β (degrees)	85°30′	89°33′	> 89°48′	> 89°54′	near 90°	near 90°	near 90°	near 90°	near 90°	near 90°	near 90°

IV. ACKNOWLEDGMENT

The whole of the work has been carried out at the Electrical Communication Engineering Section, Department of Applied Physics, University of Calcutta. The author desires to thank heartily Prof. P. N. Ghosh, Sc.D., for his very kind interest in the work and for giving him all facilities.

REFERENCES

Chakravarti and Das, 1943, Nature of Dynatron Type Negative Impedances at Frequencies from 1 to 40 Megacycles/Sec, *Ind. J. Phys.*, **17**, 51.

Chakravarti and Dutt, 1940, *Ind. J. Phys.*, **14**, 295.

Mason, 1934, *Bell System Tech. Jour.*, **13**, 360.

Mason, 1937, *Bell System Tech. Jour.*, **16**, 540.

Stanesby, 1942, *P. O. E. E. J.*, **35**, 4.

Stanesby and Broad, 1943, *P. O. E. E. J.*, **31**, 254.

Stanesby and Broad, 1941, *P. O. E. E. J.*, **33**, 176.

ELECTRICAL ENERGY OF TWO CYLINDRICAL CHARGED PARTICLES

By G. P. DUBE

(Received for publication, April 20, 1943)

ABSTRACT. Using the approximate Debye-Hückel theory, an expression for the electrical energy of two cylindrical charged particles has been worked out. This energy is found to exhibit a minimum for a certain value of the interparticle distance and may be of importance in explaining thixotropic properties.

It is well known that colloidal systems, exhibiting thixotropic phenomena, generally consist of non-spherical particles. They are rod-shaped in the thixotropic sols of vanadium pentoxide, disc-like in the sols of iron-oxide and paste of clay. A general mathematical theory of the mutual interaction energy between two spherical colloidal particles and its applications to general problems of stability of colloidal sols has been developed by the author (Dube, 1940) and has proved to be quite successful in explaining several phenomena. The same procedure has been adopted in finding out the electrical energy of two cylindrical charged particles immersed in water containing a known electrolyte.

Let us consider two parallel cylindrical particles of circular cross-section, radius a, with distance R apart and having surface charge density σ. They are immersed in water containing a known electrolyte. We are required first to find out the electrical potential at any point in the dispersion medium. The electrical potential ψ is assumed to be given by the approximate Debye-Hückel equation in the theory of strong electrolytes,

$$\nabla^2\psi = k^2\psi \qquad \ldots \quad (1)$$

where ∇^2 is the Laplacian operator and k is the characteristic quantity occurring in Debye-Hückel theory. $1/k$ is called Debye distance and is expressed in terms of the ionic strength J by the relation

$$\frac{1}{k} = 2.81 \times 10^{-10}\left(\frac{DT}{2J}\right)^{\frac{1}{2}} \text{ cms.} \qquad \ldots \quad (2)$$

It is extremely difficult to solve this equation in the two-particle case considered here. Hence to get the qualitative features of the result, we suppose a linear superposition of the two potentials, which is equivalent to the supposition that if the two particles approach one another, the distribution of charge on their surfaces and in their ionic atmospheres remains undistorted.

N.B.—On the suggestion of Prof. J. D. Bernal, F.R.S., a similar problem was being tackled by Mr. S. Levine of Toronto, but due to communication difficulties, his result could not be ascertained.

Let ψ_1, ρ_1 be the potential and charge density in the ionic atmosphere of one of the particles and ψ_2, ρ_2 be the corresponding quantities for the second particle. The energy required to bring one of the particles along with its ionic atmosphere into the electrical field of the other is now

$$F=\tfrac{1}{2}\int_V \rho_1\psi_2 dv+\int_{S_1}\sigma\psi_2 dS_1 \qquad \ldots \quad (3)$$

where S_1 is the surface area of the first particle and V is the total volume of the medium excluding the volume occupied by the two particles.

Solution for a single particle.—The potentials ψ_1, ψ_2 separately satisfy the equation (1) which in cylindrical co-ordinates becomes

$$\frac{\partial^2\psi}{\partial r^2}+\frac{1}{r}\frac{\partial\psi}{\partial r}+\frac{1}{r^2}\frac{\partial^2\psi}{\partial\theta^2}+\frac{\partial^2\psi}{\partial z^2}-k^2\psi=0.$$

Let us assume axial symmetry and confine ourselves to the plane $z=0$. Then this becomes

$$\frac{\partial^2\psi}{\partial r^2}+\frac{1}{r}\frac{\partial\psi}{\partial r}-k^2\psi=0.$$

The solution* of this will be

$$\psi=A'J_0(ikr)+B'Y_0(ikr)$$

where J_0 and Y_0 are Bessel functions of order zero (Watson, 1922). Since ψ must vanish when r tends to infinity, we have

$$\psi=AK_0(kr) \qquad \ldots \quad (4)$$

where A is a constant quantity to be determined by the boundary conditions

$$-\frac{D}{4\pi}\left(\frac{\partial\psi}{\partial r}\right)_{r=a}=\sigma, \qquad \ldots \quad (5)$$

D being the dielectric constant of the dispersion medium. Thus

$$-\frac{D}{4\pi}A\frac{\partial}{\partial r}\left\{K_0(kr)\right\}=\sigma, \quad \text{or} \quad \frac{D}{4\pi}Ak.K_1(ka)=\sigma, \quad \text{or} \quad A=\frac{4\pi\sigma}{Dk.K_1(\tau)} \qquad \ldots \quad (6)$$

where $\tau=ka$ is a dimensionless quantity. Thus the required solution becomes

$$\psi=\frac{4\pi\sigma}{Dk.K_1(\tau)}.K_0(kr). \qquad \ldots \quad (7)$$

The zeta or electrokinetic potential is then given by

$$\zeta=\frac{4\pi\sigma}{Dk}.\frac{K_0(\tau)}{K_1(\tau)}. \qquad \ldots \quad (8)$$

Evaluation of the integrals in (3).—Considering unit length of the particle

$$I'=\int_{S_1}\sigma\psi_2 dS_1=\frac{4\pi\sigma^2 a}{Dk.K_1(\tau)}.\int_0^{2\pi}K_0(kr_2)\,d\theta_1.$$

---

* In the case $k=0$, the solution is $\psi=c_1+c_2\,lnr$.

Now $$K_0(kr_2)=\sum_{m=-\infty}^{\infty} K_m(kR).I_m(kr_1).\cos m\theta_1 \quad \text{for } r_1<R$$

$$=\sum_{m=-\infty}^{\infty} K_m(kr_1).I_m(kR)\cos m\theta_1 \quad \text{for } r_1>R.$$

Hence $$\int_0^{2\pi} K_0(kr_2)\,d\theta_1=\int_0^{2\pi}\sum_{m=\infty}^{+\infty} K_m(kR).\ I_m(ka).\ \cos m\theta_1 d\theta_1$$

which is different from zero only when $m=0$ and then its value is

$$2\pi K_0(kR)I_0(\tau).$$

Therefore we have

$$P=\frac{8\pi^2\sigma^2 a}{Dk}.\ \frac{I_0(\tau)}{K_1(\tau)}.\ K_0(s\tau) \qquad \dots (9)$$

where $$R=sa.$$

The other integral is

$$Q=\tfrac{1}{2}\int_v \rho_1\psi_2 dv=-\frac{Dk^2}{8\pi}\int_v \psi_1\psi_2 dv=-\frac{2\pi\sigma^2}{DK_1^2(\tau)}\int_v K_0(kr_1)K_0(kr_2)dv.$$

The integrand can be expressed as a function of (r_1,θ_1) only and then using $Kr_1=u$ and simplifying, the integral can be shown to be

$$-\frac{4\pi^2\sigma^2}{Dk^2K_1^2(\tau)}\left[\left(\int_0^{s\tau}-2\int_0^{\tau}\right)K_0(s\tau)K_0(u).I_0(u)u.du+\int_{s\tau}^{\infty} I_0(s\tau).K_0^2(u).udu\right]$$

Therefore,

$$Q=-\frac{4\pi^2\sigma^2}{Dk^2K_1^2(\tau)}\ [K_0(s\tau)\{L(s\tau)+L(0)-2L(\tau)\}+I_0(s\tau)\{J(\infty)-J(s\tau)\}]$$

where $$J(u)=\int uK_0^2(u)du=\frac{u^2}{2}[K_0^2(u)-K_1^2(u)]$$

$$L(u)=\int K_0(u)I_0(u)udu=\frac{u^2}{2}[I_0(u)K_0(u)+I_1(u)K_1(u)].$$

For small values of u,

$$K_0(u)\simeq ln\frac{2}{\gamma u}\ ;\ K_1(u)\simeq\frac{1}{u};\ I_0(u)=1,\ I_1(u)\simeq\frac{u}{2}$$

where γ = Euler's constant.

Hence it is easy to verify that

$$L(0)=0\ ;\ J(\infty)=0.$$

Therefore,

$$Q=-\frac{4\pi^2\sigma^2}{Dk^2K_1^2(\tau)}\{K_0(s\tau)L(s\tau)-I_0(s\tau)J(s\tau-2K_0(s\tau)L(\tau)\}.$$

Now $$K_0(s\tau)L(s\tau)-I_0(s\tau)J(s\tau)=\frac{s^2\tau^2}{2}K_1(s\tau)\{K_0(s\tau)I_1(s\tau)+I_0(s\tau)K_1(s\tau)\}$$

$$=\frac{s\tau}{2}K_1(s\tau).$$

Thus

$$Q=-\frac{2\pi^2\sigma^2\tau}{Dk^2K_1^2(\tau)}[s.K_1(s\tau)-2\tau K_0(s\tau)\{I_0(\tau)K_0(\tau)+I_1(\tau)K_1(\tau)\}]. \quad \ldots \quad (10)$$

Combining (9) and (10) and defining

$$\phi(\tau)=2\tau^2\{I_0(\tau)K_2(\tau)+I_1(\tau)K_1(\tau)\} \quad \ldots \quad (11)$$

we have $$F=\frac{2\pi^2\sigma^2}{Dk^2K_1^2(\tau)}.[K_0(s\tau)\phi(\tau)-s\tau K_1(s\tau)]$$

$$=\frac{D\zeta^2}{8}\cdot\frac{1}{K_0^2(\tau)}[K_0(s\tau)\phi(\tau)-s\tau K_1(s\tau)]. \quad \ldots \quad (12)$$

This has a minimum value at a certain value of s, which is given by

$$\frac{\delta F}{\delta s}=0$$

or $$\phi(\tau)=\frac{s\tau K_0(s\tau)}{K_1(s\tau)}. \quad \ldots \quad (13)$$

This equation can be solved by numerical methods and the results are

τ = 0.1	0.5	1.0	1.5	2.0	2.5	3.0
s_m = 44.26	9.35	5.35	4.00	3.43	3.11	2.91

Then taking $\zeta=10^{-4}$ e.s.u, D=80, length of the particle $=10^{-4}$ cm. and $kT=4\times10^{-14}$, the values of $F_{\min}/kT$ are found to be 0.26, 1.4, 3.2, 7.3, 9.0, 11.3, 13.5 respectively.

The existence of an electrical energy minimum as a function of interparticle distance may be of considerable importance in explaining the thixotropic properties of non-spherical particles. The van der Waals energy must also be considered in a more rigorous treatment of the problem. Unfortunately, due to integration difficulties (Dube and Dasgupta, 1939), it has not yet been possible fo find an expression for the van der Waals energy between two cylindrical particles.

SCIENCE COLLEGE, PATNA.

REFERENCES

Dube, G. P., 1940, *Proc. 27th Ind. Sc. Congress*, Part IV, p. 61. Also Levine, S. and Dube, G. P., 1940, *Phil. Mag.*, **29**, 105. Dube, G. P. and Das Gupta, H. K. 1939, *Ind. J. Phys.*, **13**, 411.

Watson. 1922. *Theory of Bessel Functions* (Cambridge).

A NOTE ON THE OSCILLATING ROTATOR

By K. BASU

(Received for publication, May 19, 1943)

ABSTRACT. The problem of the oscillating rotator has been solved from the standpoint of Sonine's polynomials developed by the author recently.

1. The problem was first treated wave-mechanically by Fues (1926) and later by Sommerfeld (1930) considering the rotator oscillating in space and obeying the Kratzer-form of the potential energy. But the problem was hardly solved in its entirety on account of mathematical difficulty in attacking the perturbations involved in calculating the eigenvalue. Chakravarti (1938), handled the problem from the standpoint of perturbation calculations and expanded the eigenfunctions in terms of the Hermitean polynomials and calculated the dissociation energy for the diatomic molecules BeH, CdH, C_2 and N_2. In the next section I shall point out his method of approach to the problem. But in the present paper I am going to deal with it from the standpoint of Sonine's polynomials developed by me recently (Basu, 1943).

2. The wave equation we have to tackle is the following (*vide* Sommerfeld, *l.c.*, p. 28.):

$$\frac{d^2F}{d\rho^2} - \frac{m(m+1)}{\rho^2}F + \frac{8\pi^2 I}{h^2}(E-U)F = 0 \qquad \dots \quad (1)$$

where $J = \mu r_e^2$ ($\mu =$ reduced mass of the diatomic molecule, $r =$ the mean distance between the two nuclei), $\rho = 1/r_e$, and Kratzer gives

$$U(\rho) = A - J\omega_0^2\left\{\frac{1}{\rho} - \frac{1}{2\rho^2} + b(\rho-1)^3 + c(\rho-1)^4 + \dots\right\} \qquad (2)$$

wherein $\omega_0 =$ frequency of small vibration of the oscillator if the small terms $b, c, \dots$ were absent.

Chakravarti and Fues made a transformation by putting $\zeta = \rho - 1$, and in the resulting equation expanded $m(m+1)/(1+\zeta)^2$ in ascending powers of ζ ($<<1$), in order to avoid a three-term sequence relation amongst the successive coefficients of the polynomial form of the eigenfunction (Sommerfeld, *l.c.*, p. 27), but we can tackle the problem as it stands without any such transformation and expansion.

For the zero-order approximation neglect $b, c, \dots$ and get

$$\frac{d^2f}{d\rho^2} + \left\{-\beta_0^2 + \alpha^2\left(\frac{2}{\rho} - \frac{1}{\rho^2}\right) - \frac{m(m+1)}{\rho^2}\right\}f = 0 \qquad \dots \quad (3)$$

where $\beta^2 = \frac{8\pi^2 J}{h^2}(A-E)$, $\alpha = 2\pi J\omega_0/h (>>1)$, $\beta = \beta_0(b, c, \dots = 0)$, $F = f$.

Considering the asymptotic behaviour of f, *viz.*, $f \sim e^{\pm\beta_0\rho}$ and rejecting *plus* sign, we see $f=e^{-\beta_0\rho}v(\rho)$ where

$$v''-2\beta_0 v'+\left[a^2\left(\frac{2}{\rho}-\frac{1}{\rho^2}\right)-\frac{m(m+1)}{\rho^2}\right]v=0. \qquad \ldots \quad (4)$$

For the polynomial type of solution of $v(\rho)$, the index γ is given by

$$\gamma(\gamma-1)=m(m+1)+a^2, \text{ or } \gamma=\tfrac{1}{2}\pm\sqrt{(m+1/2)^2+a^2}.$$

We should take *plus* sign before the radical in order that γ may be positive and finite for $\rho=0$.

Next put $v(\rho)=\rho^\gamma u$ and obtain the $u(\rho)$ equation as

$$\rho u''+(2\gamma-2\beta_0\rho)u'+2(a^2-\beta_0\gamma)u=0, \qquad \ldots \quad (5)$$

which, when transformed by $z=2\beta_0\rho$, stands thus

$$z\frac{d^2u}{dz^2}+(2\gamma-z)\frac{du}{dz}+nu=0, \qquad \ldots \quad (6)$$

where n (an integer) $=(a^2-\beta_0\gamma)/\beta_0$ and $u=S^n_{2\gamma}(z)$, a Sonine's polynomial.

Hence

$$f \sim e^{-\beta_0\rho}\rho^\gamma S^n_{2\gamma}(z) \sim e^{-\frac{1}{2}z}z^\gamma S^n_{2\gamma}(z). \qquad \ldots \quad (7)$$

If N_r be the normalisation factor, the requirement for normalisation is

$N_r^2\int_0^\infty r^2 f^2 dr=1$, and remembering $r=\frac{r_e}{2\beta_0}z$, this means

$$N_r^2\left(\frac{r_e}{2\beta_0}\right)^3\int_0^\infty e^{-z}z^{2\gamma}S^n_{2\gamma}(z)S^n_{2\gamma}(z)dz=1. \qquad \ldots \quad (8)$$

Now the value of the integral (Basu, *l.c.*)

$$=2(n+\gamma).n![\Gamma(2\gamma)]^2/\Gamma(n+2\gamma).$$

Hence

$$N_r=2\left(\frac{\beta_0}{r_e}\right)^{\frac{3}{2}}\left\{\frac{\Gamma(n+2\gamma)}{(n+\gamma).n!}\right\}^{\frac{1}{2}}\Big/\Gamma(2\gamma). \qquad \ldots \quad (9)$$

From (6), $\beta_0=a^2/(n+\gamma)$,

$$\therefore \quad N_r=\frac{2a^3}{r_e^{\frac{3}{2}}}\,\frac{1}{(n+\gamma)^2\Gamma(2\gamma)}\sqrt{\frac{\Gamma(2\gamma+n)}{n!}}, \qquad \ldots \quad (10)$$

From this value of β_0, the energy-value $E=E_0$ was calculated by Sommerfeld and Fues by the usual polynomial method.

3. Retaining $b, c, \ldots$ terms in Eq. 1, analogous procedure gives

$$\frac{d^2F}{d\rho^2}+\left\{-\beta^2+a^2\left(\frac{2}{\rho}-\frac{1}{\rho^2}\right)-\frac{m(m+1)}{\rho^2}\right\}F=-2a^2[b(\rho-1)^3+c(\rho-1)^4]F\ldots \quad (11)$$

wherein, we have ignored $(\rho-1)^5$ and other higher order terms.

Suppose $F=e^{-\beta\rho}v(\rho)=e^{-\beta\rho}\rho^\gamma U(\rho)$, where γ will have the same value as before. The $U(\rho)$-equation becomes (by putting $z=2\beta\rho$)

$$z\frac{d^2U}{dz^2}+(2\gamma-z)\frac{dU}{dz}+NU=(f_1z+f_2z^2+\ \ldots\ +f_5z^5)U \qquad \ldots \quad (12)$$

where $f_1 = a^2(b-c)/2\beta_0^2$, $f_2 = -a^2(3b-4c)/4\beta_0^3$, $f_3 = 3a^2(b-2c)/8\beta_0^4$,

$f_4 = -a^2(b-4c)/16\beta_0^5$, $f_5 = -a^2c/32\beta_0^6$; $N = (a^2 - \beta\gamma)/\beta$.

Put $U = u + \eta$. $N = n + \epsilon$ and obtain by substitution in (12) the following perturbed equation (rejecting small quantities $f_1\eta$, etc. and $\epsilon\eta$) :

$$z\frac{d^2\eta}{dZ^2} + (2\gamma - z)\frac{d\eta}{dz} + n\eta = [-\epsilon + (f_1 z + \ \ldots \ + f_5 z^5)]u. \quad \ldots \quad (13)$$

It is to be noted that

$$\beta = \frac{a^2}{n+\gamma+\epsilon} = \frac{a^2}{n+\gamma}\left(1 - \frac{\epsilon}{n+\gamma}\right) = \beta_0\left(1 - \frac{\epsilon}{n+\gamma}\right). \quad \ldots \quad (14)$$

Suppose $$\eta = \sum_l C_l S_{2\gamma}^l(z). \quad \ldots \quad (15)$$

Substitution in (13) gives

$$\sum_l (n-l) C_l S_{2\gamma}^l(z) = -[-\epsilon + (f_1 z + \ldots\ )] S_{2\gamma}^n(z). \quad \ldots \quad (16)$$

Multiply both sides by $e^{-z} z^{2\gamma-1} S_{2\gamma}^l(z)$ and integrate between $z = 0$ to ∞. This gives (*vide* Basu, *l.c.*)

$$C_l \times \frac{n![\Gamma(2\gamma)]^2}{\Gamma(n+2\gamma)} = \frac{1}{n-l}\int_0^\infty [\epsilon - (f_1 z + \ldots\ )] S_{2\gamma}^n(z) S_{2\gamma}^l(z) e^{-z} z^{2\gamma-1}\, dz,$$

and consequently C_l (coefficients of the perturbed eigenfunction η) can be found out by evaluating the right-hand member, subject to the condition that C_n is to remain finite (notwithstanding $n = l$ makes the denominator $= 0$). This requires

$$\int_0^\infty [\epsilon - (f_1 z + \ldots\ )] e^{-z} z^{2\gamma-1} S_{2\gamma}^n(z) S_{2\gamma}^n(z)\, dz = 0 \quad \ldots \quad (17)$$

or $$\epsilon . \frac{n![\Gamma(2\gamma)]^2}{\Gamma(2\gamma+n)} = f_1\{A\} + f_2\{B\} + f_3\{C\} + f_4\{D\} + f_5\{E\} \quad \ldots \quad (18)$$

where $$\{A\} = \int_0^\infty e^{-z} z^{2\gamma} S_{2\gamma}^n(z) S_{2\gamma}^n(z)\, dz = \frac{n![\Gamma(2\gamma)]^2}{\Gamma(n+2\gamma)} g_1(n, \gamma);$$

$$\{B\} = \int_0^\infty e^{-z} z^{2\gamma+1} S_{2\gamma}^n(z) S_{2\gamma}^n(z)\, dz = \frac{n![\Gamma(2\gamma)]^2}{\Gamma(n+2\gamma)} g_2(n, \gamma);$$

$$\{C\} = \int_0^\infty e^{-z} z^{2\gamma+2} S_{2\gamma}^n(z) S_{2\gamma}^n(z)\, dz = \frac{n![\Gamma(2\gamma)]^2}{\Gamma(n+2\gamma)} g_3(n, \gamma);$$

$$\{D\} = \int_0^\infty e^{-z} z^{2\gamma+3} S_{2\gamma}^n(z) S_{2\gamma}^n(z)\, dz = \frac{n![\Gamma(2\gamma)]^2}{\Gamma(n+2\gamma)} g_4(n, \gamma);$$

$$\{E\} = \int_0^\infty e^{-z} z^{2\gamma+4} S_{2\gamma}^n(z) S_{2\gamma}^n(z)\, dz = \frac{n![\Gamma(2\gamma)]^2}{\Gamma(n+2\gamma)} g_5(n, \gamma);$$

wherein, for brevity, we have written the g's for the following :—

$$g_1=2(n+\gamma)\,;$$

$$g_2=(n+2\gamma+1)(n+2\gamma)+4n(n+2\gamma)+n(n-1)\,;$$

$$\begin{aligned}g_3=&(n+2\gamma+2)(n+2\gamma+1)(n+2\gamma)+9n(n+2\gamma+1)(n+2\gamma)+9n(n-1)(n+2\gamma)\\&+n(n-1)(n-2)\,;\end{aligned}$$

$$\begin{aligned}g_4=&(n+2\gamma+3)(n+2\gamma+2)(n+2\gamma+1)(n+2\gamma)+16n(n+2\gamma+2)(n+2\gamma+1)(n+2\gamma)\\&+36n(n-1)(n+2\gamma+1)(n+2\gamma)+16n(n-1)(n-2)(n+2\gamma)\\&+n(n-1)(n-2)(n-3)\,;\end{aligned}$$

$$\begin{aligned}g_5=&(n+2\gamma+4)(n+2\gamma+3)(n+2\gamma+2)(n+2\gamma+1)(n+2\gamma)+25n(n+2\gamma+3)\\&(n+2\gamma+2)(n+2\gamma+1)(n+2\gamma)+100n(n-1)(n+2\gamma+2)(n+2\gamma+1)(n+2\gamma)\\&+100n(n-1)(n-2)(n+2\gamma+1)(n+2\gamma.+25n(n-1)(n-2)(n-3)(n+2\gamma)\\&+n(n-1)(n-2)(n-3)(n-4).\end{aligned} \qquad \ldots \quad (19)$$

Since $\Lambda-E=\frac{h^2}{8\pi^2 J}\left(\beta_0^2-\frac{2\beta_0^3}{a^2}\epsilon\right)$ [from (3) and (4)], and

$\epsilon=f_1g_1+f_2g_2+\ \ldots\ +f_5g_5$ [from (18)]

we get $E=E_0+\frac{h^2}{4\pi^2 J}\frac{\beta_0^3}{a^2}\epsilon=E_0+E_1$, say,

where E_0 (for the unperturbed state $b=c=..0$) was obtained by Fues and Sommerfeld, and the additional energy-value $(b\neq 0,\ c\neq 0)$ is given by

$$E_1=\frac{h^2}{4\pi^2 J}\left\{\beta_0(b-c)(n+\gamma)-\tfrac{1}{4}(3b-4c)g_2(n,\gamma)+\frac{3}{8\beta_0}(b-2c)g_3(n,\gamma)\right.$$
$$\left.-\frac{1}{16\beta_0^2}(b-4c)g_4(n,\gamma)-\frac{c}{32\beta_0^3}g_5(n,\gamma)\right\}, \qquad \ldots \quad (20)$$

where $\beta_0=\frac{2\pi J\omega_0}{h}\left\{1-\tfrac{1}{2}\left(\frac{m+\frac{1}{2}}{a}\right)^2-\frac{n+\frac{1}{2}}{a}+\ldots\right\}$, $a=2\pi J\omega_0/h$.

REFERENCES

Basu, K., 1943, *Bull. Cal. Math. Soc.*, **35**, 21.
Chakravarti, S. K., 1938, *Zeit. f. Phys.*, **109**, 25.
Fues, E., 1926, *Ann. der. Phys.*, **80**, 367 ; **81**, 281.
Sommerfeld, A., 1930, *Wave Mechanics*, §3 D.

ON THE PRESENCE OF PHOSPHORUS IN THE SOLAR ATMOSPHERE

By K. NARAHARI RAO

(*Received for publication, May 7, 1943*)

ABSTRACT. Continuing the previous work of the author on the band spectrum of phosphorus, the presence of the P_2 molecule in the solar atmosphere is discussed by a study of the coincidences of the lines of two of its strong bands, (8, 27) and (9, 28), in the near ultraviolet, with the Fraunhofer lines. It has been concluded that the molecule of phosphorus exists in the Sun.

The band spectrum of phosphorus presents several extremely interesting features. The P_2 molecule has an extensive and typical band spectrum ranging from λ3500 to λ1900 corresponding to a $^1\Sigma - {}^1\Sigma$ transition. The bands are degraded towards the red, possess a simple rotational structure and exhibit an alternation in intensity of the rotational lines which is a well-known characteristic feature of all symmetrical molecules. In recent papers (Rao, 1943*a*, 1943*b*), the author has described experiments leading to the analysis of the P_2 bands in the region about λ2800, and the determination of the nuclear spin of the P_2 molecule. In continuation of this work, it was thought worthwhile to see for the possible correlations between the Fraunhofer lines and the lines due to the P_2 molecule in the near ultraviolet region. Also, it is known that a large proportion of faint solar lines (*i.e.*, those having intensities between 1 and −3 on the Rowland scale) is still unidentified and that many of these lines must be of molecular origin.

While discussing the presence of phosphorus compounds in the solar atmosphere Dorothy N. Davis (1941) excludes the study of the P_2 molecule, because the strong bands of the molecule lie in the inaccessible region, but concludes that the molecule of CP may be present in the sun. It is no doubt a fact that most of the strong bands of the molecule of phosphorus fall in the region beyond λ2800 which are of no astrophysical importance. But the (8, 27) and the (9, 28) bands, which lie in the near ultraviolet are no less strong than those that are lying in the far ultraviolet, permit a study of the presence of the molecule of phosphorus in the solar atmosphere.

These bands have been photographed by Ashley (1933) in the 2nd order of a 21-foot concave grating for studying the rotational structure of certain bands due to the P_2 molecule and determining the nuclear spin from the alternating intensity ratio. In view of the high dispersion of the instrument used by Ashley, the wavelengths of all the lines recorded by her in the two bands are used by the author and compared with those of the Fraunhofer lines in the Rowland tables. Differences of not more than 0.04 A between the laboratory measurements and the solar wavelengths have been reckoned as coincidences.

The results are summed up in the following tables—

TABLE I

(8, 27) Band

$\lambda'(P_2)$.	λ (sun).	$\Delta\lambda = \lambda$ (sun) $- \lambda'(P_2)$	Intensity of the solar line.	Identification in the Rowland atlas.	$\lambda'(P_2)$.	λ (sun).	$\Delta\lambda = \lambda$ (sun) $- \lambda'(P_2)$.	Intensity of the solar line.	Identification in the Rowland atlas
R-branch					3170.44	3170.48	0.04	−1	—
3166.43	3166.44	0.01	1	Fe	3170.66	3170.71	0.05	1	−Ni*
3166.57	3166.60	0.03	0	Zr	3170.90	—	—	—	—
3166.72	3166.68	−0.04	1	—	3171.16	3171.14	−0.02	−2	—
3166 80	3166.77	−0.03	0	—	3171.41	3171.36	−0.05	2	Fe
3166.80	3166.87	−0.02	−2	—	3171.69	3171.67	−0.02	1	Fe
3166.99	3166·99	0.00	−1	—	3171.95	3171.94	−0.01	−2	—
3167.10	—	—	—	—	3172.25	3172.30	0.05	0	—
3167.21	3167.18	−0.03	1	OH	3172.51	3172.51	0.00	0	—
3167.33	3167.30	−0.03	−3	—	3172 83	3172 85	0.02	−2	—
3167.47	3167.42	−0.05	−2N	—	3173.15	3173.21	0.06	0	OH ?
3167.60	3167.60	0.00	−1N	Zr^{+}	3173.45	3173.41	−0.04	1	Fe
3167.88	3167.86	−0.02	3	Fe	3173.75	—	—	—	—
3168.02	3168.05	0.03	−3	Co ?	3174.10	3174.06	−0 04	−1	—
3168.19	3168.15	−0.04	2	V^{+}	3174.43	3174.38	−0.05	0	OH
3168.55	3168.53	−0.02	4	Ti^{+}	3174 77	3174.79	0.02	−3	—
3168.71	3168.67	−0.04	0	OH ?	3175.13	3175.17	0.04	−3	—
3168.92	3168.96	0.04	1	OH	3175.48	3175.45	−0.03	2	Fe
3169.12	3169.08	−0.04	−2	—	3175.84	3175.82	−0.02	−3	—
3169.31	3169.37	0.06	1	—	3176.23	—	—	—	—
3169.51	—	—	—	—	3176.50	3176.45	−0.05	−1	Fe ?
3169.73	3169.75	0.02	1	Co	3176.76	3176.84	0.08	−2	Hf^{+} ?
3169.95	3170.01	0.06	−3	—	3177.14	3177.08	−0.06	−1	Mn ?
3170.18	3170.13	−0.05	−1	—	3177.54	3177.543	0.003	2	−Fe^{+}

TABLE I (*contd.*)

(8, 27) Band (*contd.*)

$\lambda(P_2)$.	λ (sun).	$\Delta\lambda=\lambda(\text{sun})-\lambda(P_2)$.	Intensity of the solar line.	Identification in the Rowland atlas.	$\lambda(P_2)$.	λ (sun).	$\Delta\lambda=\lambda(\text{sun})-\lambda(P_2)$	Intensity of the solar line.	Identification in the Rlowland atas.
3178.03	3178.02	−0.01	2	Fe	3172.15	—	—	—	—
3178.45	3178.43	−0.02	−1	—	3172.42	3172.38	−0.04	−3	—
3178.78	3178.79	0.01	−2d	—	3172.73	3172.72	0.01	−3	Ti
3179.21	3179.17	−0.04	−2N	Cr ? −	3172.99	3173.00	0.01	1	OH
3179.69	3179.67	−0.02	−2N	—	3173.33	—	—	—	—
3180.13	3180.12	−0.01	−1N	—	3173.62	3173.61	−0.01	1	Fe⁺ ?
3181.00	3180.99	−0.01	−2	—	3173.97	3173.95	−0.02	−2	—
3181.49	3181.53	0.04	1	Fe	3174.28	3174.22	−0.06	0	—
3181.95	3181.91	−0.04	1	Zr⁺	3174.62	3174.70	0.08	2	—
3182.93	3182.99	0.06	3	Fe OH	3174.99	3174.95	−0.04	1	Co—
P branch	—	—	—	—	3175.32	3175.32	0.00	1	OH-Fe ?
3167.83	3167.79	−0.04	1	—	3175.65	3175.71	0.06	−3	Mn
3168.16	3168.15	−0.01	2	V⁺	3176.02	3175.99	−0.03	1	Fe ?
3168.51	3168.53	0.02	4	Ti⁺	3176.39	3176.35	−0.04	1	Fe
3168.63	3168.67	0.04	0	OH ?	3176.64	3176.60	−0.04	−3	—
3168.87	3168.86	−0.01	1	Fe	3176.96	3176.93	−0.03	−3	—
3169.05	3169.08	0.03	−2	—	3177.42	—	—	—	—
3169.25	—	—	—	—	3177.93	—	—	—	—
3169.47	3169.43	−0.04	1	—	3178.33	3178.33	0.00	−3	—
3169.66	3169.62	−0.04	0	OH	3178.74	3178.79	0.05	−2d	—
3169.88	3169.86	−0.02	0	OH	3179.14	3179.17	0.03	−2N	Cr ?—
3170.10	3170.13	0.03	−1	—	3179.56	3179.51	−0.05	1N	Fe
3170.58	3170.48	−0.10	−1	—	3180.01	3179.97	−0.04	−1	OH
3170.81	3170.81	0.00	−3	—	3180.89	3180.88	−0.01	−2	—
3171.08	3171.14	0.06	−2	—	3181.34	3181.28	−0.06	3	Ca⁺
3171.33	3171.36	0.03	2	Fe	3181.81	3181.86	0.05	1	Fe
3171.60	3171.67	0.07	1	Fe	3182.78	3182.81	0.03	0	—
3171.85	—	—	—	—					

TABLE II

(9, 28) Band

λ (P_2)	λ (sun)	$\Delta\lambda = \lambda$ (sun) $- \lambda$(P_2)	Intensity of the solar line.	Identification in the Rowland atlas.	λ(P_2)	λ (sun)	$\Delta\lambda = \lambda$(sun) $- \lambda$(P_2)	Intensity of the solar line.	Identification in the Rowland atlas.
R branch									
3184.61	3184.62	0.01	1	−Fe	3189.12	3189.17	0.05	−3	—
3184.70	—	—	—	—	3189.38	3189.32	−0.06	0	OH
3184.78	3184.76	0.02	−3	—	3189.65	3189.64	−0.01	−3	—
3184.90	3184.90	0.00	2	Fe	3189.93	3189.96	0.03	−2	Mn
3185.01	3185.02	0.01	1N	—	3190.21	3190.17	−0.04	−2	—
3185.11	3185.09	−0.02	−3	Mo ?	3190.50	3190.54	0.04	−2	—
3185.25	3185.22	−0.03	−3N	—	3190.80	3190.85	0.05	2	Fe-Ti$^+$
3185.36	3185.39	0.03	2	V	3191.14	3191.13	−0.01	0	Fe ?
3185.51	3185.56	0.05	−1	—	3191.43	3191.42	−0.01	0	—
3185.63	3185.67	0.04	0	—	3191.74	—	—	—	—
3185.80	3185.80	0.00	−2N	—	3192.08	3192.04	−0.04	−1	—
3185.95	3185.98	0.03	0	Co-	3192.75	3192.73	−0.02	−2	OH
3186.12	3186.11	−0.01	0Nd ?	OH	3193.10	3193.06	−0.04	−1	OH
3186.32	3186.27	−0.05	−1	—	3193.41	—	—	—	—
3186.47	3186.45	−0.02	1	Ti	3193.82	3193.82	0.00	1N	Fe$^+$
3186.66	3186.64	−0.02	−3	—	3194.24	3194.24	0.00	−1	Ti$^+$?
3186.84	3186.80	−0.04	1	—	3194.55	3194.53	−0.02	−1	—
3187.03	3187.06	0.03	−3	—	3194.98	3194.97	−0.01	−1	Cb$^+$
3187.24	—	—	—	—	3195.32	3195.41	+0.09	−2N	—
3187.45	—	—	—	—	3195.65	—	—	—	—
3187.67	—	—	—	—	3196.10	3196.11	0.01	−3	Fe$^+$
3187.90	3187.90	0.00	−3	—	3196.33	3196.34	0.01	−2	—
3188.13	—	—	—	—	3197.35	3197.36	0.01	−3	—
3188.37	3188.38	0.01	0	Co	3198.22	3198.28	0.06	0	—
3188.61	3188.55	−0.06	6d ?	V$^+$−Fe	3199.13	3199.14	0.01	0	OH ?
3188.85	3188.82	−0.03	2	Fe	3200.05	3200.14	0.09	−1	—

In Tables I and II, in the intensity column 'N' indicates that the line is not clearly defined. Such a line may be considered as composed of two or

TABLE II (*contd.*)

(9, 28) Band (*contd.*)

λ (P_2)	λ (sun)	$\Delta\lambda=\lambda$(sun) $-\lambda(P_2)$	Intensity of the solar line.	Identification of the Rowland atlas.	λ(P_2)	λ (sun)	$\Delta\lambda=\lambda$(sun) $-\lambda(P_2)$	Intensity of the solar line.	Identification in the Rowland atlas.
P-branch					3191.29	3191.31	0.02	−2	Co
3186.56	--	---	—	..	3191.60	3191.57	−0.03	−3	-
3186.67	3186.64	−0.03	−3	--	3191.93	3191.89	−0.04	−1	NiZr⁺
3186.76	3186.75	−0.01	3	Fe⁺	3192.23	3192.27	−0.04	0	Ti⁺ ?
3186.82	3186.80	−0.02	1	—	3102.59	3192.62	0.03	−1	—
3187.24	—	—	—	—	3192.94	3192.92	−0.02	1N	Fe ?
3187.38	3187.31	−0.07	1	Fe⁺	3193.28	3193.30	0.02	2	Fe
3187.59	3187.56	−0.03	0Nd ?	..	3193.59	3193.55	−0.04	−2N	—
3187.82	3187.90	0.08	−3	—	3194.00	3193.98	−0.02	−2	Mo
3188.04	3188.04	0.00	1	Cr ?	3194.38	3194.34	−0.04	−3	...
3188.27	3188.20	−0.07	−3	—	3194.75	3194.70	0.01	−2	--
3188.51	3188.54	0.03	0d ?	V⁺-Fe	3195.13	3195.14	0.01	−1	-
3188.76	—	—	—	—	3195.52	--	—	—	—
3189.01	3188.94	−0.07	−2	—	3195.92	3195.88	−0.04	−3	—
3189.28	3189.32	0.04	0	OII	3196.33	3196.34	0.01	−2	—
3189.54	3189.50	−0.04	−1N	—	3197.16	3197.21	0.05	−2	—
3189.81	3189.82	0.01	−2	—	3198.02	3198.02	0.00	0	V
3190.10	3190.10	0.00	1	—	3198.90	3198.9[illegible]	0.00	−2N	Fe ?
3190.39	3190.40	0.01	−2	—	3999.82	3199.82	0.00	−3N	V ?
3190.68	3190.68	0.00	2	V⁺dFe	3200.77	3200.79	0.02	2	Fe
3190.98	3190.90	−0.08	3	—	3201.76	3201.72	−0.04	−2N	Ce⁺

more lines too close to be separated. And two lines close enough together to be considered double are indicated by a 'd', and a double whose components are very difficult to separate is indicated by a 'd?' A '−' before an element say Ni (refer* mark, in the 8, 27 band) means that Ni line is coincident with the red side of the line, the origin of the rest of the line being unknown. Similarly '−' after the element means that the origin of the red side of the line is not known.

From the above tables, we see that, in most cases where there is a large difference in wavelength between the laboratory measurement and the value of the solar line taken from the Rowland atlas, either the solar line is a blend of two or more lines which are too close to be separated or a strong atomic line in the vicinity masks the fainter molecular line. Also, we find that when the origin of the red or violet part of the solar line is unknown the P_2 line coincides with that particular portion.

Further, it is instructive to compare the observed coincidences with the number which may be expected from chance using the formula of Russell and Bowen (1929),

$$C = N(1 - e^{-2Mx/I}),$$

where N is the number of solar lines in the wavelength interval I, M is the number of lines being investigated for coincidence in the interval I and x is the size of coincidence in Angstrom units. Attention has been paid to possible systematic differences, the numbers of coincidences being determined within 0.01, from 0.01 to 0.02, 0.02 to 0.03 and 0.03 to 0.04 Angstrom units. The results obtained are summed up below :

	(8, 27) band	(9, 28) band
1 Total number of lines in the P spectrum	100	93
2 Observed coincidences (with previously identified and unidentified lines in the solar spectrum)	67	66
3 Observed coincidences with previously unidentified lines	44	4[illegible]
4 Number of coincidences from chance	49	47

Band (v', v'')	Size of coincidence in Angstroms	Number of chance coincidences	Number of observed coincidences
8, 27	0·01	14	19
	0·01-0·02	13	14
	0·02-0·03	12	14
	0·03-0·04	10	20
9, 28	0·01	14	27
	0·01-0·02	12	12
	0·02-0·03	11	13
	0·03-0·04	10	14

We can see from these two tables that in all the cases the number of observed coincidences is more in excess of that expected by chance. Also we find that about 66% of the observed coincidences are with lines previously unidentified. And a large majority of the lines coincide with faint solar lines.

These considerations, in addition to the study of the possible correlations dealt with in the beginning, indicate that with the data at present available we can conclude that the molecule of phosphorus exists in the solar atmosphere.

This conclusion is supported from physical considerations as well. The P_2 molecule is stable enough for the temperature existing in the solar atmosphere as its heat of dissociation is 5.1 volts.

The author is indebted to Dr. A. L. Narayan for his constant guidance and help during the course of these investigations.

SOLAR PHYSICS LABORATORY,
KODAIKANAL.

REFERENCES

Ashley, 1933, *Phys. Rev.*, **44**, 919.
Dorothy N. Davis, 1941, *A. P. J.*, **94**, 276.
Russell and Bowen, 1929, *A P. J.*, **69**, 196.
Rao, K. Narahari, 1943a, *Ind. J. Phys.*, **17**
1943b, *ibid.*

DIELECTRIC CONSTANT MEASUREMENTS

(*a*) *The Oscillators*—For the wavelength range from about 270 cm. to 1500 cm. an ordinary regenerative type of oscillator was employed. For the shorter wavelengths, 80 cm.—240 cm., a midget 'Acorn' tube was employed in a Hartley circuit. In the latter case, the inductance of the oscillator circuit was a single turn of copper wire of varying sizes in the wavelength range: 80 cm.—160 c.m. and was of two turns of copper wire of varying sizes in the range: 160 cm.—240 cm.

(*b*) *Experimental Method and Details*—The discharge tube A was fixed in a vertical position between two thin cylindrical metal pieces held tightly round the outside of the discharge tube. The distance between the two aluminium electrodes of the discharge tube was 7·4 cm. The diameter of the tube was 2.55 cm. and the diameter of each electrode was 2·3 cm. The cylindrical pieces, each of which was 3.5 cm. in length and 2.6 cm. in width, when straightened out, made up the terminal condenser of a pair of Lecher wires. The Lecher wires consisted of No. 18 copper wire spaced at 5.6 cm. Ultra-high frequency oscillations were then induced into the Lecher system from one or the other of the oscillators and resonance adjustments were made by sliding a short-circuiting bridge B, across the wires. The short-circuiting bridge was made of No. 14 copper wire and was mounted on a long handle. The lower side of the short-circuiting bridge was filed to give a sharp edge. A scale was kept horizontally fixed on one side of the Lecher wires and a pointer P fixed to the short-circuiting bridge indicated accurately the position of the bridge when adjusted for resonance. The resonance was indicated by a valve-detector with a galvanometer in the anode circuit. The anode current was balanced for no signal. The detector unit was coupled to the Lecher system at the input end by means of two small condensers *a* consisting of short brass tubes insulated from the Lecher wires by glass sleeves. The diagram of the entire experimental arrangement is shown in Fig. 1. The short-circuiting bridge is sketched in the same diagram. It should be noted that the bridge adjustment was made for voltage maximum across the terminal condenser of the Lecher system.

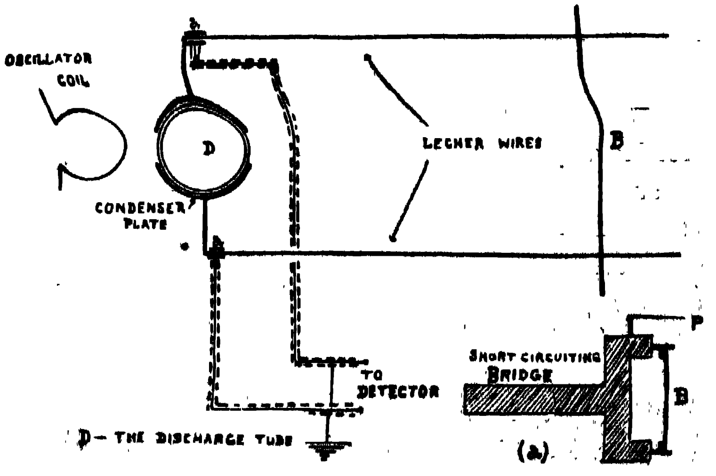

FIG. 1

Careful shielding arrangement was found essential to eliminate the induction effect of the small Rumkorff coil used for passing high voltage discharge through the discharge tube. The induction coil was enclosed in a shielded box and placed at a considerable distance from the experimental arrangement. The leads from the secondary terminals of the induction coil were properly shielded, and so also the leads from the input side of the Lecher wires to the valve-detector. The method of measuring the dielectric constant of the ionized air consisted mainly in determining the tuning position of the short-circuiting bridge when there was no discharge through the tube and in noting the shift of the tuning position when the discharge was passed through the tube.

(*c*) *Calculation of the effective dielectric constant of the ionized air.*—Let l be the length of the Lecher wire measured from the input end to the resonance point, when there is no discharge. C_0 is the capacity of the condenser which changes to the value $\epsilon . C_0$ (ϵ being the dielectric constant of the ionized air) on passing a discharge through the discharge tube. C_1 is the equivalent capacity of the two condensers with air and glass as dielectrics between the cylindrical pieces and the inner glass surface of the discharge tube. C_2 is the capacity inserted in parallel to C_0 and C_1, in order to make up for the fact that some lines of force between the cylindrical pieces do not actually pass through the discharge tube. It would also be taken to include the capacity and induction effect of the short leads to the cylindrical metal pieces.

When the length of the Lecher wire is adjusted for resonance, we have,

$$\frac{\gamma}{C} \cdot \frac{2\pi}{\lambda} \cdot \tan \frac{2\pi l}{\lambda} = 1 \qquad \ldots \quad (1)$$

where γ is the equivalent capacity of the terminal condenser, C the capacity per unit length of the Lecher system and λ the wavelength of the standing waves along the wires. Here

$$\gamma = C_2 + \frac{C_1 C_0}{C_1 + C_0} \qquad \ldots \quad (2)$$

Again, when a discharge is passed through the discharge tube, and if l' be the new resonance length of the Lecher wires from the input end we have,

$$\frac{\gamma'}{C} \cdot \frac{2\pi}{\lambda} \cdot \tan \frac{2\pi l'}{\lambda} = 1 \qquad \ldots \quad (3)$$

where

$$\gamma' = C_2 + \frac{\epsilon C_0 C_1}{C_1 + \epsilon C_0} \qquad \ldots \quad (4)$$

Now let us put $\frac{\gamma'}{\gamma} = \epsilon_u$, where ϵ_u stands for the uncorrected value of the dielectric constant of the ionized air. Thus

$$\epsilon_u = \frac{\gamma'}{\gamma} = \frac{C_2 + \frac{\epsilon C_0 C_1}{C_1 + \epsilon C_0}}{C_2 + \frac{C_0 C_1}{C_1 + \epsilon C_0}} \qquad \ldots \quad (5)$$

From (5) it can be easily shown

$$\epsilon=\epsilon_u\cdot\frac{C_1}{(1-\epsilon_u)C_0+C_1}$$

Writing δ for $(1-\epsilon_u)$, we have finally

$$\epsilon=\epsilon_u\frac{C_1/C_0}{\delta+C_1/C_0} \qquad \ldots \quad (6)$$

It is to be noted that C_2 is eliminated from the above expression. Now from (1) and (3),

$$\frac{\gamma'}{\gamma}=\epsilon_u=\frac{\tan\frac{2\pi l}{\lambda}}{\tan\frac{2\pi l}{\lambda}}, \qquad \ldots \quad (7)$$

This ratio $\frac{\gamma'}{\gamma}$ can be experimentally determined and if now we can find the ratio C_1/C_0, the exact dielectric constant of the ionized air can be determined from (6).

(*d*) *Determination of* C_1/C_0.—Three sets of observations are necessary for the evaluation of this ratio: (*i*) with only air in the discharge tube, the resonance length l should be obtained, (*ii*) with normal solution of potassium chloride * inside the discharge tube the resonance length l_1 should be found and (*iii*) with a non-polar liquid like benzene having a known dielectric constant, the resonance length l_2 should be again obtained. Thus we have for any wavelength λ

$$(i) \quad \frac{\gamma}{C}=\frac{1}{\frac{2\pi}{\lambda}\tan\frac{2\pi l}{\lambda}}, \quad \text{where } \gamma=C_2+\frac{C_1C_0}{C_0+C_1},$$

$$(ii) \quad \frac{\gamma_1}{C}=\frac{1}{\frac{2\pi}{\lambda}\tan\frac{2\pi l_1}{\lambda}}, \quad \text{where } \gamma_1=C_2+C_1$$

and

$$(iii) \quad \frac{\gamma_2}{C}=\frac{1}{\frac{2\pi}{\lambda}\tan\frac{2\pi l_2}{\lambda}}, \quad \text{where } \gamma_2=C_2+\frac{KC_0C_1}{KC_0+C_1},$$

K being the known dielectric constant of the non-polar liquid. From these three equations, we have again

$$\gamma_1-\gamma=\frac{C_1^2}{C_1+C_0}$$

and

$$\gamma_1-\gamma_2=\frac{C_1^2}{KC_0+C_1}$$

---

* Pure mercury was also used. Both mercury and the normal KCl solution gave practically the same resonance length.

so that we can write

$$\frac{\gamma_1-\gamma}{\gamma_1-\gamma_2}=A=\frac{KC_0+C_1}{C_0+C_1}$$

whence

$$\frac{C_1}{C_0}=\frac{K-A}{A-1} \qquad \dots (8)$$

K is here known and A is obtained from

$$A=\frac{\gamma_1-\gamma}{\gamma_1-\gamma_2}=\frac{\dfrac{1}{\tan\dfrac{2\pi l_1}{\lambda}}-\dfrac{1}{\tan\dfrac{2\pi l}{\lambda}}}{\dfrac{1}{\tan\dfrac{2\pi l_1}{\lambda}}-\dfrac{1}{\tan\dfrac{2\pi l_2}{\lambda}}} \qquad \dots (9)$$

The ratio C_1/C_0 can thus be determined.

(*c*) *Experimental Results.*—The pressure inside the discharge tube at the time of sealing was 3 mm. of mercury. In both sets of experiments for the two wavelength ranges; 80 cm. – 240 cm. and 270 cm. – 1500 cm., the current through the discharge tube was maintained at a constant value, *viz.*, 4.1 m.a. The ratio C_1/C_0 was determined in the manner described in the preceding sub-section.

The dielectric constant values as obtained from (6) and (7) are shown for the shorter wavelength range (80 cm.—240 cm.) in Fig. 2(*a*). The shift of the resonance point for the same range is illustrated in Fig. 2(*b*). Similar curves for the longer wavelength range (270 cm.—1500 cm.) are shown in Figs. 3(*a*) and 3(*b*).

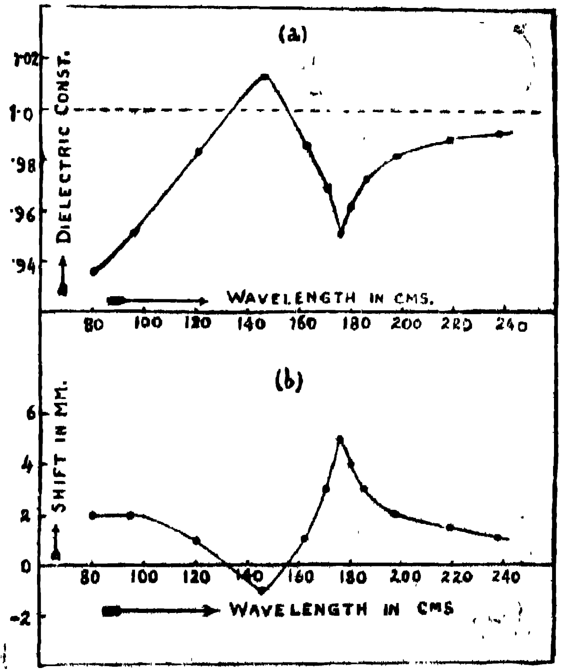

Fig. 2

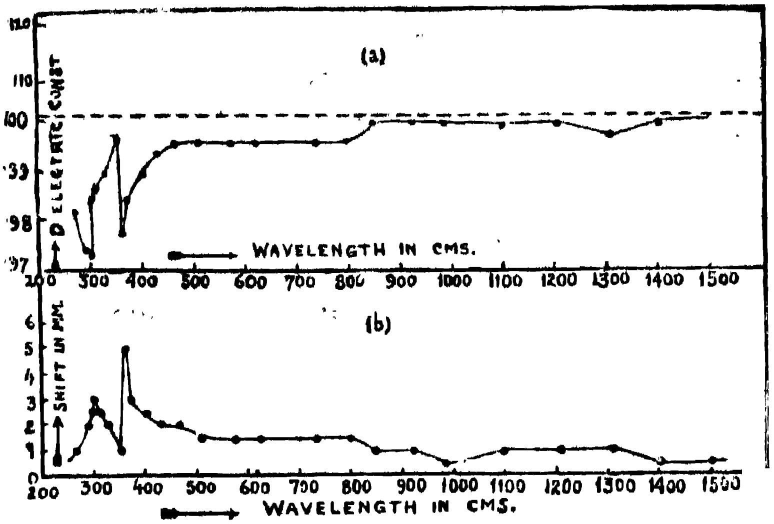

FIG 3.

The most noticeable feature in the observed variation of the dielectric constant of the ionized air with the wavelength of the measuring field is that there were three distinct minima in the dielectric constant value in the following regions:

(1) 175 cm. (2) 310 cm. (3) 370 cm.

Proceeding from the shortest wavelength (*i.e.*, about 80 cm. in these experiments) the dielectric constant of the ionized air which was less than unity, was found to increase with the increase of wavelength. It attained the value of unity, when the wavelength was about 130 cm. With further increase of wavelength, the dielectric constant became even greater than unity. Subsequently, the value decreased again showing a minimum at about 175 cm. It increased again remaining however within the value of unity and decreased subsequently attaining a minimum at 310 cm. The dielectric constant similarly increased again remaining always less than unity and later it decreased till a minimum was reached at 370 cm. Subsequently to this minimum, up to 1500 cm. the dielectric constant of the ionized air steadily increased almost approaching the value of unity.

DETECTION OF OSCILLATIONS IN THE DISCHARGE TUBE

With the discharge tube working under the same conditions as in the dielectric constant measurements and without working the oscillator, a very careful search was made for the potential nodes on the Lecher wires in order to detect any oscillations in the discharge tube. Evidence of feeble and yet very distinct oscillations at three different wavelengths was obtained. The wavelengths were obtained by measuring the distance between two successive potential nodes. The wavelengths of these oscillations in the discharge tube were: (1) 169 cm. (2) 310 cm. and (3) 362 cm. The location of the resonance points for the observed oscillations was however less precise. The positions were found to vary by a distance of about 1 cm.

It is interesting that the wavelengths of these oscillations corresponded rather well with the wavelengths, where the minima in the dielectric constant values were observed.

PREVIOUS WORK ON THE OSCILLATIONS IN THE DISCHARGE TUBE

The possibility of a resonance phenomenon in the ionized medium inside a discharge tube had long been envisaged by various investigators. A simple theory of electronic and ionic oscillations inside an ionized gas was developed by Tonks and Langmuir (1929). In the case of the electronic oscillations, the positive ions were supposed to behave like a rigid jelly of uniform positive charge density. Imbedded in it and free to move, the electrons were supposed to have a uniform distribution, so that the net charge was zero. The field arising out of the electron displacement would then be responsible for the displaced electrons to oscillate about their original positions with simple harmonic motion. The frequency of such oscillation would be given by

$$\nu = \left(\frac{Ne^2}{\pi m} \right)^{\frac{1}{2}} = 8980\sqrt{N},$$

where N is the electron density and e, m are the charge and mass of the electron. Oscillations of this type were called plasma*-electron oscillations.

J. J. Thomson (1931) also developed a similar expression for the frequency of oscillation in the case of electrodeless discharge, *viz.*,

$$\nu^2 = \frac{Ne^2}{\pi m} + \frac{c^2}{\lambda^2}$$

(c being the velocity of light and λ the wavelength of the oscillation). The lower frequency limit for long waves in this case coincides with the plasma-electron frequency of Tonks and Langmuir. Modified expressions for the Thomson formula were given by Jonescu (1931) and Placiteanu (1931). Tonks and Langmuir also considered ionic oscillations and gave an expression for the wavelength of such oscillation.

There was also experimental evidence of oscillations in a discharge tube. Tonks and Langmuir (1929) were able to detect oscillations in specially constructed mercury discharge tubes. The frequency range of the most rapid oscillations (frequency range 300 Mc/s—1000 Mc/s corresponding to the wavelength range, 30 cm —100 cm.) agreed with that predicted for the oscillations of the ultimate electrons. They also obtained evidence of positive ionic oscillations.

---

* The word 'plasma' was used by Tonks and Langmuir to designate that portion of the discharge in which the densities of the ions and electrons are high but substantially equal. It comprises the entire space not occupied by 'sheaths' of positive ions.

Previous to Tonks and Langmuir, Penning (1926) had observed oscillations of radio frequencies in low-pressure discharges in mercury vapour. J. S. Webb and L. A. Pardue (1928) also described some experiments in which they found oscillations up to 240 Kc/s in a low-pressure air discharge tube.

Gutton (1930 *a*) postulated the existence of quasi-elastically bound electrons in an ionized gas. According to his idea, the quasi-elastic force has its origin in the mutual action of the ions in the ionized gas at low pressure. The natural wavelength of the electrons under the action of the quasi-elastic force was found to follow the relation :

$$N^{\frac{3}{4}}.\lambda^2 = \frac{4\pi^2 c^2}{A},$$

where N is the electron density, A a constant and c the velocity of light. In an elaborate study of the dielectric properties of the ionized air, Gutton obtained evidence of this natural frequency of the electrons inside a discharge tube, although he was not able to detect any electron oscillation in the ionized medium. The value of Gutton's natural frequency did not however tally with Tonks' and Langmuir's value as required from their formula.

Pederson (1930), on the other hand, explained Gutton's experimental results by regarding the metal plates round the discharge tube and the latter as two condensers in series, one having air and glass as dielectrics and the other having the ionized gas as dielectric. According to Pederson, the latter behaves as if it were shunted by an inductance. The metal plates and the discharge tube in Gutton's experiments were thus equivalent to a circuit of inductance and capacity and it was the resonance of this circuit that Gutton observed. According to this view, therefore, resonance frequency would depend, within wide limits, on the distance between the plates and the discharge tube. Gutton (1930*b*) however did not notice any such influence.

Resonance dispersion in an ionic plasma was considered by W. Sigrist (1937) as a definite 'container effect,' arising from the decrease of ionic density at the confines of the spatially limited gas discharges. Sigrist made some dispersion measurements in the ionic plasma of a low-potential arc in argon, and obtained evidence of quasi-elastically bound charges with a definite resonance frequency. The experiments of Asami and Saito (1938) in Japan supported Sigrist's view.

POSSIBLE CAUSE OF MULTIPLE RESONANCE OF THE ELECTRONS IN THE PLASMA

A series of overtones in the vibrating system is of course a possible explanation (Thomson, 1931, Placiteanu, 1931, Linder, 1936) of the simultaneous appearance of electronic oscillations of different frequencies or wavelengths. Alternatively, according to the view put forward by Tonks (1931), the multiple resonance of the electrons could be attributed to the different electron densities in the plasma. Sometimes, more than one layer are plainly visible at some places inside the discharge tube. In our experiments, it is significant that the 'semi-log' curves drawn for the determination of the electron density in the discharge tube by Langmuir's probe method, showed indication of a second break, besides the main one which was unmistakable. The main break gave a value of the electron density : $N = .9 \times 10^7$ electrons per c.c. The second discontinuity gave a value : $N = .57 \times 10^7$ electrons per c.c.

The different electron densities in the plasma inside a discharge tube were previously observed by Childs (1930).

RELATION BETWEEN ELECTRON DENSITY AND NATURAL WAVELENGTH OF THE ELECTRONS IN THE PLASMA

Tonks and Langmuir's relation between the electron density N and the wavelength λ of the electronic oscillation would be given by

$$N\lambda^2 = 1.12 \times 10^{13}$$

and if in Gutton's formula $N^{\frac{3}{4}}.\lambda^2 = 4\pi^2 c^2/A$, we put $A = 6.4 \times 10^{10}$ (which fitted with Gutton's experimental results), then we have

$$N^{\frac{3}{4}}\lambda^2 = 5.5 \times 10^{10}.$$

It is worthy of notice that of the oscillations of three different wavelengths 175 cm., 310 cm. and 360 cm. which were detected in the discharge tube, the oscillation of wavelength 310 cm. appeared to correspond to the electron density $N = .9 \times 10^7$ and the oscillation of wavelength 360 cm. to $N = .57 \times 10^7$; for we find $(N\lambda^2)$ and $(N^{\frac{3}{4}}\lambda^2)$ to remain approximately constant, when calculated with the relevent values of N and λ. Thus

when $N = .90 \times 10^7$, $\lambda = 310$ cm., $N\lambda^2 = 8.63 \times 10^{10}$, $N^{\frac{3}{4}}\lambda^2 = .16 \times 10^{10}$,

and when $N = .57 \times 10^7$, $\lambda = 360$ cm., $N\lambda^2 = 7.37 \times 10^{10}$, $N^{\frac{3}{4}}.\lambda^2 = .15 \times 10^{10}$.

It is also evident that the experimental values of $(N\lambda^2)$ given above are quite different from the value calculated from Tonks and Langmuir's formula. The value of $(N^{\frac{3}{4}}\lambda^2)$, however, indicated a nearer approach to Gutton's value.

ANOMALOUS VALUES OF THE DIELECTRIC CONSTANT OF THE IONIZED AIR

Following Lorentz, the dielectric constant of an ionised gas can be written in the form :

$$\epsilon = 1 - \frac{4\pi N e^2 (\omega^2 - \omega_0^2)}{(\omega^2 - \omega_0^2) + \omega^2 \nu^2}$$

where ω = angular freqency of the measuring field

ω_0 = natural angular frequency of the electrons

N = electron density

ν = electron collision frequency

and e and m are the charge and mass of an electron, The graphical representation of this equation is the familiar curve of anomalous dispersion. Starting with a large value of ω, if we go on diminishing ω, the dielectric constant, which is less than unity, would gradually decrease and after attaining a minimum value it would increase and attain the value of unity when $\omega=\omega_0$. When ω exceeds ω_0, the dielectric constant becomes greater than unity.

If, however, there are groups of electrons, each having a distinct characteristic frequency, then considering one after another all the dispersion curves, corresponding to the various natural frequencies, it can be seen that the final curve would be a superposed effect and the resultant dielectric constant curve could be of the type actually observed in our experiments. This is illustrated in Fig. 4.

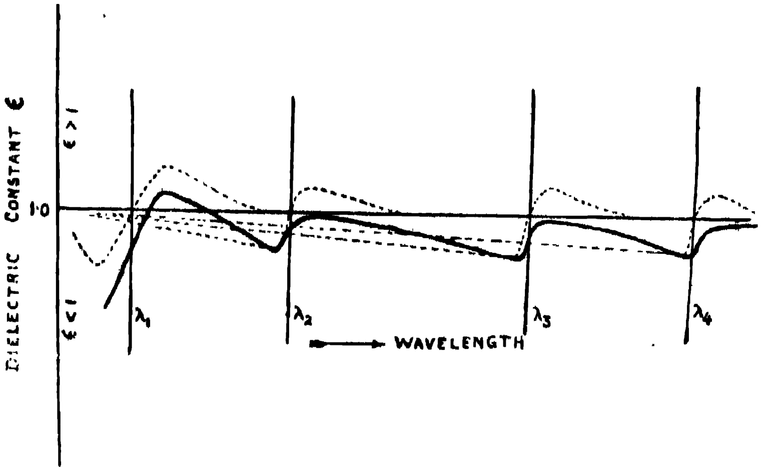

------ Individual dispersion curve

. ——— Resultant curve

FIG. 4.

Our best thanks are due to Prof. S. N. Bose, Head of the Physics Department, for his interest and help during the course of this investigation.

PHYSICS DEPARTMENT,
DACCA UNIVERSITY.

REFERENCES

Asami, X., and Saito, N., 1938, *Electrotech. Jour. Phys.*, **2**, 146.

Childs, E. C., 1930, *Phil. Mag.*, **10**, 969.

Gutton, 1930a, *Ann. de Phys.*, **13**, 68. See also Gutton and Clement, 1927, *Comptes Rendus*, 184, and Gutton's various short notes in *ComptesRendus*

Gutton, 1930b, *Comptes Rendus*, **190**, 844.

Imam Ali and Khastgir, S. R., 1937, *Phil. Mag.*, **23**, 858. See also Gangopadhyaya, S. and Khastgir, S. R., 1938, *Phil. Mag.*, *Supplement* and Emran, Md. and Khastgir, S. R., 1943, unpublished.

Jonescu, 1931, *Comptes Rendus*, **192**, 928.

Linder, 1936, *Phys. Rev.*, **49**, 645.

Pederson, 1930, *The Propagation of Radio Waves*, *Experimental Wireless and Wireless Engineer*, **7**, 16.

Penning, 1926, *Nature*, **118**, 301, and *Physics*, **6**, 241.

Placiteanu, 1931, *Comptes Rendus*, **193**, 286

Sigrist, W., 1937, *Helv. Phys. Acta.*, **10**, 73. See also Sigrist, W., 1935, *Helv. Phys. Acta.*, **8**, 317.

Thomson, J. J., 1931, *Phil. Mag.*, **11**, 697. See also Thomson, J. J., 1928, *Proc. Phys. Soc. (London)*, **40**, 82.

Tonks, 1931, *Phys. Rev.*, **37**.

Tonks and Langmuir, 1929, *Phys. Rev.*, **33**, 195 and 990.

Webb, J. S., and Pardue, L. A., 1928, *Phys. Rev.*, **31**, 1122. *Ibid.*, **32**, 946.

A NEW ULTRA-VIOLET BAND SYSTEM OF ANTIMONY MONOXIDE (SbO)

By A. K. SEN GUPTA.

(*Received for publication, June 30, 1943*).

ABSTRACT. A new ultra-violet band system, very likely due to a $^2\Sigma \longrightarrow {}^2\Pi$ transition, has been photographed under moderately high dispersion in the region λ2910 – λ2450 in the emission spectrum of antimony monoxide. The bands are degraded towards the violet and each band head is itself double. Their vibrational structure analysis shows that the lower state of this new system is identical with that of the other systems already known for the molecule.

INTRODUCTION

In a recent communication (Sen Gupta, 1939) the vibrational structure analysis of two band systems in the region λ6650 – λ3200 in the emission spectrum of SbO has been described. During this investigation the presence of a number of double-headed bands lying below λ3000 was noticed on the preliminary plates taken with a small quartz spectrograph of large light-gathering power. These bands have not been previously recorded. The analysis of their vibrational structure shows without doubt that their emitter is the diatomic molecule, SbO, inasmuch as the vibrational constants of the lower state of this band system are, within close limits, the same as those of the two existing systems. The object of the present paper is to report the analysis of these new bands.

EXPERIMENTAL

Using the same light source as previously employed, plates were taken with a Hilger E. I. quartz spectrograph, having a dispersion varying from about 2.2 A.U per m.m at λ2400 to 4.4 A.U per m.m at λ2900. Using iron arc lines as standards of comparison, the wave-lengths of band-heads were measured with a Gaertner precision comparator in the usual way.

DESCRIPTION OF THE NEW BANDS

As the separation between the sub-levels is very large in comparison to the vibrational spacings, the doublet nature of the system is not apparent at the first sight. The system is, in fact, composed of two sub-systems, the more refrangible and the less refrangible components being indicated by (*a*) and (*b*) respectively. The (0, 0) band of the *b* sub-system is a comparatively strong band at λ2663.96 (ν = 37526.9). The bands (0, 0), (0, 1), (0, 2) and (0, 3) of this sub-system are more prominent in comparison to the (1, 0), (2, 0) and (3, 0) bands. In most of the bands the heads appear double evidently due to the P-form and Q-form branches. The separation between these heads increases progressively with increasing v' – or decreasing v'' – values.

The "*a*" sub-system also shows similar characteristics with spacings practically identical with those between the bands of the "*b*" sub-system. It is further found that bands with the same v', v'' – values in the two sub-systems have an interval of approximately 2272 cm.$^{-1}$ between them. Thus the $a(0, 0)$ band is at $\lambda 2511.89$ ($\nu = 39798.6$). Like the *b*-bands, they have also two close heads, the separation between them varying in a similar manner. The bands under consideration may therefore be considered to be made up of two groups, very much identical in their appearance.

VIBRATIONAL ANALYSIS

Table I gives the wave-lengths in air of all the measured heads and also their wave numbers in vacuo. The v', v'' – values assigned to each band and the type to which its double-heads belong, are also included in the table.

As the Q-form heads are very close to the origins, it may be considered that their wave numbers would represent very approximately the positions of the respective band origins. Hence using the wave number data of the Q-heads, the following equations have been independently derived for the (*a*) and (*b*) sub-systems in the usual way.

For the *b*-sub-system

$$\nu = 37495.7 + 880.0\,(v' + \tfrac{1}{2}) - 5.80\,(v' + \tfrac{1}{2})^2 - 817.0\,(v'' + \tfrac{1}{2}) + 5.20\,(v'' + \tfrac{1}{2})^2$$

and for the *a*-sub-system

$$\nu = 39767.7 + 879.0\,(v' + \tfrac{1}{2}) - 5.90\,(v' + \tfrac{1}{2})^2 - 817.5\,(v'' + \tfrac{1}{2}) + 5.20\,(v'' + \tfrac{1}{2})^2.$$

In table II are given the differences between observed and computed wave-numbers of the band heads.

As the values of ω'_e and ω''_e do not differ very considerably, the intensity distribution of the bands would lie on a relatively narrow Condon parabola in accordance with the Frank-Condon theory. Although no actual measurement of intensity was made, a visual estimate seems to support the above view. It is further noticed that the Condon parabola in this case has one limb very short while the other limb is comparatively long.

CORRELATION OF THE BAND SYSTEMS

It may be noted at the very outset that since SbO is an odd molecule, its electronic states should be of even multiplicities. The vibrational analysis shows that as one would normally expect, only doublet electronic states are involved in the emission of three observed band systems. The data of their ν_e, ω_e and $\omega_e x_e$ values are collected together in Table III.

TABLE I.

λ In air.	ν In vacuo. in cm⁻¹.	Assignment.	Type of head	λ In air	ν In vacuo. in cm⁻¹.	Assignment.	Type of head.
2452.51	40762.2	*a* (3, 2)	Q	2617.60	38191.5	*a* (0, 2)	Q
2453.79	40740.9	*a* (3, 2)	P	2618.90	38172.6	*a* (0, 2)	P
2455.32	40715.6	*a* (2, 1)	Q	2651.20	37707.6	*b* (3, 3)	Q
2456.93	40688.0	*a* (2, 1)	P	2655.36	37648.5	*b* (2, 2)	Q
2458.25	40667.0	*a* (1, 0)	Q	2656.95	37626.0	*b* (2, 2)	P
2459.59	40645.0	*a* (1, 0)	P	2659.59	37588.7	*b* (1, 1)	Q
2493.34	40095.1	*b* (3, 0)	Q	2661.05	37568.0	*b* (1, 1)	P
2504.62	39914.2	*a* (2, 2)	Q	2663.96	37526.9	*b* (0, 0)	Q
2506.05	39891.4	*a* (2, 2)	P	2665.93	37504.8	*b* (0, 0)	P
2508.14	39858.2	*a* (1, 1)	Q	2666.14	37496.3	*a* (1, 4)	Q
2509.51	39836.4	*a* (1, 1)	P	2667.08	37483.0	*a* (1, 4)	P
2511.89	39798.7	*a* (0, 0)	Q	2672.64	37405.1	*a* (0, 3)	Q
2513.19	39778.1	*a* (0, 0)	P	2711.90	36863.6	*b* (2, 3)	Q
2542.04	39326.7	*b* (4, 2)	Q	2717.10	36793.1	*b* (1, 2)	Q
2544.17	39293.8	*b* (3, 1)	Q	2721.75	36730.2	*a* (1, 5)	Q
2545.34	39275.7	*b* (3, 1)	P	2722.44	36720.9	*b* (0, 1)	Q
2546.83	39252.7	*b* (2, 0)	Q	2724.01	36699.7	*b* (0, 1)	P
2548.63	39225.0	*b* (2, 0)	P	2729.22	36629.7	*a* (0, 4)	Q
2554.98	39127.5	*a* (2, 3)	Q	2776.66	36003.9	*b* (1, 3)	Q
2559.52	39058.1	*a* (1, 2)	Q	2778.16	35984.4	*b* (1, 3)	P
2560.89	39037.2	*a* (1, 2)	P	2782.78	35924.7	*b* (0, 2)	Q
2563.84	38992.3	*a* (0, 1)	Q	2784.15	35907.0	*b* (0, 2)	P
2565.21	38971.5	*a* (0, 1)	P	2830.42	35320.1	*b* (2, 5)	Q
2596.97	38494.9	*b* (3, 2)	Q	2831.50	35306.6	*b* (2, 5)	P
2600.30	38445.6	*b* (2, 1)	Q	2837.50	35231.9	*b* (1, 4)	Q
2601.57	38426.9	*b* (2, 1)	P	2838.66	35217.6	*b* (1, 4)	P
2603.70	38395.4	*b* (1, 0)	Q	2845.00	35139.1	*b* (0, 3)	Q
2605.40	38370.4	*b* (1, 0)	P	2846.09	35125.6	*b* (0, 3)	P
2606.58	38353.0	*a* (2, 4)	Q	2900.24	34469.8	*b* (1, 5)	Q
2611.89	38275.0	*a* (1, 3)	Q	2909.20	34363.7	*b* (0, 4)	Q

TABLE II.

Band.	O−C in cm⁻¹.	Band.	O−C in cm⁻¹.	Band.	O−C in cm⁻¹
a(0, 4)	−2.3	*a*(2, 4)	−1.6	*b*(2, 2)	−0.9
b(0, 4)	+0.7	*a*(0, 1)	+1.4	*b*(3, 3)	−1.2
a(1, 5)	−3.2	*b*(0, 1)	+0.5	*a*(1, 0)	+1.8
b(1, 5)	+3.4	*a*(1, 2)	−3.3	*b*(1, 0)	0.0
a(0, 3)	−2.8	*b*(1, 2)	+0.5	*a*(2, 1)	+2.1
b(0, 3)	+0.7	*a*(2, 3)	−3.0	*b*(2, 1)	0.0
a(1, 4)	−2.9	*b*(2, 3)	0.0	*a*(3, 2)	+1.8
b(1, 4)	+0.5	*a*(0, 0)	+0.7	*b*(3, 2)	+0.3
b(2, 5)	−3.1	*b*(0, 0)	−0.1	*b*(2, 0)	+0.5
a(0, 2)	−2.7	*a*(1, 1)	+0.1	*b*(3, 1)	+3.0
b(0, 2)	+0.5	*b*(1, 1)	−0.1	*b*(4, 2)	−1.5
a(1, 3)	−0.1	*a*(2, 2)	−2.6	*b*(3, 0)	−2.3
b(1, 3)	−2.9				

TABLE III.

Data of SbO band systems.

Designation of band system.		ν_e	ω_e'	$\omega_e'x_e'$	ω_e''	$\omega_e''x_e''$	Region of occurrence
Less Refrangible.	R	20667.5 18528.5	569.0	5.00	817.2	5.38	λ6650-λ4500
More Refrangible	R	26594.0 24322.0	582.0	6.50	817.0	5.40	λ4720-λ3245
New ultra-violet.	V	39767.7 37495.7	879.0 880.5	5.90 5.80	817.5 817.0	5.20 5.20	λ2910-λ2450

The near equality of ω_e''– and $\omega_e''x_e''$– values indicate that all the three systems have a common lower level. It is further evident that each of the more refrangible and the new ultra-violet systems has a doublet spacing of the same magnitude. One is therefore led to infer that this spacing must be between the doublet components of their common lower level since it is very unlikely that both of them have the same doublet separation in their upper states. The large value of the spacing suggests further that this common lower level is a $^2\Pi$ state. It may be noted here that in each of the homologous molecules NO, PO and AsO, the band systems so far discovered have also a common $^2\Pi$ lower level, which is considered to be the ground state of the molecule concerned. In the present case, the common lower level of the band systems may therefore be supposed to represent the ground state of SbO and an interval of 2272 cm^{-1} between its two Π-components seems also to be of the right order of magnitude.

It is, however, probable that the doublet separations in the upper levels of the above two band systems are too small to be measurable. In that case these upper levels are either $^2\Sigma$ or $^2\Delta$. Most likely each of them is a $^2\Sigma$ state. The presence of a fairly strong Q-head lends support to this view. It is therefore not unreasonable to suppose that the more refrangible and the new ultraviolet systems are due to transitions between two different excited $^2\Sigma$ states to a common $^2\Pi$ ground state. On the other hand, the less refrangible system has an interval of only 2139 cm^{-1} between its two sub-systems. This interval is less than that for each of the other two systems by 133 cm^{-1}. It seems therefore probable that the upper level of these bands has a doublet separation of this value. The absence of double heads as well as the magnitude of the separation suggest further that it is very likely a $^2\Pi$ state. Hence the less refrangible system may be assigned to the transition $^2\Pi \rightarrow {}^2\Pi$.

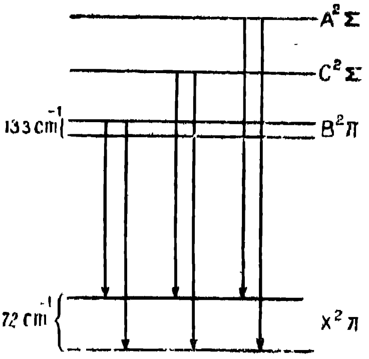

FIG. 1.

The electronic transitions concerned in the emission of the three observed band systems of SbO may be diagramitically represented as shown in Fig. 1.

It is next of interest to ascertain their analogous band systems in the spectra of the homologous molecules.

HOMOLOGOUS SPECTRA

Amongst the homologous monoxides of group V (b) elements, it is well known that NO (Jevons, 1932), which forms the first member of the series, has four overlapping band systems designated as γ, β, δ and ε bands and lying in the regions λ1665–λ3400, λ2185–λ5270, λ1900–λ2300, and λ1670–λ1880 respectively. The first three systems appear in the emission spectrum of the molecule. All of them have, however, a common lower level which is the ground state of the molecule. Excepting the bands of the β system, those of others are degraded to the violet. From an analysis of their rotational structure, γ-bands have been assigned to a transition $^2\Sigma \rightarrow {}^2\Pi$ while β-bands to $^2\Pi \rightarrow {}^2\Pi$. It is further supposed that δ-bands are also due to a $^2\Sigma \rightarrow {}^2\Pi$ transition. The nature of the upper state of the weak ε-bands, which have been observed in absorption only, is still undecided. The doublet spacing of the two Π-components of the ground level of the molecule has a value of 121 cm^{-1}.

In the spectrum of PO, (Ghosh *et al*, 1931, Sengupta *et al*, 1939), so far only two band systems are known. One of them lies in the region λ2280 – λ2790 and is considered as analogous to γ-bands of NO. The second system lies at λ3300 and is supposed to be an analogue of β-bands although it lies on the longer wave-length side of the first system. As one would expect, the doublet separation in the ground level has a higher value than that of NO, and is 224 cm^{-1}.

Two systems of bands with a common lower level have been recently analysed by Connelly (1934) and others (Jenkins *etal*, 1935, Morgan *etal*, 1935) in the spectrum of AsO. They are designated as A and B systems and lie in the regions λ2950 – λ3450 and λ2350 – λ2800 respectively. The A system degrades towards the red while the B system towards the violet. Each of them consists of double-headed bands and has been assigned to a $^2\Sigma \rightarrow {}^2\Pi$ transition their ground level having a separation of 1026 cm^{-1}. between the Π-components. In fact, the A system shows none of the characteristics of a $^2\Pi \rightarrow {}^2\Pi$ transition. Jenkins and Strait (1935) are of opinion that it is the analogue not of the β-bands but of the δ-bands of NO while the B system is analogous to the γ-bands. It is thus evident that while in the case of NO the δ-bands lie on the shorter wavelength side of the γ-bands, the order is reveresed in the spectrum of AsO.

In the spectrum of SbO, the general appearance and intensity distribution of the more refrangible system resemble closely those of A system of AsO. It is therefore vere likely analogous to the δ-bands of NO. On the other hand the new ultra-violet band system appears to be an analogue of the γ-bands, since it occurs in the expected region of the spectrum. It may be noted here that ν_e for the two sub-systems of the γ-bands of NO shifts from 43965 and 43844 cm^{-1}. to 40489 and 40265 cm^{-1}. for PO and to 40411 and 39387 cm^{-1} for AsO. In the spectrum of SbO, ν_e for the new ultra-violet bands is at 39768 and 37476 cm^{-1}. It is, however, significant that this system becomes weaker in intensity with increasing molecular weight of its emitter. In fact, it is so weakly developed in the spectrum of SbO that one may be led to predict its absence in the spectrum of BiO under similar conditions of excitation. It is further found that the more refrangible and the new ultra-violet systems of SbO are more similar to the A and B systems of AsO than to the δ and γ bands of NO as regards their intensity distribution and position. The less refrangible system of SbO is very likely analogous to the β-bands of NO since it bears a close resemblance to the latter in its intensity distribution, besides being due to a similar transition.

A correct vibrational analysis of the bands of BiO is still wanting to make the analogy complete.

ACKNOWLEDGMENT

The author desires to offer his best thanks to Prof. P. N. Ghosh for continual interest and encouragement in the course of the investigation and to Dr. P. C. Mahanti for many helpful discussions.

REFERENCES

Connelly, F. C., 1934, *Proc. Phys. Soc.*, **46**, 790.
Ghosh, P. N. and Ball, G. N., 1931, *Z. f. Phys.*, **71**, 362.
Jenkins, F. A , and Strait, L A., 1935, *Phys. Rev.* **47**, 136.
Jevons, W., Report on Band Spectra of Diatomic Molecules.
Morgan, F., and Shawhan, E. N., 1935, *Phys. Rev.* **47**, 192
Sen Gupta, A. K., 1935, *Proc. Phys. Soc.*, **47**, 247.
Sen Gupta, A. K., 1939, *Ind. Jour. Phys.*, **13**, 145.

TRANSFORMATION OF DIAZOCYANIDES

By M. A. SABOOR, M.Sc., Ph.D. (Lond.), A.I.C.

(Received for publication, 20th June, 1943)

ABSTRACT. The rate of spontaneous transformation of *cis-p*-chlorobenzenediazocyanide into the *trans*-isomeride has been followed in benzene and carbon tetrachloride solutions by means of the change in dielectric constant. The half life period thus found appears to be independent of the initial concentrations and therefore the change is of the first order.

From the measurement of the velocity constants of the transformation carried out at different temperatures the energy of activation is calculated to be about 23 kg.-cals. in either benzene or carbon tetrachloride solution.

The geometric isomerism of the *cis-trans* type in nitrogen compounds was first suggested by Hantzsch and Werner in 1890 when it was shown that certain oximes are capable of being transformed to the more stable isomeride under certain conditions. The concept was subsequently extended to doubly linked nitrogen compounds, notably to certain phenylhydrazones and diazo-compounds and from various experiments which since followed it can now be said with a fair degree of certainty that the low melting form of the diazocyanides, the form that is initially produced, is the *cis* and that the high-melting or stable form is the *trans*.

Labile form

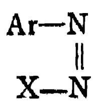

$$\begin{array}{l}\mathrm{Ar{-}N}\\ \quad\ \,\|\\ \mathrm{X{-}N}\end{array}$$

cis

Stable form

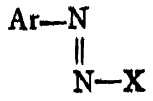

$$\begin{array}{l}\mathrm{Ar{-}N}\\ \quad\ \,\|\\ \quad\ \,\mathrm{N{-}X}\end{array}$$

trans

For various controversies extending over years leading to the establishment of these structures the following references may be seen: Hantzsch and Reddelien (1923), Hantzsch (1894), Hantzsch and Schulze (1895), Hantzsch (1895), Euler and Hantzsch (1901), Gabriel (1879), Hantzsch and Danziger (1897), Hantzsch and Schultze (1895*b*), Stephenson and Waters (1939), and Le Fèvre and Vine (1938).

When the constitutions of the diazocyanides were fairly established by all available chemical means, Hantzsch and Danziger (1897) prepared nearly twenty diazocyanides in their isomeric forms. Both isomerides were orange yellow in colour and sparingly soluble in water but gave solutions in non-polar solvents in which they were soluble. The labile form has always the lower melting point, greater solubility and couples much more easily in alcoholic solutions with β-naphthol. Hantzsch and co-workers could not determine the rate, order, etc., of this transformation owing to the difficulty in following this type of change by chemical means and to the imperfections of the physical methods of following this type of change.

In the present work an attempt has been made to follow this spontaneous isomerisation in different non-polar solvents by means of dielectric constant change, transformation of 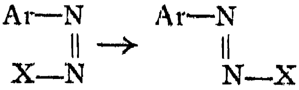 $\begin{matrix}\text{Ar—N}\\ \|\\ \text{X—N}\end{matrix} \rightarrow \begin{matrix}\text{Ar—N}\\ \|\\ \text{N—X}\end{matrix}$ being associated with a change of capacity of a condenser having $\begin{matrix}\text{Ar—N}\\ \|\\ \text{X—N}\end{matrix}$ molecules as part of the dielectric.

There are a number of difficulties for the systematic study of the *cis* ⟶ *trans* transformation of benzenediazocyanides. The unsubstituted benzenediazocyanide $C_6H_5.N=N.CN$ is difficult to obtain in the pure form and doubt has been expressed whether it exists as $C_6H_5.N=N.CN$ or as $C_6H_5.N=N.CN, HCN$ (Hantzsch, 1900) (Hantzsch and Schulze, 1895*c*). An attempt was made to prepare this substance by treating the diazotised solution of aniline with potassium cyanide in the usual way and an oily liquid was separated which was found to be highly unstable and explosive. Its benzene solution, however, showed a change of dielectric constant with time showing that the isomerisation was taking place.

Most *cis*-benzenediazocyanides are either unstable and easily isomerisable or stable and very slowly isomerisable, and in the latter case require a higher temperature for their study. These substituted benzenediazocyanides which isomerise very easily such as *p*-nitrobenzenediazocyanide are not very suitable for measurement at widely separated temperatures. On the other hand, *p*-bromobenzenediazocyanide is stable and moderately easily isomerisable so that inconveniently high temperatures are necessary to study the temperature coefficient. The variation of the dielectric constant of a non-polar liquid is not linear with temperature beyond a certain range. Besides, the high temperature introduces certain other errors connected with the experimental cell and the apparatus. Another difficulty is that the solutions of *cis*-benzenediazocyanides lose nitrogen at high temperatures. For these reasons measurements have been confined to the temperature range of 25°C and 35°C. A list of some of the very well-known *cis*-diazocyanides is given in the Table I, with their nature and characteristics. *cis*-*p*-chlorobenzenediazocyanide is seen to be stable and easily isomerisable, and the transformation to the *trans*-isomer can be obtained within moderate temperature.

TABLE I

p-Nitro-	*cis*-benzenediazocyanide	...	Unstable, very easily isomerisable.
p-Chloro-	,, ,,	...	Stable, easily isomerisable.
p-Bromo-	,, ,,	...	Stable, moderately easily isomerisable.
o-Bromo-	,, ,,	...	Very stable, difficultly isomerisable.
m-Bromo-	,, ,,	...	Unstable, not isomerisable.
2 : 6-Dibromo-	,, ,,	...	Very unstable, not directly isomerisable.
2 : 5 3 : 4 -Dibromo- 3 : 5	,, ,,	...	Stable, slowly, spontaneously isomerisable.
2 : 4- ,,	,, ,,	...	Very stable, not spontaneously isomerisable.
2 : 4 : 6-Tribromo-	,, ,,	...	Very stable, difficultly isomerisable.
2 : 4 : 6-Trichloro-	,, ,,	...	Very stable, difficultly isomerisable.
2 : 4 : 5-Trichloro-	,, ,,	...	Stable, easily isomerisable.

For those compounds which are difficultly isomerisable, their minimum temperature of isomerisation may be as high as 100°C and usual solvents such as benzene, carbon tetrachloride, etc., cannot be employed conveniently. The *cis*-form of *p*-chlorobenzenediazocyanide having a melting point of 29°C, is easily purified and convenient to handle. It was therefore chosen as the representative of the aryl-diazocyanides.

The solutions of the *cis*-diazocyanides are liable to change completely to the stable *trans*-diazocyanides or to decompose with evolution of nitrogen or hydrocyanic acid, according to the nature of the solvent and temperature used. Thus in ether solution side-reactions may occur along with the usual isomerisation, whilst in alcohol and acetone solutions *cis*-diazocyanides rapidly darken and gradually evolve nitrogen to the extent of 20%-40% of the total quantity of the diazo-group present. The isomerisation of the *cis* to the *trans*-diazocyanides is quantitative only in non-ionising solvents such as benzene and carbon tetrachloride (Stephenson and Waters, 1939). It is because of these reasons that benzene and carbon tetrachloride have been used as solvents. The choice of the benzenediazocyanides, solvents and temperatures are severely limited for a dynamic study such as that contemplated.

The recorded procedure (Hantzsch and Schutze, 1895*a*; Hantzsch and Danziger, 1897) was followed with particular modifications regarding purification and drying. *p*-Chloroaniline (0.1 g.-mol.) was dissolved in concentrated hydrochloric acid (0.45 g.-mol. or 45 c.c.) and water (45 c.c.) and diazotised with sodium nitrite (0.1 g.-mol.) with constant cooling and shaking. The resultant diazotised mixture was filtered and cooled to −10°C in solid carbon dioxide and acetone mixture, 50 c.c. of absolute alcohol being added in order to prevent the mixture from freezing. Potassium cyanide (0.2 g.-mol. or 13 g.) in water (25 c.c.) was added slowly with constant stirring so that the final mixture remained acid to litmus. The yellow precipitate was filtered off under suction, washed with chlorine-free, ice-cold water, dried as far as possible under suction, and then dissolved in cold, light petroleum with a little ether. The mixture was then shaken for ten minutes with anhydrous sodium sulphate, filtered and well-cooled in solid carbon dioxide-acetone mixture, when the labile *p*-chlorobenzenediazocyanide was deposited. The solid was washed with a little cold light petroleum and dried by evaporating off the solvent in a current of dry air.

It has been observed by the author that a dry specimen of labile *p*-chlorobenzenediazocyanide can be kept for some time in a vacuum desiccator in a refrigerator without appreciable change.

The apparatus used in determining the dielectric constant is shown diagrammatically in Fig. 1. The component parts are as follows: Q, Hilger quartz crystal (circular, 857 kilocycles per second), V_1, Valve (Mullard PM 12), V_2, Valve (Mullard PM 202), L_1, Inductance (diameter 3″ approx. with 40 turns of wire), L_2, Inductance (diameter 2.5″ approx. with 34 turns of wire), C_1 and C_2, Fixed condensers (2μF each), C_3, Variable condenser (maximum 250 μμF), C_4, Experimental cell (80 μμF with air dielectric), C_5, Fixed variable condenser (maximum

1200 $\mu\mu$F), C_6, Standard variable condenser, Sullivan type (maximum 30 $\mu\mu$F), R, Resistance (1 megohm), M Milliammeter (0 – 5 milliamps.), G, Galvanometer (Moll type, 4 volts on magnet) and B, Grid bias battery.

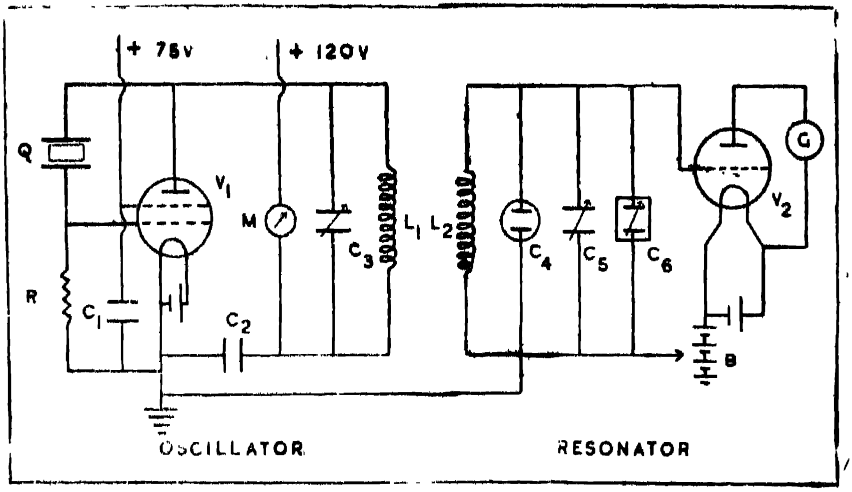

Apparatus for measuring dielectric constant

FIG. 1

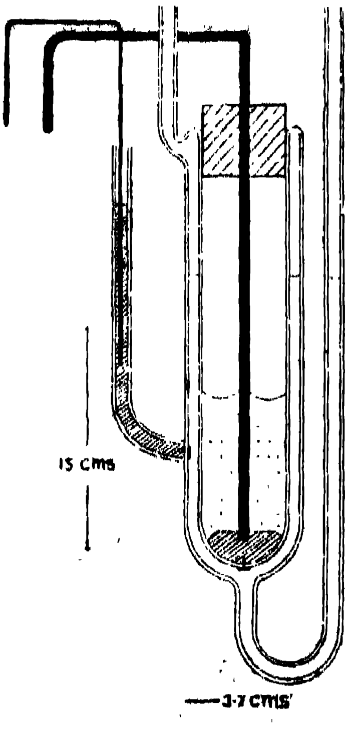

FIG. 2

Perhaps a word is necessary about the experimental cell C_4. It has therefore been shown in great detail in the adjoining sketch, Fig. 2. It is of modified Sayce and Briscoe type (Sayce and Briscoe, 1925). It consists of two concentric glass tubes similar to boiling tubes, the outer surface of the inner tube and the inner surface of the outer tube, *i.e.*, the internal surfaces of the annular space of the tubes, are coated with colloidal graphite films to form the plates of the condenser. The outer surface of the inner tube formed the high potential plate and the inner surface of the outer tube was connected to the earth and was therefore the low potential plate.

The dielectric constants of solutions of *p*-chlorobenzenediazocyanides in benzene for different weight fractions as the transformation proceeds are graphically represented in Fig. 3. The half life periods have been shown by arrows and are practically identical within the experimental error. The change is therefore a monomolecular one. The following table summarises the half life periods for benzene and carbon tetrachloride solutions at different temperatures.

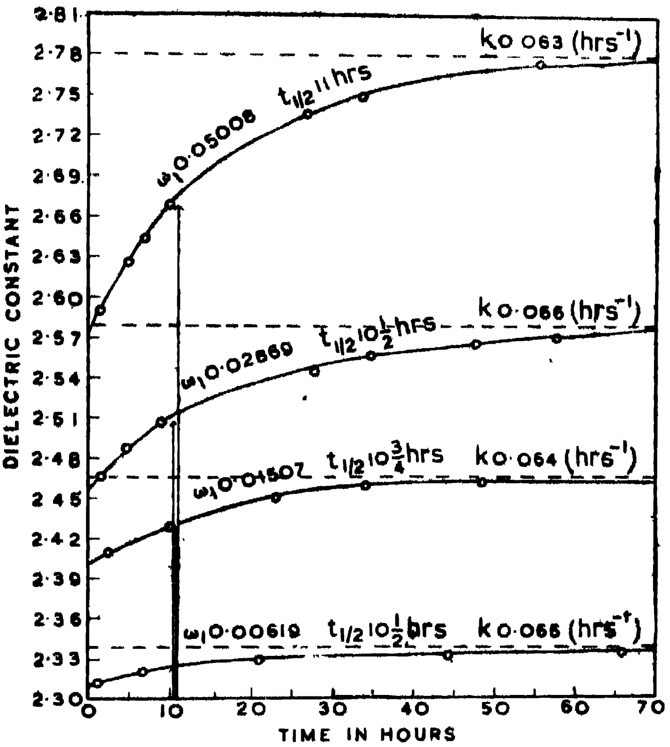

INFLUENCE OF CONCENTRATION ON ISOMERISATION
OF p-chloro-benzene diazocyanide
IN BENZENE SOLUTION AT 25°C.

FIG. 3

TABLE II

Solvents	Weight fraction	Temp.	Time of half change	$k = \frac{2.303 \log_2}{t_{\frac{1}{2}}}$	$\log_{10} k$ (hrs^{-1})	1000/T
Benzene	0·05008	25°C	11 hrs.	0.06294	−1.2010	3.356
,,	0.02461	30°C	6½ hrs.	0·10670	−0.9720	3.301
,,	0.03234	35°C	3½ hrs.	0.19810	−0.7032	3.246
Carbon tetrachloride	0 01637	25°C	16 hrs.	0.04333	−1.3632	3.356
,,	0.01513	30°C	8 hrs.	0.08666	−1.0622	3.301
,,	0·01457	35°C	4½ hrs.	0.15400	−0.8123	3.246

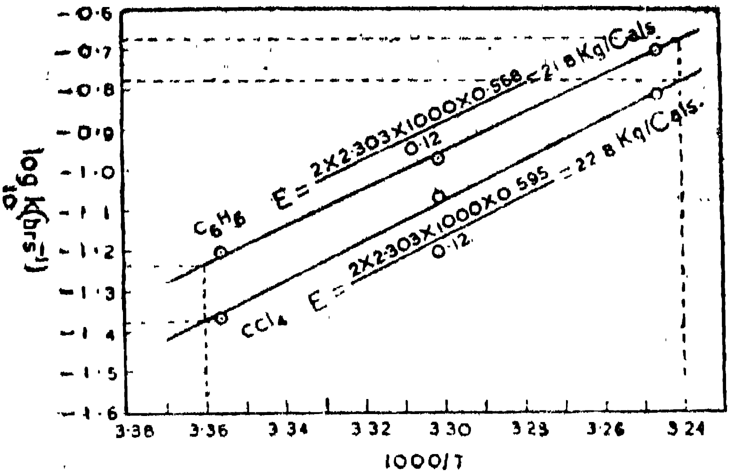

Influence of temperature and solvents on transformation of *p*-chloro-benzene diazocyanide

FIG. 4

Log k (hrs^{-1}) is shown against 1000/T multiple of reciprocal absolute temperature in the adjoining graph (Fig. 4). This bears a linear relation. The conversion therefore follows a first order equation in both solvents. As calculated from the equation $E = \frac{R \log_e (k_1/k_2)}{1/T_2 - 1/T_1}$, derived from the Arrhenius equation $k = Ae^{E/RT}$, the slopes of the lines give a mean activation energy of about 22 kg.-cals./g.-mol. for the change in benzene solution and 23 kg.-cals./g.-mol. in carbon tetrachloride solution which may be taken as identical within the experimental error and do not require a different mechanism in the two solvents.

The author wishes to express his thanks to Prof. C. K. Ingold and Dr. R. J. W. Le Fèvre for their valuable help and to the Government of Bengal in the Department of Education for grant of a State Scholarship which enabled him to carry out this work.

REFERENCES

Euler and Hantzsch, 1901, *Ber.*, **34**, 4167.
Garbiel, 1879, *Ber.*, **12**, 1637.
Hantzsch, 1894, *Ber.*, **27**, 1715.
Hantzsch, 1895, *Ber.*, **28**, 1746.
Hantzsch, 1900, *Ber.*, **33**, 2160; *ibid.*, 2178.
Hantzsch and Danziger, 1897, *Ber.*, **30**, 2529.
Hantzsch and Reddelien, 1923, *Die Diazoverbindungen.*
Hantzsch and Schulze, 1895*a*, *Ber.*, **28**, 666.
Hantzsch and Schulze, 1895*b*, *Ber.*, **28**, 2073.
Hantzsch and Schulze, 1895*c*, *Ber.*, **28**, 670.
Hantzsch and Werner, 1890, *Ber.*, **23**, 11.
Le Fèvre and Vine, 1938, *J. Chem. Soc.*, 435.
Sayce and Briscoe, 1925, *J. Chem. Soc.*, 317.
Stephenson and Waters, 1939, *J. Chem. Soc.*, 1796.

SPECTRUM OF DOUBLY-IONISED CADMIUM

By K. C. MAZUMDER

(Received for publication, June 15, 1943)

ABSTRACT. An experimental investigation of the spark spectrum of cadmium has been made, the range of spectrum extending from λ2200 to 370A. The lines corresponding to different stages of ionisation have been sorted out by introducing inductance in the spark circuit. 134 new lines of Cd III have been classified identifying 29 new terms which consist of $4d^96s$, $4d^95d$ and 7 undesignated terms. The term values have been calculated by means of the 5s-5p and 5p-6s groups of lines. The value obtained for the deepest term, $4d^{10}\ {}^1S_0$, is 308463 cm^{-1}; the corresponding ionisation potential is about 38 volts.

EXPERIMENTAL

The experimental part of this investigation was carried out at 'Upsala,' Sweden, in 1931-32 when the writer was working under the Late Prof. A. Fowler, F.R.S., in the Imperial College of Science and Technology, London, on the isoelectronic spectra of Cu, Zn, Ag, Cd, etc. Through the kindness of Prof. Siegbahn the spectra of the above elements were taken in the Physical Laboratory at Upsala with two 'grazing incidence' spectrographs. In one, the grating was of radius 1.5 metres and in the other, 1 metre. The source employed was the 'hot spark' excited by means of rectified and condensed current of tension of about 50 to 70 kilo-volts. The range of the spectra photographed was from λ2200 to 370A, the dispersion varying from 5.71A per mm. at 2200A to 2.80A per mm. at 400A. The definition was extremely good and the lines as close as 0.10A were clearly separated.

The lines belonging to the different stages of ionisation were distinguished from each other by inserting some suitable inductance in the spark circuit. By adjusting the amount of inductance and the time of exposure the lines of Cd III were obtained with approximately the same intensity with and without inductance. Cd IV lines were prominent without inductance and suppressed with inductance. The reverse was the case with the Cd II lines. The lines of which the intensities are equal with and without inductance or differ by '1' are taken to be the Cd III lines—the most prominent lines having been given the intensity '10.' The faint lines where this criterion cannot sometimes be applied have been treated as Cd III lines whenever they are found to fit into the analytical scheme.

CLASSIFICATION

The doubly-ionised cadmium is isoelectronic with singly ionised silver and neutral palladium and a general similarity of the three spectra, Cd III, Ag II and Pd I is to be expected. In accordance with Hund's theory the triplet and singlet terms arising from the atoms in the unexcited and various excited states may conveniently be represented as in Table I which indicates the types of terms arising from the more important configuration shown on the left.

TABLE I

4s	4p	4d	4f	5s	5p	5d	5f	6s	6p	Prefix	Terms
2	6	10								$4d^{10}$	$^1S_0$
2	6	9		1						$4d^9 5s$	^1D, ^3D
2	6	9			1					$4d^9 5p$	$^1(PDF)$, $^3(PDF)$
2	6	9						1		$4d^9 6s$	^1D, ^3D
2	6	9				1				$4d^9 5d$	$^1(SPDFG)$, $^3(SPDFG)$
2	6	9							1	$4d^9 6p$	$^1(PDF)$, $^3(PDF)$
2	6	8		2						$4d^8 5s^2$	$^1(SDG)$, $^3(PF)$
2	6	8		1	1					$4d^8 5s5p$	$^5(DFG)$, $^3(DFG)$, etc.

The lines corresponding with the possible combinations of the first three rows have already been measured and identified by Gibbs and White (1928), and independently by McLennan, McLay, and Crawford (1928). In the course of the present investigation all the terms shown in the fourth and the fifth row have been identified. The terms $^3F_4$, $^3F_3$, $^3F_2$ and $^3P_2$ belonging to the configuration $4d^8 5s^2$ and probably the terms $^5D_3$, $^3F_3$ belonging to the configuration $4d^8 5s5p$ for Pd I have been identified by Shenstone, (1930). But none of the terms belonging to the above two configurations have been identified in the case of Ag II. The terms $3d^8 4s^2$ and $3d^8 4s4p$ for Ni I (Russel 1929) have been found to give very bright lines in combination with the $3d^9 4p$ and $3d^9 4s$ terms respectively. No traces of these lines have, however, been found in the case of Cu II, though the spectrum was excited by the very powerful method of "hollow cathode" (Kruger, 1929).* But in the case of Zn III the terms $3d^8 4s$ (^4F) $4p^5$, $^3(DFG)$ and the terms $3d^8 4s$ (^2F) $4p^3$, $^1(DFG)$ have been identified by the present writer (Mazumder, 1936; Mazumder 1934-35). The terms $3d^8 4s^2$ $^1(SGD)$ $^3(PF)$ could not however, be located for Zn III. In the spectrum of Cd III a large number of lines giving the characteristic differences of the $4d^9 5s$ terms appeared just below λ600A. These lines do not combine into a Rydberg sequence of $4d^9 np$ terms with $4d^9 5p$ terms already known—the expected region for $4d^9(5s-6p)$ lines being in the neighbourhood of λ700A. Like Zn III these Cd III lines should then also be due to the combination of $4d^9 5s$ terms with

---

* Shenstone has, however, later identified the terms $3d^8 4s^2$ and $3d^8 4s4p$ for Cu II; *Phil. Trans. Roy. Soc*, 235A, p. 195, March 12, 1936.

$4d^8 5s5p$ terms. In the absence of the corresponding data for Ag II and Pd I it is difficult to identify the terms $4d^8 5s5p$ for Cd III. The work is, however, being continued and this part will form the subject matter for a future communication.

A few lines are still available in the region where $4d^9(5p\text{-}6s)$ and $4d^9(5p\text{-}5d)$ lines appear. Some of these residual lines give characteristic differences of $4d^9 5p$ terms. They probably arise from the combination of $4d^9 5p$ terms with $4d^8 5s^2$ terms. But most of the minor combinations being absent, the lines concerned are here shown as due to the combinations of $4d^9 5p$ terms with a few undesignated terms. It should be remembered that the transition is a double electronic one and all the satellite and intercombination lines may not appear.

There can be no doubt that the strong group of lines λ2225 to 1470A has been correctly classified by Gibbs and White as arising from the combination of $4d^9 5s$ and $4d^9 5p$ terms. The lines occur in the region which is to be expected from a comparison with corresponding groups in the isoelectronic spectra Pd I and Ag II. By applying the irregular doublet law it is found thus:

	$5s\ {}^3D_3$	−	$5p\ {}^3D_3$
Pd I	30829		
			16464
Ag II	47293		
			15149
Cd III	62442		

where the $\Delta\nu$'s are in the usual order of agreement in such comparisons. Moreover, the terms of Ag II and Cd III are arranged in the same order of magnitude and the $\Delta\nu$'s in the components of triplets have generally the same sign.

The expected regions for (5p-6s) and (5p-5d) groups of lines are in the neighbourhood of the (5s-5p) group. On examining the lines just below the (5s-5p) group a large number of differences characteristic of the 5p terms have been obtained. It has been possible to arrange the lines as due to the possible combinations of 5p terms with the 6s and 5d terms. As mentioned earlier, by means of some of the residual lines a few terms have been obtained which, though left undesignated, are most probably the $4d^8 5s^2$ group of terms.

The 5s and 6s groups having been established, it has been possible to calculate the absolute term values by means of a simple Rydberg formula. The value for the 5s ${}^3D_3$ term is found to be 228000 cm^{-1}. This places the deepest term $4d^{10}\ {}^1S_0$ at 308463 cm^{-1}; the corresponding ionization potential is about 38 volts.

Comparison of the three Isoelectronic Spectra, Pd I, Ag II and Cd III

It is of interest to compare the term values of isoelectronic spectra Pd I, Ag II and Cd III as in the following table:

The values of the $4d^9 6s$ (^{3,1}(D)) Terms

	$^3D_3$	$^3D_2$	$^3D_1$	$^1D_2$
Pd I	18476(216)	18260(3316)	14944(152)	14792
Ag II	56637(377)	56260(4215)	52045(279)	51766
Cd III	104033(488)	103545(5315)	98230(366)	97864

It will be seen that the separations of the terms have systematically increased with the nuclear charge.

Separation of the Triplet D Term

	$4d^9 5s$		$4d^9 6s$	
	(1, 2)	(2, 3)	(1, 2)	(2, 3)
Pd I	2339	1191	3316	216
Ag II	2998	1577	4215	377
Cd III	3866	1900	5315	488

The above figures show that the difference, $^3D_2 - {}^3D_1$, has increased with the quantum number, whereas $^3D_3 - {}^3D_2$ has decreased. The total separation has, however, remained practically the same. It is evident from this that the separation of the ground terms $4d^9\ {}^2D_{3,2}$ of Cd IV will approximately be—

$$(3866 + 1900) + (5315 + 488)/2 \text{ or } 5785 \text{ cm}^{-1}.$$

The actual value found by Green (1941) is 5812; thus the agreement is very close.

Application of the Irregular Doublet Law

	$5s^3D_3$	$5p^3D_3$	$5s^3D_3 - 5p^3D_3$		$(5s^3D_3)^{\frac{1}{2}} - (5p^3D_3)^{\frac{1}{2}} = \Delta(\nu^{\frac{1}{2}})$
PD I	60716	29887	30829		73.5
				16464	
Ag II	138000	90707	47293		70.3
				15147	
Cd III	228000	165560	62440		70.6

According to the irregular doublet law '$\Delta\nu^{\frac{1}{2}}$' is independent of the nuclear charge which is found to be approximately the case from the figures given in the last column. It is interesting to point out that the corresponding figures for Ni I, Cu II, and Zn III given in the author's papers mentioned earlier are 69.1, 71.8 and 72.2 respectively.

In Fig. 1 the Moseley diagrams for terms $4d^{10}\ {}^1S_0$ $4d^9 5s\ {}^3D_3$, $5p\ {}^3D_3$ and $6s\ {}^3D_3$ for the three isoelectronic spectra Pd I, Ag II and Cd III are drawn. The figures for Cd III are based upon $5s\ {}^3D_3 = 228000$ cm^{-1} calculated from the data obtained in the present investigation. The curves corresponding to the terms $5s\ {}^3D_3$ and $5p\ {}^3D_3$ run fairly parallel. All the curves bend slightly downwards with increasing Z.

In Table II the wave numbers of the lines classified as due to the combination of 5p and 6s terms are given. For completeness the (5s-5p) group of lines given by Gibbs and White is also included. The figures just above the wave numbers indicate intensities. The term values written near the respective terms are those obtained by the author.

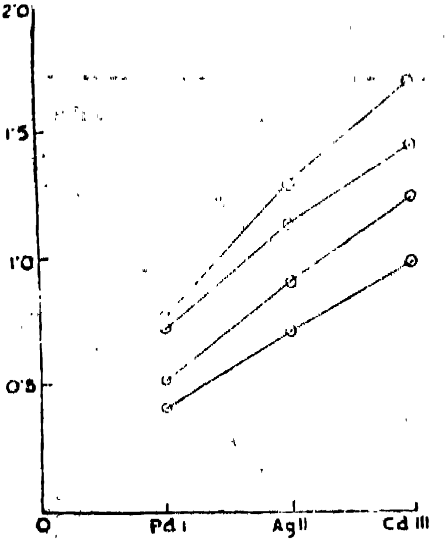

Fig. 1

Moseley diagram for Pd I, Ag II, Cd III

In Table III are given the designation of the terms and the corresponding values; in Table IV, the wave-length, wave numbers, intensities and classification. The lines against which the letters G. and W. have been written are those classified by Gibbs and White; but the wave-length, frequencies and intensities mentioned are those obtained in the present investigation except for a few lines at the end of the table where the original figures have been retained. Against some of the lines "Gr IV has been written; these have also been used by Green in his analysis of Cd IV lines. Some of these lines

TABLE II

		4*d*⁹5*s*				4*d*⁹6*s*			
4*d*⁹5*p*	4*d*¹⁰ ¹So 308463	³D₃ 228000	1900³D₂ 226100	3866³D₁ 222234	2652¹D₂ 219582	³D₃ 104033	488³D₂ 103545	5315³D₁ 98230	366¹D₂ 97864
169422 ³F₄	—	15	—	—	—	4	—	—	—
−2818		58578				65390			
172240 ³F₃	—	12	15	—	8	3	5	—	*
6541		55760	53859		47341	68207	68696		
165699 ³F₂	—	1	10	10	9	|	4	4	3
139		62300	60399	56535	53883		62152	67407	67835
165560 ³D₃	—	12	8	—	9	4	4	—	2
−2464		62439	60537		54022	61527	62015		67696
168024 ³D₂	—	1	7	12	5	†	3	4	2
7197		59971	58075	54211	51557		64478	69793	70160
160827 ³D₁	8	—	7	10	4	—	1	4	*
−13814	147637		65270	61405	58753		57282	62594	
174641 ³P₂	—	15	3	1	4	5	5	|	2
4942		53359	51459	47592	44941	70609	71096		76782
169699 ³P₁	8	—	12	5	6	—	3	1	5
3358	138765		56400	52535	49882		66153	71474	71834
166341 ³P₁		—	—	8	—	—	—	3	—
3980				55891				68112	
162361 ¹F₃	—	5	8	—	12	*	*	—	4
2372		65636	63734		57219				64497
159989 ¹D₂	—	4	5	7	12	1	*	4	3
−2389		68009	66110	62241	59595	55960		51758	62126
162378 ¹P₁	15		3	5	10	—	3	*	3
—	146085		63718	59853	57204		58834		64512

* Missing Inter-combinations. Missing satellites.

TABLE III

The term values of Cd III

Term	Value	Term	Value	Term	Value
$4d^{10}\ ^1S_0$	308463	$4d^95p\ ^3F_4$	169422	$4d^96s\ ^3D_3$	104033
$4d^95s\ ^3D_3$	228000	,, $^3F_3$	172240	,, $^3D_2$	103545
,, $^3D_2$	226100	,, $^3F_2$	165699	,, $^3D_1$	98230
,, $^3D_1$	222234	,, $^3D_3$	165560	,, $^1D_2$	97864
,, $^1D_2$	219582	,, $^3D_2$	168024		
		,, $^3D_1$	160827		
		,, $^3P_2$	174641		
		,, $^3P_1$	169699		
		,, $^3P_0$	166341		
		,, $^1F_3$	162361		
		,, $^1D_2$	159980		
		,, $^1P_1$	162378		
$4d^95d\ ^3G_5$	103332	$4d^95d\ ^3D_2$	101650	$4d^95d\ ^1G_4$	104996
,, $^3G_4$	103156	,, $^3D_1$	98304	,, $^1F_3$	88457
,, $^3G_3$	108462	,, $^3P_2$	109923	,, $^1D_2$	98789
,, $^3F_4$	98944	,, $^3P_1$	103863	,, $^1P_1$	95828
,, $^3F_3$	103045	,, $^3P_0$	101585	,, $^1S_0$	100475
,, $^3F_2$	97614	,, $^3S_1$	105485		
,, $^3D_3$	102365				

TABLE IV

The catalogue of the classified lines of doubly-ionized Cadmium

Plate II		Plate III					—
Int.	No.	Int.	No.	—	—	—	Classification
—	—	0	1	1256.834	79565		$4d^9\ 5p\ ^3D_2-4d^95d\,^1F_3$
—	—	1	1	61.538	79268		,, ,, $^3P_1-b_0$
—	—	1	1	67 245	78911		,, ,, $^3F_4-\ d_4$
—	—	0	0^+	68.838	78813		$4d^9\ 5p\ ^3P_2-4d^9\ 5d\ ^1P_1$
—	—	0^+	0^+	94.750	77235	42	,, ,, $^3F_2-$,, ,, $^1F_3$
0	0^+	0	2	1303.395	76782	IV ?	,, ,, $^3P_2-$,, $6s\ ^1D_2$
0	1	0	2	13.718	76120	IV ?	,, ,, $^3P_2-b_2$
—	—	0^+	0	26.421	75391		,, ,, $^1P_1-a_0$
—	—	0	1^+	32.335	75053	IV ?	,, ,, $^3D_3-d_4$
0	0^+	0^+	0^+	53.164	73904		,, ,, $^1F_3-4d^9\ 5d\ ^3F_3$
1	2	3	3	54.304	73839		,, ,,—$^3D_1-a_0$
0^+	0^+	0	0^+	56.389	73725		,, ,, $^3P_2-b_1$
—	—	0	0^+	61.412	73453		,, ,, $^3F_3-4d^9\ 5d\,^1D_2$
3	4	5	5	83.618	72274		,, ,, $^3P_2-$,, ,, $^3D^3$
2	3	4	5	85.156	72194		,, ,, $^3D_2-$,, ,, $^1P_1$
—	—	1	1	91.807	71850		,, ,, $^1F_3-d_4$
1	3	4	5	92.106	71834	IV ?	,, ,, $^3P_1-4d^9\,6s\ ^1D_2$
4	4	5	5	96.779	71593		,, ,, $^3P_2-$,, $5d\,^3F_3$
1^+	2^+	4	4	97.925	71535		,, ,, $^1D_2-$,, ,, $^1F_3$
—	—	1	1	99.101	71474		,, ,, $^3P_1-$,, $6s\,^3D_1$
1^+	2^+	4	5	1400.696	71393	Gr.IV	,, ,, $^3P_1-$,, $5d\ ^3D_1$
1	3	3	5	06.564	71096	Gr.IV	,, ,, $^3P_2-$,, $6s\ ^3D_2$
3	3	5	5	16.250	70609		,, ,, ,, $-$,, ,, $^3D_3$
0^+	1	1	1^+	16.627	70590		,, ,, $^3F_3-$,, $5d\ ^3D_2$
3	4	6	6^+	18.875	70478		,, ,, $^3F_4-$,, ,, $^3F_4$

TABLE IV (*contd.*)

Plate II		Plate III		—	—	—	Classification
Int.	No.	Int.	No.				
3	3	4	4$^-$	20.248	70410		$5d^9 5p\ ^3D_2 - 4d^9 5d\ ^3F_2$
3	3	4	4	20.479	70399		,, ,, $^3D_1 - b_0$
0	0$^+$	0$^+$	2	25.311	70160		,, ,, $^3D_2 - 4d^9\ 6s\ ^1D_2$
3	4	5	5	31.154	69874		$4d^8\ 5p\ ^3F_3 -$,, $5d\ ^3D_3$
3	4	5	5	1431.154	69874		$4d^9 5p\ ^3F_2 - 4d^9 5d\ ^1P_1$
2	3	3	4	32.815	69793		,, ,, $^3D_2 -$,, $6s\ ^3D_1$
—	—	0	0+	34.350	69718		,, ,, $^3D_2 -$,, $5d\ ^3D_1$
—	–	0	1	38.861	69500		,, ,, ,, $- b_2$
2	3	4	5	44.580	69224		,, ,, $^3P_1 - 4d^9 5d\ ^1S_0$
1	2	2	3	45.195	69195		,, ,, $^3F_3 -$,, ,, $^3F_3$
4	5	5	5	46.025	69155		,, ,, $^3P_2 -$,, ,, $^3S_1$
5	5	6	5	47.492	69085	Gr. IV	,, ,, $^3F_3 -$,, ,, $^3G_4$
4	4	5	5	55.684	68696		,, ,, ,, $-$,, $6s\ ^3D_2$
2	2	3	3	66.132	68207		,, ,, ,, $-$,, ,, $^3D_3$
1	1	2	3	68.175	68112		,, ,, $^3P_0 -$,, ,, $^3D_1$
,,	,,	,,	,,	,,	,,		,, ,, $^3P_1 -$,, $5d\ ^3P_0$
4	4	4	5	68.760	68085		,, ,, $^3F_2 -$,, ,, $^3F_2$
3	3	4	4	1469.495	68051		,, ,, $^3P_1 -$,, ,, $^3D_2$
1	1	2	3	69.760	68038		,, ,, $^3P_0 -$,, ,, $^3D_1$
4	4	4	4	70.400	68009	G. & W.	,, $5s\ ^3D_3 -$,, $5p\ ^1D_2$
4	4	5	5	71.896	67942		,, $5p\ ^3D_3 -$,, $5d\ ^3F_2$
0	1	2	3	74.153	67835		,, ,, $^3F_2 -$,, $6s\ ^1D_2$
0	0+	1	2	77.225	67696		,, ,, $^3D_3 -$,, ,, ,,
1	1+	3	4	82.213	67467		,, ,, $^3F_2 -$,, ,, $^3D_1$
—	—	0	0+	83.770	67396		,, ,, ,, $-$,, $5d\ ^3D_1$
2	2	3	4	91.262	67058		,, ,, $^3F_4 -$,, ,, $^3D_3$
3	5	4	5	91.785	67034	Gr. IV ?	,, ,, $^3D_3 - b_2$
3	4	4	5	1501.120	66617	Gr. IV	,, ,, ,, $- 4d^9$,, $^3F_4$
2	2	3	4	01.600	66594		,, ,, $^3F_4 - C_4$
3	4	4	5	02.680	66548		,, ,, $^1P_1 - 4d^9 5d\ ^1P_1$
3	4	4	5	06.590	66375		,, ,, $^3D_2 -$,, ,, $^3D_2$
,,	,,	,,	,,	,,	,,		,, ,, $^3F_4 -$,, ,, $^3F_3$
2	3	3	5	09.090	66265	IV ?	,, ,, ,, $-$,, ,, $^3G_4$
4	4	5	5	10.980	66182		,, ,, $^3P_2 -$,, ,, $^3G_3$
2	2	3	3	11.640	66153		,, ,, $^3P_1 -$,, $6s\ ^3D_2$
5	5	6 double	6	12.630	66110	G. & W. Gr. IV	,, $5s\ ^3D_2 -$,, $5p\ ^1F_2$
4	4	5	4	13.100	66090		,, $5p\ ^3F_4 -$,, $5d\ ^3G_5$
—	—	1	1	18.921	65836		,, ,, $^3P_1 -$,, ,, $^3P_1$
—	—	0	0+	22.988	65660		,, ,, $^3D_2 -$,, ,, $^3D_3$
5	5	6	6	23.636	65636	G. & W.	,, $5s\ ^3D_3 -$,, $5p\ ^1F_3$
4	5	5	5	28.380	65429		,, $5p\ ^3P_0 - b_1$
5	5	4	4	29.307	65390		,, ,, $^3F_4 - 4d^9 6s\ ^3D_3$
4	5	5	5	32.090	65270	G. & W.	,, $5s\ ^3D_2 -$,, $5p\ ^3D$
2	3	4	5	38.440	65001		,, $5p\ ^3D_1 -$,, $5d\ ^1P_1$
—	—	1	1	43.427	64791		,, ,, $^3F_2 - b_1$
2	3	4	4	45.170	64718		,, ,, $^3P_2 - 4d^9 5d\ ^3P_2$
1	2	2	3	50.090	64512		,, ,, $^1P_1 -$,, $6s\ ^1D_2$
3	3	4	4	50.452	64497		,, ,, $^1F_3 -$,, ,, ,,
1	3	3	3	50.910	64478	IV ?	,, ,, $^3D_2 -$,, ,, $^3D_2$
3	4	4	5	52.180	64426		,, ,, $^3F_4 -$,, $5d\ ^1G_4$
3	4	5	6	56.490	64247		,, ,, $^3P_2 - c_3$
1	1+	2	3	58.537	64163		,, $5p\ ^3D_2 - 4d^9 5d\ ^3P_1$
1	1	2	3	58.655	64158		,, ,, $^1D_2 -$,, ,, $^1P_1$
0+	1	2	1	60.311	64090		,, ,, $^3F_3 - e_2$
5	5	6	6	60.680	64075		,, ,, $^1P_1 - 4d^9 5d\ ^3D_1$
4	4	4	4	61.355	64047		,, ,, $^3F_2 -$,, ,, $^3D_2$

TABLE IV (*contd.*)

Plate II		Plate III		—	—	—	Classification
Int.	No.	Int	No.				
3	4	4	5	1566.028	63856		4d^{9}5p $^1P_1-b_2$
—	—	0	0+	66.508	63836		,, ,, $^1F_3-$,,
—	—	0+	0	68 180	63768	(78)	,, ,, $^3F_3-4d^95d\ ^3G_3$
5	4	6	6	68.988	63734	G. & W.	,, 5s $^3D_2-$,, 5p $^1F_3$
3	2	4	4	69 413	63718	,,	,, ,, ,, −,, ,, $^1P_1$
1	1	2	2	69.691	63707		,, 5p ,, $-d_2$
3	3	4	4	72 615	63588	Gr. IV	,, ,, $^1P_1-4d^95d\ ^1D_2$
3	4	3	4	73.100	63569		,, ,, $^1F_3-$,, ,, ,,
—	—	1	1	82 052	63209		,, ,, $^3D_1-$,, ,, $^3F_2$
4	4	5	6	82.408	63195		,, ,, $^3D_3-$,, ,, $^3D_3$
—	—	1	1	93.892	62740	(32)	,, ,, $^3D_3-C_4$
—	—	0	0+	96.209	62648		,, ,, $^3F_2-4d^95d\ ^3F_3$
3	3	4	4	97.598	62594		,, ,, $^3D_1-$,, 6s $^3D_1$
—	—	1	1 ?	99 092	62536		,, ,, $^3D_2-$,, 5d $^3S_1$
1	1+	2	2	99.444	62521		,, ,, $^3D_1-$,, ,, $^3D_1$
2	2	3	3	99.668	62513		,, ,, $^3D_3-$,, ,, $^3F_3$
6	5	6	5	1601.576	62439	G. & W.	,, 5s ,, −,, 5p $^3D_3$
1	1	2	2	02.500	62403		,, 5p ,, −,, 5d $^3G_4$
0	0+	2	2	03.245	62373		,, ,, $^1D_2-$,, ,, $^3F_2$
0+	1	2	3	04.891	62310		,, ,, $^3D_1-b_2$
—	—	1	1+	05.142	62300	G. & W.	,, 5s $^3D_3-4d^95p\ ^3F_2$
5	5	6	6	06.646	62241	,,	,, ,, $^3D_1-$,, ,, $^1D_2$
1	2	3	4	08 957	62152		,, 5p $^3F_2-$,, 6s $^3D_2$
1	2	2	3	09.641	62126		,, ,, $^1D_2-$,, ,, $^1D_2$
—	—	0	0+	11.858	62040		,, ,, $^3D_1-$,, 5d ,,
1	2	3	4	12.507	62015		,, ,, $^3D_3-$,, 6s $^3D_2$
—	—	0	0+	15.465	61902		,, ,, $^1P_1-$,, 5d $^1S_0$
—	—	0+	0+ ?	16.822	61850		,, ,, $^3F_3-C_3$
0	1+	2	4	19 223	61758	IV ?	,, ,, $^1D_2-4d^96s\ ^3D_1$
0+	1+	2	4 ?	21.146	61685		,, ,, ,, −,, 5d $^3D_1$
3	3	4	5	25.305	61527		,, ,, $^3D_3-$,, 6s $^3D_3$
—	—	0	0+	26.922	61466		,, ,, $^1D_2-b_2$; 4d^{9}5p $^1P_1-b_1$
5	5	8	8	28.528	61405	G. & W.	,, 5s $^3D_1-4d^95p\ ^3D_1$
—	—	1	1	29.128	61383		,, 5p $^3F_2-d_2$
—	—	1	1	33.990	61200		,, ,, $^1D_2-4d^95d\ ^1D_2$
—	—	1	1	40.470	60958		,, ,, $^3F_4-$,, ,, $^3G_3$
—	—	0	1+	42.709	60875	IV ?	,, ,, $^3D_2-C_2$
—	—	1	1	44.850	60796		,, ,, $^1P_1-4d^95d\ ^3P_0$
0+	2	2	4	46.682	60728	IV ?	,, ,, ,, −,, ,, $^3D_2$
—	—	0+	0	51.245	60560		,, ,, $^3D_3-$,, ,, $^1G_4$
5	5	6	6	51 872	60537	G. & W.	,, 5s $^3D_2-$,, 5p $^3D_3$
5	5	6	6	55 647	60399	,,	,, ,, ,, −,, ,, $^3F_2$
1	1	2	0+ ?	56.957	60352		,, 5p $^3D_1-$,, 5d $^1S_0$
—	—	0+	0 ?	60.666	60217		,, ,, $^3F_2-$,, ,, $^3S_1$
—	—	2	3	66.795	59995		,, ,, $^1F_3-$,, ,, $^3D_3$
—	—	1	1	67 484	59971	,,	,, 5s $^3D_3-$,, 5p $^3D_2$
0+	0	2	0	69 200	59909	II ?	,, 5p $^3D_1-b_1$
—	—	1	1	70.206	59873		,, ,, $^3D_2-c_2$
4	4	5	5	70.748	59853	G. & W.	,, 5s $^3D_1-4d^95p\ ^1P_1$
0	0+	1	1	73.027	59772		,, 5p $^3P_1-$,, 5d $^3P_2$
5	5	6	6	78.143	59595	G. & W.	,, 5s $^1D_3-$,, 5p $^1D_2$
—	—	1	1	78.908	59560		,, 5p $^3D_2-$,, 5d $^3G_3$
—	—	2	1	79.878	59528		,, ,, $^1F_3-c_4$
0	0+	1	2	85.846	59317		,, ,, $^1F_3-4d^95d\ ^3F_2$
0	1	2	2+	88.022	59241		,, ,, $^3D_1-$,, ,, $^3P_0$
1	2	2	3	99.704	58834		,, ,, $^1P_1-$,, 6s $^3D_2$

TABLE IV (*contd.*)

Plate II		Plate III		—	—	—	Classification
Int.	No.	Int.	No.				
3	3	4	4	1702.038	58753	G & W.	$4d^95s\ ^1D_2 - 4d^95p\ ^3D_1$
5	5	10	9	07.156	58578	,,	,, ,, $^3D_3 -$,, ,, $^3F_4$
—	—	1	0	08.056	58546		,, $5p\ ^3F_2 - C_2$
—	—	1	1	09.040	58512		,, ,, $^1P_1 - 4d^95d\ ^3P_1$
—	—	1	1	12.040	58410		,, ,, $^3D_3 - C_2$
—	—	1 double	1	21.273	58097		,, ,, $^3D_3 - 4d^95d\ ^3P_2$
5	5	8	8	21.898	58075	,,	,, $5s\ ^3D_2 -$,, $5p\ ^3D_2$
1	2	2	3	22.936	58040		,, $5p\ ^1F_3 - d_2$
—	—	0	1	43.093	57360		,, ,, ,, $-$ $4d^95d\ ^1G_4$
0	1	2	3	45.743	57282		,, ,, $^3D_1 -$,, $6s\ ^3D_2$
—	—	1	1	47.074	57239		,, ,, $^3F_2 -$,, $5d\ ^3G_3$
5	5	8	8	47.657	57219	,,	,, $5s\ ^1D_2 -$,, $5p\ ^1F_3$
5	5	5	5	48.143	57204	,,	,, ,, ,, $-$,, ,, $^1P_1$
·	—	0	0+	56.069	56945		,, $5p$,, $-$,, $5d\ ^3F_4$
5	5	8	8	68.818	56535	,,	,, $5s\ ^3D_1 -$,, $5p\ ^3F_2$
5	5	8	8	73.013	56401	,,	,, ,, $^3D_2 -$,, ,, $^3P_1$
—	—	0	0+	86.990	55960		,, $5p\ ^1D_2 -$,, $6s\ ^3D_3$
5	5	6	6	89.208	55891	,,	,, $5s\ ^3D_1 -$,, $5p\ ^3P_0$
—	—	1 double	0	92.751	55780		,, $5p\ ^3F_2$ · ,, $5d\ ^3P_2$
5	5	8	8	93.402	55760	,,	,, $5s\ ^3D_3 -$,, $5p\ ^3F_3$
—	—	0	1+	97.286	55639		,, $5p$,, $-$,, $5d\ ^3P_2$
—	—	1	1	1808.204	55303		,, ,, $^3F_2 - C_3$
—	—	1	1	43.038	54232	S ?	,, ,, $^1P_1 - c_2$
6	6	8	8	44.670	54211	G & W.	,, $5s\ ^3D_1 - 4d^95p\ ^3D_2$
5	5	6	6	51.114	54022	,,	,, ,, $^1D_2 -$,, ,, $^3D_3$
5	5	5	5	55.858	53883	,,	,, ,, ,, $-$,, ,, $^3F_2$
6	6	6	6	56.698	53859	,,	,, ,, $^3D_2 -$,, ,, $^3F_3$
6	6	10	10	74.113	53359	,,	,, ,, $^3D_3 -$,, ,, $^3P_2$
4	4	5	-	1903.492	52535	,,	,, ,, $^3D_1 -$,, ,, $^3P_1$
-	5	—	—	39.58	51557	,,	,, ,, $^1D_2 -$,, ,, $^3D_2$
—	3	—	—	43.31	51459	,,	,, ,, $^3D_2 -$,, ,, $^3P_2$
—	6	—	—	2004.73	49882	,,	,, ,, $^1D_2 -$,, ,, $^3P_1$
—	1	—	—	2101.17	47592	,,	, ,, $^3D_1 -$,, ,, $^3P_2$
—	8	—	—	2112.31	47341	,,	,, ,, $^1D_2 -$,, ,, $^3F_3$
—	4	—	—	2225.13	44941	,,	,, ,, ,, $-$,, ,, $^3P_2$

are undoubtedly Cd III lines, some may be blends and one line, namely, 71096, is more likely to be a Cd IV than a Cd III line. Out of several plates taken during the investigation only two have been measured; intensities obtained from both the plates with and without inductance are given in the table. From these figures it is easy, in the light of the variation of intensities of the lines used by Gibbs and White, to infer the stage of ionisation of the respective lines The doubtful cases have been marked 'IV' with a sign of interrogation.

It seems necessary to mention four cases where lines appear by violating the selection rule; but as they can be explained away in the following manners they have not been included in the tables. There is a line '59873' for the combination $4d^{10}5s\ ^3D_1 - 4d^{10}5p\ ^3F_3$ exactly equal to the difference of the respective term-values. Its wave-length, 1670.206, is double the wave-length of the oxygen line 835·10; but it should be mentioned that other members of this group of lines have not appeared in the 2nd order. A line appears in the place of the combination $4d^9 5p\ ^3P_0 - 4d^9 5d\ ^3P_2$. Its intensity is 'o+' and 'o' with and without inductance, so it can be a Cd II line. The combination $5p\ ^3P_1 - 5d\ ^3F_3$ seems to appear with intensity 'o+' and 'o+' with and without inductance; but on a very close examination of Plate III (only in this plate the line has appeared), its appearance without inductance is seen to be extremely doubtful. It may be then a Cd IV line. The line '73592' for the combination $5p\ ^3F_4 - 5d\ ^1P_1$ has been found and measured in both the Plates II and III with intensities 'o' and 'o+', and '1' and 'o+' with and without inductance. The author has also found a line '73597' in the zinc spectra which did neither fit into the analytical scheme for Zn II nor into that for Zn III and it could not be a Zn IV line on account of its behaviour with respect to inductance. Both these lines may be the same line and an impurity line.

In conclusion the author wishes to express his deep sense of gratitude to the late Prof. A. Fowler of the Imperial College, London, for suggesting the problem, to Prof. M. Siegbagn for permitting him to work in the Fysicum of the Upsala University, to Dr. D. M. Bose, Director of the Bose Research Institute, Calcutta, for permission to use the Library of the Institute, and to the Authority of Tata Iron & Steel Works, Ltd., for permission to continue the work in their Research Laboratory.

THE NEW CONTROL AND RESEARCH LABORATORY,
TATA IRON & STEEL WORKS.

REFERENCES

Cribbs and Write, 1928, *Phys. Rev.*, **31**, 776
Green, 1911, *Phys. Rev.*, **60**, 117.
Kruger, 1929, *Phys. Rev.*, **34**, 1122.
Mazumder, 1934-35, *Trans. Bose. Res. Inst.*, **1a**
Mazumder, 1936, *Ind. J Phys.*, **10**, 171.
McLennan, McLay and Crawford, 1928, *Trans. Roy Soc. Canada*, **22**, 45.
Russel, 1929, *Phys. Rev.*, **34**, 821.
Shenstone, 1930, *Phys. Rev.*, **36**, 669.

PROCEEDINGS

OF THE

INDIAN ASSOCIATION FOR THE CULTIVATION OF SCIENCE

A scientific meeting of the Indian Association for the Cultivation of Science was held on 6th April, 1943 in the Association Hall. Sir U. N. Brahmachari, Kt., M.A., M.D., Ph.D., presided. The papers read are given in the following pages.

J. N. Mukherjee,
Honorary Secretary.

STANDARD STATE OF DESICCATION OF DRIED BLOOD PLASMA AND THE ADVANTAGES OF DESICCATION IN THE REGION OF MOLECULAR FLOW

By J. N. MUKHERJEE

AND

B. R. MAJUMDAR

(Received for publication, May 22, 1943)

INTRODUCTION

Dried blood plasma, used for transfusion purposes, is desiccated at comparatively low temperatures to prevent the denaturation of the plasma proteins. The stability of the products depends upon the amount of residual moisture and a standard method of its estimation should be followed. It appears also from a study of the literature that a standard state of 'dry' plasma has not been specified.

Flosdorf and Webster, in 1937, measured the residual moisture of dried blood plasma from the percentage losses in weights of the product when desiccated under different conditions. The results are given in Table I.

TABLE I

Percentage loss obtained under different conditions of desiccation

Time in hours	P_2O_5, pressure 100 microns	P_2O_5, pressure 1 atmosphere	50°C, pressure 100 microns
24	0.61	0.59	0
48	1.32	0.80	0.1
72	1.28	0.82	Increased in weight
98	1.31	0.82	,, ,,

It will be seen from Table I that constant weight is attained in each case but the residual moisture content is different.

Greaves and Adair (1939) found the loss of moisture of a sample of blood plasma dried over P_2O_5 at a high vacuum (order not mentioned) at room temperature to be between 0.42 and 0.56%.

Blood plasma previously dried over silica gel at a pressure of 200 microns was desiccated over P_2O_5 at two different pressures and the results are given in the following table. In the experiments recorded in column 2 the desiccating vessel used was what is known as "drying pistol" (Gattermann 1937). A vacuum of very high order could be maintained in it. The other experiment (column 3) was carried out in a vacuum desiccator previously tested to be free from leaks.

The experiments were made at room temperature and no heat was supplied to make up for the loss due to evaporation.

TABLE II

Time in hours	% loss of moisture when desiccated, over P_2O_5 at 0.1 micron	% loss of moisture when desiccated over P_2O_5 at 100 microns
24	1.82	0.23
48	2.26	0.41
72	2.35	0.52
90	2.35	—
92	—	0.62
96	2.35	—

It is evident from the above table that losses of moisture at the two different orders of vacuum are quite different and that for a pressure of 100 microns, the percentage loss does not attain a constant value.

The rate of evaporation at a pressure of the order of 100 microns is expected to be slower than that at the region of molecular flow which is reached at a pressure of 0.1 micron or less, *i.e.*, 10^{-4} m.m. Hg.

The general equation representing the flow of gas is given by

$$T=(ap+b)\,(1+c_1p)/(1+c_2p),$$

where T represents $Q/(p_1-p_2)$, the amount of gas exhausted per unit of time and p = the mean pressure, *i.e.*, $=(p_1+p_2)/2$ where p_1 and p_2 are the pressures (Loeb, 1929) at the two extremeties of the evacuated vessel, and a, b, c_1 and c_2 are constants. In the region of molecular flow the equation reduces to $T=b$ and collisons between molecules are negligible in comparison with those between the molecules and the walls of the vessel. If we consider that P_2O_5 acts as a 'perfect sink' for molecules of water, then a steady state must be attained when no further loss in weight of the substance can take place and the product thus obtained may be taken to represent the standard state of desiccation (Table II, column 2). The dried product was found to be soluble in water but no further examination of the product was made. It is also apparent that quicker desiccation has been achieved by using vacuum which falls in the region of molecular flow.

Our thanks are due to Dr. J. B. Grant, Director of All-India Institute of Hygiene and Public Health, for the sample of dried plasma which was sent for the determination of its residual moisture.

COLLOID RESEARCH LABORATORY,
UNIVERSITY COLLEGE OF SCIENCE AND TECHNOLOGY,
CALCUTTA.

REFERENCES

Flosdorf and Webster, 1937, *J. Biol Chem.*, **121**, 353.
Gattermann, 1937, *Laboratory Methods of Organic Chemistry*, 1937 Ed., p. 14.
Greaves and Adair, 1939, *J. Hygiene*, **98**, 413.
Loeb, 1929, *Kinetic Theory of Gases*, 1929 Ed., p. 294

2

EFFECT OF SAND ON THE VISCOSITY, YIELD VALUE AND THIXOTROPIC GELATION OF MUD SUSPENSIONS

BY J. N. MUKHERJEE

AND

B. R. MAJUMDAR

(Received for publication, May 22, 1943)

Mud is now-a-days used as the lubricationg fluid for the rotary drilling of oil-wells. Properties of mud and clay suspensions are of interest to several other industries, *e.g.*, ceramics. This work was undertaken to investigate the probable causes of stuck drill pipes in oil-wells. The effect of the sand concentration in modifying the viscous properties and thixotropy of drilling mud has been studied.

EXPERIMENTAL

A. *Preparation of mud suspension.*—Powai clay from Digboi was used. A very stable suspension could be prepared from this sample by simply suspending it in water and a fairly thick suspension having thixotropic property had a weight of 78 lbs. per cubic ft. and a pH of 4.85 (determined by glass electrode). This suspension will be called PC-L1 henceforth.

B. *Sampling of sand.*—The following two grades of sand having different grain sizes were collected by sieving a sample of ordinary sand through standard sieves :

Grade I.—Passing through 48-mesh sieve but retained by 100-mesh sieve.

Grade II.—Passing through 100-mesh sieve.

These two grades of sand were incorporated into mud suspension PC-L1 to increase the sand concentration in it.

C. *Appparatus used and experimental detail.*—Stormer Viscometer (Bark, 1931) was found to be very suitable for measuring viscosities, relative yield values and the rate of thixotropic gelation. Viscosities were determined as follows: Weights required for the movement of the inner cylinder of the viscometer at 600 r.p.m. were noted and the corresponding viscosities calculated from the weight-viscosity curve of standard liquids.

The thixotropic gel strength of the mud suspension was followed by measuring the speed of the inner cylinder of the viscometer after different intervals of rest given to a freshly formed suspension.

The water filtration tests were carried out in a Jones-Babson tester. Such measurements reveal the wall-building properties of mud suspensions and this is an essential factor in characterising oil-well drilling mud.

RESULTS AND DISCUSSION

The results of chemical (Wright, 1934a) and mechanical (Wright, 1943b) analyses of the original sample are given below:

TABLE 1

Chemical Analysis			Mechanical Analysis		
Moisture	...	4.33%	Clay	...	29.38%
Loss on ignition.	...	19.58%	Silt	...	15.32%
Silica	...	50.49%	Sand	...	24.99%
Fe_2O_3	...	4.13%	Loss on solution	...	3.44%
Al_2O_3	...	19.58%			
CaO	...	1.31%			
MgO	...	0.55%			

Viscosities of mud suspension containing varying amounts of sand are given in Table 2.

TABLE 2

Sample	Grade I sand	Grade II sand
PC–L1	30.0 c.p.	30.0 c.p.
PC–L1+1% sand	33.5 ,,	34.50 ,,
PC–L1+2% ,,	34.0 ,,	34.50 ,,
PC–L1+3% ,,	32.0 ,,	32.25 ,,
PC–L1+4% ,,	30.0 ,,	34.50 ,,
PC–L1+5% ,,	31.0 ,,	45.00 ,,

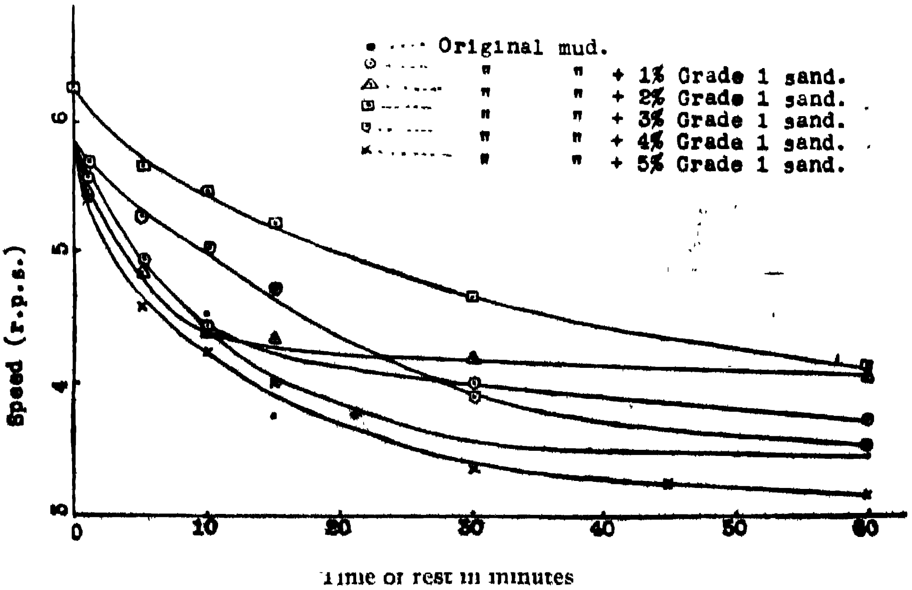

FIG. 1

With Grade I sand, there is no marked variation in the viscosity, but with Grade II sand, the viscosity of the sample whose sand concentration has been increased by 5%, is much higher than that of the other samples.

From the curves shown in Figs. 1 and 2, it appears that the thixotropic gel strength at first decreases with increase of sand concentration and above 3% of additional sand concentration, it again increases. The relation holds good for Grade I and Grade II sands. The relative yield values of the mud suspension as indicated by the same curves in Figs. 1 and 2 also vary with sand concentration.

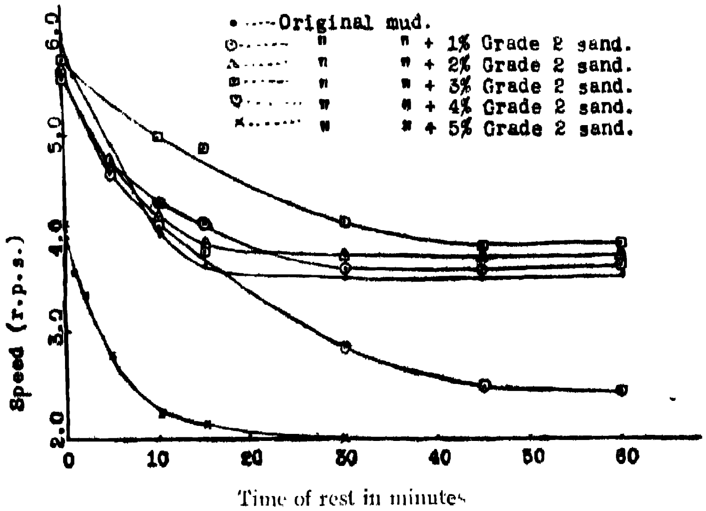

FIG. 2

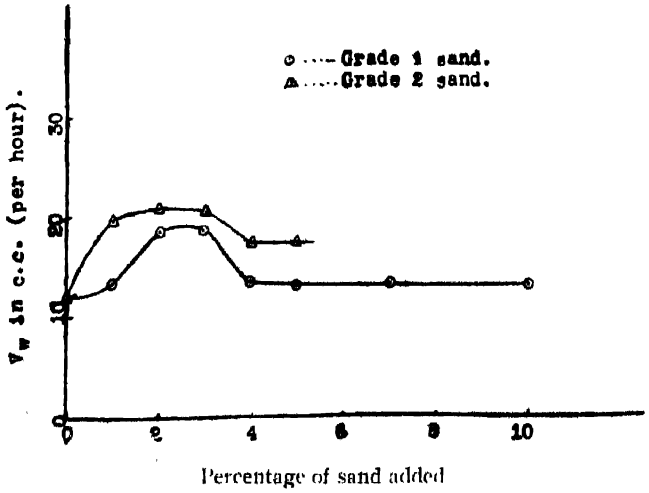

FIG. 3

Water filtration tests show that V_w (cumulative volume of water in c.c.) after 1 hour at first increases and above 3% additional sand concentration it decreases (Fig. 3). From the above results it may be concluded that there exists a critical sand concentration for this mud suspension, above which thixotropic property, the relative yield value, V_w of the mud suspension are modified. This observation throws some light on probable causes of sticking of drill pipe.

The relative permeability of sheaths formed from samples containing Grade II sand is higher than that formed from sample containing Grade I sand.

The moisture content of sheaths formed was also determined. The results are shown below:

TABLE 3

	Sample	Grade I sand Total solid %	Grade I sand Moisture %	Grade II sand Total solid %	Grade II sand Moisture %
1	PC-L1	58.61	41.39	58.61	41.39
2	PC-L1 + 1% Sand	90.42	39.58	59.58	40.02
3	PC-L1 + 2% ,,	—	-	60.47	39.53
4	PC-L1 + 3% ,,	60.71	39.29	61.11	38.89
5	PC-L1 + 4% ,,	61.41	38.59	61.81	38.18
6	PC-L1 + 5% ,,	61.50	38.50	62.19	37.81
7	PC-L1 + 7% ,,	62.10	37.90	—	—
10	PC-L1 + 10% ,,	63.59	37.41	—	—

The moisture content at sticky point (Wright, 1934c) of original mud = 28.52%. Table 3 shows that the moisture content of the sheaths formed from the mud suspension containing varying amounts of sand is higher than this value. Actually, all the sheaths were sticky.

COLLOID RESEARCH LABORATORY,
UNIVERSITY COLLEGE OF SCIENCE
AND TECHNOLOGY, CALCUTTA.

REFERENCES

Barr, *Monograph of Viscometry*, 1931 Ed., p. 235
Wright, 1934a, *Soil Analysis*, 1934 Ed., p. 153
Wright, 1934b, *Ibid.*, p. 38.
Wright, 1934c, *ibid.*, p. 20.

ON THE FLUORESCENCE OF ANTHRACENE IN PRESENCE OF NAPHTHACENE

By S. C. GANGULY

It is known that pure naphthacene crystal 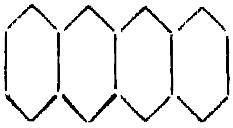 fluoresces very feebly, and in dilute solid solution of anthracene 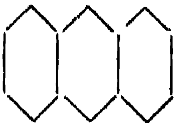, the crystal fluoresces with its characteristic yellow-green light, but the blue fluorescence of anthracene is quenched. This phenomenon is represented as follows: In dilute solid solution the anthracene molecules easily absorb light energy and releases an 'exciton' which exciton causes naphthacene to fluoresce. Not only in anthracene, but in chrysene 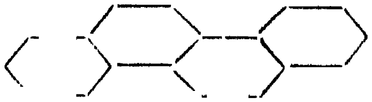 also we find solid napthacene to fluoresce, only there is little shifting of the fluorescence bands, the shifting depending on the substance with which it is mixed. In consideration of above facts, study of fluorescence spectra in alcoholic solution of anthracene, naphthacene and the mixture of the above two, is interesting. In alcoholic solution anthracene has got four fluorescence bands (excited by 3650, 4046 of Hg arc), naphtacene has three fluorescence bands on the redside of the fluorescence bands of anthracene and the mixture has both the fluorescence of anthracene and naphthacene. Three solutions are prepared, one of pure anthracene, the other of pure naphthacene and the third is the mixture of the above two. The number of gram-molecules per c.c. of anthracene and of naphthacene in the mixture are identical with those for pure substances taken separately. Exposures are given for the same time and under identical conditions. It is observed that the intensity of fluorescence bands of anthracene is not changed at all due to the presence of naphthacene. The intensity of fluorescence of napthacene also due to the presence of anthracene is not increased. Absorption spectra of the above three solutions confirm the results.

Indian Association for the Cultivation
of Science,
210, Bowbazar Street, Calcutta.

MAGNETIC STUDIES ON PERMANGANATES

By A. MOOKHERJEE

The principal susceptibilities of $KMnO_4$ and $Ba(MnO_4)_2$ crystals have been measured by the method of Krishnan and his collaborators. The anisotropy in in case of $KMnO_4$ is .07 and the effective magnetic moment=0.5 Bohr magnetons. The anisotropy is correlated with the known fine structure of the crystal in the following manner.

Krishnan and the present writer have shown that anisotropy of paramagnetic crystals arises from certain paramagnetic units. Those units are constituted as follows: each paramagnetic ion in the crystal is under the influence of the electric field of its neighbours. The magnitude and assymmetry of this field is determined by the positions of the atoms immediately surrounding the paramagnetic ion. If this field is assymmetric the crystal will exhibit magnetic anisotropy. In general there will be more than one such group in the unit cell of the crystal. So the crystal anisotropy is determined by the anisotropy of these units and their orientations relative to one another.

In ($KMnO_4$) crystal (MnO_4) group is the paramagnetic unit. From the fine structure study of $KMnO_4$ crystals by Mooney it appears that in MnO_4 group the four oxygen atoms are disposed more or less symmetrically about the manganese atom, being situated at the corners of a tetrahedron with manganese at the centre. The manganese to oxygen distances are: two oxygen atoms at 1·58 Å, one oxygen at 1.68 Å and one at 1 52 Å. So the tetrahedron of oxygens is not a regular one and the crystalline electric field will deviate from cubic symmetry; the result is that the MnO_4 group will exhibit anisotropy.

On seeking the explanation of the feeble paramagnetism by Pauling's method of directed electron pair bonds one finds that in these compounds d^3sp^3 bonds should result which make them diamagnetic but measurements show that they are feebly paramagnetic. This feeble paramagnetism can be explained by Van Vleck's electric field theory as follows.

The electric field surrounding the paramagnetic ion in this case is taken so strong that Russell Saunder's coupling between the different electrons in the ions is broken. According to Van Vleck the Stark pattern of electron consists of two levels when the symmetry of the field is cubic. Since in $KMnO_4$ crystals the crystalline electrical field deviates from cubic symmetry, one of them will further split into two and the other into three levels. This splitting exceeds $3 \times 10^4\ cm^{-1}$ in order to uncouple the individual 's'. According to Gorter the group of two levels will be lowest as the arrangement about Mn in MnO_4 is tetrahedral. The deepest state will then be obtained by assigning the four electrons responsible for paramagnetism in these two levels. All the electrons will then double up and there will be no spin free because of Pauli's exclusion principle and hence spin will contribute nothing to paramagnetism. So the only contribution to paramagnetism will be from the high frequency part of the orbital moment. Howard has shown that in case of $K_3Fe(CN)_6$ the high frequency orbital contribution to paramagnetism is about 0.5 Bohr magneton. In case of Mn^{+++} complex it is 0.5 Bohr magneton, which agrees satisfactorily with our experimental results for the permanganates.

It is interesting to note that the two lowermost levels are equally populated and hence anisotropy should be small in agreement with experimental facts.

Indian Astociation for the
Culaivation of Science
210, Bowbazar Street, Calcutta.

30

ON WHISTLING METEORS

BY S. R. KHASTGIR

(Received for publication, July 27, 1943)

ABSTRACT. Very weak whistles, usually of rapidly decreasing pitch were observed at the Delhi receiving centre of the All India Radio, located at a distance of 10 miles from the transmitters, when the receiver was tuned to the carrier waves from one of the transmitters. These were explained by the A.I.R. investigators as due to a Döppler change in the frequency of the carrier waves scattered from a rapidly moving ionized mass of air at the head of a meteor entering the earth's atmosphere, and to consequent heterodyning of these waves with the ground waves of unmodified frequency. A review of the experimental results in connection with these whistles is given in the paper. The Döppler effect theory to explain these whistles is also critically examined. The striking similarity of these whistles with the whistling tones observed by Barkhausen, Eckersley, and Burton & Boardman in audio-frequency amplifiers with large aerials, is pointed out, as suggesting a common origin for both. Accepting Eckersley's theory of the 'whistler,' the possibility of the carrier waves scattered from the ionosphere being modulated by the Fourier components of such an electrical impulse is suggested. The components of the higher frequencies travel faster in the ionospheric medium, so that the modulation frequency is a function of time. The receiver tuned to the carrier would therefore reproduce a note, the pitch of which would also be a function of time. Accordingly the whistling tones, unconnected with meteors, would also be heard by the scattered waves. It is just possible that at least some of the whistles observed at Delhi were of this origin.

In view of the observed coincidence between the appearance of meteors and the so-called Döppler whistles, it is tentatively supposed that an electrical impulse can be produced by the stoppage of meteor in the ionosphere. The modulation of the scattered waves by the various components of this impulse would then be able to produce a whistle.

The observed dependence of the pitch of the whistle on the frequency of the carrier waves is also expected according to this view.

A few test experiments are suggested.

A DÖPPLER EFFECT PRODUCED BY METEORS

Recently certain interesting observations were made by Chamanlal and Venkataraman (1941) at the Delhi receiving centre of the All-India Radio, located at a distance of 10 miles from the Delhi short wave transmitters. During these observations, when a receiver was tuned to the carrier waves from one of the transmitters, weak whistles of an unusual character were audible under certain circumstances. The whistles appeared as high-pitched notes which rapidly descended in pitch. They were of short duration, varying from about one-fifth of a second to several seconds and occurred at random time intervals. They were most frequent in the early hours of the morning and were infrequently heard during the day time. During the early morning they were found to increase greatly in number and intensity.

The observed whistles were explained by the A.I.R. investigators as due to a Döppler change in the frequency of the weak carrier waves scattered from a rapidly moving ionized mass of air at the head of a meteor entering the earth's atmosphere and to consequent heterodyning of these waves with those reaching the receiving centre as ground waves of unmodified frequency. As the meteor rushing with some high speed through the upper atmosphere gradually slows down, there would evidently be a gradual decrease in the frequency change of the waves scattered from the head of the meteor. The scattered waves on interfering with the ground waves would then give rise to a heterodyne whistle of gradually descending pitch. From a knowledge of the initial beat-frequency due to this interference, the velocity of the meteor can be calculated from

$$\Delta f = \frac{2v}{c} . f, \text{ where } \Delta f \text{ is the beat-frequency,}$$

f the carrier frequency, v the velocity of the ionized mass of air at the head of the meteor and c the velocity of light. Assuming a beat-frequency of 3Kc/s for a carrier frequency of 7 Mc/s, the calculated velocity would be 64 Km./s. This could be taken as of the same order as the maximum velocity of the meteors directly observed.

EVIDENCES IN SUPPORT OF THE DÖPPLER EFFECT THEORY

In support of the Döpplereffect theory the following facts can be adduced :

(1) The appearance of a meteor in the sky coincided with a whistle produced in the receiver.

(2) The number of whistles observed was at a maximum in the early morning, when the number and velocity of meteors entering the earth's atmosphere are greatest.

(3) No such whistle was heard with medium radio-frequency carrier waves. With such low frequency, the intensity of the scattered waves is feeble and the Döppler change is also considerably small.

The following two experimental results of the A.I.R. investigators can also be cited :

(1) The whistle heard on a carrier of 7.5 Mc/s commenced with an initial frequency about half that of the whistle heard on 15 Mc/s. The experiment was carried out by operating one transmitter near 15 Mc/s and a second transmitter near 7 Mc/s and connecting the output of the two receivers tuned separately to these frequencies to two loudspeakers or headphones, each being connected to each receiver. It was found that the whistles were first heard on the loudspeaker connected to the receiver tuned to the lower frequency and as these whistles descended in pitch, a whistle of higher pitch was heard on the other loudspeaker connected to the receiver tuned to the higher frequency. The observation of a higher pitch on the receiver tuned to the higher frequency was expected from the Döppler effect hypothesis.

(2) One of the Delhi transmitters was tuned to approximately 7 Mc/s radiating the carrier wave and a second transmitter was operated as a pulse transmitter on a slightly different frequency. In the majority of cases it was found that the entry of a meteor into the earth's upper atmosphere, as made evident by the whistle, was followed by a return from the ionosphere, as observed on a cathode-ray oscillograph.

Some special cases were also noted by the observers. While in the majority of cases the whistle was of descending pitch, in some cases, whistles were obtained with an ascending pitch. In a limited number of observations again, the whistle commenced with a descending pitch, passed through zero frequency and rose again in pitch. These special cases were explained as due to the relative velocity of the meteor at the receiving point having a component towards or away from the receiver.

REMARKS ON THE POSSIBILITY OF DETECTING DÖPPLER EFFECT UNDER THE CIRCUMSTANCES

It is well known that there are 'patchy' ionized regions in the ionosphere which cause scattering of the electromagnetic waves when they are incident on them. The whistle which was observed beyond the range of the ground wave by the A.I.R. investigators was considered by them to be an effect of interference between scattered waves from the ionosphere and the waves returned from the ionized mass of air at the head of a meteor. If a perceptible amount of ionospheric scattering is recognised, it is evident that the waves returned from the head of the meteor would only be a small fraction of the total scattered radiation reaching the receiver. The scattered waves from the ionosphere and also the ground wave have the same frequency as the carrier waves from the transmitter. These waves on interfering with relatively feeble radiation of modified frequency, scattered from the ionized mass of air at the head of a moving meteor, would hardly be able to produce a discernible beat-note. The heterodyne whistle may not therefore be heard under the circumstances. This is indeed a strong argument against the view that the observed whistles are due to Döppler effect. For a definite assertion on the point, it is however necessary to calculate, if possible, the amount of scattered radiation from the ionized mass of air which is formed at the head of a shooting star, relative to the radiation scattered from the ionosphere.

SIMILARITY OF THE OBSERVED WHISTLES WITH SOME AUDIO-FREQUENCY MUSICAL ATMOSPHERICS

It has been known for many years now that when a telephone or any audio-frequency amplifying device is placed directly in series with a large aerial, disturbances of a musical nature can be heard. It was Barkhausen (1919) who first described observations made during the last world war on whistling tones in a low frequency amplifier, the frequency of which decreased very rapidly from a high to a low value. Later T. L. Eckersley (1926-1927 and 1928) made some investigations on these musical atmospherics. He divided them into two classes, the short and the long whistlers. Both these whistlers were characterised by the fact that the disturbance started with a high pitch which dropped rapidly in the first class and slowly in the second class to a note of low pitch. The duration of a short whistler was sometimes one-fifth of a second. The long whistler was as long as 3 seconds.

In Burton and Boardman's (1933) investigations on audio-frequency atmospherics there were two distinct varieties of musical atmospherics which were given the onomatopoeic names, 'tweek' and 'swish.' A tweek consisted of a damped oscillation trailing a static impulse. It started above 2000 cycles and reduced very rapidly towards a lower limiting frequency. Its audible duration was less than one-eighth of a second. The tweeks were not usually observed during the day time, except near sunrise and sunset. Some data of tweek counts showed a very high value, some minutes before the ground sunrise. It was also found that the tweek number was considerably high during the summer and low during the winter. The swishes were also musical sounds—the frequency sometimes going downward and at other times upward. At times upward and downward progressions were observed simultaneously. The swishes were audible from ½ sec. to 4 sec., covering a frequency range from well below 800 to above 4000 cycles. The swishes appeared to have no connection with the time of the day and the time of the year or with local weather conditions. They were found to persist steadily through the early morning, bridging the transition period when the more common forms of atmospherics were found to fall off rapidly in number and intensity. According to Burton and Boardman, Eckerslsy observed both tweeks and swishes which were not however recognised by him as distinct varieties.

Whatever be the mechanism of production of these whistling tones, the similarity of these whistles with the whistles observed by the A. I. R. investigators is indeed striking. The latter observed a considerably large number of whistles in the early morning. The tweeks were also observed in large number during that period. One wonders whether the two phenomena are fundamentally the same or similar! One suggestion would be that the carrier waves were modulated in some way by the audio-frequency atmospherics which could then be heard in the receiver tuned to the frequency of the carrier waves.

ELECTRICAL IMPULSE PRODUCED BY A METEOR IN THE IONOSPHERE—A TENTATIVE SUGGESTION

Chamanlal and Venkataraman observed coincidence between the appearance of meteors and their observed whistles. If these whistles have any connection with the musical atmospherics, we would expect a correlation between the appearance of meteors and these musical atmospherics. In the few observations made by Burton and Boardman during two nights, there was no such correlation.

It can however be reasonably conjectured that an electrical impulse can be produced by the stoppage of meteors in the ionosphere. In that case, it is possible to explain the so-called Döppler whistles in a manner which is described in the next section. It should be noted that there is no experimental evidence of any electrical impulse being produced by meteors in the upper atmosphere. This suggestion means that there can be a kind of audio-frequency atmospherics which is distinct from the usual variety in its mode of production.

MODULATION OF THE CARRIER WAVES BY THE ELECTRICAL IMPULSE PRODUCED BY A METEOR IN THE IONOSPHERE

Eckersley formulated a theory based on ionospheric dispersion to explain the whistlers. Barkhausen (1930) offered two explanations—one based on multiple reflection between the earth and the ionosphere, and the other somewhat similar to Eckersley's view. Since the dispersive action of the ionosphere has the effect of transmitting different frequencies with different velocities, the various Fourier components into which an impulse is broken up, will then be drawn out into a musical note of rapidly decreasing frequency. The rate of variation with frequency would evidently depend on the amount of dispersion in the ionosphere.

The lowest pitch of the whistle, as shown by Eckersley, would be determined by

$$n_0^2 = \frac{Ne^2}{\pi m}$$

where N = number of electrons per c.c. and e and m are charge and mass of an electron.

Supposing now that an electrical impulse is produced by a meteor when it stops in the ionosphere, it is evident that its various frequency components would reach the lower fringe of the layer, one after another, in quick succession, the short wave-lengths arriving earlier than the long wave-lengths. Thus the carrier waves which are scattered from the ionosphere in the same region would be modulated by the audio-frequency oscillations—the modulation frequency being a function of time. The receiver tuned to the carrier would then reproduce a note of rapidly descending pitch.

If this view is correct, we would also expect audio-frequency atmospherics *unconnected with meteors* to produce a similar modulation of the carrier waves. Tweeks and swishes can therefore be heard by the scattered waves as modulated by these impulses in the manner already described. It is just possible that at least some of the whistles observed at Delhi were of this origin. Tweeks and some of the swishes are known to be of the descending pitch; some swishes again, are of the ascending pitch ; while a few swishes are of a mixed type. It is interesting that all these types of whistles were reported by the A.I.R. investigators. It seems probable that the whistles of the *ascending* pitch observed by these investigators are definitely unconnected with meteors. It is not, however, possible to explain these whistles as due to modulation of the carrier by the electrical impulse produced by the stoppage of meteors in the ionosphere.

It may be argued here that according to the suggested modulation theory, we would expect cross-modulation between different transmitting stations. The possibility of such 'Luxembourg effect' is however very remote. For a particular receiving centre, it is evident that the received sky-waves originally coming from the different transmitters would, in general, be reflected from widely separated regions of the ionosphere.

The dependence of the pitch of the whistle on the frequency of the carrier waves is also to be expected according to the modulation theory. We are concerned here with frequencies higher than the critical frequency for ionospheric reflection. Within this limit, the higher frequencies would penetrate the ionized layer without much refraction, whereas the lower frequencies would do the same suffering a relatively larger refraction. Consequently, corresponding to any angle of incidence, the track of the transmitted wave in the ionosphere would be at a higher level for a carrier wave of higher frequency than the corresponding track for a lower frequency. For the lower strata of the ionized layer, the electron concentration is higher at a higher level and since according to Eckersley, the lowest pitch of the whistle is proportional to the square root of the electron concentration, it is only reasonable to expect that the pitch of the whistle heard with higher frequency would be higher than that obtained with lower frequency carrier.

It should be noted that according to the modulation theory suggested in the paper, there would be side-bands on *both* sides of the carrier, for any electrical impulse modulating the latter. On the other hand, according to Chamanlal and Venkataraman's Döppler effect theory, the observed whistle would be *either* on the higher frequency side of the carrier in the case of an approaching meteor, *or* on the lower frequency side in the case of a receding meteor. For any particular variety of the whistle, it is indeed difficult to test whether or not another side-band exists simultaneously on the other side of the carrier. Taking the frequency of the whistle to be 3 Kc/s or of that order, it appears also doubtful whether such small frequency changes would be discernible in the region of such high frequency, even with a receiver of high selectivity.

SUGGESTIONS OF SOME TEST EXPERIMENTS

(*a*) Along with the receiver, if we have an audio-frequency amplifying system of high gain and high fidelity connected to a large aerial, it would be interesting to see whether both apparatus would give whistles of the same type. According to the suggested modulation theory, when the carrier waves of suitable frequency are sent up, the whistles, when produced, would be heard in both the cases. When the transmitter is off, the receiving set would fail to respond, whereas the audio-frequency amplifier would respond to the audio-frequency atmospherics.

(*b*) The return of the waves, as evidenced visually in the pulse experiments on the oscillographic screen, merely shows an increase in the electron concentration, when a meteor enters the ionosphere. Even when there are no meteors, and there is no indication of any return of the pulse, the audio-frequency amplifying system mentioned in (*a*) would respond to the audio-frequency atmospherics. When the tweeks and swishes are heard, it would be interesting to see whether these are also heard in the radio receiver, when a carrier wave of suitable frequency is sent up.

(*c*) Two receivers, one connected with a loop aerial or any suitable aerial and the other worked with a ground wave suppression aerial system and both tuned to the frequency of the carrier waves can be employed for listening to the whistles. If the whistle is really a heterodyne whistle due to interference between the ground wave and the waves of modified frequency scattered from the ionized mass of air at the head of a meteor, the receiver connected with the ground wave suppression aerial system would give no whistle, even though the meteors are visible. With the other receiver, however, the whistles would be heard. There is of course the possibility of a heterodyne whistle being produced by the interference between the waves scattered from the ionosphere and the waves returned from the head of a meteor, even when the ground waves are absent.

(*d*) Simultaneous appearance of a meteor and a whistle needs however a more convincing evidence.

It is desirable that a fuller investigation on the subject along the lines suggested in this paper should be carried out. If the Döppler effect explanation of the whistles observed by the A.I.R. investigators, is fully substantiated, this would indeed be the *first* evidence of a Döppler change of frequency in the case of wireless waves. Such experimental evidence has, however, been recently obtained by Sir Edward Appleton (1943) in connection with his simple method of demonstrating the circular polarization of ionospherically reflected radio waves. During the sunrise period (or the sunset period), when the height of ionospheric reflection is slowly decreasing (or increasing), the frequency of the ionospherically reflected waves would be slightly higher (or lower) than that of the ground waves due to Döppler effect. The ionospherically reflected waves and the ground waves, when received simultaneously in a loop aerial, would thus produce beats, causing variation in the output from the aerial. Regular fading has actually been observed during the sunrise and sunset periods,

PHYSICS DEPARTMENT,
DACCA UNIVERSITY.

REFERENCES

Appleton, E. V. 1943. *Nature*, **151**, Feb. 27.

Barkhausen, 1919, *Phys. Zeitschrift*, **20**, 401-03.

Barkhausen, 1930, *Proc. I.R.E.*, **18**, July.

Burton and Boardman, 1933, *Proc. I.R.E.*, **21**, Oct.

Chamanlal and K. Venkataraman, 1941, *Electrotechnics*, No. **14**, Nov., pp. 28-40.

T. L. Eckersley, 1925, *Phil. Mag.*, **49**, 1250; 1926, *Nature*, **112**, 821; 1928, *Nature*, **122** 17, 768.

DEVELOPMENT OF δ AND γ BANDS OF NITRIC OXIDE IN ACTIVE NITROGEN AND LYMAN BANDS IN HELIUM-NITROGEN MIXTURE

By B. M. ANAND

(Received for publication, July 6, 1948)

Plate V

ABSTRACT. The doublet structure of 0-0, 0-1, 0-2 and 0-3 bands of δ system of nitric oxide as observed in active nitrogen by a one metre normal incidence vacuum spectrograph is described.

The vibrational structure of 1,0 and 2,0 bands of γ system has been measured.

It is found that whereas δ and γ band systems are prominently present, β bands of nitric oxide lying in the vacuum region, are particularly absent in the afterglow of nitrogen under the conditions of the experiment.

Lyman-Birge-Hopfield bands of nitrogen have been developed in a mixture of helium and nitrogen. Three new bands of the system—(6,13), (0,8) and (4,9) are reported.

The band spectrum of NO molecule consists of β, γ and δ systems of bands, which are easily developed in the afterglow of nitrogen containing oxygen as an impurity. The character of bands excited in active nitrogen is characteristic of a low temperature radiating source. The number of lines are few and the heads appear prominently and the v'' progression corresponding to $v'=0$ is particularly strong in emission.

The δ bands were first observed by Knauss (1928) in active nitrogen. Six emission band heads degraded towards the short wavelength side corresponding to single progression $v'=0$, $v''=0, 1, 2, 3, 4, 5$ were recorded by him between λ 2320 and λ 1913, with a one metre vacuum grating spectrograph, using oil coated plates and a slit width of 0.25 mm. The 0,0 band lying at λ 1913 was indentified as the one previously reported by Leifson (1926) at λ 1910.6 as absorption band due to NO. Because of the large width of the slit and the use of the oil coated plates, the structure of these bands could not be observed.

Later, Schmidt (1930) observed the doublet structure of these bands with large quartz spectrograph E_1, and analysed the rotational structure of 0-3, 0-4 and 0-5 bands. His analysis showed that these bands correspond to $^2\Sigma \longrightarrow {}^2\Pi_{\frac{1}{2}, \frac{3}{2}}$ transitions, the latter being the ground level. Each sub-level gave rise to two sub-heads corresponding to P and Q branches. The values of 0,0 Q heads for each sub-level have been computed from this data, but no further attempt seems to have been made to photograph and measure the doublet structure of the 0-0 0-1, 0-2 and 0-3 band heads of this system lying in the vacuum region.

(a)

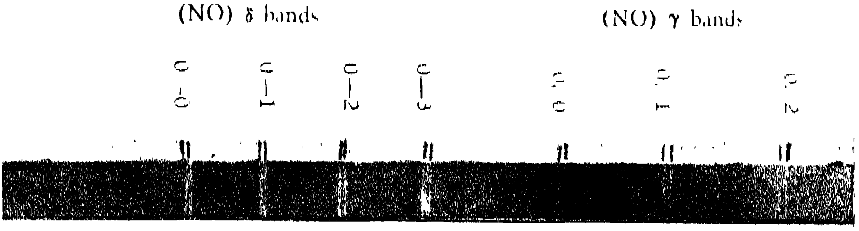

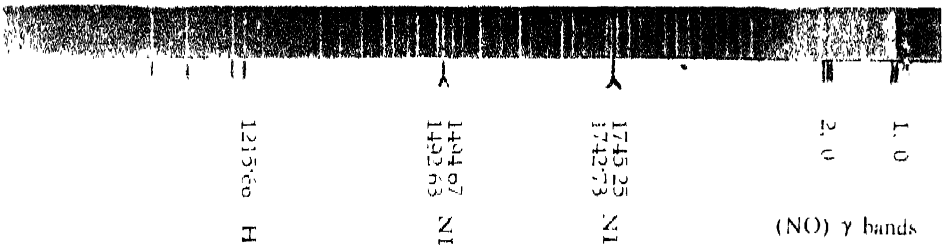

(N_2) Lyman Birge Hopfield bands

During the course of a work reported in this journal on active nitrogen in the Schumann region, the author obtained the first four bands of the progression $v''=0, 1, 2, 3$, $v'=0$ very prominently in one of the spectrograms taken with a one metre normal incidence vacuum spectrograph. The doublet structure was distinct and the results of the measurements and the corresponding values of Knauss and Schmidt are given for comparison in Table I.

TABLE I

λ in vacuum of δ bands of NO

v', v''	Present values	Intensity	Knauss values	Schmidt values
0,0	Q1	1910.2 (4)		
		1913.5 (3)	1913	
	Q2	1914.6 (3)		
0,1	Q1	1980.9 (5)		
		1984.5 (3)		
	Q2	1985.6 (4)	1987	
0,2	Q1	2056.0 (4)		
		2059.8 (2)		
	Q2	2061.3 (3)	2062	
0,3	Q1	2135.8 (4)		2135.5 Q1
		2140.1 (2)		
	Q2	2141.4 (3)	2142	2141.0 Q2

In Table II, wave numbers of the various heads are given. The differences represent the separations of the vibrational levels in the initial electronic state.

TABLE II

v', v''	0	1	2	3	Head	Transition
0	53251 (1869)	50482 (1844)	48638 (1817)	46821	Q1	$^2\Sigma-^2\Pi_{\frac{1}{2}}$
	52260 (1869)	50391 (1843)	48548 (1821)	46727		
	52230 (1867)	50363 (1843)	48520 (1822)	46698	Q2	$^2\Sigma-^2\Pi_{\frac{3}{2}}$
Δν	(1868)	(1843)	(1820)			

The intensities are relative visual estimates. The plate was measured on a Hilger comparator a number of times and the estimated error is not considered to be more than 0.1 Å.

In the same spectrogram a number of bands of γ system of NO are present, plate V (*a*). This system has been thoroughly studied by a large number of workers. However, it appears from the Identification Tables of Molecular Spectra (1941) by Pearse and Gaydon that, for the bands of this system lying below λ 2200, values corresponding to only one single head are available. In this spectrogram the doublet structure is definitely brought out though the bands are diffuse. Consequently, readings approximately at the centre of each head could only be taken.

In another spectrogram plate V (*b*) obtained by passing an uncondensed discharge in a mixture of helium and nitrogen, the vibrational structure of (1,0) and (2,0) bands of γ system has come out very well. Table III gives the measured wave-lengths and the corresponding wave numbers of the various heads of these bands along with the previous values as given in the Identification Tables of Pearse and Gaydon (1941):

TABLE III

v', v''	λ in Å	Intensity visual estimate	ν in cm.$^{-1}$	Head	Transition	Previous values
2,0	2047.0	2	48853	Q1	$A^2\Sigma - X^2\Pi_{\frac{1}{2}}$	2060
	2048.3	2	48822	P1		
	2052.2	1	48728	Q2	$A^2\Sigma - X^2\Pi_{\frac{3}{2}}$	
	2053.3	1	48702	P2		
1,0	2148.5	4	46544	Q1	$A^2\Sigma - X^2\Pi_{\frac{1}{2}}$	
	2149.5	4	46522	P1		
	2154.0	2	46426	Q2	$A^2\Sigma - X^2\Pi_{\frac{3}{2}}$	2156
	2155.3	2	46397	P2		

This plate shows prominently the well-known band system of nitrogen molecule lying in the vacuum ultra-violet and first observed by Schumann (1903). A large number of these bands degraded to the red and lying between λ1300-λ1900 were measured by Lyman (1911). Birge and Hopfield (1928) obtained this system of bands both in absorption and emission. As a result of their vibrational analysis this system was found to be due to a $^1\Pi \longrightarrow {}^1\Sigma$ transition, the latter electronic state being the ground level X of the neutral nitrogen molecule. In all their experiments purified nitrogen, *i.e.* commercial nitrogen passed over heated copper at a pressure which never exceeded 0.002 mm. was used. The most prominent impurity in these spectra was that of nitric oxide (NO). Subsequently, nitrogen was obtained by exploding sodium oxide when CO, H_2 and NO appeared as impurities.

In the present experiment pure helium at a pressure of 8 m.m. was mixed with 1% nitrogen in a Pyrex glass discharge tube 140 cm. long, 2.2 cm. in diameter, fitted with three aluminium electrodes A, B and C. The tube was sealed end-on without any window to the one-metre normal incidence vacuum spectrograph. A schematic diagram of the apparatus is shown in Fig. 1.

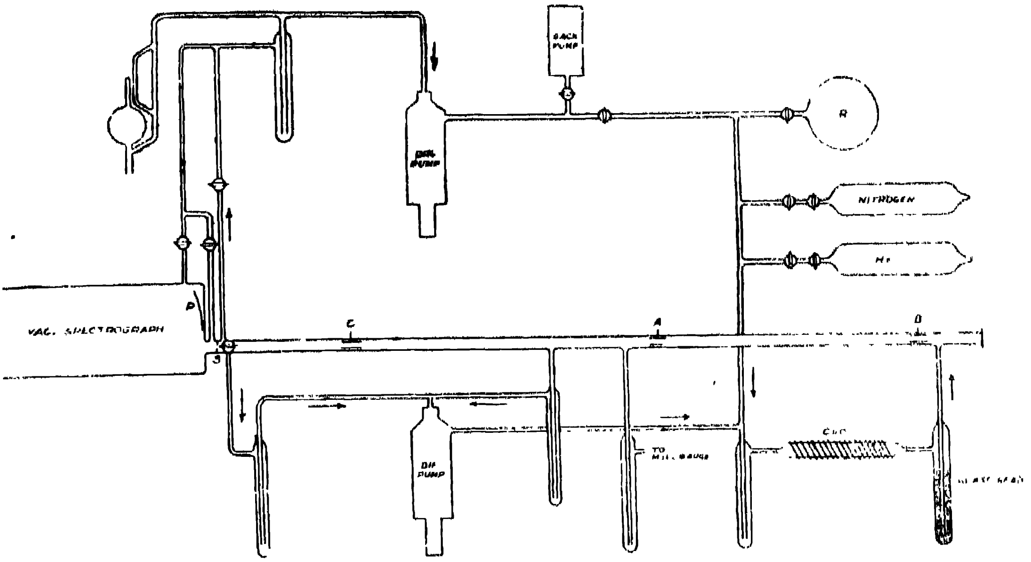

FIG. 1

Two four-stage mercury diffusion pumps maintained a difference of pressure between the discharge tube and the spectrograph. The pressure in the discharge tube was about 8 mm. while in the spectrograph it was about .01 mm. Six liquid air traps kept the discharge free from mercury and other impurities. An electrically heated quartz tube containing CuO eliminated hydrogen. A two-litre reservoir R in the main stream kept the pressure in the tube steady. The other parts are self-explanatory. For excitation of the discharge the secondary of a 15,000 volts, 450 watts transformer was connected to the terminals A and C of the discharge tube. The exposure time was one hour on a Schumann plate prepared in the Laboratory from photographic gelatine Batch 73-400 from Eastman Kodak Co.

The following impurity lines were used as comparison standards :—

1215.66 HI, 1492.63 NI, 1494.67 NI.
1742.73 NI, 1745.25 NI.

The plate was measured a number of times on two comparators (Hilger and Carl Leiss) and the mean values obtained. The intensities are the visual estimates on an arbitrary scale of 0-10. Table IV gives the mean values compared with the Birge-Hopfield values:

The values given in brackets for 6-13, 0-8 and 4-9 band heads are the computed values as calculated by Birge and Hopfield.

Some of the interesting results brought out by these experiments may be noted as follows:

(1) No attempt was made to get NO bands. The exposure was given only to get the emission spectrum of the nitrogen afterglow. A little trace of oxygen

TABLE IV

Measured values of λ in Å	Intensity	Birge-Hopfield values	Intensity	V′ − V″
2007.0	2	2007.4	2	3-11
1989.5	1	1989.9	1	2-10
1984.9	1	—	—	—
1980.2	1	(1980.06)	—	6-13
1973 5	1	1973 1	0	1-9
1962.4	1	1963.1	1	5-12
1955.1	1	(1955.96)	—	0-8
1944.7	2	1944.8	4	4-11
1927.6	2	1927.8	4	3-10
1910.9	3	1911.0	4	2-9
1894.0	2	1894 3	2	1-8
1870.7	1	1871.0	4	4-10
1853.9	3	1853.9	4	3·9
1836.9	4	1837.2	5	2-8
1820.6	4	1820.8	5	1-7
1804.5	2	1804.7	3	0-6
1800.1	1	(1800.93)	—	4-9
1784.9	1	1784.6	3	3-8
1768.0	4	1768.1	6	2-7
1751.9	5	1751.9	7	1-6
1736.0	4	1736.2	5	0-5
1702.9	2	1703.3	4	2-6
1687.2	6	1687.3	9	1-5
1671.7	6	1671.7	8	0-4
1657.5	1	1657.7	4	3-6
1626.4	2	1626.5	6	1-4
1611.4	6	1611.3	9	0-3
1600.3	1	1599.7	4	3-5
1584.1	2	1584.4	5	2-4
1576.3	1	1575.9	3	5-6
1554.2	6	1554.3	9	0-2
1529.6	3	1529.9	5	2-3
1515.0	3	1515.2	5	1-2
1500.7	5	1500.7	7	0-1
1464.0	6	1464.1	8	1-1
1450.3	3	1450.1	5	0-0
1444.0	2	1444.3	4	3-2
1429.7	3	1429.9	6	2·1
1415.7	4	1415.9	6	1-0
1412.3	2	1411.6	5	4-2
1383.7	5	1383.8	8	2-0
1953.5	4	1353 6	8	3-0
1325.7	3	1325.2	6	4-0
1311.5	1	1312.3	4	6-1
1298.9	1	1298.4	5	5-0
1226.3	1	1226.6	abs.	8-0

as an impurity was therefore responsible for the formation of NO and the development of γ and δ systems of NO bands.

(2) The doublet structure of 0,0, 0,1, 0,2, 0,3 δ bands has, so far as the author is aware, come out for the first time. Each band consists of two definite heads Q_1, Q_2 with a mean wave number difference of about 120 cm.$^{-1}$ corresponding to the interval $^2\Pi_{\frac{3}{2}} - {}^2\Pi_{\frac{1}{2}}$ of the ground state. The shorter wave-length head corresponding to $^2\Sigma - {}^2\Pi_{\frac{1}{2}}$ transition forms the Q_1 head and $^2\Sigma - {}^2\Pi_{\frac{3}{2}}$ transition forms the Q_2 head. In all the bands the Q_1 head is stronger than the Q_2 head. Moreover, whereas the Q_1 head is followed by an unresolved rotational structure up to about 4 Å towards the violet side, the Q_2 head is much sharper and there is a clear gap of about 30 cm.$^{-1}$ after which a fine structure starts towards the

shorter wave-length side. The central reading given in the tables I and II for each band corresponds to the long wave-length edge of this structure.

(3) The doublet structure of 0-0, 1-0, 2-0, 3-0, 0-1, 0-2 and 1-4 bands of γ system of NO could be roughly measured. Usually in active nitrogen the relative intensity of β and γ bands is of the same order. The strongest bands of β system, however, do not lie in the vacuum region. The 2-4 and 3-4 bands of β system lying at about λ 2490 and 2430 were searched for in the spectrogram but there was not the faintest impression of these bands. In this case, the γ bands were thus present exclusive of the β bands in this region. Possibly if the partial pressure of oxygen and, therefore, of NO were increased, the β bands would have made their appearance. One may draw the conclusion that under the conditions of the experiment, that is when the partial pressure of NO is extremely small, the maximum number of NO molecules are in the C $^2\Sigma$ state corresponding to the upper state of δ bands, a smaller number of them in A $^2\Sigma$ state, the upper state of γ bands, but comparatively very much smaller number of molecules in the B $^2\Pi$ state particularly corresponding to the vibrational states 2-4 and 3-4 giving rise to the β bands in the vacuum region.

(4) The vibrational structure of 1,0 and 2,0 bands of γ system has been measured. Values for both the P and Q heads for the two sub-levels are given. The Q heads show a prominent unresolved rotational structure towards the shorter wave-length side.

(5) Lyman-Birge Hopfield bands have been developed in nitrogen containing excess of helium. Three new bands observed at λ 1980.2 (6,13), 1955.1 (0,8), and 1800.1 (4,9) are reported. In Birge and Hopfield spectrograms bands such as 1-3, 2-5, 4-3, 4-8, 5-7, 5-10, 6-2, 6-4 and 6-9 were missing. The author was interested in finding out if some of these missing bands could be developed in nitrogen-helium mixtures. This plate does not show any one of the above-mentioned missing bands.

I take this opportunity of expressing my grateful thanks to Dr. P. K. Kichlu for many helpful discussions in the preparation of this paper.

REFERENCES

Birge, R.T., and Hopfield, J.J., 1928, *Astrophysical Journal*, **68**, 257.
Knauss, H.P., 1928, *Phys. Rev.*, **32**, 417
Leifson, S., 1926, *Astrophysical Journal*, **63**, 73
Lyman, T., 1911, *Astrophysical Journal*, **33**, 98.
Pearse, R.W.B. and Gaydon, A.G., 1941, *The Identification of Molecular Spectra.*
Schumann, V., 1903, *Smithsonian Contributions*, Nos. 1413, 16.
Schmidt, R., 1930, *Zeits f. Physik*, **64**, 279

ON THE EXPERIMENTAL STUDY OF THE EFFECT OF TRANSVERSE h.f. ELECTRIC FIELD ON THE VISCOSITY OF LIQUIDS*

By B. N. SINGH

AND

SNEHAMOY GHOSE

(*Received for publication, September* 7, 1943)

ABSTRACT. The paper contains the description of an apparatus designed by the present authors to study the effect of high-frequency transverse electric field on the rate of flow of liquids through narrow channels. The apparatus is suitable for liquids having fairly low conductivity (of the order of 10 mho or less) and for such liquids h.f. fields of the order of several kilovolts/cm. can be applied. The frequency of the h.f. field may be kept at any suitable value. The authors have used fields of the order of 10^6 cycles/sec. Incidentally the authors have found that in case of xylene (a mixture of ortho-, para- and meta-) no change in the rate of flow is recorded for fields up to 5 kilovolts cm and even more. In case of samples of amyl alcohol and ethyl acetate used by authors fields up to 1 kilovolt/cm. could be applied and for this field no change in their rate of flow was noted.

During past few years a large number of experimental investigations have been made to study the effect of electric field on the viscosity of liquids. Such investigations have been made with electric fields whose direction is either perpendicular or parallel to that of the flow of liquids. Though the results obtained by various workers appear to be rather conflicting with each other there are a few points on which more or less a general agreement may be observed. In the case of non-polar liquids there is no appreciable effect of either the longitudinal or transverse electric field. The longitudinal electric field does not appear to produce any effect even on polar liquids. The main controversy, therefore, centres round the different results obtained when the direction of the applied electric field is perpendicular to that of the flow of liquids. The recent experimental results of Menz (1939), Andrade (1940), and Prasad *etal*, (1941), however, reveal that even in this last case the effect is either negative or if positive appears to be influenced by the conductivity of the experimental liquids. But according to the results of Andrade conductivity as such is not the determining factor, because liquids like benzene conduct without showing any effect. Andrade further suggests that in case of some polar liquids there is a formation of space charges at the electrodes and hence an abnormal anode and kathode fall. If this be the case, the field in the body of the liquid is much less than the

---

* Communicated by the Indian Physical Society.

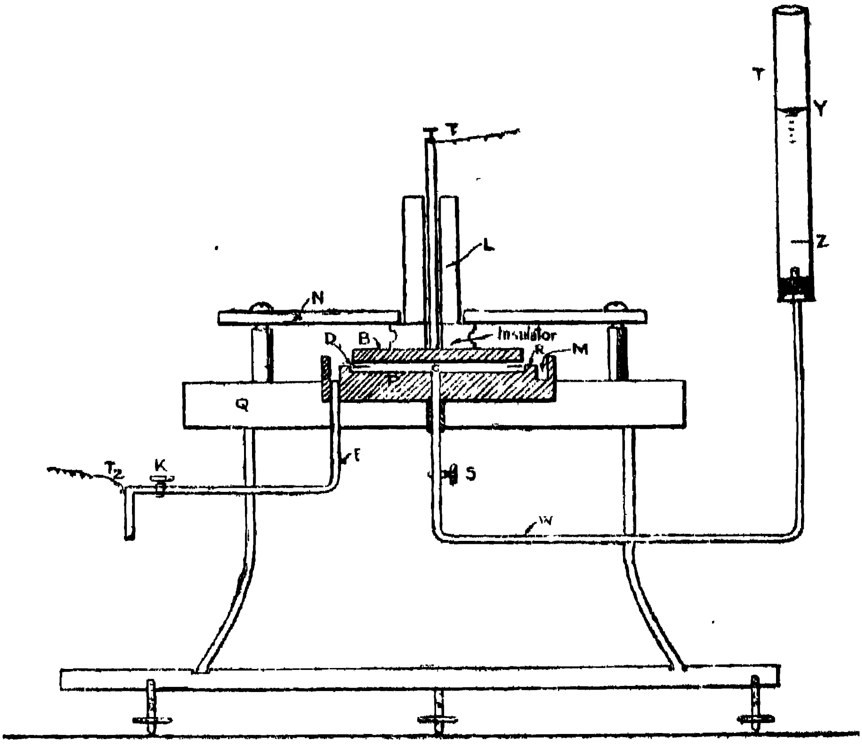

FIG. 1*a*

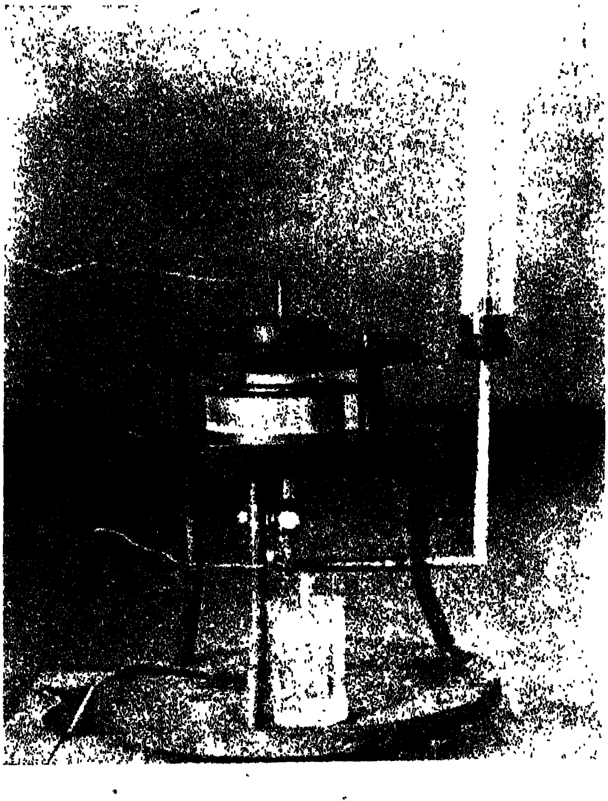

FIG. 1*b*

"apparent field", namely the applied difference of potential divided by difference between the two electrodes. In view of these possible disturbances the true viscosity effect should be sought with alternating frequency sufficiently high to prevent space charges at the electrodes and sufficiently low to avoid effects due to relaxation time. In the present paper an apparatus designed by the present authors has been described which is suitable for the experimental study of the effect of h.f. transverse electric field on the rate of flow of liquids having fairly low conductivity.

The main body of the apparatus is made of fine steel slab with a central circular platform P (shown in fig. 1*a*) on its upper surface, which is silvered and finely polished. There is a central hole C in the platform which is connected to the glass tube T through a brass U-tube fitted with a liquid-tight stopper S. Three small thin pieces of mica DD (thickness of the order of .003 cm.) are kept over the polished platform. The inside of the central hole and that of the U-tube is also silvered. A circular brass plate B of thickness 6 mm., polished and silvered at its lower surface, is kept over the strips DD. In order to keep the strips well pressed, a heavy ring of lead L is kept over the plate and made tight from above by three screws fitted in an upper circular plate N made of ebonite. The upper plate B is also provided with a handle A and terminal T_1. The central circular platform has got a rim RR about 1 mm. high and an annular space M surrounding it. The inner diameter of the circular platform is 4.3 cm. and that of the upper plate is 3.7 cm. Thus when the latter is placed over the former, between the perimeters of the two there is a fair margin of about 3 mm. When the glass tube T is filled with a liquid, the latter forces up through the hole C, passes slowly through the narrow space between the platform and the other plate B, then trickles over the rim of the platform to the annular space and finally escapes through the opening E, which is also fitted with a liquid-tight stopper K. The steel body of the apparatus is provided with another terminal T_2 and rests over a thick circular ebonite plate Q. The latter is supported by three firm rigid legs which are permanently fixed to a wooden base fitted with three levelling screws. The upper and lower ebonite plates are rigidly held together with three rods screwed to them. The glass tube T at its lower end is fitted with a rubber stopper over which a layer of mercury is kept to prevent the liquid from coming into contact with the stopper. The electric field is applied between the two terminals T_1 and T_2 of the apparatus by connecting it in parallel with the oscillating condenser of a radio-frequency oscillator, the range of oscillations in the present case being 10^5 cycles per sec. to 10^7 cycles per sec. (The connections are shown in fig. 2). The h.f. voltage impressed between the two plates of the apparatus is measured by a Moullin voltmeter. When the experimental liquid is poured into the glass tube (stopper K being closed), it flows through the U-tube and the central hole comes slowly through the narrow space between the plate and the platform and finally passes over the rim to the annular space. The level of liquid in the glass tube gradually comes down. The time required for the level of liquid to come from a particular mark say Y to another say Z may be noted with the help of a travelling telescope and a stop watch. It will be seen from the experimental

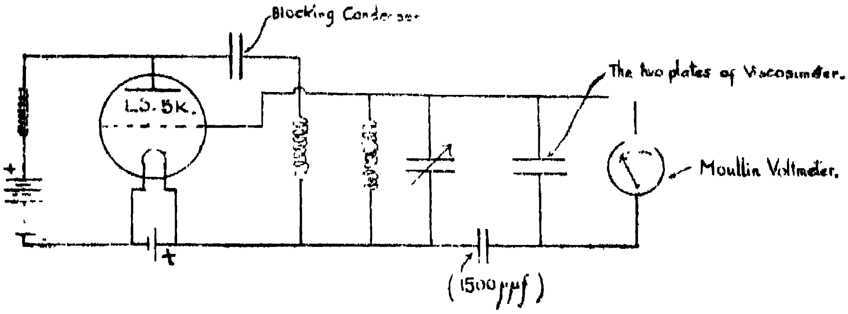

FIG. 2

data given in table 1, that the time of flow of liquid remains fairly constant, the maximum variations being not more than 3 seconds even when the time of flow exceeds 15 minutes. Provided the experimental liquid is pure, throughout the flow over such long periods, the h.f. voltage as measured by Moullin voltmeter remains practically constant. The capacity of the condenser formed by the plate B and the platform P is of the order of a few hundreds of μμF and hence suitable for introduction into h.f. oscillators of such frequencies which satisfy the condition of being sufficiently high to prevent space charges at the electrodes and sufficiently low to avoid effects due to relaxation time. In view of small separation between the plates, the effective value of the electric field acting on the liquid passing through the channel may be made considerable without the necessity of applying a field of a high order between the plates. Fig. 1*b* gives a general view of the apparatus.

EXPERIMENTAL RESULTS AND CONCLUSION

In table 1 are given the experimental data for liquids xylene (a mixture of ortho-, para- and meta-), amyl alcohol and ethyl acetate. The experimental values for the conductivity of the same samples of liquids as used for flow are also given in the last column.

The experimental data given in the above table clearly show that in the present apparatus the time of flow of the given liquid remains constant within three or four seconds even if the total time of flow extends up to 15 minutes or more. If the effect of the h.f. electric field is, therefore, to alter the rate of flow of a liquid even to a small extent it can be easily detected in the present arrangement. The only drawback in this design is that liquids not having a fairly low conductivity cannot be used. But this defect will be perhaps inevitable in every design. The fact that in the case of liquids having conductivity of the order of 10^7 mho fields up to 5 kv./cm. or even more can be obtained, shows that if after repeated distillations samples of liquids having a conductivity of a much less order be used, a much higher field may be applied and conclusive results obtained.

From the results already obtained by the present authors it may be seen that the effect of the h.f. field on the viscosity of xylene (a mixture of ortho-, para- and meta-) is negative for the fields up to the order mentioned above. In this case fields of a much higher value were actually applied but could not be

TABLE I

Liquid	Applied field volts/cm.	Frequency in cycles per sec.	Time of flow without field	Time of flow with field	Conductivity in (mho)
Xylene	5000	1.11×10^6	617 sec.	618 sec.	6.7×10^{-8}
	,,	,,	618 ,,	619 ,,	
	,,	,,	619 ,,	620 ,,	
	2000	,,	616 ,,	618 ,,	
	,,	,,	618 ,,	617 ,,	
	,,	,,	617 ,,	619 ,,	
	5000	8.1×10^5	385 ,,	386 ,,	
	,,	,,	386 ,,	387 ,,	
	,,	,,	387 ,,	388 ,,	
	3000	,,	385 ,,	386 ,,	
	,,	,,	387 ,,	386 ,,	
	,,	,,	388 ,,	387 ,,	
	5000	2.70×10^6	356 ,,	356 ,,	
	,,	,,	357 ,,	357 ,,	
	,,	,,	358 ,,	359 ,,	
	3000	,,	356 ,,	355 ,,	
	,,	,,	357 ,,	358 ,,	
	,,	,,	358 ,,	358 ,,	
Amyl alcohol	1000	1.11×10^6	1680 ,,	1681 ,,	3.16×10^{-6}
	,,	,,	1681 ,,	1682 ,,	
	,,	,,	1683 ,,	1681 ,,	
Ethyl acetate	1000	,,	936 ,,	936 ,,	2.45×10^{-6}
	,,	,,	937 ,,	938 ,,	
	,,	,,	938 ,,	938 ,,	

measured due to the absence of a voltmeter of suitable range. For the samples of amyl alcohol and ethyl acetate used by the authors h.f. fields only up to 1 Kv./cm. could be applied. It may be added that the voltage of the high frequency can be increased also by using a more powerful oscillating circuit.

The authors express their thanks to Prof. S. P. Prasad, B.A. (Cantab.) for the interest he has taken in this work. They are also thankful to Principal Kamta Prasad, B.A. (Cantab.) for his useful suggestions. One of us (S. Ghose) is also grateful to the Government of Behar for providing him with a scholarship.

PHYSICS LABORATORY,
SCIENCE COLLEGE,
PATNA.

REFERENCES

Andrade, E. N. da C., 1940, *Proc. Phys. Soc.*, **52**, 755.
Menz, H., 1939, *Ann. d. Physik*, **34**, 740.
Prasad, S. P., Singh, B. N. and Singh, B. D., 1941, *Proc. Ind. Sci. Congress*, **19**

RADIUM-CONTENT OF CEYLON THORIANITE*

By P. K. SEN CHAUDHURY

(Received for publication, Sept. 7, 1943)

ABSTRACT. A pliotron-amplifier has been set up for the study of many interesting nuclear and radio-active phenomena. With this amplifier and ionisation chamber, the radium content of a sample of Ceylon thorianite has been estimated by the well-known γ-ray method of estimation. The amount of radium present approximately amounts to 5.94×10^{-8} gms. per gm. of the mineral.

INTRODUCTION

An accurate estimation of radium present in minute traces, in different minerals has been already known to be of much commercial importance due to a large demand of this element in medical science and in making luminous paints. Besides that, estimation of radio-active elements and the equilibrium amount of their product elements in different minerals and rocks is of much theoretical interest to geophysicists. As only from such data we can calculate the age of the earth and trace the history of gradual evolution of different rocks and mountains.

The age of a rock or mineral is defined as the time elapsed since the beginning of solidification or crystallisation from the molten state. This time can be easily obtained from the experimentally determined ratio :

$$\text{Age} = \frac{\text{Accumulated amount of disintegration product element}}{\text{Rate of production of the product element}}.$$

The product element is either helium which is nothing but the accumulated α-particles emitted by the successive disintegration products, or radiogenic lead which is the end product of the three radio-active series. The amount of helium or lead present per gram of a specimen is determined by chemical analysis and suitable analytical technique. But recent investigations show that in many cases helium-method gives erroneous results due to the leakage of helium from rocks or minerals. Again as the life of parent radio-active elements, such as uranium or thorium, is very long there is negligible change in the amount of parent element since the beginning of rock-formation. Therefore the rate of production of the product element is directly proportional to the amount of uranium or thorium present in the rock or mineral. This amount can be ascertained by chemical analysis of the sample. But as the amount of uranium or thorium present is very small particularly in case of rocks, the chemical method is liable to considerable error. The alternative and much more reliable method developed and followed by Evans (1940), Nier (1941) and all the modern workers is by the comparison of ionisation current produced by certain weight of a specimen with that of a standard source. Usually α- and β-rays are cut off and the ionisation due to γ-ray only is compared. In case of very feeble source, uranium, etc., present can be directly determined by counting α-rays emitted by a thin layer of the sample. The comparison of ionisation current or the counting of α-particles being done by an ionisation chamber with an electrometer or a vacuum-tube amplifier.

---

* Communicated by the Indian Physical Society.

The present work was undertaken for a systematic estimation of radium-content and also for the age-determination of Indian minerals and rocks in co-operation with Dr. Fox, Director, Geological Survey of India and Dr. Wadia, Mineralogist to the Government of Ceylon. Both of them very kindly consented to help us in this work.

APPARATUS

The apparatus set up for this experiment is an electrometer-tube amplifier with an ionisation chamber. In recent years such an arrangement has been extensively used for the study of various nuclear and radio-active problems. Due to reliable results and very convenient manipulation it is quickly replacing electrometers and electroscope for the investigation of these problems. The electrometer-tube selected is an F. P. 54, pliotron tube designed by Metcalf and Thompson (1930). The circuit used is same in principle as that of Dubridge and Brown (1933). A Leeds and Northroup R-type of galvanometer was balanced by the plate current and the space-charge grid current of the tube. To eliminate drift and for fine control, various resistances were selected by trial. The actual circuit set up is shown in Fig. 1. Further to eliminate mechanical disturbances the ionisation chamber was carefully mounted on the Pliotron-tube enclosed in a brass cylinder. The mounting is shown in Fig. 2. Using 10^{11} ohms as the leaking resistance a sensitivity nearly 10^{-14} amp. per millimeter deflection was obtained.

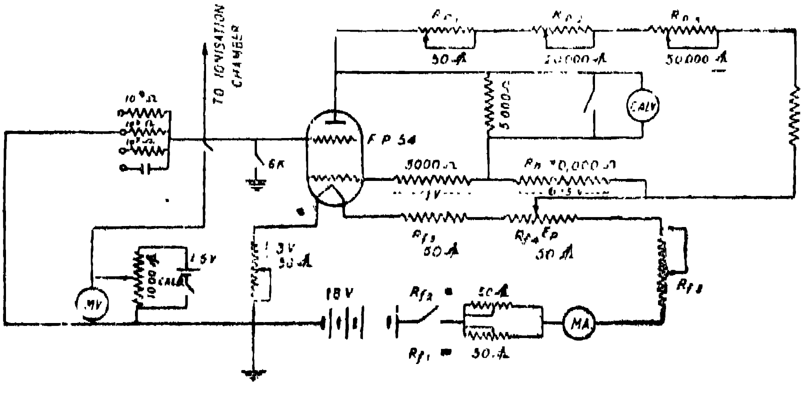

F. P. 54 - PLIOTRON AMPLIFIER CIRCUIT

FIG. 1

THE ESTIMATION OF RADIUM IN THE MINERAL THORIANITE OF CEYLON

The mineral under investigation was sent by Dr. Wadia on behalf of the Government of Ceylon for the estimation of radium-content in the mineral. A particular sample of the Ceylon Thorianite has been chemically analysed as early as about 1910 by Soddy (1910) and as referred by him, the sample contains 60 to 70% of ThO_2 and from 10 to 20% of U_3O_8. The mineral will therefore contain both radium and its isotope mesothorium 1. From this chemical analysis, the approximate amount of radium and mesothorium 1 present can be theoretically obtained from the consideration of radio-active equilibrium. As it is interesting to compare the theoretical amount with that estimated by physical process, we have calculated the theoretical amount as shown below. When a radio-active element is in equilibrium with its product elements then from the law of radio-active disintegration it follows that

$$(N_1\lambda_1)^{\overline{U}} = (N_2\lambda_2)_{Ra} \qquad \ldots \quad (1)$$

$$(N_1\lambda_1)_{Th} = (N_2\lambda_2)_{MsTh_1} \qquad \ldots \quad (2)$$

where N_1 represents the number of uranium and thorium atoms present in the respective cases and N_2 that of radium and mesothorium 1 atoms present in equilibrium, λ's represent the decay constant of the respective element.

Let us first calculate the radium-content per gm. of the mineral. It is experimentally known that $\lambda_U = 4.9 \times 10^{-18}$ sec^{-1}, $\lambda_{Ra} = 1.373 \times 10^{-11}$ sec^{-1}; and atomic wt. of U = 238 and of Ra = 226. If the percentage of U_3O_8 present be assumed to be 15%, the mean value of the chemical analysis, then 1 gm. of the mineral will contain $\frac{3 \times 714}{20 \times 842}$ gms. of U. Since 238 gms. of uranium contain 6.06×10^{23} atoms (Avogadro number) therefore 1 gm. of the mineral will contain $\frac{3 \times 714 \times 6.06 \times 10^{23}}{20 \times 842 \times 238}$ atoms of U. Therefore if there are N_{Ra} atoms of radium in equilibrium then from (1) it follows that

$$\frac{3 \times 714 \times 6.06 \times 10^{23}}{20 \times 842 \times 238} \times 4.9 \times 10^{-18} = N_{Ra} \times 1.37 \times 10^{-11}$$

$$\therefore \quad N_{Ra} = \frac{3 \times 714 \times 6.06 \times 4.9}{20 \times 842 \times 238 \times 1.37} \times 10^{16} \text{ atoms.}$$

Again 226 gm. of radium contain $(6.06) \times 10^{23}$ atoms therefore the wt. of N_{Ra} atoms of radium is

$$\frac{3 \times 714 \times 6.06 \times 4.9 \times 226 \times 10^{16}}{20 \times 842 \times 238 \times 1.37 \times 6.06 \times 10^{23}} = 4.32 \times 10^{-8} \text{ gms.}$$

$\therefore$ One gm. of the mineral contains about 4.32×10^{-8} gms. of radium.

Similarly if the percentage of ThO_2 is 70, then from the experimental value of $\lambda_{Th} = 1.33 \times 10^{-18}$ sec^{-1}, $\lambda_{MsTh_1} = 3.28 \times 10^{-9}$ sec^{-1} and the atomic wt. of thorium and mesothorium are 232 and 228 respectively, it follows that 1 gm. of the mineral contain $\frac{228 \times 70 \times 1.33 \times 10^{-11}}{264.4 \times 3.28} = 2.45 \times 10^{-10}$ gms. of MsThI.

From this calculation it follows that although the percentage of ThO_2 is much higher than that of U_3O_8 still the equilibrium amount of mesothorium 1 is much smaller, almost negligible in comparison with that of radium. This is however due to the fact that the half life of MsThI is much shorter than that of radium.

EXPERIMENTAL PROCEDURE

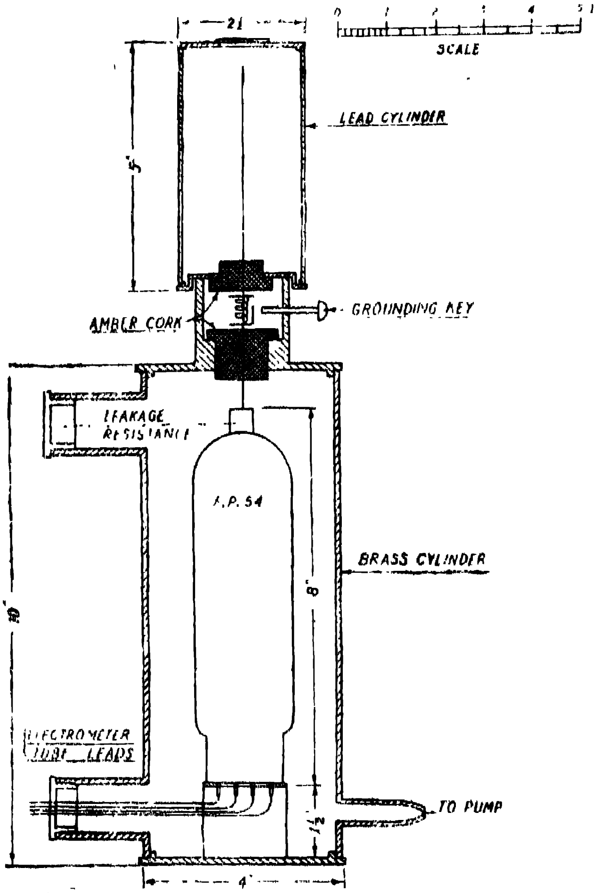

FIG. 2

The radium-content of the mineral has been estimated by the well-known γ-ray method of estimation. An ionisation chamber together with the pliotron amplifier described above has been used to compare the ionisation current due to γ-rays of a certain weight of the mineral with that of a standard γ-ray source, under exactly similar conditions. The ionisation chamber constructed is a lead cylinder about 5″ long and of internal diameter about 2″. The thickness of the wall is 1 cm. The collecting electrode is a brass wire of diameter about 1/16″, and insulated from the wall by an amber cork. About 250 volts between the wall and the central electrode was found sufficient to produce saturation current due to ionisation. The collecting electrode was connected with the grid of the pliotron tube and the mounting was done as shown in the Fig. 2. The standard sample used is 0.47 milligram of radium in the form of radium bromide. The ionisation current was compared by comparing the deflection in the galvanometer scale. The approximate linearity of the deflection was tested by taking the standard source at different distances from the ionisation chamber.

EXPERIMENTAL DATA

The mean deflection for 0.47 milligram of radium 255 mm.

,, ,, 217 gms. of thorianite 7 mm.

Radium content of per gm of the mineral $= \dfrac{47 \times 7 \times 10^{-8}}{250 \times 217} = 5.94 \times 10^{-8}$ gm.

As the mineral was spread in a thin layer of about $\frac{1}{2}$ cm. the correction due to self-absorption was small and therefore neglected.

From this experimental estimation it follows that the radium-content per gm. of the mineral of this sample is appreciably greater than that obtained theoretically from Soddy's chemical analysis assuming the percentage of U_3O_8 to be 15%. The percentage of U_3O_8 appears to be 20.63% which is very near to that of the upper limit of Soddy's estimation.

When this work was undertaken it was also the idea to estimate the age of formation of the rock. As already stated the age can be easily calculated from the well-known method of lead-uranium ratio. When radium is estimated by γ-ray method, the amount of uranium present can be calculated by the consideration of radio-active equilibrium. But for the estimation of lead, a chemical analysis of the sample is necessary. Moreover the lead present in the mineral is generally a mixture of different isotopes of lead produced by the decay of uranium, thorium, and actinium and probably some trace of ordinary lead. Therefore a mass-spectrographic analysis of the lead is necessary to ascertain the percentage of uranium or any other type of lead. For all these difficulties the work could not be proceeded further.

In conclusion I express my thanks to Professor M. N. Saha, F.R.S., for his kind guidance to complete this work. My thanks are particularly due to Dr. Wadia, Mineralogist to the Government of Ceylon for kindly supplying the mineral Thorianite and permitting me to publish the radium estimation of the sample with this apparatus. My thanks are also due to Dr. B. D. Nag Choudhury and Dr. S. C. Sirkar for many helpful suggestions. I also acknowledge my thanks to Dr. D. M. Bose, Director, Bose Research Institute, Calcutta, for kindly permitting me to complete the work.

REFERENCES

Dubridge and Brown, 1933, *R. S. I.*, **4**, 532.

Evans, 1940, *J. App. Phy.*, **12**, 297.

Metcalf and Thompson, 1930, *Phys. Rev.*, **36**, 1489.

,, 1941, *Phys. Rev*, **60**, 112.

Soddy, *Chemistry of Radio Element*, p. 94.

ON SARGENT CURVES FOR ARTIFICIALLY β-ACTIVE NUCLEI*

By P. K. SEN CHAUDHURY

(Received for publication, Sept. 7, 1943)

ABSTRACT. Sargent curves of all the known artificially made β-active nuclei together with naturally β-active nuclei have been drawn. From this Sargent plot attempt has been made to deduce the approximate spin of some nuclei of even mass-number. Further the utility of such a plot, in the study of nuclear phenomena such as nuclear isomerism which depends on spin change of the nuclei, has been pointed out.

Sargent (1933) plotted log λ against log E_{max} of all the naturally β-active nuclei and found that the points lie approximately on two lines separated by a distance of about two units on the logarithmic scale along the log λ axis. λ represents the decay constant of the nuclei and E represents the maximum energy of the emitted β-rays. Fermi's (1934) theory of β-decay provided a theoretical explanation of this experimental fact showing that the total probability of β-emission of a nucleus, *i.e.*, λ is dependent on the maximum energy of the emitted β-rays. Fermi's theory further showed that the transition probability of β-emission by the process $n \rightarrow P + \beta +$ neutrino, is dependent on the change of angular momentum or in other words spin-change say Δi of the nucleus. The probability of β-emission vanishes for all value of Δi except $\Delta i = 0$. The first Sargent curve corresponding to $\Delta i = 0$ was therefore called the allowed line. Later on it was shown that for Δi other than zero the β-emission is not completely forbidden, only the transitional probability is reduced by a factor about $(1/100)^{\Delta i}$ approximately which explains the separation of the two Sargent curves. The second line was therefore termed as the first forbidden line. Gamow and Teller (1936) considering the possibility of inversion of heavy nuclei during β-transition modified Fermi's selection rule of β-decay. According to them the permitted transitions are those for which $\Delta i = 0$. or $\Delta i = 1$.

Subsequently a few artificially made β-active nuclei were plotted by Diebner and Grassmann (1938) and found to approximately fit the Sargent curves.

As stated above according to the selection rules of β-decay, the Sargent curves provide a quick method to visualise the approximate spin change of the nuclei in β-transition. I have therefore drawn the Sargent plot with all the natural and artificial β-active nuclei known up to the date as shown in the figure. The latest and the corrected value of half lives are collected from various journals and publications. All these are represented in Table I together with the spin-change Δi in β-transition as observed from the Sargent plot. Most of these data and the reference will be found in the Table published by Livingwood and Seaborg (1940) in Review of Modern Physics, Volume XII, 1940.

---

* Communicated by the Indian Physical Society.

Following Gamow I have drawn three straight lines separated from each

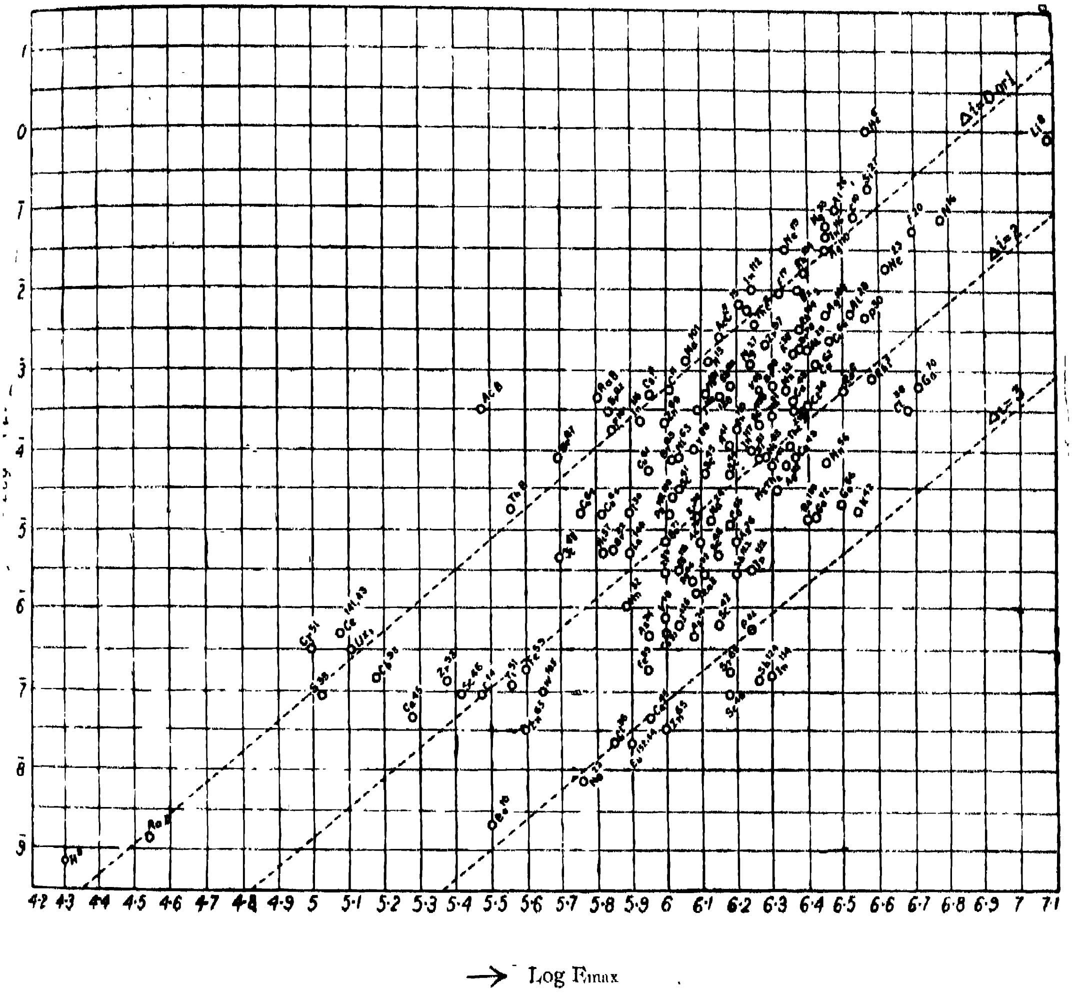

other by two logarithmic units. However it must be remembered that the two lines obtained by Sargent with naturally β-active nuclei are not exactly st. lines. Further there is also considerable controversy over the positions of the forbidden lines as yet there is no satisfactory theoretical treatment of forbidden β-emission. However the first two lines are definitely proved by experimental data of naturally β-active nuclei. As Gamow and Teller selection rule of β-decay has been found to be more true than that of Fermi, it is assumed that the first line corresponds to $\Delta i = 0$ or $\Delta i = 1$, the second line corresponds to $\Delta i = 2$ and so on. The most of the nuclei will be found to fall in the region occupied by the first and second line and some nuclei with Δi higher than two about the third line. It may be observed that the nuclei do not fall on three distinct lines. This may be partly due to the fact that the maximum energy of β-rays as determined mostly by absorption method is only approximately correct.

An important experimental fact is that nuclei having even mass number and even atomic number have the nuclear spin zero. This atonce suggests that for β-active nuclei of even mass number, Sargent plot shows not only the spin change Δi of the nuclei but also the actual spin of either the initial or the product nuclei. For a β-emission only increase or decrease the atomic number of the nuclei by one, but the mass number remains unchanged. Therefore if the radio-active nuclei be of even mass-number but of odd atomic number, then by β-emission the atomic number also becomes even and since the spin of nuclei having even mass-number and even atomic number is zero hence Δi gives the actual spin of the β-active nuclei. Similarly if the β-active nuclei be of even mass-number and even atomic number, its spin is initially zero and therefore gives the spin of the product nuclei which are of even mass-number but of odd atomic number. In this way as deduced from Sargent plot, the spin of some nuclei of comparatively heavy atomic number is shown in the Table II. The rest may be found out from the Table I.

TABLE I

Nuclei	T	λ	log λ	$E_{max} \times 10^{-6}$ e.V.	log E_{max}	Δi	Type
${}_{1}H^{3}$	31 y	$.71 \times 10^{9}$	$\overline{10}.8513$	.02	$\bar{4}.301$	0 or 1	
${}_{2}He^{6}$	.8 sec.	.995	$\bar{1}.998$	3.7	6 568	0 or 1	$\beta^{\cdot}$
${}_{3}Li^{8}$	.88 sec.	.789	$\bar{1}.897$	12	7.079	0 or 1 or 2	
${}_{4}Be^{10}$	10 yrs.	$.22 \times 10^{-8}$	$\bar{9}.3424$	.3	5.4771	3	β
${}_{5}B^{9}$	1 m.	$.115 \times 10^{-1}$	2.061				β^+
${}_{5}B_{12}$	02 s.	$.346 \times 10^{2}$	1 539	12	7.079	0 or 1	β^-
${}_{6}C^{11}$	21	$.55 \times 10^{-3}$	4.710	1.03	6.013	0 or 1	β^+
${}_{6}C^{14}$	89 days	$.897 \times 10^{-7}$	$\bar{8}.953$	.3	5.477	2	β^-
${}_{6}C^{10}$	8.8 sec.	$.79 \times 10^{-1}$	$\bar{2}.897$	3.36	6.526	0 or 1	β^+
${}_{7}N^{13}$	9.4 ms.	$.123 \times 10^{2}$	$\bar{3}.0899$	1.2	6.0792	0 or 1	β^+
${}_{7}N^{16}$	8.4 sec.	$.825 \times 10^{-1}$	2.916	6	6 778	0 or 1	β^-
${}_{8}O^{15}$	2.1 ms.	$.55 \times 10^{2}$	$\bar{3}.740$	1.7	6.230	0 or 1	β^+
${}_{8}O^{19}$	31 s.	$.224 \times 10^{-1}$	2 350				β^-
${}_{9}F^{17}$	74 s.	$.94 \times 10^{2}$	$\bar{3}.973$	2.1	6.322	0 or 1	β^+
${}_{9}F^{20}$	12	$.578 \times 10^{1}$	2.762	5	6.699	0 or 1	β^-
${}_{10}Ne^{19}$	20.3 s.	$.343 \times 10^{-1}$	$\bar{2}.535$	2.2	6.342	0 or 1	$\beta^{\cdot}$
${}_{11}Na^{22}$	3 y.	$.738 \times 10^{-9}$	$\bar{9}.868$	.58	5.76	3	β^+
${}_{11}Na^{24}$	15 h.	$.129 \times 10^{4}$	$\bar{5}.111$	1.36	6.133	2	β^-

TABLE I (*contd.*)

Nuclei	T	λ	log λ	$E_{max} \times 10^{-6}$ e.v.	log E_{max}	Δi	Type
${}_{12}Mg^{23}$	11.6 s.	$.6 \times 10^{-1}$	2.778	2.82	6.450	0 or 1	β^+
${}_{12}Mg^{24}$	10 m.	$.116 \times 10^{-2}$	3.065	1 74	6.240	0 or 1	β^-
${}_{13}Al^{24}$	20 ms.	$.578 \times 10^{-3}$	$\bar{4}.762$				
${}_{13}Al^{26}$	7	$.991 \times 10^{-1}$	$\bar{2}.996$	2.99	6.476	0 or 1	β^+
${}_{13}Al^{28}$	2.4 ms.	$.482 \times 10^{-2}$	$\bar{3}.683$	3 3	6.518	0 or 1 or 2	
${}_{13}Al^{29}$	6.7 ms.	$.173 \times 10^{-2}$	3.238	2.5	6.398	,,	β
${}_{14}Si^{31}$	2.5 h.	$.77 \times 10^{-4}$	$\bar{5}.886$	1.8	6.255	2	β
${}_{15}P^{30}$	2.6 ms.	$.445 \times 10^{-2}$	$\bar{3}$ 648	3.6	6.556	,,	β^+
${}_{15}P^{32}$	14.3 d.	$.5584 \times 10^{-6}$	$\bar{7}.7469$	1.69	6.2279	3	β
${}_{16}S^{31}$	26 ms.	$.44 \times 10^{-3}$	4.6435				β^+
${}_{16}S^{35}$	88 ds.	$.91 \times 10^{-7}$	$\bar{8}.9590$	.107	5.0294	0 or 1	β^-
${}_{17}Cl^{33}$	2.8 sec.	.25	$\bar{1}.3979$				β^+
${}_{17}Cl^{34}$	33 m.	$.34 \times 10^{-3}$	4.5315	2.5	6.3979	2	β^+
${}_{17}Cl^{36}$	1 yr.	$.22 \times 10^{-7}$	8.3424	.7	5.8451	3	β^-
${}_{17}Cl^{38}$	37 m.	$.31 \times 10^{-3}$	4 4914	4.8	6.6812	2 or 3	β
${}_{18}A^{41}$	1.8 h.	$.11 \times 10^{-3}$	4 0414	1.5	6.1761	2	β^-
${}_{18}A^{35}$	1.91 sec.	.36	$\bar{1}$ 5563				β^+
${}_{19}K^{38}$	7.7 ms.	$.15 \times 10^{-2}$	3.1761	2.3	6.3617	0 or 1 or 2	β^+
${}_{19}K^{42}$	12.5 h.	$.15 \times 10^{-4}$	$\bar{5}.1761$	3.5	6 5441	3	β^-
${}_{20}Ca^{45}$	180 ds.	$.44 \times 10^{-7}$	$\bar{8}.6435$	.19 .91	5.2788 5.0596	2 or 3	β^-
${}_{20}Ca^{49}$	2.5 h. 30 ms	$.77 \times 10^{-4}$	$\bar{5}.8865$	2.3	6.3617	2	β^-
${}_{21}Sc^{42}$	13.4 d.	$.59 \times 10^{-6}$	$\bar{7}.7704$	1.4	6.1461	3	β^+
${}_{21}Sc^{43}$	4 h.	$.48 \times 10^{-4}$	5.6812	1.3	6 1139	2	β^+
${}_{21}Sc^{44}$	4.1 h.	$.47 \times 10^{-4}$	5.6721	1.5	6.1761	2	β^-
${}_{21}Sc^{46}$	85 d.	$.94 \times 10^{-7}$	8 9731	.26 1 5	5 4150 6.1761	2 or 3	β
${}_{21}Sc^{48}$	63 h.			1.1			
${}_{21}Sc^{48}$	44 h.	$.44 \times 10^{-5}$	6.6435	1.4 .5	6.1461 5.6990	2	β
${}_{21}Sc^{49}$	57 ms.	$.2 \times 10^{-3}$	$\bar{4}.3010$	1.8	6.2553	2	β^-
${}_{22}Ti^{51}$	72 d. 2.9 m.	$.11 \times 10^{-6}$	$\bar{7}.0414$	.36	5.5563	2	β^-

TABLE I (*contd.*)

Nuclei	T	λ	log λ	$E_{max} \times 10^{6}$ e.v.	log E_{max}	Δi	Type
$_{23}V^{47}$	600 ds.	$.13 \times 10^{7}$	$\bar{8}.1130$				
$_{23}V^{48}$	10 d.	$.5 \times 10^{-6}$	7.9243	1	6.0000	2 or 3	β^{+}
$_{23}V^{49}$	33 m.	$.35 \times 10^{-3}$	$\bar{4}.5441$	1.9	6.2788	2	β^{+}
$_{24}Cr^{51}$	26.5 d.	$.3 \times 10^{-6}$	$\bar{7}.4771$	.1	5.000	0 or 1	β^{+}
$_{24}Cr^{55}$	2.27 h.	$.85 \times 10^{-4}$	5.9294				
$_{25}Mn^{51}$	46 m.	$.25 \times 10^{3}$	4.3979	2	6.3010	2	β^{-}
$_{25}Mn^{52}$	21.3 m.	54×10^{-3}	$\bar{4}.7324$	2.2	6.3424	2	β^{+}
	7.4 d.	$.11 \times 10^{6}$	6.0414	.77	5.8865	2	β^{+}
$_{25}Mn^{56}$	2.6 h.	$.74 \times 10^{-4}$	$\bar{5}.8692$	2.8	6.4472	2	β
$_{56}Fe^{59}$	47 d.	$.17 \times 10^{-6}$	$\bar{7}.2304$	.4 .9	5.6021 5.9542	2 3	β^{-}
$_{27}Co^{55}$	18h	$.11 \times 10^{-4}$	$\bar{5}.0414$	1.5	6.1761	2	β^{+}
$_{27}Co^{59}$	70d	$.11 \times 10^{-6}$	$\bar{7}.0414$				
$_{28}Ni^{57}$	36h	$.53 \times 10^{5}$	$\bar{6}.7243$	.67	5.8261	2	β^{+}
$_{28}Ni^{63}$	2.6h	$.77 \times 10^{-4}$	$\bar{5}.8865$	1.9	6.2788	2	β^{-}
$_{29}Cu^{61}$	3.4h	$.57 \times 10^{-4}$	5.7559	.9	5.9542	0 or 1	β^{+}
$_{29}Cu^{62}$	10.5m	$.11 \times 10^{-2}$	$\bar{3}.0414$	2.6	6.4150	2	β^{+}
$_{29}Cu^{64}$	12.8 h	$.15 \times 10^{-4}$	$\bar{5}.1761$	.66 .58	5.8195 5.7634	0 or 1 or 2	β^{+} β^{-}
$_{29}Cu^{66}$	5m	$.23 \times 10^{-2}$	$\bar{3}.3617$	2.9	6.4624	2	β^{-}
$_{30}Zn^{63}$	38m	$.30 \times 10^{-3}$	$\bar{4}.4771$	2.3	6.3617	2	β^{+}
$_{30}Zn^{65}$	250d	$.32 \times 10^{-7}$	$\bar{8}.5058$	.4	5.6021	2 or 3	β^{+}
$_{30}Zn^{69}$	57ms	$.2 \times 10^{3}$	$\bar{4}.3010$	1.0	6.000	0 or 1	β^{-}
$_{31}Ga^{66}$	9.4h	$.2 \times 10^{4}$	$\bar{5}.3010$	3.1	6.4914	3	β^{+}
$_{31}Ga^{70}$	20m	$.57 \times 10^{8}$	$\bar{4}.7559$	5	6.6990	2 or 3	β^{-}
$_{31}Ga^{72}$	14h	$.14 \times 10^{-4}$	$\bar{5}.1461$	2.6	6.4150	3	β^{-}
$_{33}As^{74}$	17d	$.47 \times 10^{-6}$	$\bar{7}.6721$	1.2 0.9	6.0792 5.9542	3	β^{-} β^{+}
$_{33}As^{76}$	26.8h	$.72 \times 10^{-5}$	$\bar{6}.8573$				
$_{34}Se^{79 \cdot 81}$	19m	$.61 \times 10^{-3}$	$\bar{4}.7853$	1.5	6.1761	0 or 1	β
$_{35}Br^{78}$	6.4m	$.18 \times 10^{-2}$	$\bar{3}.2553$	2.3	6.3617	0 or 1 or 2	β^{+}
$_{35}Br^{80}$	18m	$.64 \times 10^{-3}$	$\bar{4}.8062$	2.0	6.3010	2	β^{-}
$_{35}Br^{82}$	34h	$.58 \times 10^{-5}$	$\bar{6}.7634$	.7	5.8451	2	β

TABLE I (*contd.*)

Nuclei	T	λ	log λ	$E_{max} \times 10^{-6}$ e.v.	log E_{max}	Δi	Type
$_{35}Br^{83}$	2.3h	$.83 \times 10^{-4}$	$\bar{5}.9191$	1.05	6.0212	0 or 1 or 2	β^-
$_{37}Rb$	17m	$.68 \times 10^{-3}$	$\bar{4}.8325$				β^-
$_{37}Rb$	15.4m	$.75 \times 10^{-3}$	4.8751	3.8	6.5798	2	β^-
$_{37}Rb$	17.8m	$.61 \times 10^{-3}$	$\bar{4}.7853$	4.6	6.6628	2	β
$_{38}Sr^{87}$	2.5h	$.77 \times 10^{-4}$	$\bar{5}.8865$	.5	5.6990	0 or 1	β^-
$_{38}Sr^{89}$	55d	$.15 \times 10^{-6}$	$\bar{7}.1761$	1.5	6.1761	3	β^-
$_{39}Y^{88}$	2h	$.96 \times 10^{-4}$	5.9823	1.2	6.0792	0 or 1 or 2	β^+
$_{39}Y^{92}$	70h	$.27 \times 10^{-5}$	$\bar{6}.4314$	1.3	6.1139	2	β^-
$_{40}Zr^{89}$	70h	$.27 \times 10^{-5}$	$\bar{6}.4314$	1	6.0	2	β^+
$_{40}Zr^{93}$	63d	$.127 \times 10^{-7}$	$\bar{7}.1038$	.25	5.3979	2	β^-
$_{40}Zr^{95}$	17h	$.113 \times 10^{-4}$	$\bar{5}.0531$	1.25	6.0969	2	β^-
$_{41}Cb^{92}$	11d	7.26×10^{-7}	$\bar{7}.8609$	1.0	6.000	3	β
$_{41}Cb^{93}$	55d	$.145 \times 10^{-6}$	$\bar{7}.1614$	.15	5.1761	0 or 1	β
$_{42}Mo^{91}$	17m	6.76×10^{-4}	4.8299	1.85	6.2672	0 or 1 or 2	β^+
$_{42}Mo^{101}$	24m	$.493 \times 10^{-3}$	$\bar{4}.6928$	1.3	6.1139	0 or 1	β
$_{43}Ma^{101}$	9m	$.128 \times 10^{-2}$	$\bar{3}.1072$	1.16	6.0645	0 or 1	β
$_{45}Rh^{104}$	4.3m	$.267 \times 10^{-2}$	$\bar{3}.4265$	2.3	6.36	0 or 1	β^-
	42s	$.164 \times 10^{-1}$	$\bar{2}.2156$	2.3	6.36	0 or 1	
$_{47}Ag^{106}$	24.5m	$.469 \times 10^{-3}$	$\bar{4}.6712$	2.0	6.3010	2	β^+
$_{47}Ag^{108}$	2.3m	$.5 \times 10^{-2}$	$\bar{3}.6990$	2.8	6.4472	0 or 1	β^-
$_{47}Ag^{110}$	22s	$.314 \times 10^{-1}$	$\bar{2}.4969$	2.8	6.4472	0 or 1	β^-
$_{47}Ag^{112}$	3.2h	$.6 \times 10^{-4}$	$\bar{5}.7782$	2.2	6.3424	2	β^-
$_{48}Cd^{115}$	2.5d	$.329 \times 10^{-5}$	6.5172	1.11	6.0453	2	β
$_{49}In^{110}$	65m	$.177 \times 10^{-3}$	$\bar{4}.2480$	1.6	6.2041	2	β^+
$_{49}In^{113}$	2.7d	$.3 \times 10^{-5}$	$\bar{6}.4771$	1.73	6.2380	3	β^-
$_{49}In^{114}$	48d	$.168 \times 10^{-6}$	$\bar{7}.2253$	1.98	6.2967	3	β^-
$_{49}In^{116}$	54ms	$.213 \times 10^{-3}$	$\bar{4}.3284$	.85	5.9294	0 or 1	β
$_{49}In^{117}$	117m	$.983 \times 10^{-4}$	$\bar{5}.9926$	1.73	6.2380	2	β^-
$_{51}Sb^{120}$	17m	$.676 \times 10^{-3}$	$\bar{4}.8299$	1.53	6.1847	0 or 1	β^+
$_{51}Sb^{122}$	2.8d	$.285 \times 10^{-5}$	$\bar{6}.4548$	1.6	6.2041	3	β^-
$_{51}Sb^{124}$	60d	$.133 \times 10^{-6}$	$\bar{7}.1239$	1.8	6.2553	3	β^-

TABLE I (*contd.*)

Nuclei	T	λ	log λ	$E_{max} \times 10^{-6}$ e.V	log E_{max}	Δ*i*	Type
$_{53}I^{126}$	13d	$.616 \times 10^{-6}$	7.7896	1.1	6.0414	3	β^-
$_{53}I^{128}$	25ms	$4\ 6 \times 10^{-4}$	$\bar{4}.6628$	1.2, 2.1	6 0792 6.322	0 or 1 or 2	β
$_{53}I^{130}$	12.6h	1.52×10^{-5}	5 1818	.83	5.9191	2	β^-
$_{57}La^{140}$	31h	$.595 \times 10^{-5}$	$\bar{6}.7745$	.8	5.9031	2	β
$_{58}Ce^{141,43}$	15d	$.53 \times 10^{-6}$	$\bar{7}.7243$	.12	5.0792	0 or 1	β
$_{63}Eu^{152,54}$	1yr	$.219 \times 10^{-7}$	8.3404				β
$_{66}Dy^{165}$	2.5h	$.767 \times 10^{-4}$	$\bar{5}.8848$	1.9	6.2788	2	β^-
Ho^{166}	30h	$.6 \times 10^{-5}$	$\bar{6}.8062$	1.6	6.2041	2 or 3	
$_{74}W^{185}$	77 days	$.104 \times 10^{-6}$	7.0170	.45	5.6532	2	
$_{75}Re^{186}$	90 h	$.213 \times 10^{-5}$	$\bar{6}.3384$	1.2	6.0792	2 or 3	β
$_{75}Re^{188}$	18 h	1064×10^{-4}	$\bar{5}.0271$	2.5	6.3979	3	
$_{90}UX_1^{234}$	24.5d	$.3275 \times 10^{-6}$	$\bar{7}.5152$	0.13	5 1139	0 or 1	β
$_{91}UX_{II}^{234}$	1.14m	$.1013 \times 10^{-1}$	2.0055	2.32	6.3655	0 or 1	"
$_{91}UZ^{234}$	6.7h	$.287 \times 10^{-4}$	$\bar{5}.4579$	.6			"
$_{82}RaB^{214}$	26.8m	$.431 \times 10^{-3}$	$\bar{4}.6345$	0.65	5.8129	0 or 1	"
$_{83}RaC^{214}$		$.592 \times 10^{-3}$	$\bar{4}.7723$	3.15	6.4983	2	"
$_{81}RaC''^{210}$	1.32m	$.875 \times 10^{-2}$	$\bar{3}.9420$				
$_{82}RaD^{210}$	2.5y	$.137 \times 10^{-8}$	$\bar{9}.1367$	.035	4.5441	0 or 1	"
$_{83}RaE^{210}$	5.0d	$.16 \times 10^{-5}$	$\bar{6}.2041$	1.22	6.0864	2 or 3	"
$_{88}MsTh_1^{228}$	6.7y	$.328 \times 10^{-8}$	$\bar{9}.5159$				
$_{89}MsTh_2^{228}$	6.13h	$.314 \times 10^{-4}$	$\bar{5}.4960$	2.05	6.3118	2	
$_{82}ThB^{212}$	10.6h	$.182 \times 10^{-4}$	$\bar{5}.2501$	.36	5.5563	0 or 1	"
$_{83}ThC^{212}$		$.123 \times 10^{-3}$	$\bar{4}.0899$	2.25	6.3522	2	
$_{81}ThC''^{208}$	3.20m	$.361 \times 10^{-2}$	$\bar{3}.5575$	1.79	6.2529	0 or 1	
$_{89}Ac^{227}$	13.4y	$.164 \times 10^{-8}$	$\bar{9}.2148$				
$_{82}AcB^{211}$	36.0m	$.321 \times 10^{-3}$	4.5065	.30	5.4771		
$_{83}AcC^{211}$		$.16 \times 10^{-4}$	$\bar{5}.2041$				
$_{81}AcC''^{207}$	4.76m	$.243 \times 10^{-2}$	$\bar{3}.3856$	1.4	6.1461	0 or 2	

Naturally Radio-active nuclei

TABLE II

Nuclei	Spin	Nuclei	Spin	Nuclei	Spin
$_{21}Sc^{42}$	3	$_{35}Br^{80}$	2	$_{49}In^{112}$	3
$_{21}Sc^{44}$	2	$_{35}Br^{82}$	2	$_{49}In^{114}$	3
$_{21}Sc^{48}$	2	$_{41}Cb^{92}$	3	$_{49}In^{116}$	0 or 1
$_{25}Mn^{52}$	2	$_{47}Ag^{106}$	2	$_{51}Sb^{120}$	0 or 1
$_{25}Mn^{56}$	2	$_{47}Ag^{108}$	0 or 1	$_{51}Sb^{122}$	3
$_{29}Cu^{66}$	2	$_{47}Ag^{110}$	0 or 1	$_{51}Sb^{124}$	3
$_{31}Ga^{66}$	3	$_{47}Ag^{112}$	2	$_{53}I^{126}$	3
$_{31}Ga^{72}$	3	$_{49}In^{110}$	2	$_{57}La^{140}$	2

TABLE III

Isomers in Sargent Curve

Nuclei	T	Emax of β ray in M.e.v.	γ-ray if emitted and Emax in M.e v	ΔI	Reference
Ca^{49}	2.5 h 30 ms	2.3 not known	.8 not known	2	Livingwood & Seaborg (1940). ,,
Rh^{104}	4.3 ms 42 s	2.3 2.3	e.055 and .08 not known	0 or 2 0 or 1	
Ti^{51}	72 d 2,8 ms	36	1.1 energy not known	2	Walke etal (1939). Walke (1937).
Mn^{52}	21.3 ms	2.2	1.2	2	Livingwood, Seaborg (1938) and Hemendinger (1939).
	7.4 d	.77	1	2	,,
Ux_2	1.14 ms	2.32	not known	0 or 1	
Uz	6.7 h	.6	,,		
Br^{82}	34 h 40 m	.7 not known	.65 not known	2	Snell (1937) and Buck (1938). Doddson and Fowler (1939).
Y^{92}	70 h 3 h	1.3 2	not known ,,	2	
In^{112}	72 s 2.7 d	not known 1.73	,, .17 and .25	3	Lawson and Cork (1937). Barnes (1939).
In^{116}	13 s	2,8	not known		Amaldi etal (1935). Cork and Lawson (1939).
	54 ms	.85	1 8 and 1 3	0 or 1	Amaldi etal and Cork and Lawson (1937).
Br^{80}	18 ms	2		2	Snell (1937). Alichanian etal (1936).
	4.4 h		$\bar{e}$		Buck (1938).
Zn^{69}	57 m 13.8 h	1.0	not known .47	0 or 1	Livingwood & Seaborg (1939). ,,

Again the Sargent plot of nuclei may be of considerable importance in the study of nuclear isomers. For according to Weizacker's (1936) theory of nuclear isomerism the initial difference in spin of the ground state and an excited metastable state is the cause of nuclear isomerism. Therefore if the spin-change Δi of the pair in β-transition is known from Sargent plot then it may give some information about the subsequent mode of decay as suggested by Hebb and Uhlenbeck (1938). In the Table III, I have collected the isomers whose existence is now well established. The value of Δi for the isomers of which decay constant and the maximum energy of the emitted β-ray is known, is also shown in the Table. As an example the isomeric pair Rh^{104} may be considered. It will be observed from the Sargent plot that Δi for both of the pair is the same and $=0$ or 1. Therefore if initially the two nuclei have large difference of spin then this large difference persists even after β-emission. Therefore if one of the pair transforms into ground state, the other will be in an excited state even after emission. According to Hebb and Uhlenbeck this excited state is destroyed by the emission of γ-rays in steps. These γ-rays again give rise to soft conversion electrons. Probability of conversion is particularly high when the difference of spin between the ground state and the excited state is high. As a matter of fact large groups of conversion electrons have been experimentally observed with Rh^{104}.

In conclusion I express my thanks to Professor M. N. Saha, F.R.S., for his interest and encouragement in the initial stage of this work. My grateful thanks are due to various workers whose experimental data I have taken. My thanks are due to Dr. D. M. Bose, Director, Bose Research Institute, for kindly permitting me to complete the work here. My thanks are also due to Dr. S. C. Sirkar for many helpful suggestions.

BOSE RESEARCH INSTITUTE,
CALCUTTA

REFERENCES

Alichianin, 1936, *Phys. Zeits.*
Barnes, 1939, *Phys. Rev.*, **56**, 414.
Cork and Lawson, 1919, *Phys. Rev.*, **56**, 291.
" " " 1937, *Phys. Rev.*, **52**, 531.
Diebner and Grassmann, 1938, *Phys. Zeits.*, **39**, 499.
Doddson and Fowler, 1939, *Phys. Rev.*, **55**, 880.
Fermi, 1934, *Z. f. Phys.*, **88**, 161.
Hebb and Uhlenbeck, 1933, *Physica*, **5**, 605.
Lawson and Cork, 1937, *Phys. Rev.*, **62**, 531.
Livingwood and Seaborg, 1940, *Rev. Mod. Phys.*, **12**, 35.
" " " 1938, *Phys. Rev.*, **54**, 391.
" " " 1939, *Phys. Rev.*, **55**, 457.
Sargent, 1933, *Proc. Roy. Soc. A.*, **139**, 659.
Snell, 1937, *Phys. Rev.*, **52**, 1007.
Walke, 1937, *Phys. Rev*, **52**, 777.
Amaldi etal, 1935, *Proc. Roy. Soc. A.*, **149**, 522.
Buck, 1938, *Phys. Rev.*, **54**, 1025.
Gamow and Teller, 1936, *Phys. Rev.*, **49**, 895.
Hemmendinger, 1939, *Phys. Rev.*, **55**, 604.
Walke, 1939, *Proc. Roy. Soc. A.*, **171**, 360.
Weizsacker, 1936, N. Wiss, **28**, 813.

STUDIES OF ELECTRICAL INTERFERENCE TO RADIO RECEPTION*

By S. C. MAJUMDAR, S. M. SEN

AND

S. R. KHASTGIR

(Received for publication, September 7, 1943)

ABSTRACT. Studies in electrical interference from three D.C.-operated electric fans and a motor were made in three frequency ranges : (1) 7 Mc./s-20 Mc./s, (2) 3 Mc./s- 6 Mc./s and (3) .65 Mc./s- 1.5 Mc./s. The studies can be classified as follows :

I. (*a*) Measurements of the r-f radiation field of the electric noise and the corresponding a-f output for different frequencies.

(*b*) Study of the effect of speed variation on these measurements.

It was found from these studies that, in general, the noise field decreased with the increase of frequency *but for some maxima*. The corresponding a-f output was found, in general, to increase with frequency *but for some maxima*. The maxima for the r-f noise field and the a-f output were not always at the same frequencies. The maxima in the noise field appeared to depend on the interfering source. The effect of speed variation was, in general, a decrease in the field with the decrease of speed. The variation of speed did not affect the positions of the maxima.

II. Determination of the resonance frequencies of the armature-sector coils of the different motors.

The experiments were carried out over a wide range of frequencies from .5 Mc./s to 22 Mc./s. The resonance frequencies were obtained and there appeared some correspondence between the resonance frequencies thus obtained and the frequencies corresponding to the observed maxima in the noise field. It was thus conjectured that the *quasi*- continuous type of the r-f noise components would have its maximum intensity in the region of the resonance frequencies as determined by the L-C-R values of the different armature-sector coils.

III. Some measurements of the ratio of the vertical and the horizontal components of the noise field.

IV. An oscillographic study of the r-f noise components :—Evidence was obtained of damped electromagnetic waves over a wide range of frequencies.

INTRODUCTION

Every radio listener knows that reception of signals is often seriously disturbed by electric fans, electric pumps, refrigerators, electric vacuum cleaners, lifts, electric tramways, trolley buses, motor car and air-craft systems, high frequency transmission systems and various other electrical installations. Some useful and important investigations have already been carried out on this subject of electrical interference. The pioneer work of Howe (1937) on radio interference from traction systems, the work of Curtis (1932) on electrical noise from motor cars and aeroplanes, Langton and Bradshaw's (1935) work on high voltage transmission lines, the investigations of Gill and Whitehead (1938) on electrical interference from trolly buses and electro-medical equipments, etc., are worthy of special reference. We should also mention the work of Morris (1934), Neale (1935), Warren (1935-36), Schumacher (1935) and the I.E.E. Council (1934) on the methods of eliminating electric noises and the legislatures concerning them.

---

* Communicated by the Indian Physical Society.

In India some amount of work was recently done by S. P. Chakravarty and N. L. Dutt (1941) at the Kanodia Electrical Communication Engineering Laboratories of the Department of Applied Physics in the University of Calcutta. In their work they investigated electrical interference from various sources, such as, D.C.-operated electric fans, pumps and refrigerators on a wide range of wavelengths (10m.- 550m.). Measurements were made of the r-f interfering voltage input to the receiver at some distance from the different noise sources. They also measured the ratio of the horizontally polarized to the vertically polarized components on various wavelengths for the different noise sources. The effect of speed variation of the motors was also studied. An analysis was also made of the power distribution in the audio-frequency bands resulting from the r-f signal from the different sources. In their work Chakravarty and Dutt employed a directional microphone connected to an amplifier system for the measurement of the audio-frequency output. The frequency distribution of the r-f interference voltage input to the receiver as investigated by these workers over a wide range of wavelengths revealed a number of maxima. The cause or causes of these maxima were not, however, explained and this remained a very intriguing and useful subject for investigation.

SCOPE OF THE PRESENT INVESTIGATION

In the present work a study of radio interference due to the radiation field from two D.C.-operated ceiling fans, a table fan and a D.C. motor, was undertaken. Measurements were made of the normal (vertical) radiation field and the corresponding a-f output voltage across an impedance due to electrical interference from the different noise sources in three specified ranges of broadcast frequencies—low, medium and high. Maxima were observed at specified frequencies. The effect of varying the speed of the motors on these measurements was studied. A reduction in speed appeared, in general, to reduce the interference effect, while the positions of the noise maxima in relation to frequency remained the same inspite of a considerable variation in speed. The ratio of the vertically polarized to the horizontally polarized fields was also determined for the three ranges.

The works of Howe on radio interference from traction systems strongly suggested that the maxima in the r-f interference field should be associated with the resonance frequency of the armature-sector circuit in the electric-motors. In a D.C.-operated motor, it is clear that the electrical interference is due to sparking between the brushes and the approaching or receding commutator. The 'reactance voltage' in the armature coil which is developed as a result of change of current in it, frequently causes sparks and the duration of the sparking is usually somewhat prolonged due to self-inductance of the coil. With the higher speed of the motor, the reactance voltage in the armature increases, resulting in sparking of greater intensity between the brushes and the commutator segments which approach towards or recede from one or the other of the two brushes. For a particular spark, it is evident, the frequency of the damped oscillations set up would depend not only on the inductance of the armature coil in one sector and its resistance and self-capacity but also on the resistance of the air-gap across which the spark takes place. This resistance may vary between wide limits, especially under irregular spark conditions. Thus it is expected that there would be a large number of frequency components, each being associated with a distinct spark having a definite air-gap resistance. It can also be conjectured that the frequency component having the maximum intensity should lie in the region of the resonance frequency of the armature-sector circuit. Work was therefore undertaken to determine the resonance frequency or frequencies of the armature-sector coil over a wide range of frequencies, well covering the ranges for which the noise measurements weie made. The resonance frequencies of the armature-sector coils for the different motors in the specified frequency ranges showed some correlation with the positions of the maxima observed in the noise field measurements.

That the interfering elements, from sources like the fan motors, really consist of damped waves of a very wide range of frequencies was shown from the oscillographic studies of the high frequency components as picked by a suitable L-C circuit and applied after suitable amplification to the oscillograph. The low frequency oscillograms of the periodically varying curient in the armatures of the different motors were also examined.

The make, type and other details of the fans and the motor employed in the investigation are given in Table I.

TABLE I

Interfering Source	Make	Type	Remarks
A. D.C. Ceiling fans	1. Osler		Volts : 220 V Amperes : .41 A
	2. G.E.C. (Malaya)		Volts : 220 V Amperes :--
B. D.C. Table fan	Sprague Electric Co., New York.	Lundell Motor Model 30030	Volts : 225 V Amperes : .4 A
C. D.C. Motor	Adair, Dutt & Co.	G.M. 5/6	Volts : 220 V Amperes . 65 A

THE NATURE OF THE ELECTRICAL NOISE FROM D.C.-MOTORS

As has already been explained a large number of damped waves having a wide range of frequencies is expected to radiate from the noise source in a D.C.-

motor. There is also experimental evidence to show that the motor can be regarded as a source of r-f energy giving a *quasi*—continuous spectrum. The receiving set picks up a very small part of this interference spectrum and gives an a-f output in the loudspeaker. The integrated field of the interference signal within the discrete band width containing noise components can then be written

$$E_{r.f.} = a_0 \cos(\omega t + \theta_0) + a_1 \cos[(\omega + p_1)t + \theta_1] + a_2 \cos[(\omega + p_2)t + \theta_2] + \dots a_n \cos[(\omega + p_n)t + \theta_n] \dots \qquad (1)$$

where $p_1/2\pi$, $p_2/2\pi$, $p_3/2\pi$ .. are frequency differences between the interfering voltage frequencies and the frequency $\omega/2\pi$ to which the receiver is tuned, $\theta_0, \theta_1, \theta_2$ .. are the epoch angles of the components of the interference spectrum relative to the component having the same frequency as that to which the receiver is tuned and $a_0, a_1, a_2,$ are the amplitude of the several components.

It is however permissible to assume that the amplitudes of the individual components a_0, a_1, a_2, a_3, etc., of the electrical noise within the usual acceptance band (20-30 kc's) of a good receiver are of practically the same value. The expression (1) may therefore be reduced to

$$E_{r.f.} = a \sum \cos[(\omega + p_n)t + \theta_n] \qquad (2)$$

The variation of the noise field in different frequency channels would evidently depend on the energy distribution in the r-f components emanating from the noise sources in the electric motor.

In our measurements the frame aerial was tuned so that the voltage V developed due to the interference signal across the tuning condenser would be proportional to $\{E.f^2/R\}$, where E is the noise field, f the frequency and R the H. F. resistance of the aerial. If we take $R \propto \sqrt{f}$, then $V \propto E.f^{\frac{3}{2}}$. It is thus evident that the nature of variation of the input voltage V with frequency f would necessarily be different from that of the variation of the noise field with frequency. In a superheterodyne set the a-f current output i can be taken proportional to the input voltage, so that $i = K.E.f^{\frac{3}{2}}$, where K is a constant

Usually the noise field E is found to decrease with the increase of frequency f, so that $\frac{\partial E}{\partial f}$ is negative. Taking the a-f current output to be proportional to $(f^{\frac{3}{2}}.E)$, the variation of this output with frequency would be given by

$$\frac{\partial i}{\partial f} = \tfrac{3}{2} k f^{\frac{1}{2}} \left[E - \tfrac{2}{3} f \frac{\partial E}{\partial f} \right] \qquad \dots \quad (3)$$

Thus $\frac{\partial i}{\partial f}$ is negative or positive, according as $E <$ or $> \frac{2}{3} f \frac{\partial E}{\partial f}$. In other words, when the noise field is found to decrease with frequency, the acoustic output would increase or decrease with frequency according as the noise field E is greater or less than $\frac{2}{3}f\frac{CE}{Cf}$. Usually the former alternative holds; the $a-f$ output in that case increases with frequency.

EXPERIMENTAL METHOD AND DETAILS

In the present work, the $a-f$ noise output current was measured by calibrated radio receiver provided with an output valve-voltmeter, the input terminals of which were connected across the secondary of the loudspeaker transformer. The valve-voltmeter consisted of a suitable valve with a mirror galvanometer in the anode circuit. The anode current was balanced for no signal. After having tuned the frame aerial and also the receiver to a particular frequency, the fan motor was switched on and the change in the deflection of the valve-voltmeter noted. The average of a number of such observations was then determined for a particular frequency. Observations were taken in this way for several frequency channels. From the calibration graphs of the receiver obtained for the different frequencies, the noise input voltage into the receiver was obtained for these frequencies. The field-strength was then calculated from the standard formula.

In some of the measurements, R. L. Moore's (1930) integrating device was employed. The principal feature of this device was that the voltmeter responded to pulses of short duration and at the same time averaged the effect over a much longer time. The grid time-constant was about 4 m sec. and the discharge time-constant of the anode circuit, having a galvanometer in it was roughly 4 sec. This integrating device was found very sensitive.

A superhet set (Philips 313II) was employed in this work after removing the A. V. C. connections. The interfering sources were placed at a distance of about 50 ft. from the centre of the frame aerial. The vertical plane of the aerial was directed towards the noise source. To avoid the antenna effect, the aerial was earthed at the middle point of the length of wire.

All the experiments were performed in a large room with a few electric wirings in it and these wirings too were well shielded. The effect of the wirings conducting the waves from the noise source to the vicinity of the aerial to be picked up again by the receiver by radiation or induction was therefore extremely small.

EXPERIMENTAL RESULTS

Measurements of the vertical radiation field and the corresponding a-f output due to electric noise from the different motors

The measurements were made on three specified frequency ranges: (1) 7 Mc./s-20 Mc./s (2) 3 Mc./s-6 Mc./s(3) .65 Mc./s -1.5 Mc./s. The induction field can be altogether neglected for the first two frequency ranges and for the lowest frequency range also it was small. The measurements were usually made for three regulator positions of each motor. For these positions the voltages applied to the motor were 213 V, 177 V and 151 V approximately. The corresponding speeds varied between 500 and 3000 r.p.m. approximately for the different motors.

R.F. NOISE FIELD.

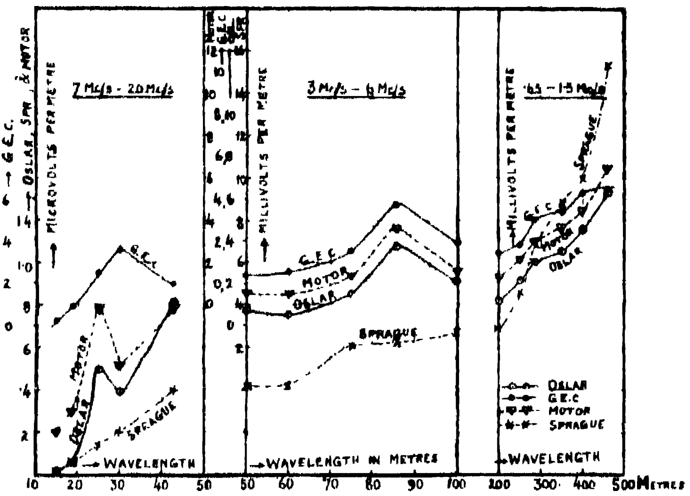

Fig. 1

A.F. Noise Output.

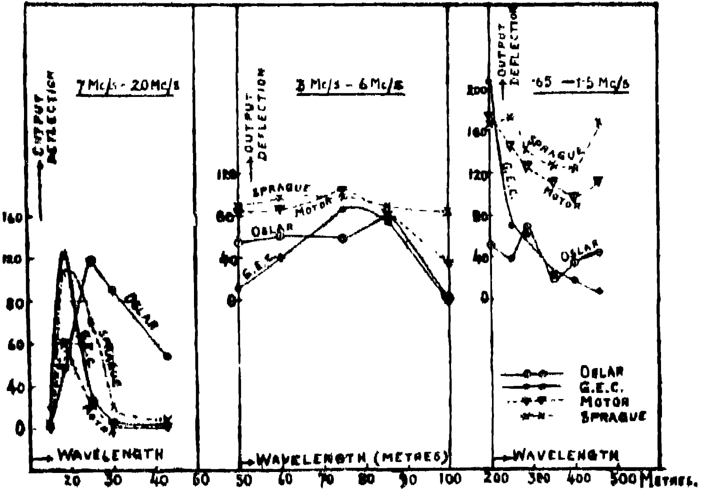

Fig. 2

Fig. 1 gives a set of typical curves showing the r-f noise field for different wavelengths from 15m to 462 meters (.65 Mc./s-20 Mc./s) for the maximum speed of the D. C. motor and the three fans. A similar curve is drawn for the a-f output in Fig. 2. The relative values of the r-f noise field and the a-f output for the different interfering sources are quite *arbitrary*. These curves clearly indicate that the noise field increased in general with wavelength, whereas the a-f current output decreased in general with the increase of wavelength, *but for some maxima at certain definite wavelengths*. The decrease of the a-f output with the increase of wavelength has been explained in the previous section.

The positions of the noise field and the acoustic output for the different interfering sources are given in Table II.

TABLE II

Frequency *f* in Mega-cycles/sec. and Wavelength λ in metres.

	Interfering Sources		Noise Field Maxima			Acoustic Output Maxima		
			.05—1.5 Mc./s	3–6 Mc./s	17–20 Mc./s	.05–1.5 Mc./s	3–6 Mc./s	17–20 Mc./s
1	D. C. Motor	f	—	3.5	12.0	-	4.0	16.0
		λ	-	85.7	25.0	—	75.0	18.75
2	Osler Ceiling fan	f		3.5	12.0	1.05	3.5	12.0
		λ	—	85.7	25.0	285.7	85.7	25.0
3	G. E. C. Ceiling fan	f		3.5	10-12.0	-	4.0	16.0
		λ	-	85.7	25-30.0	-	75.0	18.75
4	Sprague Electric Co. fan	f	-	4.0	—	1.2	4.0	16.0
		λ		75.0	—	250.0	75.0	18.75

The noticeable features in the results shown in Table II are :

(*i*) The maxima in the noise field did not appear in the same wavelength or frequency regions for all the interfering sources.

(*ii*) The maxima in the noise field and those in the acoustic output were not always at the same wavelength or frequency regions for a particular interfering source.

THE EFFECT OF VARYING THE SPEED OF THE MOTORS OF ELECTRICAL INTERFERENCE

The experimental results showed that the r-f noise field usually increased with the increase of the speed of the motors. In certain frequency channels and for some noise sources irregularities in this respect were observed—even though the experiments showing these anomalies were performed with the same degree of care and attention. Special mention should be made of the D. C. motor. The oscillograms of the current fluctuations in the armature of this motor showed secondary fluctuations due to sparks across each pair of the commutator segments, besides the main fluctuation corresponding to the periodicity of the motor. With such a complex source of electrical interference, erratic observations in respect of the effect of speed variation are to be expected.

Fig. 3 illustrates three sets of results—one set with the Osler ceiling fan on 10 Mc./s (30m.) and the other two sets with the D. C. motor on 4 Mc./s and 5 Mc./s (75m. and 60m.) respectively. The observations with the Osler fan on 10 Mc./s showed a gradual increase of the r-f noise field with the increase of speed, whereas with the D. C motor on 4 Mc./s and 5 Mc./s, the noise field at first increased and then decreased with the increase of the speed.

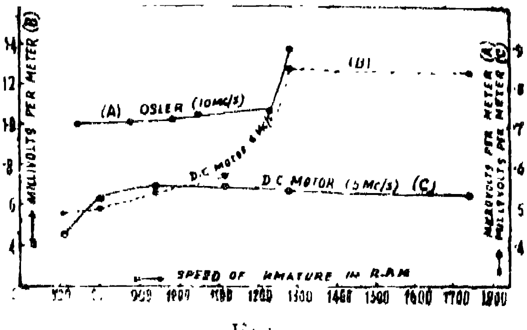

FIG. 3

RESONANCE STUDIES OF THE ARMATURE-SECTOR OF THE DIFFERENT MOTORS

The circuit diagram of the experimental arrangement is shown in Fig. 4. A particular armature-sector was placed in series with a metal-film resistance (10 ohms and sometimes 100 ohms) having no inductance and capacity. The two ends of the circuit were connected to the output terminals of a signal generator through the knife-switches at either end. Keeping the input voltage constant the alternating P.D across the metal-film resistance was then tested by a valve-voltmeter for various frequencies from 1Mc./s to 23 Mc./s and in one case from .5 Mc/s to 22 Mc./s. The valve-voltmeter had a mirror galvanometer in the anode circuit and the anode current was balanced with knife-switches on, but with the power key of the signal generator off. With the galvanometer key off in the anode circuit of the valve-voltmeter, the power key of the signal generator was then switched on and the output voltage adjusted at a definite value for a particular frequency. The galvanometer key was then closed and the position of the deflected light spot noted. The power key of the signal generator was then switched off and the change in position of the light spot recorded. Similar procedure was adopted for different frequencies and care was taken that for each frequency the output reading of the signal generator was exactly the same. The change in the galvanometer deflection could be regarded as a measure of the P.D across the metal-film resistance. When the impressed frequency would be equal to the natural frequency of the circuit containing the armature-sector of some inductance and self-capacity, the current through the circuit would be maximum and so also the P.D. across the pure resistance. The peak in the curve showing changes of galvanometer deflection for different frequencies in the present experiment would evidently enable us to locate the resonance frequency of the circuit. Outside the region of resonance, the P.D. across the resistance would increase with frequency, since the resistance would increase steadily with the increase of frequency of the H.F. current. The results are illustrated in Fig. 5 which shows the resonance peaks.

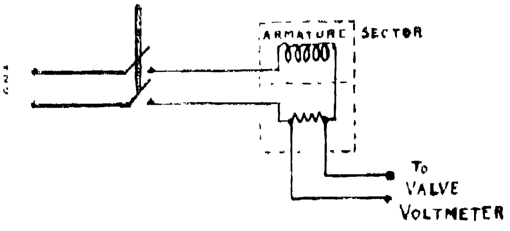

FIG. 4

The positions of the resonance peaks are given in Table III.

Considering the entire frequency range from 75 Mc./s to 20 Mc./s, a very prominent peak in the value of the ratio of vertical to horizontal noise fields was observed at 12 Mc./s (25m.). These were minor peaks. One in the region 1 Mc./s and another in the region 3-4 Mc./s. It is significant that vertical noise-field maxima appeared in these frequency regions.

TABLE III

—	Frequency range	Observed Resonance frequencies	Frequency range	Positions of Noise-field Maxima
(1) D.C. motor	.5 Mc./s to 23 Mc./s	3.5 Mc./s and 19 Mc./s	.65 Mc./s to 20 Mc./s	3.5 Mc./s and 12 Mc./s
(2) Osler fan motor	1.0 Mc./s to 23 Mc./s	3.5 Mc./s, 14 Mc./s* and 20 Mc./s*	,,	3.5 Mc./s and 12 Mc./s
(3) G. E. C. fan motor	,,	4.5 Mc./s (flat resonance)	,,	3.5 Mc./s and 12 or 10 Mc./s
(4) Sprague Electric Co. fan motor	,,	4.0 Mc./s only	,,	4.0 Mc./s only
(5) India fan motor	,,	3.6 Mc./s only (flat resonance)	No observations	—

The observed positions of the noise field maxima are also entered in the same table for comparison. The comparison, no doubt, shows some correspondence between the noise field maxima and the observed resonance frequencies. It is curious that the D.C. motor, the G.E.C. fan motor and sometimes the Osler fan motor gave noise field-strengths in the same frequency regions, *viz.*, 3.5 Mc./s and 12 Mc./s. The Sprague Electrical Co. fan did not, however, show any maximum in the high frequency region and there was also no resonance observed in the armature-sector circuit in the same range. It is indeed probable that the three motors showed the maximum noise field in the same frequency region, because of the similar L-C-R values of their armature-sectors. It is therefore much more than mere speculation to say that the noise field peaks are associated with the resonance frequencies of the armature-sector. In the case of the G.E.C. fan, there was an indication of a flat resonance peak in the region 4.5 Mc./s only. There was no evidence of any resonance in the high frequency range. The resistance of the armature coil of the G.E.C. fan was fairly high (which would account for its very low speed) and it is very likely that the high damping in the circuit was perhaps responsible for masking the resonance effect. With the motors used in the investigation, the lowest frequency where a maximum in the noise field was observed was 3.5 Mc./s. A scrutiny of the noise field curves (Fig. 1) will show 'bulges' at 1.05 Mc./s for the Osler and the G.E.C. ceiling fans and for the D.C. motor.

That the observed resonance maxima shown in Fig. 5 were real resonance effects were tested in a number of ways:

---

* For a different sector of the armature, the corresponding resonances were at 13 Mc./s and 18 Mc./s.

(1) When the armature-sector was replaced by a metallic resistance the maximum was smoothed out.

(2) When an additional inductance or capacity was added in series with the armature-sector and the metal-film resistance, the maximum shifted in the right direction.

(3) The evidence of resonance was also obtained with a different circuit arrangement.

A typical result showing the shift of the maximum towards the region of lower frequencies by inserting additional inductance or capacity in series with the actual circuit is illustrated in Fig. 6.

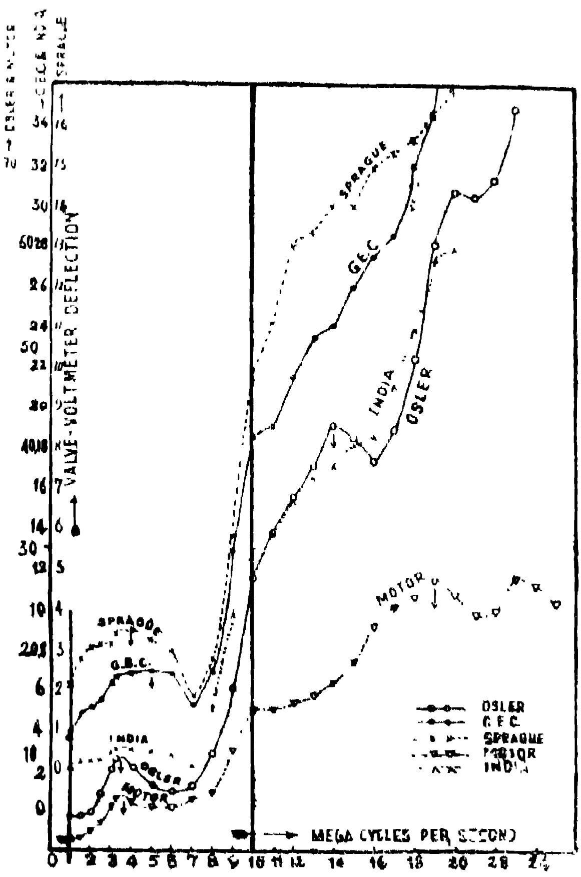

FIG. 5

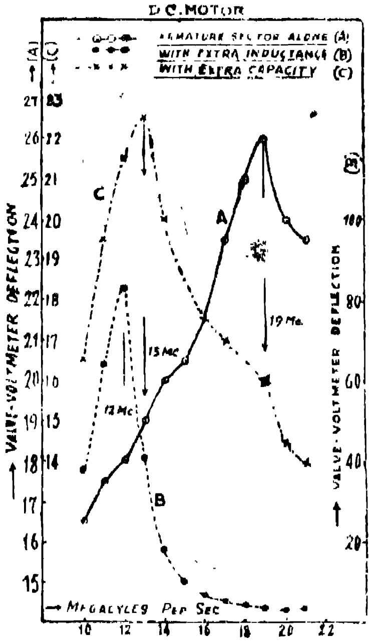

FIG. 6

MEASUREMENT OF THE RATIO OF THE VERTICAL AND THE HORIZONTAL COMPONENTS OF THE NOISE FIELD

The measured values of the ratio of the vertical and the horizontal components of the noise field in the case of the Osler ceiling fan for the three frequencey ranges are shown in Fig. 7. Regarding this variation of the ratio V/H with frequency, the following observaions can be made:

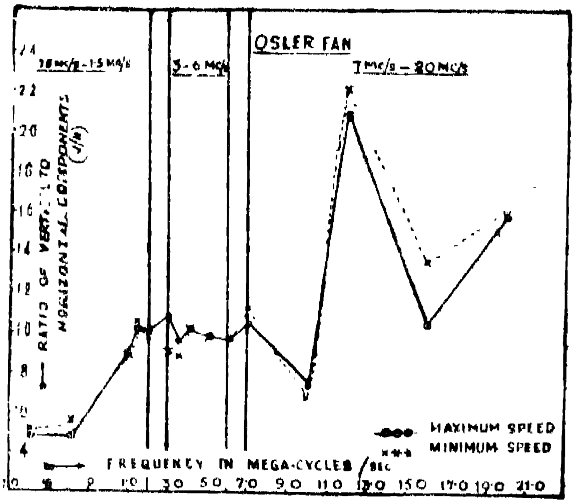

FIG. 7

Over the entire frequency range from .75 Mc./s to 20 Mc./s, there was observed a very prominent peak in the value of the ratio of vertical to horizontal noise fields at 12 Mc./s (25 m.). There were two other smaller peaks, one in the neighbourhood of 1.0 Mc./s and the other in the region, 3-4 Mc./s. It is significant that the noise field maxima appeared in the same regions.

In the region of the lowest frequency under investigation, the horizontal noise field was about twice as great as the vertical field. As the frequency increased, the vertical field increased as compared with the horizontal field and the two fields became nearly equal at 1.2 Mc./s The two fields remained fairly equal over the entire range, 3 Mc./s—6 Mc./s. (In the latter part of this range and in the first part of the high frequency range 7 Mc./s—20 Mc./s, the horizontal field was however slightly in excess). For still higher frequencies, the vertical field predominated and at its highest the vertical field was found more than double the horizontal field. The ratio V/H decreased, *in general*, as the speed of the motor was reduced.

Too much emphasis cannot be laid on this study. As the experiments were not carried out in an open space, it was possible for the aerial to have picked up reflected radiation from the walls of the room.

OSCILLOGRAMS OF THE HIGH FREQUENCY COMPONENTS OF THE DAMPED ELECTRICAL OSCILLATIONS DUE TO SPARK DISCHARGES IN THE MOTORS

A calibrated wave-meter circuit containing a variable condenser and a suitable inductance coil was arranged with the coil placed near the armature segments of the motor under investigation. The circuit picked up a particular frequency corresponding to the natural frequency of the circuit, from the various components of different frequencies present at the source, and this was amplified by the H. F. amplifier. The oscillogram did not however represent the exact wave-form of the particular component from the noise source. The damping of the wave-meter circuit introduced a certain modification in the original wave-form.

The oscillograms showed that in the range of wavelengths from 150 m. to 2000 m., the amplitude of the damped waves diminished with the increase of wavelength as effected by varying the calibrated condenser of the wave meter circuit. A typical oscillogram in the case of the D.C. motor is shown in Fig. 8. The natural frequency of the wave-meter circuit in this case was 155 m.

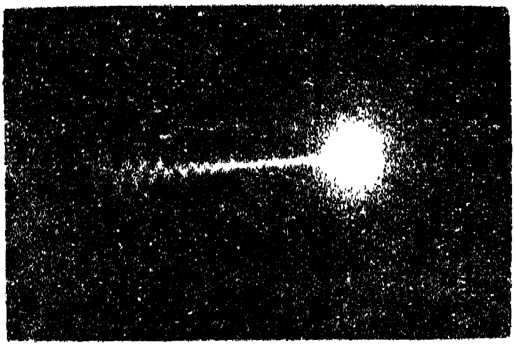

FIG. 8

In conclusion we record our thanks to Mr. S. P. Chakravarty for useful suggestions and to Prof. S. N. Bose for his interest during the progress of the work.

PHYSICS DEPARTMENT,
DACCA UNIVERSITY.

REFERENCES

Chakravarty and Dutt, 1941, *Ind. Jour. Phys.*, **14**, 305.
Curtis, 1932, *Proc. I. R. E.*, **20**, 674
Gill and Whitehead, 1938, *J. I. E. E.*, 83, 345.
Howe, 1937, *Proc. I. R. E.*, **25**, 708.
I. E. E., Council, 1934, *J. I. E. E.*, **74**, 801.
Langton and Bradshaw, 1935, *J. I. E. E.*, **75**, 613
Moore, 1939, *Proc. Phys. Soc. (Lond.)*, **51**, 972
Morris, 1934, *J. I. E. E.*, 74, 248.
Neale, 1935, *Electrical Power Engineer*, **17**, 510
Schumacher, 1935, *Proc. I. R. E.*, **23**, 779.
Warren, 1935-36, *J. P. O. E. E.*, **28**, 23.

INFLUENCE OF COMMON ION ON THE DISSOCIATION OF SOME STRONG ELECTROLYTES. PART I. SULPHURIC ACID AND BISULPHATES

By N. RAJESWARA RAO

(Received for publication, Sept. 17, 1943)

(Plate VI)

ABSTRACT. Influence of common ions on the dissociation of sulphuric acid and bisulphates is studied by taking the Raman spectra of the mixtures of these solutions with other acids which supply hydrogen ions and with normal sulphates which supply the sulphate ions. It was observed that while the addition of H ions suppressed the dissociation in all these cases, the addition of the sulphate ions to the bisulphate solutions helped further dissociation of the HSO_4 produced on dissolving the bisulphate in water. The latter result is in contradiction to the law of mass action.

INTRODUCTION

Interesting among the studies on the dissociation of strong electrolytes by Raman effect is the influence of common ion on the dissociation of an electrolyte suggested by Hibben (1937). He observed that a concentrated solution of $ZnCl_2$ gives a strong Raman line of frequency 275 which is characteristic of the undissociated $ZnCl_2$ molecules. As the solution is diluted, the line diminishes in intensity obviously due to the dissociation of $ZnCl_2$ molecules. But, when even to a comparatively dilute solution of $ZnCl_2$, NaCl is added, the line appears bright again. This was explained as arising out of the reforming of $ZnCl_2$ molecules due to the Cl ions which are supplied in abundance by the addition of NaCl. This is a natural consequence of the law of mass action. But, when he examined the influence of the kation, by adding $ZnSO_4$ the line did not increase in intensity. He explained the anomaly as due to the fact that in the latter mixture both $ZnCl_2$ and $ZnSo_4$ are homopolar. Similar investigations have been made by Venkateswaran (1935) on other halides which give Raman lines.

So far the experimental results, concerning the influence of common ion, are found to be in agreement with the law of mass action. But as the studies are extended to other strong electrolytes, to be dealt with in this series of investigations, they yield peculiar results which are difficult to understand, if one applies the law of mass action, even qualitatively. The present paper describes such investigations on sulphuric acid and bisulphates.

SULPHURIC ACID

In a previous paper (Rao, 1940) by the author, where a quantitative study of the dissociation of sulphuric acid in different concentrations was reported, it was observed that while the first stage of dissociation into H and HSO_4 ions is rapid even in highly concentrated solutions, the further dissociation of HSO_4 into H and SO_4 is very slow, even in comparatively dilute solutions. This was explained as due to the large number H ions produced during the two stages, which therefore favours recombination of H and SO_4 ions into HSO_4 ions as expected from the law of mass action.

In the present work the dissociation of sulphuric acid, as influenced by the addition of H ions, is studied. HCl is a convenient acid for the supply of H ions because it is almost completely dissociated even at high concentrations. But its addition to concentrated H_2SO_4 results in evolution of gaseous HCl. Hence it cannot be used for studying the dissociation characteristics of H_2SO_4 at high concentrations, though for dilute solutions of H_2SO_4 it is found to be very convenient. HNO_3 cannot be used as it gives a strong Raman line at 1050 which is superposed upon the 1045 line of H_2SO_4 corresponding to the HSO_4 ions, the intensity variation of which is taken as the basis for the study of the dissociation of this acid. Hence, $HClO_4$ was chosen as the source of supply of H ions for concentrated solutions of H_2SO_4. This acid, however, gives rise to a strong Raman line at 937 which is broad and falls very near the 910 line corresponding to the undissociated H_2SO_4 molecules. Thus the study of the variation of dissociation of H_2SO_4 with addition of $HClO_4$ is confined to the determination of the intensity of the 1045 line of the HS_4O ion alone in the mixture and in the pure acid.

100 cc. of concentrated sulphuric acid 30N are taken and divided into two equal parts. To one part 30 cc. of 10N $HClO_4$ is added and to the other part 30 cc. of water. The Raman spectra of the two solutions exposed under identical conditions for equal times are taken, and the intensity of the 1045 line in the two spectra are determined and are found to be 17.3 and 7.0 in the pure acid and $HClO_4$ mixture, respectively. But the water content in the former solution is more than that in the mixture with $HClO_4$. So, the above comparison requires modification to one in which the water content is the same in both. If to the concentrated sample of H_2SO_4, only that amount of water as is contained in 30 cc. of $HClO_4$ (10N) is added, its normality will be reduced to 23N and the corresponding intensity of the 1045 line, calculated from the previous work of the author on dissociation of sulphuric acid with concentration, is 12.8. Therefore, it is clear that that the decrease in the intensity of the 1045 line is more than is warranted by the smaller amount of water in the mixture with $HClO_4$ compared to that with pure water and this should be attributed to the decrease in the dissociation of H_2SO_4 brought about by the H ions supplied by $HClO_4$.

To study the second stage of dissociation, 50 cc. of 3.6N sulphuric acid is taken and divided into two parts. To one part 25 cc. of concentrated HCl is added and to the other 25 cc. of water. It is clearly seen from the microphotometric curves *a* and *b* of the spectra given in Fig. 1 that the intensity of the line at 980 corresponding to the SO_4 ions is suppressed to a large extent thereby indicating that the dissociation of HSO is diminished in the HCl mixture. It would have been interesting to see how the addition of the bisulphate ion influences the first stage of dissociation of the acid. But unfortunately, this is not practicable for the following reasons. Firstly, bisulphates dissolve but to a small extent in sulphuric acid at laboratory temperature. Secondly, even if it is possible to dissolve more at at a high temperature, the bisulphate ion contributes to a small extent to the intensity of the 910 line characteristic of undissociated H_2SO_4 molecules and therefore it is not possible to distinguish whether the changes in the intensity of the 910 line is due to the change in the dissociation of the acid or to that of the HSO_4 ions. Therefore, no attempt was made to test this.

ACID SULPHATES

It is well known that an alkaline bisulphate is completely dissociated as far as its alkaline radical is concerned and the Raman spectra of its solution which mainly consists of 4 lines at 1045, 980, 594 and 414 is therefore due to HSO_4 and SO_4 ions formed by the dissociation of HSO_4 ions. The line at 1045 is attributed by all workers to the HSO_4 ions, and that at 980 to SO_4 ions. The bands at 594 and 414 are characteristic of both the types of ions. As the solution is diluted, the line at 1045 diminishes in intensity, while that at 980 increases, thereby indicating dissociation of HSO_4 ions into SO_4 and H ions. The effect of the addition of H and SO_4 ions on the dissociation of HSO_4 in a solution of NH_4HSO_4 is studied in the following way.

A 3.4N solution of NH_4HSO_4 is taken and divided into two parts. To one part is added an equal volume of 10N HCl and to the other an equal volume of pure water. The Raman spectra of these two mixtures, exposed for equal times are taken under identical conditions. Their microphotometric curves are given in Figs. *2a* and *2b*. The spectra revealed that while the lines at 1045 and 980 are nearly of equal intensity in the water solution, in the mixture with HCl, the line at 980 is very much suppressed, which means that almost all the SO_4 ions recombined with H ions to form HSO_4 ions.

To study the influence of SO_4 ions on the dissociation of HSO_4 into SO_4 and H, the sample of the solution of NH_4HSO_4 is taken and divided into two equal parts. To one part is added solid $(NH_4)_2SO_4$, to saturation. This resulted in an increase of volume of the solution. To the other part is added pure water to make up to this volume. Raman spectra of the two mixtures exposed for equal times under identical conditions are taken. Since the 980 line in the spectrum of the sulphate mixture is due to the SO_4 ions supplied by the bisulphate as well as the sulphate, the intensity of the 1045 line only representative of the HSO_4 ion is compared in the two solutions. It is seen from the Fig. *3b* and *3a* in Plate VI that the line at 1045 is more intense in the pure bisulphate solution than in the mixture with normal sulphate. This means that the addition of the normal sulphate favours further dissociation of the HSO_4. This result is confirmed in the mixtures of $KHSO_4 + (NH_4)_2SO_4$ and $NH_4HSO_4 + Li_2SO_4$ also.

In this connection, one point requires elucidation. In the case of the mixtures with HCl, the mixture and pure solution contain very nearly the same proportion of water. But in the case of the solutions of pure acid sulphate and the mixtures of acid sulphate and normal sulphate, the latter contain less amount of water and still the dissociation of HSO_4 is more in these mixtures than in the corresponding pure solutions. It means, that the increase of dissociation brought about by the additional SO_4 ions more than compensates the opposite effect caused by the decrease in the proportion of water. This is contrary to what is to be expected from the law of mass action.

The possibility of complications arising out of the reaction $SO_4 + H_2O \rightleftharpoons HSO_4 + OH$ is excluded, because Raman spectra of solutions of normal sulphates even after long exposures do not indicate even traces of the line 1045 corresponding to the HSO_4 ions.

TO SUM UP

1. The dissociation of sulphuric acid is decreased by the addition of other electrolytes which supply H ions in abundance namely HCl and $HClO_4$ worked with in the present case.

2. The dissociation of HSO_4 into SO_4 and H is suppressed by the addition of electrolytes which supply H ions, *e.g.*, HCl used in the present case.

3. The dissociation of HSO_4 into SO_4 and H is enhanced by the addition of SO_4 ions supplied by a normal sulphate.

It is well known that the law of mass action is applicable only to very dilute solutions of weak electrolytes. For concentrated solutions, the constant is found to vary with concentration involving the formation of less number of undissociated molecules. But a case of enhancement of dissociation by the addition of one of the dissociated products is not contemplated before. Another point of interest is the discrimination between the ions involving an extreme case of inapplicability of the above law which was also not contemplated before.

Further work on the point is in progress to permit of a generalisation as regards the dissociation characteristics of strong electrolytes having an ion common to them.

In conclusion, the author takes great pleasure in recording his grateful thanks to Dr. I. Ramakrishna Rao, under whose direction this work was done.

DEPARTMENT OF PHYSICS,
ANDHRA UNIVERSITY, GUNTUR.

REFERENCES

Hibben, 1937, *J. Chem. Phys.*, **5**, 710.
Rao, N. R., 1940, *Ind. J. Phys.*, **14**, 143.
Venkateswaran, C. S., 1935, *Proc. Ind. Acad. Sci.*, **2A**, 119.

PLATE VI (A)

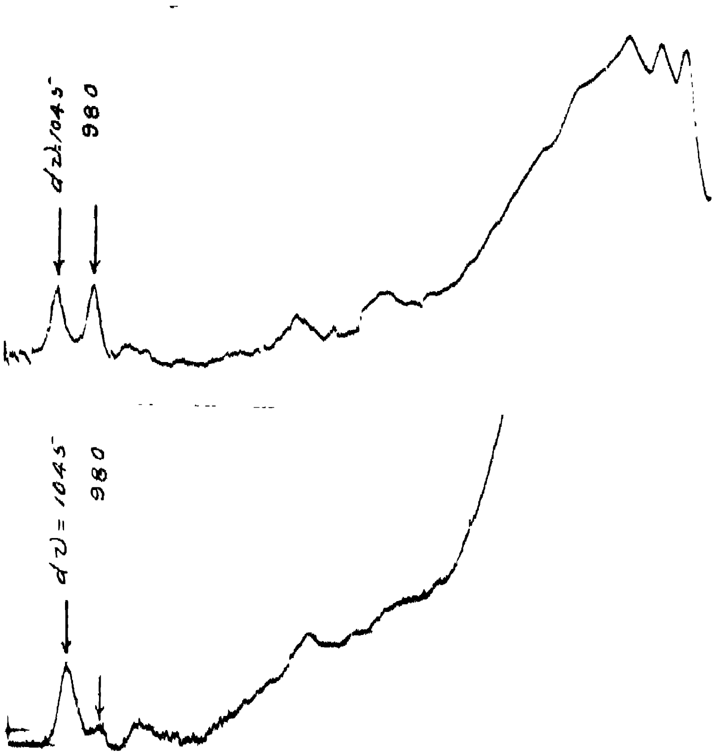

H_2SO_4 pure

H_2SO_4 + HCl

Fig. 1
Sulphuric Acid and Bisulphates

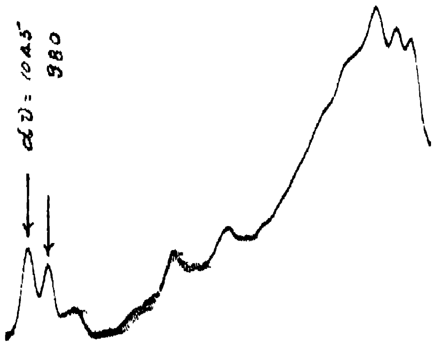

Fig. NH_4HSO_4 pure

PLATE VI (B)

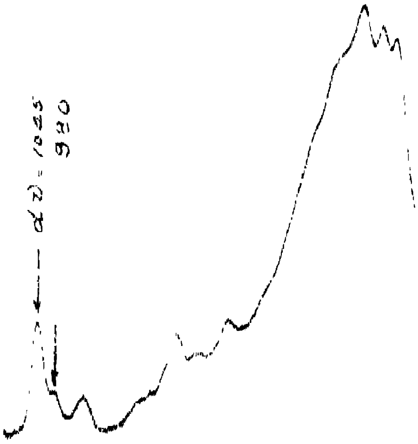

Fig. 2b. $NH_4HSO_4 + HCl$

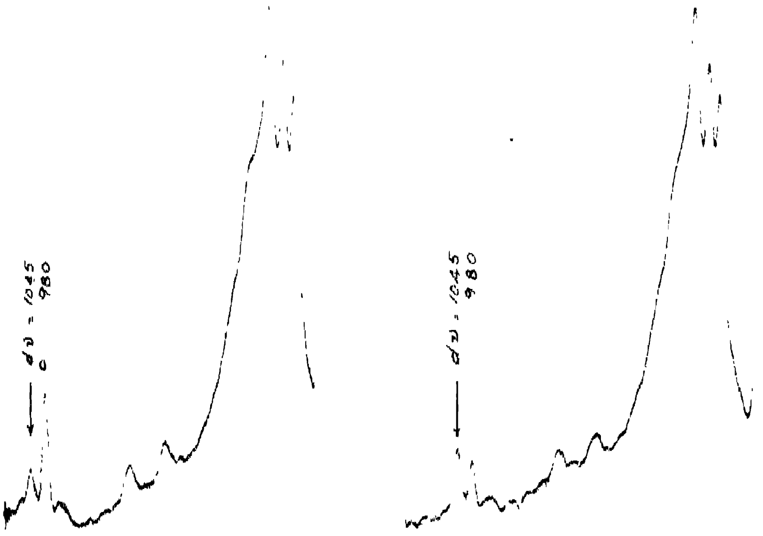

$NH_4HSO_4 + (NH_4)_2SO_4$ Fig. 3. NH_4HSO_4

EXPERIMENTS IN SCATTERED LIGHT. ANGLES OF FIRST MINIMUM

By R. V. TAMHANKAR

AND

G. R. PARANJPE

(*Received for publication, Sept. 27, 1943*)

ABSTRACT. Starting with Mie's formula, the distribution of intensity of light scattered in the region of the transmitted direction has been studied theoretically for four drop-sizes of water vapour, *viz.*, $\alpha = 15$, 20, 25 and 30, where α represents the ratio of the circumference of the drop to the wavelength of the light used. The range verified in the present investigations was 150°-180°. The calculations reveal that a sharp minimum of intensity exists in the range considered and that it has to be ascertained very carefully. This minimum, which is here termed as 'the angle of the first minimum on Mie's theory' may be correlated with the first order corona ring for the drop-sizes considered

The theoretical results have been verified experimentally for the first time. The scattered intensity has been measured by the use of a photoelectric cell coupled with a suitable amplification arrangement. The results have been compared with Mie's theory and also with the first order corona rings A fair agreement is found to exist in the cases considered

Of all the methods so far used for measuring the instantaneous size of fog droplets, the corona ring method is very convenient. By applying Babinet's principle the formula

$$\sin \theta = (n + 0.22)\frac{\lambda}{2a}$$

is obtained, giving the relationship between the average radius of the drops in the cloud, the wavelength of light and the angle subtended by the *n*th dark ring.

The theory has been studied by C. T. R. Wilson (1897), Aitken (1890-91) and (1892-93), Bricard (1938), Rayleigh (1911) and several others, who found that it gives satisfactory results. While Mecke (1920) asserts that the theory fails to give reliable results for drops smaller than 4μ. Mitra (1928) confirms Mecke's view and reveals the oscillatory nature of diffraction pattern by means of photographs in monochromatic light. Recently T. A. S. Balkrishnan (1941) has put forth, following Mecke's and Mitra's views, a correction to the theory of coronas on the assumption that the droplets in the cloud are transparent. Paranjpe and Lajami (1939), have theoretically compared the angles of the first order corona rings for various drop-sizes with the angles of first minimum in the transmitted direction on Mie's (1908) theory.

Theoretical calculations for scattering by the application of Mie's theory at very close intervals for any drop-size in the transmitted direction, near about

180′, have revealed the presence of a sharp minimum of intensity in the scattered light. Thus minimum differs for different values of α where

$$\alpha = \frac{\text{Circumference of the drop}}{\text{Wavelength of light}}.$$

This minimum of intensity is here termed 'the angle of the first minimum on Mie's theory.'

Detailed derivation of Mie's formula is treated in a paper by Paranjpe and Lajami (1940). It is only necessary to indicate here the final results.

$$J_1 = \frac{\lambda^2}{4\pi^2 r^2} \left| \sum_{n=1}^{\infty} \left\{ A_n \pi_n + P_n \left[\nu\pi_n - (1-\nu^2)\pi_n^1 \right] \right\} \right|^2$$

$$J_2 = \frac{\lambda^2}{4\pi^2 r^2} \left| \sum_{n=1}^{\infty} \left\{ A_n \left[\nu\pi_n - (1-\nu^2)\pi_n^1 \right] + P_n \pi_n \right\} \right|^2$$

where J_1 and J_2 are intensity components of scattered light polarised in horizontal and vertical planes, λ the wavelength of incident light, and r the distance of point of observation from the centre of the scattering particle. The factor $\frac{\lambda^2}{4\pi^2 r^2}$ being constant the values of J_1 and J_2 depend on $|\text{Mod}|^2$ which may be termed as I_1 and I_2. A_n and P_n are complex functions depending on (*i*) the radius of the particle (*ii*) the wavelength of light used for scattering and

$$(iii) \quad m' = \frac{m}{\ }, \ i.e., \ \frac{\text{R. I. of the material of the particle}}{\text{R. I. of the surrounding medium}}.$$

A_n and P_n are calculated by evaluating series of coefficients in terms of cylindrical functions depending on α and β where $\alpha = \frac{2\pi\rho}{\lambda}$ and $\beta = m'\alpha$. π_n and π_n^1 are functions of the scattering angle θ derived from $\nu = \cos\theta$.

In Tables I and II below are given results of calculations of angles of first minimum on Mie's theory for scattering in the transmitted direction ($\pi - \nu^\circ$) for two drop-sizes $\alpha = 15$ and $\alpha = 16.8$.

TABLE I

$\alpha = 15$, $\beta = 20$

$\pi - \nu^\circ$	I_1	I_2	$I = I_1 + I_2$
0	23027.8	23027.8	46055.6
7° 15′	9502.3	8507.3	18009.6
10°	2466.3	2325.9	4792.2
12° 30′	1279.7	901.3	2181.0
15° 51′	98.5	128.8	227.3
17° 30′	33.0	90.6	123.6
20°	242.1	164.8	406.9
22° 45′	539.1	278.3	817.4
25° 23′	562.9	288.1	851.0
27° 3′	261.5	754.6	1016.1

TABLE II

$\alpha = 16.8$, $\beta = 22.4$

$\pi - \nu^\circ$	I_1	I_2	$I = I_1 + I_2$
0	64140.5	64140.5	128281.0
7° 15	13189.3	9151.6	22340.9
10°	1823.7	1129.4	2953.1
12° 30′	359.6	342.3	701.9
15° 51′	982.6	908.5	1891.1
17° 30′	1343.1	1074.4	2417.5
20°	1074.4	994.8	2069.2

These values are plotted in Fig. 1. We see from the figure that the angles of the first minimum for the cases considered are:

Drop sizes				$\pi - r$	
α	15	β	20	16°	30′
α	16.8	β	22.4	12°	15

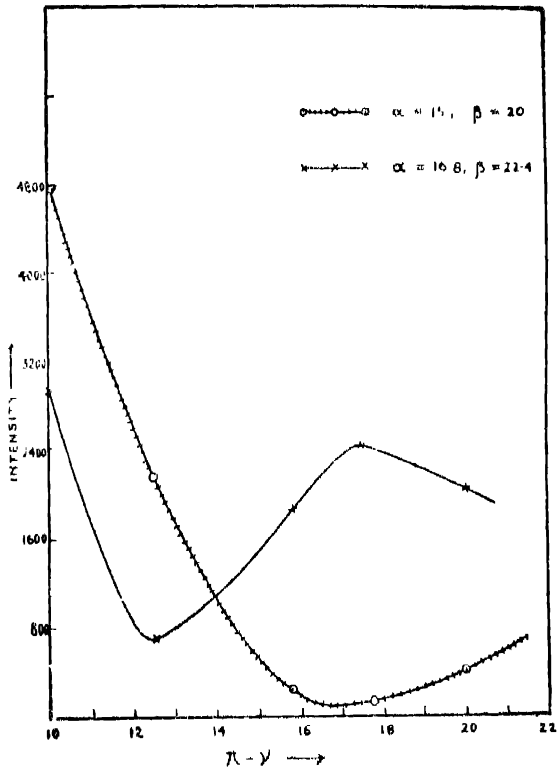

FIG. 1

It is of importance to observe that these angles $\pi - r$ are really the angles of first minimum as measured from the transmitted direction ($\pi - 0$), and that there exists no other minimum in that interval. If sufficiently small intervals are not taken both in the theoretical and experimental work it is likely that this first order minimum may be missed altogether and the higher order minima might be mistaken for the first order one.

Ray (1921) calculated intensities for $\alpha = 12$, $\beta = 16$ on Rayleigh's theory and found out the angle for the first minimum near about $\pi - 27°30'$. While Paranjpe and Lajami (1930) calculating intensities at smaller intervals for the same case according to Mie's theory found out the angle of the first minimum near about $\pi - 14°$ and the angle of the second minimum near about $\pi - 27°30'$. Considering the above results it appears that Ray's value, namely $\pi - 27°30'$, should be in reality the value of second minimum on Rayleigh's theory, particularly since Mie's theory and Rayleigh's theory do not differ so widely from each other (*vide* Note by M. M. Paranjpe, 1942). If Ray had calculated intensities for angles between $\pi - 0°$ and $\pi - 27°30'$ he would have probably found a minimum between $\pi - 0°$ and $\pi - 27°30'$ and that too at about $\pi - 14°$ since the angles of second minimum by the two theories appear to be the same.

The following method may be employed to find out theoretically the angles of the first minimum. In Table III, I_1 and I_2 are given separately. I_1 and I_2 each consists of a real component and an imaginary component, which when squared and added together give I_1 and I_2.

TABLE III

$\alpha = 15, \beta = 20$

Angle $\pi - \nu$	I_1 Real	I_1 Imaginary	I_2 Real	I_2 Imaginary
0° 0′	+ 3.0	−151.7	− 3.0	+151.7
7° 15′	+13.9	− 90.7	− 4.5	+ 92.6
10° 0′	+ 2.3	− 49.6	− 1.6	+ 48.2
12° 30′	+13.3	− 33.2	− 1.7	+ 52.2
15° 51′	+ 2.4	9.6	3.6	+ 10.8
17° 30′	− 4.8	3.1	+ 6.8	+ 6.7
20° 0′	−15.5	+ 1.1	+11.7	+ 5.2
22° 45′	−23.2	+ 1.5	+15.8	+ 5.5
25° 23′	−23.7	+ 1.1	+16.6	+ 3.6
27° 3′	− 3.4	+ 15.8	+13.5	− 23.9

A careful examination of the above table reveals the following:

For I_1

(1) The real terms are smaller than the imaginary ones up to $\pi - 17°30'$. The squares of the real terms would be therefore smaller than those of the imaginary ones, and thus it can be seen that the values of I_1 in the interval $\pi - 0°$ and $\pi - 17°30'$ depend mainly on the values of the imaginary terms.

(2) The imaginary terms of I_1 decrease gradually in magnitude from -151.7 at $\pi - 0°$ to -3.1 at $\pi - 17°30'$. At $\pi - 20°$ the (imaginary) value is $+1.1$. It is clear from this that the imaginary values pass through zero and then change the sign at some point in the interval $\pi - 17°30'$ and $\pi - 20°$.

(3) From $\pi - 17°30'$ the real quantities for I_1 are greater than the imaginary ones. This state continues thereafter, indicating that I_1 has passed through a change in the values.

For I_2

(1) The real terms in I_2 are also small as compared to the imaginary ones till about $\pi - 15°51'$. The total value of I_2 can be supposed to be due, mainly to the value of the imaginary quantities in the interval $\pi - 0°$ to $\pi - 15°51'$.

(2) The imaginary terms in I_2 decrease continuously from $+151.7$ at $\pi - 0°$ to $+3.6$ at $\pi - 25°23'$. They pass through zero and change in sign from $+3.6$ to -23.9 somewhere in the interval between $\pi - 25°23'$ and $\pi - 27°3'$.

(3) But it is seen that the preponderence of imaginary values over the real ones ceases at $\pi - 17°30'$, where both the values are almost equal, *viz.*, $+6.8$ and $+6.7$. From this point onwards the real terms are mainly responsible for the values of I_2.

These inferences show clearly that the values of I_1 and I_2 decrease gradually in the interval $\pi - 0°$ to $\pi - 17°30'$.

Somewhere near about $\pi - 17°31'$ they pass through a minimum. Since the total intensity is equal to $I_1 + I_2$ it is clear that there is no minimum in the range $\pi - 0°$ to $\pi - 17°30'$, except the one investigated presently.

Other cases can be worked out similarly.

II

Experimental determination of the intensity of scattered light in the forward direction was made for various sizes of the drop using monochromatic sodium light. Scattered light was made incident on a photoelectric cell which could be moved freely to any desired angle. A new photoelectric amplification circuit was specially designed and constructed for measuring very feeble intensities in the scattered light. The amplified current was taken proportional to the intensity of scattered light. Readings of scattering were taken at intervals of about 2°30′ round the cloud chamber by receiving the scattered light on the photocell placed at the desired angles for the clouds of required particle size.

Great difficulty was experienced in finding the position of the minimum of intensity in the transmitted direction. The scattered light in this region is superposed on the diffraction rings and also mixed with direct light and the light diffused and reflected by the glass of the chamber. The incident beam was therefore cut down to a very narrow pencil which reduced the chance of getting pronounced corona rings and also kept out the direct and the diffused light from falling on the photocell.

Results of scattering in the forward direction are given in Table IV and their curves drawn in Fig. 2. A reference to the figure shows that the angles of first minimum are not so well defined as in the cases of other minima. In fact the minimum is only to be suspected in some of these cases. The following procedure is adopted: When intensity values for consecutive scattering angles are very near to each other, that is, the ratio between these consecutive readings is much less than those of the preceding and succeeding pairs, a minimum is suspected somewhere near about that angle. The reason for lack of sharpness in the nature of these minima is that there is a vast amount of scattered light in this region, since forward scattering is much more prominent than in other regions. There is besides scattered light, a large amount of extra light in this region due to reflections and refractions of the incident beam of light by the glass of the cloud chamber.

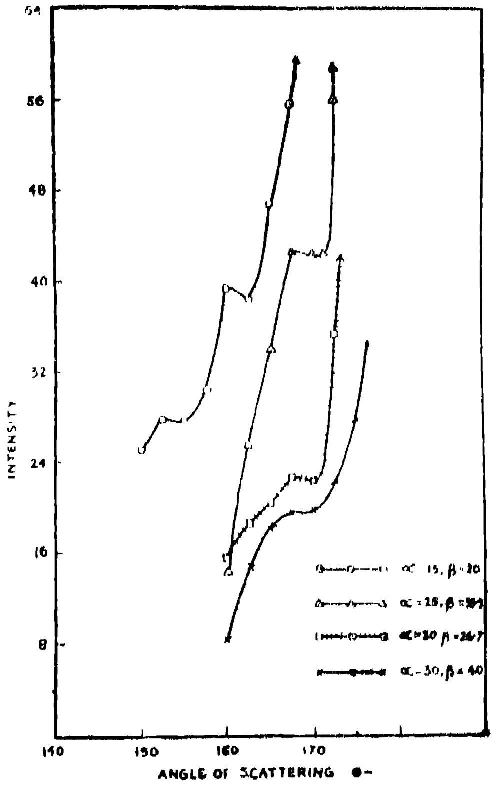

FIG. 2

In Fig. 2 the curves are drawn both for theoretical and experimental values of the drops $\alpha = 15$, 20, 25 and 30.

The curves are seen to show a fair agreement between theory and experiment.

Below is given a table showing a comparison between the theoretical and experimental data.

TABLE IV

(*a*)

$\alpha = 15$, $\beta = 20$.

Averaged over a set of 6 independent observations.

Scattering angle	Theoretical scattering	Observed scattering.
150°	1090.1	25.0
152° 57	1016.2	27.6
154° 37	851.0	27.6
157° 15′	817.4	30.4
160°	406.0	39.4
162° 30′	123.6	38.2
164° 9	227.3	40.8
167° 30′	2184.0	55.6
170°	4792.2	.
172° 45′	18099.6	Readings beyond scale
180°	46055.6	...

(*b*)

$\alpha = 20$, $\beta = 26.7$.

Averaged over a set of 4 independent observations.

Scattering angle.	Theoretical scattering.	Observed scattering
160°	1370.1	15.7
162° 30′	...	18.5
165°	...	20.1
167° 30′	...	22.6
170°	2422.0	22.1
171° 53	1481.0	...
172° 30	3327.0	35.2
175°	...	...
177° 30′	...	...
180°	91742.2	134.3

(*c*)

$\alpha = 25$, $\beta = 33.33$.

Averaged over a set of 4 independent observations.

Scattering angle.	Theoretical scattering.	Observed scattering.
160°	Theoretical values not available.	14.3
162° 30		25.5
165°		34.0
167° 30′	...	42.7
170°	...	42.5
171° 15′	...	42.4
172° 30′	...	56.0
175°	...	...
177° 30′	...	Readings beyond scale.
180°	...	

(*d*)

$\alpha = 30$, $\beta = 40$.

Averaged over a set of 4 independent observations.

Scattering angle	Theoretical scattering	Observed scattering.
160°	...	16.3
162° 30	...	29.2
165°	...	36.4
167° 30′		39.5
170°	10121.2	39.6
171° 53	22828.0	..
172° 45′	12297.0	44.5
175°	...	55.3
177° 30′	...	Readings beyond scale.
180°	391438.0	

(1) Angles of first minimum obtained on Circular Disc theory $\pi - \nu_c$, (2) angles of first minimum calculated on Mie's theory $\pi - \nu_m$ and (3) angles of first minimum obtained experimentally $\pi - \nu_e$

TABLE V

Drop-size		$\pi-\nu_c$	$\pi-\nu_m$	$\pi-\nu_e$
$\alpha=30$	$\beta=40$	7° 20′	6° 30′*	11°
$\alpha=25$	$\beta=33.3$	8° 49	...	9°
$\alpha=20$	$\beta=26.07$	11° 0	9° 0′*	10°
$\alpha=16.8$	$\beta=22.4$	13° 10	12° 15′	...
$\alpha=15$	$\beta=20$	14° 48′	16° 36′	17° 30′
$\alpha=12$	$\beta=16$	18° 30	14° 0′	...
$\alpha=10$	$\beta=13.3$	22° 30	16° 0′*	...
$\alpha=9$	$\beta=12$	25° 12	18° 0′*	...

(Results marked with asterisk are taken from calculations by Paranjpe and Lajami.)

The above values are plotted against α in Fig. 3.

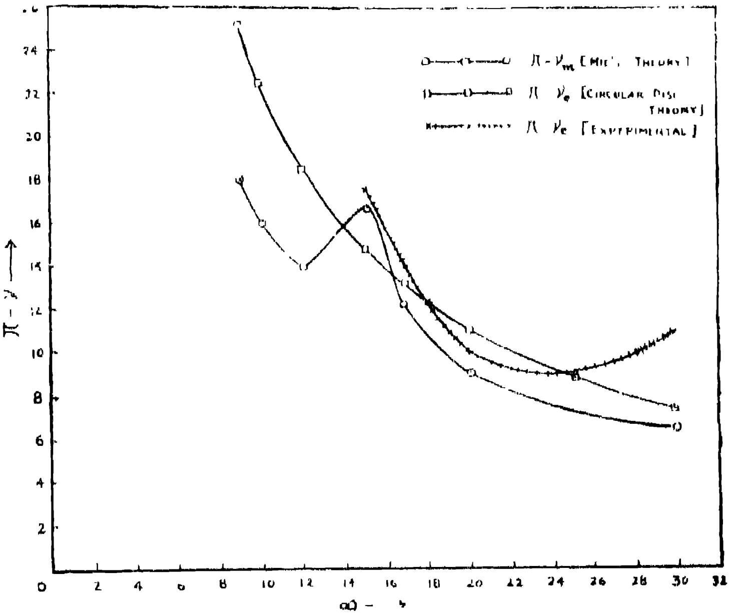

FIG. 3

The curve $\pi-\nu_c$ (Circular Disc theory) is a regular curve showing a sine relationship between α and the angle of the first minimum.

This curve $\pi-\nu_c$ shows that the value of the first minimum $\pi-\nu$ increases as the drop-size decreases. This result is perfectly in accordance with the Circular Disc Theory.

The curve $\pi-\nu_m$ (Mie's theory) exhibits the presence of a well defined maximum at $\alpha=15$ and a defined minimum at $\alpha=12$. These reversing points cannot be accounted for but it appears probable that the curve $\pi-\nu_m$ may exhibit more maxima if a sufficient number of points are plotted. It is seen from the figure that $\pi-\nu_m$ crosses $\pi-\nu_c$ at $\alpha=16.4$ and at $\alpha=14$, the two curves draw closer to each other at $\alpha=30$ and may cross at $\alpha=33$, if both of them were produced beyond 30. It thus appears that the curve $\pi-\nu_m$ is of an oscillatory nature interlinking itself with the curve $\pi-\nu_c$ by crossing it a number of times. No definite conclusion can be drawn from this behaviour because of the meagre data available. If an oscillatory nature is to be assumed for $\pi-\nu_m$ and its interlinking with $\pi-\nu_c$, this might lend support to the nature of the correction to be applied to the theory of the coronas as derived by Balkrishnan (*loc. cit.*), who concludes that the correction to the Circular Disc theory is of a periodically oscillatory nature.

The curve $\pi-\nu_e$ (Experimental) drawn with the points available appears to be of the same nature as $\pi-\nu_m$. It is seen that both these curves are almost parallel except at $\alpha=30$ where the experimental value is much higher than that expected theoretically. In other respects the curve appears to be identical with $\pi-\nu_m$ except that it is laterally shifted to higher values of $\pi-\nu$. It was not possible to extend the experimental verification below $\alpha=15$ because of the experimental limitations. If it were possible a complete relation between $\pi-\nu_m$, $\pi-\nu_e$ and $\pi-\nu_c$ could have been established.

Judging from the results available, it can be concluded that the theoretical and the experimental curves for angles of first minimum are almost identical in nature and it may be said that they agree considerably within the limits of the experimental errors. The experimental values appear to be slightly higher than the theoretical ones. But, in general, deviation from the theory is such, as would be accounted for by considering the difficulty in spotting out the minimum experimentally.

It is thus possible to employ Mie's theory as a method of determining the particle size of large water droplets. The method is found to be capable of giving reliable results in the range 1μ to 4μ.

The above discussion leads to another important conclusion, namely, that the Circular Disc theory is certainly not as defective as is thought by Mecke (*loc. cit.*) who concludes that the theory fails to give correct results below 4μ. In the present investigations drop-sizes considered were between 1μ to 4μ and the results are found to agree with those on Mie's theory, and the method can be used as a fair estimate of the size of droplets considered.

Physics Department,
Royal Institute of Science,
Bombay.

REFERENCES

Aitken (1890-91), *Proc. Roy. Soc.*, **17**, 135.
,, (1892-93), ,, **19**, 260.
Balkrishnan, T. A. S. (1941), *Proc. Ind. Acad. Sc.* A., **13**, 188.
Briend (1938), *Comptes Rendus*, **207**, 538 (Science Abstract 1802)
Mecke (1920), *Ann. der. Phys.*, **61**, 471.
Mie (1908), *Ann. der. Phys.*, **25**, 377.
Mitra (1928), *Ind. Jour. Phys.*, **3**, 175.
Paranjpe and Lajamai (1939), *Jour. Univ. Bomb.*, **8**, 3.
,, ,, (1940), ,, ,, **9**, 38.
Paranjpe (1942), ,, ,, **10**, 167
Ray (1921), *Proc. Ind. Assoc. Cult. Sc.*, **7**, 10.
,, (1923), ,, ,, ,, ,, ,, **8**, 23.
Rayleigh (1911), *Proc. Roy. Soc.*, **24**, 25.
Wilson, C. T. R. (1897), *Phil. Trans. Roy. Soc.*, **189**, 263.

EFFECT OF TEMPERATURE ON THE ELECTROLYTIC DISSOCIATION IN STRONG ELECTROLYTES.
PART I. NITRIC ACID

By N. RAJESWARA RAO

(*Received for publication, September 17, 1943*)

(Plate VII)

ABSTRACT. Electrolytic dissociation in nitric acid is studied at various concentrations and temperatures by the mechanism of Raman effect. The degree of dissociation of the acid at various temperatures is calculated by comparing the intensity of the line of Raman frequency 1050 with that of Raman frequency 1300 in the Raman spectra of the acid at these temperatures. It is found that the dissociation of the acid decreases with increasing temperature.

INTRODUCTION

It is well known that the conductivity of electrolytes increases with temperature. This increase may be due to (1) the increase in the ionic velocity and (2) larger ionisation of electrolyte. A mere study of the conductivity of the solution which is a function of the above two factors at different temperatures does not, therefore, give a direct indication of how the degree of dissociation varies with temperature. But a study of the Raman spectrum of the electrolyte at different temperatures gives, in suitable cases, an idea of how it varies, as the intensity of a Raman line is directly proportional to the ion giving rise to it. The first attempt in this direction was made by Koteswaram (1938), who, on studying the Raman spectrum of sulphuric acid at 30°C and 200°C, concluded that the acid ionises more at 200°C than at 30°C. The present work describes a similar study in nitric acid.

FACTORS TO BE TAKEN INTO ACCOUNT IN STUDYING THE DISSOCIATION OF THE ACID BY THIS METHOD

The Raman spectrum of nitric acid consists of two sets of lines corresponding respectively to the NO_3' ions and the undissociated HNO_3 molecules. The line of Raman frequency 1050 is the most intense of the first set, while that of Raman frequency 1300 is the strongest of the second set. It was first observed by I. R. Rao (1930) that as the concentration of the acid is decreased, the first set of the lines brighten up while the intensity of the latter decreases, therby showing that the acid progressively dissociates with increasing dilution. The first set of lines were observed in the spectra of the nitrates also. It was also shown by I. R. Rao (1934) that in the case of the alkali nitrates, the intensity of the 1050 line is proportional to the concentration, if the Raman spectra for different solutions are taken with equal times of exposure, thereby showing that they are completely dissociated at all concentrations. In a paper published by the author, (Rao, N. R., 1941) in which the details of the calculations are given, this result was made use of to calculate the actual degree of dissociation of the acid at various concentrations, by comparing the intensities of the 1050 line in the spectra of the nitrate solution and the acid.

To study the variation of the degree of dissociation with temperature, one may be tempted to assume that the relative intensities of particular Raman line in the spectra taken with the acid at different temperatures are a measure of the relative proportions of the radicals giving rise to this line, similar to what was done by Rao (1941) while studying its dissociation at different dilutions. This is justified only if the specific intensity (the intensity corresponding to each molecule) of a Raman line is independent of temperature. But, it is well known that there is a variation of this intensity according to the formula (Kohlrausch, 1931).

$$I\gamma \propto (\nu - d\nu)^4 \left(1 - e^{\frac{-hd\nu}{kT}}\right)^{-1}$$

Thus, a correction is necessary for this variation, to obtain the correct value of the intensity of a Raman line as a function of the number of molecules giving rise to it.

This correction is, however, eliminated by the author from the following considerations. What is required for the estimation of the degree of dissociation is the ratio of the number of the dissociated to the total number of the molecules of the acid. As was already pointed out, there are two prominent lines in the Raman spectrum of nitric acid, one of frequency 1050 and the other of 1300 characteristic of NO_3 and the HNO_3 radicals respectively. As the temperature of the acid is increased, the ratio of the intensities of these lines varies. This variation is taken as a measure of the change in the degree of dissociation.

But this is justified only if the variation in the ratio of the specific intensities of the lines with temperature is very small as otherwise it cannot be ascertained as to what proportion of this variation in the ratio is due to the change in the relative abundance of the NO_3 and the HNO_3 radicals and what due to the intrinsic change in the specific intensities of the radicals.

Let $I d\nu$ be the intensity of the 1050 line and $I d\nu'$ that of the 1300 line, then

$$I d\nu \propto (\nu - d\nu)^4 \left(1 - e^{\frac{-hd\nu}{kT}}\right)^{-1}$$

$$I d\nu' \propto (\nu - d\nu')^4 \left(1 - e^{\frac{-hd\nu'}{kT}}\right)^{-1}$$

Since $e^{\frac{-hd\nu}{kT}}$ is small compared to 1,

$$\frac{Id\nu}{Id\nu'} = \left(\frac{\nu - d\nu}{\nu - d\nu'}\right)^4 \left(1 + e^{\frac{-hd\nu}{kT}} - e^{\frac{-hd\nu'}{kT}}\right)$$

Now the expression $e^{\frac{-hd\nu}{kT}} - e^{\frac{-hd\nu'}{kT}}$ which is a difference between two small quantities that are nearly equal, is much smaller than the individual expressions. So, the variation of the ratio of the specific intensities of the lines is much smaller than their individual variation with temperature and it can be safely assumed that the ratio of the specific intensities of the lines under question is independent of temperature. This is borne out by the experimental investigations carried out in this laboratory in the case of many substances and by the quantitative measurements of the intensities of the lines in crystals made by Venkateswarlu (1942). So, any variation in the relative intensities with temperature must be due only to the change in the relative abundance of the radicals NO_3 and HNO_3 and the assumption, on the basis of which the degree of dissociation is proposed to be determined, is justified.

Now, for a fairly accurate determination of the dissociation of the acid by determining the relative intensities of the lines 1050 and 1300, the lines must be of the same order of intensity. But, as the concentration of the acid is decreased, the 1300 line characteristic of the undissociated molecules, falls off rapidly in intensity and below a concentration of about 10N the intensities of the two lines are far different from each other. Therefore, solutions of concentration below 10N cannot be studied by this method. Above about 16N, the acid gets very much coloured even by a slight rise in the temperature. Therefore only concentrations intermediate between these two limits, *viz.*, 14.50N 12.58N and 10.5N are chosen for investigation. They are studied at three temperatures 30°C, 60°C and 90°C. The solution of concentration 12.58N is studied at 5°C also.

EXPERIMENTAL

The experimental arrangement is the same as that described in a previous paper (Rao, N. R., 1940). To study the acid at higher temperatures, the copper jacket surrounding the Wood's tube is heated by a burner and the rate of flow of water and the gas adjusted to get the required steady temperature varying by not more than 5°. To work at 5°C, water cooled by large quantities of powdered ice in a trough is siphoned into the copper jacket. The mist condensed on the face of the Wood's tube is found to drain off as quickly as it is formed if the face is cleaned absolutely free from grease.

The intensities of the lines 1050 and 1300 are measured by the usual method and the degree of dissociation calculated by the following method.

CALCULATION OF THE DEGREE OF DISSOCIATION

It was suggested in a previous paper (Rao, N. R., *loc. cit.*) that the absolute degree of dissociation of the acid can be calculated by comparing the intensity of the 1050 line in the spectrum of the acid with that in an alkali nitrate solution which is assumed to be completely dissociated. If I is the intensity of the 1050 line in the spectrum of the nitrate of concentration c gm. moles. per litre, then $I/c = a$ is the intensity corresponding to one gm. mole. of NO_3 ions. If I_1, is the intensity of this line in the acid, then $I_1/\frac{I}{c} = n_1$ gives in gram-molecules the number of NO_3 ions in the acid. Subtracting n_1 from the total number of acid molecules, the number of undissociated HNO_3 molecules n_2 is obtained. While $I_1/n_1 = a$ gives the specific intensity of the NO_3 ion, $I_2/n_2 = b$ gives the specific intensity of the HNO_3 molecule where I_2 is the intensity of the 1300 line and n_2 the number of undissociated molecules. Knowing I_1, I_2 and n_1 and n_2 for one of the concentrations of the acid (a/b) is calculated. Then, the degree of dissociation

$$\alpha = \frac{n_1}{n_1 + n_2} = 1 \Big/ \left(\frac{I_2}{I_1} \cdot \frac{a}{b} + 1 \right).$$

Now, it was shown previously that (a/b), the ratio of the specific intensities can be assumed to be independent of temperature. It can also be easily seen that it is independent of concentration of the acid or of the time of exposure. It also does not vary even if the solution is slightly coloured, since the lines are very close to each other and it can be assumed that both of them will be absorbed to the same extent. Once this ratio is determined for any one convenient concentration, the value of α for any other concentration can be calculated from the ratio I_1/I_2 for this concentration. The advantage of this method is that the spectra of the solutions of the nitrate and the acid need not be taken on the same plate, every time the degree of dissociation of the acid of any particular concentration is required, and it does not matter even if the acid is slightly coloured. But, the value of this ratio (a/b) thus determined is subjected to a small error for the following reasons. The intensity of the 1300 line falls off rapidly on dilution. Therefore, only concentrated solutions which cannot be obtained in a perfectly colourless condition must be worked with, and while comparing the intensity of the 1050 line in the acid and in the nitrate solution, an error due to absorption in the case of the acid will be incurred though this error is very small and can be practically neglected, compared to the inaccuracy involved in the determination of the intensities of the Raman lines. But the absorption in the case of the 1300 line does not bring in any error at all in the calculation of the dissociation as what matters is the relative absorptions of the 1050 and the 1300 lines. It is found by a seperate experiment that the two lines are absorbed to the same extent. The intensities of the 1050 and 1300 lines are determined and the corresponding values of α for different temperatures are calculated and given in table I.

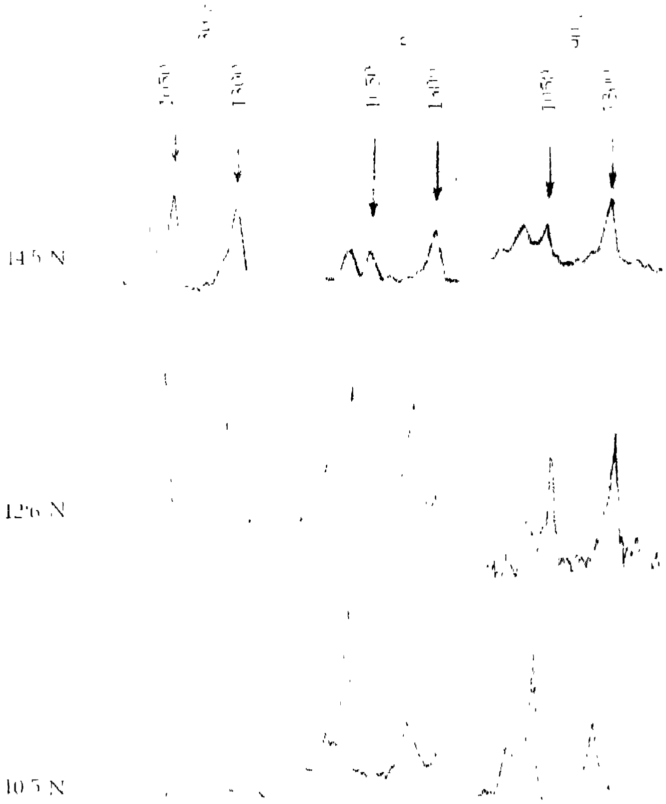

Nitric Acid

TABLE I

Percentage degree of dissociation α at various temperatures and concentrations.

Temperature / Concentration in N.	30°C	60°C	90°C
14.50N	11.4	9.5	3.2
12.58N	21.2	15.5	10.5
10.5N	35.2	30.0	22.6

The dissociation of the acid of concentration 12.58N at 5°C is found to be 29.6%.

DISCUSSION

It is clearly seen from the table that the dissociation of the acid decreases with temperature, probably due to the decrease of dielectric constant of water with temperature. This is clearly demonstrated in the microphotometric records of the spectra of the acid of different concentrations at different temperatures reproduced in Plate VII. As the temperature of the acid is increased the line at 1050 gradually decreases in intensity while that at 1300 correspondingly gets more intense.

But it is well known that the conductivity of the acid increases as its temperature is raised at all concentrations. This increase must be due to the large increase in the ionic mobility with temperature which more than compensates for the decrease in the conductivity due to the decrease in the dissociation of the acid.

In conclusion, the author wishes to express his grateful thanks to Dr. I. Ramakrishna Rao under whose direction this work is done.

DEPERTMENT OF PHYSICS,
ANDHRA UNIVERSITY, GUNTUR.

REFERENCES

Kohlrausch, K. W. F., 1931, *Smekal Raman Effect*, pp. 99.
Koteswaran, P., 1938, *Ind. Journ. Phys.*, **12**, 299.
Rao, I. R., 1930, *Proc. Roy. Soc. (London)*, **127**, 279.
,, ,, ,, ,, *(Amsterdam)*, **33**, 632.
,, . 1934, *Proc. Roy. Soc. (London)*, **144**, 159.
Rao, N. R., 1940, *Ind. Journ. Phys*, **14**, 143.
,, 1941, *Ind. Journ. Phys.*, **26**, 185.
Venkateswarlu, K., 1942, *Proc. Ind. Acad. Sci.*

A NOTE ON DIRAC EQUATIONS AND THE ZEEMAN EFFECT

By S. N. BOSE

AND

K. BASU

(*Received for publication, Sept. 22, 1943*)

ABSTRACT. A new treatment has been given for solving Dirac's equations for hydrogenic atoms, and the radial functions are expressed in terms of a combination of Sonine's polynomials $T_n^{(\mu)}(\rho)$, $T_{n-1}^{(\mu)}(\rho)$ of only two consecutive degrees n, $n-1$; and the elementary properties of such polynomials have enabled us to tackle the Zeeman effect problem in general (homogeneous field) leading to the standard quadratic equation in energy for the effect

1. With the help of the two-dimensional matrices s_x, s_y, s_z of Pauli, the wave-equations of Dirac can be put in the well-known matrix form:

$$(1.1)\qquad \frac{\iota}{\mathbf{h}c}\left[E+E_0+\frac{Ze^2}{r}\right]X+DY=0,\quad \frac{\iota}{\mathbf{h}c}\left[E-E_0+\frac{Ze^2}{r}\right]Y+DX=0$$

where D is the operator $\quad s_x\dfrac{\partial}{\partial x}+s_y\dfrac{\partial}{\partial y}+s_z\dfrac{\partial}{\partial z}$.

If, similarly $S=xs_x+ys_y+zs_z$, and $s=\frac{1}{r}(xs_x+ys_y+zs_z)$, then

$S.\,D.=r\dfrac{d}{dr}+L$, where $L=\iota(M_xs_x+M_ys_y+M_zs_z)$.

And the following commutation rules can be easily deduced:

$$s(L-1)+(L-1)s=0,\quad D(L-1)+(L-1)D=0;$$

also $\qquad s^2\equiv 1$.

Hence multiplying the equations on the left by S we have

$$(1.2)\qquad \frac{\iota}{\mathbf{h}c}\left[E+E_0+\frac{Ze^2}{r}\right]SX+\left[r\frac{d}{dr}+1\right]Y+(L-1)Y=0;$$

$$\frac{\iota}{\mathbf{h}c}\left[E-E_0+\frac{Ze^2}{r}\right]SY+\left[r\frac{d}{dr}+1\right]X+(L-1)X=0.$$

Assuming $X\equiv\begin{vmatrix}u_1\\u_2\end{vmatrix}=\dfrac{f(r)}{r}\Phi$; $Y\equiv\begin{vmatrix}u_3\\u_4\end{vmatrix}=\dfrac{g(r)}{r}\Psi$ where Φ, Ψ are similar one-column matrices and functions of (θ, ϕ), the equations can be rewritten as

$$\frac{\iota}{\mathbf{h}c} f(r)\left[E + E_0 + \frac{Ze^2}{r}\right] s\Phi + \frac{dg(r)}{dr}\cdot\Psi + \frac{g(r)}{r}(L-1)\Psi = 0, \tag{1.3}$$

$$\frac{\iota}{\mathbf{h}c} g(r)\left[E - E_0 + \frac{Ze^2}{r}\right] s\Psi + \frac{df(r)}{dr}\cdot\Phi + \frac{f(r)}{r}(L-1)\Phi = 0.$$

The equations become easily separable if the matrices Φ and Ψ are so chosen that at first $(L-1)\Psi = k\Psi$ and $s\Phi = \Psi$; and as $s^2 \equiv 1$, it follows therefore from commutation rules that

$$\Phi = s\Psi \text{ and } (L-1)\, s\Psi = -k\, s\Psi.$$

We observe at once that $L(L-1)\Psi = -\nabla_2\Psi = k(k+1)\Psi$, where

$$\nabla_2 \equiv \frac{1}{\sin\theta}\frac{\partial}{\partial\theta}\left(\sin\theta\frac{\partial}{\partial\theta}\right) + \frac{1}{\sin^2\theta}\frac{\partial^2}{\partial\phi^2};$$

and therefore k can be either a positive or a negative integer.

Secondly, if (Φ, Ψ) are the matrices for positive k, then (Ψ, Φ) are the matrices for negative k. Also remembering that the operator

$$-\left[\iota\left(x\frac{\partial}{\partial y} - y\frac{\partial}{\partial x}\right) + \frac{1}{2}s_z\right]$$

commutes with the equation-system, the angular matrices can be expressed in terms of spherical harmonics of order k and $k-1$ in the following form:

$$\Phi \equiv \begin{pmatrix} \sqrt{\frac{k+m}{2k-1}}\; Y^{\mu}_{k-1} \\[2ex] \sqrt{\frac{k-m-1}{2k-1}}\; Y^{\mu+1}_{k-1} \end{pmatrix}, \quad \Psi \equiv \begin{pmatrix} \sqrt{\frac{k-m}{2k+1}}\; Y^{\mu}_{k} \\[2ex] \sqrt{\frac{k+m+1}{2k+1}}\; Y^{\mu+1}_{k} \end{pmatrix} \quad (k, \text{ a positive integer}) \tag{1.4}$$

where $Y^{\mu}_{k} \equiv \sqrt{\frac{2k+1}{2}\cdot\frac{(k-\mu)!}{(k+\mu)!}}\;\frac{1}{2^k k!}\;\frac{d^{k+\mu}}{dx^{k+\mu}}(x^2-1)^k\;\frac{e^{i\mu\phi}}{\sqrt{2\pi}}$. $(x = \cos\theta)$

The functions are interchanged for negative values of k. Writing $f(r) = \iota F(r)$ so as to remove the imaginary from the radial equations, we get

$$\left[\frac{dG}{dr} + k\frac{G}{r}\right] - \frac{1}{\mathbf{h}c}\left[E + E_0 + \frac{Ze^2}{r}\right]F = 0, \tag{1.5}$$

$$\left[\frac{dF}{dr} - k\frac{F}{r}\right] + \frac{1}{\mathbf{h}c}\left[E - E_0 + \frac{Ze^2}{r}\right]G = 0.$$

2. To solve the equations we assume

$$F = f_0 e^{-\lambda r} r^{\mu} F_1(r),\quad G = g_0 e^{-\lambda r} r^{\mu} G_1(r),\ \text{and } N = \alpha E/(E_0^2 - E^2)^{\frac{1}{2}} \tag{2.1}$$

where $Ze^2/\mathbf{h}c = \alpha$.

Substituting in (1.5), F_1 and G_1 are easily seen to satisfy the following equations:

$$(2.2)\qquad \begin{aligned} &\frac{dG_1}{dr} - \lambda G_1 + \lambda F_1 + \frac{k+\mu}{r}G_1 + \frac{N}{E}(E_0 - E)\frac{F_1}{r} = 0,\\ &\frac{dF_1}{dr} - \lambda F_1 + \lambda G_1 - \frac{k-\mu}{r}F_1 - \frac{N}{E}(E_0 + E)\frac{G_1}{r} = 0, \end{aligned}$$

$$(2.3)\qquad \text{where } f_0/g_0 = -(E_0 - E)/\mathbf{h}c\lambda = \frac{\lambda \mathbf{h}c}{E_0 + E} = -\left(\frac{E_0 - E}{E_0 + E}\right)^{\frac{1}{2}} \text{ and } \lambda = \left(\frac{E_0^2 - E^2}{\mathbf{h}c}\right)^{\frac{1}{2}}$$

If $F_1 + G_1 = 2\chi^+$, $G_1 - F_1 = 2\chi^-$, elimination leads easily to the following equations:

$$(2.4)\qquad r\frac{d^2\chi^+}{dr^2} + (2\mu + 1 - 2\lambda r)\frac{d\chi^+}{dr} + 2\lambda(N - \mu)\chi^+ = 0,$$

$$(2.5)\qquad r\frac{d\chi^+}{dr} - (N - \mu)\chi^+ = \left(N\frac{E_0}{E} - k\right)\chi^-,$$

provided $\qquad k^2 - \mu^2 = N^2(E_0^2 - E^2)/E^2 = \alpha^2.$

Taking the first equation it can be easily seen that it admits of polynomial solutions if $N - \mu = n$ (an integer). Writing ρ for $2\lambda r$, and writing a Sonine polynomial in the form

$$T_n^{(\mu)}(\rho) = B_n^{(\mu)}\left[\rho^n - \frac{n(n+2\mu)}{1!}\rho^{n-1} + \frac{n(n-1)(n+2\mu)(n+2\mu-1)}{2!}\rho^{n-2} - \dots\dots\right]$$

$$(2.6)\qquad = B_n^{(\mu)}(-1)^n e^{\rho}\rho^{-2\mu}\frac{d^n}{d\rho^n}\left[e^{-\rho}\rho^{n+2\mu}\right]$$

with constant $B_n^{(\mu)}$ so chosen that it is normalized according to

$$\int_0^\infty e^{-\rho}\rho^{2\mu}T_n^{(\mu)}(\rho)T_n^{(\mu)}(\rho)d\rho = 1$$

we get $B_n^{(\mu)} = 1/\{n!\Gamma(n + 2\mu + 1)\}^{\frac{1}{2}}$.

Hence it easily follows that χ^+ and χ^- will have solutions as given below:

$$(2.7)\qquad \chi^+ = \delta\left(N\frac{E_0}{E} - k\right)^{\frac{1}{2}}T_n^{(\mu)}(\rho)$$

$$(2.8)\qquad \chi^- = \delta\left(N\frac{E_0}{E} + k\right)^{\frac{1}{2}}T_{n-1}^{(\mu)}(\rho)$$

$$\left[N = n + \mu = \frac{\alpha}{\sqrt{1 - \epsilon^2}}\ ;\ \epsilon = \frac{E}{E_0}\right]$$

where the normalising factor δ is to be determined presently.

Our radial functions of eqs. (2.1) stand thus

$$(2.9)\qquad F = -\delta\sqrt{\left(1 - \frac{E}{E_0}\right)}e^{-\frac{\rho}{2}}\rho^{\mu}\left[\left(N\frac{E_0}{E} - k\right)^{\frac{1}{2}}T_n^{(\mu)}(\rho) - \left(N\frac{E_0}{E} + k\right)^{\frac{1}{2}}T_{n-1}^{(\mu)}(\rho)\right]$$

$$(2.10)\qquad G = \delta\sqrt{\left(1 + \frac{E_0}{E_0}\right)}e^{-\frac{\rho}{2}}\rho^{\mu}\left[\left(N\frac{E_0}{E} - k\right)^{\frac{1}{2}}T_n^{(\mu)}(\rho) + \left(N\frac{E_0}{E} + k\right)^{\frac{1}{2}}T_{n-1}^{(\mu)}(\rho)\right]$$

Normalisation requires

$$\int^{\infty} (F^2+G^2)\,dr = 1,$$

which gives
$$\delta = \sqrt{\frac{\lambda}{2N}\,\frac{E}{E_0}}.$$

We can write the two solutions (A) and (B), corresponding to positive and negative values of k respectively.

$$
(A)\quad
\begin{array}{|ll|}
u_1 = \sqrt{\frac{k+\mu}{2k-1}}\; i\,\frac{f_+(r)}{r}\,Y^{\mu}_{k-1}, & u_3 = \sqrt{\frac{k-\mu}{2k+1}}\;\frac{g_+(r)}{r}\,Y^{\mu}_{k} \\
u_2 = -\sqrt{\frac{k-\mu-1}{2k-1}}\; i\,\frac{f_+(r)}{r}\,Y^{\mu+1}_{k-1}, & u_4 = \sqrt{\frac{k+\mu+1}{2k+1}}\;\frac{g_+(r)}{r}\,Y^{\mu+1}_{k}
\end{array}
$$

$$
(B)\quad
\begin{array}{|ll|}
v_1 = \sqrt{\frac{k-\mu}{2k+1}}\; i\,\frac{f_-(r)}{r}\,Y^{\mu}_{k}, & v_3 = \sqrt{\frac{k+\mu}{2k-1}}\;\frac{g_-(r)}{r}\,Y^{\mu}_{k-1} \\
v_2 = \sqrt{\frac{k+\mu+1}{2k+1}}\; i\,\frac{f_-(r)}{r}\,Y^{\mu+1}_{k}, & v_4 = -\sqrt{\frac{k-\mu-1}{2k-1}}\;\frac{g_-(r)}{r}\,Y^{\mu+1}_{k-1}
\end{array}
$$

wherein it is understood that f_- and g_- are obtained by changing the sign of k, in the expressions for F and G in (1.5) above.

3. When the atom is in an electromagnetic field defined by the vector-potential $(A_x A_y A_z)$, the Dirac-equations become

$$(3.1)\qquad \frac{i}{\mathbf{h}c}\left[E+E_0+\frac{Ze^2}{r}\right]X + DY + \frac{e}{\mathbf{h}c}AY = 0$$

$$(3.2)\qquad \frac{i}{\mathbf{h}c}\left[E-E_0+\frac{Ze^2}{r}\right]Y + DX + \frac{e}{\mathbf{h}c}AX = 0$$

where
$$A = i\,[A_x s_x + A_y s_y + A_z s_z]$$

In the case of a constant magnetic field H, in the direction of Z-axis

$$(3.3)\qquad A = \tfrac{1}{2}Hr \begin{vmatrix} 0 & e^{-i\mu\phi}\sin\theta \\ -e^{i\mu\phi}\sin\theta & 0 \end{vmatrix} = \tfrac{1}{2}Hr\mathbf{a}.$$

We observe in passing that in the absence of A, the wave function X is generally small compared with Y—the radial component of $F(r)$ has the factor $\sqrt{1-\frac{E}{E_0}}$, while $G(r)$ has $\sqrt{1+\frac{E}{E_0}}$; so that the perturbation effect of $\frac{e}{\mathbf{h}c}AX$ is small as compared with effect due to the term $\frac{e}{\mathbf{h}c}AY$ in eq. (3.1).

Remembering

$$e^{-\iota\phi}\, Y_k^{\mu+1} \sin\theta = -\sqrt{\frac{(k-\mu)(k-\mu+1)}{(2k+1)(2k+3)}}\, Y_{k+1}^{\mu} + \sqrt{\frac{(k+\mu)(k+\mu+1)}{(2k+1)(2k-1)}}\, Y_{k-1}^{\mu};$$

$$e^{\iota\phi}\, Y_k^{\mu} \sin\theta = \sqrt{\frac{(k+\mu+1)(k+\mu+2)}{(2k+1)(2k+3)}}\, Y_{k+1}^{\mu+1} - \sqrt{\frac{(k-\mu)(k-\mu-1)}{(2k-1)(2k+1)}}\, Y_{k-1}^{\mu+1};$$

we seek an approximate solution of the equation by choosing one set of angular function $(Y_k^{\mu}, Y_k^{\mu+1})$, and assuming the existence of both the sets $(Y_{k-1}^{\mu}, Y_{k-1}^{\mu+1})$ and $(Y_{k+1}^{\mu}, Y_{k+1}^{\mu+1})$ in X. This can be done by suitably combining the (A) and (B) types, thus

Take $u_j = C_l^+ u_j^+ + C_{-(l+1)}^- v_j^-$, $(j = 1, 2, 3, 4)$, where $(u_1^+, u_2^+, u_3^+, u_4^+)$ corresponds to $k = +l$; and $(v_1^-, v_2^-, v_3^-, v_4^-)$ corresponds to $k = -(l+1)$. More explicitly, their values are

$$u_1^+ = \sqrt{\frac{l+\mu}{2l-1}}\ \iota\, \frac{f_+(r)}{r}\, Y_{l-1}^{\mu}; \qquad v_1^- = \sqrt{\frac{l-\mu+1}{2l+3}}\, Y_{l+1}^{\mu}\ \iota\, \frac{f_-(r)}{r};$$

$$u_2^+ = -\sqrt{\frac{l-\mu-1}{2l-1}}\ \iota\, \frac{f_+(r)}{r}\, Y_{l-1}^{\mu+1}, \quad v_2^- = \sqrt{\frac{l+\mu+2}{2l+3}}\, Y_{l+1}^{\mu+1}\ \iota\, \frac{f_-(r)}{r};$$

$$u_3^+ = \sqrt{\frac{l-\mu}{2l+1}}\, \frac{g_+(r)}{r}\, Y_l^{\mu}; \qquad v_3^- = \sqrt{\frac{l+\mu+1}{2l+1}}\, \frac{g_-(r)}{r}\, Y_l^{\mu};$$

$$u_4^+ = \sqrt{\frac{l+\mu+1}{2l+1}}\, \frac{g_+(r)}{r}\, Y_l^{\mu+1}; \qquad v_4^- = -\sqrt{\frac{l-\mu}{2l+1}}\, \frac{g_-(r)}{r}\, Y_l^{\mu+1}.$$

The constants λ, N, μ of the two types of solutions are different and are expressed by the following relations

$$(3.4) \qquad \lambda_+ = (E_0^2 - E_+^2)^{\frac{1}{2}}/\mathbf{h}c,\ l^2 - \alpha^2 = \mu_+^2,\ N_+ = \alpha E_+/[E_0^2 - E_+^2]^{\frac{1}{2}},$$

and $\qquad N_+ = n_+ + \mu_+$ [for (A) – type with $k = l$].

$$(3.5) \qquad \lambda_- = (E_0^2 - E_-^2)^{\frac{1}{2}}/\mathbf{h}c),\ (l+1)^2 - \alpha^2 = \mu_-^2,\ N_- = \alpha E_-/[E_0^2 - E_-^2]^{\frac{1}{2}},$$

and $\qquad N_- = n_- + \mu_-$ [for (B) – type with $k = -(l+1)$].

If E_+ and E_- differ slightly from one another, we have the following approximate relations

$$(3.6) \qquad \lambda_+ = \lambda_-,\ \mu_- = \mu_+ + 1,\ N_+ = N_-,\ n_- = n_+ - 1, \text{ and } \frac{E_+ - E_-}{E_0} \ll 1.$$

By following the usual method of perturbation we see easily that the characteristic equation for determining the Eigen value E would be

$$(3.7) \qquad \begin{vmatrix} \dfrac{\iota}{\mathbf{h}c}\left[E - E_+\right] + p\alpha_{11} & p\alpha_{12} \\ p\alpha_{21} & \dfrac{\iota}{\mathbf{h}c}\left[E - E_-\right] + p\alpha_{22} \end{vmatrix} = 0$$

where $p = eH/2\mathbf{h}c$, and

$$
\begin{aligned}
a_{11} &= \int \left[X_+^* \, r\mathbf{a}Y_+ + Y_+^* \, r\mathbf{a}X_+ \right] dV \\
a_{22} &= \int \left[X_-^* \, r\mathbf{a}Y_- + Y_-^* \, r\mathbf{a}X_- \right] dV \\
a_{12} &= \int \left[X_+^* \, r\mathbf{a}Y_- + Y_+^* \, r\mathbf{a}X_- \right] dV \\
a_{21} &= \int \left[X_-^* \, r\mathbf{a}Y_+ + Y_-^* \, r\mathbf{a}X_+ \right] dV
\end{aligned}
\tag{3.8}
$$

and X_+^* etc. are transposed conjugates of X_+ (the **a** is given in (3.3))

Carrying out integrations over the angle-variable-space we get

$$a_{11} = -\frac{2i(4\mu+2)\,l}{(2l-1)(2l+1)} \int_0^\infty r f_+ g_+ \, dr\,;$$

$$a_{22} = \frac{2i(4\mu+2)(l+1)}{(2l+1)(2l+3)} \int_0^\infty r f_- g_- \, dr\,;$$

$$a_{12} = a_{21} = \frac{i\sqrt{(l-\mu)(l+\mu+1)}}{2l+1} \int_0^\infty r(f_- g_+ + f_+ g_-)\, dr.$$

4. To evaluate the integral $\{I\}$ or $\{II\}$, we substitute the values of the corresponding f, g, and remembering $r = \rho/2\lambda$, we obtain

$$
\begin{aligned}
\{I\} = -\frac{\lambda_+}{2N_+}\,\frac{E_+}{E_0^2}\,\frac{(E_0^2-E_+^2)^{\frac{1}{2}}}{4\lambda^2}\Bigg\{ &\left(N_+\frac{E_0}{E_+} - k\right)\int_0^\infty e^{-\rho}\rho^{2\mu+1}\left[T_n^{(\mu)}(\rho)\right]^2 d\rho \\
&- \left(N_+\frac{E_0}{E_+} + k\right)\int_0^\infty e^{-\rho}\rho^{2\mu+1}\left[T_{n-1}^{(\mu)}(\rho)\right]^2 d\rho \Bigg\}.
\end{aligned}
$$

The integrals are evaluated quickly by repeated partial integrations ; thus

$$
\begin{aligned}
\int_0^\infty e^{-\rho}\rho^{2\mu+1}\left|T_n^{(\mu)}(\rho)\right|^2 d\rho &= \frac{(-)^n}{\sqrt{n!\,\Gamma(n+2\mu+1)}}\int_0^\infty \rho T_n^{(\mu)}(\rho)\,\frac{d^n}{d\rho^n}\left[e^{-\rho}\rho^{2\mu+n}\right]d\rho \\
&= \int_0^\infty e^{-\rho}\,\frac{\rho^{2\mu+n}}{n!\;\Gamma(n+2\mu+1)}\,d\rho .\ \frac{d^n}{d\rho^n}\left[\rho\left(\rho^n - \frac{n(n+2\mu)}{1!}\rho^{n-1} + \dots\right)\right]_- \\
&= (n+1)(n+2\mu+1) - n(n+2\mu) = 2N_+ + 1.
\end{aligned}
$$

Similarly

$$\int_0^\infty e^{-\rho}\rho^{2\mu+1}\left[T_{n-1}^{(\mu)}(\rho)\right]^2 d\rho = 2N_+ - 1.$$

An easy substitution of the value of λ_+ in the foregoing leads to the following results :

$$\int_0^\infty r f_+ g_+ \, dr = -\frac{\mathbf{h}c}{4E_0}\left(1 - 2l\frac{E_0}{E_+}\right); \tag{4.1}$$

$$(4.2)\qquad \int_0^\infty r f_- g_- dr = -\frac{\mathbf{h}c}{4E_0}\left(1+2(l+1)\frac{E_0}{E_-}\right).$$

The evaluation of the third integral cannot, however, be exactly expressed in a neat form; for the simple reason that λ_+, N_+, E_+ as well as λ_-, N_-, E_- are different in the two solutions, as also $\rho_+ = 2\lambda_+ r$ and $\rho_- = 2\lambda_- r$. If, however, we introduce approximations in the beginning, and take

$$(4.3)\qquad \lambda_+ = \lambda_- = |\lambda|,\ E_+ = E_-,\ \mu_- = \mu_+ + 1,\ n_- = n_+ - 1,\ \rho_+ = \rho_-,$$

we see the third integral

$$\{III\} = -\frac{2|\lambda|}{2N}\frac{|E|}{E_0^2}\frac{(E_0^2-|E|^2)^{\frac{1}{2}}}{4|\lambda|^2}\left\{\left(N\frac{E_0}{E}-l\right)^{\frac{1}{2}}\left(N\frac{E_0}{E}+l+1\right)^{\frac{1}{2}}\times\right.$$
$$\int_0^\infty e^{-\rho}\rho^{2\mu+2}T_n^{(\mu)}(\rho)T_{n-1}^{(\mu+1)}(\rho)d\rho-\left(N\frac{E_0}{E}+l\right)^{\frac{1}{2}}\left(N\frac{E_0}{E}-l-1\right)^{\frac{1}{2}}$$
$$\left.\times\int_0^\infty e^{-\rho}\rho^{2\mu+2}T_{n-1}^{(\mu)}(\rho)T_{n-2}^{(\mu+2)}(\rho)d\rho\right\}.$$

The two definite integrals can be easily evaluated in the same way as before. We give the results below.

$$(4.4)\qquad \int_0^\infty e^{-\rho}\rho^{2\mu+2}T_n^{(\mu)}(\rho)T_{n-1}^{(\mu+1)}(\rho)d\rho = \int_0^\infty \frac{e^{-\rho}\rho^{n+2\mu}}{\sqrt{\,n-1\,!\,n\,!\,\Gamma(n+2\mu+1)\Gamma(n+2\mu+2)}}$$
$$\times\frac{d^n}{d\rho^n}\left[\rho^{n+1}-(n-1)(n+2\mu+1)\rho^n+\ldots\right] = 2\sqrt{(N-l)(N+l+1)}.$$

$$(4.5)\qquad \int_0^\infty e^{-\rho}\rho^{2\mu+2}T_{n-1}^{(\mu)}(\rho)T_{n-2}^{(\mu+1)}d\rho = 2\sqrt{(N+l)(N-l-1)}.$$

Hence

$$\{III\} = -\frac{1}{2N}\frac{\mathbf{h}c}{E_0}\left[\sqrt{N\frac{E_0}{E}-l}\ \sqrt{N\frac{E_0}{E}+l+1}\ \sqrt{N-l}\ \sqrt{N+l+1}\right.$$
$$\left.-\sqrt{N\frac{E_0}{E}+l}\ \sqrt{N\frac{E_0}{E}-l-1}\ \sqrt{N+l}\ \sqrt{N-l-1}\right].$$

Observing $E_0/E \rightarrow 1$, we see

$$\{III\} = -\frac{1}{2N}\cdot\frac{\mathbf{h}c}{E_0}2N = -\frac{\mathbf{h}c}{E_0}.$$

Finally, putting $p = eH/2\mathbf{h}c$, and $e\mathbf{h}/2m_0c = \mu_0$ (Bohr-magneton) and substituting the values of the three integrals (and making $E_0/E \rightarrow 1$) we see that the determinantal equation (3.7) takes the form

$$(4.6)\qquad \begin{vmatrix} E-E_+-\frac{2l}{2l+1}m\mu_0H & -\frac{\mu_0H}{2l+1}\sqrt{(l-m+\frac{1}{2})(l+m+\frac{1}{2})} \\ -\frac{\mu_0H}{2l+1}\sqrt{(l-m+\frac{1}{2})(l+m+\frac{1}{2})} & E-E_--\frac{2l+2}{2l+1}m\mu_0H \end{vmatrix} = 0$$

wherein we have put $\mu+\frac{1}{2}=m$ (magnetic quantum number).

The result (4.6) agrees completely with that quoted by Bethe (1933) supposed to have been worked out by him from Pauli's equations. Condon and Shortley (1935) obtained similar determinant from principles of quantum mechanics by applying two-fold perturbations (spin-orbit and magnetic) simultaneously. It may be noted that Darwin (1928) has many similar features with our mode of attack, and we can claim some elegance by our introduction of Sonine's properties, which exhibit our solutions in a good perspective.

DACCA UNIVERSITY,
RAMNA, DACCA.

CALCUTTA UNIVERSITY,
92, UPPER CIRCULAR ROAD, CALCUTTA.

REFERENCES

Bethe, H., 1933, *Handbuch der Physik*, **24**, p. 306.

Condon, E. U. and Shortley, G. H., 1935, *The Theory of Atomic Spectra* (Cambridge University Press), p. 233.

Darwin, C. G., 1928, *Proc. Roy. Soc.*, London (A), **118** p. 654-680.

INFLUENCE OF TEMPERATURE ON THE INTENSITIES OF RAMAN LINES DUE TO SOME ORGANIC LIQUIDS

By S. C. SIRKAR

AND

S. B. SANYAL

(Received for publication, October 26, 1945)

ABSTRACT The intensities of a few Raman lines of benzyl alcohol, benzyl amine and benzoyl chloride at the room temperature and at higher temperatures, a few degrees below the boiling points of the liquids, have been measured quantitatively, using the method of photographic spectrophotometry. It has been observed that in the case of the lines 616, 794 and 1003 of benzyl alcohol and of the line 1003 of benzoyl chloride, the intensities increase with the increase of temperature in accordance with the predictions of the polarisability theory. In the case of the Raman lines of larger frequency-shifts the intensities are observed to remain almost constant with the increase in the temperature of the liquids as indicated by the said theory.

INTRODUCTION

It is well known that according to the theory put forward by Placzek (1931) the intensity of the Raman lines of frequencies $\nu-\nu_i$ should increase with the temperature in accordance with the relation $I_{(\nu-\nu_i)} \propto 1/(1-e^{-h\nu_i/kT})$ ... (1) Several attempts have been made to test the correctness of these predictions of the theory besides those regarding the ratio of the intensities of the Stokes and anti-Stokes Raman lines. Before this theory was published, Landsberg and Mandelstam (1930) had investigated the intensities of Raman line 465 of quartz at temperatures 22°C and 537°C. They observed that the intensity at the higher temperature was 1.29 times that at the lower temperature. The same problem was also studied qualitatively by Ney (1931) who reported that the influence of the increase of temperature on the intensities of the Raman lines of quartz was different for different Raman lines, so that the relative intensities of the Raman lines on the Stokes side were observed to change with the increase of temperature of the crystal. The microphotometric curves of the spectrogram reproduced by Ney show that the line 465 of quartz shifts to 458 and its intensity diminishes considerably at the higher temperature. Careful examination of the records, however, also shows that this line becomes much broader at the higher temperature than at the lower temperature. Ornstein and Went (1935), besides measuring the ratio of the intensities of Stokes and anti-Stokes Raman lines, also investigated quantitatively the changes in the intensities of the lines

127 and 465 of quartz with the change of temperature of the crystal from 90°K to 420°K, and of the lines 153, 282, 714 and 1088 of calcite with the change of temperature from 293°K to 426°K. They observed that in the case of both the Raman lines of quartz mentioned above the intensity diminished with the increase of temperature, and the same effect was observed also in the case of the three lines 155, 282 and 714 of calcite, while the intensity of the line 1088 remained constant with the change of temperature. It has not been mentioned by these authors, however, whether they measured the integrated intensity or the peak intensity. It has been pointed out above that the microphotometric records reproduced by Ney indicate a broadening of the line 465 at the higher temperature. Hence the intensity is smaller at the higher temperature than at the lower temperature if the peak intensity is considered, but if the integrated intensity were taken into consideration the conclusion would probably be different, at least for this line.

The same problem was investigated in the case of some crystals more recently by Venkateswarlu (1941). He first studied the intensities of the Raman lines 465 of quartz, 1065 of sodium nitrate and 315 of mercuric chloride at different temperatures and observed in each case a diminution in intensity with the increase of temperature up to about 493°K. He mentioned that the width of the lines did not increase with the increase in temperature and hence only the peak intensities were measured. In a later paper Venkateswarlu (1942) reported the results of similar investigations in the case of calcite. In this case also the intensities of the Raman lines 155, 280, 710 and 1085 of calcite were observed to diminish with the increase of temperature from 305°K up to 493°K. It has been mentioned by him that the lines were of same width at the lower and higher temperatures and so only the peak intensities were measured. If, however, the spectrogram reproduced by him be examined carefully it is found that the line 280 of calcite becomes appreciably broader at higher temperatures. Besides this, the intensities of the Rayleigh lines also appear to diminish at the higher temperatures almost in the same ratio as those of the Raman lines mentioned above. If this be not due to any systematic diminution of the intensity of the incident light at higher temperatures, it is difficult to understand how the intensity of the Rayleigh scattering diminishes with the increase of temperature, because experimentally it has been observed by Landsberg and Mandelstam (1930) that in the case of quartz the intensity of the Rayleigh scattering is proportional to the absolute temperature of the crystal.

The validity of relation (1) in the case of liquids was first tested by Ananthakrishnan (1938) who investigated the intensities of the Raman lines of CCl_4 at temperatures ranging from 25°C to 200°C. He observed that the integrated intensity of the Stokes Raman lines of CCl_4 does not increase with the increase of temperature. He has also discussed various other changes, *e.g.*, broadening, and change of frequency of the Raman lines which are observed with the increase of temperature as well as the difficulties which are experienced in making the experimental conditions identical at both high and low temperatures.

Besides the difficulties mentioned by Ananthakrishnan, *e.g.*, the widening of the lines, the change of refractive index of the liquid causing a change in the intensity of the incident light, and the expansion of the liquid, there is another difficulty not mentioned by him, namely, the birefringence of the window of the tube containing the liquid caused by high pressures developed when the liquid is heated much above its boiling point in the closed tube. The present investigation was undertaken with the object of testing the validity of relation (1) given by Placzek in the case of a few aromatic liquids having high boiling points so that no high pressure could be developed inside the tube containing them. Some of the other sources of error have also been taken into account as will be evident from the discussions of the results.

EXPERIMENTAL

The liquids chosen for the present investigation are benzyl alcohol, benzylamine and benzoyl chloride. These were obtained from Kahlbaum's sealed bottles. They were distilled in vacuum before use. The experimental tube had a plane window and its other end was bent into the form of a horn terminating in a bulb to hold the increased volume of liquid at the higher temperature. A narrow tube was joined to the bulb and after the tube was filled with the distilled liquid upto a level below the bottom of the bulb, the tube was evacuated and a constriction in the narrow tube was sealed off. The heater consisted of a few coils of nichrome wire enclosed between two coaxial brass cylinders, insulated by asbestos and a window was left open parallel to the length of the cylinder. This gap was closed by a transparent thin sheet of mica. The tube was thrust into the heater through one of its mouth and the scattered light was observed through the other mouth, the open regions of which were closed with asbestos packing. Light from a horizontal Heraus type mercury arc condensed by a five-inch glass condenser was used as the incident light which passed through the mica window. The arc was started before the commencement of the exposure and was allowed to run at a stretch undisturbed throughout the exposure for both the hot and the cold liquid. As the room was closed on all sides, the intensity of the arc did not fluctuate during the exposure. Also, as the liquids were heated upto temperatures a few degrees below their boiling points, the plane windows of the experimental tubes did not develop any extra birefringence at the higher temperature. The levels of the liquid in the tail of the experimental tube at the room temperature and at the higher temperatures were noted and from the measured volumes upto these levels the increase in the volume of the liquid was estimated. The temperature was measured with a mercury thermometer which was placed in contact with the glass tube containing the liquid inside the heater.

The Raman spectrum for the hot liquid was photographed first in order to take into account any chemical change in the liquid which might take place with the rise of temperature. The current in the heater was switched off and the spectrum for the cold liquid was next photographed on the same plate using the same time of exposure as for the hot liquid. A few intensity marks were also obtained on the same plate using different known widths of the slit of the spectrograph and light from an ordinary tungsten filament lamp reflected by a piece of thick white paper as source of continuous radiation. A Hilger two-prism spectrograph of high light-gathering power was used. Microphotometric records of the spectrograms were obtained with the help of a Kipp and Zonen self-recording microphotometer. The intensities of the background on both sides of each line relative to the unexposed portion of the plate were determined in the case of each line in question with the help of the blackening log.-intensity curves and were subtracted from the total intensity of both the background and the line in order to obtain the intensity of the line. In the case of each liquid only a selected few Raman lines have been taken into consideration. Also, in order to investigate the question whether the intensity of the Rayleigh lines increases with the increase of the temperature of liquids, the intensities of the line λ4916 recorded at the two temperatures have been compared. The results are discussed in the following section.

RESULTS AND DISCUSSION

The ratios of intensities of particular Raman lines at the higher temperature to the corresponding intensities at the room temperature as deduced from the blackening produced on the plate by the lines with the help of the blackening log-intensity curves for the corresponding wavelengths are given in column 2 of tables I, II and III. These have been corrected for the dilatation of the liquid at the higher temperatures. The correction factors as calculated from the observed increase of volume of the liquids have been found to be approximately 1.09, 1.09 and 1.08 for benzyl alcohol, benzoyl chloride and benzyl amine respectively. The corrected values of the intensities are given in column 3 of the tables. These intensity-ratios as calculated from relation (1) are given in the last column of the tables. Only Raman lines excited by the Hg line λ4358 have been investigated in each case. The ratio of the intensity of the Rayleigh line λ4916 at the higher temperature to that at the room temperature as deduced from the spectrograms has also been entered in the last column of each of the said tables. The widths of the lines investigated are observed to remain unchanged at the higher temperatures and therefore the peak intensity has been measured in each case.

It can be seen from tables I, II and III that the intensity of the Raman lines 610, 794 and 1000 of benzyl alcohol and 1003 of benzoyl chloride increases with the rise of temperature of the liquids and the increase observed in each case is fairly in agreement with that predicted by the theory within experimental error. In the case of the lines 1001 and 3055 of benzyl amine the corrected intensity ratio is slightly lower than the calculated value, but this diminution is probably due to some experimental error, which taking into consideration

TABLE I

Benzyl alcohol. B. P. 478°K

Raman line.	I_{466}/I_{303} observed	I_{466}/I_{303} corrected for dilatation	I_{466}/I_{303} calculated
c-610	1.067	1.10	1.135
c-704	1.00	1.09	1.06
c-1000	0.96	1.05	1.03
c-3050	0.90	0.98	1.00
Rayleigh line 4916	1.05	1.14	...

TABLE II

Benzoyl chloride B. P. 470°K

Raman line.	I_{453}/I_{303} observed	I_{453}/I_{303} corrected for dilatation.	I_{453}/I_{303} calculated
c-1003	0.953	1.04	1.03
c-1592	0.92	1.00	1.004
c-3067	0.90	0.98	1.00
Rayleigh line 4916	1.11	1.21	..

TABLE III

Benzyl amine. B. P. 457°K

Raman line.	I_{436}/I_{303} observed.	I_{436}/I_{303} corrected for dilatation.	I_{436}/I_{303} calculated.
c-1001	0.90	0.97	1.02
c-3055	0.88	0.95	1.00
Rayleigh line 4916	1.08	1.16	...

all the factors involved cannot be claimed to be much less than 5%. The results, however, show that there is no large diminution of the intensities of the Raman lines with the increase in the temperature of the liquids as observed by previous workers in the case of some crystals and also by Ananthakrishnan in the case of carbon tetrachloride. On the contrary, the intensity of the Raman lines of smaller frequency-shift increases more than that of the lines of larger frequency-shift with the rise of temperature of the liquid as indicated by relation (1), and therefore the relative intensities of these lines undergo changes with the change of temperature. The microphotometric records of the lines obtained in the case of benzyl alcohol are reproduced in Fig. 1 and it can be seen that the ratio of the intensity of the line 610 to that of the line 1003 increases at the higher temperature.

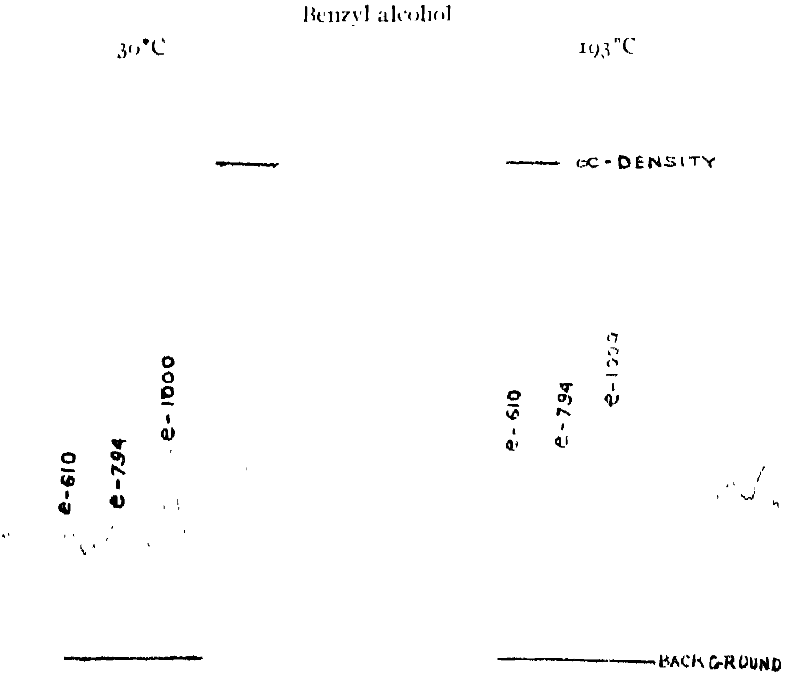

FIG. 1

As regards the intensity of the Rayleigh line the results observed at the two temperatures for the line λ4916 in each case are given in the tables, because, there is no appreciable absorption in this region. It is observed that in each case the intensity of the Rayleigh line increases with the increase of temperature. Since the intensity of the Raman line due to C-H vibration excited by λ4358 and situated close to the line λ4916 does not change with the increase of temperature, the ratio of the intensity of the line λ4916 to that of the Raman line mentioned above increases with the increase of temperature. This can be seen from the microphotometric records reproduced in Fig. 2. Since there was some feeble stray light mixed with the scattered light, the observed increase is

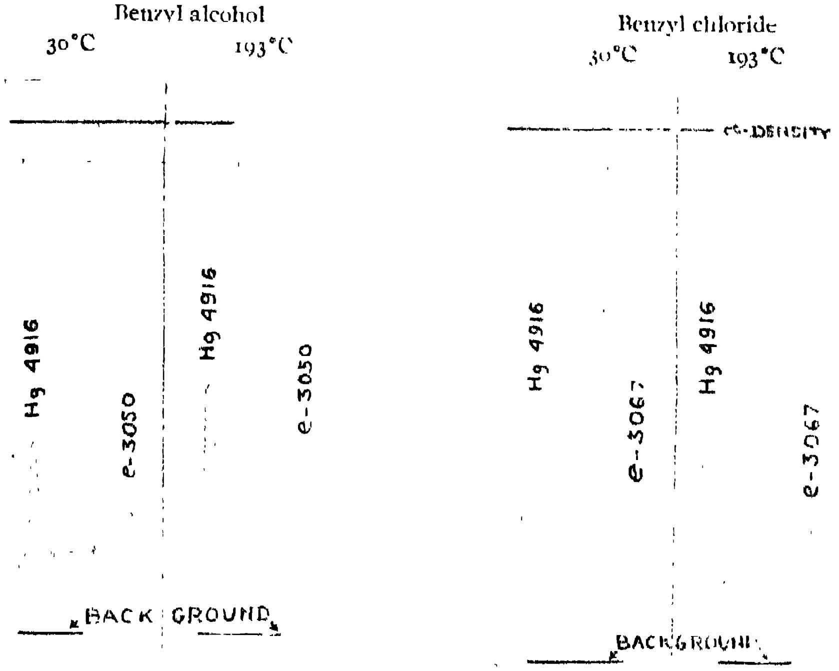

FIG. 2

slightly less than the actual increase in each case. The increase expected theoretically in these cases cannot be calculated, because the values of compressibility, and refractive index at the different temperatures are not known.

The authors are indebted to Prof. M. N. Saha, F.R.S. for kindly allowing them to use the microphotometer of the Palit Laboratory of the Physics Department, University College of Science, Calcutta, and for a loan of the Hilger two-prism spectrograph used in the investigation. The authors are also indebted to the authorities of the Indian Association for the Cultivation of Science for kindly providing facilities for carrying out the investigation at the laboratories of the Association.

INDIAN ASSOCIATION FOR THE
CULTIVATION OF SCIENCE
210, BOWBAZAR STREET, CALCUTTA

REFERENCES

Ananthakrishnan, R., 1938, Effect of temperature on the Raman spectrum of liquid carbontetrachloride, *Proc. Ind. Acad. Sci.*, **7A**, 196.

Landsberg, G. and Mandelstam, L., 1930, Light scattering in crystals at higher temperature, *Z. f. Phys.*, **60**, 364.

Ney, M. J., 1931, Influence of temperature on the Raman spectrum of quartz, *Z. f. Phys.*, **68**, 551

Ornstein, L. S and Went, J. J., 1935, Influence of temperature on the Raman rays of crystals, *Physica*, **2**, 503.

Placzek, G., 1931, Intensity and polarisation of Raman scattering due to polyatomic molecules, *Z. f. Phys.*, **70**, 84.

Venkateswarlu, K., 1941, Effect of temperature on the intensities of Raman lines, I, *Proc. Ind. Acad. Sci.* **14A**, 529.

Venkateswarlu, K., 1942, Effect of temperature on the intensities of Raman lines II. *Proc. Ind. Acad. Sci.*, **16A**, 45.

A SELF CONSISTENT METHOD OF DETERMINING THE MASS OF MESOTRON

By K. C. KAR

AND

R. R. ROY

(Received for publication, Aug. [illegible], 1943)

ABSTRACT A new method is developed for finding the mass of mesotron existing in neutrons and protons. The method is self-consistent. The accuracy of the mass thus determined, which is 110 electron unit, depends on the accurate value of the binding energy of deuteron already known from the experiment of Chadwick. The interaction potential is taken in the form suggested by Yukawa. The mass determined by the present method is the same as the mass obtained by Kar (1942) from the theory of proton-proton scattering.

In the present paper we shall discuss a new method of determining the mass of mesotron. The method is perfectly rigorous and self-consistent. The accuracy with which the mass is determined depends on the knowledge of the accurate value of the binding energy of deuteron.

It is well known that the neutron-proton attractive force in a deuteron is of Yukawa type, derivable from a potential of the form

$$V = -\frac{A}{r}e^{-ar} \qquad \ldots \quad (1)$$

Again, because there is a special affinity between a neutron and a proton, the attractive force between them should be of *exchange type*. The particle which takes part in the exchange is evidently the mesotron. The experiments done so far prove definitely that the charge of this particle is e the electronic charge; but the mass determined by several experimenters till now varies between 100⟶400 electron mass approximately. Our proposed self-consistent method gives the mass accurately inasmuch as the binding energy of deuteron is known with fairly great accuracy.

Now, it is already known (Bethe and Bacher, 1936-37) that in an α-particle the exchange force is completely saturated both with respect to the spatial and spin coordinates, whereas in a deuteron it is saturated with respect to the spatial coordinates only. Consequently the interaction potential between a neutron and a proton should be as given by Majorana. Thus referring the motion to the centre of mass of the interacting neutron and proton and assuming the potential to be spherically symmetrical and of Yukawa type, we have for the wave equation of the neutron or proton initially at $\mathbf{r}(r, \theta, \phi)$ and after exchange at $-\mathbf{r}(r, \pi-\theta, \pi+\phi)$

$$\frac{h^2}{4\pi^2 M}\,\Delta\chi(\mathbf{r}) + E\chi(\mathbf{r}) = -\frac{A}{r}e^{-ar}\,\chi(-\mathbf{r}) \qquad \ldots \quad (2)$$

where M is the mass of the proton or neutron and E the binding energy being negative. Now, because

$$\chi(-\mathbf{r}) = R(r)P_l^m(\cos(\pi-\theta))e^{im(\pi+\phi)}$$

$$= (-1)^l R(r)P_l^m(\cos\theta)e^{im\phi}$$

and

$$\chi(\mathbf{r}) = R(r)P_l^m(\cos\theta)e^{im\phi}$$

we at once get from (2)

$$\frac{h^2}{4\pi^2 M}\left\{\frac{d^2}{dr^2}(rR) - \frac{l(l+1)}{r^2}(rR)\right\} + E.(rR) = -(-1)^l\frac{A}{r}e^{-ar}(rR) \qquad \ldots \quad (3)$$

There are reasons to believe that no excited state of the deuteron exists which differs from the ground state with respect to the orbital motion. Thus $l=0$ and so (3) becomes

$$\frac{h^2}{4\pi^2 M}\cdot\frac{d^2}{dr^2}(rR) + E.(rR) = -\frac{A}{r}e^{-ar}.(rR) \qquad \ldots \quad (3.1)$$

Even at the ground state the deuteron may have two varieties according as the spins of proton and neutron are parallel and antiparallel. In the former case the deuteron is in a triplet state having threefold degeneracy, while in the latter it is in a non-degenerate singlet state. However, if we assume Yukawa interaction of purely Majorana type, the binding energies should be same in both the cases.

Now, because a is very great, the Yukawa potential is appreciably changed for a very slight variation of r due to the exponential factor e^{-ar}, the factor A/r practically remaining constant. Thus to solve the wave equation (3.1) for deuteron, we may take A/r to be constant to a first approximation and equal to $A/\bar{r}$, where $\bar{r}$ is, strictly, the mean distance between neutron and proton. More rigorous solution of of (3.1) may, however, be obtained by using δ-function. Thus putting $V_0 = A/\bar{r}$, we have from (3·1) up to first approximation

$$\frac{h^2}{4\pi^2 M}\,\frac{d^2}{dr^2}(rR) + (E + V_0 e^{-ar})\,(rR) = 0 \qquad \ldots \quad (3.2)$$

If we put $x = e^{-ar}$, (3.2) reduces to

$$x\frac{d}{dx}\left\{x\frac{d}{dx}(rR)\right\} + \frac{4\pi^2 M}{a^2 h^2}(E + V_0 x)\,(rR) = 0 \qquad \ldots \quad (3.3)$$

Let us again put

$$z = \frac{4\pi M^{\frac{1}{2}} V_0^{\frac{1}{2}} x^{\frac{1}{2}}}{} \qquad \ldots \quad (3.4)$$

Hence (3.3) reduces to

$$\frac{d^2}{dz^2}(rR)+\frac{1}{z}\frac{d}{dz}(rR)+\left(1+\frac{16\pi^2 ME}{a^2h^2}\cdot\frac{1}{z^2}\right)(rR)=0 \qquad \ldots \quad (3.5)$$

which is the usual Bessel equation, when E is negative. Its well known solution is

$$rR=CJ_s\left(\frac{4\pi M^{\frac{1}{2}}V_0^{\frac{1}{2}}e^{-\frac{1}{2}ar}}{ah}\right) \qquad \ldots \quad (4)$$

where

$$s=\frac{4\pi(-EM)^{\frac{1}{2}}}{ah} \qquad \ldots \quad (4.1)$$

and C the averaging factor. Because R should be bounded at $r=0$, we have from (4)

$$J_s\left(\frac{4\pi M^{\frac{1}{2}}V_0^{\frac{1}{2}}}{ah}\right)=0 \qquad \ldots \quad (5)$$

From tables of Bessel Functions $J_s(z)$ one can easily find the value of $z=z_s$ (say) for which the function is zero for a given s. In the same way one finds easily that for a given s, Eq(5) is satisfied if

$$\frac{4\pi^{\frac{1}{2}}M^{\frac{1}{2}}V_0^{\frac{1}{2}}}{ah}=B_s \qquad \ldots \quad (5.1)$$

where the numerical value of B_s is obtained from tables of Bessel Functions (Watson.)

Now, from (3.2) we have for the wavestatistical value of the binding energy of deuteron

$$E=-\frac{h^2}{4\pi^2 M}\int_0^\infty \frac{d^2}{dr^2}(rR).\,rR.\,dr-V_0\int_0^\infty e^{-ar}.\,R^2r^2dr \qquad \ldots \quad (6)$$

where (rR) is given in (4). From the substitutions already made (*vide* (3.4)) we have

$$\frac{dz}{dr}=-\frac{a}{2}z$$

and therefore

$$\frac{d^2J_s}{dr^2}=\frac{a^2}{4}z\left(\frac{d^2J_s}{dz^2}.\,z+\frac{dJ_s}{dz}\right)$$

and also

$$e^{-ar}=\frac{a^2h^2}{16\pi^2 MV_0}.\,z^2$$

Thus we easily get from (6), denoting differentiation with respect to the argument by dash

$$E=\frac{h^2c^2}{4\pi^2 M}.\,\frac{a}{2}\int_0^{B_s}J_s\,(zJ_s''+J_s')\,dz-\frac{h^2c^2}{4\pi^2 M}.\,\frac{a}{2}\int_0^{B_s}J_s^2 z\,dz \qquad \ldots \quad (6.1)$$

where B_s is given in (5.1). The averaging factor C in (6.1) is determined in the usual way from the condition

$$C^2\int_0^\infty J_s^2 dr = \frac{2C^2}{\alpha}\int_0^{B_s} J_s^2(z)\frac{dz}{z} = 1 \qquad \ldots \quad (6.2)$$

Again, from the wellknown recurrence formulae of Bessel functions, *viz.*,

$$J_{s-1}(z) + J_{s+1}(z) = \frac{2s}{z}J_s(z)$$

$$J_s'(z) = \frac{s}{z}J_s(z) - J_{s+1}(z)$$

we have

$$J_s'(z) = \tfrac{1}{2}\{J_{s-1}(z) - J_{s+1}(z)\}$$

$$J_s''(z) = \tfrac{1}{4}\{J_{s-2}(z) - 2J_s(z) + J_{s+2}(z)\}$$

On using the above relations, (6.1) may be easily transformed to

$$E = -\frac{\alpha h^2C^2}{8\pi^2M}\left\{\frac{1}{2}\int_0^{B_s} J_s^2(z)z\,dz - \int_0^{B_s} J_{s+1}(z)J_s(z)dz + s\int_0^{B_s} J_s^2(z)\frac{dz}{z}\right.$$
$$\left. + \frac{1}{4}\int_0^{B_s} J_{s+2}(z)J_s(z)z\,dz + \frac{1}{4}\int_0^{B_s} J_{s-2}(z)J_s(z)z\,dz\right\} \qquad .. \quad (6.3)$$

On substituting the experimental values of binding energy (E) *viz.*, 2.15 MV $= 3.421 \times 10^{-6}$ erg, we get sets of values of *s* and *α* satisfying (4.1). Of these only one set will obviously be correct. To find out these correct values we make use of the wavestatistical eq. (6.3) of binding energy. Now, for a given value of s, B_s is known from tables and so the integrals in (6.3) are evaluated by the graphical method. The averaging factor C may also be determined from the condition (6.2). Thus the binding energy is calculated from (6.3) for a given set of values of *s* and *α* satisfying (4.1). The binding energy so calculated is not in general the correct one. We, therefore, calculate a number of binding energies from (6.3) for different values of *s* and *α* satisfying (4.1) and draw a graph giving E for different values of *s* and *α* taken. This enables us to find the exact values of *s* and *α* for which the binding energy is just what is obtained experimentally. Having got the correct values of *s* and *α* by the above method which is evidently self-consistent, we get the mass of mesotron from the usual formula

$$m = \frac{\alpha h}{2\pi c} \qquad \ldots \quad (7)$$

The accuracy of the mass so determined depends on the accuracy with which the binding energy of deuteron is known. The values of *s* and *α* calculated by the present method are 1.59 and $.2848 \times 10^{13}$ respectively. With the above value of *α* in (7) the mass of mesotron is found to be 110 e.u. This is the value obtained experimentally by Corson and Brode (1938).

It should be noted that from the theory of proton-proton scattering already developed by one of us, (Kar, 1942) the value of *α* has been obtained as

$.2866 \times 10^{13}$ and the corresponding mass calculated from (7) is 110.8 e.u. It is in very good agreement with the mass calculated by the present method. This strongly suggests that the origin of the short range attractive force must be same in both the cases. The attraction is due to meson field surrounding a neutron and a proton.

If, however, it is assumed that the proton-proton interaction is due to exchange and the attractive force is of Majorana type, then, it is clear, the particle taking part in the exchange cannot be mesotron having charge e. It should be 'neutretto' having the same mass but without the free charge e. As, however, in the formation of nucleus, the proton is not found to exhibit any affinity for proton, it appears to us that there is no exchange although there is attraction between the protons. Accordingly, the assumption regarding the existence of a new kind of exchange particle, *e.g.*, neutretto, is unnecessary.

It is thus evident that the attraction between a neutron and a proton or between two protons is due to the meson field. In the former case there is exchange while in the latter case there is none. Accordingly the interaction between protons cannot be of Majorana type. It should be that given by Wigner. But for $l=0$, the wave equation is same as (3.1). The next question that is to be settled is whether the short range meson field permanently exists in the protons and neutrons. As, however, the short range force is always found to be attractive and never repulsive, it appears likely that the field is of electrical origin and is temporarily developed during close interaction, due to polorisation of neutrons and protons and consequent creation of mesotrons within the particles.

In conclusion we may note that as α and B_ϵ are already determined we readily evaluate V_0 *i.e.*, $A/\bar{r}$ from (5.1). The unknown parameter A of Yukawa potential cannot be determined by the present method. It is determined from neutron-proton scattering which we shall discuss on a different occasion. However, we may just mention at present that the value of $\sqrt{A}$ so determined is $\sim 6e$ which is just the value obtained from proton-proton scattering (Kar, 1942). On comparing the values of A and V_0 we find $\bar{r} \sim 3.118 \times 10^{-13}$ from which a rough estimate of the scattering cross-section may be made.

PHYSICAL LABORATORY,
PRESIDENCY COLLEGE,
CALCUTTA.

REFERENCES

Bethe and Bacher, 1936-37, *Rev. Mod. Phys.*, **8**.
Corson and Brode, 1938, *Phys. Rev.*, **53**, 773.
Kar, K. C., 1942, *Ind. Jour. Phys.*, **16**, 187.
Watson, G. N., Bessel Functions, Cambridge.

THE THEORY ON NEUTRON-PROTON SCATTERING

By K. C. KAR

AND

R. R. ROY

(*Received for publication, August 17, 1938*)

ABSTRACT. The Wavestatistical Theory of Neutron-Proton Scattering is developed using an interaction potential of Yukawa type, *viz*, $V = \frac{A}{r} e^{-\alpha r}$. The theoretical formula for the intensity of scattering is found to agree with the experiment of Harkins and others for $\sqrt{A} = 6e$ and $\alpha = .2848 \times 10^{13}$. This value of α gives 110 *e.m.* as the mass of mesotron taking part in the exchange in neutron-proton interaction. The mass so determined is exactly the same as that obtained from the binding energy of deuteron and from proton-proton scattering.

In the theory of neutron-proton scattering recently developed by one of the authors (Kar and Basu, 1939) the interaction potential has been taken in the form $V = -V_0 e^{-\alpha r}$. The formula derived has been found to agree only qualitatively with the experiments of Chadwick (1933) and others. In the present paper it is proposed to develop the theory of scattering somewhat on similar lines, on the basis of an interaction potential suggested by Yukawa.

The wave equations of the incident neutron inside and outside the potential field of the proton, the motion being referred to C-system, are

$$\Delta\chi + k^2\left(1 - \frac{V}{E}\right)\chi = 0 \qquad .. \quad (1)$$

and

$$\Delta\chi_0 + k^2\chi_0 = 0 \qquad .. \quad (1.1)$$

where $k = \frac{\pi M v}{h}$ and $E = \frac{1}{4}Mv^2$. Proceeding in the usual manner (Kar, *et al* 1937), we have for the first order scattering function

$$\lambda_1\chi_1(r_2) = -\frac{1}{4\pi} \cdot \frac{k^2}{E}\int V(r_1)\chi_0(r_1) \cdot \frac{e^{ikr_{12}}}{r_{12}}\, d\tau_1 \qquad \ldots \quad (2)$$

where

$$\chi_0 = \frac{1}{\sqrt{v}} e^{ikx_1}, \qquad \ldots \quad (2.1)$$

the incident wave being supposed to move along the x-axis. On integrating (2) as before (Kar, 1937), we have

$$\lambda_1\chi_1(r_2) = -\frac{2k \operatorname{cosec} \frac{1}{2}\psi}{Mv^2} \cdot \frac{e^{ikr_2}}{\sqrt{v}\, r_2} \int_{r_0}^{\infty} \sin k'r\, V(r)\, r\, dr \qquad \ldots \quad (2.2)$$

where $$k' = 2k \sin \tfrac{1}{2}\phi.$$

Eq (2.2) may be written in the simple form

$$\lambda_1 \chi_1(r) = \frac{\operatorname{cosec}^2 \frac{1}{2}\phi}{Mv^2} \cdot \frac{e^{ikr}}{\sqrt{v}\,r} F(r_0) \qquad \ldots \quad (2.3)$$

where $$F(r_0) = -k' \int_{r_0}^{\infty} \sin k' r V(r) r dr \qquad \ldots \quad (2.4)$$

Proceeding in the usual way it may be easily shown that the critical approach r_0, which must be always positive, is given, for an attractive force of interaction, by the formula (Kar, 1942)

$$r_0 = \frac{\operatorname{cosec}^2 \frac{1}{2}\phi}{Mv^2} \cdot 2\rho(\sin \tfrac{1}{2}\phi - \sin^2 \tfrac{1}{2}\phi) G(r_0) \qquad \ldots \quad (3)$$

where $$G(r_0) = -k' \int_{r_0}^{\infty} \sin k'(r - r_0) V(r) r dr \qquad \ldots \quad (3.1)$$

Now, taking the interaction potential to be of Yukawa type, *viz.*, $V(r) = -\frac{A}{r} e^{-\alpha r}$, we find the values of $F(r_0)$ and $G(r_0)$. On substituting these values in (2.3) and (3) we get for the scattering function and the critical approach

$$\lambda_1 \chi_1 = \frac{4\pi^2 MA}{h^2} \cdot \frac{e^{-\alpha r_0}\left\{\cos k' r_0 + \frac{\alpha}{k'} \sin k' r_0\right\}}{\alpha^2 + k'^2} \cdot \frac{e^{ikr}}{\sqrt{v}\,r} \qquad \ldots \quad (4)$$

$$r_0 = 2.7 \times \frac{4\pi^2 MA}{h^2} \cdot \frac{e^{\alpha r_0}}{\alpha^2 + k'^2} (\sin \tfrac{1}{2}\phi - \sin^2 \tfrac{1}{2}\phi) \qquad \ldots \quad (4.1)$$

If θ is the angle of scattering in the laboratory system, we have $2\theta = \phi$. Thus we have for the relative intensity of scattering and the critical approach in L-system

$$I = g^2 f^2 \, 4 \cos \theta \, . \, 2\pi \sin \theta d\theta \qquad \ldots \quad (5)$$

and $$r_0 = 2.7 \times (\sin \theta - \sin^2 \theta) g \qquad \ldots \quad (5.1)$$

where $$g = \frac{4\pi^2 MA}{h^2} \cdot \frac{e^{-\alpha r_0}}{\alpha^2 + k'^2} \qquad \ldots \quad (5.2)$$

and $$f = \cos k' r_0 + \frac{\alpha}{k'} \sin k' r_0 \qquad \ldots \quad (5.3)$$

In order to verify our formula (5) quantitatively we have to depend on the only experiment done so far by Harkins, Kamen, Newson and Gans (1936). Their experimental values are, however, given for angular ranges of ten degrees and so it is necessary to integrate (5) between θ_1 and θ_2. Because the angular range is small we may take g and f outside the sign of integration giving them their mean values, *viz.*, g_m and f_m. We have then from (5) after integration

$$I(\theta_1, \theta_2) = 2\pi g_m^2 f_m^2 (\cos 2\theta_1 - \cos 2\theta_2) \qquad (5.4)$$

where $$g_m=\frac{4\pi^2 MA}{h^2}\frac{r_{0m}}{a^2+k'^2_m} \qquad (5.5)$$

$$f_m=\cos k'_m r_{0m}+\frac{a}{k'_m}\sin k'_m r_{0m} \qquad (5.6)$$

and $$r_{0m}=2.7\times(\sin\theta_m-\sin^2\theta_m)g_m \qquad \ldots \quad (5.7)$$

Again, because the absolute values of the intensity are not given in the experiment cited above, formula (5.4) cannot be verified directly. However, it is obvious that the experimental values which are proportional to the absolute values, are given by the formula

$$I(\theta_1,\theta_2)=B\times 2\pi g_m^2 f_m^2(\cos 2\theta_1-\cos 2\theta_2) \qquad \ldots \quad (5.8)$$

where B is the unknown constant of proportion. On using tentatively the values, *viz.*, $\sqrt{\Lambda}=6e$ already determined from proton-proton scattering (Kar, 1942) and $\alpha=.2848\times10^{13}$ obtained in our previous paper (Kar and Roy, 1943), we easily find the unknown constant of proportion B from one experimental value at a given angular range. Having got the value of B once for all we are in a position to calculate the values of the intensity of scattering at any other angular range. The theoretical values so obtained from (5.8) and the experimental values are given respectively by the continuous and the dotted curves in Fig. 1.

It is apparent from Fig. 1 that the theoretical curve has a peak at 45°, showing that in C-system the scattering is isotropic. This is confirmed by the experiments of Chadwick (1933) and others. The peak of the experimental curve is, however, at 65°. It it is evident that if this difference is neglected, the agreement it as is should be. Now it has been pointed out by Dee and Gilbert (1937), that the shift of the maximum intensity towards large angle, as observed by Harkins and others is due to inhomogeneity of the incident beam of neutrons from the source taken by them.

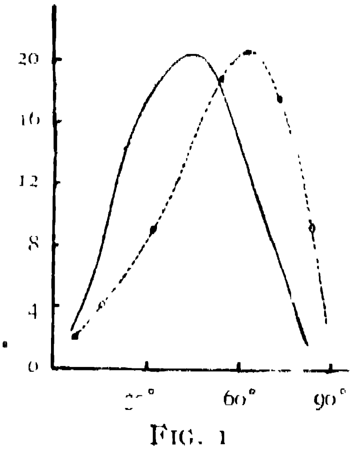

FIG. 1

It should be noted that the values of Λ and *a* for which the theoretical curve is in agreement with the experiment are very nearly the same as those obtained from proton-proton scattering (Kar 1942), and also same as the value of *a* obtained from the binding energy of deuteron (Kar and Roy, 1943). This shows that the nature of the short range force is essentially the same in neutron-proton and proton-proton interactions. Now, because *a* has the same value in the different theories, the mass of mesotron which is responsible for the short range force in neutron and proton, is also same. And it has been found to be 110 electron unit from the usual formula

If, now, formula (5) for the intensity of scattering for the elementary solid angle $2\pi \sin \theta d\theta$ be integrated over the limits 0 and $\pi/2$, we get the total scattering cross-section σ. Logarithms of the cross-sections thus determined for different velocities are plotted against the logarithms of incident energy. And the curve is given in Fig. 2

The circles indicate the experimental values. It is obvious that there is very good agreement for thermal neutrons having low velocity. However, for higher velocities there are some departures.

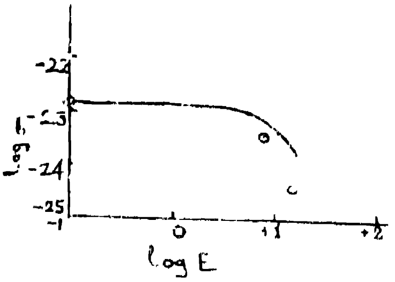

FIG. 2

Before concluding, we shall make a few remarks on some of the special features of the wavestatistical theories of scattering so far developed (Kar, *et al*, 1942), for different kinds of interactions. The fundamental assumption made in the above theories, is that the incident particle approaches the scattering particle only up to a certain distance r_0 which is called the 'critical approach.' It has nothing to do with the size of the nucleus and, in fact, it is much greater than the size. It has been shown that the critical approach depends on the velocity of the incident particle and also on the angle of scattering. It is obvious that it decreases with the increase of the incident velocity for a given angle of scattering, and also for a given incident velocity it decreases with the increase of scattering angle. Now, the volume round the scatterer which is unperturbed by the incident particle due to the critical approach may be called the 'excluded volume.' This volume has evidently no contribution to the total intensity of scattering. Now, in deriving Born-Rutherford, Holtzmark and other wave-mechanical formulæ of scattering the above excluded volume has been wholly neglected. In other words, the scattering by the excluded volume is taken into consideration. As a result their theoretical values are always much higher than the experimental values. It is well known (Mott and Massey, 1933), that at high velocity of incidence and large angles of scattering, Born-Rutherford formula is found to agree fairly well with the experiment. At this region the excluded volume is obviously negligible. Thus we find that the wave mechanical formulæ generally give much higher values, whereas the wavestatistical formulæ are decidedly in better agreement with the experiment. And in some cases the agreement is found to be almost exact.

Apart from the experimental evidences which confirm the wavestatistical theories, there are theoretical justifications in support of the fundamental assumption of critical approach. The incident beam of particles moving in straight line in a given direction is deflected due to the presence of the scatterer. Thus the scatterer acts as a source of perturbation and imposes some boundary conditions on the motion of the incident beam of particles. On account of these boundary conditions, the incident beam approaches the scatter only upto a certain limit. If the wave character of the particles is completely disregarded, the critical approach is evidently given for Coulomb field by the distance of the vertex of the hyperbolic path from the centre of the scattering particle. However, the wavestatistical character of the particles constituting the incident beam cannot be ignored. Accordingly, in the different wavestatistical theories of scattering the critical approach r_0 for any potential field is always determined by the wavestatistical method using the boundary conditions at $r = r_0$

$$\left.\begin{aligned} \chi_0 + \lambda_1 \chi_1 &= 0, \\ \frac{d\chi_0}{dr} + \lambda_1 \frac{d\chi_1}{dr} &, \end{aligned}\right\} \qquad \dots \quad (6)$$

It is interesting to note that for Coulomb field the wavestatistical method gives exactly the same value of the critical approach as the dynamical method except an additional numerical factor 1.35, which is known as the dynamical defect factor.

PHYSICAL LABORATORY,
PRESIDENCY COLLEGE,
CALCUTTA

REFERENCES

Chadwick, 1933, *Proc. Roy. Soc. A.*, **142**, 1.
Dee and Gilbert, 1937, *Proc. Roy. Soc. A.*, **163**, 265.
Harkins, Kamen, Newson and Gans, 1936, *Phys. Rev.*, **50**, 980.
Kar, K. C. and Basu, D., 1939, *Phil. Mag.*, **27**, 76.
Kar, K. C., Ghosh, M. and Mukherjee, K. K., 1937, *Phil. Mag.*, **24**, 964
Kar, K. C., 1937, *Phil. Mag.*, **24**, 971
Kar, K. C., 1942, *Ind. Jour. Phys.*, **16**, 187.
Kar, K. C. and Roy, R. R., 1943, *Ind. Jour. Phys.* (in Press).
Kar, K. C., and Sen Gupta R. L., 1942, *Science and Culture*, **8**, 191
Mott and Massey, 1933, *Atomic Collisions*, Oxford Press.

MOLECULAR ASSOCIATION IN OXYACIDS

By N. RAJESWARA RAO

(Received for publication, September 17, 1943)

ABSTRACT. In the present paper, molecular association in solutions of oxyacids is studied with the help of Raman effect. On comparing the associating nature of these substances with their strength, it is found that the stronger the acid the smaller is the tendency for its molecules to polymerise To study this point further, a comparative study of molecular association in solutions of acetic and chloracetic acids, which are known to be of increasing order of strength but of quite similar structure, is made and the above point is confirmed.

It is also found that increase in the hydrogen-ion concentration in these solutions will have the effect of diminishing the molecular association contrary to what is to be expected from the law of mass action

INTRODUCTION

Koteswaram (1940) succesfully employed Raman effect to study molecular association in a number of associated liquids and arrived at the conclusions that substances must have both a donor and and an acceptor atom for association to take place in pure state, *e.g.*, water, fatty acids. From this it appears as if oxyacids, which contain both H and O atoms, form ideal substances for molecular association. It is well known that in the oxyacids, the hydrogen-ion is attached to the oxygen atom forming the OH link which on dissociation breaks off. Thus, nitric acid is considered to be having the formula $NO_2.OH$, sulphuric acid $SO_2.(OH)_2$, iodic acid $IO_2.OH$ and so on. This contention has been further verified by the Raman spectra of these acids in the pure state by Venkateswaran (1936) and Dadieu and Kohorausch (1931) who observed the OH band in these spectra. Also, all these molecules must necessarily be polar because of their unsymmetrical structures. Thus, the condition for molecular association is satisfied and one must expect associated molecules in solutions of these oxyacids. But a study of the solutions of H_2SO_4, HNO_3, $HClO_4$ or H_3PO_4 does not show any evidence of the existence of associated molecules of the type $(HNO_3)_2$ or $(H_2SO_4)_2$, etc., though in solutions of acetic acid the determination of molecular weights of H_2SO_4, H_3PO_4 and $HClO_4$ revealed the existence of unstable dimers, which were found to be very unstable and to decompose with time. In solutions of iodic acid, evidence for associated molecules could be found in higher concentrations (Rao, N. R., 1942). Its Raman spectra in different concentrations show lines which are found to vary with concentration, which was interpreted on the basis of the splitting up of polymerised molecules into normal molecules with dilution. In trichloracetic acid also, evidence for polymers, which split up very fast on dilution, was found from a study of its Raman spectrum in different concentrations and temperatures.* But in acetic acid, studied in detail by Koteswaram (1938), associated molecules were found even in dilute solutions.

In the present paper, the association of the oxyacids and its dependence on their strengths will be studied, by making a comparative study of the acetic and chloracetic acids, which are known to be of increasing order of strength.

ACETIC ACID

Koteswaram observed that the Raman spectrum of acetic acid consists of sharp lines of frequencies 446, 601, 620, 872, 893, 1010, 1270, 1368, 1433, 2889, 2946, 2996 and a band which can be regarded as composed of components at 1673, 1700, 1720 and 1770. On examining the intensities and the changes in the frequencies of the lines 872, 893, 1010 and the band at 1700 in the spectra of this acid in different concentrations in water and other polar liquids and at different temperatures, he observed that (1) the line at 872 appears only in the spectrum of the pure acid, (2) the second line 893 gets diffuse on dilution and increase of temperature, (3) the line at 1010, which he attributed to the C-O band, shifts to a higher Raman frequency on dilution and temperature and (4) the lower frequency components of the 1700 band disappear under these conditions. He attributed these changes to the depolymerisation of the acid molecules.

Now on dilution, the polymerised molecules split up into simple ones which on further dilution split up into ions. They can be represented by the equation :

$$(CH_3COOH)_2 \rightleftharpoons 2CH_3COOH \rightleftharpoons 2H^+ + 2CH_3COO^-.$$

Now if, in a dilute solution, the hydrogen ion concentration is increased, the backward reactions must be favoured resulting in an increase of the polymerised molecules. To test this, 3 sets of aqueous solutions, 82% acetic acid, and 82% acetic acid + 1N HCl, 50% acetic acid, and 50% acetic acid + 1N HCl and 25% acetic acid + 1N HCl are prepared and their Raman spectra are obtained with times of exposure inversely proportional to the concentration of acetic acid in them. For each pair of solutions, the weight of acetic acid per 100 c.c. of solution was the same, so that the spectra for any pair should be identical for equal exposures under identical conditions, if the acetic acid is unaffected by HCl. The changes in the spectra of the mixture compared to the pure solutions are very slight and of uncertain nature. Only there is a slight indication that the lower frequency components of the band at 1700 are further diminished in intensity in the mixture with HCl. This is surprising in view of the above expectation, which is expected to show an increase in the intensity of components which correspond to the polymers.

MONOCHLORACETIC ACID

Due to substitution of one of the hydrogen atoms in the CH_3 group of acetic acid by chlorine, this acid is known to be stronger than acetic acid. In the following pages are given the results on the molecular association of this acid on lines similar to those in the case of acetic acid.

---

* Unpublished work of the author.

The Raman spectrum of this acid in the solid and the molten states has been studied by a few authors including Parthasarathy (1934), Thatte and Ganesan (1931), Cheng (1929), and Dadieu and Kohlrausch (1929). All the above authors reported that their spectra were superposed by an intense continuous background. Parthasarathy seems to have obtained a fairly good spectrum of the acid in the solid state. Thatte and Ganesan recorded only two feeble lines of frequencies 433 and 2994. Cheng made a comparative study of the infra-red and the Raman spectra of the acid. Kohlrausch seems to have obtained the best spectrum with the molten acid, though he reported to have observed intense continuum superposed on this spectrum. But, so far, no attempt was made to study its molecular association by this method.

EXPERIMENTAL

The Raman spectra of this acid are usually superposed by an intense continuum, making it sometimes difficult to observe the lines clearly. In order to avoid this, the acid is distilled a number of times and the final distillate is collected direct into the Wood's tube. The spectrum of the molten acid is taken by maintaining the copper jacket at about 60°C and exposing the acid for about 2 hours. Aqueous solutions of concentrations 10·5N, 5N, 2·5N, 1·25N and 0·5N are prepared and treated with pure carbon while hot. The solution is filtered through a quantitative filter paper in a sintered glass funnel. In a similar way, a 2.5N solution of the sodium salt of this acid is also prepared. To study the effect of increasing the hydrogen-ion concentraion, two solutions, one of normality 1.35 and another a mixture of 1.25N of this acid and 1N of HCl, are prepared with the weight of $CH_2ClCOOH$ per 100 c c. of solution in both being the same.

The experimental arrangement is the same as that employed in the previous work. Spectra of the acid of different concentrations are photographed with times of exposures nearly inversely proportional to the concentration of the acid. Spectra of concentrations 10.5N, 5N, 2.5N and 1.25N are photographed at 80°C also, to study the temperature effect.

RAMAN LINES

Raman lines in spectra obtained by the previous authors are given in Table I and those obtained by the author in Table II.

TABLE I

Author	Raman frequencies in cm^{-}
Parthasarathy	242 (3), 294 (3), 333 (3), 426 (4), 575 (4), 648 (0), 789 (2), 991 (1), 1235 (2), 1366 (1b).
Thatte and Ganesan	433 (w), 2994 (m).
Cheng Raman lines	794 868, 920, 1191, 1437
Infra Red	12.58, 11.52, 10.85, 8.39, 6 96.
Kohlrausch	168 (2b, e), 232 (3b, e, c), 414 (6sb), 561 (½b), 669 (1sb), 790 (10 sb), 901 (3sb), 1181 (1), 1405 (3sb), 1670-1760(½), 2957 (3b).

TABLE II

Molten 60°C	10·5N 30°C	10·5N 80°C	5·0N 30°C	5·0N 80°C	2·5N 30°C	2·5N 80°C	1·25N 30°C	1·25N 80°C	1·25N in HCl	0·5N 30°C	Salt 3N
230	242	242	242	242	242	242	242	242	242	242	242
414	438	438	438	438	438	438	438	438	438	438	450
560	610	610	610	610	610	610	610	610	610	610	610
670	682	682	682	682	682	682	682	682	682	682	682
790	790	790	790	790	790	790	790	790	790	790	790
900	915	915	920	920	920	920	920	920	920	920	930
1180	1200	1200	1200	1200	1200	1200	1200	1200	1200	1200	1200
1415	1405	1405	1405	1405	1405	1405	1405	1405	1405	1405	1405
			1590	1590	1590	1590	1590	1590	1590	1590	—
1710	1710	1710	1710	1710	1710	1710	1710	1710	1710	1710	
							1650	1650	1650	1650	1650
2950	2950	2950	2950	2950	2950	2950	2950	2950	2950	2950	2950

DISCUSSION

The Raman spectrum of this acid is in many respects similar to that of acetic acid. The lines 242, 438, 610, 682, 790, 1205 and 2950 undergo very little change on dilution. On comparing the assignment of the lines for acetic acid studied by Koteswaram it can be seen that the lines of frequencies 790, 915, 1405 and 1590-1710 can be attributed respectively to C-C, C-O, CH_2 and C-O bonds. The other lines are due to some external oscillations.

The line at 915 changes in frequency from 900 in molten acid to 930 in the salt, similar to the C-O lines in acetic acid, probably for similar reasons, i.e., due to the splitting up of the polymers into simple molecules. The band at 1590-1710 and the line 1405 undergo conspicuous changes on dilution and variation of temperature.

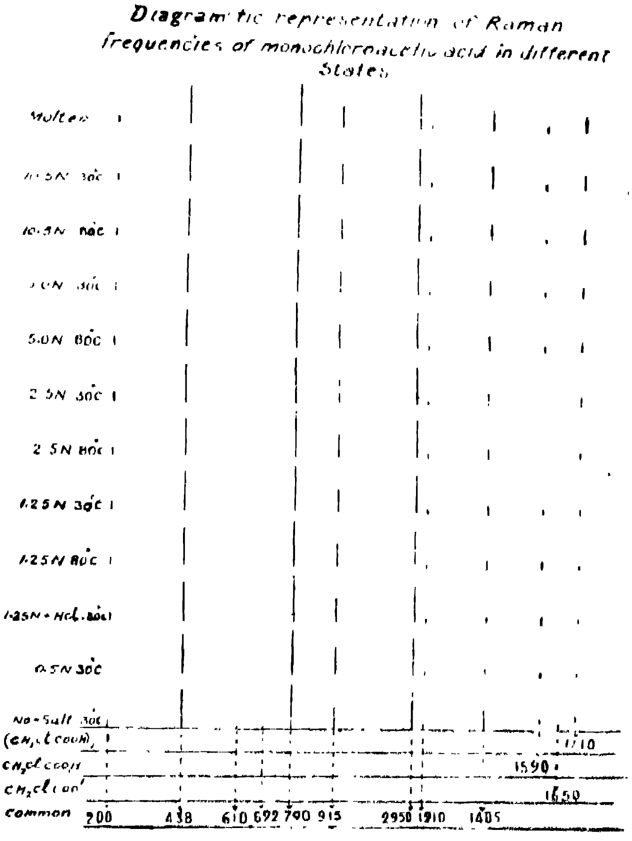

DIAGRAM

As in the case of acetic acid, this band can be regarded as composed of components due to the polymers, simple molecules and ions. With increasing dilution and temperature, this band shifts to a lower frequency due to increase in the intensity of the component 1590 attributed to $CH_2ClCOOH$ molecules, due to splitting up of the polymers $(CH_2ClCOOH)_2$. On further dilution, *i.e.*, from 2.5 to 1.25 and from 1.25 to 0.5N, the band shifts to a higher frequency due to the increase in the intensity of the component 1650, which is the frequency of the band in the spectrum of the salt solution. This shows the evidence for the electrolytic dissociation of the acid. Since the band is very diffuse and is composed of components very close to it, a quantitative determination of the degree of dissociation is not possible.

The line at 1405 behaves in a peculiar way. It is found to be common in all the solutions, but its intensity falls off rapidly on dilution and rise in temperature. In the salt solution, however, it is very intense. Probably, the line is common to all the radicals but its specific intensity corresponding to the normal molecules is perhaps very small. The feebleness of this line even in 0·5N solution shows that the dissociation of the acid in this solution also is small.

On adding HCl, the band at 1590-1710 shows (1) an increase in the intensity on the lower frequency and (2) a diminution in intensity on the higher frequency side indicating a large increase in the number of normal $CH_2ClCOOH$ molecules due to (1) a decrease in the dissociation and (2) a large splitting of the polymers. The latter result is in conformity with that obtained in the case of acetic acid and the former with those reported in a previous paper by the author "On the effect of common ion on the dissociation of strong electrolytes" (Rao, N. R., 1941).

IODIC AND TRICHLORACETIC ACIDS

Studies on these acids are given in detail in the previous papers of the author (Rao, N. R., 1942). But a brief account of the results obtained will be given below, as far as it relates to the present paper. In iodic acid, concentrated solutions show diffuse Raman lines at 636 and 790. The latter was regarded as composed of components at 770 and 825 characteristic of $(HIO_3)_2$ and HIO_3 respectively. With dilution, the former diminished in intensity with a corresponding increase in the intensity of the latter, indicating gradual splitting up of the polymers into monomers. The effect of increasing the hydrogen-ions on the molecular association of this acid could not be studied as it does not dissolve to a sufficiently large extent in solutions of other acids.

In trichloracetic acid, the C-O band at about 1700 shows similar behaviour as in acetic acid, with this difference that in this case the diminution in the intensity of the component due to the polymers is very rapid and is almost absent even in 6N solution.

GENERAL CONCLUSIONS

From the foregoing work, the following conclusions can be drawn as regards molecular association in oxyacids :—

1. No evidence for polymerisation could be found in solutions of strong acids, *viz.*, H_2SO_4, HNO_3, $HClO_4$ and H_3PO_4.

2. Weak oxyacids like acetic, formic and benzoic acids show the presence of polymerised molecules in their solutions. Evidence for this can be gathered from the work of previous authors, *e.g.*, Koteswaram, already referred to in the course of this paper.

3. Oxyacids of intermediate strength, *e.g.*, iodic, monochloracetic, and trichloracetic acids, contain polymers in their solutions.

4. From the above results, it can be seen that the weaker the acid, the larger the tendency for the molecules to polymerise. This can also be seen on examining acetic, monochloracetic and trichloracetic acids which have similar structures but have a decreasing tendency for exhibiting association and increasing tendency for dissociation.

5. These results show that while the presence of donor and acceptor atoms is essential for the formation of polymers, this is not the only factor. The nature of both the solvent and the solute plays a great part in determining the degree of association.

6. Addition of hydrogen ions will diminish polymerisation. This could be definitely tested only in the case of monochloracetic acid.

It is likely that due to the supply of a large number of ions by HCl, the dielectric constant of the solutions is increased, exerting more electrical pressure on the polymers and hence the suppression of association on the addition of ions.

In conclusion, the author takes great pleasure in recording his grateful thanks to Dr. I. Ramakrishna Rao, under whose direction the present work was done.

DEPARTMENT OF PHYSICS,
ANDHRA UNIVERSITY,
GUNTUR.

REFERENCES

Cheng, 1929, *Ann. Phys.* (11), **5**, 427.

Dadieu and Kohlrausch, 1929, *Wien. Ber.*, **138**, 635. Also, 1930, *Monatchefte. f. Chem.*, **55**, 58.

Dadieu and Kohlrausch, 1931, *Naturwissenshaften*, **19**, 690

Koteswaram, P., 1938, *Zeits. f. Phys.*, **110**, 118.

Koteswaram, P., 1940, *Ind. Jour. Phys.*, **14**, 353

Parthasarathy, 1939, *Phil. Mag.* (suppl.), **77**, 471.

Rao, N R., 1941, *Current Science*, **11**, 13.

Rao, N. R., 1942, *Ind. Jour. Phys.*, **16**, 71.

Thatte and Ganesan, 1931, *Phil. Mag.*, **12**, 823.

Venkateswaran, 1936, *Proc. Ind. Acad. Sci.*, **4A**, 174.

STUDY OF ELECTROLYTIC DISSOCIATION IN STRONG ELECTROLYTES BY RAMAN EFFECT

TRICHLORACETIC ACID

BY N. RAJESWARA RAO

(Received for publication, September 17, 1943)

ABSTRACT The Raman spectrum of trichloracetic acid exhibits conspicuous changes on dilution of the acid. On comparing the spectra of the acid at different concentrations and of lithium and sodium salts of this acid, the lines of this acid are attributed to different kinds of radicals, $(CCl_3COOH)_2$, CCl_3COOH and CCl_3COO. This assignment is further supported by the corresponding changes that these lines undergo on increasing the temperature and the hydrogen-ion concentration by adding hydrochloric acid to this acid. Also, on comparing this acid with acetic acid, the lines are attributed to different bonds, C−C, C−O, C=O, etc.

INTRODUCTION

It is well known that trichloracetic acid is a very strong acid, comparable to nitric or hydrochloric acids in dilute solutions. But there is no evidence to show how it dissociates in concentrated solutions as the electrochemical methods, usually adopted for such studies, are applicable only to dilute solutions. But the method suggested by I. R. Rao (1930), *i.e.*, by Raman effect is best suited for such studies and has been adopted by the author for this acid also.

The Raman spectrum of trichloracetic acid has been studied by Woodward (1931), Parthasarathy (1934), Thatte and Ganesan (1931), Kohlrausch (1933), Ghosh and Kar (1931) and Cheng (1936). The studies were confined only to concentrated solutions and it was generally found that the Raman spectra were superposed by an intense continuous background. Woodward reported no apparent change in the Raman spectrum of the acid with dilution and came to the conclusion that no relation could be found between Raman effect and electrolytic dissociation of this acid from his spectra. No other systematic attempt was made to study the dissociation of the acid at various concentrations by this method. The present work is an attempt in that direction.

EXPERIMENTAL

The acid was distilled under reduced pressure by continuously drawing out the decomposition vapours and the distillate is collected direct in the Wood's tube. This is found to diminish the continuous spectrum to a large extent. With this sample, solutions of concentrations 9.0, 6.0, 3.0, and 1.5N are prepared with double distilled water. Also, solutions of CCl_3COONa and CCl_3COOLi of concentrations 3.0N each are prepared with pure substances. In order to help correct assignment of the Raman lines to various radicals, a mixture containing 1.5N of this acid with 2N HCl is also prepared.

While studying the acid at higher temperature, it was experienced that the decomposed vapours formed bubbles near the surface of the tube, which strongly diffused the direct mercury arc light. In order to avoid this, the tube is kept vertical and the scattered light is reflected, by means of a mirror set at 45°, to the slit of the spectrograph. With this arrangement, the spectra of the molten acid (at 60°C) and of 9N and 6N solutions at 80°C are taken.

RAMAN LINES

The lines and corresponding intensities are presented in the diagram. Table I gives the frequencies obtained by different authors, while Table II gives those of the author.

TABLE I

Author		Raman lines in cm⁻¹
Woodward	8.8N	190(s), 286(s), 436(s), 689(m,d), 843(m,d)
	1.6N	190(s), 286(s), 436(s), 680(m,d), 843(m,d)
Parthasarathy (solid)		250(1), 286(1), 327(1), 453(2), 600(2)
Thatte and Ganesan		433(w), 685(st), 2091(diffuse)
Cheng		671, 700, 835, 947, 1210 (Raman lines) 14.88, 14.29, 11.96, 10.56, 8.26 (Infra red)
Kohlrausch (molten)		200(10b), 277(10b), 318(3), 433(10b), 447(10b), 676(8b), 833(5sb), 946(3b), 1413(1b), 1689(0), 1743(1sb)

In the above table, the numbers and letters in the brackets represent intensities of the lines, the letters having the usual significance.

TABLE II

Molten	9.0N	9.0N 80°C	6.0N	6.0N 80°C	3.0N	1.5N	1.5N HCl	Li-salt
200(6)	200(6)	200(6)	200(6)	200(6)	200(6)	200(6)	200(6)	200(6)
284(8)	284(8)	284(8)	284(8)	284(8)	284(8)	284(8)	284(8)	284(8)
316(0)	316(0)	...	...	...	...	...	...	..
438(10)	438(10)	438(10)	438(10)	438(10)	438(10)	438(10)	438(10)	438(10)
690(4d)	712(4d)	712(4d)	712(4d)	712(4d)	712(4d)	712(4d)	712(4d)	712(4d)
...	730(3½)	730(1)	730(3)	730(3½)	730(2)	730(1)	730(2)	...
...	...	...	...	...	750(1)	750(2)	750(0)	750(2)
832(4d)	856(4)	856(4)	856(4)	856(4)	856(4)	856(4)	856(4)	856(4)
946(1)	960(1)	960(1)	960(1)	960(1)	960(1)	960(1)	960(1)	960(1)
...	...	...	...	...	1295(1)	1295(3)	1295(0)	1295(6)
1415(½)	1415(0)	1415(0)	...	...	...	...	...	..
1650(d)	1680(½)	1700(½)	1700(0)	1700(½)	1700(0)	1630(0)	1630(0)	1630(0

From a comparison of the Raman frequencies and the intensities of the lines obtained by various authors, it can be seen that except that of Kohlrausch all the other spectra were superposed by an intense continuous background which masked the lines. On comparing the results obtained by Kohlrausch with that of the author, it is seen that there are discrepancies in the values for the frequencies. This may be due to the fact that the lines are diffuse and exact location of the maxima is difficult.

The bands at 1689 and 1743, observed by Kohlrausch, are not found to be sufficiently resolved, nor are the two lines of frequencies 433 and 447. All the above authors, except Woodward, observed the Raman spectrum either in one concentration or in the molten acid only. Woodward studied the spectra of the acid in two solutions but could not observe the important line 1295, and thus came to the conclusion that nothing can be said from his results as regards dissociation of the acid.

In the diagram the bands 712, 730, 750; 856, 863 and 1630, 1680, 1700 are not as resolved as represented. Their resolution is exaggerated in order to make the assignment clear.

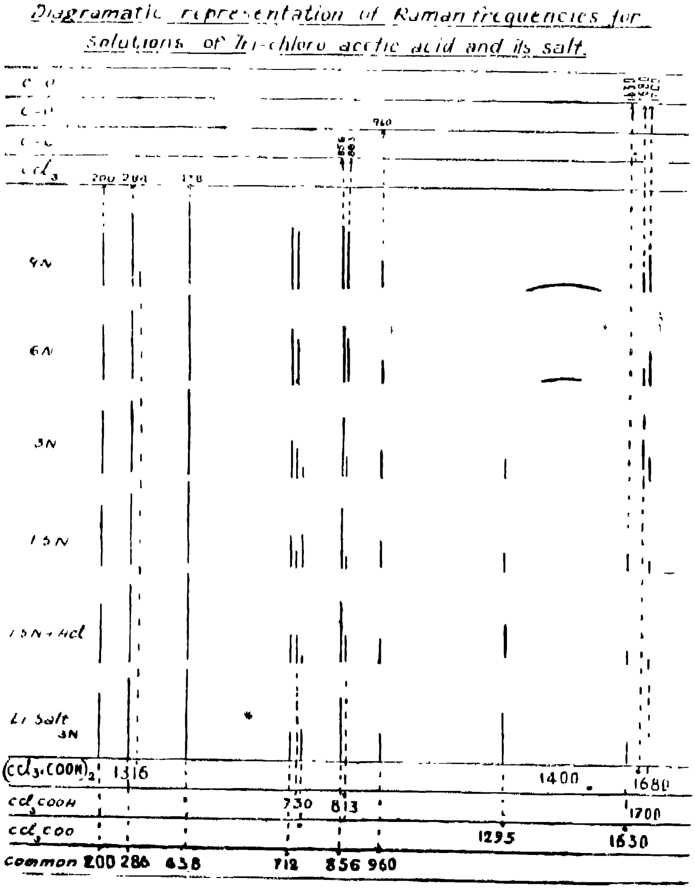

DIAGRAM

ASSIGNMENT OF THE LINES

The Raman spectrum of this acid is similar to that of acetic acid. Koteswaram (1938) assigned lines of frequencies 872 and 893 to C-C link, 1010 to C-O, the composite band at about 1700 to C=O, the group of lines 2880, 2940, 2996 to CH_3, in the spectrum of acetic acid. Similar considerations help assignment of lines in trichloracetic acid also to different bands. This assignment is also represented in the diagram.

From the diagram it can be clearly seen that the Raman spectrum of the acid changes with dilution, temperature and with increase of concentration of the hydrogen-ions by adding HCl. These variations can be interpreted on the basis of the changes in the dissociation of the acid.

The band 1630-1700 is found to be common to all components having the C-O band and hence can be attributed to it. In solutions of acetic acid, this band was observed by Koteswaram to be increasing in frequency on dilution and temperature. He explained that it can be regarded as composed of two components corresponding to molecules of the type $(CH_3COOH)_2$ and CH_3COOH, the lower frequency components belonging to the former. On increasing the dilution or the temperature, the lower frequency side diminishes in intensity indicating a diminution in the number of polymers which split up into monomers. Similarly, in the spectrum of the trichloracetic acid, the component 1680 which diminishes in intensity with dilution of the acid may be attributed to the $(CCl_3COOH)_2$ molecules, which, on dilution, split up into normal CCl_3COOH molecules, giving rise to the component at 1700. The rapid diminution of the intensities of the Raman lines 316 and 1400 also can be explained on the above basis.

The bands 712-750, 856-863 and 1630-1700 can be regarded as composed of a number of components as shown in the diagram. The components 730, 863 and 1700 diminish in intensity on dilution and are absent in the salt solution. This can be explained if they are attributed to the normal CCl_3COOH molecules, which dissociate into ions on dilution. The brightening up of these lines in the HCl mixture, from suppression of dissociation, may be expected to support the above view.

The components 730, 1295 and 1630 are absent in concentrated solution of the acid, but first make their appearance in the spectrum of the 3N solution. With dilution they become more intense and are brightest in that of the salt solution. Those lines can be regarded as characteristic of the CCl_3COO' ions. The absence of this line in the HCl-mixture corresponding to the suppression of dissociation also is in support of the above view.

The other lines 200, 284, 438, 712, 856 and 960 are found in all these solutions and can, therefore, be regarded as common to all the three types of radicals, $(CCl_3COOH)_2$, CCl_3COOH and CCl_3COO'. The gradual diminution of the line 712 with dilution suggests that its specific intensity corresponding to the ions is less than that for the normal molecules.

The above assignment of the lines to various radicals and bonds is clearly demonstrated in the diagram.

TEMPERATURE EFFECT

On comparing the intensities of the components 712, 730, 1700, for the concentrations 9N and 6N at 30°C and 80°C, the following points can be noticed. At higher temperature,

1. The component at 730 increased in intensity, indicating an increase in the number of normal CCl_3COOH molecules.

2. The C=O band at 1680 shifts to higher frequency (1700), indicating a diminution in the number of polymers.

Therefore, it should be stated that just as in the case of other associated molecules like acetic acid, this acid also exhibits depolymerisation with temperature.

HYDROGEN-ION EFFECT

In a previous communication by the author (Rao, N. R., 1942), it was reported that if in a solution of a strong acid the concentration of the H ions is increased, the dissociation of the acid will be strongly suppressed. This point is tested in the case of this acid also. In the diagram, it can be seen clearly that the intensity of the lines corresponding to the ions are strongly suppressed in the mixture with HCl, compared to the pure solution of the same concentration (1.5N) This is a further proof of the correctness of the assignment of the lines to different radicals.

DISCUSSION

The above changes in the lines of the acid with dilution show clear evidence for the dissociation of the acid. A quantitative investigation of the degree of dissociation is not possible for the following reasons. On exposure to the incident radiation, the solutions develop, owing perhaps to photochemical decomposition, a slight violet colour, which is different for different-concentrations. Hence, they absorb light to different extents. On account of the fact that this colour increases with time, it was not possible to determine the actual absorption, with a view to eliminating its effect on the relative intensities of the lines. The continuous background is also found to increase on dilution.

But a rough estimate of the dissociation in 1.5N solution of the acid is made by comparing the intensity of the line 1295, corresponding to the CCl_3COO' ions in these solutions with that in the salt solution. Such a comparison shows that the degree of dissociation in 1.5N solution is only 60%, while the corresponding value for nitric acid is about 95%. Hence, it should be concluded that this acid is much weaker than nitric acid in concentrated solutions. In dilute solutions, the two acids are of the same strength, as revealed by conductivity data.

In conclusion, the author wishes to record his grateful thanks to Dr. I. Ramakrishna Rao, D.Sc. (Lond.), under whose direction the present work was undertaken.

REFERENCES

Cheng, 1930, *Ann. Phys.* (11) **5**, 427.
Ghosh and Kar, 1931, *J. Phys. Chem.*, **35**, 1735.
Kohlrausch, 1933, *Z. f. Physik. Chem.*, **21B**, 242.
Koteswaram, 1938, *Zeit. f. Phys.*, **110**, 118
Parthasarathy, S., 1934, *Phil. Mag.* (*suppl.*), **77**, 471
Rao, I. R., 1930, *Proc. Roy. Soc.* (*Amsterdam*), **127**
,, ,, (*London*), **33**, 632.
Rao, N. R., 1942, *Current Science*, **1**, 13
Thatte and Ganesan, 1931, *Phil. Mag.*, **12**, 823
Woodward, L., 1931, *Physik. Z.*, **32**, 777.

FLUID FLOW THROUGH POROUS MEDIA. PART III. AIR PERMEABILITY OF CONSOLIDATED SANDS PARTLY SATURATED WITH WATER*

By N. C. SEN GUPTA

(Received for publication, Nov. 11, 1943)

ABSTRACT An apparatus suitable for measuring gas permeabilities of consolidated sands, partly saturated with liquids is described The maximum rates of flow of air beyond which the observed permeabilities tend to diminish were found for seven samples of dry consolidated oilwell sands from Assam oil fields. Air permeabilities of these core samples at different degrees of water saturation were obtained keeping the rate of flow of air within the above limit. When the relative air permeabilities were plotted against the corresponding water saturations the curves obtained with the different core samples could be divided into two types In the first type the air permeability was constant within the limits of experimental error until the liquid saturation exceeded a certain value (5—15%) beyond which the permeability diminished, and finally became zero as the liquid saturation approached 100%. With the second type of curve the permeability began to diminish as the liquid saturation increased from zero. The remaining portions of the curve were similar to those of the first type

INTRODUCTION

In the first and second parts of this series (Sengupta and Mg. Thein Nyun, 1942, 1943) measurements on the use of gases for measuring true permeabilities of porous media, and the relations between porosity, permeability and average grain size of a number of oilsands obtained from Burma were reported. In these measurements the cores were extracted with chloroform and then thoroughly dried before measuring their permeabilities. In all technical problems associated with flow of fluids through porous media the latter are almost always partially saturated with one or more fluids. For example, oilsands may contain, in addition to crude oil, either water or natural gas or both. It is desirable in such cases to investigate conditions of flow of one fluid through consolidated sands partly saturated with another fluid. In the present paper results on flow of air through cores partially saturated with water have been reported.

The permeabilities K_a were calculated using the relation:—

$$K_a = \frac{2V \cdot p \cdot \eta \cdot L}{(p_2^2 - p_1^2)A}$$

where V in the volumes of air in *c. c.* flowing per second at atmospheric pressure through the cylindrical core of length L *cm.* and area A sq. *cm.*, p_2 is the pressure of the inflowing and p_1 that of the outflowing air, p the atmospheric pressure all expressed in atmospheres and η the viscosity of air in centipoises (0.0189 *c.p.* at 25°C the temperature of measurements).

---

* Communicated by Prof J N Mukherjee

The permeabilities of the partly saturated cores were expressed as fractions of the permeabilities of the dry cores and the liquid saturations were expressed in percentages, those of the completely saturated cores being taken as 100%.

EXPERIMENTAL

The apparatus used for the present measurements is shown in Figure 1.

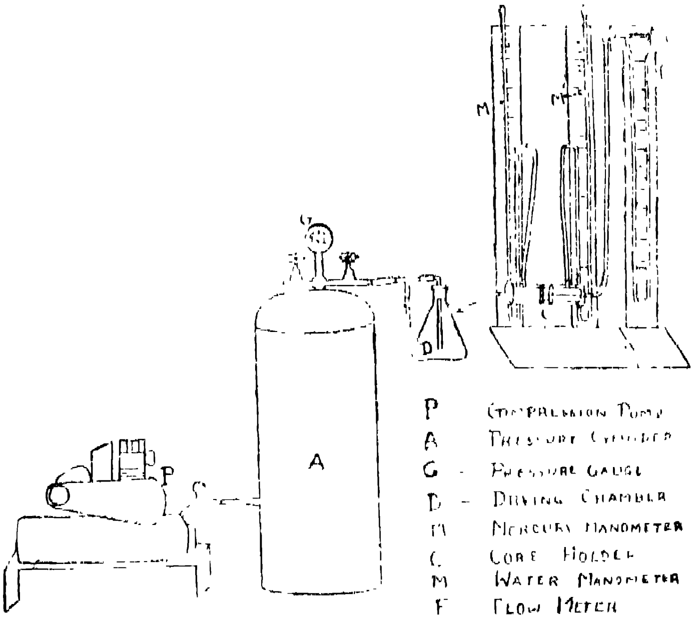

FIG. 1

It is different from that described in Part I of the series. The core holder is very similar to that used by Muscat (1937) and others except that the cores were sealed in brass cylinders and held in position in the core holder by rubber washers. The brass cylinders were removed from the core holders from time to time and weighed to determine the relative saturations. Air was taken from a pressure cylinder and dried by passing through a chamber containing fused calcium chloride. The pressure of the inflowing air was obtained from a mercury manometer and that of the outflowing air from a water manometer. The rate of flow of air was measured with a capillary flow-meter previously calibrated using a gas burette.

The core samples were first cut to the proper size, extracted with chloroform and thoroughly dried. Each core was then sealed in position with sealing wax in a brass ring. The brass rings containing the cores were weighed when dry and again when completely saturated with water, the difference giving the weight of the liquid filling the pores.

It was shown in Part I of this series that the measured permeability diminishes when the rate of flow of the gas exceeds a certain limit. Similar measurements were also made with the seven core samples used in the present measurements and the limiting rates of flow below which the measured permeability remained constant were ascertained. In measurements with partially saturated cores the rates of flow of air were kept within this limit.

RESULTS AND DISCUSSION

The rates of flow at different pressure gradients through several core samples are given in Figure 2 and in Tables I and II.

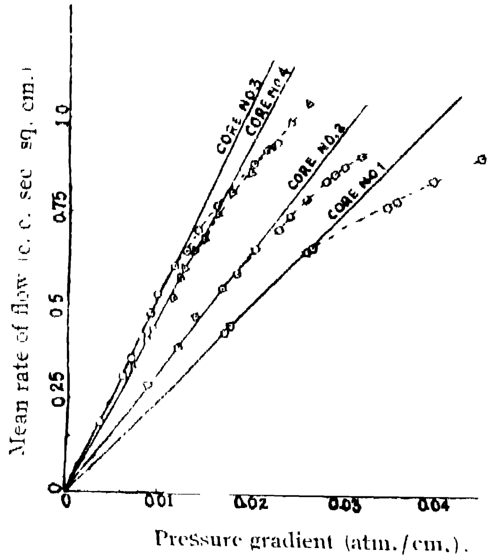

FIG. 2

TABLE I

Core No. 6 Length—2.00 cm. Area of cross section—9.26 sq. cm.

Pressure gradient (atm./cm.)	Rate of flow (c.c./sec., sq. cm.	Permeability (millidarcy).	Percentage deviation from permeability at zero rate of flow.
0.0241	0.1315	103	−0.5
0.0362	0.1974	103	−0.5
0.0483	0.2650	104	+0.5
0.0602	0.3348	105	+1.5
0.0729	0.4025	104	+0.5
0.0849	0.4581	102	−1.5
0.0969	0.5183	101	−2.4
0.1094	0.5776	100	−3.4
0.1213	0.6250	97.4	−5.9
0.1339	0.6712	95.3	−8.0
0.1457	0.7191	93.3	−9.9

Permeability at zero rate of flow from graphical extrapolation—103.5 millidarcy.

TABLE II

Core No. 3 Length—1.90 cm. Area of cross section—9.05 sq. cm.

Pressure gradient (atm./cm.)	Rate of flow (c.c./sec./sq. cm.)	Permeability (millidarcy).	Percentage deviation from permeability at zero rate of flow.
0.00352	0.102	1030	+2.5
0.00612	0.317	980	-2.5
0.00705	0.360	980	-2.5
0.00802	0.418	981	-2.4
0.00890	0.482	1020	+1.5
0.00975	0.531	1035	+3.0
0.01280	0.641	942	−6.5
0.01413	0.714	956	−4.9
0.01613	0.770	903	10.1
0.02027	0.891	834	-17.0
0.02164	0.930	803	20.1
0.02305	0.940	771	23.3

Permeability at zero rate of flow from graphical extrapolation—1005 millidarcy.

The permeability remains constant (within a maximum error of ±2.5%) until the rate of flow exceeds a value of 0.5—0.6 c.c./sec./sq. cm. Similar results were also obtained by Carlson and Eastman (1940). In the measurements reported below the rates of flow were kept below 0.5 c.c. per sec. per sq. cm.

Air permeability at different degrees of water saturation are shown in Figures 3 and 4 and Tables III and IV.

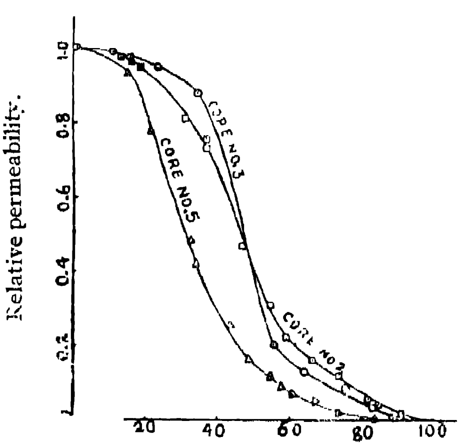

Percent water saturation.

FIG. 3

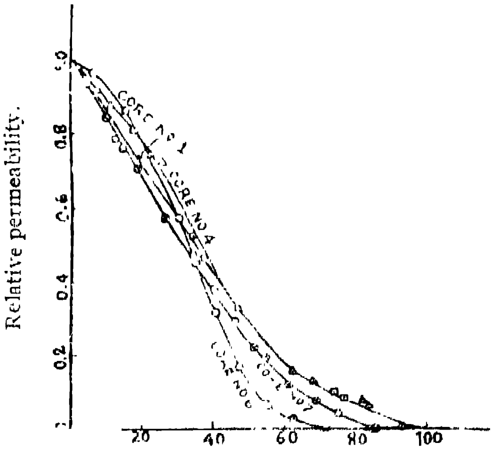

Percent water saturation.

FIG. 4

TABLE III

Core No. 7 Length—1.95 cm. Area of cross section—9.58 sq. cm.

Percentage water saturation	Permeability (millidarcy)	Relative permeability
95.8	0	—
89.6	0	—
83.9	0	—
76.0	3.8	0.045
69.0	6.9	0.083
61.0	10.2	0.122
55.0	17.2	0.206
51.1	18.2	0.218
46.3	25.2	0.302
39.7	32.2	0.386
34.6	38.4	0.460
30.2	47.3	0.566
25.8	49.1	0.581
18.9	60.9	0.720
14.6	64.9	0.768
10.1	72.6	0.859
0.0	83.5	1.00

TABLE IV

Core No. 5 Length 2.00 cm. Area of cross section 9.26 sq.cm

Percentage water saturation	Permeability (millidarcy)	Relative permeability
83.9	0	—
74.0	1.75	0.0215
67.3	4.05	0.0498
61.5	5.67	0.0698
58.1	7.43	0.0914
55.3	9.06	0.1167
49.2	12.86	0.1582
43.8	21.05	0.2589
33.4	34.08	0.4193
32.7	39.59	0.4871
21.2	63.39	0.7798
14.9	76.72	0.9439
1.0	81.28	1.00
0.0	81.28	1.00
—	—	—
—	—	—
—	—	—

While curves plotted in Figure 3 approach zero liquid saturation asymptotically those plotted in Figure 4 make an angle at zero liquid saturation. Otherwise the curves are all alike in shape. The slopes at the point of zero liquid saturation do not seem to depend on the permeability of the cores. Again, some cores attain zero air permeability long before complete liquid saturation is obtained while others approach zero permeability as the liquid saturation approaches 100%; cores showing the former behaviour generally have lower permeabilities.

Krutter (1941) made measurements similar to those reported in this paper. The author is not aware of any other work of similar nature although the simultaneous flow of two or three fluids through loose as well as consolidated sands was studied by Wyckoff, and others. (Wyckoff and Botset, 1936; Leverett, 1938, Botset, 1939 ; Leverett and Lewis, 1940). Wyckoff and others made measurements using very highly permeable cores and obtained curves which resembled in some respect those reported in Figure 3. Krutter found that different core samples produced curves of different shapes although his average curve was similar to those of Wyckoff and others. The reason why different cores would show different permeability/liquid saturation curves does not appear to be very clear.

ACKNOWLEDGEMENTS

I have much pleasure in acknowledging my indebtedness to Professor J. N. Mukherjee, C.B.E., D.Sc., and Mr. A. Reid, M.A., B.Sc., for their criticisms and kind interest in the present work. My thanks are due to the Manager of the Burmah Oil Co. (India Concessions) Ltd., for permission to publish this paper and to the University of Calcutta for providing laboratory facilities.

COLLOID RESEARCH LABORATORY
UNIVERSITY COLLEGE OF SCIENCE,
92, UPPER CIRCULAR ROAD,
CALCUTTA

REFERENCES

Botset, H. G., 1939, *Petroleum Technology*, Oct., T. P. 1111.

Carlson, A. J. and Eastman, M. C., 1940, *Petroleum Technology*, May, T. P. 1196.

Krutter, H., 1941, *Oil and Gas Journal*, June **12**, 49.

Leverett, M. C., 1938, *Petroleum Technology*, November, T. P. 1003.

Leverett, M. C., and Lewis, W. B., 1940, *Petroleum Technology*, T. P. 1206.

Muscat, M., 1937, *The flow of Homogeneous Fluids through Porous Media*, McGraw Hill Book Co., Ltd.

Sengupta, N. C. and Mg. Thein Nyun, 1942, *Ind. J. Phys.*, **16**, 119.

Sengupta, N. C. and Mg. Thein Nyun, 1943, *Ind. J. Phys.*, **17**, 39.

Wyckoff, R. D. and Botset, H. G., 1936, *Physics*, **7**, 325.

ON THE THEORY OF EMISSION OF ALPHA-PARTICLES FROM RADIOACTIVE NUCLEI*

By G. P. DUBE

AND

S. N. JHA

(Received for publication, Nov 27, 1943)

ABSTRACT. The rectangular potential hole of Condon-Gurney-Gamow model has been replaced by an exponential potential function $V = -V_0 e^{-r/r_0}$ and an expression has been worked out for the decay constant λ. It is found that the exact form and magnitude of the potential function inside the nucleus plays a very insignificant rôle in the problem. In the two limiting cases V_0 very small and V_0 very large, the decay constants λ_0 and λ_∞ are both independent of V_0 and ratio λ_∞/λ_0 is of the order 5 only. The nuclear radius r_0 has been calculated using the experimental data for the decay constant λ and the energy E and all the radii except those of ThC', RaC' are found to be between 7.8 and 9.7 × 10^{-13} cm. which is of the right order of magnitude and agrees in a satisfactory manner with those obtained by the previous workers with the one-body picture of the nucleus.

A satisfactory explanation of the emission of alpha-particles from certain radioactive substances was first given by Condon and Gurney (1929) and independently, by Gamow (1928), who considered the problem as a transmission of alpha particles through the nuclear potential barrier. For ease in calculation the nucleus was represented by a rectangular potential hole of a certain constant depth and a width r_0 where r_0 is defined as the nuclear radius. In the range $r_0 \leqq r \geqq \infty$ the potential function was taken to be the Coulomb one, *i.e.*, $V = \frac{2Ze^2}{r}$ where Z is the atomic number of the product nucleus and $2e$ is the charge of the alpha-particle. Such a picture of the nucleus is very crude. As a matter of fact, experimental evidences go to prove definitely that the nucleus consists of protons and neutrons held together by strong and short-range exchange forces. Thus the nuclear problems must be regarded as many-body problems and not as one-body problems. The extreme ease, with which energy is interchanged between densely packed particles inside the nucleus, can be easily understood with this model. The emission of an alpha-particle into free space after crossing the potential barrier which surrounds the nucleus is understood in this way, *viz.*, the interaction between the several constituents of the nucleus leaves an alpha-particle with a certain kinetic energy; possessed of this kinetic energy the alpha-particle penetrates through the barrier. The ideal calculation would be to find out the probability of the formation of alpha-particles from neutrons and protons and their being left with a certain kinetic energy and the next task would be to find out the penetrability of the alpha-particles through the nuclear potential barrier. This is how the problem should be tackled if the nucleus is considered as a many-body problem. Unfortunately the mathematical complexities are so great that the many-body problem may remain unsolved for a considerably long time.

---

* Communicated by Prof. M. N. Saha, F.R.S.

The exact law of force between an alpha-particle and other nuclear particles is at present unknown. It may be expected that the exact form of the potential function inside the nucleus will not drastically modify the results obtained in the rectangular potential hole model but a detailed mathematical analysis of this expected result has not been attempted. Bethe (1937) mentions that the exact value of the potential depth is of no great importance. It was therefore thought necessary to examine this problem in detail.

In the present paper, the rectangular potential hole of Condon-Gurney-Gamow model has been replaced by an exponential function given by,

$$V = -V_0 e^{-r/r_0} \qquad \dots \quad (1)$$

and an expression has been worked out for the decay constant λ. It has been found that the decay constant λ does not sensibly depend on the magnitude of V_0 and in the two limiting cases, V_0 very small and V_0 very large it is in fact independent of V_0 and the ratio λ_∞/λ_0 is of the order 5 only. It is entirely a new result and provides a clear and detailed analysis and in support of a hitherto expected result. Using the experimental data for the decay constant, the nuclear radii have been calculated and the values obtained are quite satisfactory and agree well with those given by previous workers with the one-body picture of the nucleus. In view of the more correct many-body picture of the nucleus, the results presented in this paper are purely of theoretical interest.

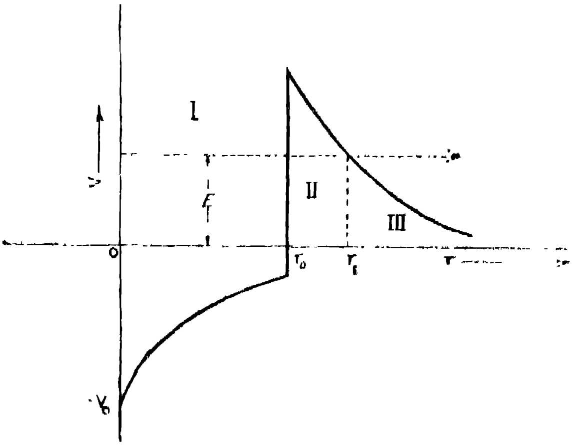

FIG. 1

The exponential potential function is shown in Fig. 1 as a function of r the distance from the centre of the nucleus. If we consider alpha-particles of a given energy E, we may divide the whole space into three regions as indicated in Fig. 1.

(*i*) The interior of the nucleus $0 < r \leq r_0$, where the potential energy

$$V = -V_0 e^{-r/r_0}$$

(*ii*) The region of the potential barrier $r_0 \leq r \leq r_1$ where r_1 is the classical distance of closest approach of an alpha-particle of energy E falling on the nucleus from outside. In this region the potential energy is greater than the energy of the alpha-particle.

(*iii*) The outside region $r > r_1$ in which the potential energy is less than E.

We consider the case when the wave function of the alpha-particle is spherically symmetrical. This corresponds to an alpha-particle of orbital momentum $l=0$ or what is known as the *s*-state of the particle. The wave function of an alpha-particle can then be written in the form,

$$\phi = \frac{\psi}{r}$$

where ψ satisfies the equation

$$\frac{d^2\psi}{dr^2} + \frac{2M}{\mathbf{h}^2}(E - V)\psi = 0$$

where M is the mass of an alpha-particle and **h** is Planck's constant divided 2π. We take the values (Birge, 1941)

$$M = 6.644 \times 10^{-24} \text{ gm.}$$

$$\mathbf{h} = 1.0541 \times 10^{-27} \text{ erg-sec}$$

In the three regions marked in the figure 1, the equations are

Region I, $$\frac{d^2\psi}{dr^2} + \frac{2M}{\mathbf{h}^2}\left(E + V_0 e^{-r/r_0}\right)\psi = 0 \qquad \ldots \quad (2)$$

Region II, $$\frac{d^2\psi}{dr^2} + \frac{2M}{\mathbf{h}^2}(E - V)\psi = 0 \qquad \ldots \quad (3)$$

Region III, $$\frac{d^2\psi}{dr^2} + \frac{2M}{\mathbf{h}^2}(E - V)\psi = 0 \qquad \ldots \quad (4)$$

In equation (3), $V = \frac{2Ze^2}{r}$ and $E - V$ is negative whereas in equation (4) V is again $\frac{2Z\epsilon^2}{r}$ but $E - V$ is positive.

First of all we give the solution of equation (2).

Putting

$$y = e^{-r/2r_0}$$

we have $$\frac{d\psi}{dr} = -\frac{y}{2r_0} \cdot \frac{d\psi}{dy} \quad \text{and} \quad \frac{d^2\psi}{dr^2} = \left(\frac{y}{2r_0}\right)^2 \left\{ \frac{d^2\psi}{dy^2} + \frac{1}{y}\frac{d\psi}{dy} \right\}$$

Hence the equation (2) transforms itself to

$$\frac{d^2\psi}{dy^2} + \frac{1}{y}\frac{d\psi}{dy^2} + \frac{2M}{\mathbf{h}^2}(2r_0)^2\left(V_0 + \frac{E}{y^2}\right)\psi = 0 \qquad \ldots \quad (5)$$

We define
$$p^2 = \frac{2M}{\mathbf{h}^2}\,.\,(2r_0)^2.\,V_0 \qquad \ldots \quad (6)$$

$$\mu^2 = -\frac{2M}{\mathbf{h}^2}\,.(2r_0)^2.E = -p^2\frac{E}{V_0} = i^2n^2. \qquad \ldots \quad (7)$$

Therefore the equation (5) takes the form,

$$\frac{d^2\psi}{dy^2} + \frac{1}{y}\frac{d\psi}{dy} + \left(p^2 - \frac{\mu^2}{y^2}\right)\psi = 0 \qquad \ldots \quad (8)$$

This is a standard type of equation and is known as Bessel's equation and has been well-studied by mathematicians. Here μ is not an integer, therefore the general solution of this equation is,

$$\psi_1 = C.J_{\mu}(py) + D.J_{-\mu}(py)$$

or
$$\psi_1 = C.J_{ni}(pe^{-r/2r_0}) + D.J_{-ni}(pe^{-r/2r_0}) \qquad \ldots \quad (9)$$

where C and D are constants to be determined by the boundary conditions. The first term corresponds to a wave travelling towards the right and the second one to a wave travelling towards the left after being reflected at the potential barrier.

We next consider the equation (3) in which case $E-V$ is negative. Let us define

$$\phi(r) = \frac{2M}{\mathbf{h}^2}\left(\frac{2Ze^2}{r} - E\right), \text{ (positive)} \qquad . \quad (10)$$

The solution ψ_{II} in this region is of an exponential character rather than of a wave type. As has been shown by Jeffreys (1924) and later on, independently by Kramers (1926), the two fundamental solutions of (3) approximate very closely to

$$\psi_1 = B_1\left\{\phi(r)\right\}^{-\frac{1}{4}}.\,\text{exp.}\left\{\int_r^{r_1}\left[\phi(r)\right]^{\frac{1}{2}}dr\right\}$$
$$\psi_2 = \tfrac{1}{2}B_2.\left\{\phi(r)\right\}^{-\frac{1}{4}}.\,\text{exp.}\left\{-\int_r^{r_1}\left[\phi(r)\right]^{\frac{1}{2}}dr\right\} \qquad \ldots \quad (11)$$

It is to be noted that ψ_1 decreases from the nucleus outwards and ψ_2 increases. At the boundary of the nucleus, function $\psi_1(r_0)$ will be much greater than $\psi_2(r_0)$ because ψ_1 contains an exponential with a large positive exponent while ψ_2 contains one with a large negative exponent.

Lastly we consider the equation (4) in which case $E-V$ is positive. At large distances from the nucleus, V is very small and therefore it can be neglected. The equation then becomes

$$\frac{d^2\psi}{dr^2}+\frac{2M}{\mathbf{h}^2}E\psi=0$$

of which a general solution is

$$\psi=Ae^{ikr}+Be^{-ikr}$$

where $$k^2=\frac{2M}{\mathbf{h}^2}E$$

and A and B are some constants. By multiplying it with the time factor $\exp.\left(\frac{-iEt}{\mathbf{h}}\right)$, it can be seen that the first term represents an outgoing wave while the second term gives an incoming wave. In the physical problem considered here, the alpha-particle leaves the nucleus and none comes towards it from outside, hence we put $B=0$.

Therefore, $$\psi=Ae^{ikr} \qquad \ldots \quad (12)$$

To obtain the wave function for smaller values of r, it is again convenient to use the Wenzel- Kramers- Brillouin (1932) approximation in the form given by Kramers (1926). According to this method, the two fairly good approximate solutions of the equation (4), which fit in smoothly at $r=r_1$ with the two solutions given in (11) respectively are,

$$\psi_3=\{\phi(r)\}^{-\frac{1}{4}}\cos\left\{\int_{r_1}^{r}|\phi(r)|^{\frac{1}{2}}dr+\frac{\pi}{4}\right\}$$

$$\ldots \quad (13)$$

$$\psi_4=\{\phi(r)\}^{-\frac{1}{4}}\cos\left\{\int_{r_1}^{r}[\phi(r)]^{\frac{1}{2}}dr-\frac{\pi}{4}\right\}$$

The most general solution of the equation (4) is then,

$$\psi_{\rm III}=B_1\psi_3+B_2\psi_4 \qquad \ldots \quad (14)$$

In order that (14) may be of the same form as (12), we must choose

$$B_2=iB_1$$

Since, for large r, V can be neglected $\phi(r)=k^2$ and therefore,

$$\psi_{\rm III}\longrightarrow B_1k^{-\frac{1}{2}}e^{ikr} \qquad \ldots \quad (15)$$

Comparing (12) and (15) we have,

$$A=B_1k^{-\frac{1}{2}} \qquad \ldots \quad (16)$$

At the boundary of the nucleus $r=r_0$, the wave function of the region I will be equal to that of region II and so will their first derivatives be. As has already been pointed, $\psi_1(r_0)$ will be much greater than $\psi_2(r_0)$, hence we may neglect $\psi_2(r_0)$ and put,

$$\psi_{\rm I}(r_0)=\psi_1(r_0);\quad \left(\frac{d\psi_{\rm I}}{dr}\right)_{r_0}=\left(\frac{d\psi_1}{dr}\right)_{r_0}$$

or $$*\mathrm{C}J_{ni}(pe^{-\frac{1}{2}})+\mathrm{D}J_{-ni}(pe^{-\frac{1}{2}})=\mathrm{B}_1\{\phi(r_0)\}^{-\frac{1}{4}}\ \exp.\left\{\int_{r_0}^{r}[\phi(r)]^{\frac{1}{2}}dr\right\}$$

and, $$\mathrm{C}J'_{ni}(pe^{-\frac{1}{2}})+\mathrm{D}J'_{-ni}(pe^{-\frac{1}{2}})=\frac{2r_0}{pe^{-\frac{1}{2}}}.\mathrm{B}_1.\{\phi(r_0)\}^{\frac{1}{4}}\ \exp.\left\{\int_{r_0}^{r}[\phi(r_0)]^{\frac{1}{2}}dr\right\}.$$

where $J'_{\mu}(pe^{-\frac{1}{2}})=\left\{\frac{\partial J_{\mu}(pe^{-r/2r_0})}{\partial(pe^{-r/2r_0})}\right\}_{r=r_0}$ and we have neglected a term $\frac{1}{4}\phi^{-\frac{5}{4}}.\frac{d\phi}{dr}$ in comparison with $\phi^{\frac{1}{4}}$; as it is numerically very small.

We define,

$$\left.\begin{aligned} pe^{-\frac{1}{2}}&=x\\ J_{ni}(x)&=\alpha\\ J'_{ni}(x)&=\alpha'\\ J_{-ni}(x)&=\beta\\ J'_{-ni}(x)&=\beta'\\ \frac{2r_0}{x}&=m\\ \int_{r_0}^{r}[\phi(r)]^{\frac{1}{2}}dr&=\mathrm{P}\end{aligned}\right\}\qquad\ldots\quad(17)$$

Therefore,

$$\mathrm{C}\alpha+\mathrm{D}\beta-\mathrm{B}_1\{\phi(r_0)\}^{-\frac{1}{4}}e^{\mathrm{P}}=0$$

$$\mathrm{C}\alpha'+\mathrm{D}\beta'-\mathrm{B}_1 m\{\phi(r_0)\}^{\frac{1}{4}}e^{\mathrm{P}}=0.$$

This gives us

$$\frac{\mathrm{C}}{\beta'\{\phi(r_0)\}^{-\frac{1}{4}}e^{\mathrm{P}}-m\beta\{\phi(r_0)\}^{\frac{1}{4}}e^{\mathrm{P}}}=\frac{\mathrm{D}}{m\alpha\{\phi(r_0)\}^{\frac{1}{4}}e^{\mathrm{P}}-\alpha'\{\phi(r_0)\}^{-\frac{1}{4}}e^{\mathrm{P}}}=\frac{\mathrm{B}_1}{\alpha\beta'-\alpha'\beta}.$$

or $$\mathrm{B}_1=\mathrm{C}.\frac{\alpha\beta'-\alpha'\beta.}{\beta'\{\phi(r_0)\}^{-\frac{1}{4}}-m\beta\{\phi(r_0)\}^{\frac{1}{4}}}.e^{-\mathrm{P}}\qquad\ldots\quad(18)$$

The decay constant λ is given by

$$d\mathrm{N}=-\lambda\mathrm{N}dt$$

or $$\lambda=-\frac{1}{\mathrm{N}}.\frac{d\mathrm{N}}{dt}.$$

where $\frac{1}{\mathrm{N}}\frac{d\mathrm{N}}{dt}$ is the ratio of all the particles coming out per second from the nucleus to the total number incident. Thus we have,

$$\lambda=4\pi r^2.v.|\Phi|^2$$

$$=4\pi.v.|\mathrm{A}|^2.$$

$$=\frac{4\pi v}{k}.|\mathrm{B}_1|^2$$

---

* $e^{-\frac{1}{2}}$ is exp.$(-\frac{1}{2})$ and should not be confused with the electronic charge, for which the greek symbol ϵ (epsilon) has been used.

Now $\frac{v}{k}=\frac{\mathbf{h}}{M}$ and $\phi(r_0)=\frac{2M}{\mathbf{h}^2}.(V_1-E)$ where $V_1=\frac{2Ze^2}{r_0}$ and defining

$$\gamma=\alpha\beta'-\alpha'\beta \qquad \dots \quad (19)$$

we have,

$$\lambda=\frac{4\pi\mathbf{h}}{M}.|C|.^2\left|\frac{\gamma}{m\{\phi(r_0)\}^{\frac{1}{2}}\beta\left[\frac{\beta'}{\beta m\{\phi(r_0)\}^{\frac{1}{2}}}-1\right]}\right|^2.e^{-2P} \qquad \dots \quad (20)$$

It has been proved on page 43, Theory of Bessel Functions, Watson (1922), that if ν be not an integer,

$$J_\nu(z)J'_{-\nu}(z)-J_{-\nu}(z)J'_\nu(z)=-\frac{2\sin\nu\pi}{\pi z}$$

Replacing ν by in and the argument z by x, this becomes identical with γ defined in (19). Therefore we have,

$$\gamma=-\frac{2\sin(in\pi)}{\pi x} \quad \text{and} \quad \gamma^2=\frac{4\sinh^2 n\pi}{\pi^2x^2} \qquad \dots \quad (21)$$

Using the expression for m and $\phi(r_0)$, we have

$$m\{\phi(r_0)\}^{\frac{1}{2}}=\frac{2r_0}{x}.\frac{\sqrt{2M}}{\mathbf{h}}.(V_1-E)^{\frac{1}{2}}=e^{\frac{1}{2}}.\left(\frac{V_1-E}{V_0}\right)^{\frac{1}{2}} \qquad \dots \quad (22)$$

Also, $$m^2x^2=(2r_0)^2$$

Hence,

$$\lambda=\frac{4\mathbf{h}^2}{\sqrt{2}.\pi M^{\frac{3}{2}}r_0^2}.\frac{\sinh^2 n\pi}{(V_1-E)^{\frac{1}{2}}}.\left|\frac{C}{\beta}\right|^2\left|\frac{e^{-2P}}{\frac{\beta'}{\beta e^{\frac{1}{2}}}\left(\frac{V_0}{V_1-E}\right)^{\frac{1}{2}}-1}\right|^2 \qquad \dots \quad (23)$$

$|C|^2$ can be determined from the condition that the intensity of the incident wave is unity. Therefore we have,

$$4\pi|C|^2\int_0^{r_0}J_{in}(pe^{-r/2r_0}).J_{-in}(pe^{-r/2r_0}).dr=1$$

Putting $z=pe^{-r/2r_0}$, $dr=-\frac{2r_0}{z}dz$ then $-8\pi r_0|C|^2.\int_p^x\frac{J_{in}(z)J_{-in}(z)}{z}dz=1$

To perform this integration, we make use of the relation (7), page 147, Watson (1922), *viz.*,

$$J_\nu(z)J_{-\nu}(z)=\sum_{s=0}^{\infty}\frac{(-1)^s(\frac{1}{2}-z)^{2s}.(2s)!}{(s!)^2\Gamma(\nu+s+1)\Gamma(-\nu+s+1)}$$

Putting $$\nu=,in$$

$$\frac{J_{in}(z)J_{-in}(z)}{z}=\sum_{s=0}^{\infty}\frac{(-1)^s.(2s)!z^{2s-1}}{2^{2s}.(s!)^2\Gamma(in+s+1)\Gamma(-in+s+1)}$$

Therefore we have,

$$\int_p^x \frac{J_{in}(z)J_{-in}(z)}{z}dz = \frac{1}{\Gamma(1+in)\Gamma(1-in)}\log\frac{x}{p} + \sum_{s=1}^{\infty}\frac{(-1)^s(2s-1)!(x^{2s}-p^{2s})}{2^{2s}.(s!)^2\Gamma(in+s+1)\Gamma(-in+s+1)}$$

$$= -\frac{1}{2\Gamma(1+in)\Gamma(1+in)} + \sum_{s=1}^{\infty}\frac{(-1)^{s+1}(2s-1)!\,.\,p^{2s}(1-e^{-s})}{2^{2s}.(s!)^2\Gamma(in+s+1)\Gamma(-in+s+1)} \quad . \qquad (24)$$

For small values of p and hence of V_0, we can neglect all the terms containing p^2 and higher powers and we have,

$$|C|^2 = \frac{1}{4\pi r_0}\,.\,\Gamma(1+in)\Gamma(1-in) = \frac{1}{4\pi r_0}\,.\,\frac{n\pi}{\sinh n\pi} = \frac{n}{4r_0\sinh n\pi} \quad \ldots \quad (25)$$

If p and hence V_0 be not negligible, we have to retain three or four terms of the series containing p. The the range of integration being small, a sufficiently accurate value is given by

$$\int_p^x J_{in}\frac{(z)J_{-in}(z)}{z}dz = J_{in}\left(\frac{x+p}{2}\right).J_{-in}\left(\frac{x+p}{2}\right).\log\frac{x}{p} = -\tfrac{1}{2}J_{in}\left(\frac{x+p}{2}\right)J_{-in}\left(\frac{x+p}{2}\right)$$

or

$$|C|^2 = \frac{1}{4\pi r_0\left|J_{in}\left(\frac{x+p}{2}\right)\right|^2} \quad . \qquad (26)$$

Next we turn to the evaluation of the terms containing β and β'. For all values of ν, the Bessel function $J_\nu(z)$ is defined by,

$$J_\nu(z) = \sum_{s=0}^{\infty}\frac{(-1)^s\,.\,(\frac{1}{2}z)^{\nu+2s}}{s!\,\Gamma(\nu+s+1)}$$

Hence, $$\beta = J_{-in}(x) = \frac{(\frac{1}{2}x)^{-in}}{\Gamma(1+in)}\,.\left\{1-\frac{(\frac{1}{2}x)^2}{1-in}+\ldots\right\}$$

For small values of x, we have,

$$\beta = \frac{(\frac{1}{2}x)^{-in}}{\Gamma(1-in)} \qquad \frac{1}{|\beta|^2} = |\Gamma(1-in)|^2 = \frac{n\pi}{\sinh n\pi} \quad \ldots \quad (27)$$

When order and argument both are large and comparable, a very good approximation to the Bessel function $J_\nu(z)$ is Watson (1922), page 229,

$$J_\nu(z) = M_\nu\cos\left(Q_\nu - \frac{\pi}{4}\right)$$

where $$M_\nu = \left(\frac{2}{\pi\sqrt{z^2-\nu^2}}\right)^{\frac{1}{2}} \text{ and } Q_\nu = \sqrt{z^2-\nu^2} - \frac{\nu\pi}{z} + \nu\sin^{-1}\frac{\nu}{z}\,.$$

In the problem considered here $\nu = in$, hence

$$|\beta|^2 = |J_{-in}(x)|^2 = \frac{2}{\pi}\frac{\cosh^2(n\pi/2)}{\sqrt{x^2+n^2}}$$

or

$$|\beta|^2 = \frac{\sinh n\pi}{\pi\sqrt{x^2+n^2}} \qquad \dots \quad (28)$$

and also

$$|C|^2 = \frac{\{(\frac{x+p}{2})^2+n^2\}^{\frac{1}{2}}}{4r.\sinh n\pi}$$

Therefore, we have the following results,

$$\left.\begin{aligned}
\left|\frac{C}{\beta}\right|^2 &= \frac{n^2\pi}{4r_0\sinh^2 n\pi} \quad \text{for small } V_0 \\
\left|\frac{C}{\beta}\right|^2 &= \frac{\pi[(x^2+n^2)\{(\frac{x+p}{2})^2+n^2\}]^{\frac{1}{2}}}{4r_0\sinh^2 n\pi} \quad \text{for } x \text{ and } n \text{ large and comparable.} \\
\left|\frac{C}{\beta}\right|^2 &= \frac{\pi x(x+p)}{8r.\sinh^2 n\pi} \quad \text{for } x \text{ large and} >> n.
\end{aligned}\right\} \quad \dots \quad (29)$$

Making use of the relation

$$J'_\nu(z) = -\frac{\nu}{z}J_\nu(z) + J_{\nu-1}(z)$$

we have

$$\frac{\beta'}{\beta} = \frac{J'_{-in}(x)}{J_{-in}(x)} = \frac{ni}{x} + \frac{J_{-(in+1)}(x)}{J_{-in}(x)}$$

Since we have the relation

$$\frac{J_\nu(x)}{J_{\nu-1}(x)} = \frac{\frac{1}{2}\frac{x}{\nu}}{1-\frac{\frac{1}{4}\frac{x^2}{\nu(\nu+1)}}{1-\dots\dots}} = \frac{1}{2}\frac{x}{\nu}\left\{1+\frac{x^2}{4\nu(\nu+1)}+\dots\right\}$$

therefore, for small values of x,

$$\frac{J_\nu(x)}{J_{\nu-1}(x)} = \frac{1}{2}\frac{x}{\nu}$$

or

$$\frac{\beta'}{\beta} = \frac{ni}{x} - \frac{2ni}{x} = -\frac{ni}{x} = -ie^{\frac{1}{2}}\cdot\left(\frac{E}{V_0}\right)^{\frac{1}{2}} \qquad \dots \quad (30)$$

For large n and for large values of x, we have

$$J_{-(in+1)}(x) \backsim J_{-in}(x).$$

Therefore

$$\frac{\beta'}{\beta} = 1+\frac{ni}{x} = 1+ie^{\frac{1}{2}}\sqrt{\frac{E}{V_0}} \qquad \dots \quad (31)$$

Using these relations, we get,

$$\left|\frac{\beta'}{\beta e^{\frac{1}{2}}}\cdot\left(\frac{V_0}{V_1-E}\right)^{\frac{1}{2}} - 1\right|^2 = 1+\frac{E}{V_1-E} = \frac{V_1}{V_1-E} \quad \text{for small values of } V_0. \qquad \dots \quad (32)$$

$$\left|\frac{\beta'}{\beta c^{\frac12}}\left(\frac{V_0}{V_1-E}\right)^{\frac12}-1\right|^2=\frac{1}{c(V_1-E)}\left\{V_0+cV_1-2\sqrt{cV_0(V_1-E)}\right\} \quad \ldots \quad (33)$$

for V_0 comparable with E,

and $$=\frac{V_0}{c(V_1-E)} \text{ for } V_0 \text{ large.}$$

By the help of the relations (7), (23), (29) and (31), for very small values of V_0 we therefore have,

$$\lambda_0=\frac{4\sqrt{2}}{r_0\sqrt{M}}\cdot\frac{E}{V_1}(V_1-E)^{\frac12}e^{-2P} \quad \ldots \quad (34)$$

For very large values of V_0, we have, using the relations (6), (17), (23), (29) and (33),

$$\lambda_\infty=\frac{1(c^{\frac12}+1)}{r_0\sqrt{2M}}\cdot(V_1-E)^{\frac12}.e^{-2P} \quad \ldots \quad (35)$$

For values of V_0 comparable with E, we have, using (23), (29) and (33),

$$\lambda=\frac{4}{r_0}.\sqrt{\frac{2}{M}}\cdot(V_1-E)^{\frac12}.\frac{(V_0+cE)^{\frac12}\cdot\left\{\left(\frac{c^{\frac12}+1}{2}\right)^2V_0+cE\right\}^{\frac12}}{V_0+cV_1-2\sqrt{cV_0(V_1-E)}}.e^{-2P} \quad \ldots \quad (36)$$

It is to be noticed that λ_0 and λ_∞ are both independent of V_0 and that (36) reduces to (34) and (35) in the limiting case of V_0 very small and V_0 very large respectively. Also we have

$$\frac{\lambda_0}{\lambda_\infty}=\frac{\text{[illegible]}}{c^{\frac12}+1}\cdot\frac{E}{V_1}=.76\,\frac{E}{V_1} \quad \ldots \quad (37)$$

If we choose for r_0 the nuclear radius the value 9×10^{-13}cm. derived with one body model from experiment, Bethe (1937), for Z the average nuclear charge of radioactive elements, about 86, V_1 comes out to be 27 MV; and for E we choose an average energy 6 MV. Therefore the ratio λ_0/λ_∞ comes out to be .17 only. This leads us to conclude that the decay constant λ does not depend sensibly on the exact form and magnitude of the potential function inside the nucleus. The most important factor is the exponential term and for the sake of completeness we discuss its nature. As defined in (17),

$$P=\frac{\sqrt{2M}}{h}\int_{r_0}^{r_1}\left(\frac{2Ze^2}{r}-E\right)^{\frac12}dr.$$

Substituting $\cos^2\alpha=\frac{Er}{2Ze^2}$, we have;

$$P=\frac{\sqrt{2M}}{h}\cdot\frac{4Ze^2}{\sqrt{E}}\int_0^{\alpha_0}\sin^2\alpha\,d\alpha=\frac{\sqrt{2M}}{h}\cdot\frac{Ze^2}{\sqrt{E}}\left[2\alpha_0-\sin 2\alpha_0\right]$$

where
$$\theta_0 = \cos^{-1}\sqrt{\frac{E}{V_1}}\,.$$

Therefore
$$P = \left\{\frac{\sqrt{2M}}{h}\cdot\frac{2Ze^2}{\sqrt{E}}\right\}\left\{\cos^{-1}\sqrt{\frac{E}{V_1}} - \left(\frac{E}{V_1}\right)^{\frac{1}{2}}\left(1-\frac{E}{V_1}\right)^{\frac{1}{2}}\right\}$$

Defining
$$\frac{E}{V_1} = \theta$$

$$P = \frac{1.26Z}{\sqrt{E}}\,g(\theta) \qquad \ldots \quad (38)$$

where E is in million volts and

$$g(\theta) = \cos^{-1}\theta^{\frac{1}{2}} - \theta^{\frac{1}{2}}(1-\theta)^{\frac{1}{2}} \qquad \ldots \quad (39)$$

The values of $g(\theta)$ as a function of θ are given below :

TABLE I

θ	$g(\theta)$	θ	$g(\theta)$	θ	$g(\theta)$
.12	.8873	.18	.7485	.24	.6317
.13	.8651	.19	.7275	.25	.6142
.14	.8404	.20	.7071	.26	.5972
.15	.8161	.21	.6875	.27	.5822
.16	.7926	.22	.6683	.28	.5631
.17	.7702	.23	.6498	.29	.5483
				.30	.5328

For comparison with the experimental data, it is found convenient to use the experimental data for the decay constant and the energy of the alpha-paricle and to compute the nuclear radius from these data with the help of the derived theoretical formula. If the formula is correct, the radius r_0 must come out to be nearly the same for all radioactive nuclei. It has already been shown that the exact shape and magnitude of the potential function inside the nucleus plays only a very insignificant role in the problem and the ratio λ_r/λ_0 is of the order 5 (eq. 37), hence we adopt as the final formula,

$$\lambda = 2.5\lambda_0 = \frac{5\sqrt{2}\,E}{e^2\sqrt{M}\,Z}(V_1 - E)^{\frac{1}{2}}e^{-2P} \qquad \ldots \quad (40)$$

This can be written in the form

$$\lambda = A(E, Z, r_0)e^{-2P}$$

or
$$\log_{10}\lambda = \log_{10}A - {\cdot}8686P$$

where $$\log_{10} A = 22.3822 + \log_{10}\frac{E}{Z} - \tfrac{1}{2}\log_{10}(V_1 - E)$$

E, V_1 being in million volts. In calculating A, we have taken the value of V_1 corresponding to $r_0 = 9.0 \times 10^{-13}$ cm. Thus we have, if V_1 be in million volts,

$$V_1 = .32Z.$$

Using the relation (38),

$$g(\theta) = \frac{\sqrt{E}}{1.005\,Z}(\log_{10} A - \log_{10}\lambda) \qquad \ldots \quad (41)$$

This enables us to calculate $g(\theta)$ from the experimental data of the decay constant λ and the energy E in million volts. The results given in Table I have been used to calculate θ and then the nuclear radius r_0 is given by the relation,

$$\log_{10} r_0 = -13.1591 + \tfrac{1}{2}\log_{10} A - \log_{10}\frac{E}{Z} \qquad \ldots \quad (42)$$

The calculated values of the nuclear radius r_0 are given in Table II and all radii except those of ThC, RaC lie between 7.8 and 9.7 × 10^{-13} cms. These are of the right order of magnitude and compare in a satisfactory manner with those obtained by Gamow (1929), (1937) and by Bethe (1937).

TABLE II

Disintegrating Nucleus	Product		Energy E MV	Decay constant λ in sec⁻¹	Nuclear radius r_0 in 10^{-13} cm. calculated from (42)
Th	MThI	88	4.31	1.2×10^{-18}	7.77
RdTh	ThX	88	5.52	1.15×10^{-8}	8.71
ThX	Thn	86	5.70	2.20×10^{-6}	9.63
Thn	ThA	84	6.40	1.27×10^{-2}	8.63
ThA	ThB	82	6.90	5.0	8.22
ThC	ThC″	81	6.20	6.7×10^{-5}	7.07
ThC′	ThD	82	8.95	?	—
UI	UXI	90	4.15	5.0×10^{-18}	9.67
Io	Ra	88	4.67	2.9×20^{-13}	9.25
Ra	Rn	86	4.88	1.37×10^{-11}	8.68
Rn	RaA	84	5.59	2.10×10^{-6}	8.66
RaA	RaB	82	6.11	3.8×10^{-3}	8.48
RaC	RaC″	81	5.61	5.3×10^{-7}	7.21
RaC′	RaD	82	7.83	7×10^{4}	9.07
RaF	RaG	82	5.40	5.7×10^{-8}	7.95
Pa	Ac	89	5.16	6.9×10^{-13}	7.95
RdAc	AcX	88	6.16	4.25×10^{-7}	7.81
AcX	An	86	5.82	7.2×10^{-7}	8.49
An	AcA	84	6.95	1.77×10^{-1}	8.61
AcA	AcB	82	7.51	3.5×10^{2}	8.25
AcC	AcC″	81	6.74	5.3×10^{-3}	6.80
AcC′	AcD	82	7.58	?	—

? No experimental values available

Our thanks are due to Principal Kamta Prosad, I.E.S., for his keen interest in this work.

PHYSICAL LABORATORY,
SCIENCE COLLEGE,
PATNA

REFERENCES

Bethe, H. A., 1937, Nuclear Physics, B. Nuclear Dynamics, Theoretical, *Rev. Mod Phys.*, **9**, 166

Birge, R. T., 1941, A new Table of value of the general physical constants, *Rev. Mod. Phys*, **13**, 237.

Brillouin, L., 1932, Notions de mécanique ondulatoire, les méthode d' approximations, *Actualities Scientifique et Industrielles*, **39**, Hermann, Paris, p 11.

Condon, E. U. and Gurney, R. W., 1929, Quantum Mechanics and Radioactive Disintegration, *Phys Rev*, **33**, 127.

Gamow, G., 1928, Zur Quantentheorie des Atomkerns, *Zeits f. Phys*, **41**, 204

Gamow, G. and Houtermans, F., 1929, Zur Quantentheorie des radioaktiven Kerns, *Zeits f Phys*, **42**, 496.

Gamow, G. and Houtermans, F, 1937, *Atomic Nuclei and Radioactivity*, Camb. Univ Press, Sec 68.

Jeffreys, H., 1924, On certain approximate solution of linear differential equations of the second order, *Proc. Lond. Math Soc*, **23**, 428.

Kramers, H. A., 1926, Wellenmechanik und halbzahlige Quantisierung, *Zeits. f Phys.*, **39**, 828

Watson, G. N., 1922, *Theory of Bessel Function*, Camb. Univ. Press.

Wenzel, G., 1926, Eine Verallgemeinerung der Quantenbedingungen fur die Zwecke der Wellenmechanik, *Zeits f Phys.*, **38**, 518.

STUDY OF ELECTROLYTIC DISSOCIATION IN STRONG ELECTROLYTES BY RAMAN EFFECT

MISCELLANEOUS SUBSTANCES : PHOSPHORIC ACID, BICARBONATES AND PERCHLORIC ACID

By N. RAJESWARA RAO

(*Received for publication, September 17, 1943*)

ABSTRACT. In this paper, a detailed study of electrolytic dissociation in phosphoric acid and phosphates, bicarbonates and perchloric acid is described. Raman spectra of solutions of phosphoric acid are quite similar to that of sulphuric acid and the lines attributed to various kinds of radicals, H_3PO_4, H_2PO_4, HPO_4 and PO_4. A study of these lines in solutions of the acid and of the salt revealed that the dissociation of phosphoric acid is quite rapid as far as the removal of the first hydrogen ion is concerned, while further dissociation is very slow. No evidence for the dissociation of the ions is found in solutions of phosphates and bicarbonates could be traced from these studies. In solutions of perchloric acid, below 70%, evidence for the presence of undissociated molecules is found. It is concluded that this acid is not as strong as was supposed to be.

PHOSPHORIC ACID

Introduction.—Electrolytic dissociation in phosphoric acid and phosphates has been studied by a number of investigators including Nisi (1929), Bell and Jeppesen (1935), Schaefer, Matosi and Aderhold (1930), Hibben (1931), and C. S. Venkateswaran (1936). Nisi observed lines of frequencies 356, 498 and 911 for 84% acid, 512 and 906 for 50%, and 505 and 895 for 25% solutions of the acid. These results have been confirmed by Bell and Jeppesen. Nisi obtained lines at 358, 518, 889 and 1061 for a 38% solution of dihydrogen sodium phosphate and Schaefer and co-workers recorded a line at 924 for crystals of tertiary phosphate of ammonium. Venkateswaran worked with the acid in a number of concentrations. He also worked with solutions of a number of salts. The author attempted to study this acid also along with the substances published in this series (Rao, N. R., 1940, 1941, 1942) of investigations, and found that the results and conclusions of the previous authors require modification.

EXPERIMENTAL

The reason why comparatively little work is done in this acid by Raman effect is that its Raman spectrum is invariably found to be superposed by an intense spectrum. Somehow, it is found very difficult to remove this by purification of the acid. Therefore, other methods of diminishing this, *i.e.*, by making use of filters is resorted to.

First, the acid in the concentrated state is mixed with a little nitric acid—as in the case of sulphuric acid (Rao, N. R. 1940)—and heated up to 200°C, when most of the impurities would have oxidised. This is found to improve the spectrum to a large extent. Then the acid is filtered through a sintered glass funnel while hot. This removed the dust in the solution. Solutions of the salts are purified by treating them with purified carbon and then filtering through quantitative filter paper in a sintered glass funnel. Thus, solutions of the acid of concentrations, 75%, 50%, 30% and 15% of sodium dihydrogen phosphate of concentrations 5.7, 2.85, and 1.43N, of sodium monohydrogen phosphate of concentrations 2.5, and 1.5N and tertiary phosphate of concentration 1.0N are prepared.

Inspite of this laborious purification, continuous spectrum could not be avoided without the use of filters. Also, in the cases of dilute solutions of the acid and for the solutions of the salts, concentration being low, long exposures were required to get tolerably good spectra. In these cases, the continuous spectrum was suppressed to some extent, by using a double jacketted Wood's tube. The experimental liquid was placed in the innermost tube and two outer jackets were filled with solutions of sodium nitrite and of iodine in carbontetrachloride, in order to isolate the 4358 line of the mercury arc as much as possible.

RAMAN LINES OF PHOSPHORIC ACID AND PHOSPHATES

Of the work done by various authors, that of Venkateswaran (*loc. cit.*) is the most recent and in many respects exhaustive. Therefore, the Raman lines obtained by Venkateswaran are given here in Table I for the sake of convenience of comparison with those of the author given in table II.

TABLE I

Substance		Raman frequencies in cm^{-1}.						
H_3PO_4	85%	361 (w.d),	495 (w.d),	914 (st),	—	—	—	—
	60%	361 (w.d),	495 (w.d),	903 (st),	—	—	—	—
	30%	361 (w.d),	495 (w d),	890 (v.st),	950 (v.w)	—	4200 (v.w)	—
	15%	316 (w d),	495 (w.d),	886 (v st),	959 (w),	1082 (w),	1194 (w),	1427 (w)
	7·5%	316 (w.d),	495 (w.d),	886 (st),	959 (w),	1082 (w),	1194 (w),	1427 (w)
	3·0%	316 (w d),	495 (w.d),	886 (st),	959 (v.w)	1082 (v.w)	—	—
NaH_2PO_4	27%	356 (w),	495 (v.w),	886 (st),	—	1085 (m).		
$(NH_4)_2HPO_4$	30%	363 (v.w),	515 (v.w),	889 (w),	975 (st),	1070 (w).		
$(NH_4)_3PO_4$	31%	363 (v.w),	515 (v.w),		985 (m),	1080 (v.w).		
$(NH_4)_3PO_4$crystal					951 (w),	—		

TABLE II

Substance		Raman frequencies in cm^{-1}					
H_3PO_4	75%	360(w.d),	480(w.d),	914(st),	1060(v.w),	—	
	50%	360(w.d),	480(w.d),	903(st),	1060(v.w),	—	
	30%	360(w.d),	480(w.d),	890(st.b),	1060(v.w),	—	
	15%	360(w.d),	480(w.d),	886(st.b),	1060(v.w),	1200(v.w),	1450(v.w)
NaH_2PO_4	5.70N	360(m.d),	500(m.d),	886(st),	1060(st),	1200(v.w),	1450
	2.85N	380(m.d),	505(m.d),	886(st),	1070(st),	1200(v.w),	1450
	1.13N	380(m.d),	505(m.d),	886(st),	1080(st),	1200(v.w),	1450
Na_2HPO_4	2.50N	380(m.d),	515(m.d),	880(w),	990(st),	1080(v.w),	1450
	1.50N	385(m.d),	515(m.d),	880(w),	990(st),	1080(v.w),	1450
Na_3PO_4	1.90N	390(m.d),	515(m.d),	—	950(st),	1080(v.w),	1450

In the above tables, the letters in the brackets represent the intensities. w-weak; v. w-very weak; v. w. d-very weak and diffuse; w. d-weak and diffuse; m-medium; m. d-medium and diffuse; st-strong, st. b-strong and broad.

ASSIGNMENT OF RAMAN LINES TO DIFFERENT RADICALS

The Raman spectrum of phosphoric acid is quite similar to that of sulphuric acid and the assignment of lines to different radicals in the former can, therefore, be made on lines similar to that of the latter.

Venkateswaran assigned the lines at 1085, 980, 515, and 363 to PO_4, 1080, 975, 880, 515 and 363 to HPO_4, 1085, 885, 515 and 360 to H_2PO_4 ions. He did not assign any lines to H_3PO_4 molecules. He suggested that the line at 914 shifts to 880 as the acid is diluted from 85% to 3%. He seems to have regarded this as a concentration effect, and considered the acid to be largely dissociated into H_2PO_4 ions. This warrants a high conductivity for the acid even at high concentrations, while experiment shows that it is so even in comparatively weak acid.

Another point to be considered is that he gives 980 and 975 for the values of the lines characteristic of PO_4 and HPO_4 ions, while the corresponding lines in the spectra of the tertiary and secondary salts obtained by the author, are found to be well separated with a frequency difference of 40 cm^{-1}, the frequency difference in the spectrum of the secondary salt being greater than that of the tertiary, contrary to what is represented by Venkateswaran.

The groups of lines at 360, 515, 890 and can 1060 be regarded as composed of components corresponding to PO_4, HPO_4, H_2PO_4 and H_3PO_4, similar to those at 420, 550 and 900 in solutions of sulphuric acid, where they were considered to be composed of components corresponding to radicals SO_4, HSO_4 and

H_2SO_4. The line at 900 in sulphuric acid has a component at 860 corresponding to HSO_4 ions but with its specific intensity much less than its neighbour 910, characteristic of H_2SO_4. Similarly, for phosphoric acid, the line 890 appears to be very feeble and to have a little lower frequency in the spectrum of the secondary salt while in the the primary salt and acid, it is the most intense line.

On the above basis, the lines are assigned to different radicals and are represented in the diagram. The three groups of lines mentioned above are not resolved as represented in the diagram. Their resolution is exaggerated in order to make the assignment clear.

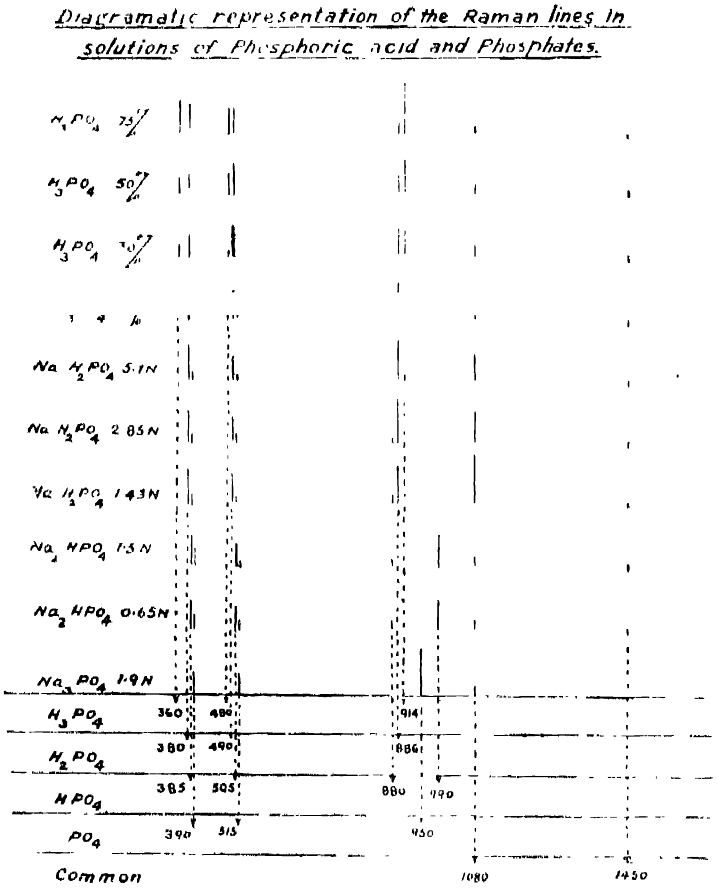

DIAGRAM

The line at 1080 which appears in all the spectra is of doubtful origin. It is most intense in the spectra of the primary salt. It is very diffuse in the most concentrated solutions and gets sharper with dilution. From its large intensity in the spectra of the primary salt solution, it is likely, that it is characteristic of the H_2PO_4 ions. Its appearance in the secondary and the tertiary salts may be due to the hydrolysis of these salts giving rise to the H_2PO_4 ions, which seem to the most stable of all the radicals mentioned above, both in the acid and salt solutions.

DISSOCIATION OF PHOSPHORIC ACID

The comparatively good intensity of the 886 line in the various spectra, it can be even in dilute solutions, indicates the predominence of H_2PO_4 ions even in very dilute solutions as was observed by Nisi, Venkateswaran and others. Also the absence of the 990 line in the spectra of the acid indicates that the further dissociation of H_2PO_4 into HPO_4 and H is very small even in dilute solutions of the acid. The behaviour of the acid in this respect is quite similar to that of sulphuric acid, and obviously due to similar reasons.

There is one important difference between sulphuric and phosphoric acids in this respect. While even in very concentrated solutions, ranging from about 15N, we find lines corresponding SO_4 ions, lines corresponding to HPO_4 or PO_4, are not found in the spectra with these concentrations of the acid. Venkateswaran, who worked with dilute solutions also, reported a weak line at about 950 corresponding to HPO_4 ions which he attributed to the further dissociation of HPO_4. Considering the fact that this line is very intense in the corresponding salts, it should be concluded that the number of HPO_4 ions in the acid solutions is very small.

The rapid shifting of the line 914 to 886 as the concentration is reduced from 75% to 15%, shows that the dissociation of the acid is quite rapid. But the conductivity data shows that the degree of dissociation is only 18% even in 16% acid. Since the calculation of the dissociation made in the later case involves many unfulfilled assumptions, which are well known, the value given for the degree of dissociation should be taken with some reserve. The acid is fairly strong as far as the removal of the first hydrogen ion is concerned.

DISSOCIATION OF PHOSPHATES

In solutions of NaH_2PO_4, the line at 1080 gets sharp and intense on dilution, but the line due to HPO_4 at 990 does not appear at all, thereby showing that the dissociation of H_2PO_4 into HPO_4 and H is very slow even in these concentrations, contrary to the dissociation of HSO_4 into SO_4 and H in solutions of acid sulphates.

The spectrum of Na_2HPO_4 does not change with dilution, and there are no lines in this spectrum corresponding to PO_4 ions, thereby showing that the dissociation of HPO_4 into PO_4 is also very slow.

DISSOCIATION OF BICARBONATES

Raman spectra of bicarbonates have been studied only by a few investigators, namely Dickinson and Dillon (1929) and I. R. Rao and C. R. Rao (1936). Dickinson and Dillon worked with a 26% solution of $KHCO_3$ and reported a line of frequency 1035. I. R. Rao and C. S. Rao referred to bicarbonates also in their note on "Electrolytic dissociation in strong electrolytes" and reported that the bicarbonates dissociate completely as far as the alkali radical is concerned and the acid radical dissociates progressively on dilution. A study of dissociation of bicarbonates with dilution will be described in the following.

EXPERIMENTAL

Raman spectra of these substances are found to be superposed by an intense continuous spectrum, which is found difficult to avoid even after laborious purification of the solutions. Therefore, two filters, a solution of quinine sulphate in dilute HCl and of iodine in carbon tetrachloride, are used. Since, quinine sulphate had to be replaced very often, the usual arrangement employing double jacketted Wood's tube could not be used. Light from a mercury arc is condensed by a condenser on to the Woods tube. Filters containing in rectangular glass cells are placed near the Wood's tube Long exposures of nearly 50 hrs. were required to get tolerably good spectra. Another difficulty experienced in this connection is that though clear solutions are prepared, after some time, they are found to attack the glass container a little and become slightly turbid. Since, this happens only after a long time, it is not very serious. Solutions of sodium carbonate (3.06N) and potassium bicarbonate (2.35N, 1.18N, 0.59N) are prepared with pure substances and treated as usual with carbon and filtered through a sintered glass funnel. The Raman spectra are photographed for times inversely proportional to the concentration.

RESULTS AND DISCUSSION

Only a few lines could be recorded with some intensity and the frequencies measured and are given in table III.

TABLE III

Substance	Raman frequencies in cm^{-1}.		
Na_2CO_3 3.06N		1060 (st)	—
$KHCO_3$ 2.35N	1040 (st)	1060 (v.w)	1400 (st)
1.18N	1040 (st)	1060 (v.w)	1400 (st)
0.59N	1040 (st)	1060 (v.w)	1400 (st)

It is quite probable that there may be many other weak lines of lower frequencies, but they could not be recorded. Raman spectra of carbonates both in crystals and solutions are taken by a number of investigators (Kohlrausch, 1931*a*). The crystals give rise to a number of sharp lines, while in solutions only one line could be recorded. Its frequency slightly varies from substance to substance also.

It can be seen from the Table III that the 1060 line is common to both solutions, carbonate and bicarbonate and can be taken to be characteristic of the CO_3 group. Lines of frequencies 1040 and 1400 are taken to be characteristic of HCO_3 ions. Now, for CO_2 there is a Raman line at 1408 (Kohlrausch, 1931*b*). From this it can be concluded that the HCO_3 ion has a structure $CO_2.OH$, where H is attached to O, as in the case of all the other acids. The 1040 line seems to correspond to the 1010 line of acetic acid attributed to C-O bond.

The spectra of the bicarbonate solutions show little changes in the intensities of the lines with dilution, thereby showing that the dissociation in these solutions vary very little with dilution, as in the case of phosphates. Now, carbonic acid H_2CO_3 is known to be very weak and hence in solution of sodium carbonate, hydrolysis can be expected to take place resulting in the production of HCO_3 ions. The absence of lines due to HCO_3 in the carbonate solution indicates that this process is also very slow.

PERCHLORIC ACID

Perchloric acid is well known to be a very strong acid. Investigators (Kohlrausch, 1931*c*) in this field found that even a 70% acid gives the same Raman lines as the solution of the corresponding salt, unlike in the case of nitric acid and other acids which show two sets of lines attributable to the undissociated molecules and their ions. This suggests that this acid is completely dissociated in solutions below 70%. The present work is intended to test this point.

Perchloric acid has been successfully studied by Fontoyne (1936) at different concentrations. For pure acid, he observed lines of frequencies 422(1), 570(5), 730(5), 922(0), 1025(4), and 1190(0), corresponding to $HClO_4$ molecules and for $NaClO_4$ at 463(1), 626(1), 935(8), and 1110(0), corresponding to ClO_4 ions. It can be seen that these spectra are quite similar to those of H_2SO_4 and its ions. Table IV gives the lines and their intensities in these solutions as studied by the author.

TABLE IV

Solution	Raman frequencies in cm^{-1}			
$HClO_4$ 10N	450(1)	610(1)	930(5)	1120(0)
$NaClO_4$ 10N	463(1)	626(1)	935(8)	1110(1)
$HClO_4$ 7.5N	455(1)	610(1)	930(6½)	1120(0)
$NaClO_4$ 7.5N	462(1)	462(1)	935(8)	1110(0)
$HClO_4$ 5.0N	455(1)	610(1)	930(7½)	1120(0)
$NaClO_4$ 5.0N	462(1)	626(1)	935(8)	1110(0)

The above spectra are taken under identical conditions with times of exposure inversely proportional to concentration. From the above table the following points can be clearly seen.

1. At the outset, it appears that the Raman spectra of the acid and the salt consist of the same lines, that is those characteristic of only the acid radical, and the lines due to undissociated acid molecules could not be observed in these solutions.

2. The lines of frequencies 463 and 626 slightly shift to shorter frequencies in the spectra of the acid compared to that in the salt.

3. The intensity of the line at 935 characteristic of the ions becomes larger with increasing dilution of the acid, while that in the salt solution is the same in all concentrations.

4. For each concentration, the intensity of this line is larger in the spectrum of the salt than in that of the acid.

DISCUSSION

The results 2-4 are not to be expected if the acid is completely dissociated. (2) indicates the presence of the lower frequency components due to the undissociated molecules. From 3 and 4, it is evident that the acid is not completely dissociated in these solutions, as was thought by the previous investigators. The absence of the lines due to the undissociated molecules simply means that the specific intensity of the lines due to these molecules is very small compared to those due to the ions. This view is further supported by the fact, that in the case of sulphuric and nitric acids also, where a quantitative investigation of the dissociations are reported by the author, it was found that the lines corresponding to the undissociated molecules have less specific intensity than those of the ions.

In conclusion, the author takes great pleasure in recording his grateful thanks to Dr. I. Ramakrishna Rao, D.Sc. (Lond.), under whose direction the present work was done.

Department of Physics,
Andhra University, Guntur.

REFERENCES

Bell and Jeppesen, 1935, *Jour. Chem. Phys.*, **3**, 363.
Dickinson and Dillon, 1929, *Proc. Nat. Acad. Amer.*, **15**, 334.
Fontoyne, 1936, *Nature*, **138**, 886
Hibben, 1931, *Jour. Amer. Chem. Soc.*, **53**, 2418.
Kohlrausch, 1931*a* "*Der Smekal-Raman Effect.*" Page 343 (references).
,, 1931*b* page 352 (references).
,, 1931*c* page 3 (references).
Nisi, 1929, *Jap. Jour. Phys.*, **5**, 119.
Rao, I. R., and Rao, C. S., 1936, *Nature*, April.
Rao, N. R., 1940, *Ind. Jour. Phys.*, **14**, 143.
Rao, N. R., 1941, *Ind. Jour. Phys.*, **15**, 185
Rao, N. R , 1942, *Ind. Jour. Phys* , **16**, 71
Schaefer, Matossi and Aderhold, 1930, *Zeit. f. Phys* , **65**, 289
Venkateswaran, C. S., 1936, *Proc. Ind. Acad. Sc.*, **3**, 26.